School of Earth & Planetary Sciences

The subduction history of the Paleo-Pacific Oceanic plate from the Mesozoic to early Cenozoic in NE China and Sikhote-Alin, Russian Far East

Kai Liu

This thesis is presented for the Degree of

Doctor of Philosophy

At

Curtin University

May 2021

Declaration

This thesis is completed from a jointly supervised PhD program with an agreement between Curtin University, Western Australia and Peking University, China. The thesis is submitted to both universities for the doctoral degree. Peking University has already received the thesis and I have passed the thesis defense.

To the best of my knowledge and belief this thesis contains no material previously published by any other person except where due acknowledgement has been made. This thesis contains no material which has been accepted for the award of any other degree or diploma at any university, other than Peking University, China.

Kai Liu

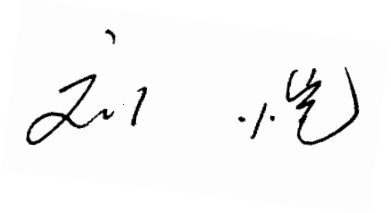

Date: 27/01/2021

Abstract

The Pacific domain is characterized by several oceanic plates that were subducted beneath the Asian and American plates during the past hundreds of millions of years. The NE Asian continental margin, including NE China and Sikhote-Alin, Russian Far East, was affected by the subduction of the Paleo-Pacific oceanic plates in the Mesozoic and the Pacific plate in the Cenozoic. Thus, the study area preserves essential geological evidence for understanding the subduction history in the NW Pacific and its geological responses along the continental margin. Detailed field investigations along several traverses, large-scale mapping, whole-rock geochemistry, zircon U-Pb dating and Lu-Hf isotope analysis were carried out on igneous and sedimentary rocks in the NE China and Sikhote-Alin areas. Based on the data, it will be discussed when and how the subduction process influenced magmatism, deformation and terrane motion along the continental margin.

NE China is separated into several continental blocks, including the Songliao Block in the west and the Bureya-Jiamusi-Khanka Block in the east. The earliest arc magmatism related to Paleo-Pacific plate subduction in the area is represented by the Khanka Lake granitoids in the northern Khanka Block. Zircon LA-ICP-MS dating identified two major magmatic episodes: Triassic (ca. 249 Ma) granodiorite and Late Triassic to Early Jurassic (209-199 Ma) syenogranite. Later felsic veins intruded these granitoids between 195-184 Ma. The granodiorite (ca. 249 Ma) has abundant mafic enclaves and shows adakite-like geochemical features, such as high Sr, Sr/Y and La/Yb, with zircon εHf(t) values of −0.65 to 1.61, indicating magma mixing between older lower crust and juvenile basaltic magma was important. The syenogranite (209-199 Ma) belongs to the highly fractionated I-type granites, showing high SiO_2, Na_2O, K_2O and very low Mg, Fe, Ni and Cr. The zircon εHf(t) values are positive, ranging from 1.72 to 5.12, suggesting the importance of juvenile materials in its source. The zircon εHf(t) values from granodiorite, syenogranite and felsic veins become more positive as the zircon

ages become younger, recording the consistent increase of juvenile crustal melting. The Khanka Lake granitoids provide evidence of the early-stage subduction of the Paleo-Pacific plate in NE China and the eastern Central Asian Orogenic Belt (CAOB).

Subduction-related magmatism was also active along the eastern margin of the Songliao Block, namely the Lesser Xing'an-Zhangguangcai Range. The ancient Mudanjiang Ocean was located between the Songliao and Jiamusi-Khanka blocks before the Cretaceous, and may be a part of the Paleo-Pacific Ocean in NE China. Volcanic rocks were sampled and analyzed in order to understand their genesis and relationship to subduction. Zircon SHRIMP U-Pb dating and whole-rock geochemical analyses were carried out on these volcanic rocks. The results show that most samples are Early Jurassic in age (189-178 Ma), including andesite, trachyandesite, trachydacite and rhyolite. The rhyolite is a highly fractionated I-type, similar to the coeval granites in the Lesser Xing'an-Zhangguangcai Range. The andesitic to trachytic rocks were affected by magma mixing along an active continental margin. The samples from the Jiamusi Block and one sample from the Lesser Xing'an Range record late Early Cretaceous (ca. 100 Ma) ages. In contrast, fractional crystallization was the most important genesis mechanism for the basalts and trachydacites. However, magma mixing or crustal contamination was also involved in the genesis of several andesitic samples. It is proposed that Jurassic arc magma was generated by westward subduction of the Mudanjiang Ocean. After closure of the Mudanjiang Ocean, the Paleo-Pacific Ocean began to govern the tectonic evolution of the eastern CAOB. The roll-back of the Paleo-Pacific slab triggered back-arc extension in NE China and resulted in extensive volcanism in the Jiamusi Block during the late Early Cretaceous.

During the Jurassic to Cretaceous, numerous components were accreted along the eastern margin of the Jiamusi-Khanka Block to form the Sikhote-Alin accretionary orogenic belt. These accretionary units are mainly N-S trending and separated by thrusts and strike-slip faults. Six sandstone samples were collected along an E-W traverse in the southern Sikhote-Alin orogenic belt for zircon U-Pb dating and Lu-Hf

isotopic analysis. They indicate that the Jiamusi-Khanka Block was the most important source area for sediments in the Samarka accretionary complex. However, the Zhuravlevka turbidite basin, separated by the Central Sikhote-Alin Fault from the Samarka belt, was supplied by both the Jiamusi-Khanka Block and the North China Craton. The easternmost belt, the Taukha accretionary complex shows no signal of the Jiamusi-Khanka Block, but was only fed from the North China Craton. East to west trending accretionary processes cannot explain the data, so it is proposed that the eastern Sikhote-Alin belts were initially deposited farther south during the Early Cretaceous. Afterwards, sinistral strike-slip faulting transported the eastern Sikhote-Alin belts northward after their deposition.

The arc-related granitoids and volcanic rocks moved eastwards to the coastal Sikhote-Alin area after major sinistral strike-slip motion during the late Early Cretaceous, implying the consistent roll-back of the Paleo-Pacific slab. The whole-rock Sr-Nd isotopes of the granitoids show significant enriched features in the Late Cretaceous. However, after a magmatic gap (ca. 55-45 Ma), mantle-derived or juvenile crustal materials increased abruptly indicated by their depleted isotopic characteristics. The I & S-type granitoids and volcanic rocks were superseded by A-type granite and intra-plate basalts and adakitic volcanic rocks. This change in magma is proposed to represent a slab window opening during the early Cenozoic under the continental margin, caused by the Izanagi-Pacific ridge subduction. At ca. 55 Ma, MORB-like gabbros intruded into the coeval accretionary complexes in Hokkaido, NE Japan, whereas A- and S-type granites were emplaced into the coeval fore-arc basins in Sakhalin, SE Russian, further supporting the ridge subduction model. Ridge subduction and the migration of a triple junction caused a change in the regional stress field. The Pacific Plate moved in a WNW or W direction after the consumption of the Izanagi Plate which was subducted to the NNW. This important change triggered the sinistral strike-slip faulting in Sikhote-Alin, NE China and Korea to change to dextral motion. This ridge subduction event is also supported by evidence from the ocean side. New research based on magnetic anomalies, seamount chains and plate reconstructions

indicates that the Izanagi-Pacific ridge arrived at the eastern Asian margin at ca. 60 Ma, resulting in plate reorganization in the west Pacific domain.

Acknowledgements

This research could never be completed without the support of the following people and institutes.

My supervisors, Profs. Simon A. Wilde at Curtin and Jinjiang Zhang at Peking University (PKU), contributed much during my research in the past years. Simon was very kind to agree to my application for the joint PhD program when I sent him my first email and helped a lot to achieve the complicated process. As a famous geologist, he taught me how to analyze the data and tell a story based on the known facts, and even, how to make a mount by myself. Prof. Zhang and I had lots of discussions on NE China and Sikhote-Alin. He showed me the great importance of good scientific questions because no good research will be carried out before posing an interesting question. He is also an honorable person and motivated geologist. By studying under Prof. Zhang during my PhD career, I learned much about how to organize a scientific project in the first place, which will be a great asset during my future career.

The colleagues in both Curtin and PKU helped me a lot with experiments, fields and daily life. They are deeply appreciated because of their kindness and friendship. Guys from Room 3330, 3315 and 3327, Yifu'er Building in PKU, include Meng Wang, Jiamin Wang, Maohui Ge, Yiyun Ling, Hongling Deng, Chao Lin, Shan Shang, Tianli Huang, Yang Wang, Congyuan Yin, Sheng Ai, Wei Du and Bei Zhu. Mr. Adam Frew is thanked for his patience and kind help with SHRIMP dating, and Ms. Elaine Miller for assisting with CL imaging. Thank you to my Chinese friends in Perth for your beer, meal and shelter, especially Peter Chen, Nicole Zhan, Zongying Huang, Zhuocheng Wang, Siyu Hu and Nan Zhang.

Special thanks are given to Profs. Jianbo Zhou and Feng Guo. Prof. Zhou kindly guided us in the trip after my supervisor and I decided to have the very first field

investigation in NE China. When I prepared my papers, Jianbo always gave me useful suggestions about tectonics and Feng helped me a lot on geochemical and isotopic analyses. Also, the support of geologists from the Far East Geological Institute, Far East Branch, Russian Academy of Sciences is deeply appreciated. The Sikhote-Alin Mountains impress me so deeply. Mr. Sergey A. Kasatkin, a very happy man, taught me how to find outcrops, collect appropriate samples, chop woods and catch fish in the dense coniferous forest. Prof. Vladimir V. Golozoubov knows every rock and structure in his area, even more precise than the geological maps. Mr. Igor Alexandrov and Victor P. Nechaev are kind friends who discussed both geological and cultural differences between China and Russia, opening my eyes to see their beautiful country and the rocks in Sikhote-Alin. Prof. Bei Xu gave me many comments on the sedimentary geology. Without Prof. Xu, the chief scientist of a big project which funded my research, it would not even be possible for me to go to Russia as a researcher. Pan Zhao was good company in the field, as well as a respectable brother. I will never forget the beautiful view along the coast of Sea of Japan with these friends and colleagues. The co-operation between us will hopefully continue in my future work and their help will always be remembered with thanks.

Ms. Yi-wen Ren spent many years with me. We learned how to respect and love people who we care during the thousands of days. I shall never forget the life we went through together and the lessons I learned from these days. Wish smile never disappear on your face. “If I cannot see you tomorrow, good morning, good afternoon and good night”. Ms. Manqi Liao took care of me when I felt disappointed and depressed in the last year of my study career. She is a lovely girl and can always joke, although things go not well sometimes, which is the most important character I have earnt from her.

Last but not least, I feel grateful and honored to be your son, Mr. Mingjun Liu and Mrs. Hongyu Li. I do not know how much you worried when I lived in Australia and travelled during the field trips all over the world, thousands of miles away from my hometown. The life I spent after graduation from the China University of Geosciences

has been beyond your knowledge and I totally understand that you felt losing control of your only child. But I always keep in mind that I come from a small county in central China and a great family built by you. I hope that you can always smile and feel proud when thinking of me.

I also acknowledge Profs. Tatsuaki Kimura and Alexander Khanchuk, and many other geologists from China, Japan, and Korea who contributed to the paleophytogeography and tectonic reconstruction of East Asia. Their excellent work inspired me when I was confused by the Pacific accretionary orogens, the giant south-north strike-slip motion and the subduction process of the Paleo-Pacific plates.

This research was financially supported by the State Key Program of National Natural Science Foundation of China (41730210) and the Major State Basic Research Development Program of China (2013CB429804) and was partly funded by the Fundamental Research Funds for the Central Universities (310827161010).

Table of Contents

List of figures

List of publications included as part of the thesis

The thesis includes the following three published papers and one manuscript in review:

Liu, K., Zhang, J., Wilde, S. A., Zhou, J., Wang, M., Ge, M., ... & Ling, Y. (2017). *Initial subduction of the Paleo-Pacific Oceanic plate in NE China: Constraints from whole-rock geochemistry and zircon U–Pb and Lu–Hf isotopes of the Khanka Lake granitoids*. Lithos, 274, 254-270.
Available at:
http://dx.doi.org/10.1016/j.lithos.2016.12.022

Liu, K., Zhang, J., Wilde, S. A., Liu, S., Guo, F., Kasatkin, S. A., ... & Wang, J. (2017). *U-Pb Dating and Lu-Hf Isotopes of Detrital Zircons From the Southern Sikhote-Alin Orogenic Belt, Russian Far East: Tectonic Implications for the Early Cretaceous Evolution of the Northwest Pacific Margin*. Tectonics, 36(11), 2555-2598.
Available at:
https://doi.org/10.1002/2017TC004599

Liu, K., Zhang, J., Wilde, S. A., Xiao, W. J., Wang, M. and Ge, M. H. (2019). *Zircon U-Pb dating and whole-rock geochemistry of volcanic rocks in eastern Heilongjiang Province, NE China: Implications for the tectonic evolution of the Mudanjiang and Paleo-Pacific oceans from the Jurassic to Cretaceous*. Geological Journal, 1-24.
Available at:
https://doi.org/10.1002/gj.3623

Liu, K., Zhang, J., Wilde, S. A. and Xiao, W. J. *Izanagi-Pacific ridge subduction in NE Asia in the early Cenozoic: A review of geological evidence from NE Asia*. Earth-Science Reviews. **In review.**

Statement of contribution of others

This thesis was supported by the School of Earth & Planetary Sciences, Curtin University and the School of Earth and Space Sciences, Peking University. The individual chapters, consisting of three published papers and one unpublished manuscript which is under review when writing this thesis, were conducted under the supervision of Prof. Simon A. Wilde at Curtin University and Prof. Jinjiang Zhang at Peking University. Field trips, sample preparation and data acquisition were undertaken through collaboration between Curtin University, Peking University, Institute of Tibetan Plateau Research (Chinese Academy of Sciences) and China University of Geosciences (Wuhan). As the author of this thesis, and the first author of all published papers and the unpublished manuscript contained within, I declare that I have been primarily responsible for all subsequent research, analysis, data interpretation and writing up of these papers/chapters.

Kai Liu

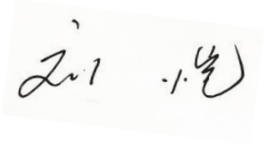

06/11/2019

An approximate breakdown of persentage contributions by each co-author is provided below.

Paper 1:

Title: Initial subduction of the Paleo-Pacific Oceanic plate in NE China: Constraints from whole-rock geochemistry and zircon U–Pb and Lu–Hf isotopes of the Khanka Lake granitoids.

Journal: Lithos. Year: 2017. Volume: 274. Pages: 254-270.

Author list (and contributions): Kai Liu (60%), Jinjiang Zhang (10%), Simon A. Wilde (10%), Jianbo Zhou (5%), Meng Wang (5%), Maohui Ge (5%), Jiamin Wang (3%), YiyunLing (2%).

Paper 2:

Title: U-Pb Dating and Lu-Hf Isotopes of Detrital Zircons From the Southern Sikhote-Alin Orogenic Belt, Russian Far East: Tectonic Implications for the Early Cretaceous Evolution of the Northwest Pacific Margin.

Journal: Tectonics. Year: 2017. Volume: 36. Pages: 2555-2598.

Author list (and contributions): Kai Liu (60%), Jinjiang Zhang (10%), Simon A. Wilde (10%), Shiran Liu (3%), Feng Guo (3%), Sergey A. Kasatkin (3%), Vladimir V. Golozoubov (3%), Maohui Ge (3%), Meng Wang (3%), Jiamin Wang (2%).

Paper 3:

Title: Zircon U-Pb dating and whole-rock geochemistry of volcanic rocks in eastern Heilongjiang Province, NE China: Implications for the tectonic evolution of the Mudanjiang and Paleo-Pacific oceans from the Jurassic to Cretaceous.

Journal: Geological Journal. Year: 2019. Volume: Special Issue.

Author list (and contributions): Kai Liu (60%), Simon A. Wilde (10%), Jinjiang Zhang (10%), Wenjiao Xiao (10%), Meng Wang (5%), Maohui Ge (5%).

Paper 4:

Izanagi-Pacific ridge subduction in the early Cenozoic: A review of magmatism and deformation history of the NE Asian continental margin.

Journal: Earth-Science Reviews. **In review**.

Author list (and contributions): Kai Liu (70%), Jinjiang Zhang (10%), Wenjiao Xiao (10%), Simon A. Wilde (10%).

I, Simon A. Wilde, as one of the co-authors and Kai Liu's PhD supervisor, endorse that the level of contribution indicated above is appropriate.

Simon A. Wilde

Date: 06/11/2019

I, Jinjiang Zhang, as one of the co-authors and Kai Liu's PhD supervisor, endorse that the level of contribution indicated above is appropriate.

Jinjiang Zhang

Date: 30/10/2019

I, Wenjiao Xiao, as one of the co-authors, endorse that the level of contribution

indicated above is appropriate.

Wenjiao Xiao

Date: 04/11/2019

I, Jianbo Zhou, as one of the co-authors, endorse that the level of contribution indicated above is appropriate.

Jianbo Zhou

Date: 03/11/2019

I, Feng Guo, as one of the co-authors, endorse that the level of contribution indicated above is appropriate.

Feng Guo

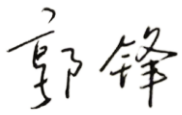

Date: 03/11/2019

I, Sergey A. Kasatkin, as one of the co-authors, endorse that the level of contribution indicated above is appropriate.

Sergey A. Kasatkin

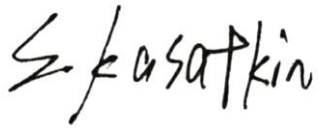

Date: 06/10/2019

I, Vladimir V. Golozoubov, as one of the co-authors, endorse that the level of contribution indicated above is appropriate.

Vladimir V. Golozoubov

Date: 06/10/2019

I, Meng Wang, as one of the co-authors, endorse that the level of contribution indicated above is appropriate.

Meng Wang

Date: 06/11/2019

I, Jiamin Wang, as one of the co-authors, endorse that the level of contribution indicated above is appropriate.

Jiamin Wang

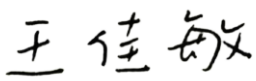

Date: 05/11/2019

I, Maohui Ge, as one of the co-authors, endorse that the level of contribution indicated above is appropriate.

Maohui Ge

Date: 06/11/2019

I, Yiyun Ling, as one of the co-authors, endorse that the level of contribution indicated above is appropriate.

Yiyun Ling

Date: 05/11/2019

I, Shiran Liu, as one of the co-authors, endorse that the level of contribution indicated above is appropriate.

Shiran Liu

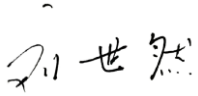

Date: 06/11/2019

Chapter 1 Introduction

1.1 Research background

1.1.1 Accretionary orogens

Orogens are mainly built along convergent plate margins, such as subduction zones and active continental margins. Accretionary orogens are always accompanied by the subduction of an oceanic plate and are characterized by intraoceanic or continental arcs, fore-arc accretionary prisms and basins and back-arc basins (Cawood et al., 2009; Xiao et al., 2003). The most notable present-day accretionary orogeny is the western Pacific, from the Tonga, Philippines, Japanese Islands to the Kuril and Aleutian subduction zones (Fig. 1.1). In an accretionary orogeny, various kinds of massifs, blocks, arcs or tectonostratigraphic terranes can be transported towards the trench and finally welded together. Long-term accretion of these assemblages last for hundreds of million years, forming wide accretionary complexes, whereas no typical "hard" continental-continental collision occured. During the accretionary process, multiple linear ophiolites, granitoids, and arc-related basins are juxtaposed and several collisional events between arc, microcontinent block and overriding continent/arc may happen. Rotation and lateral displacement occur when the linear geological units are influenced by interaction between the convergent plates. Thus, the preserved architecture and tectonic history of an accretionary orogeny are always complicated. In addition, subduction-related metamorphism is commonly observed in accretionary orogens, such as paired metamorphic belts; the high-T with low-P belts near the magmatic arc and high-P with low-T belts near the trench (Miyashiro, 1973).

Depending on the kinematics of the convergent plates, the accretionary orogens are subdivided into "retreat" type and "advance" type (Royden, 1993; Cawood et al., 2009). The retreat type is characterized by the rollback of the oceanic slab and retreat of the trench. The advance type is the opposite and shows a faster rate of the advancing oceanic plate than the overriding plate.

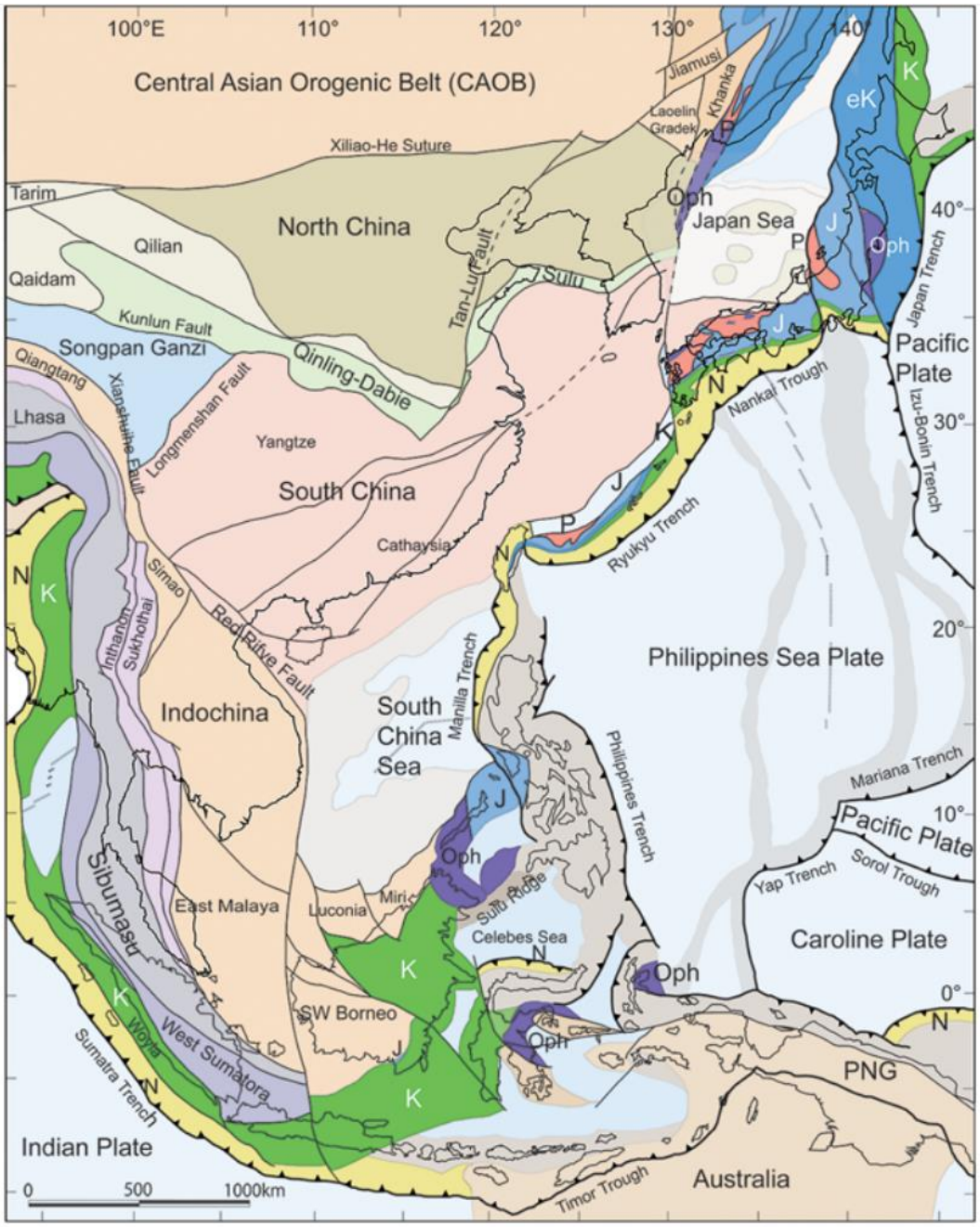

Fig 1.1 Accretionary complexes and arcs in the west Pacific rim (after Wakita et al., 2018). P=Permian, T=Triassic, J=Jurassic, K=Cretaceous, N=Neogene, Oph=Ophiolite.

1.1.2 The identification of accretionary orogens: Materials and structures of accretionary wedges

In an accretionary orogen, continuous accretionary assemblages are docked to a main continent or craton which is named the “host continent” and the orogeny is finally ended by the closure of the ocean characterized by the collision of the other continent or continents, forming what is know as a “Wilson cycle”. Thus, the architecture of a

long-term evolved accretionary orogen always contains deformed, bent and dismembered multiple island arcs/mature arcs, basins, and accretionary complexes with complicated subduction directions.

The most significant signatures to determine an accretionary orogen in both ancient and modern orogens are accretionary wedges, magmatic arcs (especially arc magma intruding into ancient accretionary wedges) and subduction-related metamorphism.

An accretionary wedge, also named accretionary prism or complex, is the most important geological unit that characterizes an accretionary orogen. When an oceanic plate is subducted beneath a continental margin, the materials on the oceanic crust are scraped into the trench and subduction channel (Isozaki, 1997), including basic/ultrabasic rocks (oceanic crust), chert (pelagic chemical sediments), mudstone (deep water terrigenous sediments in oceanic basins) and carbonate (shallow sea shelf and some seamount caps). All these sediments are deposited in the ocean and finally incorporated into the accretionary wedge during the subduction process, contributing to the ocean-ward growth of the wedge. Thick turbidites in the trench and fore-arc basins are also deformed and mixed with these oceanic components, which is also one of the most important signatures of accretionary wedges. Subduction may last for several hundreds of millions of years as multiple oceanic basins between arc/microcontinents are closed. Thus, several parallel/sub-parallel ophiolite belts are often observed in accretionary orogens. However, it does not mean a lot of major oceans were present because the scraping of oceanic crustal components is commonly discrete even before the closure of an ocean. For example, in the modern circum-Pacific region, countless ophiolites with various ages are identified in the Japanese Islands, Russian Far East and Cordillera of North America. But the Pacific Ocean is not close to closure and these ancient ophiolites can only indicate the disappearance of margin seas or ocean basins between arcs and continents.

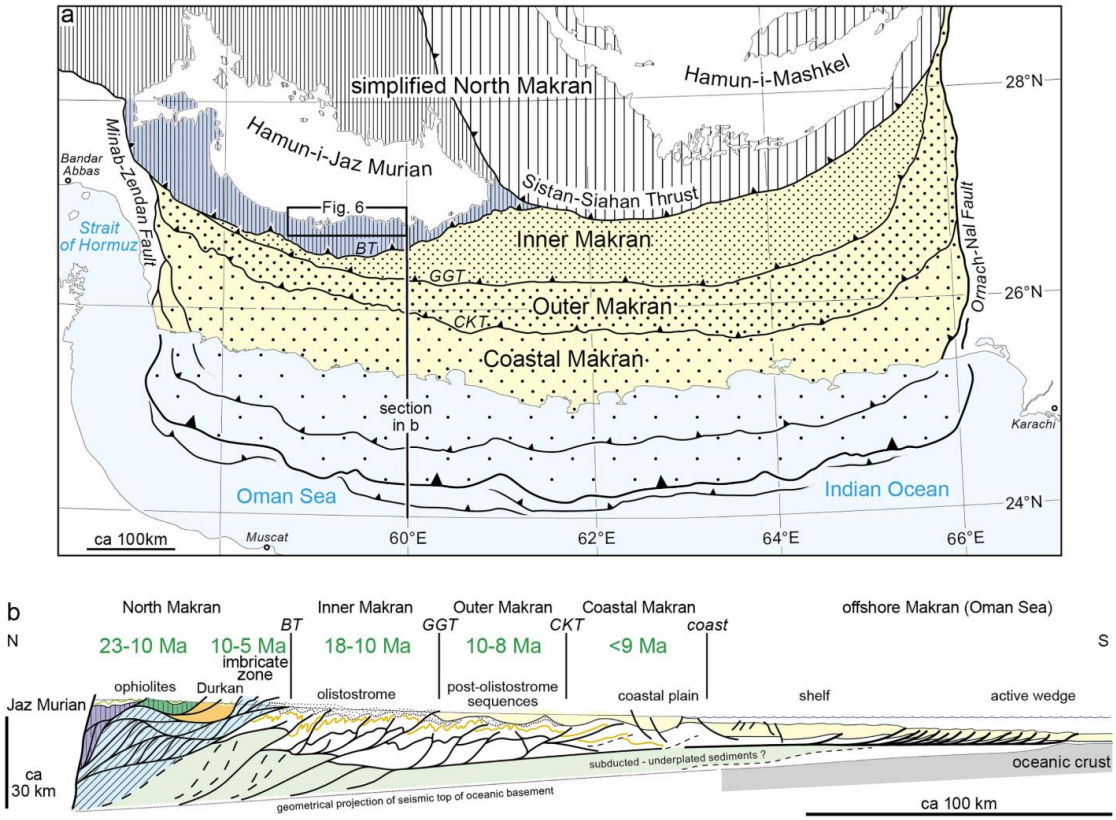

Fig. 1.2 Accretionary wedge/prism in the Iranian Makran area (Burg, 2018). Accretionary belts are separated by parallel thrusts, showing intensely out-of-sequence deformation and the oceanwards younging accretion process.

The deformation and structure of accretionary wedges is the most distinguishing feature to be identified. Normally, an accretionary wedge is separated by major faults from surrounding geological units (Fig. 1.2), which are commonly thrusts or strike-slip faults. The overriding plate can also be deformed during the subduction process, but commonly presents as a "coherent unit" with stable volcanic and sedimentary sequences. As proposed by Raymond (1984), the "broken unit" in the overriding plate margin shows thin-skinned thrusting during advancing subduction and extension in retreating subduction and its deformation style is always not as complicated as in the accretionary wedge. In the "dismembered unit" and "mélange", the major part of the accretionary wedge, imbricate structure and thrust duplexes are usually observed, showing strongly deformed materials scraped from the oceanic crust, and involving terrigenous components from the overriding plate. The original sedimentary sequences are rarely preserved in the mélange. "Matrix and block" structures are prevalent in the strongly-deformed part of accretionary wedges. The matrix is always comprised of

mudstone and siltstone that act as weak layers during compression, whereas the blocks can be of various types, including lenses of hard basic/ultrabasic rocks, coarse sandstones and fragments of chert.

Another important feature of a well-preserved accretionary wedge is the oceanwards younging emplacement age of the accretionary components. This is because the special growth style of the accretionary wedge. When an oceanic plate is subducted, the older accretionary components arrive at the trench earlier and become the hanging wall, whereas the late-stage materials are thrust under the older ones as the footwall (Taira, 2001). Thus, the age of an accretionary wedge will be younger to the subducting ocean side, which can be clearly observed in the Cordillera and Japanese Islands (Dickinson, 1976; Isozaki et al., 2010; Fig. 1.2). Although the sedimentary sequences are destroyed by deformation, stratigraphic sequence can be preserved locally in some places, from bottom to top presenting as cherts, basalts, mudstones, siltstones and sandstones.

1.1.3 The identification of accretionary orogens: Magmatism and crustal growth

The other important signature of an accretionary orogen is the various kinds of magmatic rocks that are included. The most significant magmatic rocks are produced by subduction-related arc magmatism. When the oceanic slab enters a subduction zone, the remaining sediments on the crust experience higher temperature and pressure, leading to dehydration reactions. The released fluids essentially metasomatize the overlying mantle wedge and calc-alkaline basaltic magma is generated from the partial melting of the mantle wedge. The dehydration reaction is normally triggered at 90-150 km depth of the slab surface, and the distribution maximum is 110 ± 38 or 128 ± 38 km (Tatsumi, 1986). Total dehydration happens at 70-300 km depending on the different slab angles (Schmidt and Poli, 1998). The arc-related basalt shows more oxidized features (Fe^{3+}/total Fe) than mid-ocean ridge and intraplate basalts, caused by the SO_2 degassing process (Kelly and Cottrell, 2012). The content of H_2O (average

1.7%) is also higher than the primitive MOR basalt (< 0.5%; Sobolev and Chaussidon, 1996). The fluids derived from oceanic sediments are enriched in incompatible elements (K, Na, Rb, LREEs etc.) and depleted in high field strength elements (HFSEs), HREEs and Nb-Ta-Ti, which are the predominant geochemical features of arc magma (Kelemen et al., 1990; Fig. 1.3).

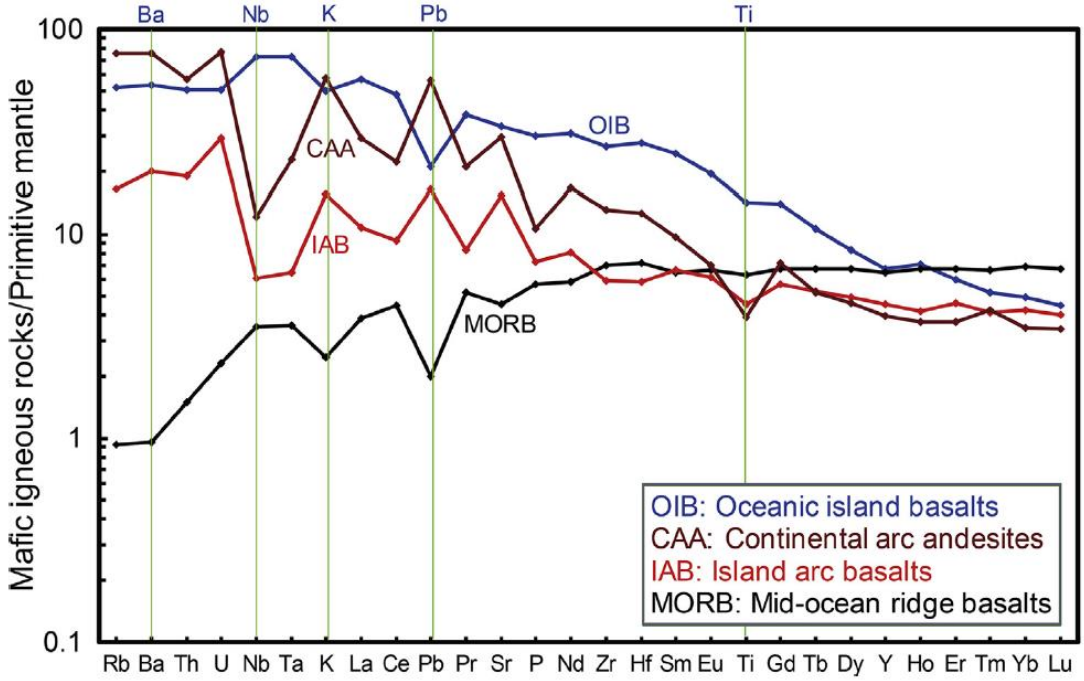

Fig. 1.3 The geochemical difference between arc magma, MORB and OIB (Zheng et al., 2019).

Some subduction-related magmatic rocks in accretionary orogens show distinguishing geochemical features, depending on their genesis. For example, high-Mg andesite, boninite, Nb-enriched basalt and adakite are widespread in a subduction zone. The high-Mg andesite shows higher MgO and Mg# than normal andesite and granodiorite. The distribution of these high-Mg rocks is typically associated with hot and young oceanic crust (Katz et al., 2004). In the "subduction of young and hot oceanic crust" situation, adakite and boninite commonly occur. Boninite is proposed to result from the initial subduction of an island arc or the interaction between a spreading center and island arc (Meffre et al., 1996; Stern, 2004), whereas adakite is considered to be the partial melt of a young oceanic slab, during which process it shows importantly high Sr, low Y and Yb that are in equilibrium with residual eclogite (Defant and Drummond,

1990). However, slab melt can also interact with peridotite of the mantle wedge to produce adakite and Nb-enriched basalt. In some thickened continental areas, such as Tibet, adakite is also widely reported (Chung et al., 2003). Although these rocks occur in various tectonic settings, the magmatic associations can be the signature for accretionary orogens when they are related to coeval accretionary complexes and long-term accretion without "hard" continental-continental collision.

I- and S-type granites are characteristic of collisional and accretionary orogens and can be distinguished by geochemical and isotopic features in the Lachlan orogen in eastern Australia, one of the most famous accretionary orogens in the Paleozoic (Chappell et al., 1988). The I-type granites have been considered to be the predominant magmatic rock type in both continental and oceanic arcs, whereas the S-type is related to syn-collision or post-collision orogeny (Barbarin, 1998). However, in the circum-Pacific accretionary orogens, S-type granites are extensively distributed where rare continental-continental collision occurred (Collins and Richards, 2008). A tripartite association including inboard S-type granite, outboard oceanic arc and intervening backarc basin is identified in long-term accretionary orogens (Collins and Richards, 2008). When the oceanic slab rolls back, extension dominates the overriding plate to generate a back-arc basin and I-type granite in the thinned supra-subduction crust. However, when repeated transient trench advancing happens, the back-arc area experiences short-lived compression and crustal thickening. At the late stage of contraction, enough meta-sedimentary materials are buried deeply to be partially melted and S-type granites are generated, following a new episode of I-type granites (Collins and Richards, 2008). Thus, S-type followed by I-type granites are also important in accretionary orogens. This tripartite association is one of the signatures to identify a long-term accretionary orogeny accompanied by repeated trench advance.

One of the most remarkable features of the magmatism in accretionary orogens is that the arc magma may migrate into the previously docked accretionary assemblages including arc, microcontinent and accretionary complexes. The mechanisms include

trench and arc retreat caused by slab roll-back and lateral growth of crust. For the former mechanism, the slab angle becomes steeper when the downgoing slab is anchored at 410-660 km depth and thus the arc migrates oceanwards. For the latter case, the exotic arcs, tectonostratigraphic terranes or blocks are docked and welded to the host continent, which results in the closure of oceanic basins between host continent and old accretionary assemblages. New subduction is initiated along the new margin after the accretion event, causing the passive migration of arc magmatism to the trench side. In some cases, slab roll-back, trench retreat and docking of accretionary assemblages are coeval in a giant accretionary orogen, such as the Paleozoic Central Asian Orogenic Belt (Xiao et al., 2015). No matter whether it is slab roll-back or lateral growth, the long-distance migration of magmatism, with the newly born magma intruding into the previous accretionary complexes, is a unique features that distinguishes accretionary orogens.

Continental growth is a significant process in long-lived accretionary orogens. Convergent plate margins, represented by subduction zones, have been treated as a major site to reduce the bulk volume of crust because of the sinking of oceanic crust into the mantle. However, in major accretionary orogens, continental growth is extensive. In the Central Asian Orogenic Belt (CAOB), a large volume of granites was formed by the subduction process and continued to the post-collisional stage after the North China Craton collided with the CAOB (Xiao et al., 2003; Jahn et al., 2000).

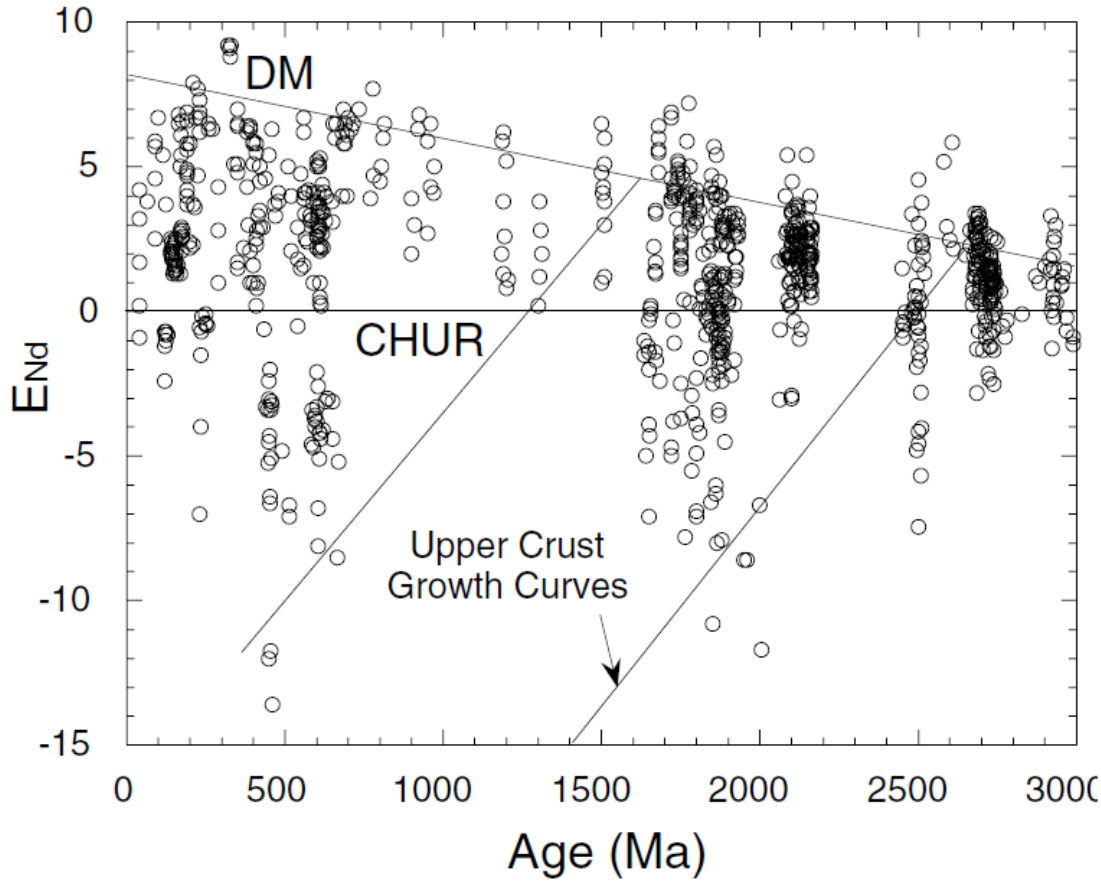

Fig. 1.4 Continental growth revealed by whole-rock Nd isotopes in accretionary orogens worldwide (Condie, 2007).

Nd-Sr isotopes in the granitoids (500-100 Ma) of the CAOB show remarkably high proportions (60 to 100 %) of mantle-derived materials (Jahn, 2004). The alkaline and peralkaline granitoids in the CAOB are post-accretionary, with mantle-derived basaltic magma underplating the accretionary assemblages and heating the crust to generate extensive partial melting in the CAOB. After crystallization, the bulk crust grew significantly by the input of granitic plutons. However, enriched Nd-Hf isotopes are also present in the areas dominated by microcontinental blocks, indicating that both juvenile growth and reworking of old crust are important in the CAOB (Jahn, 2004; Kröner et al., 2014). The growth rate globally depends on the duration of the orogeny and the materials involved in the accretionary orogens. The orogens comprised of island arc and accretionary complexes are named “simple orogens”, where mantle-derived components increase the volume of the bulk continental crust during the accretionary history. In contrast, the “complexes orogens” contain microcontinents or

ancient blocks, which may experience more reworking of old crust (Condie, 2007). For Phanerozoic accretionary orogens, the average accretion rates reached 70 to 150 km^3/km/m.y. (Condie, 2007). Thus, crustal growth in accretionary orogens is mainly associated with young oceanic arcs or accretionary complexes, whereas reworking of old crust and mixing between juvenile mantle input and crustal basement can also play an important role in the more complicated cases.

1.2 Accretionary orogens in the NW Pacific

The accretionary orogens in the western Pacific include a long belt extending over 5000 km from Taiwan in the south to Kamchatka in the north, which were called the "Nipponides" (Sengör and Natal'In, 1996) or "Pacific-type" and "Miyashiro-type" orogens (Maruyama et al., 1997). The west Pacific accretionary orogen is characterized by long-term history, multiple accretionary components and complicated tectonic scenarios.

The life span of the orogen has lasted over 500 Ma since the Devonian or even the Cambrian (Isozaki, 1997). The Japanese Islands extended towards the ocean side by ~400 km (Maruyama, 1997) and >200 km for the Sikhote-Alin accretionary complexes. Some components in the accretionary orogens are identified to be rifted from the mainland of Chinese cratons or blocks, such as the Oki and South Kitakami in Japan that were derived from the South China Craton (Maruyama et al., 1997; Isozaki et al., 2015) and Sergeevka in Russia derived from the northeast China blocks (Khanchuk, 2001). During 700-500 Ma, the Japanese Islands experienced a passive continental margin stage. After ca. 500 Ma (Isozaki et al., 2010) or 450 Ma (Maruyama et al., 1997), the initial subduction of the Paleo-Pacific oceanic plate began to control the whole area. Since then, episodic accretion of autochthonous prisms and calc-alkaline arc magma was accompanied by coeval high P/T metamorphism. One episode of accretionary orogeny reached its climax when a spreading center arrived at the trench, which produced numerous intrusive and eruptive rocks along with high P/T

metamorphic rocks and tectonic erosion (Maruyama et al., 1997; Isozaki et al., 2010). After the spreading ridge passed away, a new Pacific-type orogeny continued. Thus, an orogenic cycle in the western Pacific includes subduction-related magma, accretionary complexes, exhumation of high P/T metamorphic schists and emplacement of ophiolite and ridge subduction at its end. Five complete cycles are identified in the Japanese Islands, witnessing the long-term subduction history of the Paleo-Pacific plates, including the Renge, Farallon, Izanagi, Kula and Pacific plates (Taira, 2001; Isozaki et al., 2010).

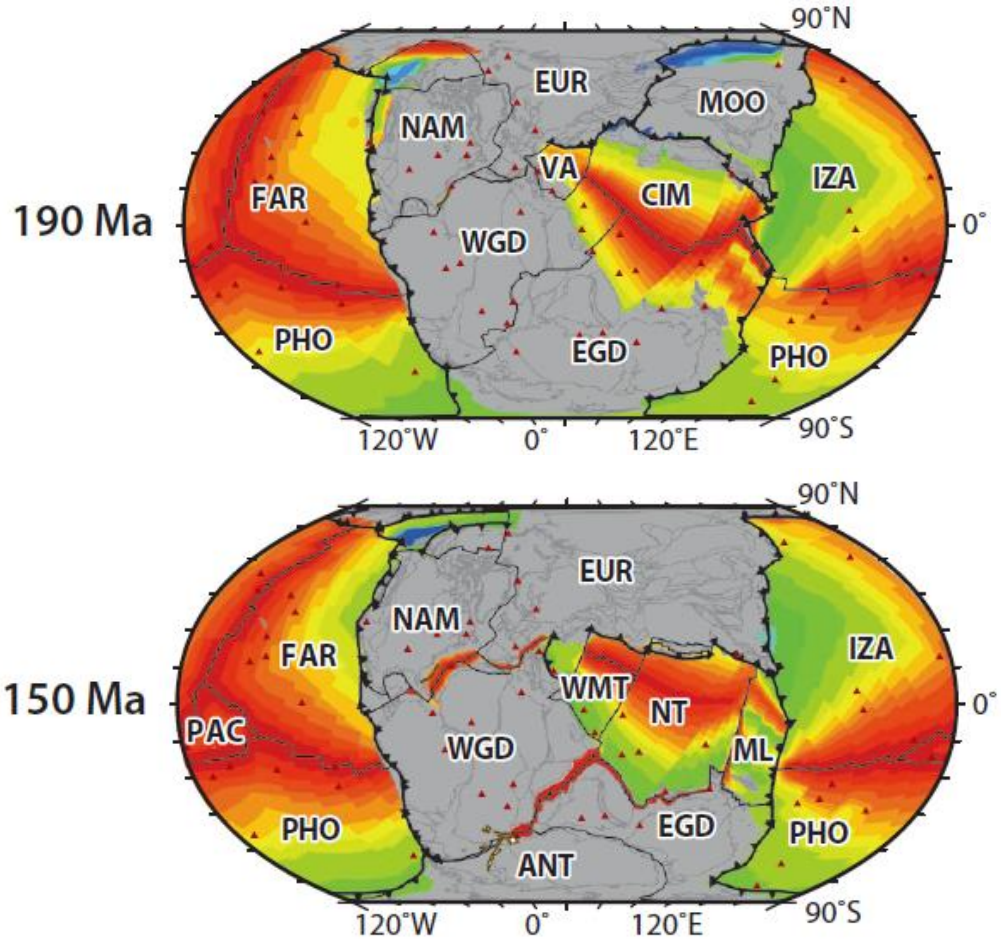

Fig. 1.5 Plate reconstruction at 190 and 150 Ma to show the oceanic plates in the Pacific domain (Müller et al., 2016). Abbreviations: FAR-Farallon Plate, PHO-Pheonix Plate, PAC-Pacific Plate, NAM-North American Plate, WGD-west Gondwana Plate, ANT-Antarctic Plate, EUR-Eurasian Plate, VA- Vardar Plate, WMT- west Meso-Tethys Ocean, NT- Neo-Tethys Ocean, ML- Proto-Molucca Plate, EGD-east Gondwana Plate, IZA-Izanagi Plate.

The components in these accretionary orogens in the NW Pacific vary from

autochthonous arc, accretionary complex, continental blocks and exotic oceanic materials.

Although the accretionary complexes include many fragments from the oceanic crust, the clastic materials are mainly terrigenous and derived from the island arc or continental arc and sometimes the interior of the mainland. Detailed detrital zircon dating of the sandstones in Japan, Korea, China and the Russian Far East show the striking abundance of old components. In SW Japan, ages of 1.8 to 2.5 Ga are reported in the Jurassic and Early Cretaceous schists, indicating the contribution of the Chinese Cratons, although controversy remains because it is difficult to distinguish the provenance between the North and South China cratons (Fujisaki et al., 2014). The situation is similar in NE China (Zhou and Li, 2017), Sikhote-Alin (Liu et al., 2017) and Sakhalin (Zhao et al., 2017). Old zircon ages are commonly detected there, indicating the affinity between those accretionary complexes and the active margin of cratons.

Accretion of oceanic materials travelling long distances is also important in the NW Pacific accretionary orogens. They are components of oceanic crust before being scraped by the thrusts at the trench and in subduction channels. The main lithologies can be divided into three major groups (Isozaki, et al., 1990), 1) magmatic rocks, mainly including basaltic rocks in seamounts and oceanic plateaus with hot spot or plume features, and pillow lava from the middle-ocean ridge (MOR), back- and fore-arc oceanic crusts; 2) metamorphic rocks, including serpentinized ultramafic rocks, high P/T metamorphic schists and greenschist-facies meta-volcanic rocks; and 3) oceanic sedimentary rocks without terrigenous infinities, such as limestone and chert.

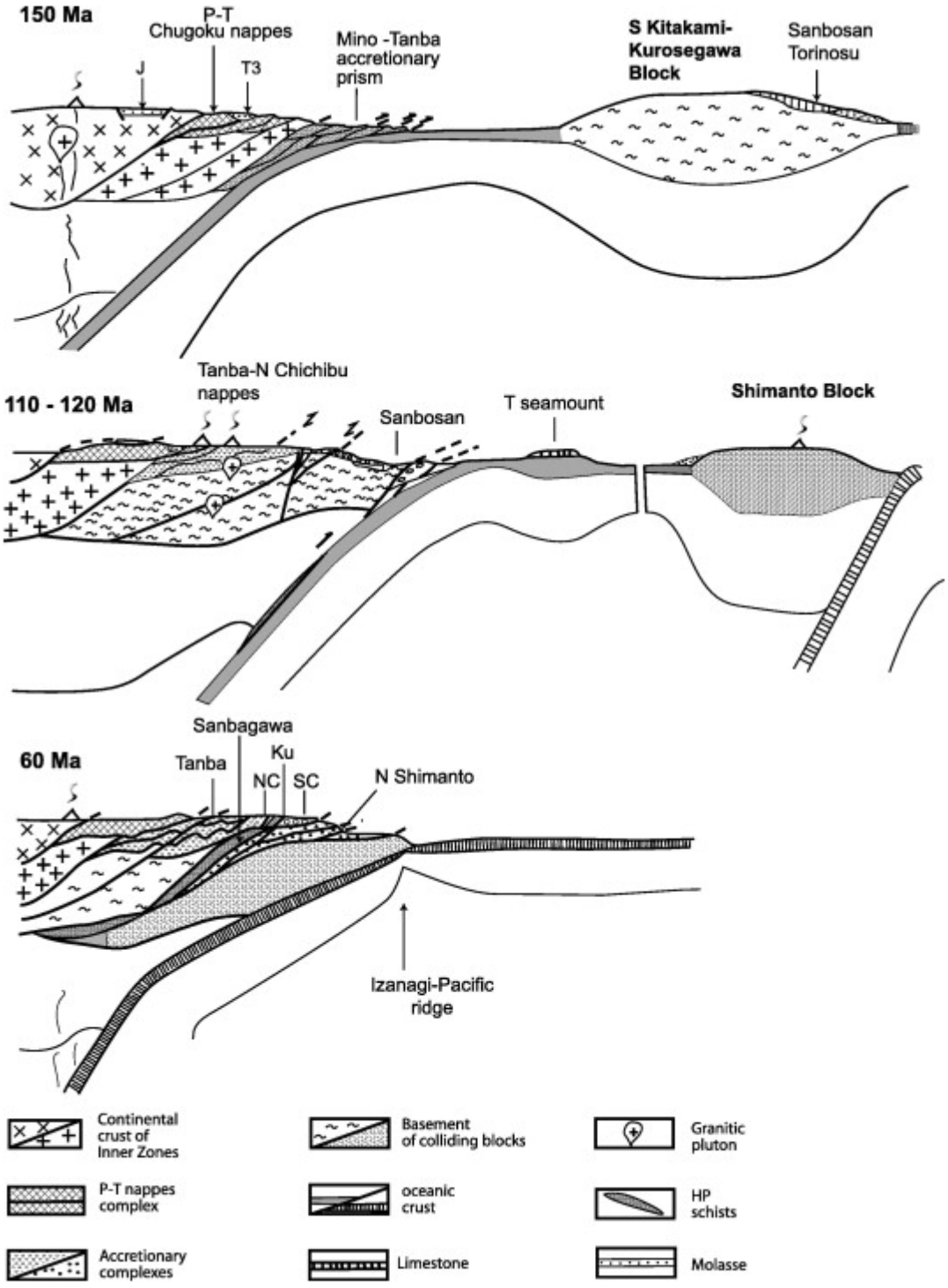

Fig. 1.6 Tectonic model showing block collision process in SW Japan (Charvet, 2013).

Several microcontinental blocks were docked onto the eastern Asian margin during the long-term subduction history. Despite the predominantly accretionary nature of the orogeny in the NW Pacific, collisions took place several times when continental blocks and mature arcs (continental arcs) arrived. The main signatures of the collision events

are presented by following evidence: 1) Extensive thrust sheets and nappes in SW Japan (Faure et al., 1986) and southern Sikhote-Alin (Khanchuk, 2001) are identified. Charvet et al. (1985) recognized an "Alpine-type orogen in an island-arc position". The Oga nappe consists of limestones and was proposed to be a component or fragment of the continental margin of the North China Craton (Chough et al., 2000). The Sergeevka nappes in Sikhote-Alin are underlain by high P/T blueschists and were proposed to be parts of the Paleozoic continental blocks (Khanchuk et al., 2016). Oceanic plateaus may also contribute to the lateral growth in the subduction history. However, in the case of Ontong Java Plateau, only 20% are thrust upon to the upper plate whereas the remaining 80% is subducted into the mantle (Mann and Taira, 2004), which means only buoyant arc and blocks with continental nature and lower density form the majorities of exotic materials preserved in accretionary orogens (Charvet, 2013). Whole-rock Sr-Nd isotopes support the existence of extensively hidden mature basement in SW Japan and Sikhote-Alin. In both areas, the Sr-Nd isotopes are mainly enriched, indicating important components from older crust (Jahn, 2010; Jahn et al., 2015). This characteristic is different from the CAOB, even if both the circum-Pacific and CAOB are proposed to be the most typical examples of accretionary orogens.

1.3 Major geological events in NE China and Sikhote-Alin: Consensus and controversy

NE China includes the easternmost Central Asian Orogenic Belt (CAOB), bounded by the Siberia Craton and Mongol-Okhotsk suture zone to the north and the North China Craton to the south. Tectonically, the eastern part of the CAOB includes the Songliao Block in the west and the Bureya-Jiamusi-Khanka blocks in the east, which are the major microcontinental blocks in the area (Fig. 1.7). The CAOB includes numerous blocks, accretionary prims, basins and arcs in Mongolia, southern Russia, Inner Mongolia and Xinjiang Province in China (Xiao et al., 2003; Wilde, 2015). It is characterized by roughly E-W trending suture zones separating the accretionary assemblages of the giant oroclines in central Asia (Xiao et al., 2015). In the NE China

part, the eastern CAOB was affected by the subduction of the Mongol-Okhotsk and Paleo-Pacific oceanic plates in the Mesozoic. The eastern Songliao and Bureya-Jiamusi-Khanka blocks experienced extensive magmatism at the continental margin (Wu et al., 2011) and strong deformation and high P/T metamorphism in the accretionary complexes (Zhou et al., 2009) in the Mesozoic. This process shaped the tectonic framework of the eastern CAOB, resulting in N-S trending accretionary complexes, magmatic belts and deep faults (Fig. 1.7), which is different from the central and western CAOB.

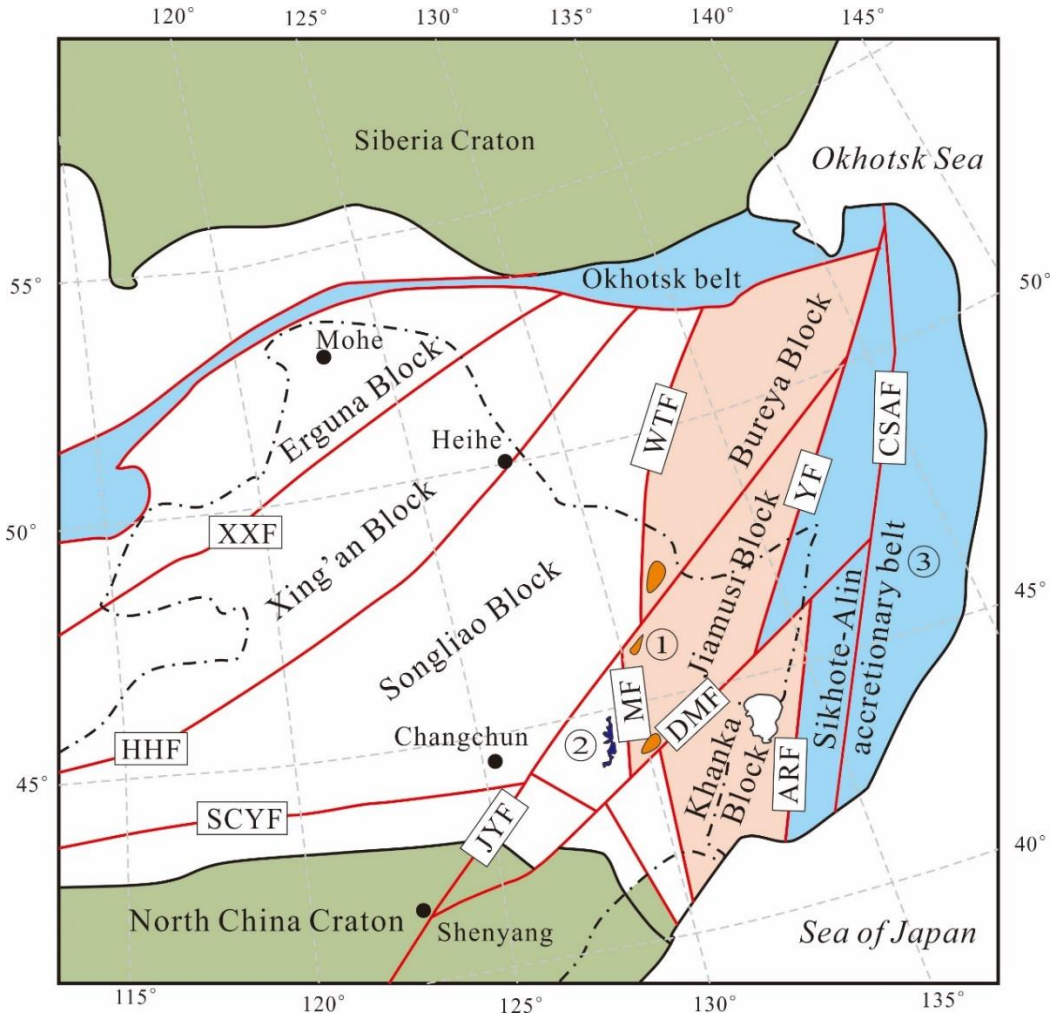

Fig. 1.7 The geological units in NE China and Sikhote-Alin (Liu et al., 2017a). ① =Heilongjiang Complex, ②=Zhangguangcai Complex. Both accretionary complexes are related to the ancient ocean crust between the Songliao and Jiamusi blocks.

The Sikhote-Alin accretionary complex, also called the Sikhote-Alin orogenic belt (Jahn et al., 2015), is one of the most typical accretionary belts/orogens in NW Pacific.

The Jurassic to Cretaceous accretionary complex in Sikhote-Alin is comparable with SW Japan before the opening of the Sea of Japan in the Miocene (Kojimo, 1989; Khanchuk, 2001). The Nadanhada accretionary complex or terrane belongs to the west part of the Sikhote-Alin accretionary complex, although it is situated within the Chinese territory. The other Mesozoic accretionary complex in NE China is named the "Heilongjiang Complex" or "Heilongjiang high-pressure metamorphic belt" (Zhou et al., 2009). The Nadanhada and Heilongjiang complexes are the only preserved Mesozoic accretionary prisms on the Chinese mainland, attracting many geologists who focus on the subduction history of the Paleo-Pacific Ocean in eastern China (Fig. 1.7).

Studies on the NE China and Sikhote-Alin areas have been popular since the 1990s. In the past 30 years, a lot of new data have been collected and important consensus has been reached, although controversies still exist. The major advances and debated issues are summarized below.

1.3.1 The recognition of early Neoproterozoic basement and the late Pan-African orogen in NE China

Although granitic gneiss was speculated as Paleoproterozoic in age because of the strong deformation and high-grade metamorphism, initial zircon U-Pb dating yielded ages of 274-256 Ma (Wu et al., 2001). Precambrian basement of the Bureya-Jiamusi-Khanka blocks appeared unfounded for a long time until several papers were published recently.

The first Neoproterozoic protolith age was published by Khanchuk et al. (2010), with a zircon SHRIMP U-Pb age of 757±4 Ma from the granulite complex of the Khanka Block, defining the Iman Group on the Russian side of the border. The analyzed samples are two- pyroxene–amphibole schists with tholeiitic basalt infinities for their protoliths, that then experienced granulite facies metamorphism at ca. 507±3 Ma,

constrained by metamorphic zircons and rims on the inherited zircons. However, the content of SiO_2 in the samples is low at 47.16% (Khanchuk et al., 2010), which seems unsaturated for the crystallization of zircons. Because of the lack of detailed petrological and isotopic analysis, this age has been tentatively considered as the protolith age of the metamorphic basement.

Unlike the basaltic features of the granulite complex in the Russian Far East, the recently-obtained ages are mainly from orthogneiss and sedimentary rocks.

Yang et al. (2017) described orthogneisses in the southern Jiamusi Block, adjacent to the Dun-Mi Fault that separates the Jiamusi and Khanka blocks. SIMS and LA-ICP-MS zircon U-Pb dating yielded weighted mean ages varying from 898±4 to 891±13 Ma. The rims of these early Neoproterozoic zircons and metamorphic zircons have two metamorphic ages, at ca. 563 Ma and 518-496 Ma. In the central Jiamusi Block, protolith ages of 757 to 751 Ma were reported later in the Mashan Complex, with the metamorphic ages ranging from 476 to 530 Ma (Yang et al., 2018). Geochemical data shows that the oldest orthogneisses were partially melted from a low-pressure crustal source consisting of mainly sedimentary rocks (Yang et al., 2017). The granitic gneiss with ages of 757 to 751 Ma was generated by a rifting event. The late Neoproterozoic metamorphism was linked to collision and post-collision in east Gondwana (Yang et al., 2018).

Detrital zircon U-Pb dating results in the Jiamusi Block show that the Mashan and Ximashan complexes in NE China and the Kimkanskaya groups in the Russian Far East were deposited in the Neoproterozoic (Luan et al., 2017). They were intruded by the Pan-African plutons and involved in the granulite-facies metamorphism at ca. 500 Ma (Wilde et al., 2003). The spectra of detrital zircons indicate the Jiamusi Block may have infinities with the Tarim Craton, due to the abundant zircon ages of 1.4 Ga (Luan et al., 2017).

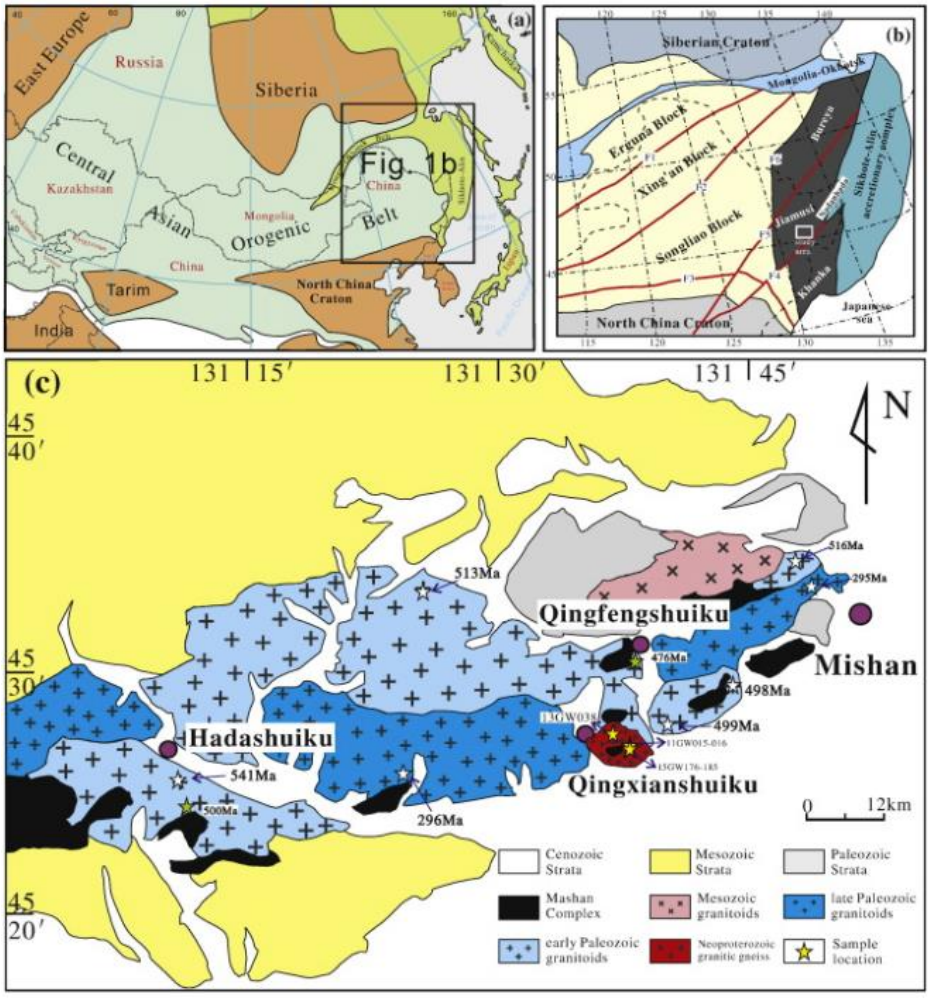

Fig. 1.8 The location of Neoproterozoic granitic basement of the Jiamusi Block in NE China (Yang et al., 2017).

The SHRIMP dating of both magmatic and metamorphic rocks in the Jiamusi Block by Wilde et al. (2003) also supports the correlation with north Australia, Tarim, and the North and South China cratons (Fig. 1.9).

However, the tectonic infinity of the blocks in NE China is controversial. The evolution of the Jiamusi-Khanka Block was associated with the Sayang-Baikal Orogen at the southern margin of the Siberia Craton according to the identification of a khondalite belt, including sillimanite- and garnet-bearing gneisses, amphibolite-plagioclase gneiss, cordierite- and graphite-bearing gneiss (Zhou et al., 2010). The belt extends > 1300 km in the southern CAOB margin, involving the Erguna, Xing'an, Songliao and Jiamusi-Khanka blocks (Zhou et al., 2011).

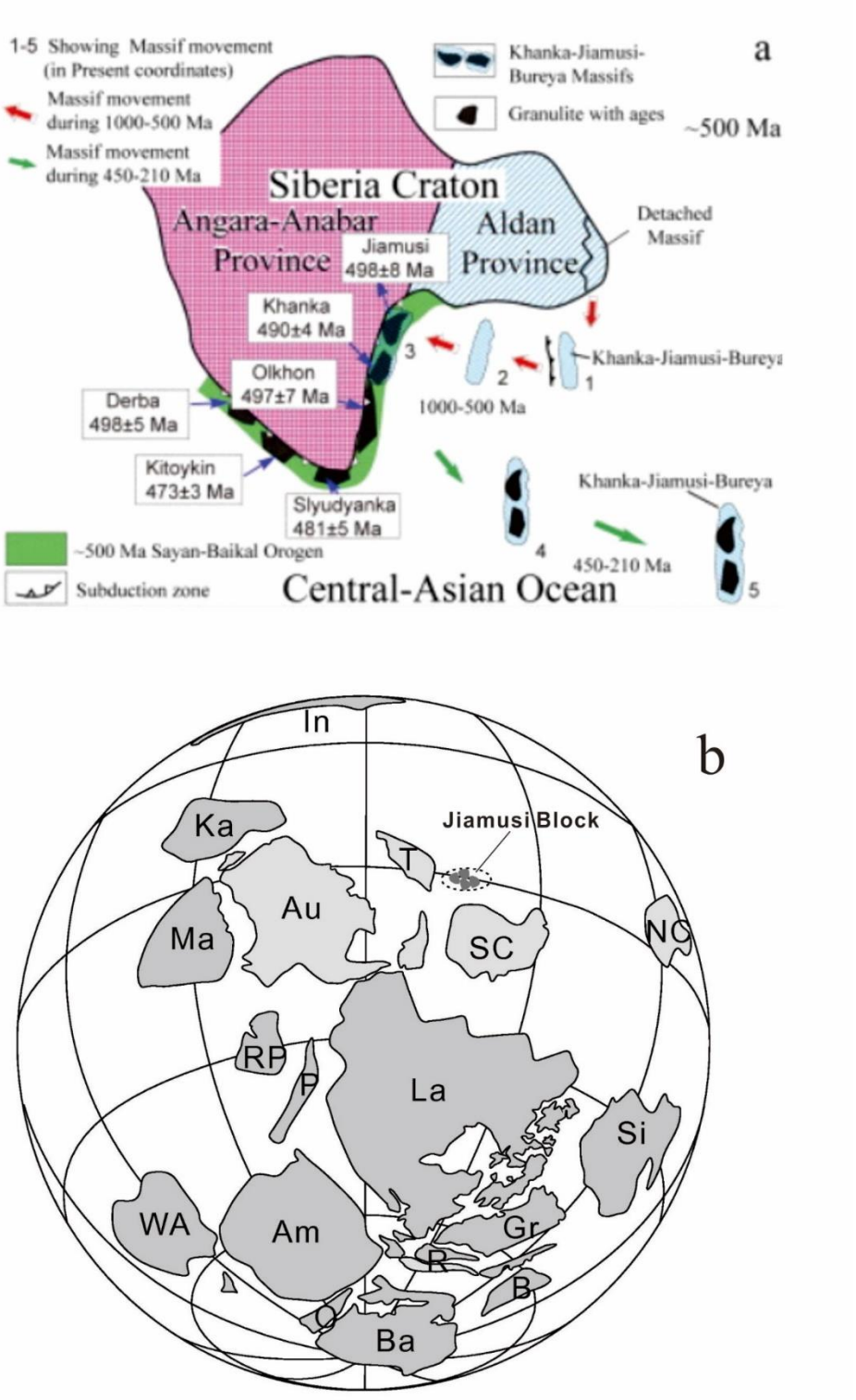

Fig. 1.9 Different models to explain the origin of the Jiamusi and Khanka blocks. a. The Siberia affinity of the Khanka-Jiamusi-Bureya Block (Zhou et al., 2010). b. The infinity afinity of Tarim Craton with theand Jiamusi Block (Luan et al., 2017).

The similarities of the basement information of the Bureya, Jiamusi and Khanka blocks support the viewpoint that they were one large continental block, separated by strike-

slip faults at a later stage (Zhou et al., 2010). This giant late Pan-African orogen indicates that the blocks in the eastern CAOB may have been welded together in the earliest Paleozoic and argues against the idea that the blocks were exotic and traveled a long distance before accreted onto the CAOB (Wu et al., 2007).

1.3.2 The opening and closure of the Mudanjiang Ocean: Magmatic and metamorphic history of the Heilongjiang blueschist

The Mudanjiang Ocean was identified by recent detailed research on the Heilongjiang Complex. The Heilongjiang Complex is located on the western margin of the Jiamusi Block and adjacent to the Lesser Xing'an-Zhangguangcai Range in the eastern Songliao Block. The main lithologies include metagabbro, amphibolite, marble, quartzite, blueschist and mica schist, typically the remnants of an oceanic crust scraped at the trench. High P/T conditions are recognized by the research on the blueschist and mica schist. Magmatic zircons in the blueschist yield protolith ages ranging from ca. 280 Ma to 210 Ma (Ge et al., 2016; Zhou et al., 2009). The geochemical features of the meta-basalt and gabbros show affinities to both E-MORB and OIB, indicating the accretion of oceanic crust and seamounts in the Mudanjiang Ocean. The blueschist-facies metamorphism is dated as Early Jurassic (190-170 Ma), which coincides with the abundant Early Jurassic granitoids and volcanic rocks in the Lesser Xing'an-Zhangguangcai Range with a continental arc signature (Wu et al., 2007, 2011; Zhou et al., 2009; Xu et al., 2013; Ge et al., 2016). Thus, the westward subduction model for the Mudanjiang Ocean beginning at the Early Jurassic is accepted by most researchers.

However, questions remain about the Late Triassic to Early Jurassic tectonic settings in NE China. Some studies proposed a rift or back-arc extension model for the Lesser Xing'an-Zhangguangcai Range. The main evidence is the "bimodal magmatic rocks" (Yu et al., 2012) and "A-type" rhyolites and granites (Xu et al., 2009). Five mafic-ultramafic plutons were studied in the Lesser Xing'an-Zhangguangcai Range (Yu et al., 2012). The LA-ICP-MS zircon U-Pb dating shows Early Jurassic ages ranging

from 186 to 182 Ma. Geochemical and zircon Lu-Hf isotopic data from these plutons indicate they were generated from the partial melting of a depleted mantle influenced significantly by slab-released fluids (Yu et al., 2012). The mafic plutons were proposed to be components of "bimodal magmatism" with the coeval granitoids, revealing a back-arc extension environment during the Paleo-Pacific Plate subduction. The A-type granites and rhyolites in the eastern Heilongjiang Province are Late Triassic in age (217 to 208 Ma; Xu et al., 2009). The Nd isotopes indicate an origin of mainly juvenile lower crust. Although no typical alkaline minerals have been found in the rocks, the high-SiO_2 rhyolites are classified as A-type, based on high contents of K_2O+Na_2O and Zr+Nb+Ce+Y and it has further been proposed that they represent post-collisional magmatism related to closure of the Paleo-Asian Ocean (Xu et al., 2009).

Another important issue is that the previously accepted closure time of the Mudanjiang Ocean (Early to Middle Jurassic; see Zhou and Li, 2017 and references therein) has been challenged by new data. According to the high-pressure metamorphic ages, the subduction of the Mudanjiang Ocean was believed to be active in the Early Jurassic (Zhou et al., 2009). The closure time is speculated to be before the Middle Jurassic because of the angular unconformities of fluvial sedimentary rocks overlying the blueschists (Zhou and Li, 2017). Recently, Zhu et al. (2015) published a protolith age of 142±1 Ma, sampled from an alkaline blueschist in the Yilan area, NE China. This age is proposed to represent the youngest age of the oceanic crust of the Mudanjiang Ocean. Thus, they argued that the Mudanjiang Ocean was not closed by ca. 141 Ma. However, no similar ages have been reported and the metamorphic age of this sample is unknown. It therefore needs further investigation to verify a possible metamorphic event in the Cretaceous.

1.3.3 The subduction of the Paleo-Pacific Ocean in NE China and Sikhote-Alin areas

In the Sikhote-Alin area, the tectonostratigraphic terranes were accretionary belts associated with the movement of the Paleo-Pacific plates, such as the Farallon Plate and Kula-Izanagi Plate. There were three different types of terranes formed during the Jurassic to Cretaceous: 1) the accretionary complex, 2) the turbidite basin related to the sinistral strike-slip faults; and 3) arc-related basins related to the subduction of the Paleo-Pacific Ocean. The first type is represented by the Jurassic to Early Cretaceous Khabarovsk, Nadanhada-Bikin and Samarka terranes in the west and Taukha Terrane in the east (Fig. 1.10). The accretionary complexes are characterized by abundant faults and folds. In some local areas, continuous sedimentary strata can be recognized which consists of, from bottom to top, basalt, chert, mudstone, siltstone and turbiditic sandstone, revealing the changing sedimentary facies from ocean to continental margin (Kemkin, 2008; Kojima, 1989; Matsuda and Isozaki, 1991). The Nadanhada Terrane or accretionary complex in NE China is the western part of the Jurassic accretionary complex in Sikhote-Alin. The lithologies, deformation and post-accretion magmatism in Nadanhada are similar to the Samarka accretionary complexes in the Russian Far East (Zhou et al., 2014). The second type of terrane includes the Early Cretaceous Zhuravlevk-Amur terrane which was transported northwards along with the Central Sikhote-Alin Fault (Fig. 1.10). The main rock type in the terrane is sandstone interlayered by siltstone (Malinovsky and Golozubov, 2011). The third type of terrane is represented by the late Early Cretaceous Kema Terrane, which is composed of arc-related basins and components of island arc (Malinovsky et al., 2006, 2008). The main rock types are siltstone, sandstone, conglomerate, tuff and basaltic volcanics (Malinovsky et al., 2005). The Sikhote-Alin terranes were accreted one by one to the eastern margin of the Bureya-Jiamusi-Khanka Block before the Late Cretaceous (Golozoubov et al., 1999; Khanchuk, 2001; Khanchuk et al., 2016). Cretaceous to Cenozoic magmatism is widespread in this area, and is mainly recorded by granitoids and extrusive equivalents, with minor basaltic rocks (Jahn et al., 2015; Kruk et al., 2014; Fig. 1.11). The ages of the magmatic rocks range from the Early Cretaceous in the west to the Paleogene in the southeast (Jahn et al., 2015; Khanchuk et al., 2016; Tang et al., 2016). Younger volcanic rocks are also reported, and the subduction-related

felsic magmatism was replaced by intra-plate basaltic and andesitic lava from the Eocene to Miocene (Martynov et al., 2017).

The subduction and accretionary orogeny associated with the Paleo-Pacific Ocean is recognized by the studies of the Sikhote-Alin accretionary complexes. The presently accepted consensus includes: 1) the terranes or accretionary complexes in Sikhote-Alin are associated with the Jurassic to Cretaceous accretionary belts in SW Japan before the opening of the Sea of Japan (Kojima, 1989; Khanchuk, 2001; Jahn et al., 2015); 2) the various kinds of accretionary terranes were built in the Pacific domain at low latitude and travelled northwards in a short time period, probably related to the large-scale sinistral strike-slip faults in the NE Asian margin (Khanchuk et al., 2016); and 3) magmatism from the Early Cretaceous to Paleocene was generated by the oblique subduction of the Izanagi plate and slab roll-back forcing magmatism to migrate to the southeast (Fig. 1.11; Jahn et al., 2015; Khanchuk et al., 2016; Tang et al., 2016).

However, major controversies about the tectonic evolution of the Sikhote-Alin accretionary orogen still remain. The first important issue focuses on the existence of hidden continental crust under the accretionary materials. Jahn et al. (2015) carried out detailed whole-rock Sr-Nd and zircon Hf isotopic research in the southern Sikhote-Alin. The results show that the granitoids are significantly enriched in Nd isotopes.

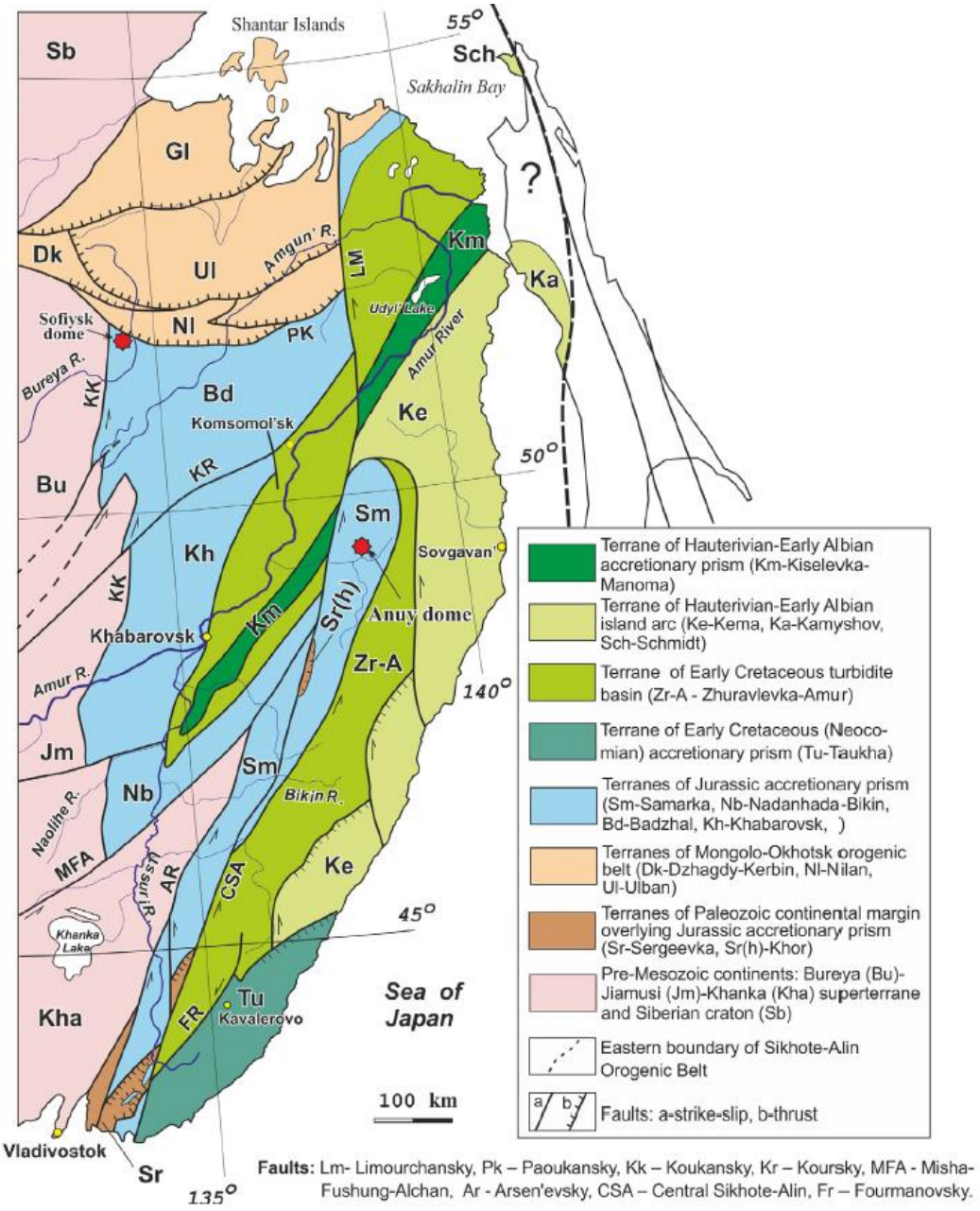

Fig. 1.10 Jurassic to Cretaceous accretionary belts in Sikhote-Alin, Russian Far East (Khanchuk et al., 2016).

Combined with the unusual continental thichness (>30 km), it is proposed that there may be old crustal basement hidden under the accretionary complexes (Jahn et al., 2015). However, Khanchuk et al. (2016) explained the signatures of old basement by the mixing of the sedimentary rocks that contains a lot of terrigenous materials with old ages. No outcrop of crystallized basement rocks has been discovered in the Sikhote-Alin accretionary orogen. The second debated issue in the area is about the role played by the strike-slip faults during the accretionary orogeny. Most Russian

literature emphasizes the importance of the sinistral strike-slip faults in the Cretaceous and proposes that the Sikhote-Alin area was a transform continental margin, similar to present-day California (Golozoubov et al., 1999; Khanchuk, 2001; Khanchuk et al., 2016; Grebennikov et al., 2016). However, the collisional orogeny model proposed by Faure et al. (1995) and Natal'in (1993) was based on research on the Anuy dome, a high-grade metamorphic complex in the northern Sikhote-Alin. The Anuy dome represents a microcontinental block, named the Anuy microcontinental block, in their model (Fig. 1.12). Although strike-slip faulting was important in the area, it only truncated the orogen without significantly changing the tectonic framework in the area.

1.4 Research objectives

The above summary of the history of the accretionary orogen in the NW Pacific, and specifically in NE China and Sikhote-Alin, introduces the important geological events revealed by previous research. The most significant tectono-thermal events include: 1) the formation of Neoproterozoic basement experiencing widespread late Pan-African (ca. 500 Ma) high-grade metamorphism, as recorded by the Mashan Complex in NE China; 2) the opening, subduction and closure of the Mudanjiang Ocean during the Permian to Jurassic, corresponding to the Heilongjiang Complex and magmatism in NE China; and 3) the subduction of the Paleo-Pacific ocean in the eastern Jiamusi-Khanka Block, generating magmatic rocks and wide accretionary complexes in both NE China and Sikhote-Alin.

As mentioned in Section 1.1, these key scientific questions in the area remain highly controversial. The first issue about the basement of the Jiamusi and Khanka blocks concerns the origin of these blocks and their position in supercontinental reconstructions.

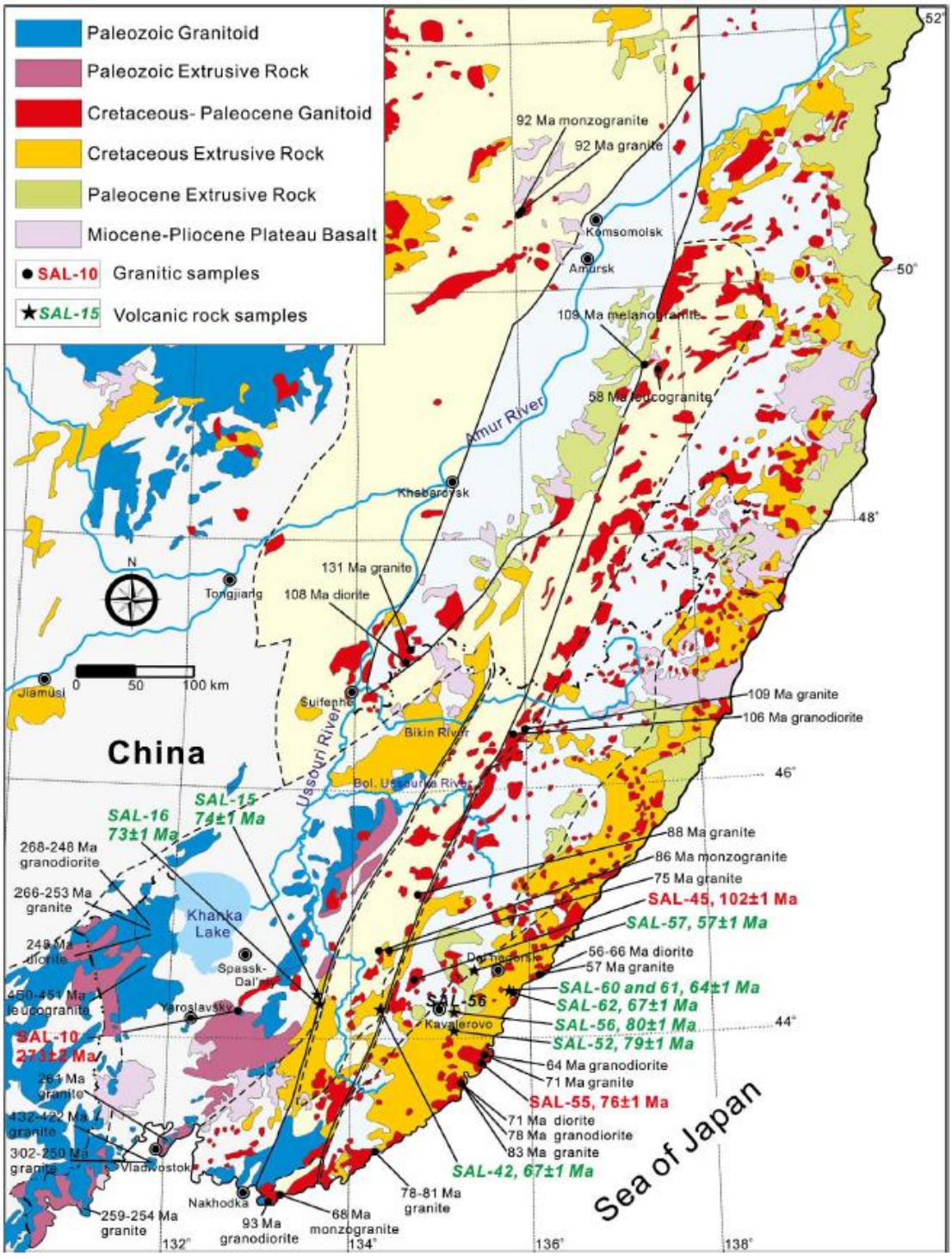

Fig. 1.11 Granitoids in Sikhote-Alin (Zhao et al., 2017).

However, the fundamental tectonic framework of present-day NE Asia was not built before the westward subduction of the Mudanjiang and Paleo-Pacific oceans was initiated in the Mesozoic. Thus, this thesis will focus on two main questions, e.g. the subduction of the Mudanjiang and Paleo-Pacific oceans in NE China and in Sikhote-

Alin, in the Russian Far East.

The essential geological records of subduction include the magmatic rocks and accretionary complexes.

Mesozoic magmatic rocks in NE China are represented by voluminous granitoids that occupy over 80% of the area (Wu et al., 2011). The Zhangguangcai-Lesser Xing'an Range in NE China is the largest magmatic belt in the eastern CAOB; > 600 km long and 150-300 km wide. The majority of this belt is comprised of late Permian to Early Jurassic granitoids, related to subduction of the Mudanjiang Ocean (Wu et al., 2011; Ge et al., 2016). Minor components include Jurassic to Cretaceous volcanic rocks (Xu et al., 2013) and mafic-ultramafic plutons (Yu et al., 2012). In the Jiamusi Block, Triassic to Jurassic magmatic rocks have not been reported so far, and the Mesozoic magmatic rocks are represented by extensive Cretaceous volcanic rocks (Sun et al., 2013). In the Khanka Block, research on magma genesis and its relationship with tectonic evolution has been studied much less than in the Zhangguangcai-Lesser Xing'an Range.

The most important accretionary complexes in the area are the Heilongjiang Complex in the western Jiamusi Block and the Sikhote-Alin accretionary complex to the east. The former complex has been studied in detail during the past decade, including the protolith and metamorphic ages, P/T conditions and provenance of the meta-sedimentary rocks (Wu et al., 2007; Zhou et al., 2009; Ge et al., 2016).

However, the Sikhote-Alin accretionary complex, which is much larger and directly related to Paleo-Pacific subduction, has not been well understood. The published research has focused on magmatism and dating by fossils. The provenance of the sedimentary rocks remains unclear, including the faulted and folded sandstones in the accretionary wedges and turbidite basins, which make up the majority of the accretionary complexes.

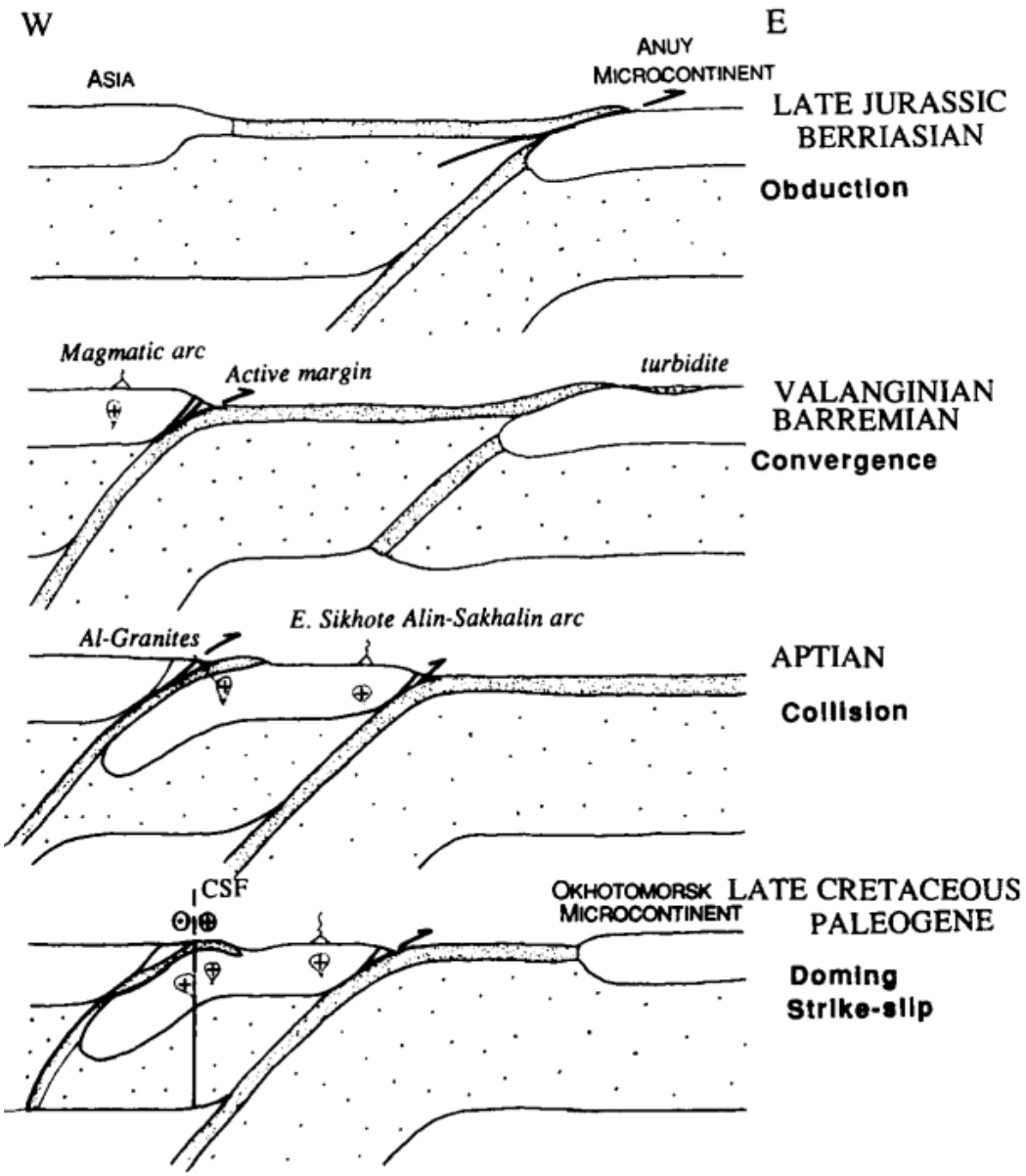

Fig. 1.12 Collision model of microcontinental blocks in Sikhote-Alin area (Faure et al., 1995).

This constrains our understanding of the origin of the sediments and the context of the Sikhote-Alin accretionary orogeny.

The research objectives were carefully selected depending on their importance scientifically and the scarcity of data:

1) Determine the lithology, emplacement age, geochemistry and isotope signature of the major batholith in the north Khanka Block. Although detailed data about the batholiths/plutons in the Zhangguangcai-Lesser Xing'an Range

are abundant, details of the magmatism in the northern Khanka Block are absent. This research focuses on a batholith to the north of the Khanka Lake, the Khanka Lake batholith. The magmatic genesis and tectonic setting are discussed and compared to the adjacent magmatism.

2) Investigate the lithological associations and deformation style of the rocks in the southern Sikhote-Alin accretionary orogen. The relationships between the belts/terranes in Sikhote-Alin will also be discussed based on the field observations. The provenance of these belts/terranes has been determined by zircon U-Pb dating and Lu-Hf isotopes of the detrital zircons in the southern Sikhote-Alin. Tectonic reconstruction is made according to the published data in the orogen and the new data on detrital zircons.
3) Determine the lithology, eruptive age and geochemistry of the volcanic rocks in the Lesser Xing'an-Zhangguangcai Range and Jiamusi Block. There has been some data published on granitoids in the area, however, detailed geochemical and geochronological data are absent. The magmatic genesis of the volcanic rocks and their tectonic implications is discussed in detail. Depending on these and published data, a new model for the subduction process of the Mudanjiang and Paleo-Pacific oceans is proposed.
4) Review the recently published data on structures, basins, magmatism, geomagnetism and low-temperature geochronology from the Cretaceous to Eocene in NE China and Sikhote-Alin. A major change of tectono-thermal conditions along the NE Asian margin is recognized, including all aspects of the geological records. This change is attributed to the Izanagi-Pacific Ridge subduction along the NE Asian margin, the total consumption of the Izanagi plate and the different subduction direction of the Pacific plate.

1.5 Research methods

1.5.1 Field work and petrological observations

The field investigation in this thesis is the foremost work and field observations are the most important evidence to judge the geochronological relationship against existing geological records. Detailed field work was carried out in several key areas, from west to east, including the Lesser Xing'an-Zhangguangcai Range, the Jiamusi-Khanka Block in NE China and the southern Sikhote-Alin area in the Russian Far East. In NE China, the sampling focused on both intrusive and eruptive rocks following the large-scale mapping and detailed description of the distribution, lithological associations of the igneous rocks, and their relationship with local structures and sedimentary rocks. At each outcrop of volcanic and plutonic rocks, 5 to 6 specimens (> 10 kg) were collected for zircon U-Pb dating and geochemical analysis. In the southern Sikhote-Alin, samples for detrital zircon U-Pb dating and Lu-Hf analysis were collected along a ca. 200 km long traverse, across the main terranes/belts in the accretionary orogen. The attitudes of sedimentary rocks, folds and faults were measured at the sampling sites. The boundary faults between belts/terranes were specifically observed where the outcrop was available. However, the most important fault in the area, the Central Sikhote-Alin Fault, is represented by a narrow river valley in the southern Sikhote-Alin area, where no available outcrop was found in the field. Samples in this area are mostly turbidites in the accretionary wedges or turbidite basin. In the easternmost belt/terrane, one sandstone sample was collected from the lenses in a tectonic mélange. For each sample, 5 kg was collected for zircon U-Pb geochronology and Lu-Hf isotope analysis.

Thin-sections were cut from all the samples for petrological investigation. The texture and mineral assemblages were characterized for both igneous and sedimentary rocks in order to classify the lithological types.

1.5.2 Zircon U-Pb dating

The methods used in the thesis for zircon U-Pb dating include LA-ICP-MS and SHRIMP. Zircons were selected and mounted to prepare them for the cathodoluminescence (CL) imaging, which was carried out before the U-Pb analysis in order to examine the internal structures of the zircons. Zircons with magmatic oscillatory zones and appropriate sizes (> 100 μm) were selected for LA-ICP-MS analysis, whereas smaller ones from the volcanic rocks, especially the andesitic and basaltic rocks (50-100 μm) were analyzed by SHRIMP.

1.5.3 Zircon Lu-Hf isotopes

The LA-MC-ICP-MS method was used for in-situ zircon Lu-Hf isotopes analysis after the zircon U-Pb dating. The aim was to determine the contribution from enriched and depleted sources when the zircons were crystallized. The analyzed spots were placed over the U-Pb spots when the zircons were large enough (>200 μm). In the smaller zircons (<200 μm), the Lu-Hf spots were placed adjacent to the U-Pb sites to avoid excessive damage by laser erosion and inaccuracy of data. Analytical details are provided in each Chapter.

1.5.4 Whole-rock geochemistry

X-ray fluorescence (XRF) and ICP-MS methods were utilized, repectively, for major and trace elements analysis for the intrusive and eruptive rocks. The major and trace elements presented in the thesis were used to determine the genesis and help to determine the tectonic implications, when compared with other regional geological records. Precise details of the methods are presented in each Chapter.

1.6 Thesis structure

The thesis opens with an introductory chapter (Chapter 1) to summarize the present understanding of accretionary orogens, the general subduction process in the NW

Pacific region and the subduction history of the blocks and accretionary complexes in NE China and Sikhote-Alin. The subduction of the Mudanjiang and Paleo-Pacific oceans in NE China and Sikhote-Alin is a focus of the thesis. The results of the research on the subduction history are presented in four chapters (Chapter 2, 3, 4 and 5), which are the majority of the thesis. Chapter 2 has been published in *Lithos*, Chapter 3 in *Tectonics*, and Chapter 4 in The *Geological Journal*. Chapter 5 is under review in *Earth-Science Reviews*.

Chapter 2 Initial subduction of the Paleo-Pacific Oceanic plate in NE China: Constraints from whole-rock geochemistry and zircon U–Pb and Lu–Hf isotopes of the Khanka Lake granitoids. This chapter focuses on the very early-stage subduction of the Mudanjiang and Paleo-Pacific oceans during the earliest Triassic to Early Jurassic, based on the geochronological, geochemical and isotopic research on granitoids in the north Khanka Block. In this chapter, it is proposed that the Triassic to Jurassic I-type granitoids in the Khanka Block are comparable with the coeval magmatism in the giant N-S trending Lesser Xing'an-Zhangguangcai Range, where they resulted from the subduction-related arc magmatism.

Chapter 3 U-Pb Dating and Lu-Hf Isotopes of Detrital Zircons From the Southern Sikhote-Alin Orogenic Belt, Russian Far East: Tectonic Implications for the Early Cretaceous Evolution of the Northwest Pacific Margin. This chapter describes the field investigations in the southern Sikhote-Alin orogenic belt and discusses the orogenic process according to the U-Pb and Lu-Hf analyses of detrital zircons from the sandstones in various belts/terranes. Provenance analysis is firstly carried out in this important area. Sinistral strike-slip faulting during the late Early Cretaceous is proposed to be responsible for the northward motion of the terranes/belts, which contain the signature of the North China Craton/Korean Peninsula, reflected by old zircon groups in the sandstones.

Chapter 4 Zircon U-Pb dating and whole-rock geochemistry of volcanic rocks in

eastern Heilongjiang Province, NE China: Implications for the tectonic evolution of the Mudanjiang and Paleo-Pacific oceans from the Jurassic to Cretaceous. The Jurassic to Cretaceous volcanism in the Lesser Xing'an-Zhangguangcai Range and the Jiamusi Block is discussed in this chapter. The main data include SHRIMP zircon U-Pb dating, major and trace element geochemistry. Isotopes were not analyzed in this study because all the granitoids and available volcanic rocks show signs of reworking of juvenile crust or mantle input revealed by previous research. The results of this study support the view that NE China experienced a subduction setting during the Jurassic, with back-arc extension in the Cretaceous. In addition, this paper also connects the magmatism in Sikhote-Alin and NE China, indicating that Paleo-Pacific subduction controlled the whole of NE Asia after the final closure of the Mudanjiang Ocean before the Cretaceous. Since then, the arc magmatism moved to Sikhote-Alin, turning NE China into a back-arc extension environment.

Chapter 5 Izanagi-Pacific ridge subduction in NE Asia in the early Cenozoic: A review of geological evidence from NE Asia. This chapter is a review paper, which focuses on an important change of tectonic settings in NE Asia in the early Cenozoic (65-50 Ma). The manuscript summarizes the recently published data in Sikhote-Alin, NE China and adjacent areas, concentrating on zircon U-Pb geochronology, geochemistry and isotopes of igneous rocks, structural analysis of faults and basins, low-temperature geochronology of basins and mountains and geomagnetism. The major changes in the magmatic nature and kinematics of plates are discussed based on the reviewed data. These significant changes are attributed to the Izanagi-Pacific ridge subduction during the early Cenozoic and the following subduction of the Pacific plate at the NE Asian margin. This review paper supplies essential evidence from the continental side to support the Izanagi-Pacific ridge subduction event proposed by research mainly based on the oceanic plates.

The thesis ends with a chapter (Chapter 6) briefly summarizing the major conclusions of the four papers and a chapter listing all the references (Chapter 7). The data used in

this thesis are not listed, but are available from the Author by email (k.liu@mail.iggcas.ac.cn).

1.7 References

Barbarin, B. (1999). A review of the relationships between granitoid types, their origins and their geodynamic environments. Lithos, 46(3), 605-626.

Burg, J. P. (2018). Geology of the onshore Makran accretionary wedge: Synthesis and tectonic interpretation. Earth-Science Reviews, 185, 1210-1231.

Cawood, P. A., Kröner, A., Collins, W. J., Kusky, T. M., Mooney, W. D., & Windley, B. F. (2009). Accretionary orogens through Earth history. Geological Society, London, Special Publications, 318(1), 1-36.

Chappell, B. W., & Stephens, W. E. (1988). Origin of infracrustal (I-type) granite magmas. Earth and Environmental Science Transactions of the Royal Society of Edinburgh, 79(2-3), 71-86.

Charvet, J. (1985). Some tectonic and tectogenetic aspects of SW Japan. An alpine-type oregon in an island-arc position. Formation of Active Ocean Margins, 791-817.

Charvet, J. (2013). Late Paleozoic–Mesozoic tectonic evolution of SW Japan: A review–Reappraisal of the accretionary orogeny and revalidation of the collisional model. Journal of Asian Earth Sciences, 72, 88-101.

Chough, S. K., Kwon, S. T., Ree, J. H., & Choi, D. K. (2000). Tectonic and sedimentary evolution of the Korean peninsula: a review and new view. Earth-Science Reviews, 52(1-3), 175-235.

Chung, S. L., Liu, D., Ji, J., Chu, M. F., Lee, H. Y., Wen, D. J., ... & Zhang, Q. (2003). Adakites from continental collision zones: melting of thickened lower crust beneath southern Tibet. Geology, 31(11), 1021-1024.

Collins, W. J., & Richards, S. W. (2008). Geodynamic significance of S-type granites in circum-Pacific orogens. Geology, 36(7), 559-562.

Condie, K. C. (2007). Accretionary orogens in space and time. Memoirs-Geological Society of America, 200, 145-158.

Defant, M. J., & Drummond, M. S. (1990). Derivation of some modern arc magmas by melting of young subducted lithosphere. Nature, 347(6294), 662.

Dickinson, W. R. (1976). Sedimentary basins developed during evolution of Mesozoic–Cenozoic arc–trench system in western North America. Canadian Journal of Earth Sciences, 13(9), 1268-1287.

Faure, M., Caridroit, M., & Charvet, J. (1986). The late Jurassic oblique collisional orogen of SW Japan. New structural data and synthesis. Tectonics, 5(7), 1089-1114.

Faure, M., Natal'In, B. A., Monie, P., Vrublevsky, A. A., Borukaiev, C., & Prikhodko, V. (1995). Tectonic evolution of the Anuy metamorphic rocks (Sikhote Alin, Russia) and their place in the Mesozoic geodynamic framework of East Asia. Tectonophysics, 241(3-4), 279-301.

Fujisaki, W., Isozaki, Y., Maki, K., Sakata, S., Hirata, T., & Maruyama, S. (2014). Age spectra of detrital zircon of the Jurassic clastic rocks of the Mino-Tanba AC belt in SW Japan: Constraints to the provenance of the mid-Mesozoic trench in East Asia. Journal of Asian Earth Sciences, 88, 62-73.

Ge, M. H., Zhang, J. J., Liu, K., Ling, Y. Y., Wang, M., & Wang, J. M. (2016). Geochemistry and geochronology of the blueschist in the Heilongjiang Complex and its implications in the late Paleozoic tectonics of eastern NE China. Lithos, 261, 232-249.

Golozoubov, V. V., Markevich, V. S., & Bugdaeva, E. V. (1999). Early Cretaceous changes of vegetation and environment in East Asia. Palaeogeography, Palaeoclimatology, Palaeoecology, 153(1-4), 139-146.

Grebennikov, A. V., Khanchuk, A. I., Gonevchuk, V. G., & Kovalenko, S. V. (2016). Cretaceous and Paleogene granitoid suites of the Sikhote-Alin area (Far East Russia): Geochemistry and tectonic implications. Lithos, 261, 250-261.

Isozaki, Y. (1997). Jurassic accretion tectonics of Japan. Island Arc, 6(1), 25-51.

Isozaki, Y., Aoki, K., Nakama, T., & Yanai, S. (2010). New insight into a subduction-

related orogen: a reappraisal of the geotectonic framework and evolution of the Japanese Islands. Gondwana Research, 18(1), 82-105.

Isozaki, Y., Ehiro, M., Nakahata, H., Aoki, K., Sakata, S., & Hirata, T. (2015). Cambrian plutonism in Northeast Japan and its significance for the earliest arc-trench system of proto-Japan: New U–Pb zircon ages of the oldest granitoids in the Kitakami and Ou Mountains. Journal of Asian Earth Sciences, 108, 136-149.

Isozaki, Y., Maruyama, S., & Furuoka, F. (1990). Accreted oceanic materials in Japan. Tectonophysics, 181(1-4), 179-205.

Jahn, B. M. (2004). The Central Asian Orogenic Belt and growth of the continental crust in the Phanerozoic. Geological Society, London, Special Publications, 226(1), 73-100.

Jahn, B. M., Valui, G., Kruk, N., Gonevchuk, V., Usuki, M., & Wu, J. T. (2015). Emplacement ages, geochemical and Sr–Nd–Hf isotopic characterization of Mesozoic to early Cenozoic granitoids of the Sikhote-Alin Orogenic Belt, Russian Far East: Crustal growth and regional tectonic evolution. Journal of Asian Earth Sciences, 111, 872-918.

Jahn, B. M., Wu, F., & Chen, B. (2000). Granitoids of the Central Asian Orogenic Belt and continental growth in the Phanerozoic. Earth and Environmental Science Transactions of the Royal Society of Edinburgh, 91(1-2), 181-193.

Katz, O., Beyth, M., Miller, N., Stern, R., Avigad, D., Basu, A., & Anbar, A. (2004). A Late Neoproterozoic (~630 Ma) high-magnesium andesite suite from southern Israel: implications for the consolidation of Gondwanaland. Earth and Planetary Science Letters, 218(3-4), 475-490.

Kelemen, P. B., Johnson, K. T. M., Kinzler, R. J., & Irving, A. J. (1990). High-field-strength element depletions in arc basalts due to mantle–magma interaction. Nature, 345(6275), 521.

Kelley, K. A., & Cottrell, E. (2012). The influence of magmatic differentiation on the oxidation state of Fe in a basaltic arc magma. Earth and Planetary Science Letters, 329, 109-121.

Kemkin, I. V. (2008). Structure of terranes in a Jurassic accretionary prism in the

Sikhote-Alin-Amur area: implications for the Jurassic geodynamic history of the Asian eastern margin. Russian Geology and Geophysics, 49(10), 759-770.

Khanchuk, A. I. (2001). Pre-Neogene tectonics of the Sea-of-Japan region: A view from the Russian side. in Special issue: *Geotectonic framework of eastern Asia before the opening of the Japan Sea*, *Part 2*, Earth Science (Chikyu Kagaku), 55(5), 275-291.

Khanchuk, A. I., Kemkin, I. V., & Kruk, N. N. (2016). The Sikhote-Alin orogenic belt, Russian South East: Terranes and the formation of continental lithosphere based on geological and isotopic data. Journal of Asian Earth Sciences, 120, 117-138.

Khanchuk, A. I., Vovna, G. M., Kiselev, V. I., Mishkin, M. A., & Lavrik, S. N. (2010). First results of zircon LA-ICP-MS U-Pb dating of the rocks from the Granulite complex of Khanka massif in the Primorye region. In Doklady Earth Sciences, 434 (1), 1164-1167.

Kojima, S. (1989). Mesozoic terrane accretion in northeast China, Sikhote-Alin and Japan regions. Palaeogeography, Palaeoclimatology, Palaeoecology, 69, 213-232.

Kröner, A., Kovach, V., Belousova, E., Hegner, E., Armstrong, R., Dolgopolova, A., ... & Sun, M. (2014). Reassessment of continental growth during the accretionary history of the Central Asian Orogenic Belt. Gondwana Research, 25(1), 103-125.

Kruk, N. N., Simanenko, V. P., Gvozdev, V. I., Golozubov, V. V., Kovach, V. P., Serov, P. I., ... & Kuibida, M. L. (2014). Early Cretaceous granitoids of the Samarka terrane (Sikhote-Alin'): geochemistry and sources of melts. Russian Geology and Geophysics, 55(2), 216-236.

Liu, K., Zhang, J., Wilde, S. A., Liu, S., Guo, F., Kasatkin, S. A., ... & Wang, J. (2017). U‐Pb Dating and Lu‐Hf Isotopes of Detrital Zircons From the Southern Sikhote‐Alin Orogenic Belt, Russian Far East: Tectonic Implications for the Early Cretaceous Evolution of the Northwest Pacific Margin. Tectonics, 36(11), 2555-2598.

Luan, J. P., Wang, F., Xu, W. L., Ge, W. C., Sorokin, A. A., Wang, Z. W., & Guo, P. (2017). Provenance, age, and tectonic implications of Neoproterozoic strata in the Jiamusi Massif: evidence from U–Pb ages and Hf isotope compositions of detrital

and magmatic zircons. Precambrian Research, 297, 19-32.

Malinovsky, A. I., & Golozubov, V. V. (2011). Lithology and depositional settings of the terrigenous sediments along transform plate boundaries: Evidence from the early Cretaceous Zhuravlevka terrane in Southern Sikhote Alin. Russian Journal of Pacific Geology, 5(5), 400.

Malinovsky, A. I., Golozoubov, V. V., & Simanenko, V. P. (2006). The Kema island-arc terrane, eastern Sikhote Alin: Formation settings and geodynamics. Doklady Earth Sciences, 410 (1), 1026-1029.

Malinovsky, A. I., Golozoubov, V. V., Simanenko, V. P., & Simanenko, L. F. (2008). Kema terrane: A fragment of a back‐arc basin of the early Cretaceous Moneron–Samarga island‐arc system, East Sikhote–Alin range, Russian Far East. Island Arc, 17(3), 285-304.

Malinovsky, A. I., Golozubov, V. V., & Simanenko, V. P. (2005). Composition and depositional settings of Lower Cretaceous terrigenous rocks of the Kema River Basin, eastern Sikhote Alin. Lithology and Mineral Resources, 40(5), 429-447.

Mann, P., & Taira, A. (2004). Global tectonic significance of the Solomon Islands and Ontong Java Plateau convergent zone. Tectonophysics, 389(3-4), 137-190.

Martynov, Y. A., Khanchuk, A. I., Grebennikov, A. V., Chashchin, A. A., & Popov, V. K. (2017). Late Mesozoic and Cenozoic volcanism of the East Sikhote-Alin area (Russian Far East): a new synthesis of geological and petrological data. Gondwana Research, 47, 358-371.

Maruyama, S., Isozaki, Y., Kimura, G., & Terabayashi, M. (1997). Paleogeographic maps of the Japanese Islands: plate tectonic synthesis from 750 Ma to the present. Island Arc, 6(1), 121-142.

Matsuda, T., & Isozaki, Y. (1991). Well‐documented travel history of Mesozoic pelagic chert in Japan: From remote ocean to subduction zone. Tectonics, 10(2), 475-499.

Meffre, S., Aitchison, J. C., & Crawford, A. J. (1996). Geochemical evolution and tectonic significance of boninites and tholeiites from the Koh ophiolite, New Caledonia. Tectonics, 15(1), 67-83.

Miyashiro, A. (1973). Paired and unpaired metamorphic belts. Tectonophysics, 17(3), 241-254.

Müller, R. D., Seton, M., Zahirovic, S., Williams, S. E., Matthews, K. J., Wright, N. M., ... & Bower, D. J. (2016). Ocean basin evolution and global-scale plate reorganization events since Pangea breakup. Annual Review of Earth and Planetary Sciences, 44, 107-138.

Natal'in, B. (1993). History and modes of Mesozoic accretion in southeastern Russia. Island Arc, 2(1), 15-34.

Raymond, L. A. (1984). Classification of mélanges. Mélanges: their nature, origin, and significance: Geological Society of America Special Paper, 198, 7-20.

Royden, L. H. (1993). The steady state thermal structure of eroding orogenic belts and accretionary prisms. Journal of Geophysical Research: Solid Earth, 98(B3), 4487-4507.

Schmidt, M. W., & Poli, S. (1998). Experimentally based water budgets for dehydrating slabs and consequences for arc magma generation. Earth and Planetary Science Letters, 163(1-4), 361-379.

Sengör, A. C., & Natal'In, B. A. (1996). Turkic-type orogeny and its role in the making of the continental crust. Annual Review of Earth and Planetary Sciences, 24(1), 263-337.

Sobolev, A. V., & Chaussidon, M. (1996). H_2O concentrations in primary melts from supra-subduction zones and mid-ocean ridges: implications for H_2O storage and recycling in the mantle. Earth and Planetary Science Letters, 137(1-4), 45-55.

Stern, R. J. (2004). Subduction initiation: spontaneous and induced. Earth and Planetary Science Letters, 226(3-4), 275-292.

Sun, M. D., Chen, H. L., Zhang, F. Q., Wilde, S. A., Dong, C. W., & Yang, S. F. (2013). A 100 Ma bimodal composite dyke complex in the Jiamusi Block, NE China: an indication for lithospheric extension driven by Paleo-Pacific roll-back. Lithos, 162, 317-330.

Taira, A. (2001). Tectonic evolution of the Japanese island arc system. Annual Review of Earth and Planetary Sciences, 29(1), 109-134.

Tang, J., Xu, W., Niu, Y., Wang, F., Ge, W., Sorokin, A. A., & Chekryzhov, I. Y. (2016). Geochronology and geochemistry of Late Cretaceous–Paleocene granitoids in the Sikhote-Alin Orogenic Belt: Petrogenesis and implications for the oblique subduction of the paleo-Pacific plate. Lithos, 266, 202-212.

Tatsumi, Y. (1986). Formation of the volcanic front in subduction zones. Geophysical Research Letters, 13(8), 717-720.

Wakita, K., Nakagawa, T., Sakata, M., Tanaka, N., & Oyama, N. (2018). Phanerozoic accretionary history of Japan and the western Pacific margin. Geological Magazine, 1-17.

Wilde, S. A. (2015). Final amalgamation of the Central Asian Orogenic Belt in NE China: Paleo-Asian Ocean closure versus Paleo-Pacific plate subduction—A review of the evidence. Tectonophysics, 662, 345-362.

Wilde, S. A., Wu, F., & Zhang, X. (2003). Late Pan-African magmatism in northeastern China: SHRIMP U–Pb zircon evidence from granitoids in the Jiamusi Massif. Precambrian Research, 122(1-4), 311-327.

Wu, F. Y., Sun, D. Y., Ge, W. C., Zhang, Y. B., Grant, M. L., Wilde, S. A., & Jahn, B. M. (2011). Geochronology of the Phanerozoic granitoids in northeastern China. Journal of Asian Earth Sciences, 41(1), 1-30.

Wu, F. Y., Yang, J. H., Lo, C. H., Wilde, S. A., Sun, D. Y., & Jahn, B. M. (2007). The Heilongjiang Group: a Jurassic accretionary complex in the Jiamusi Massif at the western Pacific margin of northeastern China. Island Arc, 16(1), 156-172.

Wu, F.Y., Wilde, S. A., Sun, D. Y. (2001). Zircon SHRIMP U-Pb ages of gneissic granites in Jiamusi massif. Acta Petrologica Sinica, 17(3), 443-452.

Xiao, W., Windley, B. F., Hao, J., & Zhai, M. (2003). Accretion leading to collision and the Permian Solonker suture, Inner Mongolia, China: Termination of the central Asian orogenic belt. Tectonics, 22(6).

Xiao, W., Windley, B. F., Sun, S., Li, J., Huang, B., Han, C., ... & Chen, H. (2015). A tale of amalgamation of three Permo-Triassic collage systems in Central Asia: oroclines, sutures, and terminal accretion. Annual Review of Earth and Planetary Sciences, 43, 477-507.

Xu, W. L., Ji, W. Q., Pei, F. P., Meng, E., Yu, Y., Yang, D. B., & Zhang, X. (2009). Triassic volcanism in eastern Heilongjiang and Jilin provinces, NE China: chronology, geochemistry, and tectonic implications. Journal of Asian Earth Sciences, 34(3), 392-402.

Xu, W. L., Pei, F. P., Wang, F., Meng, E., Ji, W. Q., Yang, D. B., & Wang, W. (2013). Spatial–temporal relationships of Mesozoic volcanic rocks in NE China: constraints on tectonic overprinting and transformations between multiple tectonic regimes. Journal of Asian Earth Sciences, 74, 167-193.

Yang, H., Ge, W. C., Bi, J. H., Wang, Z. H., Tian, D. X., Dong, Y., & Chen, H. J. (2018). The Neoproterozoic-early Paleozoic evolution of the Jiamusi Block, NE China and its East Gondwana connection: Geochemical and zircon U–Pb–Hf isotopic constraints from the Mashan Complex. Gondwana Research, 54, 102-121.

Yang, H., Ge, W. C., Zhao, G. C., Bi, J. H., Wang, Z. H., Dong, Y., & Xu, W. L. (2017). Zircon U–Pb ages and geochemistry of newly discovered Neoproterozoic orthogneisses in the Mishan region, NE China: Constraints on the high-grade metamorphism and tectonic affinity of the Jiamusi–Khanka Block. Lithos, 268, 16-31.

Yu, J. J., Wang, F., Xu, W. L., Gao, F. H., & Pei, F. P. (2012). Early Jurassic mafic magmatism in the Lesser Xing'an–Zhangguangcai Range, NE China, and its tectonic implications: constraints from zircon U–Pb chronology and geochemistry. Lithos, 142, 256-266.

Zhao, P., Li, J. J., Alexandrov, I., Ivin, V., & Jahn, B. M. (2017). Involvement of old crustal materials during formation of the Sakhalin Island (Russian Far East) and its paleogeographic implication: Constraints from detrital zircon ages of modern river sand and Miocene sandstone. Journal of Asian Earth Sciences, 146, 412-430.

Zheng, Y. F. (2019). Subduction zone geochemistry. Geoscience Frontiers, 10(4), 1223-1254.

Zhou, J. B., & Li, L. (2017). The Mesozoic accretionary complex in Northeast China: Evidence for the accretion history of Paleo-Pacific subduction. Journal of Asian Earth Sciences, 145, 91-100.

Zhou, J. B., Cao, J. L., Wilde, S. A., Zhao, G. C., Zhang, J. J., & Wang, B. (2014). Paleo-Pacific subduction-accretion: Evidence from Geochemical and U-Pb zircon dating of the Nadanhada accretionary complex, NE China. Tectonics, 33(12), 2444-2466.

Zhou, J. B., Wilde, S. A., Zhang, X. Z., Zhao, G. C., Liu, F. L., Qiao, D. W., ... & Liu, J. H. (2011). A >1300 km late Pan-African metamorphic belt in NE China: New evidence from the Xing'an block and its tectonic implications. Tectonophysics, 509(3-4), 280-292.

Zhou, J. B., Wilde, S. A., Zhang, X. Z., Zhao, G. C., Zheng, C. Q., Wang, Y. J., & Zhang, X. H. (2009). The onset of Pacific margin accretion in NE China: evidence from the Heilongjiang high-pressure metamorphic belt. Tectonophysics, 478(3-4), 230-246.

Zhou, J. B., Wilde, S. A., Zhao, G. C., Zhang, X. Z., Zheng, C. Q., Wang, H. U., & Zeng, W. S. (2010). Pan-African metamorphic and magmatic rocks of the Khanka Massif, NE China: further evidence regarding their affinity. Geological magazine, 147(5), 737-749.

Zhu, C. Y., Zhao, G., Sun, M., Liu, Q., Han, Y., Hou, W., ... & Eizenhofer, P. R. (2015). Geochronology and geochemistry of the Yilan blueschists in the Heilongjiang Complex, northeastern China and tectonic implications. Lithos, 216, 241-253.

Chapter 2 Initial subduction of the Paleo-Pacific Oceanic plate in NE China: Constraints from whole-rock geochemistry and zircon U–Pb and Lu–Hf isotopes of the Khanka Lake granitoids

2.0 Abstract

Northeast China is located in the eastern part of the Central Asian Orogenic Belt (CAOB) and was influenced by Paleo-Pacific subduction during the Mesozoic. Abundant granitoids from the late Paleozoic to early Mesozoic in NE China record this process, including the Khanka Lake granitoids, which resulted in extensive growth of continental crust in the area. However, the question of how and when the Paleo-Pacific tectonic system began to affect NE China is still highly controversial. The Khanka Lake granitoids can be subdivided into two main components based on their geochemical characteristics, namely granodiorite and syenogranite. The granodiorite has a U–Pb age of 249 Ma and is adakite-like (enriched in LREE and LILEs with high Mg#, Sr, La/Yb, Sr/Y and Na_2O/K_2O), with zircon εHf(t) values of −0.65 to 1.61, produced by the magma mixing between melting of the lower continental crust and juvenile basaltic magma. The syenogranite has zircon U–Pb ages of 209 to 199 Ma and geochemical features of highly fractionated I-type granites, with high SiO_2, total alkalis and low Mg (and Mg#), Fe, Cr and Ni, and positive zircon εHf(t) of 1.72 to 5.12, indicating an origin from remelting of juvenile crust. The granitoids were intruded by felsic veins between 195 and 184 Ma with positive zircon εHf(t) from 0.57 to 5.32. The εHf(t) values of the granitoids become more positive as the zircon U–Pb ages become younger, suggesting continuous melting of juvenile crust during subduction. It is concluded that the Khanka Lake granitoids record the early stage of subduction of the Paleo-Pacific Oceanic plate, which commenced at least ca. 250 Ma ago.

2.1. Introduction

Northeast China (NE China) is located in the eastern part of the Central Asian Orogenic Belt (CAOB). It is a region of great importance with respect to understanding the tectonic evolution of Northeast Asia (Figs. 2.1 and 2.2; Wilde et al., 2010; Xu et al., 2013, 2014). One feature of this region is the complicated interaction between three tectonic realms: the Paleo-Asian Ocean, the Mongol-Okhotsk Ocean, and the Paleo-Pacific Ocean. The Paleo-Asian Ocean closed during the late Paleozoic, resulting in many E–W trending suture zones between the Siberia and North China cratons (Wilde, 2015; Wilde and Zhou, 2015; Zhou et al., 2013). In the northeastern part of the CAOB, a similar trending suture zone (the Mongol-Okhotsk Suture zone) was produced by the final collision between the Siberia Craton and the amalgamated NE China blocks during the Late Jurassic to Early Cretaceous (Khanchuk et al., 2015; Kravchinsky et al., 2002; Zonenshain et al., 1990). During the early Mesozoic, the Paleo-Pacific Ocean began to influence and then dominate the tectonic framework of the eastern CAOB and even the whole of eastern Asia (Guo et al., 2015; Wilde, 2015; Wu et al., 2003a, 2003b, 2011; Xu et al., 2013). This complicated process has left magmatic records, making NE China a crucial site for studying the relationship between the Paleo-Pacific Ocean and Paleo-Asian Ocean realms, with wider implications for other accretionary orogens.

The most fundamental and controversial question related to NE China is the initial time of the Paleo-Pacific subduction, ons which many studies have been initiated (Li, 2006; Meng et al., 2010; Wu et al., 2007; Xu et al., 2013; Zhou et al., 2009a, 2009b).

There are several blocks (or massifs) consisting mainly of Phanerozoic magmatic rocks, volcano-sedimentary rocks and minor Precambrian basement in the eastern CAOB (Fig. 2.2.2).

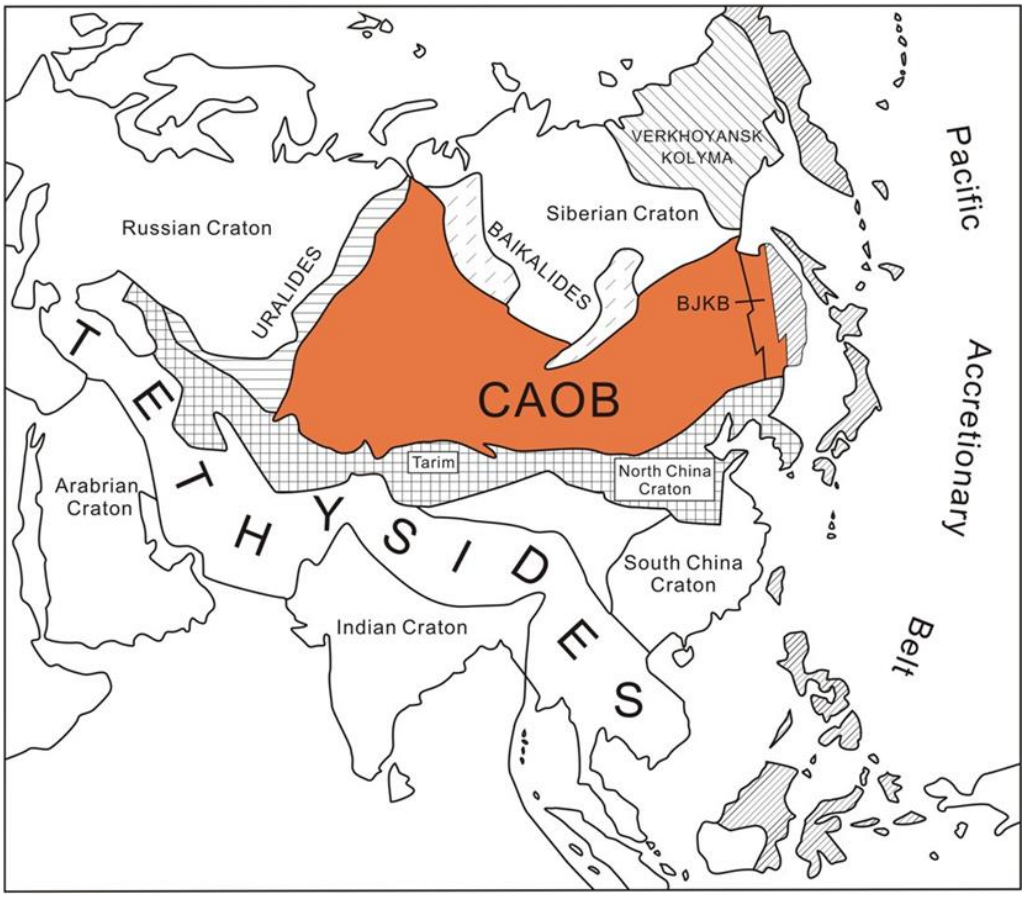

Fig. 2.1. Sketch map showing Asian tectonics and the Central Asian Orogenic Belt (CAOB). BJKB is the abbreviation for the Bureya–Jiamusi–Khanka Block, easternmost segment of the CAOB. Modified after Sengör and Natal'in (1996) and Wilde (2015).

Previous research has confirmed that the Erguna, Xing'an, and Songliao Blocks are mainly amalgamated arcs (with minor Precambrian basement) influenced by the Paleo-Asian and Mongol-Okhotsk realms, whereas the Nadanhada Terrane and Sikhote-Alin terranes in the east are accretionary prisms or basins related to subduction of the Paleo-Pacific Oceanic plate during the Late Triassic to Early Cretaceous (Cheng et al., 2006; Zhou et al., 2014). However, the formation, affinity and tectonic evolution of the central block that lies between the eastern CAOB and the accretionary terranes—the Bureya-Jiamusi-Khanka Block—is still open to debate (Meng et al., 2010; Wilde et al., 1997; Wu et al., 2011; Zhou et al., 2009a, 2009b). Wilde et al. (1999) and Wu et al. (2007) proposed that this united block was an exotic block probably derived from a peri-Gondwana position that traveled northwards until it collided with the CAOB in the Jurassic. Some researchers have also suggested that the Bureya–Jiamusi–Khanka

Block might have been connected to the Siberia Craton during the early Paleozoic based on the widespread late Pan-African rocks in both the southern Siberia Craton and NE China (Wilde et al., 1997; Zhou et al., 2009a, 2010). In this model, after ca. 450 Ma, the Bureya–Jiamusi–Khanka Block broke away from southern Siberia and moved eastwards, with final accretion to the CAOB taking place in the Jurassic (Zhou et al., 2010, 2014).

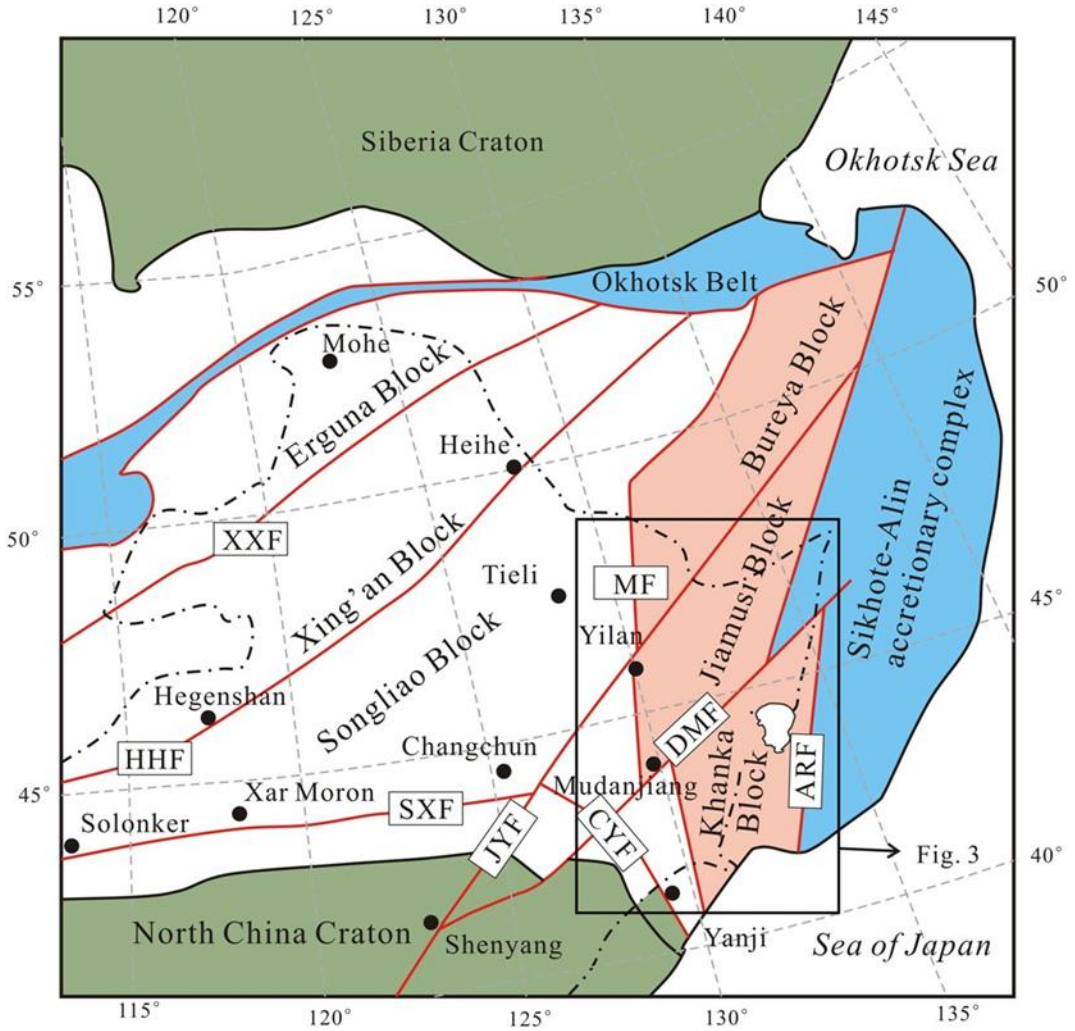

Fig. 2.2. Tectonic framework of NE China (modified from Wilde et al., 2000; Wu et al., 2007; Zhou et al., 2010). The main tectonic boundaries: ARF: Arsen'evsky Fault; SXF: Solonker-Xar Moron Fault; CYF: Changchun-Yanji Fault; MF: Mudanjiang Fault; DMF: Dunhua-Mishan Fault; JYF: Jiamusi-Yitong Fault; HHF: Hegenshan-Heihe Fault; XXF: Xinlin-Xiguitu Fault.

The tectonic setting of the Bureya–Jiamusi–Khanka Block during the early Mesozoic is likewise unclear. Xu et al. (2009, 2013) hold the view that post-collision delamination of the CAOB controlled this region during the whole of the Triassic and

that Paleo-Pacific subduction began after the Early Jurassic. Other researchers consider that Paleo-Pacific subduction had already started in the Triassic (Guo et al., 2015; Shao et al., 2013; Wu et al., 2007, 2011; Zhou et al., 2009a, 2010, 2014), or even the Early Permian (Sun et al., 2015).

2.2. Geological setting

The Jiamusi–Khanka Block is located at the southeastern margin of the CAOB (Fig. 2.2). The accretionary Sikhote-Alin terranes (including the Nadanhada Terrane) are adjacent to its eastern margin, whereas the Heilongjiang Complex (another accretionary complex) lies in the west (Jahn et al., 2015; Kemkin, 2008; Khanchuk, 2010a). The Jiamusi and Khanka Blocks are separated by the Dunhua- Mishan strike-slip fault (the Dun-Mi Fault), a branch of the Tan-Lu Fault (Fig. 2.2.3; Zhou et al., 2009b, 2010). To the southwest, the Khanka Block was bounded by the Changchun-Yanji suture zone (Fig. 2.2.2; Zhou et al., 2013).

The Bureya–Jiamusi–Khanka Block shares a ~500 Ma Pan-African basement (Fig. 2.2.3; Khanchuk, 2010b; Wilde et al., 2000; Zhou et al., 2010), namely the Mashan Complex, which consist of granulite facies metamorphic rocks (Wilde et al., 1997; Zhou et al., 2010). At the western edge of the Jiamusi–Khanka Block, the Heilongjiang Complex (Fig. 2. 2.3; Zhou et al., 2009a, 2009b) extends north to south and is composed of clastic sediments, chemical sediments and basalts including blueschists. It records the subduction history related to the Mudanjiang Ocean during the Mesozoic, which was an ocean between the Bureya–Jiamusi–Khanka Block and Songliao Block, lying roughly parallel to the N–S trending Mudanjiang Fault (Wu et al., 2007; Zhou et al., 2009a, 2009b).

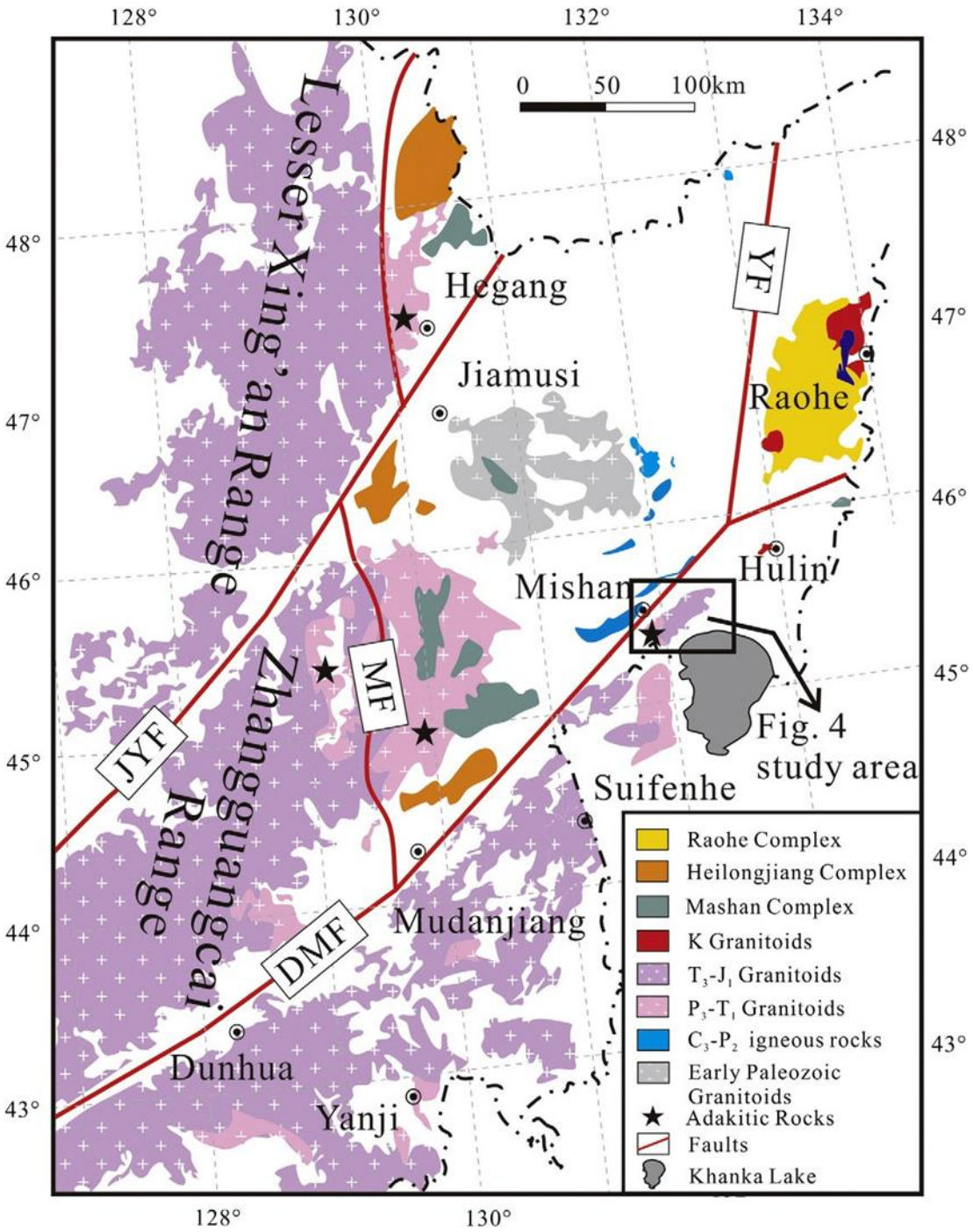

Fig. 2.3. Distribution of magmatic rocks in eastern NE China (modified from Wu et al., 2011). The age data of igneous rocks are from Cheng et al. (2006), Wei et al. (2008), Wu et al. (2011), Shao et al. (2013), Yang et al. (2012) and references therein. DMF: Dunhua-Mishan Fault; JYF: Jiamusi-Yitong Fault; MF: Mudanjiang Fault; YF: Yuejinshan Fault.

There are also voluminous magmatic rocks of late Paleozoic to early Mesozoic age exposed extensively with a general N–S trend within the Jiamusi–Khanka Block and the adjacent Lesser Xing'an–Zhangguangcai Range (Fig. 2.3; Wu et al., 2011; Xu et

al., 2013). The ages of these granitoids become younger in the Jiamusi–Khanka Block westwards to the Lesser Xing'an–Zhangguangcai Range (Fig. 2.3). At the eastern margin of the Jiamusi–Khanka Block, dacites, rhyolites, andesitic tuffs, and granitoids have Late Carboniferous to middle Permian ages (Meng et al., 2008; Yu et al., 2012), whereas at the western margin of the Jiamusi– Khanka Block, adjacent to the eastern Lesser Xing'an–Zhangguangcai Range, granitoids are late Permian to Early Triassic in age (mainly I-type granitoids with some adakite-like granodiorites; Huang et al., 2008; Khanchuk, 2010a; Song et al., 1994; Wu et al., 2001, 2011). Farther west, the granitoids are mainly of Late Triassic to Early Jurassic age with highly fractionated I-type characteristics (Guo et al., 2010; Wu et al., 2003a, 2003b, 2011).

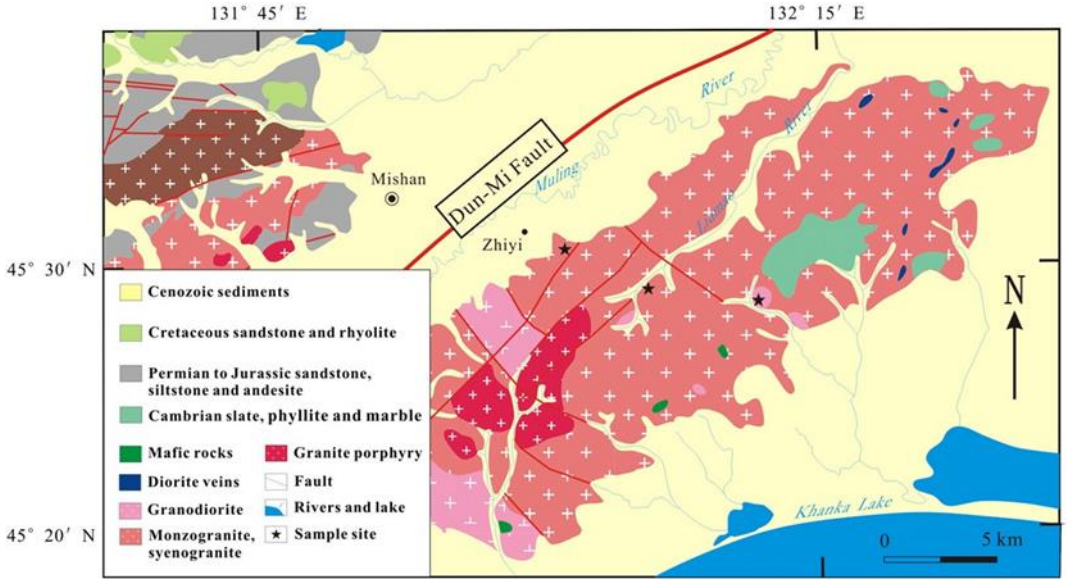

Fig. 2.4. Geological map of the Khanka Lake granitoids showing the sample locations (modified from the 1:200,000 Hulin and Mishan geological maps).

The Khanka Lake granitoids in the northwestern Khanka Block outcrop along the northwest bank of Khanka Lake (Figs. 2.3 and 2.4). This composite batholith occupies an area of ca. 450 km2 and consists of granodiorite (Fig. 2.2.5a, b), syenogranite (Fig. 2.2.5c), and later felsic and diorite dikes/veins. The granites account for 60% of the batholith and intruded into early Paleozoic slate, phyllite, and marl (Fig. 2.2.4), producing marble by contact metamorphism. Locally, granodiorites are also intruded by granite (Fig. 2.2.5c and d). The other major component of the Khanka Lake

granitoids is granodiorite, which contains more Fe–Mg minerals and abundant elliptical mafic enclaves (Fig. 2.2.5a). However, few contact relations between the granodiorite and biotite syenogranite can be found because of the extensive soil cover. There are also some other intermediate veins and mafic dikes intruding the granite, varying from diorite and granodiorite to pegmatite in composition, throughout the batholith (Fig. 2.2.5b).

2.3 Sample descriptions

The sample locations are shown in Fig. 2.2. 3 and listed in Appendix 1.

2.3.1 Granodiorite

The granodiorite is mainly exposed in the western part of the intrusion, accounting for 25–30% of the area. Samples NE13-30 to 36 were collected from outcrops in the central part of the Khanka Lake batholith (Fig. 2.2. 4). The samples are medium- to coarse-grained with an allotriomorphic granular texture (Fig. 2.2.5e). The mineral assemblage consists of plagioclase (~55%), quartz (~20%), hornblende (~10%), and biotite (~ 5%), with accessory titanite. Samples NE13-30 and 31 were selected for zircon U–Pb dating and Lu–Hf isotopic analysis, whereas samples NE13-32 to 36 were prepared for geochemical analysis.

2.3.2 Syenogranite

Samples NE13-38 to 47, LJ-190 to 194, LJ-200 to 204, and LJ-208 to 212 were collected from the syenogranite (Fig. 2.2.4).

Samples NE13-38, 40, 41 42, LJ-190 to 194, and LJ-208 to 212 are fine- to medium-grained biotite syenogranite (Fig. 2.2.5f), which are porphyritic with phenocrysts of K-feldspar and quartz. The main mineral assemblage is quartz (~40%), K-feldspar (~35%), plagioclase (15–20%), and biotite (5–8%).

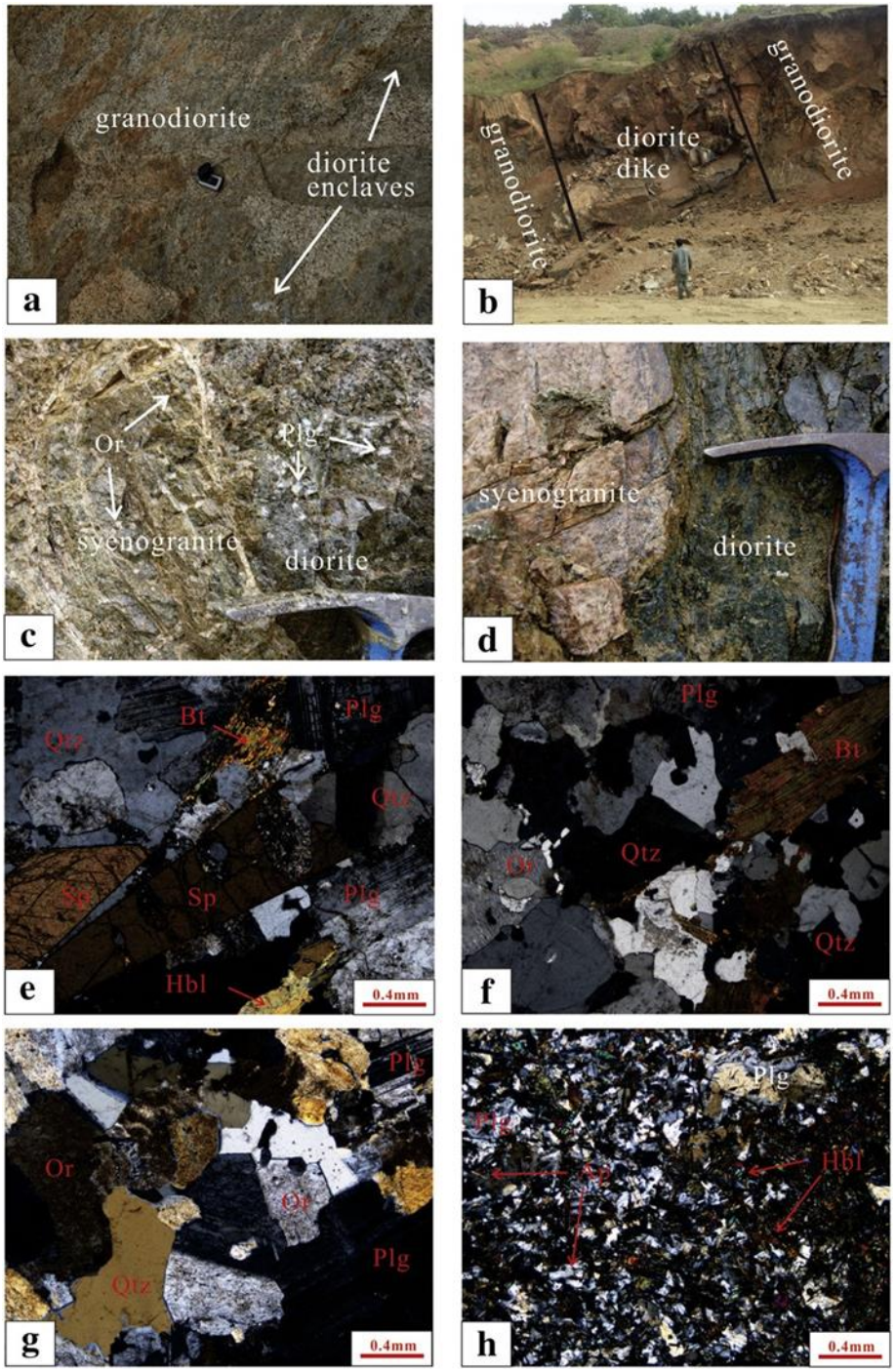

Fig. 2.5. (a), (b), (c) and (d) are the outcrops and (e), (f), (g) and (h) are photomircrographs of the studied granitoids. (a) Granodiorite with diorite enclaves; (b) a diorite dike intruding granodiorite; (c) contact between granite and diorite; (d) contact between syenogranite and diorite; (e) granodiorite sample NE13-30; (f) syenogranite sample NE13-38; (g) syenogranite sample LJ-200; (h) diorite vein sample LJ-205. Mineral abbreviations: Qtz = quartz; Or = orthoclase; Plg = plagioclase; Bt = biotite; Hbl = hornblende; Ttn = titanite; Ap = apatite. All photomicrographs are in cross-polarized light.

Whereas samples NE13-39, NE13-43 to 47, LJ-200 to 204 are fine- to medium-grained biotite-bearing syenogranite with medium- to coarse-grained allotriomorphic granular textures (Fig. 2.2. 5g). However, the mineral content varies: quartz (25–40%), perthite (45–60%), plagioclase (15–20%), with minor biotite. Samples LJ-201 and 204 contain apatite as the main accessory mineral and relatively more plagioclase.

Fig. 2.6. Representative CL images of zircons from the studied granitoids. Solid and dashed circles represent analytical spots of U–Pb and Lu–Hf isotopes, respectively, while the digits beside the circles are U–Pb ages and εHf(t) values.

Zircons were selected from samples NE13-38, 39 and 43 for U–Pb dating and Lu–Hf isotopic measurements. The other 22 samples were prepared for geochemical analysis.

2.3.3 Pegmatite and diorite veins

Pegmatite contains mainly quartz (~40%) and K-feldspar (~60%), whereas the diorite consists of plagioclase (~55%), hornblende (~35%), and minor quartz (Fig. 2.5h). The hornblende occurs in small dark patches in the diorite veins (Fig. 2.5h). Samples LJ-205 and 206 were collected from two separated diorite veins for zircon U–Pb and Lu–Hf isotopic analysis. No geochemical analyses were conducted because of the strong weathering.

2.4 Analytical methods

2.4.1 Zircon U–Pb dating

Zircons were separated by standard heavy-liquid and magnetic techniques, and picked under a binocular microscope. About 300 zircons from each sample were embedded in a 25-mm epoxy resin disk and polished to reveal approximately half of the grain's thickness. Cathodoluminescence (CL) imaging was used to observe the internal structure of zircons, utilizing the Quanta 200 FEG Scanning Electron Microscope at the Key Laboratory of Orogenic Belts and Crustal Evolution of the Education Ministry of China, Peking University.

Zircon U–Pb isotopic analyses were carried out using laser ablation inductively coupled plasma mass spectrometry (LA-ICP-MS) at the Key Laboratory of Continental Collision and Plateau Uplift, Chinese Academy of Sciences, Beijing. Laser sampling was performed on a NewWave and ATL 193 nm ArF excimer laser ablation system (UP193FX), with short pulse times (<4 ns). Element and isotope signal intensities were acquired by an Agilent 7500a ICP-MS. Both high-purity helium and argon were used as carrier gases, which were mixed via a T-connector before entering the ICP-MS. Helium gas was controlled by a mass flow controller installed in the laser system, whereas argon gas was controlled by the ICP-MS. Helium and argon carrier gas flows were optimized by ablating NIST SRM 612 reference glass to obtain maximum signal intensity for ^{238}U and ^{208}Pb, minimum oxide and double-charge interference, minimum gas blank, and most stable signal intensity. With spots of 35 μm, the analyses consist of 15–20s gas blank acquisition (warm up), 40s data acquisition from the sample aerosol (ablation) and 45–55s washout time in the spot sampling mode of the laser system and TRF data acquisition mode of the Agilent ChemStation. The 91500 and Plesovice standard zircons were used as external standards for the matrix-matched calibration. NIST SRM 612 reference glass was analyzed as an external standard for the trace element content calibration. Plesovice, 91500, and NIST SRM 612 standards were analyzed after each five to ten analyses of the samples. Off-line isotope ratios and trace element concentrations were calculated

using the GLITTER_Ver4.0 program (Van Achterbergh et al., 2001); U–Pb concordia diagrams, weighted mean calculations, and probability density plots of U–Pb ages were made by using Isoplot/Ex_ver 2.49 (Ludwig, 2001).

2.4.2 Zircon Lu–Hf isotopes

Zircon Lu–Hf isotopes were analyzed at the State Key Laboratory of Geological Processes and Mineral Resources of the China University of Geosciences, Wuhan. The Lu–Hf isotopes were obtained from locations adjacent to the LA-LCP-MS sites using a Neptune MC-ICP-MS (Thermo Fisher Scientific, Germany) in combination with a Geolas 2005 excimer ArF laser ablation system (Lambda Physik, Göttingen, Germany). Based on the instrumentation and data acquisition protocols (Hu et al., 2012), the analyses were conducted with a beam of 44 μm, using the ICPMSDataCal to conduct the off-line signal selection and integration and mass bias calibrations (Liu et al., 2010). The parameters that were used to calculate the isotopes were as follows: 176Hf/177Hf ratios were 0.282793 (chondrite) and 0.28325 (depleted mantle), 176Lu/177Hf ratios were 0.0338 (chondrite) and 0.0384 (depleted mantle), the radioactive decay coefficient of 176Lu to 176Hf was 1.867 × 10−11a−1, and the 176Lu/177Hf ratio of bulk continental crust was 0.015 (Griffin et al., 2004; Iizuka et al., 2015; Söderlund et al., 2004).

2.4.3 Major and trace element geochemistry

All the samples for whole-rock geochemical analysis were trimmed to remove the weathered surfaces, and the fresh inner portions that remained were washed and crushed to a 200-mesh size in an agate mill. The analyses of major and trace elements were obtained by ICP-emission spectrometry and inductively coupled plasma-mass spectrometry (ICP-MS) using natural rock standards as reference samples for calibration at the Acme Analytical Laboratories in Vancouver, Canada. Before the analysis of major elements, 0.2g of rock-powder was fused with 1.5g $LiBO_2$ and then dissolved in 100 mL 5% HNO_3.

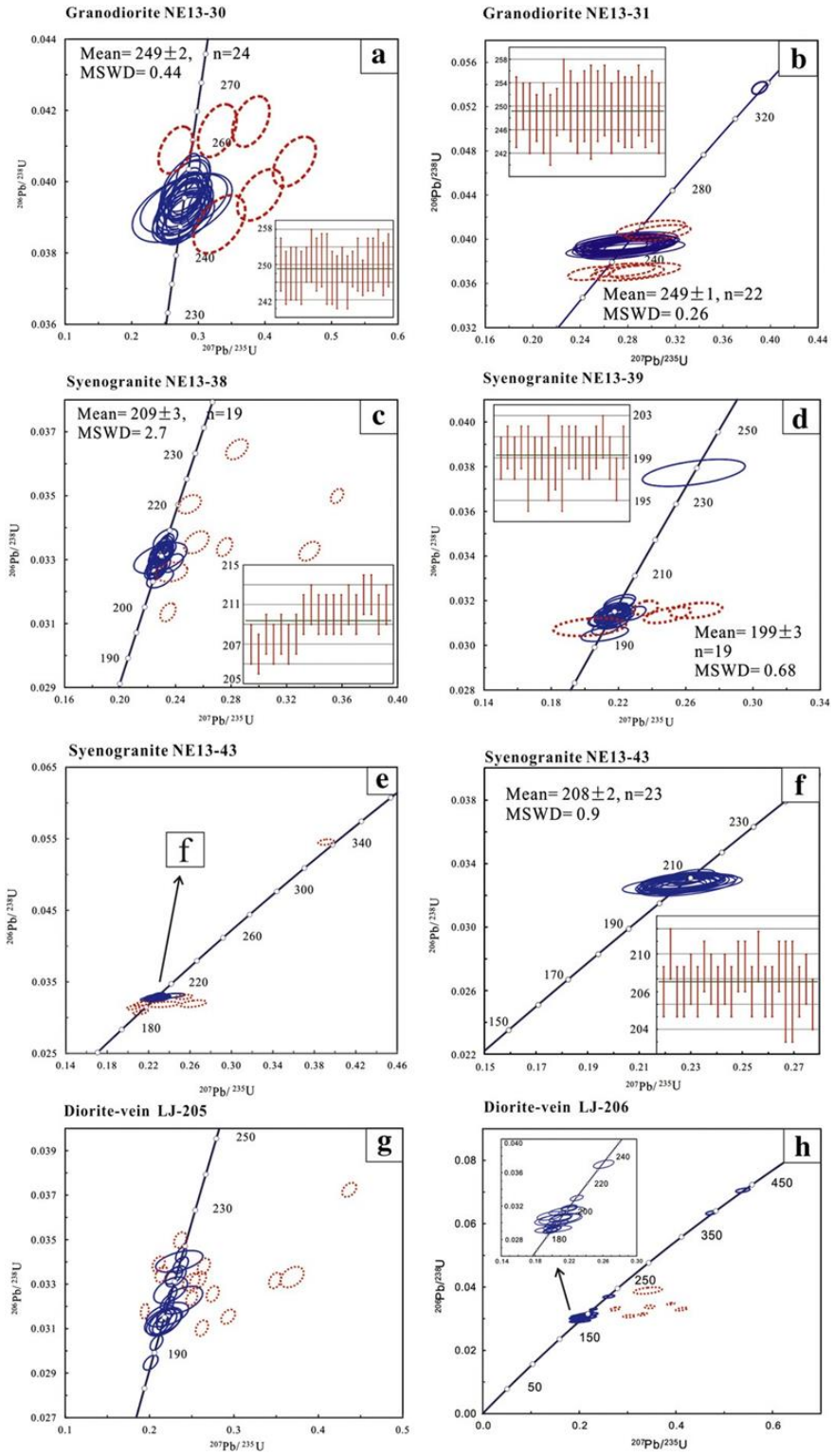

Fig. 2.7. Zircon U–Pb concordia diagrams. (a) and (b) granodiorite sample NE13-30 and NE13-31; (c) syenogranite sample NE13-38; (d) syenogranite sample NE13-39; (e) and (f) syenogranite sample NE13-43; (g) and (h) diorite vein sample LJ-205 and LJ-206, respectively. The blue ellipses are concordant ages and the red dashed ellipses are discordant ones. The data used for calculating the mean 206Pb/238U ages are shown in the small rectangles in (a), (b), (c), (d) and (f).

One gram of each sample was placed in a furnace at 1000 °C for several hours before being cooled in desiccators and reweighed to calibrate the loss on ignition (LOI). The detection limit of ICP-emission spectrometry is 0.01%. Trace elements (including rare earth elements, REEs) were analyzed by ICP-MS on pulps after 0.25 g of rock-powder was dissolved with four acid digestions.

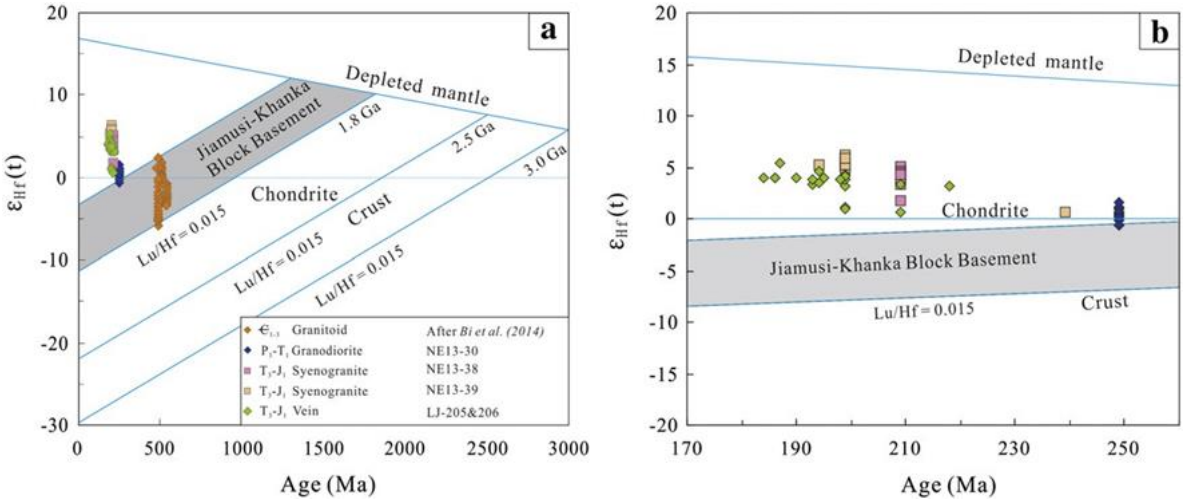

Fig. 2.8. Zircon εHf(t) values vs. crystallization ages for five samples: NE13-30 (granodiorite), NE13-38 (syenogranite), NE13-43 (syenogranite), LJ-205 and LJ-206 (felsic veins). (a) shows the zircons from samples in this study and those from the Pan-African granitoids, which represent the Lu–Hf isotopic field of basement in the Jiamusi–Khanka Block (Bi et al., 2014). (b) is an enlargement of (a) from 260 to 170 Ma, showing the positive trending of zircon εHf(t) values with a decrease in zircon U–Pb ages in the Khanka Lake granitoids.

2.5 Results

2.5.1 Zircon U–Pb and Lu–Hf isotopes

Seven samples (NE13-30, NE13-31, NE13-38, NE13-39, NE13-43, LJ-205, LJ-206) were analyzed for dating. Lu–Hf isotopes were analyzed for five of these samples: NE13-30, NE13-38, NE13-39, LJ-205, and LJ-206. The U–Pb and Lu–Hf isotopic analytical results are presented in Appendices 2 and 3, respectively, and typical CL images of zircons are shown in Fig. 2.6.

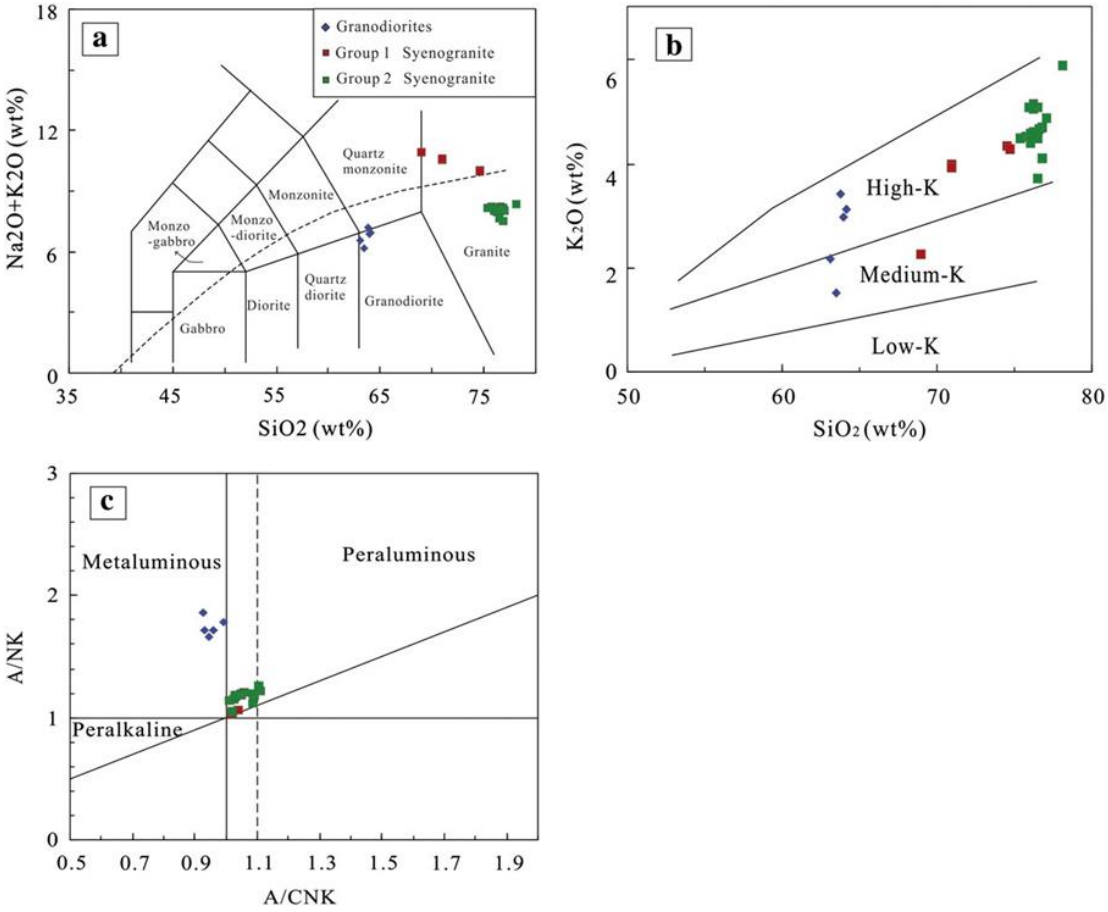

Fig. 2.9. Classification diagrams of major elements in the Khanka Lake granitoids. (a) Total alkalis vs. silica classification (TAS classification diagram, after Middlemost, 1994); (b) K2O vs. SiO2 (Peccerillo and Taylor, 1976); (c) A/CNK vs. A/NK (A/NK = [molar Al2O3 / (Na2O + K2O)], A/CNK = [molar Al2O3 / (CaO + Na2O + K2O)]; Maniar and Piccoli, 1989).

2.5.1.1. Granodiorite (samples NE13-30 and NE13-31)

The zircons from the granodiorite samples NE13-30 and NE13-31 are elliptical or rounded in shape with length/width ratios varying from 1.5:1 to 4:1, and the lengths range from 100 μm to 350 μm (Fig. 2.6). Most of the zircons show weak oscillatory zones. The Th/U ratios range from 0.37–0.95 for sample NE13-30 and 0.11–0.65 for sample NE13-31 (Appendix 2), indicating a magmatic origin. Thirty-three sites were analyzed from sample NE13-30, and 26 concordant data were obtained, which cluster between 246 and 252 Ma with a weighted mean age of 249 ± 2 Ma (MSWD = 0.44; Fig. 2.7a). For sample NE13-31, the 206Pb/238U ages range from 246 to 251 Ma, with a weighted mean age of 249 ± 1 Ma (MSWD = 0.26, n = 22; Fig. 2.7b) and with one inherited grain with an age of 337 Ma.

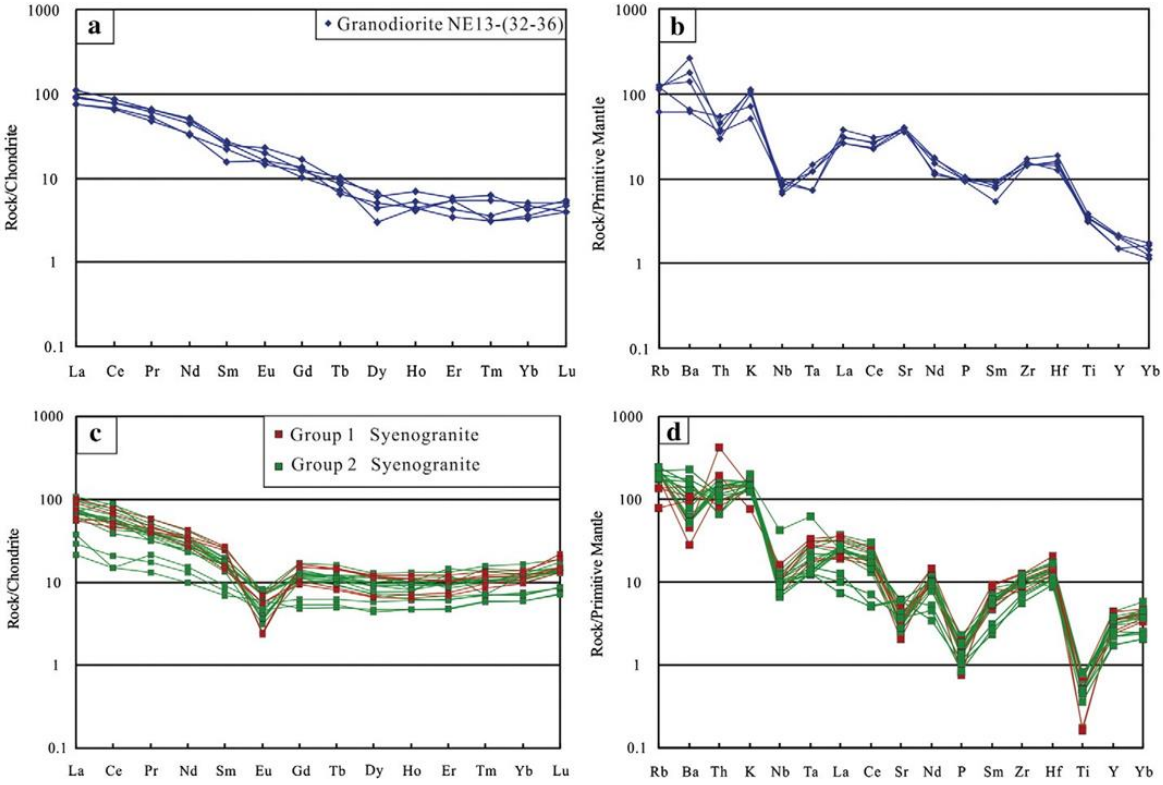

Fig. 2.10. Chondrite-normalized REE patterns and primitive mantle-normalized trace element spider diagrams for Early Triassic granodiorites (a and b) and Late Triassic to Early Jurassic granites (c and d). Chondrite and primitive mantle normalization values are from Sun and McDonough (1989).

Sample NE13-30 was chosen for in-situ Lu–Hf isotope analyses on 25 zircons with concordant U–Pb ages. The $^{176}Hf/^{177}Hf$ ratios range from 0.282601 to 0.282666, the $\varepsilon_{Hf}(t)$ values vary from -1.29 to 0.97 (Fig. 2. 8b), and their T_C model ages from 1057 to 1182 Ma (Appendix 3).

2.5.1.2. Syenogranite (samples NE13-38, NE13-39, and NE13-43)

The zircons from biotite syenogranite sample NE13-38, NE13-39 and NE13-43 have rounded or elongate shapes with lengths of 100–380 μm and length/width ratios of 1:1–4.5:1 (Fig. 2.6). Most of the zircons show magmatic oscillatory zones in the CL images, but some zircons from sample NE13-39 are dark in CL and without obvious oscillatory zones (Fig. 2.6). The Th/U ratios range from 0.31–1.07 for sample NE13-38, 0.34–0.84 for sample NE13-39, and 0.11–0.97 for sample NE13-43 (Appendix 2),

supporting a magmatic origin.

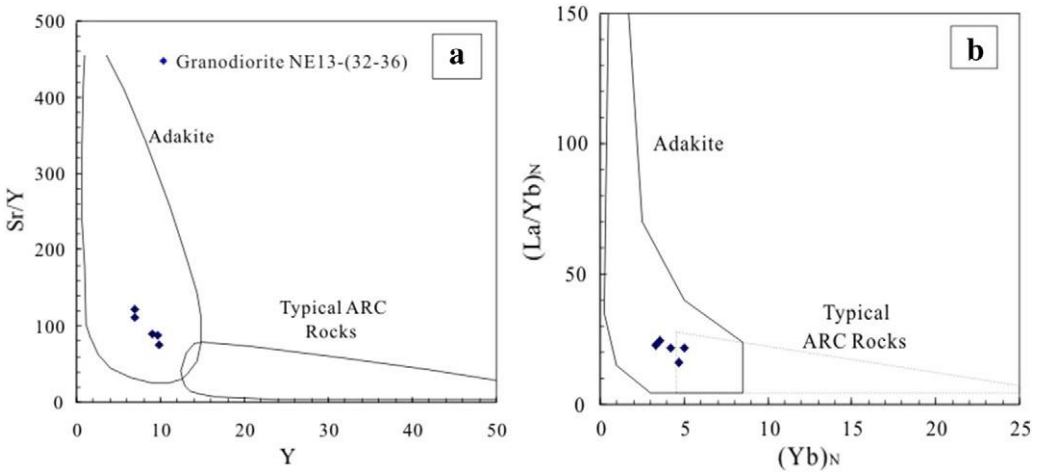

Fig. 2.11. Petrogenetic diagrams for the Early Triassic Khanka Late granodiorite. (a) Sr/Y vs. Y and (b) $(La/Yb)_N$ vs. $(Yb)_N$; both indicate adakite-like features.

Nineteen and 23 concordant data for samples NE13-38 and NE13- 43, record weighted mean ages of 209 ± 3 Ma (MSWD = 2.7; Fig. 2.7c) and 208 ± 2 Ma (MSWD = 0.9; Fig. 2.7e), respectively. Nineteen concordant data for sample NE13-39 give a weighted mean $^{206}Pb/^{238}U$age of 199 ± 3 Ma (MSWD = 0.79; Fig. 2.7d). It is notable that one zircon with similar CL features to those in the granodiorites (NE13-30, NE13-31) records a $^{206}Pb/^{238}U$ age of 239 Ma. In sample NE13-43, there is also one inherited zircon with an age of ca. 340 Ma.

According to the two ages of emplacement (199 Ma and ~ 208 Ma), in-situ zircon Lu–Hf isotope analyses were conducted on 22 zircons from sample NE13-38 (~ 209 Ma) and 22 zircons from sample NE13- 39 (~ 199 Ma). The $^{176}Hf/^{177}Hf$ ratios of zircons from sample NE13-38 are 0.282698–0.282792, and the εHf(t) values range from 1.04 to 4.44 (Fig. 2.8b), with T_C model ages from 831 to 1020 Ma. However, the zircons from sample NE13-39 show higher $^{176}Hf/^{177}Hf$ ratios of 0.282791–0.282832 and more positive εHf(t) values of 4.26–5.56 and younger T_C model ages from 760 to 832 Ma (Appendix 3). The single zircon with an age of 239 Ma has an εHf(t) value of 0.04 and a T_C model age of 1099 Ma, which is similar to that of zircons in the granodiorite (~249 Ma).

2.5.1.3. Diorite veins (samples LJ-205 and LJ-206)

Two samples (LJ-205, LJ-206) from diorite veins were selected for U–Pb and Lu–Hf isotopic analyses. The zircons can be divided into two groups according to their different characteristics in the CL images. The length of the first group ranges from 50 to 260 μm, with length/ width ratios of 1.5:1–4:1 (Fig. 2.6). Zircons from the other group are smaller in size with lengths of 50–150 μm and length/width ratios of 1.1–2:1. All the zircons of the first group have typical magmatic oscillatory zones, but the other group shows only weak zoning (Fig. 2.6). The high Th/U ratios of 0.22–1.20 confirm a magmatic origin (Appendix 2). Thirty-four sites were analyzed in sample LJ-205 and 18 concordant data were obtained, with ages ranging from 187 Ma to 218 Ma (Fig. 2.7g). Sample LJ-206 yielded 17 concordant ages from 30 analyses, and they ranged in age from 184 Ma to 209 Ma (Fig. 2.7h). In both samples, zircons from 199 Ma to 218 Ma were similar to those from the biotite syenogranite, indicating that these are likely inherited zircons captured from the surrounding rocks. It is considered that the younger zircons with ages of 184–195 Ma mark the intrusion age of the two veins. Twelve zircons with concordant ages from sample LJ-205 were selected for Lu–Hf isotopic analyses. The $^{176}Hf/^{177}Hf$ ratios and εHf(t) values are 0.282668–0.282819 and −0.04–4.65 (Fig. 2.8b), respectively. The T_C model ages range from 801 Ma to 1080 Ma. From sample LJ-206, 10 Lu–Hf isotopic data were obtained, having εHf(t) values of 2.90–3.92 and T_C model ages of 847–904 Ma.

2.5.2 Major and trace elements

Geochemical analyses were carried out on 5 samples of granodiorite and 22 samples of syenogranite; results are listed in Appendix 1.

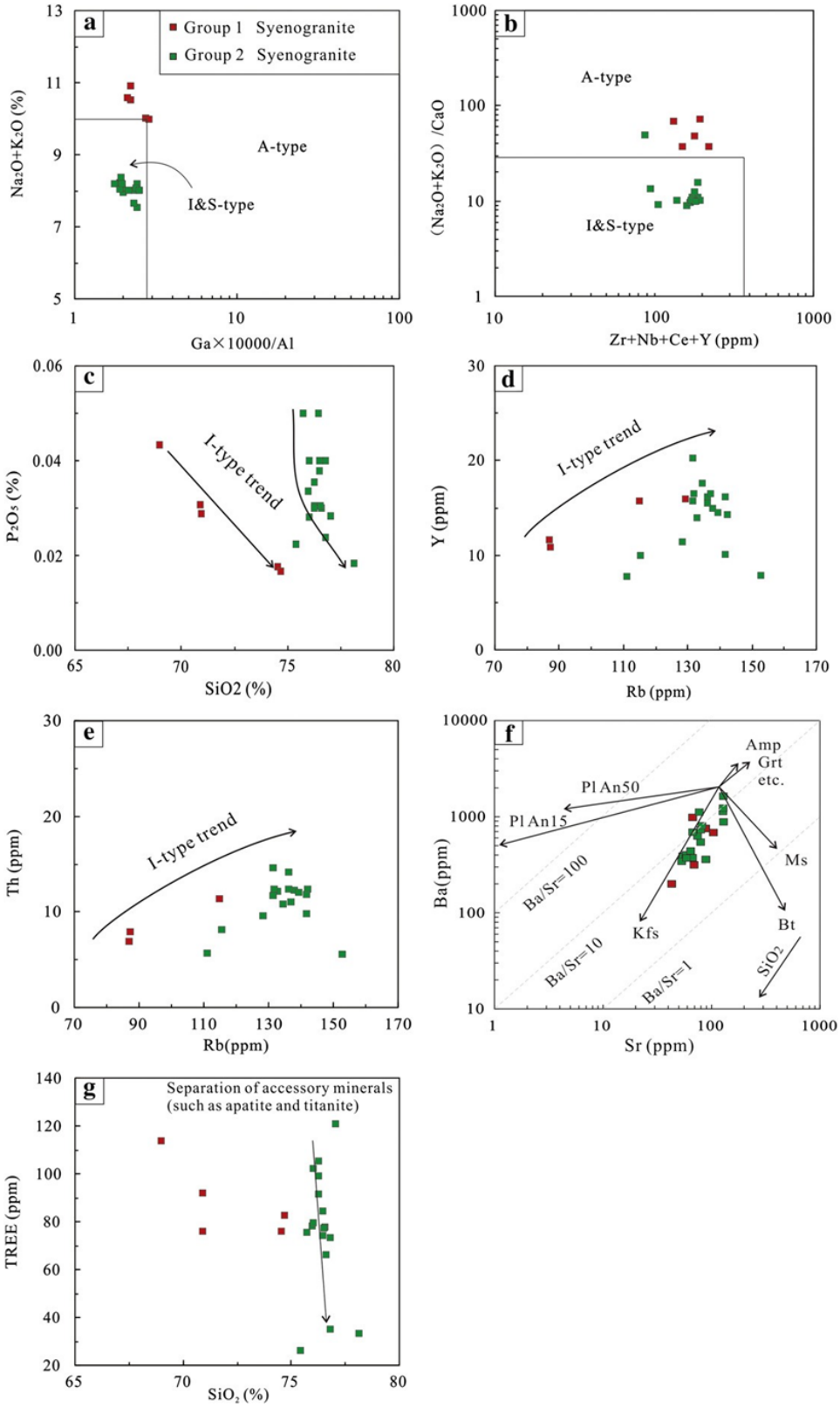

Fig. 2.12. Petrogenetic diagrams for the Late Triassic to Early Jurassic Khanka Lake syenogranite. (a) ($Na_2O + K_2O$) vs. (Ga × 10,000/Al) and (b) ($Na_2O + K2O$) vs. (Zr + Nb + Ce + Y) (after Whalen et al., 1987). (c) P_2O_5 vs. SiO_2, (d) Y vs. Rb and (e) Th vs. Rb (after Chappell, 1999; Li et al., 2007). (f) Ba vs. Sr (after Janoušek et al., 2004). (g) Total REE vs. SiO_2.

2.5.2.1. Granodiorite

The five samples plot near the intersection of granodiorite, quartz diorite, and quartz monzonite on the $Na_2O + K_2O$ vs. SiO_2 diagram (Fig. 2.9a). With K_2O contents of 1.51–3.42%, they plot in the medium- to high-K calc-alkaline series in the K_2O vs. SiO2 diagram (Fig. 2.9b). The K_2O/Na_2O ratios range from 0.33–0.90, and the ratios of A/CNK (Al_2O_3 / $(CaO + Na_2O + K_2O)_{mol}$) range from 0.92 to 0.99 (<1.0), displaying a metaluminous character (Fig. 2.9c). An important characteristic of the granodiorites is the relatively high Al_2O_3 contents (16.54–17.20%) and low MgO contents (1.60–1.83%), which means they plot in the field of adakites (Defant and Drummond, 1990). The Mg# of 48–50 ($Mg\# = 100 \times Mg / (Mg + Fe_{total})$ as atomic ratio) are higher than normal crust-derived granitoids (Rapp and Watson, 1995; Rapp et al., 1991).

All five samples show strongly fractionated chondrite- normalized REE patterns (Fig. 2.10a; Sun and McDonough, 1989) with total REE concentrations from 86 to 122 and $(La/Yb)_N$ from 16 to 25 (Appendix 1). The HREE pattern is relatively flat and the Eu anomalies are negative to weakly positive (δEu = 0.87–1.27; $\delta Eu = (Eu_N/SQRT (Sm_N \times Gd_N))$) (Appendix 1). The samples show high Sr (743–840 ppm) but low Yb (0.56–0.85) and Y (6.90–9.80) concentrations, with high Sr/Y ratios (76–122; Appendix 1). Rubidium, Ba, Sr, Zr, and Hf show positive anomalies, whereas Nb, Ta, and P have negative anomalies (Fig. 2.10b).

2.5.2.2. Syenogranite

Twenty-two samples of granite (NE13-(40–42); LJ-(190–194); NE13-(44–47), LJ-(200–204), and LJ-(208–212)) plot in the field of granite in the plutonic igneous rock diagram (Fig. 2.9a), and they can be subdivided into two groups. Group 1 includes 5 syenogranite samples: LJ-200 to LJ-204, whereas Group 2 includes the 17 syenogranite samples: NE13-(44–47), LJ-(190–194) and LJ-(208–212). Group 1 has relatively low SiO_2 contents (68.97–74.67%) and K_2O/Na_2O ratios (0.26–0.76), compared to Group 2 which has extremely high SiO_2 contents (75.74–78.15%) and

higher K_2O/Na_2O ratios (0.95–2.37) (Appendix 1). However, Group 1 and 2 share some similarities. The A/CNK values of both groups cluster between 0.92–1.11, mostly from 1 to 1.1, indicating a weak peraluminous character (Fig. 2.9c). $Fe_2O_3^T$ and MgO are relatively low (0.26–1.62% and 0.05–0.23%, respectively), and the Mg# values are from 19.9 to 32.2. In addition, the samples show enrichment in LREEs and LILEs, depletion in Rb, Ba, Th, K, Zr, and Hf, and negative anomalies of Nb, Ta, P, and Ti (Fig. 2.10d).

In addition, samples LJ-200 and LJ-202 in Group 1 have the highest total REE contents and strongest negative Eu anomalies (Fig. 2.10c). Samples LJ-(208–212) in Group 2 can be distinguished from the other high-SiO_2 granite samples (Fig. 2.9c) by showing lower total REE concentrations (26.12–79.64 ppm) and weaker Eu anomalies (δEu = 0.50–1.06), whereas other high-SiO_2 samples have total REE of 66.44–121.04 ppm and δEu of 0.12–0.56 (Fig. 2.10c).

2.6 Petrogenesis of the Khanka Lake granitoids

2.6.1 Petrogenesis of the granodiorites (ca. 249 Ma)

The most outstanding feature of the granodiorites is that they plot in the field of adakites (Fig. 2.11a). High Sr (743–840 ppm, average 799), Sr/Y (76–122, average 97), $(La/Yb)_N$ ratios (16–25; Fig. 2.11b), Al_2O_3 (ca. 17%) and Na_2O (3.8–4.6%) with low Y, Yb (<10 and 1, respectively) are similar to classical adakites (Defant and Drummond, 1990; Peacock et al., 1994; Smithies, 2000).

Adakites were originally attributed to the partial melting of young subducted slabs (<25 Ma; Defant and Drummond, 1990), but later studies have proposed alternative mechanisms for the origins of such rocks. These models include: partial melting of thickened lithosphere (Atherton and Petford, 1993; Barnes et al., 1996; Chung et al., 2003; Condie, 2005; Gao et al., 2004; Hou et al., 2004), magma mixing between crust and slab-modified mantle (Guo et al., 2007, 2009), assimilation and fractional

crystallization of melts from the mantle wedge metasomatized by fluids from a subducted oceanic slab (Castillo et al., 1999) and partial melting from the mafic lower crust under normal pressure (Ma et al., 2015; Qian and Hermann, 2013).

Melting of the mantle wedge does not explain the petrogenesis of the Khanka Lake granodiorite, since the low contents of Fe, Mg, Cr and Ni preclude the possibility that these adakite-like magmas could be generated from the mafic-ultramafic mantle wedge or the interaction between the parent magma with mantle peridotite (Castillo et al., 1999; Defant and Drummond, 1990; Guo et al., 2007). In the present case, the slab-melting model also cannot explain the chemical features of the Khanka Lake granodiorite. Oceanic crust is tholeiitic with low potassium contents, which is the reason why adakites always show low K_2O and K_2O/Na_2O (<0.6; Xiao and Clemens, 2007). However, the Khanka Lake granodiorites show medium-high K calc-alkalic features with relatively high K_2O/Na_2O ratios (>0.5), indicating that the source material could be basaltic rocks from the lower continental crust which have more potassium and shows Nb-Ta-Zr-Hf anomalies, different from MORB. The studied rocks have moderate Si_2O contents (<70%), low Rb/Ba (<0.1), Nb/U (<15), which is similar to melts derived from mafic lower crust (Gao et al., 2004; Ma et al., 2015). Magma mixing between melts from the mafic lower crust and juvenile magma is more appropriate to explain the genesis of the Khanka Lake granodiorite. The εHf(t) values of the Khanka Lake granodiorite shows a small range from −0.9 to 1.3 (average 0.3, Fig. 2.8a) with two- stage model ages from 1182 to 1057 Ma, implying that the Mesoto Neoproterozoic basement of the Jiamusi–Khanka Block is important in the magma genesis (Griffin et al., 2000; Yang et al., 2015c). The low εHf(t) values of zircons also rule out the possibility of slab-melting. However, participation of juvenile crust is required because the εHf(t) values of zircons are beyond the range of the Pan-African basement of the Jiamusi–Khanka Block. There are extensive elliptical or elongated mafic enclaves in the granodiorite (Fig. 2.5a). The boundary between the enclaves and granodiorite is diffuse, indicating that both the mafic magma and felsic magma did not solidify during the mixing. The magma mixing explanation is also consistent with the

high Mg# of ~ 50, which is higher than the Mg# of melting from the lower crust (Rapp and Watson, 1995; Rapp et al., 1991).

Traditionally, the high Sr/Y and La/Yb ratios in adakites with high K_2O/Na_2O are considered to be the signatures of partial melts from a thickened crust or foundered lower crust (depth >50 km; Chung et al., 2003; Gao et al., 2004). However, new experimental petrological research proposes that these adakite-like rocks are most likely derived from the partial melting of mafic lower crust at condition of 800–950 °C and 10–12.5 kbar, which corresponds to a depth of 30–40 km (Qian and Hermann, 2013). By starting with a protolith composition of mafic lower crust in the North China Craton, the adakite-like characteristics can be generated in partial melts that are in equilibrium with two-pyroxene granulite (<33 km), garnet-bearing granulite (33–45 km) or eclogite (>45 km), which means a thickened crustal setting is possible but not necessary (Ma et al., 2015). In the Jiamusi–Khanka Block, however, the known granulite is not two- pyroxene granulite or garnet-bearing granulite, but khondalite with a sedimentary protolith (Wilde et al., 1997), which cannot form the protolith of the adakite-like granodiorite (Qian and Hermann, 2013; Ma et al., 2015). Thus, it is difficult to estimate the partial melting P–T conditions of the Khanka Lake granodiorite, although the adakite-like characteristics are recognized.

In summary, magma mixing between the melts from the old mafic lower crust and juvenile basaltic magma is responsible for the origin and evolution of the adakitic granodiorite during the earliest Triassic (ca. 249 Ma). A high-pressure environment is possible but not necessary in the source area.

2.6.2 Petrogenesis of the syenogranite (209–199 Ma)

Syenogranite samples of Group 1 plot in the field of A-type granite, whereas Group 2 plots as highly fractionated I&S-type granite (Fig. 2.12a and b; Whalen et al., 1987).

However, Group 1 is different from typical A-type granite because of much lower Ga × 10,000/Al and Zr + Nb + Ce + Y (Fig. 2.12a, b; Whalen et al., 1987). There is also no mafic alkaline mineral, such as arfvedsonite or riebeckite, to confirm that they are A-type granite (Wu et al., 2003a, 2003b). Furthermore, the P_2O_5 content decreases with higher SiO_2 within each group, indicating that they are I-type granites (Fig. 2.12c; Chappell, 1999; Deng et al., 2014; Li et al., 2007; Wolf and London, 1994; Wu et al., 2003a), which is consistent with the plots of Th vs. Rb and Y vs. Rb (Fig. 2.12d, e; Chappell, 1999; Deng et al., 2014; Li et al., 2007).

All granitoids show depletion of Ba, Nb, Ta, Sr, P and Ti, similar to the widespread highly-fractionated I-type granites in NE China, Tibet and South China (Chen and Tang, 2015; Li et al., 2007; Wu et al., 2003a, 2003b; Zhu et al., 2009). Both Sr and Ba decrease rapidly, which can be interpreted as the separation of either K-feldspar or the assemblage of plagioclase and biotite (Fig. 2.12f; Janoušek et al., 2004; Li et al., 2007; Zhu et al., 2009). However, the proportion of biotite and plagioclase decreases as the quartz and K-feldspar increase in the syenogranite, indicating that biotite and plagioclase are the dominant fractionated mineral phases. This differentiation also explains why, as the SiO_2 content increases, the contents of Na_2O and Al_2O_3 decrease, whereas K_2O and Rb increase (figures not shown). The negative anomalies of Nb, Ta and Ti probably result from the fractionation of titanite in the parent magma (Xiong, 2006), whereas the separation of apatite contributes to the decrease of P_2O_5 and REE content (Fig. 2.12c and g). The separation of these accessory minerals also fits the geochemical characteristic that some element contents (including P_2O_5, CaO, $Fe_2O_3^T$ and TREEs) vary considerably when the SiO_2 content stabilizes between 71%–74%.

The T_C model age range of 1020–831 Ma indicates that Neoproterozoic granitoids in the gneissic basement were likely the protolith of the syenogranite (Fig. 2.8b; Guo et al., 2010; Yang et al., 2015a). However, the εHf(t) values become more positive as the zircon age becomes younger and some zircons are more positive than the values of the basement of the Jiamusi–Khanka Block, indicating that the proportion of juvenile material in the parent magma increases with time (Fig. 2.8; Jahn et al., 2000; Jahn, 2001; Wu et al., 2003b). In addition, they belong to the medium- to high-K calc-alkalic

series and depleted in HREE and HFSE and enriched in LREE and LILE, indicating an active continental margin environment (Grove et al., 2003; Pearce, 1982; Wang et al., 2015a, 2015b; Yang et al., 2015a, 2015b).The low Sr, Sr/Y, and Mg# and strongly negative Eu anomalies suggest that these granites are crust-derived at low-pressure because there is probably residual plagioclase in the source and no mixing with mantle magma occurred (Rapp and Watson, 1995; Zhang et al., 2006).

It is concluded that the syenogranite was generated from reworking and remelting of basement, with some juvenile input, under low- pressure conditions within an active continental marginal setting. They then experienced strong fractionation of plagioclase, biotite and some accessory minerals (including apatite and titanite).

2.7 Tectonic implications

2.7.1 Paleogeographic position of the Khanka Lake granitoids during the early Mesozoic

In order to understand the tectonic setting of the Khanka Lake batholith, it is necessary to discuss the paleogeographic position of the Khanka Lake granitoids because after their emplacement they were likely moved northeastwards due to the Dun-Mi Fault, the northern segment of the Tan-Lu Fault (Fig. 2.2. 3; Wu et al., 2007, 2011; Xu et al., 2013; Zhou et al., 2009a, 2009b). The initial activity on the Dun-Mi Fault has been dated along the ductile shear zone at ca. 161 Ma by the biotite Ar–Ar method, although the most important sinistral movement took place in the late Early Cretaceous, which produced pull-apart or graben basins in NE China (Sun et al., 2010). Most researchers suggest a sinistral displacement of 150–250 km based on studies of geological units which were cut by the strike-slip fault (Fig. 2.13). The Hulin and Jixi basins shared the similar uplifted basement, which was overlain by similar strata since the Early Cretaceous, indicating they belonged to an intact basin before being separated by the Dun-Mi Fault (Zhao et al., 2009). The Changchun-Yanji Fault and related accretionary complexes were also dislocated by the Dun-Mi Fault (Li et al., 2002; Wang et al., 2000).

It was estimated that a left-lateral offset of approximately 200 km occurred along the Dun-Mi Fault based on the above evidence. Therefore, the Khanka Lake granitoids should be moved southwest by ca. 200 km from their present location and thus should be near the present site of Mudanjiang and aligned with the Zhangguangcai Range in an N–S trending magma belt formed in the early Mesozoic (Fig. 2.13b).

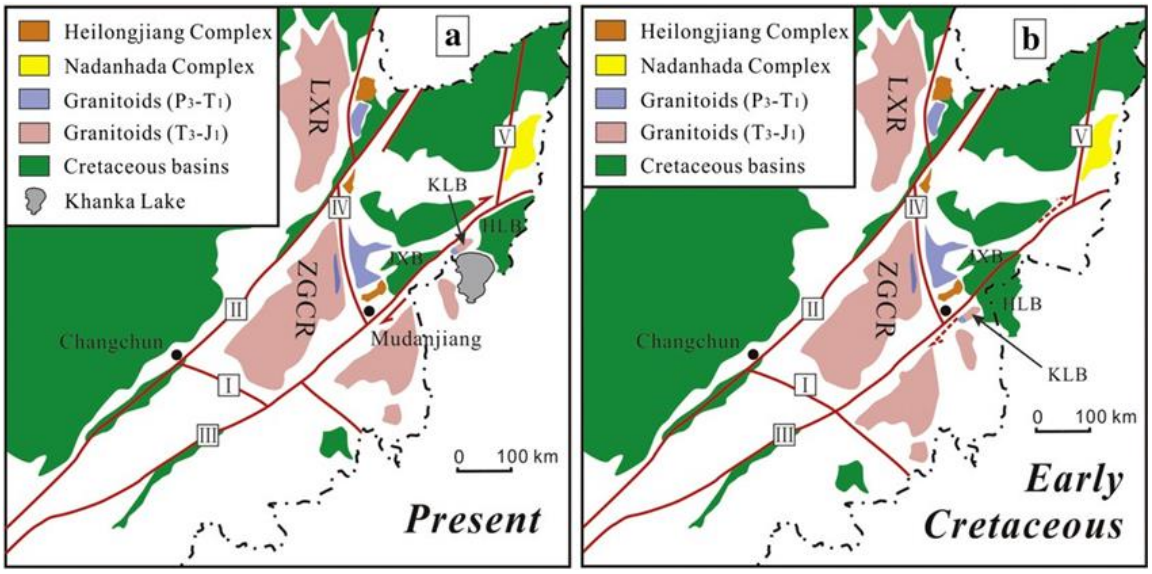

Fig. 2.13. Sketch map of major geological units in eastern NE China, including the granitoids, accretionary complexes, Cretaceous basins and major faults. (a) Present setting and (b) Early Cretaceous setting before major movement along the Dun-Mi Fault. Modified after Zhao et al. (2009) and Zhou et al. (2009b, 2013). LXR = Lesser Xing'an Range. ZGCR = Zhangguangcai Range. KLB = Khanka Lake batholith. JXB = Jixi Basin. HLB = Hulin Basin. Fault names: I. Changchun-Yanji Fault; II. Jia-Yi Fault; III. Dun-Mi Fault; IV. Mudanjiang Fault; V. Yuejinshan Fault

2.7.2 The N–S trending magmatic belt in NE China

The magmatic rocks along the western Jiamusi and Khanka Blocks and those in the Lesser Xing'an–Zhangguangcai Range constitute a N–S trending magmatic belt in NE China. Recently, more magmatic rocks of late Paleozoic to early Mesozoic age have been identified in the belt, which has two peak ages: late Permian to Early Triassic and Late Triassic to Early Jurassic (Fig. 2.2.3; Guo et al., 2010; Huang et al., 2008; Wu et al., 2001; Xu et al., 2013).

Most plutons of the first stage are calc-alkali I-type granitoids (Guo et al., 2010; Wu et al., 2011), some of which are adakite-like granodiorites (black stars in Fig. 2.3).

Adakite-like granodiorites with zircon U–Pb ages of 244 Ma (Sr/Y = 28.0–127.6, δEu = 0.68–1.38) were reported to the northwest of Jiamusi city (Wei et al., 2008). Granitoids of ca. 245 Ma were also discovered in the middle Zhangguangcai Range, with a high Sr/Y ratio of 72 and δEu of 1.07 (Shao et al., 2013). Furthermore, a huge N–S trending granodiorite batholith with an age of 270–254 Ma crops out to the northeast of Mudanjiang city in the western Jiamusi Block, and part of it is also characterized by high Sr/Y ratios (18.04–90.95; Wu et al., 2001). If the offset on the Dun-Mi Fault were removed, the adakite-like granodiorites in the Khanka Lake batholith with ages of ca. 249 Ma would form the southern part of the belt of I-type and adakite-like rocks near Mudanjiang.

The later stage of magmatism at 210–180 Ma is found around the northern and western margin of Khanka Lake (Khanchuk, 2010a; Yang et al., 2015a). These granites all have positive εNd(t) and/or zircon εHf(t) values (Guo et al., 2010; Wu et al., 2011). Contemporary igneous rocks (T3–J1) in the N–S trending magmatic rocks include various rock types. In the Lesser Xing'an–Zhangguangcai Range and western Khanka Block, intermediate to mafic rocks are found, including andesite, basalt, basaltic andesite and gabbro-diabase (228–202 Ma; Shao et al., 2013; Wang et al., 2015a, 2015b) and olivine norite, gabbro, hornblendite and diorite (190–180 Ma; Guo et al., 2015; Yu et al., 2012). Further research on geochemistry and isotopes indicates that they show island-arc characteristics and probably related to the mantle wedge metasomatized by slab-deriving fluids, resulting from the subduction of the Paleo-Pacific Oceanic plate. Felsic rocks, such as granitoids, are more extensively distributed in the eastern NE China. The highly-fractionated I-type granitoids in the Lesser Xing'an–Zhangguangcai Range are the majority of the N–S trending magmatic belt (Wu et al., 2003a, 2003b, 2011). Recently, similar granitoids are found in the western Khanka Block and the Bureya Block. The granitoids and diorite enclaves (211–208 Ma) in the Jidong area were generated by the magma mixing during the westwards subduction of the Paleo-Pacific Oceanic plate (Yang et al., 2015b). Whereas in the central Bureya Block, the N–S trending magmatic belt includes I-type leucogranite

and trachyrhyolite (210–199 Ma), which are proposed to be related to the amalgamation between the Bureya Block and western CAOB blocks (Sorokin et al., 2016).

2.7.3 Tectonic setting of the Jiamusi–Khanka Block during the early Mesozoic

The early Mesozoic magmatism in NE China is poorly understood with respect to the tectonic setting. The granitoids (including the adakite-like rocks) of Permian to Early Triassic age in the western Jiamusi–Khanka Block show typical I-type characteristics, such as A/CNK<1.0, Na_2O/K_2O>1, enrichment of LILEs and LREEs, relatively high CaO, and positive εNd(t) and/or εHf(t) values, which are consistent with an active continental margin setting. Igneous rocks formed in the active continental margin are also reported in the adjacent areas, with ages ranging from Early Permian to Early Triassic, such as andesite, dacite, rhyolite and granitoids in the eastern Jiamusi Block (Meng et al., 2008; Yang et al., 2015a), and gabbros in the Dongfanghong area (Bi et al., 2015; Sun et al., 2015). The detailed studies on these igneous rocks show that they are generated along an active continental margin. Thus, it is proposed that the late Permian to Early Triassic granitoids are related to an N–S trending subduction system (Ge et al., 2016; Huang et al., 2008; Wu et al., 2001).

For the Late Triassic to Early Jurassic granitoids, however, two extremely different hypotheses have been proposed: delamination during the post-collision stage of the eastern CAOB related to the closure of the Paleo-Asian Ocean (Xu et al., 2009, 2013; Yu et al., 2012) and subduction related to the Mudanjiang Ocean or the Paleo-Pacific Plate (Guo et al., 2015; Wilde and Zhou, 2015; Wu et al., 2011; Zhou et al., 2009a, 2013, 2014).

In order to discuss the tectonics of NE China during the early Mesozoic, it is important to understand the accretionary complexes along the eastern and western margins of the

Jiamusi–Khanka Block (Fig. 2.2.3). They are both Triassic to Middle Jurassic in age related to the Paleo-Pacific Ocean and Mudanjiang Ocean, respectively (Zhou et al., 2009a, 2009b, 2014). In the west, the Heilongjiang Complex contains blueschists which are considered to be slices scraped from the Mudangjiang Ocean. The protoliths of these blueschists are OIB and E-MORB type basalts with zircon U–Pb ages from 280 Ma to 210 Ma (Ge et al., 2016; Zhou et al., 2009a, 2009b), indicating that the Mudanjiang Ocean between the Jiamusi–Khanka Block and the eastern CAOB existed during the early Permian to Early Triassic, which denies the possibility of collision (including post-collision delamination) between the Jiamusi–Khanka Block and the western blocks. To the east, the Nadanhada Terrane is part of the Sikhote-Alin accretionary terranes which are the tectonostratigraphic terranes related to Paleo-Pacific subduction (Cheng et al., 2006; Jahn et al., 2015; Khanchuk et al., 2016). Sediments ranging from pelagic chert to terrigenous turbidite in the Nadanhada Terrane were mainly deposited from the Triassic to Middle Jurassic (Shao et al., 1991). Mafic to ultramafic rocks are separated from these sedimentary rocks by faults, and include OIB with an age of ca. 170 Ma and minor N-MORB with an age of 216 Ma (Cheng et al., 2006; Zhou et al., 2014). However, the final assemblage between the Nadanhada Terrane and Jiamusi Block took place between 150 Ma and 130 Ma, as is constrained by the youngest paleontological age of sediments and the zircon U–Pb age of an undeformed S-type granite intruding the Nadanhada Terrane (Zhou et al., 2014). So during the early Mesozoic, the effect of subduction of the Paleo-Pacific and the Mudanjiang Oceanic plates is of great importance in the eastern CAOB and can explain the sub-parallel N–S trending magmatic belt.

The closure of the Paleo-Asian Ocean and final collision of the CAOB in this area, along the Changchun-Yanji suture zone at the southwestern margin of Khanka Block, was completed before the late Paleozoic (Li et al., 2014; Xu et al., 2014; Zhao et al., 2013). Some Late Triassic A-type rhyolites were generated in the Suifenhe area, indicating local post-collision extension of the southeastern CAOB (Xu et al., 2009). However, this kind of A-type rhyolite is rare in the Lesser Xing'an–

Zhangguangcai Range, which is instead dominated by I-type granitoids, indicating the different tectonic realm from the Paleo-Asian Ocean (Wu et al., 2003a, 2003b, 2011). In addition, the trend of the magmatic belts associated with different tectonic realms are distinct: the N–S trending magma belt in the Lesser Xing'an–Zhangguangcai Range and western Khanka Block is consistent with the subduction direction of the Paleo-Pacific Ocean and Mudanjiang Ocean, whereas the magmatic belts associated with the Paleo-Asian Ocean trend roughly E–W along some large suture zones, including the Xinlin-Xiguitu suture zone and the Xar Moron-Changchun-Yanji Fault zone (Figs. 2.1 and 2.2; Li, 2006; Xiao et al., 2003; Xu et al., 2014).

Another important question about the Mesozoic tectonic setting in NE China is the relationship between the Mudanjiang Ocean and Paleo-Pacific Ocean. The Mudanjiang Ocean was located between the Bureya–Jiamusi–Khanka Block and the Songliao Block, represented by the Heilongjiang Complex that consists of the accretionary complex and remnant oceanic crust of the oceanic crust (Zhou et al., 2009a). The Mudanjiang Ocean was considered to be a small ocean, alike to the Red Sea (Zhou et al., 2009a). However, some new data from the blueschist near Yilan indicate that the ocean was opened at least from ca. 280 Ma and closed before the Late Jurassic, indicating the width of the oceanic crust is possibly larger than the previously estimated scale (Ge et al., 2007). However, it is proposed that the subduction of the Mudanjiang Ocean is under the Paleo-Pacific Ocean tectonic realm based on the following evidence. Firstly, the Bureya–Jiamusi–Khanka Block is a continental crust fragment. No matter deriving from the northern Gondwana (Wu et al., 2007) or the CAOB (Zhou et al., 2010), the area of the Bureya–Jiamusi–Khanka Block is only ~ 300,000 km2, not large enough to separate two different oceans, suggesting the Mudanjiang Ocean is probably a branch of the Paleo-Pacific Ocean. Secondly, the N–S trending magmatic belt indicate the subduction of the oceanic crust is E–W trending, which is consistent with the tectonic realm of the Paleo-Pacific Ocean (Maruyama et al., 1997).

Therefore, the weight of evidence indicates that the Bureya–Jiamusi– Khanka Block was within the realm of the Paleo-Pacific Ocean, not the Paleo-Asian Ocean. This is further substantiated by the fauna of the southwestern Khanka Block, including early to late Permian fusulinids and ammonoids from limestone in the Yanji area, establishing that the Khanka Block has similarities to other circum-Pacific terranes (Shao et al., 1995). As a result, the continental arc associated with Paleo-Pacific subduction resulted in a N–S trending belt of thickened lithosphere from the late Permian to Early Triassic, with continuous subduction of the Paleo-Pacific Oceanic plate causing remelting of juvenile crust throughout this period.

2.8 Conclusions

(1) The Khanka Lake granitoids in NE China consist of granodiorite with zircon U–Pb ages of ca. 249 Ma, together with syenogranite between 209 and 199 Ma. Some diorite veins intruded the batholith between 195 and 184 Ma.

(2) The ca. 249 Ma granodiorites are medium-high potassium, adakite-like rocks produced by magma mixing between the melts from lower continental crust and juvenile basaltic rocks.

(3) The 199–209 Ma granitoids are highly fractionated I-types derived from remelting of juvenile lower crust under low pressure.

(4) The Khanka Lake batholith was most likely the southern part of the N–S trending Lesser Xing'an–Zhangguangcai Range in NE China before activity along the Dun-Mi Fault moved it ca. 200 km to the northeast. This belt formed at an active continental margin from the late Permian to Early Triassic, with Paleo-Pacific (and Mudanjiang) Ocean subduction was responsible for the remelting of juvenile crust during the Late Triassic to Early Jurassic.

(5) The Khanka Block was thus in a subduction setting of the PaleoPacific Ocean realm during the earliest Mesozoic.

2.9 Acknowledgments

Y.H. Yue and W. Yao from the Institute of Tibetan Plateau Research, Chinese Academy of Sciences are thanked for their kind help with LA-ICP-MS dating. In addition, Z.C. Liu, L. Xu and other staff at the State Key Laboratory of Geological Processes and Mineral Resources, China University of Geosciences (Wuhan) gave valuable advice on the zircon Lu–Hf isotopes. We are especially grateful to Editor Sun-Lin Chung, Professor Feng Guo and another anonymous reviewer for their comments which help us improve this paper significantly. This research was financially supported by the Major State Basic Research Development Program of China (No. 2013 CB429804) and the Fundamental Research Funds for the Central Universities (310827161010).

2.10 References

Atherton, M.P., Petford, N., 1993. Generation of sodium-rich magmas from newly underplated basaltic crust. Nature 362, 144–146.

Barnes, C.G., Petersen, S.W., Kistler, R.W., Murray, R., Kays, M.A., 1996. Source and tectonic implications of tonalite-trondhjemite magmatism in the Klamath Mountains. Contributions to Mineralogy and Petrology 123, 40–60.

Bi, J., Ge, W., Yang, H., Zhao, G., Yu, J., Zhang, Y., Wang, Z., Tian, D., 2014. Petrogenesis and tectonic implications of early Paleozoic granitic magmatism in the Jiamusi Massif, NE China: geochronological, geochemical and Hf isotopic evidence. Journal of Asian Earth Sciences 96, 308–331.

Bi, J.H., Ge, W.C., Yang, H., Zhao, G.C., Xu, W.L., Wang, Z.H., 2015. Geochronology, geochemistry and zircon Hf isotopes of the Dongfanghong gabbroic complex at the eastern margin of the Jiamusi Massif, NE China: Petrogensis and tectonic implications. Lithos 234, 27–46.

Castillo, P.R., Janney, P.E., Solidum, R.U., 1999. Petrology and geochemistry of

Camiguin island, southern Philippines: insights to the source of adakites and other lavas in a complex arc setting. Contributions to Mineralogy and Petrology 134, 33–51.

Chappell, B.W., 1999. Aluminium saturation in I- and S-type granites and the characterization of fractionated haplogranites. Lithos 46, 535–551.

Chen, J.Y., Tang, J.H., 2015. Petrogenesis of the Fogang highly fractionated I-type granitoids: constraints from Nb, Ta, Zr and Hf. Acta Petrologica Sinica 31, 846–854 (in Chinese with English abstract).

Cheng, R.Y., Wu, F.Y., Ge, W.C., Sun, D.Y., Liu, X.M., Yang, J.H., 2006. Emplacement age of the Raohe Complex in eastern Heilongjiang Province and the tectonic evolution of the eastern part of Northeastern China. Acta Petrologica Sinica 22, 353–376 (in Chinese with English abstract).

Chung, S., Zhang, Q., Liu, D., Ji, J., Chu, M., Lee, H.Y., Lo, C., Lee, T., Qian, Q., 2003. Adakites from continental collision zones: melting of thickened lower crust beneath southern Tibet. Geology 31, 1021–1024.

Condie, K.C., 2005. TTGs and adakites: are they both slab melts? Lithos 80, 33–44.

Defant, M.J., Drummond, M.S., 1990. Derivation of some modern arc magmas by melting of young subducted lithosphere. Nature 347, 662–665.

Deng, Z., Liu, S., Zhang, L., Wang, Z., Wang, W., Yang, P., Luo, P., Guo, B., 2014. Geochemistry, zircon U–Pb and Lu–Hf isotopes of an Early Cretaceous intrusive suite in northeastern Jiangxi Province, South China Block: implications for petrogenesis, crust/mantle interactions and geodynamic processes. Lithos 200–201, 334–354.

Gao, S., Rudnick, R.L., Yuan, H.L., Liu, X.M., Liu, Y.S., Xu, W.L., Lin, W.L., Ayers, J., Wang, X.C.,

Wang, Q.H., 2004. Recycling lower continental crust in the North China craton. Nature 432, 892–897.

Ge, W.C., Wu, F.Y., Zhou, C.Y., Zhang, J., 2007. Porphyry Cu-Mo deposits in the eastern Xing'an-Mongolian Orogenic Belt: mineralization ages and their geodynamic implications. Chinese Science Bulletin 52, 3416–3427 (in Chinese

with English abstract).

Ge, M.H., Zhang, J.J., Liu, K., Ling, Y.Y., Wang, M., Wang, J.M., 2016. Geochemistry and geochronology of the blueschist in the Heilongjiang Complex and its implications in the late Paleozoic tectonics of eastern NE China. Lithos 261, 232–249.

Griffin, W.L., Pearson, N.J., Belousova, E., Jackson, S.E., Achterbergh, E., O'Reilly, S.Y., Shee, S.R., 2000. The Hf isotope composition of cratonic mantle: LAM–MC–PIMCS analysis of zircon megacrysts in kimberlites. Geochimica et Cosmochimica Acta 64, 133–147.

Griffin, W.L., Belousova, E., Shee, S.R., Pearson, N.J., O'Reilly, S.Y., 2004. Archean crustal evolution in the northern Yilgarn Craton: U–Pb and Hf isotope evidence from detrital zircons. Precambrian Research 131, 231–282.

Grove, T.L., Elkins-Tanton, L.T., Parman, S.W., Cartterjee, N., Muntener, O., Gaetani, G.A., 2003. Fractional crystallization and mantle melting controls on calk-alkaline differentiation trends. Contributions to Mineralogy and Petrology 145, 515–533.

Guo, F., Nakamura, E., Fan, W., Kobayashi, K., Li, C., 2007. Generation of Palaeocene adakitic andesites by magma mixing, Yanji area, NE China. Journal of Petrology 48, 661–692.

Guo, F., Nakamura, E., Fan, W., Kobayashi, K., Li, C., Gao, X., 2009. Mineralogical and geochemical constraints on magmatic evolution of Paleocene adakitic andesites from the Yanji area, NE China. Lithos 112, 321–341.

Guo, F., Fan, W., Gao, X., Li, C., Miao, L., Zhao, L., Li, H., 2010. Sr–Nd–Pb isotope mapping of mesozoic igneous rocks in NE China: constraints on tectonic framework and Phanerozoic crustal growth. Lithos 120, 563–578.

Guo, F., Li, H., Fan, W., Li, J., Zhao, L., Huang, M., Xu, W., 2015. Early Jurassic subduction of the Paleo-Pacific Ocean in NE China: petrologic and geochemical evidence from the Tumen mafic intrusive complex. Lithos 224–225, 46–60.

Hou, Z.Q., Gao, Y.F., Qu, X.M., Rui, Z.Y., Mo, X.X., 2004. Origin of adakitic intrusives generated during mid-Miocene east–west extension in southern Tibet.

Earth and Planetary Science Letters 220, 139–155.

Hu, Z.C., Liu, Y.S., Gao, S., Liu, W.G., Zhang, W., Tong, X.R., Lin, L., Zong, K.Q., Li, M., Chen,

H.H., Zhou, L., Yang, L., 2012. Improved in situ Hf isotope ratio analysis of zircon using newly designed X skimmer cone and jet sample cone in combination with the addition of nitrogen by laser ablation multiple collector ICP–MS. Journal of Analytical Atomic Spectrometry 27, 1391–1399.

Huang, Y.C., Ren, D.H., Zhang, X.Z., Xiong, X.S., Zhang, C.Y., Wang, Y., Zhao, L.L., 2008. Zircon U–Pb dating of the Meizuo granite and geological significance in the Huanan Uplift, East Heilongjiang Province. Journal of Jilin University (Earth Science Edition) 38, 631–638 (in Chinese with English abstract).

Iizuka, T., Yamaguchi, T., Hibiya, Y., Amelin, Y., 2015. Meteorite zircon constraints on the bulk Lu− Hf isotope composition and early differentiation of the Earth. Proceedings of the National Academy of Sciences 112 (17), 5331–5336.

Jahn, B.M., 2001. Highly evolved juvenile granites with tetrad REE patterns: the Woduhe and Baerzhe granites from the Great Xing'an Mountains in NE China. Lithos 59, 171–198.

Jahn, B.M., Griffin, W.L., Windley, B., 2000. Continental growth in the Phanerozoic: evidence from Central Asia. Tectonophysics 328, vii–vix.

Jahn, B.M., Valui, G., Kruk, N., Gonevchuk, V., Usuki, M., Wu, J.T., 2015. Emplacement ages, geochemical and Sr–Nd–Hf isotopic characterization of Mesozoic to early Cenozoic granitoids of the Sikhote-Alin Orogenic Belt, Russian Far East: Crustal growth and regional tectonic evolution. Journal of Asian Earth Sciences 111, 872–918.

Janoušek, V., Finger, F., Roberts, M., Frýda, J., Pin, C., Dolejš, D., 2004. Deciphering the petrogenesis of deeply buried granites: whole-rock geochemical constraints on the origin of largely undepleted granulites from the Moldanubian Zone of the Bohemian Massif. Transactions of the Royal Society of Edinburgh: Earth Sciences 95, 141–159.

Kemkin, I.V., 2008. Structure of terranes in a Jurassic accretionary prism in the

Sikhote- Alin-Amur area: implications for the Jurassic geodynamic history of the Asian eastern margin. Russian Geology and Geophysics 49, 759–770.

Khanchuk, A.I., 2010a. First SHRIMP U–Pb zircon dating of magmatic complexes in the southwestern Primor'e region. Russian Geology and Geophysics 49, 759–770.

Khanchuk, A.I., 2010b. First results of zircon LA ICP MS U–Pb dating of the rocks from the granulite complex of Khanka massif in the Primorye region. Doklady Earth Sciences 434, 1164–1167.

Khanchuk, A.I., Didenko, A.N., Popeko, L.I., Sorokin, A.A., Scevchenko, B.F., 2015. Structure and evolution of the Mongol–Okhotsk Orogenic Belt. In: Kroner, A. (Ed.), The Central Asian Orogenic BeltContributions to the Regional Geology of the Earth. E. Schweitzerbart Science Publishers, Stuttgart, Germany, pp. 211–234.

Khanchuk, A.I., Kemkin, V.I., Kruk, N.N., 2016. The Sikhote-Alin orogenic belt, Russian South East: terranes and the formation of continental lithosphere based on geological and isotopic data. Journal of Asian Earth Sciences 120, 117–138.

Kravchinsky, V.A., Sorokin, A.A., Courtillot, V., 2002. Paleomagnetism of Paleozoic and Mesozoic sediments from the southern margin of Mongol-Okhotsk Ocean, far eastern Russia. Journal of Geophysical Research - Solid Earth 107 (B10).

Li, J.Y., 2006. Permian geodynamic setting of Northeast China and adjacent regions: closure of the Paleo-Asian Ocean and subduction of the Paleo-Pacific Plate. Journal of Asian Earth Sciences 26, 207–224.

Li, B.L., Sun, F.Y., Yao, F.L., 2002. Large scale sinistral strike-slip movement of Dunhua-Mishan fracture zone and its control on gold metallogeny in the Mesozoic. Geotectonica et Metallogenia 26, 390–395 (in Chinese with English abstract).

Li, X., Li, Z., Li, W., Liu, Y., Yuan, C., Wei, G., Qi, C., 2007. U–Pb zircon, geochemical and Sr–Nd–Hf isotopic constraints on age and origin of Jurassic I- and A-type granites from central Guangdong, SE China: a major igneous event in response to foundering of a subducted flat-slab? Lithos 96, 186–204.

Li, S., Wilde, S.A., He, Z., Jiang, X., Liu, R., Zhao, L., 2014. Triassic sedimentation and postaccretionary crustal evolution along the Solonker suture zone in Inner

Mongolia, China. Tectonics 33, 960–981.

Liu, Y., Gao, S., Hu, Z., Gao, C., Zong, K., Wang, D., 2010. Continental and oceanic crust recycling-induced melt–peridotite interactions in the Trans-North China Orogen: U–Pb dating, Hf isotopes and trace elements in zircons from mantle xenoliths. Journal of Petrology egp082.

Ludwig, K.R., 2001. Isoplot/Ex Version 2.49: A Geochronological Toolkit for Microsoft Excel. Special Publication. Berkeley Geochronology Center, pp. 1–55.

Ma, Q., Zheng, J.P., Xu, Y.G., Griffin, W.L., Zhang, R.S., 2015. Are continental "adakites" derived from thickened or foundered lower crust? Earth and Planetary Science Letters 419, 125–133.

Maniar, P.D., Piccoli, P.M., 1989. Tectonic discrimination of granitoids. Geological Society of America Bulletin 101, 635–643.

Maruyama, S., Isozaki, Y., Kimura, G., Terabayashi, M., 1997. Paleogeographic maps of the Japanese Islands: plate tectonic synthesis from 750 Ma to the present. Island arc 6 (1), 121–142.

Meng, E., Xu, W.L., Yang, D.B., Pei, F.P., Yu, Y., Zhang, X.Z., 2008. Permian volcanisms in eastern and southeastern margins of the Jiamusi Massif, northeastern China, zircon U–Pb chronology, geochemistry and its tectonic implications. Chinese Science Bulletin 53, 1231–1245 (in Chinese with English abstract).

Meng, E., Xu, W.L., Pei, F., Yang, D., Yu, Y., Zhang, X., 2010. Detrital-zircon geochronology of Late Paleozoic sedimentary rocks in eastern Heilongjiang Province, NE China: implications for the tectonic evolution of the eastern segment of the Central Asian Orogenic Belt. Tectonophysics 485, 42–51.

Middlemost, E., 1994. Naming materials in the magma/igneous rock system. Earth-Science Reviews 37, 215–224.

Peacock, S.M., Rusher, T., Thompson, A.B., 1994. Partial melting of subducting oceanic crust. Earth and Planetary Science Letters 121, 224–227.

Pearce, J.A., 1982. Trace Element Characteristics of Lavas From Destructive Plate Boundaries. John Wiley & Sons, Chichester, United Kingdom (GBR), pp. 525–

548.

Peccerillo, A., Taylor, S.R., 1976. Geochemistry of Eocene calc-alkaline volcanic rocks from the Kastamonu area, northern Turkey. Contributions to Mineralogy and Petrology 58, 63–81.

Rapp, R.P., Watson, E.B., 1995. Dehydration melting of metabasalt at 8–32 kbar, implications for continental growth and crust–mantle recycling. Journal of Petrology 36, 891–931.

Rapp, R.P., Watson, E.B., Miller, C.F., 1991. Partial melting of amphibolite/eclogite and the origin of Archaean trondhjemites and tonalites. Precambrian Research 51, 1–25.

Qian, Q., Hermann, J., 2013. Partial melting of lower crust at 10–15 kbar: constraints on adakite and TTG formation. Contributions to Mineralogy and Petrology 165 (6), 1195–1224.

Sengör, A.M.C., Natal'in, B.A., 1996. Paleotectonics of Asia: fragments of a synthesis. In: Yin, A., Harrison, M. (Eds.), The Tectonic Evolution of Asia. Cambridge University Press, Cambridge, pp. 486–640.

Shao, J.A., Tang, K.D., Wang, C.Y., Zang, Q.J., Zhang, Y.P., 1991. The tectonic characteristics and evolution of Nadanhada Terrane. Science in China. Series B 7, 744 (in Chinese).

Shao, J.A., Tang, K.D., Zhan, L.P., 1995. Reconstruction of an ancient continental margin and its implication: new progress on the study of geology of Yanbian region, northeast China. Science in China. Series B 25, 548–555.

Shao, J.A., Li, Y.F., Tang, K.D., 2013. Restoration of the orogenic processes of Zhangguangcailing Range. Acta Petrologica Sinica 29, 2959–2970 (in Chinese with English abstract).

Smithies, R.H., 2000. The Archaean tonalite–trondhjemite–granodiorite (TTG) series is not an analogue of Cenozoic adakite. Earth and Planetary Science Letters 182 (1), 115–125.

Söderlund, U., Patchett, P.J., Vervoort, J.D., Isachsen, C.E., 2004. The 176Lu decay constant determined by Lu–Hf and U–Pb isotope systematics of Precambrian

mafic intrusions. Earth and Planetary Science Letters 219, 311–324.

Song, B., Niu, B.G., Li, J.Y., Xu, W.X., 1994. Isotope geochronology of granitoids in Mudanjiang-Jixi area. Acta Petrologica et Mineralogica 13, 204–213 (in Chinese with English abstract).

Sun, S., McDonough, F., 1989. Chemical and isotopic systematics of oceanic basalts: implication for mantle composition and processes. In: Saunders, A.D., Norry, M.J. (Eds.), Magmatism in the Ocean Basins. Geological Society London: Special Publications 42, pp. 313–345.

Sun, X., Wang, S., Wang, Y., Du, J., Xu, Q., 2010. The structural feature and evolutionary series in the northern segment of Tancheng-Lujiang fault zone. Acta Petrologica Sinica 26, 165–176.

Sun, M.D., Xu, Y.G., Wilde, S., Chen, H.L., Yang, S.F., 2015. The Permian Dongfanghong island-arc gabbro of the Wandashan Orogen, NE China: implications for Paleo-Pacific subduction. Tectonophysics 30, 122–136.

Sorokin, A.A., Kotov, A.B., Kudryashov, N.M., Kovach, V.P., 2016. Early Mesozoic granitoid and rhyolite magmatism of the Bureya Terrane of the Central Asian Orogenic Belt: Age and geodynamic setting. Litho 261, 181–194.

Van Achterbergh, E., Ryan, C.G., Jackson, S.E., Griffin, W.L., 2001. Data reduction software for LA–ICP–MS. Laser–Ablation–ICPMS in the Earth Sciences—Principles and Applications. Mineralogical Association of Canada Short Course Series 29, pp. 239–243.

Wang, X.F., Li, Z.J., Chen, B.L., 2000. Tan-Lu Fault Zone. Geol. Publ. House, Beijing, pp. 122–258 (in Chinese).

Wang, F., Xu, W.L., Xu, Y.G., Gao, F.H., Ge, W.C., 2015a. Late Triassic bimodal igneous rocks in eastern Heilongjiang Province, NE China: implications for the initiation of subduction of the Paleo-Pacific Plate beneath Eurasia. Journal of Asian Earth Sciences 97 (part B), 406–423.

Wang, M., Zhang, J., Zhang, B., Qi, G., 2015b. An Early Paleozoic collisional event along the northern margin of the Central Tianshan Block: constraints from geochemistry and geochronology of granitic rocks. Journal of Asian Earth

Sciences 113, 325–338.

Wei, H.Y., Sun, D.Y., Ye, S.Q., Yang, Y.C., Liu, Z.H., Liu, X.M., Liu, Z.C., 2008. Zircon U–Pb ages and its geological significance of the granitic rocks in the Yichun-Hegang region, southeastern Xiao Hinggan Mountains. Earth Science - Journal of China University of Geosciences 37, 50–59 (in Chinese with English abstract).

Whalen, J.B., Currie, K.L., Chappell, B.W., 1987. A-type granites: geochemical characteristics, discrimination and petrogenesis. Contributions to Mineralogy and Petrology 95, 407–419.

Wilde, S.A., 2015. Final amalgamation of the Central Asian Orogenic Belt in NE China: Paleo-Asian Ocean closure versus Paleo-Pacifiplcate subduction— a review of the evidence. Tectonophysics 662, 345–362.

Wilde, S.A., Zhou, J., 2015. The late Paleozoic to Mesozoic evolution of the eastern margin of the Central Asian Orogenic Belt in China. Journal of Asian Earth Sciences 113, 909–921.

Wilde, S.A., Dorsett-Bain, H., Liu, J.L., 1997. The indentificaiton of a pre-African granulite faces event in Northeastern China, SHRIMP U–Pb zircon dating of the Mashan Group at Liu Mao, Heilongjiang Province, China. Proceedings of the 30th IGC: Precambrian Geology and Metamorphic Petrology 17, pp. 59–74.

Wilde, S.A., Dorsett-Bain, H.L., Lennon, R.G., 1999. Geological setting and controls on the development of graphite, sillimanite and phosphate mineralization within the Jiamusi Massif: an exotic fragment of Gondwanaland located in north-eastern China? Gondwana Research 2 (1), 21–46.

Wilde, S.A., Wu, F.Y., Zhao, G., 2010. The Khanka Block (NE China) and its significance for the evolution of the Central Asian Orogenic Belt and continental accretion. Geological Society, London, Special Publications 338, 117–137.

Wilde, S.A., Zhang, X., Wu, F., 2000. Extension of a newly identified 500Ma metamorphic terrane in North East China: further U–Pb SHRIMP dating of the Mashan Complex, Heilongjiang Province. China.Tectonophysics 328 (1), 115–130.

Wolf, M., London, D., 1994. Apatite dissolution into peraluminous haplogranitic melts: an experimental study of solubilities and mechanisms. Geochimica et Cosmochimica Acta 58, 4127–4145.

Wu, F., Wilde, S.A., Sun, D.Y., 2001. Zircon SHRIMP U–Pb ages of gneissic granites in Jiamusi Massif, northeastern China. Acta Petrologica Sinica 17, 443–452 (in Chinese with English abstract).

Wu, F., Jahn, B., Wilde, S.A., Lo, C., Yu, T., Lin, Q., Ge, W., Sun, D., 2003a. Highly fractionated I-type granites in NE China I: geochronology and petrogenesis. Lithos 66, 241–273.

Wu, F., Jahn, B., Wilde, S.A., Lo, C., Yu, T., Lin, Q., Ge, W., Sun, D., 2003b. Highly fractionated I-type granites in NE China II: isotopic geochemistry and implications for crustal growth in the Phanerozoic. Lithos 67, 191–204.

Wu, F., Yang, J., Lo, C., Wilde, S.A., Sun, D., Jahn, B., 2007. The Heilongjiang Group: a Jurassic accretionary complex in the Jiamusi Massif at the western Pacific margin of northeastern China. Island Arc 16, 156–172.

Wu, F., Sun, D., Ge, W., Zhang, Y., Grant, M.L., Wilde, S.A., Jahn, B., 2011. Geochronology of the Phanerozoic granitoids in northeastern China. Journal of Asian Earth Sciences 41, 1–30.

Xiao, L., Clemens, J.D., 2007. Origin of potassic C-type. adakite magmas: experimental and field constraints. Lithos 95, 399–414.

Xiao, W., Windley, B., Hao, J., Zhai, M., 2003. Accretion leading to collision and the Permian Solonker suture, Inner Mongolia, China: termination of the central Asian orogenic belt. Tectonics 22, 1069–1089.

Xiong, X.L., 2006. Trace element evidence for the growth of early continental crust by melting of rutile-bearing hydrous eclogite. Geology 34, 945–948.

Xu, W.L., Ji, W., Pei, F.P., Meng, E., Yu, Y., Yang, D., Zhang, X., 2009. Triassic volcanism in eastern Heilongjiang and Jilin provinces, NE China: chronology, geochemistry, and tectonic implications. Journal of Asian Earth Sciences 34, 392–402.

Xu, W.L., Pei, F.P., Wang, F., Meng, E., Ji, W., Yang, D., Wang, W., 2013. Spatial–

temporal relationships of Mesozoic volcanic rocks in NE China: constraints on tectonic overprinting and transformations between multiple tectonic regimes. Journal of Asian Earth Sciences 74, 167–193.

Xu, B., Zhao, P., Bao, Q.Z., Zhou, Y.H., Wang, Y.Y., Luo, Z.W., 2014. Preliminary study on the pre-Mesozoic tectonic unit division of the Xing-Meng Orogenic Belt XMOB. Acta Petrologica Sinica 30, 1841–1857 (in Chinese with English abstract).

Yang, H., Zhang, Y.L., Chen, H.J., Ge, W.C., 2012. Zircon U–Pb ages of Khanka Lake granitic complex and its geological implication. Global Geology 31, 621–630 (in Chinese with English abstract).

Yang, H., Ge, W.C., Zhao, G.C., Yu, J.J., Zhang, Y.L., 2015a. Early Permian-Late Triassic granitic magmatism in the Jiamusi–Khanka Massif, eastern segment of the Central Asian Orogenic Belt and its implications. Gondwana Research 27, 1509–1533.

Yang, H., Ge, W.C., Zhao, G.C., Dong, Y., Xu, W.L., Wang, Z.H., Ji, Z., Yu, J.J., 2015b. Late Triassic intrusive complex in the Jidong region, Jiamusi–Khanka Block, NE China: geochemistry, zircon U–Pb ages, Lu–Hf isotopes, and implications for magma mingling and mixing. Lithos 224–225, 143–159.

Yang, H., Ge, W.C., Zhao, G.C., Bi, J.H., Wang, Z.H., Dong, Y., 2015c. The zircon U–Pb ages of the Neoproterozoic granitic gneiss and Pan-African S-type granites and the geological significance. Journal of Jilin University (Earth Science Edition) (S1) (in Chinese).

Yu, J., Wang, F., Xu, W.L., Gao, F., Pei, F., 2012. Early Jurassic mafic magmatism in the Lesser Xing'an–Zhangguangcai Range, NE China, and its tectonic implications: constraints from zircon U–Pb chronology and geochemistry. Lithos 142–143, 256–266.

Zhang, Q., Wang, Y., Li, C.D., Wang, Y.L., Jin, W.J., Jia, X.Q., 2006. Granite classification on the basis of Sr and Yb contents and its implications. Acta Petrologica Sinica 22, 2249–2269 (in Chinese with English abstract).

Zhao, Y.L., Liu, Y.J., Han, G.Q., Wen, Q.B., Li, W., Liang, J.D., 2009. 3D finite

element simulation on sinistral strike-slip of Dunhua-Mishan fault. Global Geology 28, 310–317 (in Chinese with English abstract).

Zhao, P., Chen, Y., Xu, B., Faure, M., Shi, G., Choulet, F., 2013. Did the Paleo-Asian Ocean between North China Block and Mongolia Block exist during the late Paleozoic? First paleomagnetic evidence from central-eastern Inner Mongolia, China. Journal of Geophysical Research - Solid Earth 118, 1873–1894.

Zhou, J.B., Wilde, S.A., Zhang, X., Zhao, G., Zheng, C., Wang, Y., Zhang, X., 2009a. The onset of Pacific margin accretion in NE China: evidence from the Heilongjiang high- pressure metamorphic belt. Tectonophysics 4, 230–246.

Zhou, J.B., Zhang, X., Ma, Z., Liu, L., Jin, W., Zhang, M., Wang, C., Chi, X., 2009b. Tectonic framework and basin evolution in Northeast China. Oil and Gas Geology 30, 530–538 (in Chinese with English Abstract).

Zhou, J.B., Wilde, S.A., Zhao, G., Zhang, X., Zheng, C., Wang, H., Zeng, W., 2010. Pan-African metamorphic and magmatic rocks of the Khanka Massif, NE China: further evidence regarding their affinity. Geological Magazine 147, 737–749.

Zhou, J.B., Han, J., Wilde, S.A., Guo, X.D., Zeng, W.S., Cao, J.L., 2013. A primary study of the Jilin-Heilongjiang high-pressure metamorphic belt: evidence and tectonic implications. Acta Petrologica Sinica 29, 386–398 (in Chinese with English abstract).

Zhou, J.B., Cao, J., Wilde, S.A., Zhao, G., Zhang, J., Wang, B., 2014. Paleo-Pacific subduction accretion: evidence from geochemical and U–Pb zircon dating of the Nadanhada accretionary complex, NE China. Tectonics 33, 2444–2466.

Zhu, D., Mo, X., Wang, L., Zhao, Z., Niu, Y., Zhou, C., Yang, Y., 2009. Petrogenesis of highly fractionated I-type granites in the Chayu area of eastern Gangdese, Tibet: constraints from zircon U–Pb geochronology, geochemistry and Sr-Nd-Hf isotopes. Science in China Series D-Earth Sciences 39, 833–848.

Zonenshain, L.P., Kuzmin, M.I., Natapov, L.M. (Eds.), 1990. Geology of the USSR: a plate tectonic synthesis. American Geophysical Union, Geodynamics Series 21.

Chapter 3 U-Pb Dating and Lu-Hf Isotopes of Detrital Zircons From the Southern Sikhote-Alin Orogenic Belt, Russian Far East: Tectonic Implications for the Early Cretaceous Evolution of the Northwest Pacific Margin

3.0 Abstract

The Sikhote-Alin orogenic belt in Russian Far East is comprised of several N-S trending belts, including the Late Jurassic to Early Cretaceous accretionary prisms and turbidite basin which are now separated by thrusts and strike-slip faults. The origin and collage of the belts have been studied for decades. However, the provenance of the belts remains unclear. Six sandstone samples were collected along a 200 km long east-west traverse across the major belts in the southern Sikhote-Alin for U-Pb dating and Lu-Hf isotope analysis to constrain the provenance and evaluate the evolution of the northwest Pacific margin at this time. The result reveals that the sediments from the main Samarka belt was mainly from the adjacent Bureya-Jiamusi-Khanka Block (BJKB); the eastern Samarka belt and the Zhuravlevka turbidite basin were supplied by detritus from both the North China Craton (NCC) and the BJKB; the Taukha belt was mainly fed by sediments from the NCC; whereas the data from the Sergeevka nappes are insufficient to resolve their provenance. In the Late Jurassic to Early Cretaceous, collision and subduction was important in the initial collage of most belts in Sikhote-Alin. However, merely E-W trending collage cannot explain the increasing importance of the NCC provenance from west to east. It is proposed that the main Samarka belt was located adjacent to the BJKB when deposited, whereas the other belts were farther south to accept the materials from the NCC. Sinistral strike-slip faulting transported the eastern belts northward after their initial collage by thrusting.

3.1 Introduction

The East Asian continent consists of three major cratons which are, from north to south, the Siberia Craton, North China Craton, and South China Craton (Fig. 3.1). Several orogenic belts/suture zones welded the cratons to form the tectonic framework of northeastern Asian continent.

The Central Asian Orogenic Belt (CAOB) is located between the Siberia and North China cratons. This gigantic orogenic belt is composed of many arcs, basins, and continental blocks within the Paleo-Asian Ocean which was closed in the Late Paleozoic (Chen et al., 2016; Rowley et al., 1985; Şengör, 1984; Şengör et al., 1993; Sengör & Natal'In, 1996; Song et al., 2015; Wilde, 2015; Windley et al., 2007; Xiao et al., 2003; Xu et al., 2015; Zhao et al., 2013; Zonenshain, 1973). The eastern segment of the Mongol-Okhotsk Ocean between the CAOB and Siberia Craton did not close until the Early Cretaceous (Donskaya et al., 2013; Khanchuk, Didenko, Popeko, et al., 2015; Kravchinsky et al., 2002). The South China Craton (SCC) collided with and was subducted beneath the North China Craton (NCC) along the Dabie-Sulu Orogen between ca. 240–225 Ma, resulting in high-pressure and ultrahigh-pressure metamorphism (Liu & Liou, 2011; Wu & Zheng, 2013; R. Zhang et al., 2009), whereas the orogenic belt along the East Asian margin belongs to the Pacific tectonic realm or the Pacific orogenic belt, which was active after the collage of the three major cratons (Zhou & Li, 2017). There are numerous Mesozoic to Cenozoic accretionary complexes, arcs, and continental blocks in the Pacific tectonic realm, extending from Taiwan to Kamchatka for ~3,000 km. The Pacific orogenic belt is named as "Nipponides" by Sengör and Natal'In (1996).

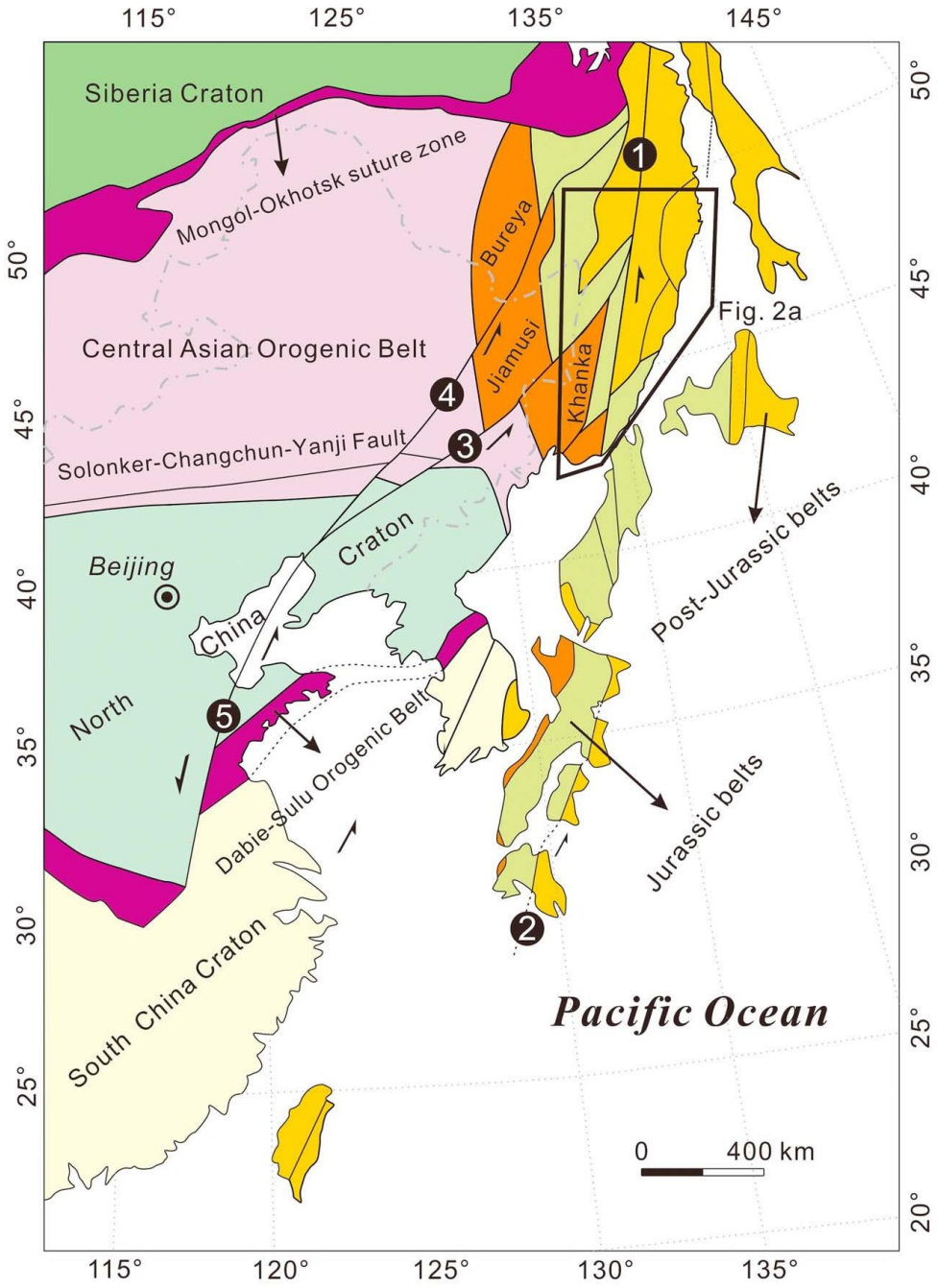

Fig. 3.1. Tectonic framework of East Asia at the end of the Early Cretaceous after termination of northward transport. Modified after Sun, Xu, Wilde, & Chen (2015) and Xu et al. (1987). Japanese Islands are moved back to the Asian continental margin before the opening of the Sea of Japan (Khanchuk, 2001; Kojima, 1989; Taira, 2001). The main strike-slip faults in East Asia are (numbers in black circles): 1. Central Sikhote-Alin Fault; 2. Median Tectonic Line; 3. Dun-Mi Fault; 4. Jia-Yi Fault; and 5. Tan-Lu Fault.

The Sikhote-Alin orogenic belt is part of the Pacific orogenic belt and is located along the eastern margin of the CAOB (Figs. 3.1 and 3.2). Over the past 30 years, many

studies on paleontology, stratigraphy, and paleomagnetism were carried out to reveal the geological history of the NNE trending belts of the Sikhote-Alin orogenic belt and adjacent areas. The lithology and structural features of belts in Sikhote-Alin were compared and associated with the Japanese Islands, especially SW Japan. However, the origin and tectonic evolution of these belts are still very controversial. Based on the "terrane tectonics" theory, many late Mesozoic "tectonostratigraphic terranes" were identified in NE China, Sikhote-Alin, and Japanese Islands (Fig. 3.1; Howell et al., 1985; Khanchuk, 2001; Kojima, 1989; Kojima et al., 2000; Mizutani, 1987; Shao & Tang, 1995). Most boundaries between these terranes/belts are thrusts or strike-slip faults. The terranes were believed to be transported from south to north by the strike-slip faults, and the displacement was estimated from hundreds to thousands of kilometers (Gilder et al., 1999; Khanchuk, 2001, 2016; Lee, 1999; Xu et al., 1987; Xu & Zhu, 1994; Yin & Nie, 1993). However, collisional orgeny was recognized in SW Japan and some other places in the continental margin (Charvet et al., 1985; Faure et al., 1986; Natal'in, 1993; Otsuki, 1992). The collision of buoyant blocks (mature arcs or continental blocks) onto the hinterland is considered to be very important to shape the tectonics of the East Asia, such as the large thrust sheet/nappe tectonics. There are some other studies suggesting that the Pacific tectonic realm is a typical "accretionary orogen," especially for the Japanese Islands. In their models, Japanese Islands were basically an accretionary complex built in long-term subduction of the Paleo-Pacific Ocean. High-pressure metamorphism and ridge subduction were important for the deformation and magmatism in the SW Japan according to their models (Isozaki et al., 2010; Maruyama, 1997).

In Sikhote-Alin, detailed research has been implemented on structural geology, micropaleontology, and magmatism (Golozoubov et al., 1999; Jahn et al., 2015; Khanchuk, 2001; Khanchuk et al., 1996; Kemkin & Kemkina, 2000; Kojima, 1989; Kojima et al., 2008; Tang et al., 2016). However, the provenance issue, which is very significant to understand the origin and tectonic history of the belts, remains unclear. U-Pb dating and Lu-Hf isotopes of detrital zircons are an effective means for

determining the provenance of sediments (Bingen et al., 2001; Cawood et al., 2012; Fernández et al., 2010; Fernandez-Suarez et al., 2002; Gehrels, 2014; Grasse et al., 2001; Gutiérrez-Alonso et al., 2003; Wyld & Wright, 2001). Here we present U-Pb dating and Lu-Hf isotopic data for detrital zircons from the southern Sikhote-Alin orogenic belt in order to ascertain their maximum depositional age, their provenance, and to better understand the tectonic processes operating along the eastern Asian continental margin during the Late Jurassic to Early Cretaceous.

3.2 Geological Outline of the Southern Sikhote-Alin Orogenic Belt

The southern Sikhote-Alin orogenic belt is located to the east of the Bureya-Jiamusi-Khanka block (BJKB), which has a Neoproterozoic basement ca. 850–960 Ma in age and records late Pan-African granulite-facies metamorphism at ~500 Ma (Fig. 3.1; Wilde et al., 1997; Wilde et al., 2003; Yang et al., 2017). After Jurassic, the BJKB became the easternmost part of the CAOB. However, the location of the BJKB prior to the Jurassic is controversial, with some authors considering it to be part of the CAOB that underwent rifting in the Triassic (Zhou et al., 2009), whereas others have considered it is an exotic block that was accreted to the CAOB in the Jurassic (Wu, Han, et al., 2007), possibly being derived from Gondwana (Wilde et al., 1999) or Siberia (Zhou et al., 2009). New detrital zircon data show that the Jiamusi Block may have affinity of the Tarim Craton (Luan et al., 2017). These various hypotheses have been invoked to explain the origin of the Heilongjiang Complex, developed along the western margin of the Jiamusi Block, which is an accretionary complex that welded the Jiamusi Block to the Songliao Block of the CAOB in the Early Jurassic (Wu, Han, et al., 2007; Zhou et al., 2009). Significantly, terrigenous rocks in the Sikhote-Alin orogenic belt along the eastern margin of the BJKB were mainly deposited after the Early Jurassic. The N-S trending belts/zones investigated in this study are, from west to east, the Samarka accretionary complex (Jurassic), the Zhuravlevka turbidite basin (Early Cretaceous), and the Taukha accretionary complex (Early Cretaceous). In addition, the Sergeevka nappes are thrust over the southern Samarka accretionary

complex. The northwestern boundary of the Taukha belt and the boundary between the Kema and Zhuravlevka belts are likely thrusts. However, the western boundary of the Taukha belt is sinistral strike-slip fault. Likewise, the Central Sikhote-Alin Fault, the boundary between the Samarka belt and the Zhuravlevka basin, is a famous sinistral strike-slip fault in the Russian Far East (Fig. 3.2a and 3.2b).

The oldest units in the Sikhote-Alin are the Sergeevka nappes (SR on Fig. 3.2a), which include several separate early Paleozoic continental fragments that were thrust over the Samarka belt (SM on Fig. 3.2a). These nappes are also known as the Sergeevka Terrane in the Russian literatures (Khanchuk et al., 2016), although it is inappropriate to refer to these as a terrane because they are present in several areas and do not form a coherent geological unit (Fig. 3.2a). The Sergeevka nappes contain Early Ordovician granitoids with a biotite Ar-Ar age of 491 Ma (Fig. 3.2a; Khanchuk et al., 1996). The fragments mainly comprise gabbro, diorite, migmatite, and amphibolite and are themselves overlain by Jurassic conglomerate and sandstone (Fig. 3.3, 3.4, and 3.5c and 3.5d). Some blueschist-facies metamorphic rocks are present between the Jurassic sedimentary rocks and Early Paleozoic continental fragments, representing a pre-Cretaceous orogeny (Khanchuk, 2006; Khanchuk et al., 2016).

The Samarka belt is a Late Jurassic accretionary complex (SM on Fig. 3.2a) that consists of several deformed tectonic slices or thrust sheets (Fig. 3. 4). The boundaries between slices are reverse faults/thrusts. In each slice, the depositional sequence changes from chert and siltstone upward into sandstone. At the top of some slices, sedimentary rocks were faulted and folded into mélange that is characterized by strong deformation and contains blocks of various sizes (Fig. 3.3 and 3.5a and 3.5b; Kemkin, 2008). The chert varies in age from Late Permian to Early Jurassic and represents pelagic sediments. In contrast, the clastic rocks are mainly terrigenous and Late Jurassic in age (Kemkin et al., 2006).

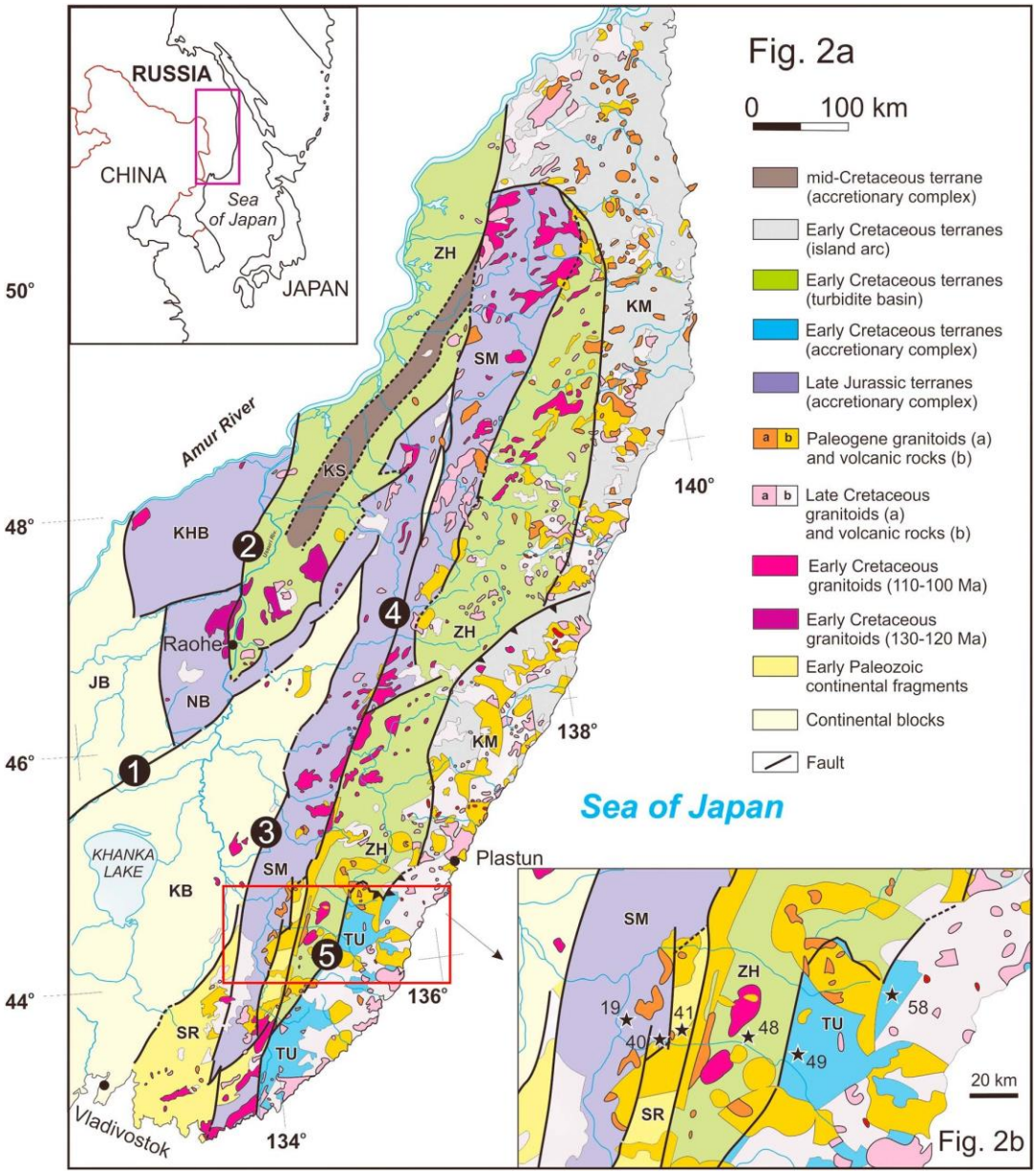

Fig. 3.2. (a) Geological map of the southern Sikhote-Alin. Modified after Grebennikov et al. (2016). Abbreviations: JB = Jiamusi Block; KB = Khanka Block; SR = Sergeevka nappes; KHB = Khabarovsk belt; NB = Nadanhada-Bikin belt; SM = Samarka belt; KS: Kisilevsky belt; ZH = Zhuravlevka turbidite basin; TU = Taukha accretionary complex; KM = Kema arc. Faults (numbers in black circles): (1) Dun-Mi Fault, (2) Koukansky Fault, (3) Arsen'evsky Fault, (4) Central Sikhote-Alin Fault, and (5) Fourmanovsky Fault. (b) Sample locations in the southern Sikhote-Alin belts. Numbers are abbreviated from samples SAL-19, SAL-40, SAL-41, SAL-48, SAL-49, and SAL-58.

The mélange contains blocks of limestone, chert, and basalt within a siltstone matrix. Another feature of the Samarka accretionary complex is that it contains fragments of

Paleozoic ophiolites, including peridotite, gabbro, and basalt pillows, interpreted as components from an oceanic plateau but now outcropped as nappe/klippe in the Samarka accretionary complex (Khanchuk & Vysotskiy, 2016). The age of ophiolite was estimated as Late Devonian to Early Carboniferous based on the conodont and foraminifera research in the sedimentary rocks contacting the pillow basalts (Khanchuk & Vysotskiy, 2016).

To the east, the Zhuravlevka turbidite basin (ZH on Fig. 3.2a) is truncated by the Central Sikhote-Alin Fault (Fig. 3.2a). The basin was mainly filled by turbidites showing well-developed Bouma sequences (Fig. 3.5e), with some chert and conglomerates cropping out locally. Faults accompanied by vertically dipping strata are present near the boundaries of the basin, whereas deformation in the interior is represented by broad folds, less steeply inclined strata and several NNE trending strike-slip faults and thrusts (Fig. 3.4). Heavy mineral studies and paleontological evidence suggest that depositional age spans the whole of the Early Cretaceous (from the late Berriasian to late Albian) and that these sediments were mainly derived from mature continental crust (Malinovsky & Golozubov, 2011).

Along the margin of the Sea of Japan, the Taukha belt (TU on Fig. 3.2a) is a Late Jurassic to Early Cretaceous accretionary complex lying to the east of the Zhuravlevka turbidite basin and to the south of the Kema belt, an Early Cretaceous island arc (KM on Fig. 3.2a). The boundary between the Taukha belt and the Zhuravlevka basin is mainly sinistral strike slip with thrust characteristic in the north segment (Fig. 3.4; Golozoubov, 2006; Kemkin & Kemkina, 2000). The rock types in the Taukha accretionary complex are similar to those in the Samarka accretionary complex although the age is younger.

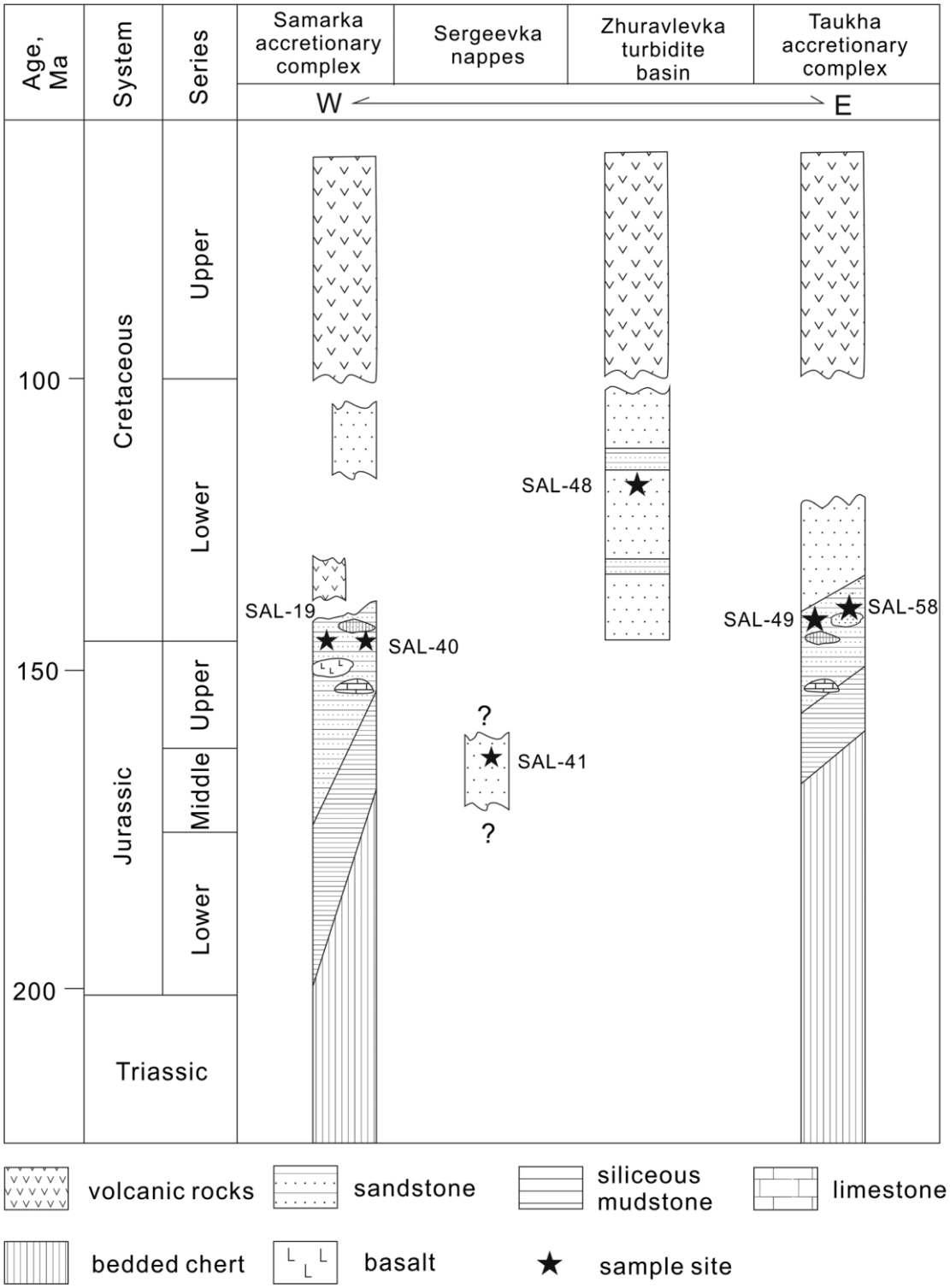

Fig. 3.3. Tectonostratigraphic column of the southern Sikhote-Alin belts, modified after Kemkin (2008), Kemkin and Kemkina (2015), Khanchuk et al. (2016), and Malinovsky and Golozubov (2011). Only part of the Sergeevka nappes is shown on this figure because the stratigraphic information is incomplete.

For example, in some areas where the original stratigraphic sequence has survived, the chert that has been dated from Late Triassic to Late Jurassic in age, changes upward to chert-mudstone, siltstone, turbidite, and olistostromes, which are latest Jurassic to Early Cretaceous in age (Fig. 3.3 and 3.5f; Kemkin & Kemkina, 2000). This chert-siltstone-sandstone sequence is considered to represent oceanic plate stratigraphy (Berger & Winterer, 1974; Isozaki et al., 1990). Some mélange zones crop out where the siltstone and sandstone are strongly deformed by folds and faults in the northern Taukha belt. Jurassic basalts overlain by Late Jurassic chert are found locally in the northwest Taukha belt (Kemkin & Kemkina, 2000; Kemkin et al., 2016). Radiolarian research suggests that the limestone and chert blocks in the mélange could be as old as Late Devonian or Permian (Fig. 3.2b; Kemkin & Kemkina, 2000, 2015).

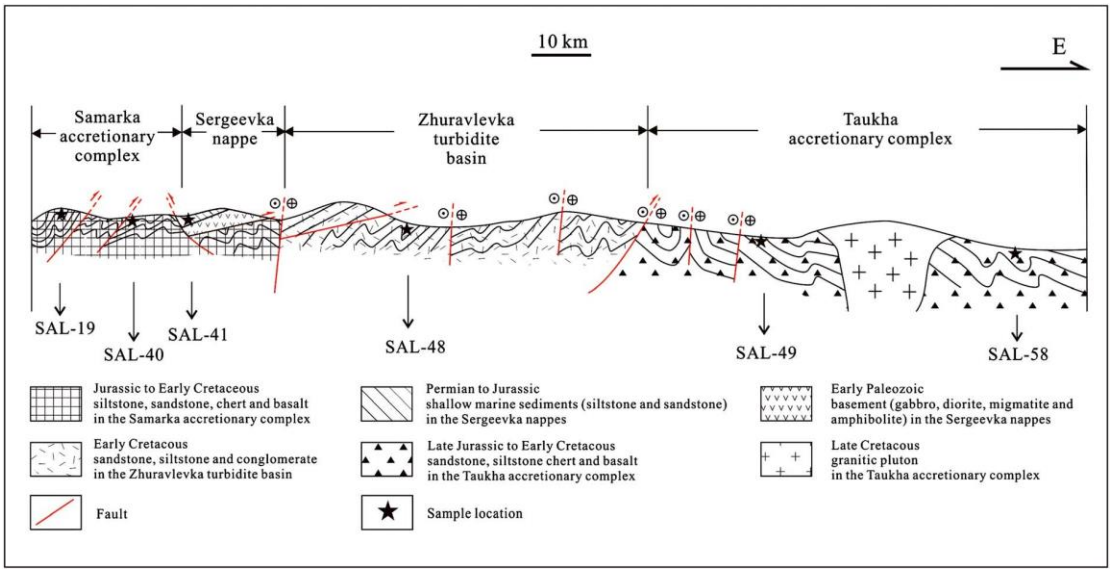

Fig. 3.4. Cross section along the sampling traverse in the southern Sikhote-Alin orogenic belt.

The Jurassic to Cretaceous belts in the southern Sikhote-Alin are separated by a series of faults which are, from west to east, the Arsen'evsky Fault, the Central Sikhote-Alin Fault, and the Fourmanovsky Fault (Faults 3, 4, and 5, respectively, on Fig. 3.2a). The Central Sikhote-Alin Fault is a sinistral strike-slip fault which is traceable for over 1,000 km in length (Utkin, 2013), and the offset on this fault may be greater than 200 km, based on the dislocated Samarka and Zhuravlevka belts (Fig. 3.1 and 3.2a; Utkin, 1993). Deep seismic sounding shows that the Arsen'evsky and Central Sikhote-Alin

faults cut the Moho at a depth of ~40 km (Argentov et al., 1976). The Fourmanovsky Fault is characterized by sinistral strike slip in the western part with thrusting in the north part (Fig. 3.2).

Fig. 3.5. Outcrop photographs of the southern Sikhote-Alin belts. (a) Foliated siltstone in the Samarka accretionary complex, (b) folded chert in the Samarka accretionary complex. Red curves mark the folds, (c) conglomerate in the Sergeevka nappes, including clasts of gabbro, sandstone, chert and quartzite, (d) cumulate gabbro in the Sergeevka nappes, (e) turbidite in the Zhuravlevka turbidite basin; (f) mélange in the Taukha accretionary complex, involving different-size sandstone lenses in foliated siltstone.

During the Early Cretaceous to Paleogene, felsic magmatic rocks were emplaced

extensively into the belts of the southern Sikhote-Alin (Fig. 3.2a). The earliest granitoids are 131 to 124 Ma in age and are rare, only being found in the Nadanhada-Bikin accretionary complex and the adjacent part of the Zhuravlevka turbidite basin (Fig. 3.2a; Cheng et al., 2006; Grebennikov et al., 2016; Jahn et al., 2015). However, magmatism was interrupted between 130 and 110 Ma in the other belts, after which it was reactivated by rapid oblique Paleo-Pacific subduction (the Izanagi Plate) and became quasi-continuous from 110 Ma to 56 Ma (Jahn et al., 2015; Kruk et al., 2014; Tang et al., 2016).

The correlation between the Jurassic to Cretaceous belts in NE China, Sikhote-Alin, and SW Japan has been discussed for decades. Based on paleontological and paleomagnetic data, Kojima (1989) proposed that the Late Jurassic Nadanhada-Bikin accretionary complex in NE China and Sikhote-Alin are the northern extension of the Tanba-Mino belt in SW Japan (Fig. 3.1). Khanchuk (2001) also connected the arc magmatism and accretionary complexes in the Sikhote-Alin with equivalents in SW Japan. The correlation between the Taukha belt and the Northern Kitakami belt was supported by the paleontological research and stratigraphic characteristic (Kojima et al., 2008).

3.3 Sample Locations and Petrology

Six sandstone samples were collected along a 200 km traverse, extending from west to east in the southern Sikhote-Alin orogenic belt, in order to evaluate any changes in provenance within the belts, especially across the Central Sikhote-Alin Fault (Fig. 3.2b, 3.3, and 3.4).

Sample SAL-19 was collected in the central part of the Samarka belt. It is a sandstone within a fine- to medium-grained Bouma sequence. However, the chert-siltstone-sandstone stratigraphic sequence is disrupted because of faults and folds (Fig. 3.5a). Some basalt blocks are present near the contact between the sandstone and the underlying folded and thinly bedded chert. Sample SAL-19 is a dark grey, fine-grained

sandstone that is poorly sorted with angular quartz grains that are 15–30 μm in length (Fig. 3.6a) and composed mainly of quartz (25%) and plagioclase (30%), with minor muscovite (1%). The space between the grains is filled by lithic fragments (45%), which are mainly felsic volcanic fragments.

Sample SAL-40 was collected from the eastern Samarka belt, separated from sample SAL-19 by an unnamed fault (Fig. 3.2b). This fault cuts Paleogene granitoids, indicating movement after granitoid emplacement, although the precise timing of movement is unknown. Sample SAL-40 is a dark grey, coarse-grained sandstone that is poorly sorted or rounded (Fig. 3.6b). The main minerals are quartz (45%), plagioclase (25%), K-feldspar (10%), sericite (3%), and clay minerals (2%), with felsic lithic fragments (15%). The clastic grains are mainly 70–100 μm in length. Subgrained quartz and local quartz veins are observed in thin section (Fig. 3.6c). Adjacent to these areas, K-feldspar and quartz are weakly oriented and reduced in grain size (15–40 μm) due to granulation (Fig. 3.6c).

Sample SAL-41 was collected from a Jurassic sandstone interbedded with conglomerate from one of the Sergeevka nappes. The conglomerate contains fragments of gabbro, chert, sandstone, and quartzite (Fig. 3.5c). Because the sample is small in size and was used to obtain zircons as a whole, no thin section was made of this sample. However, based on the outcrop, it is a grey, medium- to coarse-grained sandstone that is poorly sorted or rounded. Some small angular fragments of chert and gabbro, 0.5–2 cm in diameter, were observed.

Sample SAL-48 was obtained from the Zhuravlevka turbidite basin, located 50 km to the east of sample SAL-41. Sample SAL-48 is separated from samples SAL-40 and SAL-41 by the Central Sikhote-Alin Fault (Fault 4 on Fig. 3.2a). The outcrop consists of turbidite with interbedded mudstone and siltstone defining a Bouma sequence. Grains in sample SAL-41 are angular and poorly sorted and 30–150 μm in length (Fig. 3.6d). It mainly comprises quartz (60%), plagioclase (25%), opaque minerals (10%),

and lithic fragments (5%).

Two samples (SAL-49 and SAL-58) were collected from the Taukha accretionary belt (Fig. 3.2b). The former was located 40 km to the east of sample SAL-48 and the latter 110 km northeast of SAL-48. Both samples from the Taukha accretionary complex are separated from sample SAL-48 (in the Zhuravlevka basin) by the Fourmanovsky Fault (Fault 5 on Fig. 3.2a). Sample SAL-49 is a coarse sandstone that contains minor subangular chert fragments (0.5–3 cm), and it is moderately well sorted and with poorly rounded grains that range in length from 100–200 μm. The main minerals are quartz (55%), K-feldspar (35%), and muscovite (5%), with lithic fragments (5%; Fig. 3.6e). Sample SAL-58 was collected from a mélange that occurs in the northern Taukha belt, 60 km to the southwest of Plastun (Fig. 3.2a). There are numerous sandstone blocks within a matrix of siltstone (Fig. 3.5f), with the size of blocks varying from 5 to 150 cm in diameter. Sample SAL-58 shows no sign of deformation and the mineralogy consists of quartz (70%), K-feldspar (15%), and muscovite (5%), with lithic fragments (10%). The grains are poorly sorted with lengths from 20 to 150 μm (Fig. 3.6f).

Overall, in the southern Sikhote-Alin orogenic belt, sandstones are always interbedded with mudstones and underlain by folded and/or faulted chert, showing a change from a typical pelagic marine sequence to terrigenous sedimentation. Some sandstones include angular fragments of chert and/or mudstone and show graded bedding (including Bouma sequences), suggesting strong hydrodynamic conditions related to turbidity currents. The quartz and feldspar grains are all poorly sorted and angular, with lithic fragments and feldspar collectively greater than quartz in some units. All these features are typical of sediments deposited on a continental slope and trench, resulting from erosion of an adjacent continental margin or an arc, with deposition by turbidity currents after short-distance transport.

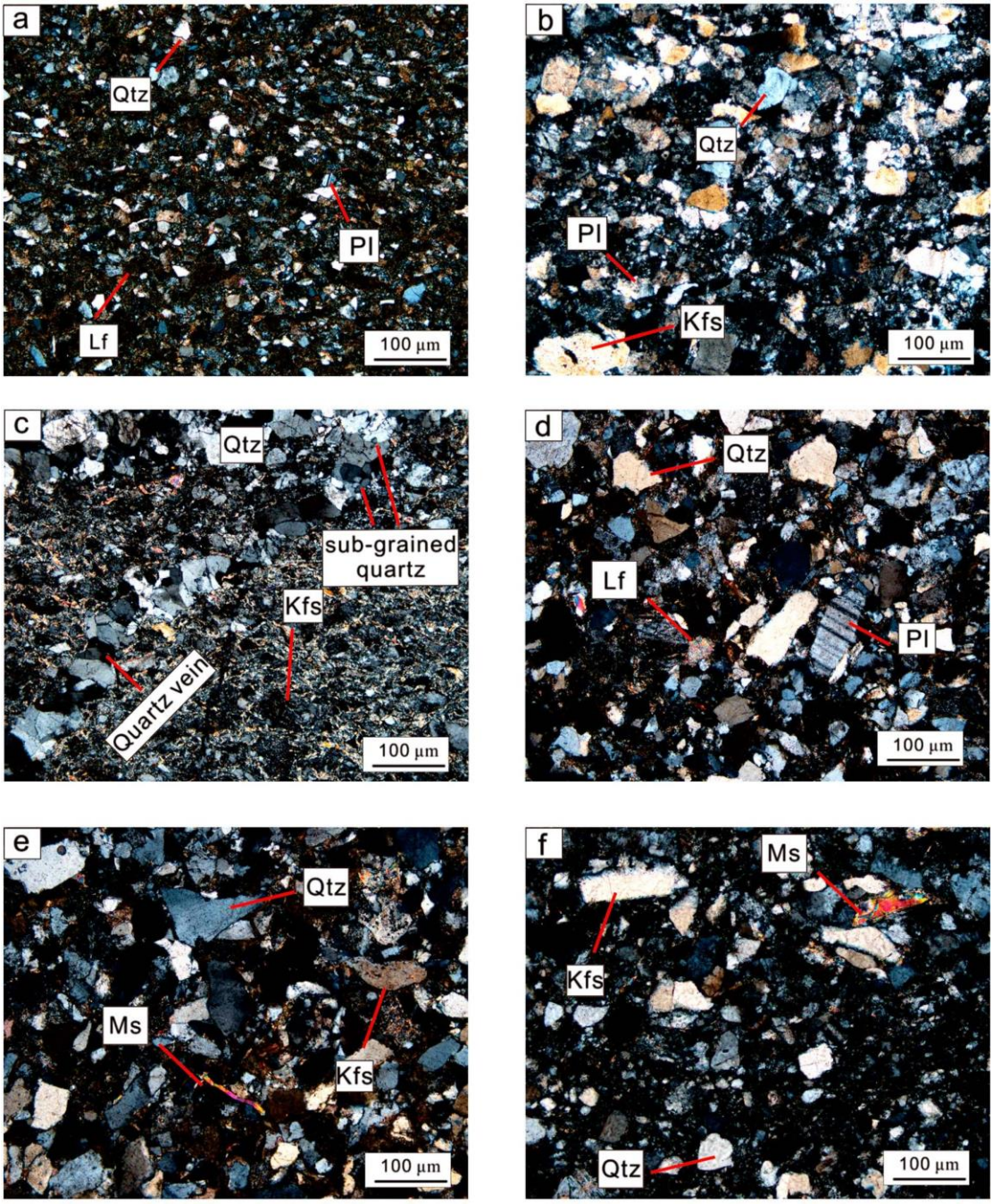

Fig. 3.6. Photomicrographs of sandstone samples. (a) Sample SAL-19, (b) sample SAL-40, (c) deformed zone of sample SAL-40, in which weak deformation and sub-grained quartz can be observed, (d) sample SAL-48, (e) sample SAL-49; and (f) sample SAL-58. Abbreviation: Qtz = quartz; Pl = plagioclase; Kfs = K-feldspar; Lf = lithic fragments; Ms = muscovite.

3.4 Methodology

Zircons were separated from the six samples by standard heavy-liquid and magnetic

techniques and handpicked under a binocular microscope. About 200 zircon grains from each sample were embedded in a 25 mm epoxy resin disk and polished to approximately half of the grain's thickness. Cathodoluminescence (CL) imaging was obtained using a Quanta 200 FEG Scanning Electron Microscope at the Key Laboratory of Orogenic Belts and Crustal Evolution of the Education Ministry of China, Peking University in order to observe the internal structure of the zircons.

Zircon U-Pb isotopic analyses were carried out using laser ablation inductively coupled plasma mass spectrometry (LA-ICP-MS) at the Key Laboratory of Continental Collision and Plateau Uplift, Chinese Academy of Sciences, Beijing. Laser sampling was performed using a NewWave and ATL 193 nm ArF excimer laser ablation system (UP193FX), with short pulses (<4 ns) and a spot size of 35 μm. Element and isotope ion-signal intensities were acquired by an Agilent 7500a ICP-MS. Both high-purity helium and argon were used as carrier gases, which were mixed via a T-connector before entering the MS. Helium was adjusted by a mass flow controller installed in the laser system, whereas argon was controlled by the ICP-MS. Helium and argon carrier gas flows were optimized by ablating National Institute of Standards and Technology (NIST) Standard Reference Material (SRM) 612 reference glass to obtain maximum signal intensity for 238U and 208Pb, minimum oxide, and double-charge interference, minimum gas blank, and most stable signal intensity. The analytical procedure was 15–20 s gas blank acquisition (warm up), 40 s data acquisition from the sample aerosol (ablation), and 45–55 s washout time in the spot sampling mode and TRF data acquisition mode of the Agilent ChemStation. Zircon 91500 was used as an external standard for the matrix-matched calibration. NIST SRM 612 reference glass was analyzed as an external standard for the trace element content calibration. The 91500 zircon and NIST SRM 612 standards were analyzed after each 5 to 10 analyses. Off-line isotope ratios and trace element concentrations were calculated using the GLITTER_Ver4.0 program (Van Achterbergh et al., 2001); U-Pb concordia diagrams, weighted mean calculations, and probability density plots of U-Pb ages were made using Isoplot/Ex_ver 3 (Ludwig, 2001).

The zircon Lu-Hf isotopes were analyzed at the State Key Laboratory of Geological Processes and Mineral Resources of the China University of Geosciences, Wuhan. Based on the in-house instrumentation and data acquisition protocols (Hu et al., 2012), the analyses were conducted with a beam of 44 μm, using the ICPMSDataCal program to conduct the off-line signal selection and integration and mass bias calibrations (Liu et al., 2010). The Lu-Hf isotopes of zircons were obtained from the same LA-LCP-MS sites or adjacent domains of same CL structure when insufficient material was available. Data were acquired using a Neptune MC-ICP-MS (Thermo Fisher Scientific, Germany) in combination with a Geolas 2005 excimer ArF laser ablation system (Lambda Physik, Göttingen, Germany). In order to correct for isobaric interferences, the mass bias of Hf (βHf) and Yb (βYb) were calculated using 179Hf/177Hf = 0.7325 and 173Yb/171Yb = 1.13017, which were normalized by an exponential correction for mass bias (Segal et al., 2003). By measuring the interference-free 173Yb isotope and using 176Yb/173Yb = 0.79381, the interference of 176Yb on 176Hf was corrected (Segal et al., 2003). Similarly, the interference of 176Lu on 176Hf was corrected by measuring the interference-free 175Lu and using 176Lu/175Lu = 0.02656 (Blichert-Toft & Albarède, 1997). Because of the similarity between Yb and Lu, the mass bias of Yb (βYb) was used to calculate the mass fractionation of Lu (Hu et al., 2012). Other parameters used to calculate the isotopes were as follows: 176Hf/177Hf ratios were 0.282793 (chondrite) and 0.28325 (depleted mantle), 176Lu/177Hf ratios were 0.0338 (chondrite) and 0.0384 (depleted mantle), the radioactive decay coefficient of 176Lu to 176Hf was 1.867 × 10-11 a-1, and the 176Lu/177Hf ratio of bulk continental crust was 0.015 (Griffin et al., 2004; Iizuka et al., 2015; Söderlund et al., 2004).

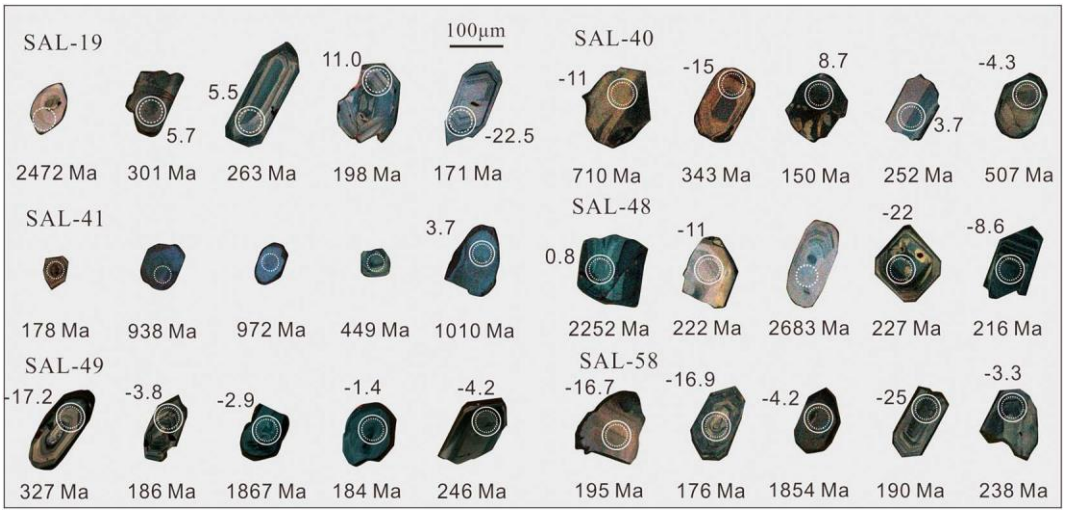

Fig. 3.7. Representative CL images of detrital zircons. Dashed and solid circles represent analytical spots of U-Pb and Lu-Hf isotopes, respectively. The numbers beside the circles are U-Pb ages and εHf(t) values.

3.5 Results

Representative CL images of the analyzed detrital zircons are shown in Fig. 3.7. The results of U-Pb dating and Lu-Hf isotopic analysis are shown in Fig. 3.8 and 3.9, respectively, with detailed analytical data presented in Tables 1 and 2, respectively. The ages of young zircons (<1,000 Ma) are shown by 206Pb/238U ages in Fig. 3.8 and 9, whereas the old ones (>1,000 Ma) use 207Pb/206Pb ages. Zircon U-Pb ages with high discordance (>10%) were excluded from the calculations.

When the age$^{206Pb/238U}$ of zircon is younger than 1,000 Ma,

$$\text{Discordance} = (\text{Age}^{206Pb/238U}/\text{Age}^{207Pb/235U} - 1) \times 100\%;$$

When the age$^{206Pb/238U}$ of zircon is older than 1,000 Ma,

$$\text{Discordance} = (\text{Age}^{207Pb/235U}/\text{Age}^{207Pb/Pb206} - 1) \times 100\%;$$

Discordance is expressed by absolute value.

Because of their sizes (<50 μm), not all the zircons could be analysed for Lu-Hf isotopes. Most detrital zircons are from felsic magmatic rocks which were melted from crust. Thus, εHf(t) and TDM2 are used here to evaluate the characteristics of the Lu-Hf isotopes, representing the isotopic feature of the crust in which the zircons were

crystallized.

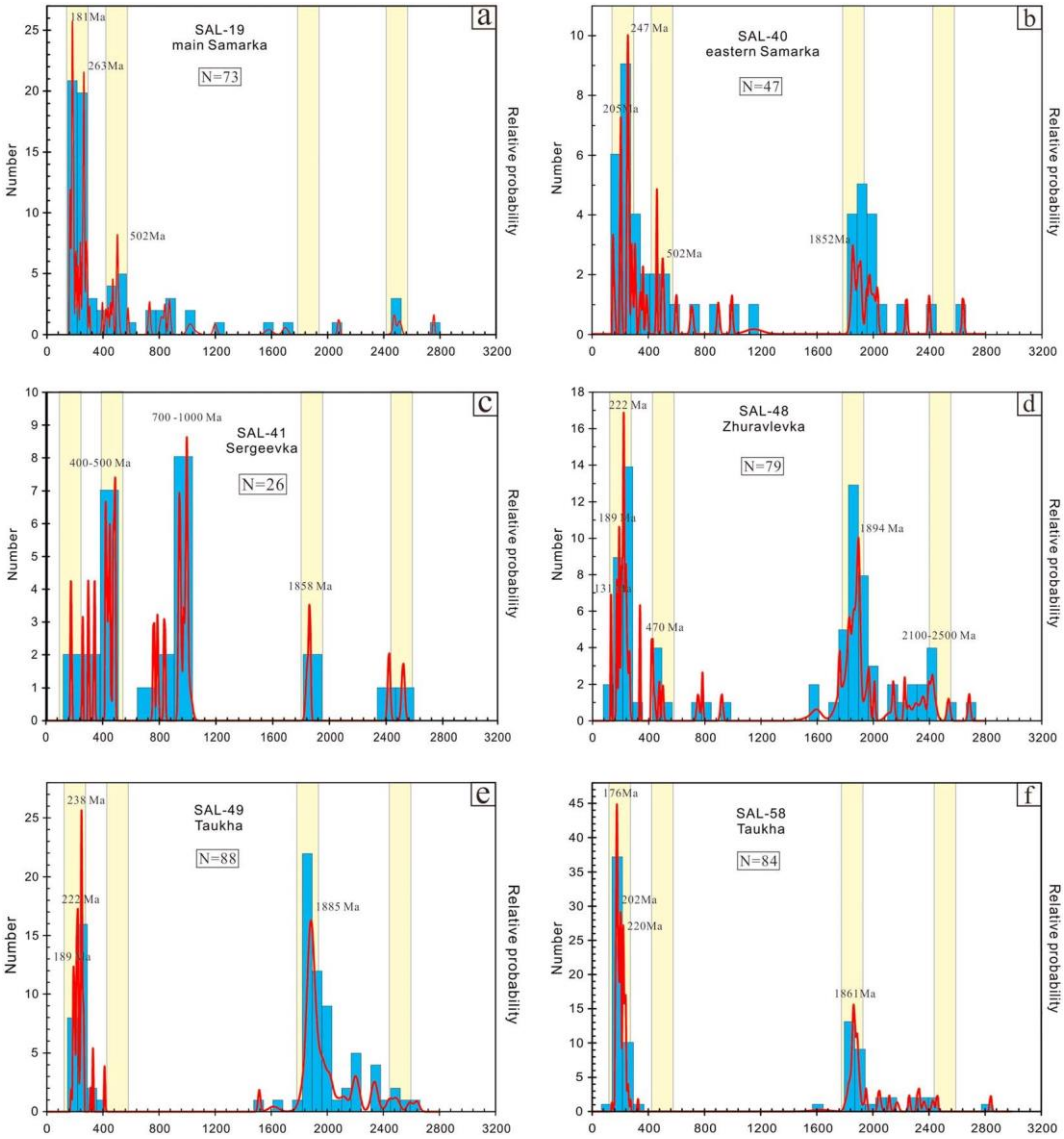

Fig. 3.8. Age spectra of detrital zircons. The spectra diagram uses 206Pb/238U ages for young zircons (<1,000 Ma) and 207Pb/206Pb ages for old ones (>1,000 Ma). Zircons with high discordance (>10%) are excluded. (a) Sample SAL-19 from the central Samarka accretionary complex, (b) sample SAL-40 from the eastern Samarka accretionary complex, (c) sample SAL-41 from the Sergeevka nappes, (d) sample SAL-48 from the Zhuravlevka turbidite basin, (e) sample SAL-49 from the Taukha accretionary complex, and (f) sample SAL-58 from the Taukha accretionary complex. Four common age groups are marked by yellow bands, namely, 170–260 Ma, 450–550 Ma, 1.6–1.9 Ga, and 2.3–2.6 Ga. The late Pan-African age of 450–550 Ma is important in the BJKB, whereas the ~1.8 Ga and 2.5 Ga ages are dominant in the NCC.

3.5.1 The Samarka Accretionary Complex

3.5.1.2 Sample SAL-19

Most zircons are 30–200 μm in length and show magmatic oscillatory zones (Fig. 3.7), although a few zircons have core-rim structures. Seventy-three concordant ages were obtained from 95 analyses and define six age groups (Fig. 3.8a): 162–227 Ma (33%), 236–268 Ma (19%), 275–434 Ma (12%), 452–579 Ma, 729–1,197 Ma (12%), and 1,580–2,756 Ma (11%). Three peak ages are shown in the spectrum, 181 Ma, 263 Ma, and 502 Ma (Fig. 3.8a). The Th/U ratios of 72 of the concordant analyses vary from 0.19 to 2.38, indicating a magmatic origin, and only one zircon with an age of 503 Ma has a Th/U ratio of 0.07, possibly indicating a metamorphic origin. Zircons from the Early Permian to Early Jurassic account for 59% of the analyses. Thirty zircons were analyzed for Lu-Hf isotopes and the εHf(t) values of 23 of these vary between -3 and 11 (Fig. 3.9a), with TDM2 model ages from 494 to 1,456 Ma. However, four zircons with ages of 162–180 Ma show quite different εHf(t), ranging from -23 to -6, with TDM2 model ages of 3.8–2.1 Ga.

3.5.1.2 Sample SAL-40

Zircons from sample SAL-40 range from 40 to 150 μm in length and have a variety of structures and crystal forms. Some zircons show magmatic oscillatory zones, whereas some are sector zoned and others are only weakly zoned (Fig.3.7). Sixty-two zircons were analyzed, and 47 concordant ages were obtained with the Th/U ratios ranging from 0.1 to 7.1. In this sample, 36% of zircon ages range from 1.8 to 2.6 Ga with a peak age at 1.85 Ga, forming a major age group. There are five other age populations defined by Phanerozoic and Neoproterozoic zircons (Fig. 3.8b): 150–210 Ma (15%), 246–285 Ma (19%), 302–389 Ma (11%), 458–507 Ma (9%), and 599–1,151 Ma (11%). Two age peaks are defined by the Phanerozoic zircons, namely, 205 Ma and 247 Ma. The εHf(t) values of the Phanerozoic zircons (507–150 Ma) are similar to those in sample SAL-19, mostly ranging from -0.7 to 10.7 (Fig. 3.9b), with TDM2 model ages from 1,211 to 508 Ma. One zircon with an age of 898 Ma recorded the most positive εHf(t) value of 11.2. The εHf(t) values of 2.4–1.9 Ga zircons range from -2 to 1.6, with

TDM2 model ages from 2.8 to 2.2 Ga.

3.5.2 The Sergeevka Nappes

Approximately 100 zircons were obtained from sample SAL-41, and most were too small to analyze (15–40 μm in diameter). Suitable zircons ranged from 40 to 100 μm in diameter and show weak or no zoning (Fig. 3.7), with Th/U ratios of 0.30–1.96. There were 26 concordant U-Pb ages from 49 analyses, with 11 Neoproterozoic zircons (761–1,010 Ma) accounting for 42% of the total, much higher than in other samples (Fig. 3.8c). The late Pan-African and Paleozoic zircons are the second most important population (seven zircons with ages from 301 to 489 Ma), whereas only one Mesozoic zircon was obtained with an age of 178 Ma. Only six zircons were large enough to be analyzed for Lu-Hf isotopes. Two Pan-African zircons show positive εHf(t) values of 0.5 and 10.5 (Fig. 3.9c); two other zircons with ages of ~1.0 Ga have εHf(t) values of -1.3 and 3.7, whereas those of two zircons ~1.8 Ga in age are -0.1 and 1.0 (Fig. 3.9c).

3.5.3 The Zhuravlevka Turbidite Basin

Zircons from sample SAL-48 can be divided into two groups. One group is characterized by oscillatory zones and the grains are 80–200 μm in length, whereas the other group has weak oscillatory zoning, sector zoning, or no zoning at all and these grains have lengths from 80 to 150 μm (Fig. 3.7). Seventy-nine concordant zircon U-Pb ages were recorded from 99 analyses. The Th/U ratios mostly range from 0.05 to 1.92, although two zircons have Th/U ratios of 0.04 and 0.05 possibly indicating a metamorphic origin. The age populations (Fig. 3.8d) are 129–132 Ma (3%), 175–209 Ma (11%), 216–228 Ma (10%), 240–267 Ma (6%), 337–502 Ma (8%), 752–920 Ma (4%), 1.6–2.1 Ga (43%), and 2.2–2.7 Ga (14%). There are five age peaks in the spectrum: 131 Ma, 189 Ma, 222 Ma, 470 Ma, and 1.9 Ga. Two zircons with ages of 129 and 132 Ma are the youngest recorded in this study. The Hf isotopic features are distinct from the previous samples, with most Phanerozoic zircons (72%) having

negative εHf(t) values (-23.5 to -1.3), with TDM2 model ages from 2.4 to 1.3 Ga, whereas only six zircons (21%) record positive values (1.6 to 9.4), with TDM2 model ages from 636 to 1,029 Ma.

3.5.4 The Taukha Accretionary Complex

3.5.4.1 Sample SAL-49

Zircons from sample SAL-49 are 50 to 150 μm in length. Of 98 analyses, 88 were concordant. The Phanerozoic zircons show weak oscillatory zones with small inclusions of opaque material, whereas the Precambrian ones are weakly zoned, sector zoned, or no zoning at all (Fig. 3.7). The Th/U ratios range from 0.22 to 1.55. About 70% of the zircons are in the range 1.5–2.6 Ga with a peak age at 1.9 Ga (Fig. 3.8e). The other 30% range in age from 414 Ma to 176 Ma, with three age ranges, 176–226 Ma (17%), 239–262 Ma (10%), and 309–414 Ma (3%). Five zircons with ages ranging from 1.5 to 2.6 Ga were selected for Lu-Hf isotope analysis, recording εHf(t) values of -10.1 to -2.1 (Fig. 3.9e). Seventeen Phanerozoic zircons were also analyzed for Lu-Hf isotopes, and their εHf(t) values vary from -17.2 to 7.9. However, ~70% record negative values from -17.2 to -1, with TDM2 model ages from 2.1 to 1.1 Ga.

3.5.4.2 Sample SAL-58

Zircons from sample SAL-58 range from 50 to 200 μm in length/diameter. Most show magmatic oscillatory zones in CL, with some showing sector zones (Fig. 3.7). Eighty-eight concordant ages were obtained from a total of 96 analyses. The Th/U ratios are >0.5, which are the highest of the six samples. The age spectrum is similar to sample SAL-49; however, the proportion of 1.5–2.6 Ga zircons (41%) is smaller (Fig. 3.8f). Phanerozoic zircons account for 59%, with three age ranges: 145–210 Ma (35%), 217–239 Ma (15%), and 250–270 Ma (5%).

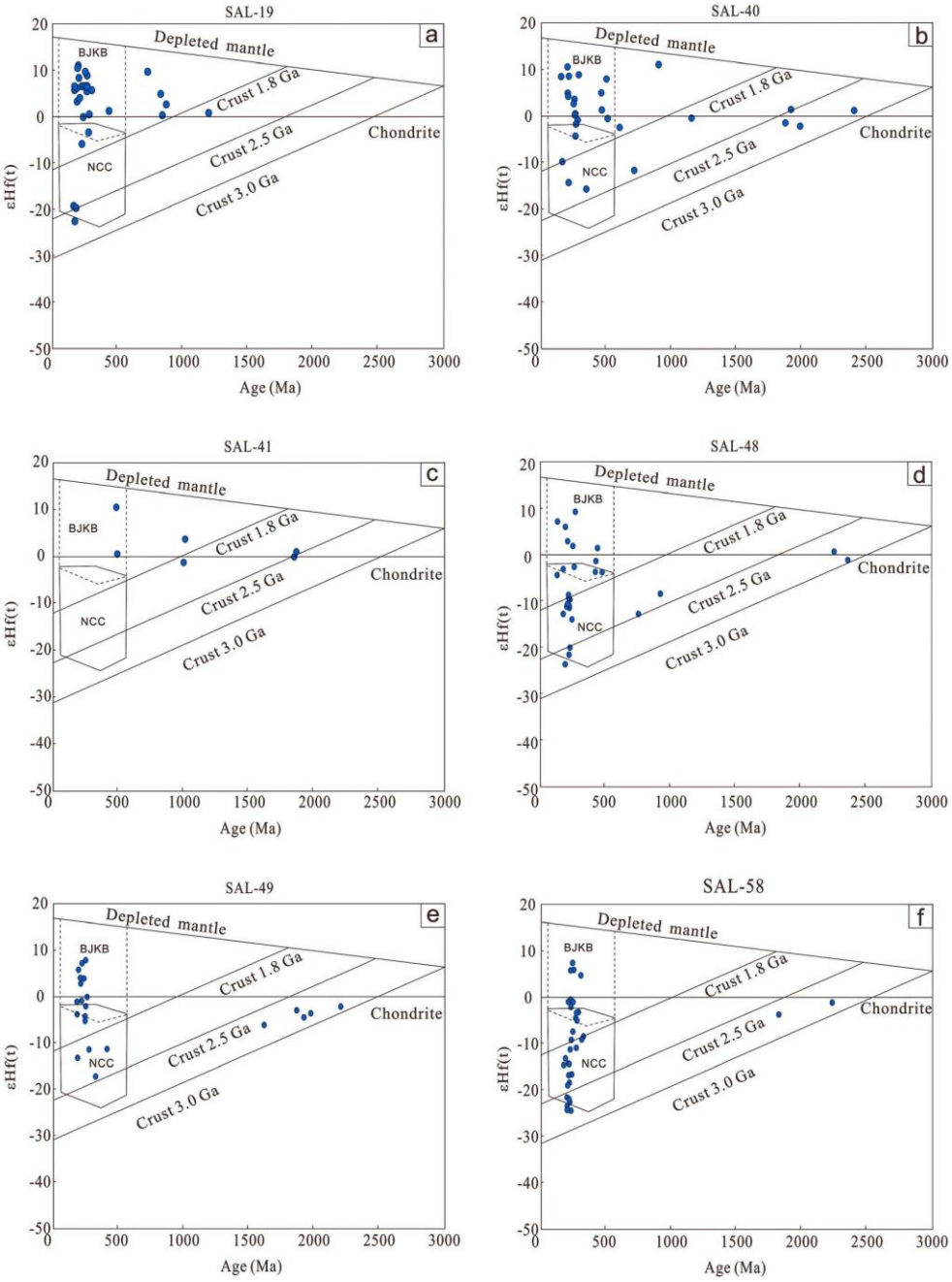

Fig. 3.9. Zircon εHf(t) values versus 206Pb/238U ages. (a) Sample SAL-19 from the central Samarka accretionary complex, (b) sample SAL-40 from the eastern Samarka accretionary complex, (c) sample SAL-41 from the Sergeevka nappes, (d) sample SAL-48 from the Zhuravlevka turbidite basin, (e) sample SAL-49 from the Taukha accretionary complex, and(f) sample SAL-58 from the Taukha accretionary complex. The fields of zircon εHf(t) values of the BJKB and NCC are modified after Cheong et al. (2013) and Yang et al. (2006).

Two Precambrian zircons and 32 Phanerozoic zircons were analyzed for Lu-Hf isotopes. The εHf(t) of the Phanerozoic zircons is mainly negative (80%), ranging from -24.5 to -0.5, with TDM2 model ages from 2.5 to 1.1 Ga, whereas the εHf(t) of the two

Precambrian zircons (~1.8 Ga and 2.3 Ga) are -4.2 and -1.2, respectively, with TDM2 model ages of 2.6 Ga and 2.8 Ga, respectively (Fig. 3.9f).

3.6 Discussion

3.6.1 Depositional Ages of Sandstones in the Southern Sikhote-Alin Orogenic Belt

Detrital zircon data can help determine the maximum depositional age of the analyzed sandstone sample (Dickinson & Gehrels, 2009; Gehrels, 2014). Generally, in the active continental margin, the youngest zircon age is close to the depositional age because the supply of volcanic materials from arc magmatism. However, only one youngest zircon age is not enough to constrain the depositional age. In this study, the youngest peak age in the spectrum (Gehrels, 2014) and previous paleontological research are applied together to solve this issue.

In the Samarka belt, the youngest zircon ages recorded from samples SAL-19 and SAL-40 are 162 Ma and 150 Ma, respectively, implying that they were deposited after the Middle Jurassic. According to Russian paleontological research, sandstone near sample SAL-19 is underlain by the Olenekian-Bathonian chert and the Oxfordian-Tithonian mudstone and siltstone (Kemkin, 2008; Khanchuk, 2001), which means the sandstone was deposited after the Late Jurassic.

In the Sergeevka nappes, a shallow-marine and clastic rock assemblage ranges in age ranging from Devonian to Jurassic (Khanchuk, 2006; Khanchuk et al., 2016). The youngest zircon U-Pb age recorded in this study is 178 Ma in sample SAL-41. However, no fossil data in the outcrop of sample SAL-41 are available to further constrain this, so it is proposed that deposition may occur in or after the Middle Jurassic.

The Zhuravlevka basin is composed mainly of turbidites with depositional ages

ranging from the Berriasian to Albian (Malinovsky & Golozubov, 2011). But the youngest zircon in sample SAL-48 has an age of 129 Ma and the youngest peak is ~131 Ma, constraining the depositional age in the late Early Cretaceous. This maximum depositional age is verified by the faunal research in the sandstone and siltstone from the same outcrop, showing an Aptian to Albian age (Golozoubov, 2006). In the Taukha accretionary complex, the age of turbidite is Berriasian to Valanginian (i.e., Early Cretaceous: 145–133 Ma) according to detailed faunal research (Golozoubov et al., 1992; Kemkin & Kemkina, 2000). The new zircon ages support this result, with the youngest zircon U-Pb age constraining the maximum depositional age of the sandstone at 145 Ma.

3.6.2 Possible Provenance of the Detrital Zircons

In the Late Jurassic to Early Cretaceous of NE Asia, four geological units had the potential to feed the southern Sikhote-Alin orogenic belt (Fig.3.1): the Siberia Craton (SC), the eastern CAOB, especially the Bureya-Jiamusi- Khanka Block (BJKB), the North China Craton (NCC), and the South China Craton (SCC).

Although the northern Korean Peninsula is a contiguous part of the eastern NCC (Zhao et al., 2005), the southern Korean Peninsula has tectonic affinities with the SCC because of the similarities in rock assemblages and metamorphic history from the Neoproterozoic to Mesozoic. With respect to the provenance of the Sikhote-Alin area, we will discuss the whole of the Korean Peninsula along with the eastern NCC because they have been a united source area following collision along the Imjingang Belt in the Middle Triassic (Fig.3.1; Cheong et al., 2013; Kim et al., 2008).

3.6.2.1 Possible Provenance of the Precambrian Detrital Zircons

The Precambrian zircons in the southern Sikhote-Alin show two major peaks at 2.5 and 1.8 Ga, with a much smaller population at around 0.8 Ga (Fig.3.8b–8f).

Late Archean and Paleoproterozoic ages (2.5 and 1.8 Ga) are most widespread in the eastern NCC. The oldest units in the eastern NCC are early Archean in age, including ~3.8 Ga, 3.7–3.6 Ga, and 3.3–3.1 Ga rocks (Wu et al., 2008). However, the predominant rocks are 2.7–2.5 Ga in age, including high-grade tonalitic-trondhjemitic-granodioritic (TTG) gneisses and granitoids (Zhao & Zhai, 2013). Paleoproterozoic rocks (1.95–1.85 Ga) mainly crop out in three linear tectonic belts in the western, central, and eastern NCC. One view is that these belts represent continent-continent collisional belts (Wilde et al., 2002; Zhai & Santosh, 2011; Zhao et al., 2012, 2005, 2001; Zhao & Zhai, 2013), whereas other researchers propose that they were generated as continental rifts within a single continent (Li et al., 2005, 2004, 2006; Zhang & Yang, 1988). Minor mafic dykes were emplaced in the NCC from ~1.8 to 0.9 Ga (Peng et al., 2008, 2011). Precambrian granitoids and metamorphic rocks are also found in the Korean Peninsula. In North Korea, the TTG gneisses and granitic rocks have ages ranging from 1.93 to 1.85 Ga (Zhai et al., 2007; Zhao et al., 2006). In the Ryeongnam massif of South Korea, granite gneisses with ages of 1.9–2.1 Ga are likewise reported (Turek & Kim, 1996). The detrital zircons from the river mouths in North Korea are also dominated by Paleoproterozoic populations (~2.2–2.1 Ga and 1.9–1.8 Ga) with minor Archean zircons (~2.5 Ga; Wu, Yang, Lo, et al., 2007).

In the Hida metamorphic complex of Japan, zircons with ages of 1.8 Ga and 1.1 Ga were obtained from meta- sedimentary gneiss and a few Permian to Triassic granites, and the 1.1 Ga peak is less important (Horie et al., 2010; Sano et al., 2000). Thus, there is a possibility that the Hida metamorphic complex contributed Precambrian zircon to the Sikhote-Alin orogenic belt. However, the 2.5–2.0 Ga zircons are absent in both gneiss and granite, indicating that the Hida metamorphic complex cannot be the main source area.

Paleoproterozoic A- and S-type granites formed at 1.9–1.8 Ga are also found in South China (Chen et al., 2015; Qiu et al., 2000; Zheng et al., 2004, 2006). However, the most widespread magmatic and metamorphic rocks in the SCC are from 1.0 to 0.75

Ga, for example, the igneous rocks of 1,000–850 Ma related to the collision between the Yangtze and Cathaysia blocks, and the bimodal magmatism at 850–750 Ma due to rifting of the Rodinia supercontinent (Charvet, 2013; Charvet et al., 2010; Li et al., 1999; Z. X. Li et al., 2002; X. H. Li et al., 2002; Li & Li, 2007). The 1.0–0.75 Ga zircons are always well represented in sandstones from the SCC (Jia et al., 2010; Yang et al., 2012). However, the age population of 1.0 to 0.75 Ga in age is small in the southern Sikhote-Alin orogenic belt, so it is considered that the SCC is unlikely to be the source area. Instead, the 1.0–0.75 Ga zircons in the southern Sikhote-Alin are most likely derived from the Neoproterozoic basement of the BJKB (Kim et al., 2008; Lee et al., 1998, 2003; Luan et al., 2017; Wilde et al., 2015; Wu et al., 2011; Yang et al., 2017).

Zircon age spectra with peak ages at 3.3, 3.0, 2.6, and 1.8 Ga, especially the 1.8 Ga ages, were also reported in the southern Siberia Craton (Rojas-Agramonte et al., 2011), which is consistent with zircon ages from the Zhuravlevka and Taukha belts. However, the eastern segment of the Mongol-Okhotsk Ocean between the Siberia Craton and the eastern CAOB was not closed before the Early Cretaceous, which makes it unlikely that sediments were transported to the Sikhote-Alin, because the transport distance would be too large given that the sedimentary characteristics of sandstones from the Sikhote-Alin indicate that they resulted from near- source deposition (Fig. 3.5; Donskaya et al., 2013; Khanchuk et al., 2016; Kravchinsky et al., 2002). Thus, it is proposed that the Siberia Craton could not be the source area for the southern Sikhote-Alin orogenic belt.

3.6.2.2 Potential Provenance of Phanerozoic Zircons

In the BJKB, the Pan-African metamorphic and igneous rocks range in age from 540 to 480 Ma with a peak of ~500 Ma (Wilde et al., 2000; Zhou et al., 2011). In the middle Paleozoic, only a few inherited zircons with 390–290 Ma ages are reported in the granitic rocks along the western BJKB (Miao et al., 2015). A magmatic arc belt (290–

274 Ma in age) was generated along the eastern margin of the Jiamusi Block (Bi et al., 2015; Meng et al., 2008; Sun, Xu, Wilde, Chen, et al., 2015; Yu et al., 2013), whereas there are 270–244 Ma I-type granodiorites and 220–170 Ma highly fractionated I-type granitoids in the western BJKB and adjacent areas(Jahn et al., 2015; Liu et al., 2017; Wu et al., 2003a, 2003b, 2011; Xu et al., 2013; Yang et al., 2015b). These granites are mostly the result of reworking of juvenile crust, commonly with weak negative to positive zircon εHf(t) values from -4 to 16 (Cao et al., 2011; Meng et al., 2011; Yang et al., 2006; Yu et al., 2012).

In the Phanerozoic, Mesozoic magmatism, especially the granitoids and relevant volcanic rocks, was generated in the NCC (Griffin et al., 1998; Menzies et al., 2007, 1993; Qi et al., 2015; Wilde et al., 2003; Yang et al., 2008; Zhang et al., 2014; Zhu et al., 2012). Intrusive and volcanic rocks were emplaced in the NCC from the Early Triassic to Late Cretaceous, with the Triassic magmatic rocks mainly located along the western segment of the northern margin of the NCC. Thus, it is unlikely to be the source of the Sikhote-Alin orogenic belt. After the Jurassic, magmatism moved eastward and also increased in volume (Zhang et al., 2014). The most important zircon age populations are 180–150 Ma and 130–110 Ma, usually with negative to weakly positive zircon εHf(t) values of -32 to 5, because of the involvement of basement in the magma source (Yang et al., 2009; Zhang et al., 2007; R. Zhang et al., 2009; S. H. Zhang et al., 2009; Zheng et al., 2004; Zhu et al., 2012). Similar magmatic events also took place in the Korean Peninsula at this time. The northern Korean Peninsula is characterized by middle Cretaceous granites (~110 Ma) and also contains some granites ranging in age from 250 to 170 Ma (Wu, Yang, Lo, et al., 2007). In the southern Korean Peninsula, 190–160 Ma is the most important magmatic episode, with local early Paleozoic arc magmatism at 440–370 Ma and Triassic granites at 260–220 Ma (Cheong et al., 2013, 2014; S. Kim et al., 2011; J. Kim et al., 2011; Kim et al., 2015). In addition, zircon Lu-Hf isotopes of Korean Peninsula rocks imply that Paleoarchean to Paleoproterozoic crust provided important source materials to these granitoids, and thus, the zircon εHf(t) values are negative from -31 to -2 (Cheong et

al., 2013, 2014, 2015). However, there are minor granitoids (265–252 Ma) recording positive zircon εHf(t) values of 10 to 15, with TDM2 model ages from 600 to 400 Ma (Cheong et al., 2013).

In the eastern Siberia Craton and adjacent coastal areas, the Paleo-Pacific subduction-related magmatism mainly took place in the Late Cretaceous, located along an active continental margin (up to 3,000 km long) and is the most important magmatic event regionally (Kirillova, 2003). However, it is younger than the depositional age of sandstones in the southern Sikhote-Alin, meaning that eastern Siberia and adjacent areas cannot be the source area for these rocks.

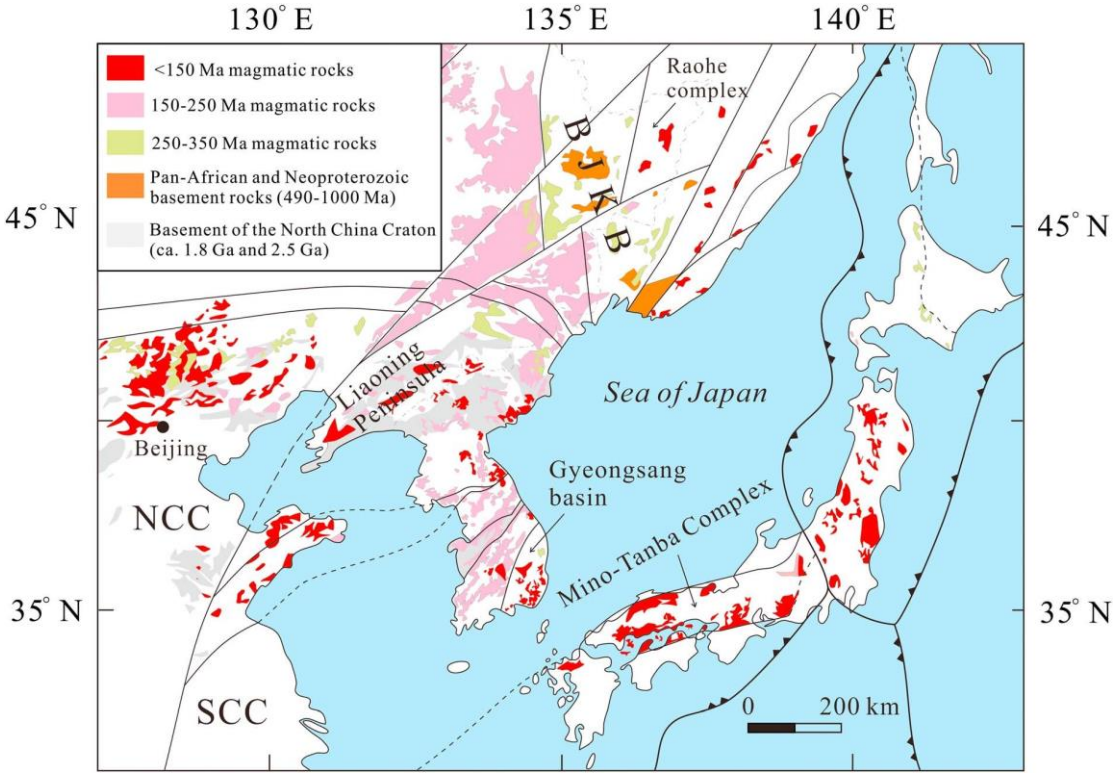

Fig. 3.10. Distribution of Archean to Early Cretaceous magmatism in the possible source areas for the Sikhote-Alin belts (Cheong et al., 2013; Jiang et al., 2013; Kim et al., 2011; Wu, Yang, Wilde, et al., 2007; Zhang et al., 2013; Zhao & Zhai, 2013).

3.6.3 Provenance Analysis in the Southern Sikhote-Alin Orogenic Belt

3.6.3.1 The Samarka Accretionary Complex

The spectrum of zircon ages in sample SAL-19 is similar to that of the Nadanhada

accretionary belt, which is located along the eastern margin of the BJKB, where the sediments were shown to be derived from the eastern CAOB, especially the BJKB, although no Archean zircons were reported from the latter (Sun, Xu, Wilde, & Chen, 2015; Zhou et al., 2014; Fig. 3.8a, 3.8g, and 3.10).

In sample SAL-19, zircons with ages of 268–236 Ma and 227–162 Ma were most likely derived from the adjacent magmatic rocks in the western BJKB, whereas the Early Permian ages (275–302 Ma) mostly likely came from the magmatic rocks in the eastern and central BJKB (Bi et al., 2015; Sun, Xu, Wilde, Chen, et al., 2015; Sun, Xu, Wilde, & Chen, 2015; Wu et al., 2011; Yang et al., 2015). The Phanerozoic zircons show weakly negative to positive εHf(t) values from -6 to 11 which are similar to those from the BJKB (Fig. 3.9a). In addition, the age groups of ~502 Ma and 1,000–700 Ma are in accord with the Pan-African and Neoproterozoic basement ages, respectively, in the Jiamusi-Khanka Block (Yang et al., 2017; Zhou et al., 2014). However, there are some zircons with ages of 1.6–2.7 Ga (<10%), indicating a possible minor contribution from the eastern NCC, which is consistent with the evidence that three Jurassic zircons have negative εHf(t) values (-20 to -22.5).

Although collected in the same belt, sample SAL-40 shows a different provenance (Fig. 3.8b). Late Pan-African (458–507 Ma) and Neoproterozoic (599–1,151 Ma) zircon ages indicate that the BJKB likewise supplied sediments to the unit hosting sample SAL-40, with most Phanerozoic zircons showing positive εHf(t) values with young TDM2 model ages, further supporting this view (Fig. 3.9b). However, ages from 1.8 to 2.6 Ga are more important in sample SAL-40, accounting for 36%, which implies that the eastern NCC and/or Korean Peninsula provided more detritus to this part of the Samarka accretionary complex.

There is an unnamed but significant fault that separates the two sample sites, marking the boundary between different components or thrust sheets/slices within the Samarka accretionary complex, which are called the main Samarka belt (sample SAL-19) and

eastern Samarka belt (sample SAL-40), respectively. According torecently published data, detrital zircons from the “coastal Samarka belt” (the southernmost part of the Samarka accretionary complex adjacent to the coast of the Sea of Japan) show an age spectrum with peaks at 189 Ma, 247 Ma, and 1.8 Ga, similar to sample SAL-40 in this study, implying that significant detritus was derived from the NCC and Korean Peninsula (Tsutsumi et al., 2016). Thus, the Samarka accretionary is not a single geological unit and was divided into several thrust slices/sheets according to the structural analysis and geometry (Fig. 3.4). Different components of the Samarka belt show at least two kinds of provenance characteristic, one is the BJKB and the other is the NCC.

3.6.3.2 The Sergeevka Nappes

The nappes include fragments of the Paleozoic continental margin, and the major rock types are silica-unsaturated mafic rocks containing much fewer zircons than the granitoids (Fig. 3.7). The number of zircons in sample SAL-41 is thus too small for a valid provenance analysis. However, it is inferred that the Neoproterozoic zircons and late Pan-African zircons with positive εHf(t) values may have originated from the BJKB or the local denudation of mafic and metamorphic rocks (Fig. 3.8c and 3.9c). The zircons with Paleoproterzoic ages could have been supplied from the NCC or the Korean Peninsula. A source in the SCC is also possible for this sandstone because of the abundance of zircons with ages from 700 to 1,000 Ma. Thus, the provenance of the Sergeevka nappes remains uncertain based on this study and requires further research.

3.6.3.3 The Zhuravlevka Turbidite Basin

The zircon age spectrum of sample SAL-48 is similar to that of sample SAL-40, suggesting derivation from both the NCC and BJKB (Fig. 3.8d).

Zircons with an age of 420–500 Ma are an important component of the BJKB and the adjacent blocks of the eastern CAOB. However, the abundance of 420–500 Ma zircons

is much lower than that of the Neoproterozoic and Archean zircons, suggesting the eastern NCC and Korean Peninsula was also an important source of detritus. Precambrian zircons make up 57% of the population and show major peaks at 1.8 Ga and 2.5 Ga, which is characteristic of the eastern NCC and Korean Peninsula (Darby & Gehrels, 2006; Li & Huang, 2013; Zhao et al., 2005; Zhu et al., 2012). This is further verified by the Phanerozoic zircon Lu-Hf isotopes, with up to 73% having negative εHf(t) values (Fig. 3.9d). The age population at ~250 Ma is small, whereas zircons with Middle Jurassic to Cretaceous ages are abundant, which correlates with the most important period of Mesozoic magmatism in the eastern NCC and Korean Peninsula (Cheong et al., 2013, 2014; Qi et al., 2015; Zhang et al., 2013; Zhu et al., 2012).

3.6.3.4 The Taukha Accretionary Complex

Both samples SAL-49 and SAL-58 from the Taukha accretionary complex are characterized by two main age groups; one Paleoproterozoic and the other Phanerozoic (Fig. 3.8e and 3.8f). The absence of late Pan-African and Neoproterozoic ages indicates that the BJKB did not supply sediments to the Taukha accretionary complex during the Late Jurassic to Early Cretaceous. Thus, the eastern NCC (including the Korean Peninsula) was the most likely source. The zircons with ages of ~2.5 Ga and 1.8 Ga record basement ages of the NCC (Zhao et al., 2005). The zircons with ages of 420–300 Ma could be derived from arc magmatism in the central Korean Peninsula (Kim et al., 2015), and those with ages of 260–230 Ma might be related to arc magmatism and the continent-continent collision belt along the Imjingang Belt (the possible extension of the Sulu-Dabie orogenic belt into the Korean Peninsula; Cheong et al., 2014; J. Kim et al., 2011). Zircons with ages of 220–150 Ma are likely related to collisional magmatism in the eastern NCC and/or Paleo-Pacific subduction-related magmatism in the southern Korean Peninsula (Kusky et al., 2007; Li et al., 2013; S. H. Zhang et al., 2009; Zhang et al., 2013). About 70–80% of the Phanerozoic zircons have negative εHf(t) values in samples SAL-49 and SAL-58, consistent with a NCC source (Fig. 3.9e and 3.9f; Yang et al., 2006; Sun, Xu, Wilde, & Chen, 2015). However,

there are also a few zircons with positive εHf(t) values; for example, five Mesozoic zircons in sample SAL-49 show positive εHf(t) values from 2.8 to 7.9. These values are consistent with the Neoproterozoic juvenile crustal component in South Korea (Cheong et al., 2013).

3.6.4 Provenance Variation in the Southern Sikhote-Alin Orogenic Belt

According to the composition of sandstones in the southern Sikhote-Alin orogenic belt, different samples show different tectonic settings for the provenance area, changing gradually from an arc to a continental setting (Fig. 3.11).

For sample SAL-19, a transitional arc setting fits the absence of a zircon age peak at 1.8 Ga from the NCC and the abundance of Jurassic zircons most likely derived from the continental arc in the eastern CAOB, which is supported by their negative εHf(t) values. Sample SAL-40 has less lithic fragments and more quartz, illustrating the growing importance of sediments from the Asian continental basement. Samples SAL-48 and SAL-49 plot in the transitional continental area, implying that the deformation belt at the northern margin of the NCC and Korean Peninsula was the main source area. For sample SAL-49, a likely minor contribution from South Korea is indicated by the similar positive ε(Hf) t values of five Mesozoic zircons (Cheong et al., 2013).

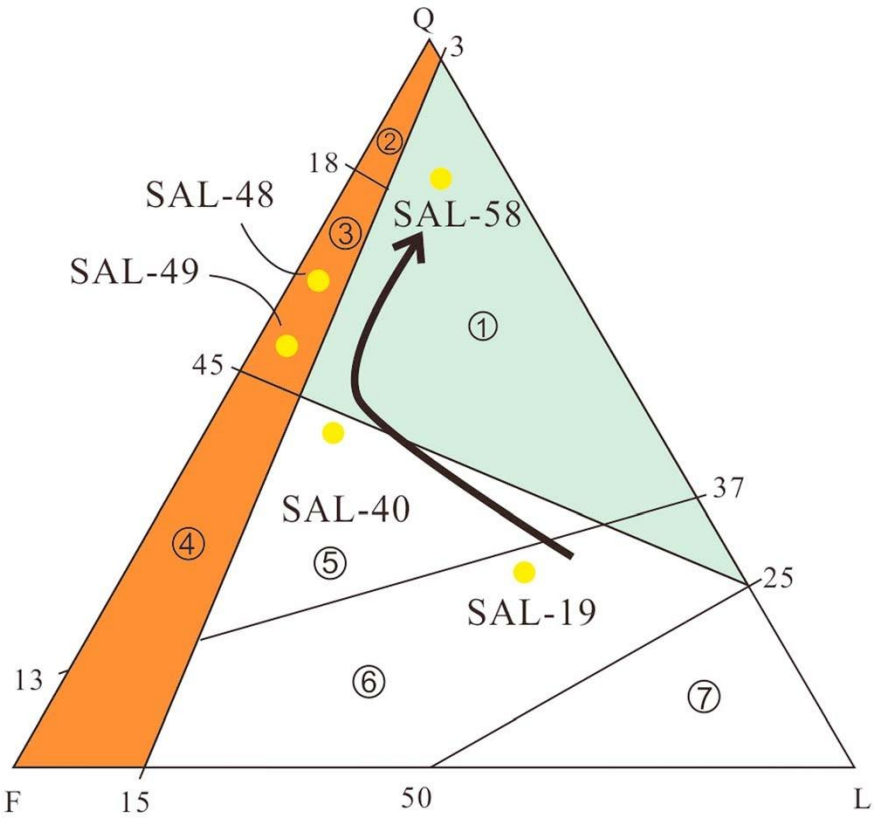

Fig. 3.11. Q-P-L diagram for the sandstones in the Samarka, Zhuravlevka, and Taukha belts (Dickinson, 1985; Dickinson et al., 1983). Numbers in the figure: 1. Recycled orogen; 2. Craton interior; 3. Transitional continent; 4. Basement uplift;5. Dissected arc; 6. Transitional arc; 7. Undissected arc. The arrow shows the change in trend of the tectonic setting of the provenance area from an arc to a transitional continent and finally to a recycled orogen, during which the contribution from the old craton is increasingly important.

Finally, sample SAL-58 was likely fed by a recycled orogen, such as existedaccretionary complex and suture zone/fold-thrust belts of collision orogen (Dickinson et al., 1983). Collision events between mature block/arcs happened in the Japanese Island from Late Paleozoic to Mesozoic and accretionary complexes were built in the gaps of collision (Charvet, 2013; Charvet et al., 1983; Isozaki, 1997; Maruyama, 1997). The highlands associated with the pre-Early Cretaceous subduction and collision events were possible to supply detritus to the Taukha accretionary complex. However, the first-cycle of sediments shows that the eastern NCC and Korean Peninsula were the initial source areas indicated by the bimodal zircon age spectrum.

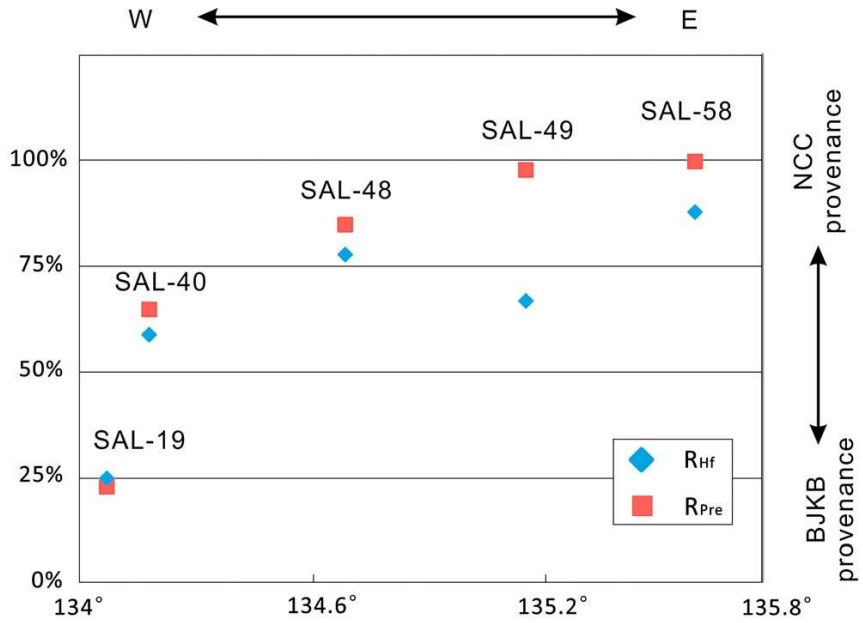

Fig. 3.12. Ratios (RHf and RPre) versus the longitude of the sample locations. The two ratios are calculated to show the different provenance of samples investigated in this study. RHf is the ratio of the number of Phanerozoic zircons with positive εHf(t) values divided the number of the Phanerozoic zircons in each sample. RPre is the ratio of the number of Archean and Paleoproterozoic zircons in each sample divided the number of Precambrian zircons. Both ratios increase from west to east, meaning that in these samples the contribution from the eastern NCC and/or Korean Peninsula increases from west to east. This is because the Phanerozoic zircons with positive εHf(t) values are mostly from the eastern BJKB, whereas the Archean and Proterozoic zircons are mostly from the eastern NCC. Sample SAL-41 is not shown because the number of analyses is insufficient for a meaningful result.

Along the sample traverse (Fig. 3.2b), the proportion of zircons with 1.8 and 2.5 Ga ages and Phanerozoic zircons with negative zircon $\varepsilon_{Hf}(t)$ values increases from west to east, which likewise indicates the growing importance of the NCC and/or Korean Peninsula as the source (Fig. 3.12). For sample SAL-49, the decoupling of R_{Pre} and R_{Hf} in Fig. 3.10 is attributed to the five Mesozoic zircons with positive $\varepsilon_{Hf}(t)$ values, most likely showing the minor proportion contributed by Neoproterozoic juvenile crust in South Korea (Cheong et al., 2013).

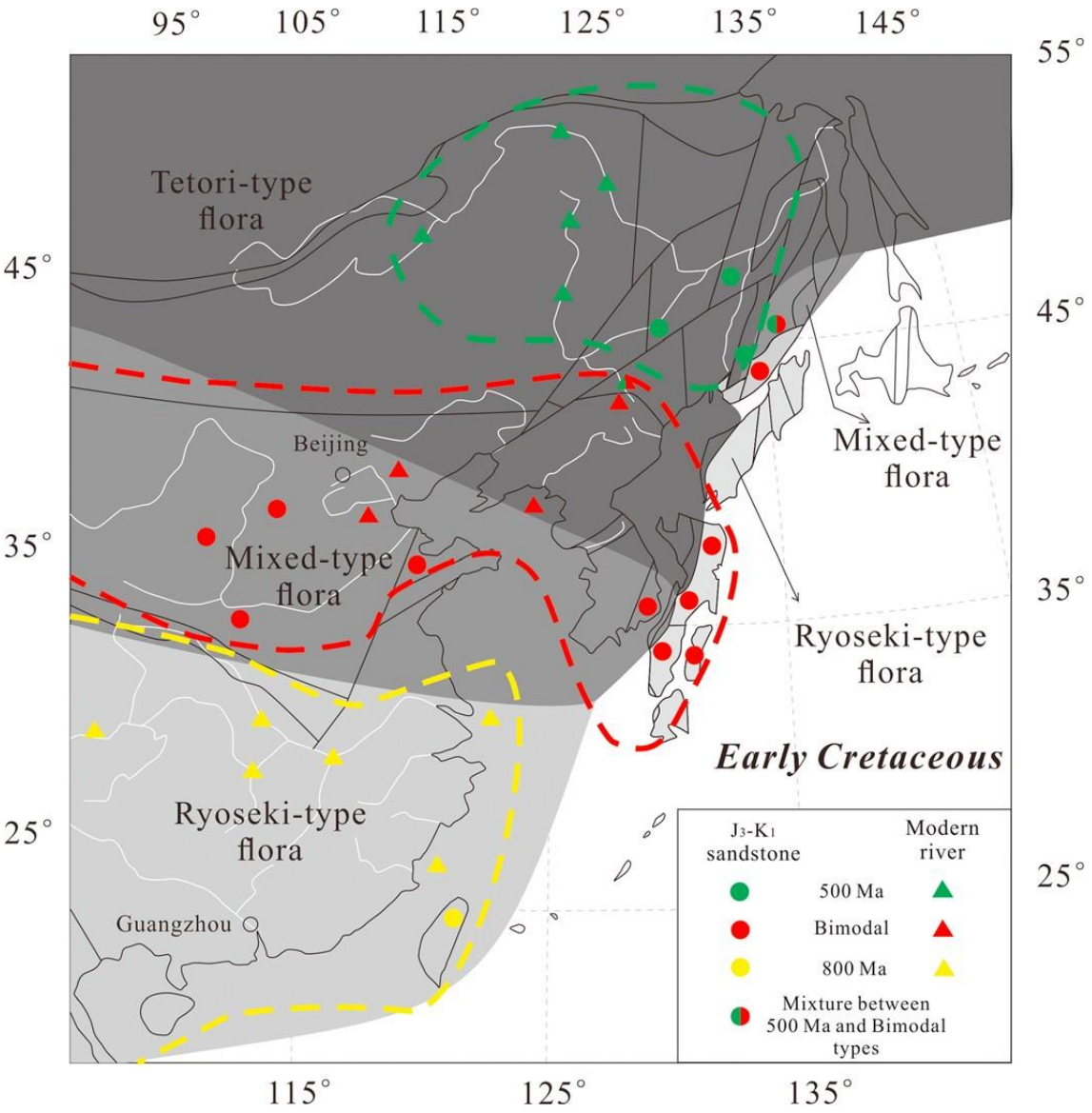

Fig. 3.13. Provinces in the Early Cretaceous East Asia show different types of detrital zircon spectra. The dashed lines show the range of each province. The green dashed line shows the 500 Ma-type province; the red one shows the bimodal-type province; the yellow one shows the 800 Ma-type province. The paleophytogeograhic provinces are also shown, modified after Kimura (1979, 2000) and Golozoubov et al. (1999).

3.7 Tectonic Implications

Three provinces with different zircon age spectra can be recognized along the eastern Asian continental margin from southeastern Russia to south China (Fig. 3.13), based on the U-Pb age data of detrital zircons collected from the Late Jurassic to Early Cretaceous sandstones and modern river sands. Each zircon age spectrum is generally limited to within a particular area, which helps us better understand the specific

geological characteristics in different areas and thus allows to compare that with the southern Sikhote-Alin orogenic belt.

1. Bimodal type: This type of zircon age spectrum shows two important age groups, that is, a Phanerozoic group and a Paleoproterozoic to Archean group (with peaks at ~1.8 and 2.5 Ga; Fig. 3.14a). Very few, if any, zircons with ages between the two major groups have been found. The bimodal-type spectrum appears in the Late Jurassic to Early Cretaceous sandstones from the basins in the interior of the NCC (Li & Huang, 2013; Wang et al., 2016), SW Japan (Aoki et al., 2014; Fujisaki et al., 2014; Isozaki et al., 2010; Nakama et al., 2010) and South Korea (Lee et al., 2015). Modern river sands along the coast of the eastern NCC and Korean Peninsula also have similar spectra (Wu, Yang, Lo, et al., 2007; Yang et al., 2009).
2. 500 Ma type: This type of zircon age spectrum is characterized by important peaks at ~180, 220, 250, and 500 Ma, but ages around ~1.8 or 2.5 Ga are much lesser abundant than in the Bimodal type, or, indeed, sometimes absent (Fig. 3.14b). A minor age group from 0.7 to 1.0 Ga can also be found in the interior of the eastern CAOB, consistent with the Neoproterozoic basement of the BJKB (Khanchuk et al., 2010; Wilde et al., 1997; Yang et al., 2017). The 500 Ma-type spectrum is also found around the BJKB, such as the Heilongjiang Complex and Nadanhada belt (Zhou et al., 2009, 2015; Sun, Xu, Wilde, & Chen, 2015), and the river sands from the middle reach of the Amur River.
3. 800 Ma type: The spectra in the eastern SCC always contain a prominent age peak at ~0.8 Ga, which is the most significant characteristic of this area (Fig. 3.14c; Wang et al., 2014; Yui et al., 2012). Zircon peaks at ~130 Ma, 170 Ma, 1.8 Ga, and 2.5 Ga are also present in this type, derived from Jurassic- Cretaceous magmatism and basement rocks of the SCC. This type of spectrum is dominant in almost all of the modern river sands collected from the Yangtze River and its branches (Yang et al., 2012). However, very few Late Jurassic to Early Cretaceous sandstones can be found in the present SCC, except perhaps the Tananao complex in Taiwan which fits well with the 800 Ma-type spectrums (Li et al., 2012; Yui et

al., 2012).

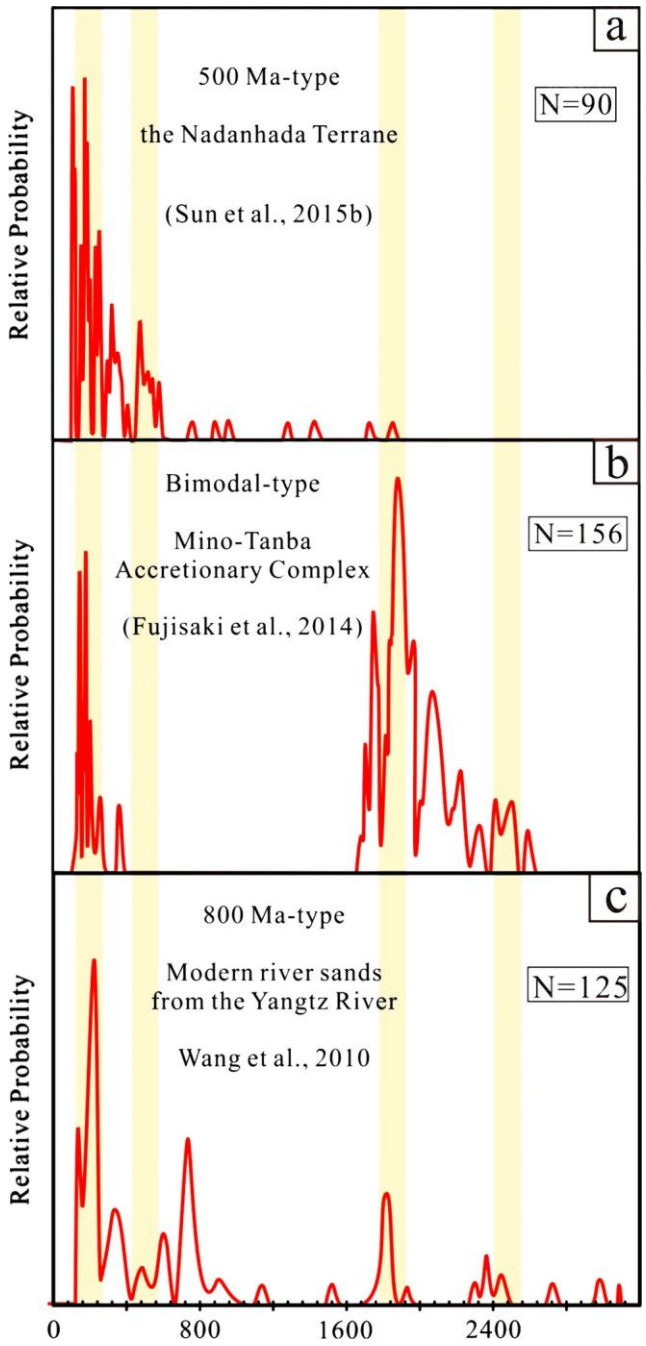

Fig. 3.14. Typical spectra of detrital zircons in the (a) 500 Ma-type, (b) bimodal-type, and (c) 800 Ma-type provinces in the Early Cretaceous of East Asia.

In the southern Sikhote-Alin, sample SAL-19 from the main Samarka accretionary complex shows a 500 Ma- type spectrum. Samples SAL-49 and SAL-58 from the Taukha accretionary complex have typical bimodal-type spectra. However, sample SAL-40 from the eastern Samarka belt and sample SAL-48 from the Zhuravlevka basin are a mixture of sediments with the 500 Ma type and bimodal type. The detrital

monazite ages in the Samarka belt and Zhuravlevka basin also support this viewpoint (Tsutsumi et al., 2016). In the main Samarka belt, there is a significant peak at ~500 Ma, which is not shown in the monazite data from the Zhuravlevka or Taukha (Fig. 3.15). Thus, the influence from the BJKB to the Zhuravlevka and Taukha was quite weak. Importantly, located in their present geographic positions, it is difficult for the eastern Samarka accretionary complex, the Zhuravlevka turbidite basin, and the Taukha accretionary complex to be fed by sediments from the eastern NCC or Korean Peninsula (Fig. 3.1 and 3.10).

It is also virtually impossible for the Taukha belt to exclude sediments from the BJKB in its present location. This strongly indicates that the belts in the southern Sikhote-Alin area were moved by tectonic movement significantly, such as subduction, collision, and strike slip. Therefore, discussing the tectonic settings will be very necessary in order to explain the abrupt changing of provenance types across the Central Sikhote-Alin Fault.

Many hypotheses have been raised in the past decades in the Pacific tectonic realm to explain the collage of the numerous belts in this region, including the (1) collision orogeny, (2) accretionary orogeny, and (3) strike-slip faulting along a transform margin. In SW Japan, collision orogeny was identified based on the discovery of large thrust sheet and nappes (Charvet et al., 1985; Faure et al., 1986). These nappe tectonics are explained by the intermittent docking of continental blocks/mature arcs to the hinterland.

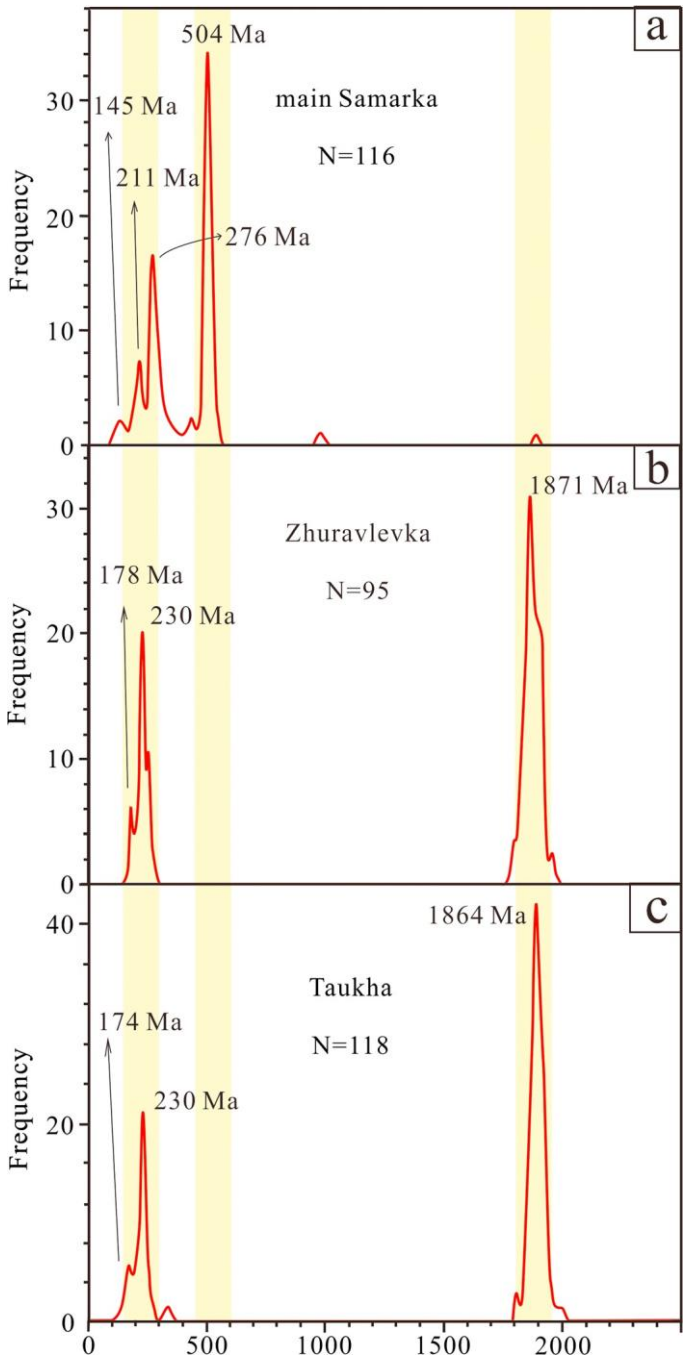

Fig. 3.15. Spectra of detrital monazite collected in (a) the main Samarka, (b) the Zhuravlevka, and (c) the Taukha belts (Tsutsumi et al., 2016).

The Sr-Nd isotopic research of granitoids in SW Japan supports this viewpoint because the participation of old crust can be detected in the felsic magmatism (Jahn, 2010). Structural geological analysis also reveals nappe/thrust tectonics similar to that in the classical collisional orogenic belt (Charvet et al., 1985). Faure et al. (1995) proposed similar model in Sikhote-Alin, underlining the importance of continental blocks in orogeny. Recently, Jahn et al. (2015) studied the Sr-Nd isotopes in the granitoids in

Sikhote-Alin. The result also supports the possible existence of an old crust basement. However, the explanation of Sr-Nd isotopes is argued because the remelting of the sedimentary rocks in Sikhote-Alin, including abundant detritus from old continental blocks/cratons, can also explain the isotopic data (Khanchuk et al., 2016; Kruk et al., 2014).

Some other studies suggest that accretionary orogeny, instead of collision, was dominant in the Japanese Island (Isozaki et al., 2010; Maruyama, 1997). In their models, the Japanese Islands are basically a large accretionary prism which was influenced by high-pressure metamorphism, accretion of sea mount/plateau, and ridge subduction.

As a result, the Japanese Islands grew continuously eastward due to persistent subduction and underthrusting of the oceanic plate. The age of the thrust sheets, therefore, tends to be younger from hinterland to the ocean side.

According to some Russian geologists, the eastern Asian margin was a transform plate boundary in Early Cretaceous, alike to the modern plate margin in California, alike to the Saint Andreas Fault (Golozoubov, 2006; Golozoubov et al., 1999; Khanchuk, 2001; Khanchuk et al., 2016). Accretionary orogeny associated with subduction took place in the Jurassic and Late Cretaceous in their representative model (Khanchuk et al., 2016). Whereas in the Early Cretaceous (145–100 Ma), the collage of some major units in Sikhote-Alin was attributed to the northward displacement by strike-slip faults. It is noted that strike-slip faulting is also emphasized by the “collisional orogeny” and “accretionary orogeny” models, although it is not considered to be the only/major geodynamic mechanism. For example, the post- collision strike-slip faulting was important in reworking of the south Kitakami-Kurosegawa continental block after its collision with the hinterland of Japan (Charvet, 2013; Kato & Saka, 2003, 2006). In the previous models for Sikhote-Alin, the “terranes” were suggested to be built near South China and then moved northward to its present location by sinistral strike-slip

faulting (Natal'in, 1993).

In the southern Sikhote-Alin, nappe/thrust tectonics can be identified in the Sergeevka nappes (Fig. 3.2 and 3.4), in which the two-stage evolution is similar to that of the south Kitakami-Kurosegawa block in Japan, namely, the thrusting at the early stage and reworking by strike-slip faulting at the later stage (Fig. 3.16a). High-pressure metamorphism (blueschist facies) happened when the slab was subducted and then exhumed during the collsion. These nappes were thrust upon the Samarka accretionary complex, suggesting a collisional orogeny (Khanchuk et al., 2016). At the first stage, the subduction and collision between the Sergeevka and Samarka were responsible for the emplacement of the nappes (Fig. 3.16a). At the later stage, the continental block was dismembered into several fragments, which is clearly shown on the regional geological map (Fig. 3.2).

One of the key questions about the tectonics in Sikhote-Alin is that if the collisional orogeny played an important role. In the northern Sikhote-Alin area, Faure et al. (1995) identified a continental block, the Anuy microcontinent, which was proposed to collide with the western belts in the middle Cretaceous. Nd isotopes of granites also indicate that the basement of the Sikhote-Alin orogenic belt may be an old crust, instead of a juvenile one (Jahn et al., 2015). However, this conclusion should be drawn carefully now. In reality, there is no valid geochronological data showing any evidence of "old continental basement" so far. Thus, in addition to the Sergeevka block, the existence of other old crust/continental block is difficult to assure, making it difficult to identify the collisional orogeny in Sikhote-Alin. This issue still needs more detailed research in future.

Anyway, no matter accretion or collision model of the belts from east to west does not fit the new data in this study. The detrital zircon dating and Lu-Hf isotopes reveal that the provenance features of belts separated by the Central Sikhote-Alin Fault are quite different. The affinity of NCC/Korean Peninsula is recognized in the eastern Samarka

belt, Zhuravlevka basin, and Taukha accretionary complex, whereas the Nadanhada and main Samarka accretionary complexes were dominated by the BJKB. The provenance of the Nadanhada and main Samarka belts is comprehensible because they are adjacent to the BJKB. But it is very difficult to explain the weak signal of the BJKB and strong influence from the NCC in other belts because they are adjacent to the eastern CAOB as well. In this study, the sinistral strike-slip faulting, represented by the Central Sikhote-Alin Fault, is proposed to be responsible for this issue. It is suggested that the eastern Samarka, Zhuravlevka, and Taukha belts were not located adjacent to the BJKB when deposited, but farther south than their present locations, possibly near the Korean Peninsula to accept the sediments from the NCC (Fig. 3.16b). The sinistral strike-slip faulting system transported the belts to north. This strike-slip faulting system should be active after the collision of the Sergeevka nappes and the initial collage between the Zhuravlevka, Kema, and Taukha belts (Fig. 3.16c) because the Central Sikhote-Alin Fault cuts the Samarka belt, Sergeevka nappes, and most boundaries between the major belts (Fig. 3.2). It should be noted that thrusting was the initial contact relationship between most belts in Sikhote-Alin except the Zhruavlevka turbidite basin which was deposited along the Central Sikhote- Alin Fault at the very beginning (Khanchuk et al., 2016; Malinovsky & Golozubov, 2011).

Evidence for northward transport is also recorded by the floral distribution in the sedimentary rocks. Two major paleophytogeographic provinces are recognized in the area, the Tetori-type floral province in the north and the Ryoseki-type floral province in the south (Fig. 3.12; Batten, 1984; Kimura, 1979; Vakhrameev, 1987; Yabe et al., 2003). A mixed-type floral province is further recognized between these two (Kimura et al., 1988; Kimura, 2000). Although the province boundaries are roughly latitudinal, more detailed research shows an irregular flora distribution in the southern Sikhote-Alin (Fig. 3.12). Plants from the southernmost Sikhote-Alin are similar to the Ryoseki-type flora, whereas some areas in the Sikhote-Alin are assigned to the mixed-type flora domain (Golozoubov et al., 1999; Kimura, 2000). Tectonic reconstruction based on the floral assemblages in East Asia indicates that northward movement could be more than

5° of latitude in SW Japan and 15° of latitude in the southern Sikhote-Alin (Golozoubov et al., 1999). However, there remain uncertainties about the affinity of belts as recorded by the detrital zircon, monazite, and flora. The reason is that the floral assemblage is mainly determined by latitude, whereas the provenance of sediments is mainly constrained by their paleogeographic location when deposited. However, in this instance, both pieces of evidence are consistent with northward transport after the initial collision, including the paleomagnetic research published recently, showing that northward movement was important for some belts in Sikhote-Alin (Didenko et al., 2014; Khanchuk, Didenko, Tikhomirova, et al., 2015).

The exact offset is very difficult to evaluate for the Cental Sikhote-Alin Fault because (1) the sinistral displacement may be changed by the complicated deformations in the region, for example, the dextral movement at later stage, faulting and folding due to subduction or collision; (2) the Central Sikhote-Alin Fault has been an inactive fault for dozens of million years, making the direct evidence used to evaluate the offset, such as rivers and ranges, very obscure; and (3) the forest almost cover the whole Sikhote-Alin area and there is even no good outcrop of the fault founded for now. Thus, the offset of the sinistral faults in the Sikhote-Alin area is still an unsolved issue which needs more detailed research and direct evidence.

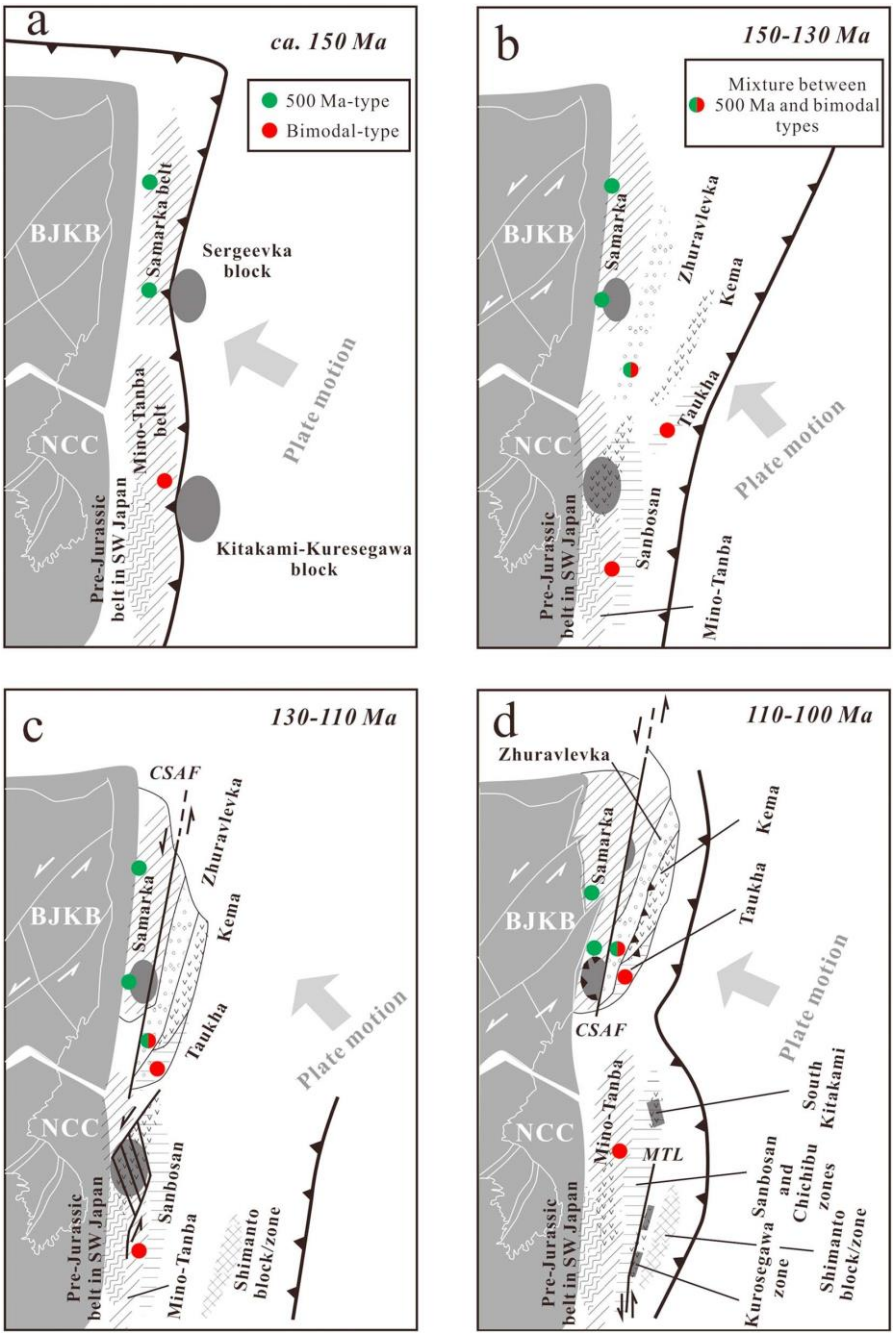

Fig. 3.16. Tectonic reconstruction of the East Asian continental margin at 150 to 100 Ma. Faults: CSAF = the Central Sikhote-Alin Fault; MTL = the Median Tectonic Line in Japan. The reconstruction in SW Japan is modified after Kato and Saka (2003) and Charvet (2013). The plate motion direction is according to Müller et al. (2008).

The timing of this northward transport with parallel-margin left-lateral motion has not been well constrained. However, in the southern Sikhote-Alin it can be inferred that the northward movement occurred in the late Early Cretaceous based on the magmatic and floral evidence. There is also a magmatic gap between 130 and 110 Ma in the

Sikhote-Alin, probably due to plate motion parallel to the continental margin, which weakened the effect of subduction beneath the continent and thus reduced arc magmatism (Jahn et al., 2015; Khanchuk, 2001; Khanchuk et al., 2016; Maruyama, 1997). After ~110 Ma, magmatism in the Sikhote-Alin became quasi-continuous from 100 to 56 Ma as a result of westward subduction of the Izanagi and Pacific plates (Jahn et al., 2015; Kruk et al., 2014). The floral assemblages were different in various basins of the southern Sikhote-Alin prior to this magmatic gap (Golozoubov et al., 1999). However, the flora were similar between 110 and 100 Ma (Golozobov et al., 1999), providing some constraint on the timing of sinistral movement on the major strike-slip faults.

3.8 Conclusions

The southern Sihote-Alin orogenic belt is composed, from west to east, of the Samarka, Zhuravlevka, and Taukha belts, which are separated by thrusts and strike-slip faults. The Sergeevka nappes include Paleozoic continental margin fragments that were covered by late Paleozoic to Mesozoic sedimentary rocks and were thrust over the Samarka accretionary complex.

Detrital zircon U-Pb ages and Lu-Hf isotopes of sandstones in the various belts constrain the provenance as follows: (1) the main Samarka belt mainly received terrigenous sediments from the eastern CAOB (mainly from the BJKB); (2) the Zhuravlevka basin and eastern Samarka belt were fed by both the eastern CAOB and NCC (probably including the Korean Peninsula); (3) the sediments of the Taukha belt were derived from the eastern NCC and Korean Peninsula; and (4) the provenance of the Jurassic sediments in the Sergeevka nappes is largely unconstrained due to insufficient data and needs to be further investigated.

The initial contact relationship between most belts in the Sikhote-Alin orogenic belt is thrust resulted from collisional orogeny and subduction of the Paleo-Pacific Ocean.

However, the Zhuravlevka turbidite basin was deposited along the Central Sikhote-Alin Fault.

The Sergeevka nappes were thrust upon the Samarka belt before the Early Cretaceous and then reworked by sinistral strike-slip faults. The Taukha belt and Kema arc collided with the Zhuravlevka basin before the Late Cretaceous. However, sinistral strike-slip faulting was important in the final collage of the Sikhote-Alin orogenic belt after the initial thrusting. The eastern Samarka belt, Zhuravlevka basin, and Taukha belt were transported northward from the margin of the NCC to their present location. The timing of this northward movement is estimated as the late Early Cretaceous.

3.9 Acknowledgments

We would like to thank Igor Alexandrov, Victor P. Nechaev, Bei Xu, and Pan Zhao for their help with the fieldwork and their important suggestions for this manuscript. The comments from Editor John Geissman, Associate Editor Andrei Khudoley, Jian-bo Zhou, Jacques Charvet, and an anonymous reviewer are essential to improve the quality of our manuscript, especially for the part of tectonic reconstruction. We acknowledge Tatsuaki Kimura and other geologists from China, Japan, and Korea who contributed to the paleophyto- geography and tectonic reconstruction of East Asia. Y. H. Yue from the Institute of Tibetan Plateau Research, Chinese Academy of Sciences, is thanked for her kind help with LA-ICP-MS dating. In addition, Z.C. Liu, L. Xu and other staff at the State Key Laboratory of Geological Processes and Mineral Resources, China University of Geosciences (Wuhan), gave valuable advice on the analysis of zircon Lu-Hf isotopes. The data presented in this paper are available in Tables 3.1 and 3.2. This research was financially supported by the State Key Program of National Natural Science Foundation of China (41730210) and the Major State Basic Research Development Program of China (2013 CB429804) and partly funded by the Fundamental Research Funds for the Central Universities (310827161010).

3.10 References

Aoki, K., Isozaki, Y., Kofukuda, D., Sato, T., Yamamoto, A., Maki, K., … Hirata, T. (2014). Provenance diversification within an arc-trench system induced by batholith development: The Cretaceous Japan case. Terra Nova, 26(2), 139–149. https://doi.org/10.1111/ter.12080

Argentov, V., Gnibidenko, G., Popov, A., & Potap'ev, S. (1976). Deep Structure of Primorye. Moscow (in Russian): Nauka.

Batten, D. (1984). Palynology, climate and the development of Late Cretaceous floral provinces in the Northern Hemisphere; a review. In Fossils and Climate, (pp. 127–164). Chichester, UK: John Wiley.

Berger, W., & Winterer, E. (1974). Plate stratigraphy and the fluctuating carbonate line. In Pelagic sediments: On land and under the sea (pp. 11–48). International Association of Sedimentologists. Special Publication Number 1, Oxford, UK: Blackwell Scientific Publications.

Bi, J. H., Ge, W. C., Yang, H., Zhao, G. C., Xu, W. L., & Wang, Z. H. (2015). Geochronology, geochemistry and zircon Hf isotopes of the Dongfanghong gabbroic complex at the eastern margin of the Jiamusi Massif, NE China: Petrogensis and tectonic implications. Lithos, 234, 27–46.

Bingen, B., Birkeland, A., Nordgulen, & Sigmond, E. M. (2001). Correlation of supracrustal sequences and origin of terranes in the Sveconorwegian orogen of SW Scandinavia: SIMS data on zircon in clastic metasediments. Precambrian Research, 108(3-4), 293–318. https://doi.org/10.1016/S0301-9268(01)00133-4

Blichert-Toft, J., & Albarède, F. (1997). The Lu-Hf isotope geochemistry of chondrites and the evolution of the mantle-crust system. Earth and Planetary Science Letters, 148(1-2), 243–258. https://doi.org/10.1016/S0012-821X(97)00040-X

Cao, H., Wenliang, X., Fuping, P., & Xingzhou, Z. (2011). Permian tectonic evolution in southwestern Khanka Massif: Evidence from Zircon U-Pb chronology, Hf isotope and Geochemistry of gabbro and diorite. Acta Geologica Sinica (English Edition), 85(6), 1390–1402.

Cawood, P. A., Hawkesworth, C., & Dhuime, B. (2012). Detrital zircon record and tectonic setting. Geology, 40(10), 875–878. https://doi.org/ 10.1130/G32945.1

Charvet, J. (2013). The neoproterozoic–early paleozoic tectonic evolution of the South China Block: An overview. Journal of Asian Earth Sciences, 74, 198–209.

Charvet, J., Shu, L., Faure, M., Choulet, F., Wang, B., Lu, H., & Le Breton, N. (2010). Structural development of the Lower Paleozoic belt of South China: Genesis of an intracontinental orogen. Journal of Asian Earth Sciences, 39(4), 309–330. https://doi.org/10.1016/ j.jseaes.2010.03.006

Chen, Z. H., Xing, G. F., & Zhao, X. L. (2015). Palaeoproterozoic A-type magmatism in northern Wuyishan terrane, Southeast China: Petrogenesis and tectonic implications. International Geology Review, 1–14.

Chen, Y., Zhang, Z., Li, K., Yu, H., & Wu, T. (2016). Detrital zircon U–Pb ages and Hf isotopes of Permo-Carboniferous sandstones in central Inner Mongolia, China: Implications for provenance and tectonic evolution of the southeastern Central Asian Orogenic Belt. Tectonophysics, 671, 183–201. https://doi.org/10.1016/j.tecto.2016.01.018

Cheng, R., Wu, F., Ge, W., Sun, D., Liu, X., & Yang, J. (2006). Emplacement age of Raohe Complex in eastern Heilongjiang Province and the tectonic evolution of the eastern part of Northeastern China. Acta Petrologica Sinica, 22(2), 353–376. (in Chinese with English abstract)

Cheong, C. s., Yi, K., Kim, N., Lee, T. H., Lee, S. R., Geng, J. Z., & Li, H. K. (2013). Tracking source materials of Phanerozoic granitoids in South Korea by zircon Hf isotopes. Terra Nova, 25(3), 228–235. https://doi.org/10.1111/ter.12027

Cheong, C. S., Kim, N., Kim, J., Yi, K., Jeong, Y. J., Park, C. S., … Cho, M. (2014). Petrogenesis of Late Permian sodic metagranitoids in southeastern Korea: SHRIMP zircon geochronology and elemental and Nd–Hf isotope geochemistry. Journal of Asian Earth Sciences, 95, 228–242. https://doi.org/10.1016/j.jseaes.2014.06.005

Cheong, C. S., Kim, N., Jo, H. J., Cho, M., Choi, S. H., Zhou, H., & Geng, J. Z. (2015). Lithospheric mantle signatures as revealed by zircon Hf isotopes of Late Triassic post-collisional plutons from the central Korean peninsula, and their tectonic implications. Terra Nova, 27(2), 97–105. https://doi.org/10.1111/ter.12135

Darby, B. J., & Gehrels, G. (2006). Detrital zircon reference for the North China block. Journal of Asian Earth Sciences, 26(6), 637–648. https://doi. org/10.1016/j.jseaes.2004.12.005

Dickinson, W. R. (1985). Interpreting provenance relations from detrital modes of sandstones. In G. G. Zuffa (Eds.), Provenance of Arenites (pp. 333–361). Dordrecht, Netherlands: Reidel. https://doi.org/10.1007/978-94-017-2809-6_15

Dickinson, W. R., & Gehrels, G. E. (2009). Use of U–Pb ages of detrital zircons to infer maximum depositional ages of strata: A test against a Colorado Plateau Mesozoic database. Earth and Planetary Science Letters, 288(1-2), 115–125. https://doi.org/10.1016/j.epsl.2009.09.013

Dickinson, W. R., Beard, L. S., Brakenridge, G. R., Erjavec, J. L., Ferguson, R. C., Inman, K. F., … Ryberg, P. T. (1983). Provenance of North American Phanerozoic sandstones in relation to tectonic setting. Geological Society of America Bulletin, 94(2), 222–235.

Didenko, A., Khanchuk, A., Tikhomirova, A., & Voinova, I. (2014). Eastern segment of the Kiselevka-Manoma terrane (Northern Sikhote Alin): Paleomagnetism and geodynamic implications. Russian Journal of Pacific Geology, 8(1), 18–37. https://doi.org/10.1134/ S1819714014010023

Donskaya, T., Gladkochub, D., Mazukabzov, A., & Ivanov, A. (2013). Late Paleozoic–Mesozoic subduction-related magmatism at the southern margin of the Siberian continent and the 150 million-year history of the Mongol-Okhotsk Ocean. Journal of Asian Earth Sciences, 62, 79–97. https://doi.org/10.1016/j.jseaes.2012.07.023

Faure, M., Caridroit, M., & Charvet, J. (1986). The late Jurassic oblique collisional orogen of SW Japan—New structural data and synthesis. Tectonics, 5(7), 1089–1114. https://doi.org/10.1029/TC005i007p01089

Faure, M., Natal'In, B. A., Monie, P., Vrublevsky, A. A., Borukaiev, C., & Prikhodko, V. (1995). Tectonic evolution of the Anuy metamorphic rocks (Sikhote Alin, Russia) and their place in the Mesozoic geodynamic framework of East Asia. Tectonophysics, 241(3–4), 279–301. https://doi. org/10.1016/0040-1951(94)00186-D

Fernández, R. D., Catalán, J. R. M., Gerdes, A., Abati, J., Arenas, R., & Fernández-Suárez, J. (2010). U–Pb ages of detrital zircons from the Basal allochthonous units of NW Iberia: Provenance and paleoposition on the northern margin of Gondwana during the Neoproterozoic and Paleozoic. Gondwana Research, 18(2–3), 385–399. https://doi.org/10.1016/j.gr.2009.12.006

Fernandez-Suarez, J., Alonso, G. G., Cox, R., & Jenner, G. A. (2002). Assembly of the Armorica microplate: A strike-slip terrane delivery? Evidence from U-Pb ages of detrital zircons. The Journal of Geology, 110(5), 619–626. https://doi.org/10.1086/341760

Fujisaki, W., Isozaki, Y., Maki, K., Sakata, S., Hirata, T., & Maruyama, S. (2014). Age spectra of detrital zircon of the Jurassic clastic rocks of the Mino-Tanba AC belt in SW Japan: Constraints to the provenance of the mid-Mesozoic trench in East Asia. Journal of Asian Earth Sciences, 88, 62–73. https://doi.org/10.1016/j.jseaes.2014.02.006

Gehrels, G. (2014). Detrital zircon U-Pb geochronology applied to tectonics. Annual Review of Earth and Planetary Sciences, 42(1), 127–149. https://doi.org/10.1146/annurev-earth-050212-124012

Gilder, S. A., Leloup, P. H., Courtillot, V., Chen, Y., Coe, R. S., Zhao, X., … Zhu, R. (1999). Tectonic evolution of the Tancheng-Lujiang (Tan-Lu) fault via middle Triassic to Early Cenozoic paleomagnetic data. Journal of Geophysical Research, 104(B7), 15,365–15,390. https://doi.org/ 10.1029/1999JB900123

Golozoubov, V. V. (2006). Tectonics of the Jurassic and Lower Cretaceous Complexes of the North-Western Farming of the Pacific Ocean (p. 231). Vladivostok: Dal'nauka. (in Russian)

Golozoubov, V. V., Khanchuk, A. I., Kemkin, I. V., Panchenko, I. V., & Simanenko, V. P. (1992). Taukha and Zhuravlevka Terranes (South SikhoteAlin), (p. 83). Vladivostok: Preprint. (in Russian)

Golozoubov, V. V., Markevich, V. S., & Bugdaeva, E. (1999). Early Cretaceous changes of vegetation and environment in East Asia. Palaeogeography, Palaeoclimatology, Palaeoecology, 153(1–4), 139–146.

https://doi.org/10.1016/S0031-0182(99)00074-7

Grasse, S. W., Gehrels, G. E., Lahren, M. M., Schweickert, R. A., & Barth, A. P. (2001). U-Pb geochronology of detrital zircons from the Snow Lake pendant, central Sierra Nevada—Implications for Late Jurassic–Early Cretaceous dextral strike-slip faulting. Geology, 29(4), 307–310.

Grebennikov, A. V., Khanchuk, A. I., Gonevchuk, V. G., & Kovalenko, S. V. (2016). Cretaceous and Paleogene granitoid suites of the Sikhote-Alin area (Far East Russia): Geochemistry and tectonic implications. Lithos, 261, 250–261. https://doi.org/10.1016/j.lithos.2015.12.020

Griffin, W. L., Zhang, A., O'Reilly, S. Y., Ryan, C. G., Flower, M., Chung, S. L., … Lee, T. Y. (1998). Phanerozoic evolution of the lithosphere beneath the Sino-Korean Craton. In Mantle dynamics and plate interactions in East Asia, Geographical Series (Vol. 27, pp. 107–126). Washington, DC: American Geophysical Union.

Griffin, W., Belousova, E., Shee, S., Pearson, N., & O'reilly, S. (2004). Archean crustal evolution in the northern Yilgarn Craton: U–Pb and Hf- isotope evidence from detrital zircons. Precambrian Research, 131(3–4), 231–282. https://doi.org/10.1016/j.precamres.2003.12.011

Gutiérrez-Alonso, G., Fernández-Suárez, J., Jeffries, T., Jenner, G., Tubrett, M., Cox, R., & Jackson, S. (2003). Terrane accretion and dispersal in the northern Gondwana margin. An Early Paleozoic analogue of a long-lived active margin. Tectonophysics, 365(1–4), 221–232. https://doi. org/10.1016/S0040-1951(03)00023-4

Horie, K., Yamashita, M., Hayasaka, Y., Katoh, Y., Tsutsumi, Y., Katsube, A., … Cho, M. (2010). Eoarchean–Paleoproterozoic zircon inheritance in Japanese Permo-Triassic granites (Unazuki area, Hida Metamorphic Complex): Unearthing more old crust and identifying source terrranes. Precambrian Research, 183(1), 145–157. https://doi.org/10.1016/j.precamres.2010.06.014

Howell, D. G., Jones, D. L., & Schermer, E. R. (1985). Tectonostratigraphic Terranes of the Circum-Pacific Region. In D. G. Howell (Ed.), Tectonostratigraphic

terranes of the Circum-Pacific region. Circum-Pacific Council for Energy and Mineral Resources, Earth Science Series 1 (pp. 3–30). Houston, TX: AAPG.

Hu, Z., Liu, Y., Gao, S., Liu, W., Zhang, W., Tong, X., … Chen, H. (2012). Improved in situ Hf isotope ratio analysis of zircon using newly designed X skimmer cone and jet sample cone in combination with the addition of nitrogen by laser ablation multiple collector ICP-MS. Journal of Analytical Atomic Spectrometry, 27(9), 1391–1399. https://doi.org/10.1039/c2ja30078h

Iizuka, T., Yamaguchi, T., Hibiya, Y., & Amelin, Y. (2015). Meteorite zircon constraints on the bulk Lu—Hf isotope composition and early differentiation of the Earth. Proceedings of the National Academy of Sciences, 112(17), 5331–5336. https://doi.org/10.1073/pnas.1501658112

Isozaki, Y. (1997). Contrasting two types of orogen in Permo-Triassic Japan: Accretionary versus collisional. Island Arc, 6(1), 2–24. https://doi.org/10.1111/j.1440-1738.1997.tb00038.x

Isozaki, Y., Maruyama, S., & Furuoka, F. (1990). Accreted oceanic materials in Japan. Tectonophysics, 181(1–4), 179–205. https://doi.org/ 10.1016/0040-1951(90)90016-2

Isozaki, Y., Aoki, K., Nakama, T., & Yanai, S. (2010). New insight into a subduction-related orogen: A reappraisal of the geotectonic framework and evolution of the Japanese Islands. Gondwana Research, 18(1), 82–105. https://doi.org/10.1016/j.gr.2010.02.015

Jahn, B. M. (2010). Accretionary orogen and evolution of the Japanese Islands: Implications from a Sr-Nd isotopic study of the Phanerozoic granitoids from SW Japan. American Journal of Science, 310(10), 1210–1249.

Jahn, B. M., Valui, G., Kruk, N., Gonevchuk, V., Usuki, M., & Wu, J. T. (2015). Emplacement ages, geochemical and Sr–Nd–Hf isotopic characterization of Mesozoic to early Cenozoic granitoids of the Sikhote-Alin Orogenic Belt, Russian Far East: Crustal growth and regional tectonic evolution. Journal of Asian Earth Sciences, 111, 872–918. https://doi.org/10.1016/j.jseaes.2015.08.012

Jia, J., Zheng, H., Huang, X., Wu, F., Yang, S., Wang, K., & He, M. (2010). Detrital

zircon U-Pb ages of Late Cenozoic sediments from the Yangtze delta: Implication for the evolution of the Yangtze River. Chinese Science Bulletin, 55(15), 1520–1528. https://doi.org/10.1007/s11434-010- 3091-x

Kato, K., & Saka, Y. (2003). Kurosegawa terrane as a transform fault zone in southwest Japan. Gondwana Research, 6(4), 669–686. https://doi. org/10.1016/S1342-937X(05)71016-9

Kato, K., & Saka, Y. (2006). New model for the Early Cretaceous development of SW Japan based on basic rocks of the Chichibu Composite Terrane. Geosciences Journal, 10(3), 275–289. https://doi.org/10.1007/BF02910370

Kemkin, I. (2008). Structure of terranes in a Jurassic accretionary prism in the Sikhote-Alin-Amur area: Implications for the Jurassic geodynamic history of the Asian eastern margin. Russian Geology and Geophysics, 49(10), 759–770. https://doi.org/10.1016/j.rgg.2007.12.014

Kemkin, I., & Kemkina, R. (2000). Jurassic-Early Cretaceous biostratigraphic cherty and terrigenous deposits of the Dalnegorsk Ore region (Southern Sikhote-Alin). Geology of the Pacific Ocean, 15(1), 85–106.

Kemkin, I. V., & Kemkina, R. A. (2015). Geochemistry of chert rocks from the Sikhote-Alin Taukha terrane, Russia far east: Significance for determination of their depositional environment. Environmental Earth Sciences, 73(5), 2253–2268. https://doi.org/10.1007/s12665-014-3574-1

Kemkin, I., Filippov, A., & Khanchuk, A. (2006). New data on the structure of the Khabarovsk Terrane of the Jurassic accretionary prism (Sikhote-Alin). Doklady Earth Sciences, 406(1), 28–31. https://doi.org/10.1134/S1028334X06010089

Kemkin, I., Khanchuk, A., & Kemkina, R. (2016). Accretionary prisms of the Sikhote-Alin Orogenic Belt: Composition, structure and significance for reconstruction of the geodynamic evolution of the eastern Asian margin. Journal of Geodynamics, 102, 202–230. https://doi.org/ 10.1016/j.jog.2016.10.002

Khanchuk, A. I. (2001). Pre-Neogene tectonics of the Sea-of-Japan region: A view from the Russian side. Earth Science, 55(5), 275–291. Khanchuk, A. I. (Ed.) (2006). Geodynamics, Magmatism and Metallogeny of the Russian East, Book1

(p. 572). Vladivostok: Dal'nauka. (in Russian)

Khanchuk, A. I., Didenko, A. N., Popeko, L. I., Sorokin, A. A., & Shevchenko, B. F. (2015). Structure and evolution of the Mongol-Okhotsk Orogenic Belt. In A. Kroner (Ed.), The Central Asian Orogenic Belt. Contributions to the Regional Geology of the Earth (pp. 211–234). Stuttgart, Germany: E. Schweitzerbart Science Publishers.

Khanchuk, A. I., Didenko, A. N., Tikhomirova, A. I., & Voinova, I. P. (2015). Paleomagnetism and geochemistry of the Kiselevka block of the Kiselevka-Manoma terrane (northern Sikhote-Alin): Geodynamic significance. Geological Society of America Special Papers, 513, 513–514.

Khanchuk, A. I., Kemkin, I. V., & Kruk, N. N. (2016). The Sikhote-Alin orogenic belt, Russian South East: Terranes and the formation of continental lithosphere based on geological and isotopic data. Journal of Asian Earth Sciences, 120, 117–138. https://doi.org/10.1016/ j.jseaes.2015.10.023

Khanchuk, A. I., Ratkin, V. V., Ryazantseva, M. D., Golozubov, V. V., & Gonokhova, N. G. (1996). Geology and Mineral Deposits of Primorskiy Krai, (p. 61). Dalnauka: Vladivostok.

Khanchuk, A. I., & Vysotskiy, S. (2016). Different-depth gabbro–ultrabasite associations in the Sikhote-Alin ophiolites (Russian Far East). Russian Geology and Geophysics, 57(1), 141–154. https://doi.org/10.1016/j.rgg.2016.01.010

Kim, S. W., Williams, I. S., Kwon, S., & Oh, C. W. (2008). SHRIMP zircon geochronology, and geochemical characteristics of metaplutonic rocks from the south-western Gyeonggi Block, Korea: Implications for Paleoproterozoic to Mesozoic tectonic links between the Korean Peninsula and eastern China. Precambrian Research, 162(3–4), 475–497. https://doi.org/10.1016/j.precamres.2007.10.006

Kim, J., Yi, K., Jeong, Y. J., & Cheong, C. S. (2011). Geochronological and geochemical constraints on the petrogenesis of Mesozoic high-K granitoids in the central Korean peninsula. Gondwana Research, 20(2–3), 608–620.

https://doi.org/10.1016/j.gr.2010.12.005

Kim, S. W., Kwon, S., Koh, H. J., Yi, K., Jeong, Y. J., & Santosh, M. (2011). Geotectonic framework of Permo–Triassic magmatism within the Korean Peninsula. Gondwana Research, 20(4), 865–889. https://doi.org/10.1016/j.gr.2011.05.005

Kim, S. W., Kwon, S., Park, S. I., Yi, K., Santosh, M., & Ryu, I. C. (2015). Early to Middle Paleozoic arc magmatism in the Korean Peninsula: Constraints from zircon geochronology and geochemistry. Journal of Asian Earth Sciences, 113, 866–882. https://doi.org/10.1016/ j.jseaes.2015.09.017

Kimura, T. (1979). Late Mesozoic palaeofloristic provinces in east Asia. Proceedings of the Japan Academy, Series B Physical and Biological Sciences, 55(9), 425–430. https://doi.org/10.2183/pjab.55.425

Kimura, T., Ohana, T., & Mimoto, K. (1988). Discovery of a podocarpaceous plant from the Lower Cretaceous of Kochi Prefecture, in the Outer Zone of southwest Japan. Proceedings of the Japan Academy, Series B, 64(8), 213–216.

Kimura, T. (2000). Early Cretaceous climatic provinces in Japan and adjacent regions on the basis. Cretaceous Environments of Asia, 17, 155. https://doi.org/10.1016/S0920-5446(00)80029-1

Kirillova, G. L. (2003). Cretaceous tectonics and geological environments in East Russia. Journal of Asian Earth Sciences, 21(8), 967–977. https:// doi.org/10.1016/S1367-9120(02)00093-7

Kojima, S. (1989). Mesozoic terrane accretion in northeast China, Sikhote-Alin and Japan regions. Palaeogeography, Palaeoclimatology, Palaeoecology, 69, 213–232. https://doi.org/10.1016/0031-0182(89)90165-X

Kojima, S., Igor'V, K., Kametaka, M., & Ando, A. (2000). A correlation of accretionary complexes of southern Sikhote-Alin of Russia and the Inner Zone of Southwest Japan. Geosciences Journal, 4(3), 175–185. https://doi.org/10.1007/BF02910136

Kojima, S., Tsukada, K., Otoh, S., Yamakita, S., Ehiro, M., Dia, C., … Eichwald, L. P. (2008). Geological relationship between Anyui metamorphic complex and

Samarka terrane, Far East Russia. Island Arc, 17(4), 502–516. https://doi.org/10.1111/j.1440-1738.2008.00644.x

Kravchinsky, V. A., Cogné, J.-P., Harbert, W. P., & Kuzmin, M. I. (2002). Evolution of the Mongol-Okhotsk Ocean as constrained by new palaeomagnetic data from the Mongol-Okhotsk suture zone, Siberia. Geophysical Journal International, 148(1), 34–57. https://doi.org/ 10.1046/j.1365-246x.2002.01557.x

Kruk, N. N., Simanenko, V. P., Golozubov, V. V., Kovach, V. P., Vladimirov, V. G., & Kasatkin, S. A. (2014). Geochemistry of rocks in the Anuy metamorphic dome, Sikhote-Alin: Composition of the protoliths and the possible nature of metamorphism. Geochemistry International, 52(3), 229–246. https://doi.org/10.1134/S0016702914010030

Kusky, T., Windley, B., & Zhai, M. G. (2007). Tectonic evolution of the North China Block: From orogen to craton to orogen. Geological Society, London, Special Publications, 280(1), 1–34. https://doi.org/10.1144/SP280.1

Lee, D. W. (1999). Strike–slip fault tectonics and basin formation during the Cretaceous in the Korean Peninsula. Island Arc, 8(2), 218–231. https://doi.org/10.1046/j.1440-1738.1999.00233.x

Lee, K. S., Chang, H. W., & Park, K. H. (1998). Neoproterozoic bimodal volcanism in the central Ogcheon belt, Korea: Age and tectonic implication. Precambrian Research, 89(1–2), 47–57. https://doi.org/10.1016/S0301-9268(97)00077-6

Lee, S. R., Cho, M., Cheong, C. S., Kim, H., & Wingate, M. T. (2003). Age, geochemistry, and tectonic significance of Neoproterozoic alkaline granitoids in the northwestern margin of the Gyeonggi massif, South Korea. Precambrian Research, 122(1–4), 297–310. https://doi.org/ 10.1016/S0301-9268(02)00216-4

Lee, T. H., Park, K. H., Yi, K., Geng, J. Z., & Li, H. K. (2015). SHRIMP U-Pb ages and Hf isotopic composition of the detrital zircons from the Myogok Formation, SE Korea: Development of terrestrial basin and igneous activity during the early Cretaceous. Geosciences Journal, 19(2), 189–203. https://doi.org/10.1007/s12303-014-0042-6

Li, H. Y., & Huang, X. L. (2013). Constraints on the paleogeographic evolution of the

North China Craton during the Late Triassic–Jurassic. Journal of Asian Earth Sciences, 70, 308–320.

Li, Z. X., & Li, X. H. (2007). Formation of the 1300-km-wide intracontinental orogen and postorogenic magmatic province in Mesozoic South China: A flat-slab subduction model. Geology, 35(2), 179–182. https://doi.org/10.1130/G23193A.1

Li, Z., Li, X., Kinny, P., & Wang, J. (1999). The breakup of Rodinia: Did it start with a mantle plume beneath South China? Earth and Planetary Science Letters, 173(3), 171–181. https://doi.org/10.1016/S0012-821X(99)00240-X

Li, Z. X., Li, X. H., Zhou, H., & Kinny, P. D. (2002). Grenvillian continental collision in south China: New SHRIMP U-Pb zircon results and implications for the configuration of Rodinia. Geology, 30(2), 163–166.

Li, X. H., Li, Z. X., Zhou, H., Liu, Y., & Kinny, P. D. (2002). U–Pb zircon geochronology, geochemistry and Nd isotopic study of Neoproterozoic bimodal volcanic rocks in the Kangdian Rift of South China: Implications for the initial rifting of Rodinia. Precambrian Research, 113(1–2), 135–154. https://doi.org/10.1016/S0301-9268(01)00207-8

Li, S. Z., Zhao, G. C., Sun, M., Wu, F. Y., Liu, J. Z., Hao, D. F., … Luo, Y. (2004). Mesozoic, not Paleoproterozoic SHRIMP U–Pb zircon ages of two Liaoji granites, Eastern Block, North China Craton. International Geology Review, 46(2), 162–176. https://doi.org/10.2747/0020- 6814.46.2.162

Li, S. Z., Zhao, G. C., Sun, M., Wu, F. Y., Hao, D. F., Han, Z. Z., … Xia, X. P. (2005). Deformational history of the Paleoproterozoic Liaohe Group in the Eastern Block of the North China Craton. Journal of Asian Earth Sciences, 24, 654–669.

Li, S. Z., Zhao, G. C., Sun, M., Zhao, G. T., & Hao, D. F. (2006). Are the South and North Liaohe Groups of the North China Craton different exotic terranes? Nd isotope constraints. Gondwana Research, 9(1–2), 198–208. https://doi.org/10.1016/j.gr.2005.06.011

Li, Z. X., Li, X. H., Chung, S. L., Lo, C. H., Xu, X., & Li, W. X. (2012). Magmatic switch-on and switch-off along the South China continental margin since the Permian: Transition from an Andean-type to a Western Pacific-type plate

boundary. Tectonophysics, 532, 271–290.

Liu, F., & Liou, J. (2011). Zircon as the best mineral for P–T–time history of UHP metamorphism: A review on mineral inclusions and U–Pb SHRIMP ages of zircons from the Dabie–Sulu UHP rocks. Journal of Asian Earth Sciences, 40(1), 1–39. https://doi.org/10.1016/ j.jseaes.2010.08.007

Liu, Y., Hu, Z., Zong, K., Gao, C., Gao, S., Xu, J., & Chen, H. (2010). Reappraisement and refinement of zircon U-Pb isotope and trace element analyses by LA-ICP-MS. Chinese Science Bulletin, 55(15), 1535–1546. https://doi.org/10.1007/s11434-010-3052-4

Liu, K., Zhang, J., Wilde, S. A., Zhou, J., Wang, M., Ge, M., … Ling, Y. (2017). Initial subduction of the Paleo-Pacific Oceanic plate in NE China: Constraints from whole-rock geochemistry and zircon U–Pb and Lu–Hf isotopes of the Khanka Lake granitoids. Lithos, 274–275, 254–270. https://doi.org/10.1016/j.lithos.2016.12.022

Luan, J. P., Wang, F., Xu, W. L., Ge, W. C., Sorokin, A. A., Wang, Z. W., & Guo, P. (2017). Provenance, age, and tectonic implications of Neoproterozoic strata in the Jiamusi Massif: evidence from U–Pb ages and Hf isotope compositions of detrital and magmatic zircons. Precambrian Research, 297, 19–32.

Ludwig, K. (2001). Isoplot 3.0—A geochronological toolkit for Microsoft Excel, Special Publication No. 4, Berkeley Geochronology Center, Berkeley, Calif.

Malinovsky, A., & Golozubov, V. (2011). Lithology and depositional settings of the terrigenous sediments along transform plate boundaries: Evidence from the early cretaceous Zhuravlevka terrane in Southern Sikhote Alin. Russian Journal of Pacific Geology, 5(5), 400–417. https:// doi.org/10.1134/S1819714011050058

Maruyama, S. (1997). Pacific-type orogeny revisited: Miyashiro-type orogeny proposed. Island Arc, 6(1), 91–120. https://doi.org/10.1111/ j.1440-1738.1997.tb00042.x

Meng, E., Xu, W., Yang, D., Pei, F., Yu, Y., & Zhang, X. (2008). Permian volcanisms in eastern and southeastern margins of the Jiamusi Massif, northeastern China: Zircon U-Pb chronology, geochemistry and its tectonic implications. Chinese

Science Bulletin, 53(8), 1231–1245.

Meng, E., Xu, W., Pei, F., Yang, D., Wang, F., & Zhang, X. (2011). Permian bimodal volcanism in the Zhangguangcai Range of eastern Heilongjiang Province, NE China: Zircon U–Pb–Hf isotopes and geochemical evidence. Journal of Asian Earth Sciences, 41(2), 119–132. https://doi.org/10.1016/j.jseaes.2011.01.005

Menzies, M. A., Fan, W., & Zhang, M. (1993). Palaeozoic and Cenozoic lithoprobes and the loss of >120 km of Archaean lithosphere,

Sino-Korean craton, China. Geological Society, London, Special Publications, 76(1), 71–81. https://doi.org/10.1144/GSL.SP.1993.076.01.04 Menzies, M., Xu, Y., Zhang, H., & Fan, W. (2007). Integration of geology, geophysics and geochemistry: A key to understanding the North China Craton. Lithos, 96(1–2), 1–21. https://doi.org/10.1016/j.lithos.2006.09.008

Miao, L., Zhang, F., Zhu, M., & Liu, D. (2015). Zircon SHRIMP U–Pb dating of metamorphic complexes in the conjunction of the Greater and Lesser Xing'an ranges, NE China: Timing of formation and metamorphism and tectonic implications. Journal of Asian Earth Sciences, 114, 634–648. https://doi.org/10.1016/j.jseaes.2014.09.035

Mizutani, S. (1987). Mesozoic terranes in the Japanese Islands and neighbouring East Asia. In E. Scheibner (Eds). Terrane accretion and orogenic belts, American Geophysical Union, Geodynamic Series 19, (pp. 263–273). https://doi.org/10.1029/GD019p0263

Müller, R. D., Sdrolias, M., Gaina, C., Steinberger, B., & Heine, C. (2008). Long-term sea-level fluctuations driven by ocean basin dynamics. Science, 319(5868), 1357–1362. https://doi.org/10.1126/science.1151540

Nakama, T., Hirata, T., Otoh, S., Aoki, K., Yanai, S., & Maruyama, S. (2010). Paleogeography of the Japanese Islands: Age spectra of detrital zircon and provenance history of the orogen. Journal of Geography, 119(6), 1161–1172. https://doi.org/10.5026/jgeography.119.1161

Natal'in, B. (1993). History and modes of Mesozoic accretion in southeastern Russia. Island Arc, 2(1), 15–34. https://doi.org/10.1111/ j.1440-1738.1993.tb00072.x

Peng, P., Zhai, M., Ernst, R. E., Guo, J., Liu, F., & Hu, B. (2008). A 1.78 Ga large igneous province in the North China craton: The Xiong'er Volcanic Province and the North China dyke swarm. Lithos, 101(3–4), 260–280. https://doi.org/10.1016/j.lithos.2007.07.006

Peng, P., Bleeker, W., Ernst, R. E., Söderlund, U., & McNicoll, V. (2011). U–Pb baddeleyite ages, distribution and geochemistry of 925Ma mafic dykes and 900Ma sills in the North China craton: Evidence for a Neoproterozoic mantle plume. Lithos, 127(1–2), 210 – 221. https://doi.org/ 10.1016/j.lithos.2011.08.018

Qi, G., Zhang, J., & Wang, M. (2015). Mesozoic tectonic setting of rift basins in eastern North China and implications for destruction of the North China Craton. Journal of Asian Earth Sciences, 111, 414–427. https://doi.org/10.1016/j.jseaes.2015.06.022

Qiu, Y. M., Gao, S., McNaughton, N. J., Groves, D. I., & Ling, W. (2000). First evidence of> 3.2 Ga continental crust in the Yangtze craton of south China and its implications for Archean crustal evolution and Phanerozoic tectonics. Geology, 28(1), 11–14.

Rojas-Agramonte, Y., Kröner, A., Demoux, A., Xia, X., Wang, W., Donskaya, T., … Sun, M. (2011). Detrital and xenocrystic zircon ages from Neoproterozoic to Palaeozoic arc terranesof Mongolia: Significance for the origin of crustal fragments in the Central Asian Orogenic Belt. Gondwana Research, 19(3), 751–763. https://doi.org/10.1016/j.gr.2010.10.004

Rowley, D. B., Raymond, A., Parrish, J. T., Lottes, A. L., Scotese, C. R., & Ziegler, A. M. (1985). Carboniferous paleogeographic, phytogeographic, and paleoclimatic reconstructions. International Journal of Coal Geology, 5(1–2), 7–42. https://doi.org/10.1016/0166-5162(85)90009-6

Sano, Y., Hidaka, H., Terada, K., Shimizu, H., & Suzuki, M. (2000). Ion microprobe U-Pb zircon geochronology of the Hida gneiss: Finding of the oldest minerals in Japan. Geochemical Journal, 34(2), 135–153. https://doi.org/10.2343/geochemj.34.135

Segal, I., Halicz, L., & Platzner, I. T. (2003). Accurate isotope ratio measurements of

ytterbium by multiple collection inductively coupled plasma mass spectrometry applying erbium and hafnium in an improved double external normalization procedure. Journal of Analytical Atomic Spectrometry, 18(10), 1217–1223. https://doi.org/10.1039/b307016f

Sengör, A. C., & Natal'In, B. A. (1996). Turkic-type orogeny and its role in the making of the continental crust. Annual Review of Earth and Planetary Sciences, 24(1), 263–337. https://doi.org/10.1146/annurev.earth.24.1.263

Şengör, A., Natal'In, B., & Burtman, V. (1993). Evolution of the Altaid tectonic collage and Palaeozoic crustal growth in Eurasia. Nature, 364, 22.

Shao, J., & Tang, K. (1995). Terranes in Northeast China and Evolution of Northeast Asia Continental Margin, edited, Seismic Press, Beijing.

Söderlund, U., Patchett, P. J., Vervoort, J. D., & Isachsen, C. E. (2004). The 176 Lu decay constant determined by Lu–Hf and U–Pb isotope systematics of Precambrian mafic intrusions. Earth and Planetary Science Letters, 219(3–4), 311–324. https://doi.org/10.1016/S0012- 821X(04)00012-3

Song, S., Wang, M. M., Xu, X., Wang, C., Niu, Y., Allen, M. B., & Su, L. (2015). Ophiolites in the Xing'an-Inner Mongolia accretionary belt of the CAOB: Implications for two cycles of seafloor spreading and accretionary orogenic events. Tectonics, 34, 2221–2248. https://doi.org/ 10.1002/2015TC003948

Sun, M. D., Xu, Y. G., Wilde, S. A., & Chen, H. L. (2015). Provenance of Cretaceous trench slope sediments from the Mesozoic Wandashan Orogen, NE China: Implications for determining ancient drainage systems and tectonics of the Paleo-Pacific. Tectonics, 34, 1269–1289. https://doi.org/10.1002/2015TC003870

Sun, M. D., Xu, Y. G., Wilde, S. A., Chen, H. L., & Yang, S. F. (2015). The Permian Dongfanghong island-arc gabbro of the Wandashan Orogen, NE China: Implications for Paleo-Pacific subduction. Tectonophysics, 659, 122–136. https://doi.org/10.1016/j.tecto.2015.07.034

Taira, A. (2001). Tectonic evolution of the Japanese island arc system. Annual Review of Earth and Planetary Sciences, 29(1), 109–134. https://doi.org/10.1146/annurev.earth.29.1.109

Tang, J., Xu, W., Niu, Y., Wang, F., Ge, W., Sorokin, A. A., & Chekryzhov, I. Y. (2016). Geochronology and geochemistry of Late Cretaceous– Paleocene granitoids in the Sikhote-Alin Orogenic Belt: Petrogenesis and implications for the oblique subduction of the paleo-Pacific plate. Lithos, 266, 202–212.

Tsutsumi, Y., Yokoyama, K., Kasatkin, S. A., & Golozubov, V. V. (2016). Provenance study of accretionary complexes in Primorye, Far East Russia, using ages and compositions of detrital minerals. Memoirs of the National Museum of Nature and Science, 51, 79–87.

Turek, A., & Kim, C.-B. (1996). U-Pb zircon ages for Precambrian rocks in southwestern Ryeongnam and southwestern Gyeonggi massifs, Korea. Geochemical Journal, 30(4), 231–249. https://doi.org/10.2343/geochemj.30.231

Utkin, V. (1993). Wrench faults of Sikhote-Alin and accretionary and destructive types of fault dislocation in the Asia-Pacific transition zone. The Tancheng-Lujiang wrench fault system, 225–237.

Utkin, V. (2013). Shear structural paragenesis and its role in continental rifting of the East Asian margin. Russian Journal of Pacific Geology, 7(3), 167–188. https://doi.org/10.1134/S181971401303007X

Vakhrameev, V. (1987). Climates and the distribution of some gymsosperms in Asia during the Jurassic and Cretaceous. Review of Palaeobotany and Palynology, 51(1–3), 205–212. https://doi.org/10.1016/0034-6667(87)90030-3

Van Achterbergh, E., Ryan, C., & Griffin, W. (2001). GLITTER On-Line Interactive Data Reduction for the LA-ICPMS Microprobe. Sydney: Macquarie Research Ltd.

Wang, Q., Deng, J., Li, C., Li, G., Yu, L., & Qiao, L. (2014). The boundary between the Simao and Yangtze blocks and their locations in Gondwana and Rodinia: Constraints from detrital and inherited zircons. Gondwana Research, 26(2), 438–448. https://doi.org/10.1016/ j.gr.2013.10.002

Wang, J., Chang, S.-C., Lu, H.-B., & Zhang, H.-C. (2016). Detrital zircon provenance of the Wangshi and Laiyang groups of the Jiaolai basin: Evidence for Early Cretaceous uplift of the Sulu orogen, Eastern China. International Geology

Review, 58(6), 719–736. https://doi.org/ 10.1080/00206814.2015.1105728

Wilde, S. A. (2015). Final amalgamation of the Central Asian Orogenic Belt in NE China: Paleo-Asian Ocean closure versus Paleo-Pacific plate subduction—A review of the evidence. Tectonophysics, 662, 345–362. https://doi.org/10.1016/j.tecto.2015.05.006

Wilde, S., Dorsett-Bain, H., & Liu, J. (1997). The identification of a Late Pan-African granulite facies event in northeastern China: SHRIMP U–Pb zircon dating of the Mashan Group at Liu Mao, Heilongjiang Province, China. Proceedings of the 30th IGC: Precambrian Geology and Metamorphic Petrology, 17, 59–74.

Wilde, S. A., Dorsett-Bain, H. L., & Lennon, R. G. (1999). Geological setting and controls on the development of graphite, sillimanite and phosphate mineralization within the Jiamusi Massif: An exotic fragment of Gondwanaland located in north-eastern China? Gondwana Research, 2(1), 21–46. https://doi.org/10.1016/S1342-937X(05)70125-8

Wilde, S. A., Zhang, X., & Wu, F. (2000). Extension of a newly identified 500Ma metamorphic terrane in North East China: Further U–Pb SHRIMP dating of the Mashan Complex, Heilongjiang Province, China. Tectonophysics, 328(1–2), 115–130. https://doi.org/10.1016/S0040- 1951(00)00180-3

Wilde, S. A., Zhao, G., & Sun, M. (2002). Development of the North China Craton during the late Archaean and its final amalgamation at 1.8 Ga: Some speculations on its position within a global Palaeoproterozoic supercontinent. Gondwana Research, 5(1), 85–94. https://doi.org/ 10.1016/S1342-937X(05)70892-3

Wilde, S. A., Wu, F., & Zhang, X. (2003). Late Pan-African magmatism in northeastern China: SHRIMP U–Pb zircon evidence from granitoids in the Jiamusi Massif. Precambrian Research, 122(1–4), 311–327. https://doi.org/10.1016/S0301-9268(02)00217-6

Windley, B. F., Alexeiev, D., Xiao, W., Kröner, A., & Badarch, G. (2007). Tectonic models for accretion of the Central Asian Orogenic Belt. Journal of the Geological Society, 164(1), 31–47. https://doi.org/10.1144/0016-76492006-022

Wu, Y. B., & Zheng, Y. F. (2013). Tectonic evolution of a composite collision orogen:

An overview on the Qinling–Tongbai–Hong'an–Dabie– Sulu orogenic belt in central China. Gondwana Research, 23(4), 1402–1428. https://doi.org/10.1016/j.gr.2012.09.007

Wu, F. Y., Jahn, B. M., Wilde, S. A., Lo, C. H., Yui, T. F., Lin, Q., … Sun, D. Y. (2003a). Highly fractionated I-type granites in NE China (I): Geochronology and petrogenesis. Lithos, 66(3–4), 241–273. https://doi.org/10.1016/S0024-4937(02)00222-0

Wu, F. Y., Jahn, B. M., Wilde, S. A., Lo, C. H., Yui, T. F., Lin, Q., … Sun, D. Y. (2003b). Highly fractionated I-type granites in NE China (II): Isotopic geochemistry and implications for crustal growth in the Phanerozoic. Lithos, 67(3–4), 191–204. https://doi.org/10.1016/S0024- 4937(03)00015-X

Wu, F. Y., Han, R. H., Yang, J. H., Wilde, S. A., Zhai, M. G., & Park, S. C. (2007). Initial constraints on the timing of granitic magmatism in North Korea using U–Pb zircon geochronology. Chemical Geology, 238(3–4), 232–248. https://doi.org/10.1016/j.chemgeo.2006.11.012

Wu, F. Y., Yang, J. H., Lo, C. H., Wilde, S. A., Sun, D. Y., & Jahn, B. M. (2007). The Heilongjiang Group: A Jurassic accretionary complex in the Jiamusi Massif at the western Pacific margin of northeastern China. Island Arc, 16(1), 156–172. https://doi.org/10.1111/j.1440- 1738.2007.00564.x

Wu, F. Y., Yang, J. H., Wilde, S. A., Liu, X. M., Guo, J. H., & Zhai, M. G. (2007). Detrital zircon U–Pb and Hf isotopic constraints on the crustal evolution of North Korea. Precambrian Research, 159(3–4), 155–177. https://doi.org/10.1016/j.precamres.2007.06.007

Wu, F. Y., Zhang, Y. B., Yang, J. H., Xie, L. W., & Yang, Y. H. (2008). Zircon U–Pb and Hf isotopic constraints on the Early Archean crustal evolution in Anshan of the North China Craton. Precambrian Research, 167(3–4), 339–362. https://doi.org/10.1016/j.precamres.2008.10.002

Wu, F. Y., Sun, D. Y., Ge, W. C., Zhang, Y. B., Grant, M. L., Wilde, S. A., & Jahn, B. M. (2011). Geochronology of the Phanerozoic granitoids in northeastern China. Journal of Asian Earth Sciences, 41(1), 1–30.

https://doi.org/10.1016/j.jseaes.2010.11.014

Wyld, S. J., & Wright, J. E. (2001). New evidence for Cretaceous strike-slip faulting in the United States Cordillera and implications for terrane- displacement, deformation patterns, and plutonism. American Journal of Science, 301(2), 150–181. https://doi.org/10.2475/ajs.301.2.150

Xiao, W., Windley, B. F., Hao, J., & Zhai, M. (2003). Accretion leading to collision and the Permian Solonker suture, Inner Mongolia, China: termination of the central Asian orogenic belt. Tectonics, 22(6), 1069. https://doi.org/10.1029/2002TC001484

Xu, J. W., & Zhu, G. (1994). Tectonic models of the Tan-Lu fault zone, eastern China. International Geology Review, 36(8), 771–784.

Xu, J., Zhu, G., Tong, W., Cui, K., & Liu, Q. (1987). Formation and evolution of the Tancheng-Lujiang wrench fault system: A major shear system to the northwest of the Pacific Ocean. Tectonophysics, 134(4), 273–310. https://doi.org/10.1016/0040-1951(87)90342-8

Xu, W. L., Pei, F. P., Wang, F., Meng, E., Ji, W. Q., Yang, D. B., & Wang, W. (2013). Spatial–temporal relationships of Mesozoic volcanic rocks in NE China: Constraints on tectonic overprinting and transformations between multiple tectonic regimes. Journal of Asian Earth Sciences, 74, 167–193. https://doi.org/10.1016/j.jseaes.2013.04.003

Xu, B., Zhao, P., Wang, Y., Liao, W., Luo, Z., Bao, Q., & Zhou, Y. (2015). The pre-Devonian tectonic framework of Xing'an–Mongolia orogenic belt (XMOB) in north China. Journal of Asian Earth Sciences, 97, 183–196. https://doi.org/10.1016/j.jseaes.2014.07.020

Yabe, A., Terada, K., & Sekido, S. (2003). The Tetori-type flora, revised: A review. Memoir of the Fukui Prefectural Dinosaur Museum, 2, 23–42. Yang, J. H., Wu, F. Y., Shao, J. A., Wilde, S. A., Xie, L. W., & Liu, X. M. (2006). Constraints on the timing of uplift of the Yanshan Fold and Thrust

Belt, North China. Earth and Planetary Science Letters, 246(3–4), 336–352. https://doi.org/10.1016/j.epsl.2006.04.029

Yang, J. H., Wu, F. Y., Wilde, S. A., Belousova, E., & Griffin, W. L. (2008). Mesozoic decratonization of the North China block. Geology, 36(6), 467–470. https://doi.org/10.1130/G24518A.1

Yang, J., Gao, S., Chen, C., Tang, Y., Yuan, H., Gong, H., … Wang, J. (2009). Episodic crustal growth of North China as revealed by U–Pb age and Hf isotopes of detrital zircons from modern rivers. Geochimica et Cosmochimica Acta, 73(9), 2660–2673. https://doi.org/10.1016/ j.gca.2009.02.007

Yang, S., Zhang, F., & Wang, Z. (2012). Grain size distribution and age population of detrital zircons from the Changjiang (Yangtze) River system, China. Chemical Geology, 296, 26–38.

Yang, H., Ge, W., Zhao, G., Yu, J., & Zhang, Y. (2015). Early Permian–Late Triassic granitic magmatism in the Jiamusi–Khanka Massif, eastern segment of the Central Asian Orogenic Belt and its implications. Gondwana Research, 27(4), 1509–1533. https://doi.org/10.1016/j. gr.2014.01.011

Yang, H., Ge, W., Zhao, G., Bi, J., Wang, Z., Dong, Y., & Xu, W. (2017). Zircon U–Pb ages and geochemistry of newly discovered Neoproterozoic orthogneisses in the Mishan region, NE China: Constraints on the high-grade metamorphism and tectonic affinity of the Jiamusi–Khanka Block. Lithos, 268, 16–31.

Yin, A., & Nie, S. (1993). An indentation model for the North and South China collision and the development of the Tan-Lu and Honam fault systems, eastern Asia. Tectonics, 12(4), 801–813. https://doi.org/10.1029/93TC00313

Yu, J., Wang, F., Xu, W., Gao, F., & Pei, F. (2012). Early Jurassic mafic magmatism in the Lesser Xing'an–Zhangguangcai Range, NE China, and its tectonic implications: Constraints from zircon U–Pb chronology and geochemistry. Lithos, 142, 256–266.

Yu, J., Hou, X., Zhang, Y., & Liu, J. (2013). Magma mixing genesis of the Early Permian Liulian pluton at the northeastern margin of the Jiamusi massif in NE China: Evidence from petrology, geochronology and geochemistry. Acta

Petrologica Sinica, 29(9), 2971–2986.

Yui, T., Maki, K., Lan, C., Hirata, T., Chu, H., Kon, Y., … Ernst, W. (2012). Detrital zircons from the Tananao metamorphic complex of Taiwan: Implications for sediment provenance and Mesozoic tectonics. Tectonophysics, 541, 31–42.

Zhai, M. G., & Santosh, M. (2011). The early Precambrian odyssey of the North China Craton: A synoptic overview. Gondwana Research, 20(1), 6–25. https://doi.org/10.1016/j.gr.2011.02.005

Zhai, M. G., Guo, J. H., Peng, P., & Hu, B. (2007). U-Pb zircon age dating of a rapakivi granite batholith in Rangnim massif, North Korea. Geological Magazine, 114, 547–552.

Zhang, Q. S., & Yang, Z. S. (1988). Early Crust and Mineral Deposits of Liaodong Peninsula, China. Beijing: Geological Publishing House.

Zhang, S. H., Zhao, Y., Song, B., Yang, Z. Y., Hu, J. M., & Wu, H. (2007). Carboniferous granitic plutons from the northern margin of the North China block: Implications for a late Palaeozoic active continental margin. Journal of the Geological Society, 164(2), 451–463. https://doi.org/ 10.1144/0016-76492005-190

Zhang, R., Liou, J., & Ernst, W. (2009). The Dabie–Sulu continental collision zone: A comprehensive review. Gondwana Research, 16(1), 1–26. https://doi.org/10.1016/j.gr.2009.03.008

Zhang, S. H., Zhao, Y., Song, B., Hu, J. M., Liu, S. W., Yang, Y. H., … Liu, J. (2009). Contrasting Late Carboniferous and Late Permian–Middle Triassic intrusive suites from the northern margin of the North China craton: Geochronology, petrogenesis, and tectonic implications. Geological Society of America Bulletin, 121(1–2), 181–200.

Zhang, H. F., Zhu, R. X., Santosh, M., Ying, J. F., Su, B. X., & Hu, Y. (2013). Episodic widespread magma underplating beneath the North China Craton in the Phanerozoic: Implications for craton destruction. Gondwana Research, 23(1), 95–107. https://doi.org/10.1016/j.gr.2011.12.006

Zhang, S. H., Zhao, Y., Davis, G. A., Ye, H., & Wu, F. (2014). Temporal and spatial

variations of Mesozoic magmatism and deformation in the North China Craton: Implications for lithospheric thinning and decratonization. Earth-Science Reviews, 131, 49–87. https://doi.org/10.1016/j.earscirev.2013.12.004

Zhao, G., & Zhai, M. (2013). Lithotectonic elements of Precambrian basement in the North China Craton: Review and tectonic implications. Gondwana Research, 23(4), 1207–1240. https://doi.org/10.1016/j.gr.2012.08.016

Zhao, G., Wilde, S. A., Cawood, P. A., & Sun, M. (2001). Archean blocks and their boundaries in the North China Craton: Lithological, geochemical, structural and P–T path constraints and tectonic evolution. Precambrian Research, 107(1–2), 45–73. https://doi.org/10.1016/ S0301-9268(00)00154-6

Zhao, G., Sun, M., Wilde, S. A., & Sanzhong, L. (2005). Late Archean to Paleoproterozoic evolution of the North China Craton: Key issues revisited. Precambrian Research, 136(2), 177–202. https://doi.org/10.1016/j.precamres.2004.10.002

Zhao, G. C., Cao, L., Wilde, S. A., Sun, M., Choe, W. J., & Li, S. Z. (2006). Implications based on the first SHRIMP U-Pb zircon dating on Precambrian granitoid rocks in North Korea. Earth and Planetary Science Letters, 251(3–4), 365–379. https://doi.org/10.1016/j. epsl.2006.09.021

Zhao, G., Cawood, P. A., Li, S., Wilde, S. A., Sun, M., Zhang, J., … Yin, C. (2012). Amalgamation of the North China Craton: Key issues and discussion. Precambrian Research, 222, 55–76.

Zhao, P., Chen, Y., Xu, B., Faure, M., Shi, G., & Choulet, F. (2013). Did the Paleo-Asian Ocean between North China Block and Mongolia Block exist during the late Paleozoic? First paleomagnetic evidence from central-eastern Inner Mongolia, China. Journal of Geophysical Research: Solid Earth, 118, 1873–1894.

Zheng, J., Griffin, W., O'Reilly, S. Y., Lu, F., Yu, C., Zhang, M., & Li, H. (2004). U–Pb and Hf-isotope analysis of zircons in mafic xenoliths from Fuxian kimberlites: Evolution of the lower crust beneath the North China Craton. Contributions to Mineralogy and Petrology, 148(1), 79–103. https://doi.org/10.1007/s00410-004-0587-x

Zheng, J., Griffin, W., O'Reilly, S. Y., Zhang, M., Pearson, N., & Pan, Y. (2006). Widespread Archean basement beneath the Yangtze craton. Geology, 34(6), 417–420. https://doi.org/10.1130/G22282.1

Zhou, J. B., & Li, L. (2017). The Mesozoic accretionary complex in Northeast China: Evidence for the accretion history of Paleo-Pacific subduction. Journal of Asian Earth Sciences, 145, 91–100. https://doi.org/10.1016/j.jseaes.2017.04.013

Zhou, J. B., Wilde, S. A., Zhang, X. Z., Zhao, G. C., Zheng, C. Q., Wang, Y. J., & Zhang, X. H. (2009). The onset of Pacific margin accretion in NE China: Evidence from the Heilongjiang high-pressure metamorphic belt. Tectonophysics, 478(3–4), 230–246. https://doi.org/10.1016/ j.tecto.2009.08.009

Zhou, J. B., Wilde, S. A., Zhang, X. Z., Zhao, G. C., Liu, F. L., Qiao, D. W., … Liu, J. H. (2011). A> 1300km late Pan-African metamorphic belt in NE China: New evidence from the Xing'an block and its tectonic implications. Tectonophysics, 509(3–4), 280–292. https://doi.org/10.1016/ j.tecto.2011.06.018

Zhou, J. B., Cao, J. L., Wilde, S. A., Zhao, G. C., Zhang, J. J., & Wang, B. (2014). Paleo-Pacific subduction-accretion: Evidence from Geochemical and U-Pb zircon dating of the Nadanhada accretionary complex, NE China. Tectonics, 33, 2444–2466. https://doi.org/10.1002/ 2014TC003637

Zhu, R. X., Yang, J. H., & Wu, F. Y. (2012). Timing of destruction of the North China Craton. Lithos, 149, 51–60. https://doi.org/10.1016/ j.lithos.2012.05.013

Zonenshain, L. (1973). The evolution of Central Asiatic geosynclines through sea-floor spreading. Tectonophysics, 19(3), 213–232. https://doi. org/10.1016/0040-1951(73)90020-6

Chapter 4 Zircon U-Pb dating and whole-rock geochemistry of volcanic rocks in eastern Heilongjiang Province, NE China: Implications for the tectonic evolution of the Mudanjiang and Paleo-Pacific oceans from the Jurassic to Cretaceous

4.0 Abstract

The eastern Heilongjiang Province, NE China is located in the eastern CAOB (Central Asian Orogenic Belt). Previous studies suggest that subduction of the Mudanjiang and Paleo-Pacific oceans had been initiated in this area during the early Mesozoic. However, research on the Mesozoic volcanic rocks is insufficient, limiting our understanding of the relationship between magmatism and subduction process. To solve the problem, seven volcanic rocks in the Lesser Xing'an-Zhangguangcai Range and the Jiamusi Block were collected for zircon U-Pb dating (SHRIMP) and whole-rock geochemical analysis. Most samples from the Lesser Xing'an-Zhangguangcai Range are Jurassic in age (189 – 178 Ma), including andesite, trachyandesite, trachydacite and rhyolite. The andesitic to trachytic rocks were generated by magma mixing at an active continental margin, whereas the rhyolite is highly fractionated I-type. All the samples from the Jiamusi Block and one basaltic andesite from the Lesser Xing'an Range are middle Cretaceous in age (ca. 100 Ma) and were formed in a back-arc extensional setting (roll-back). Fractional crystallization was important in the generation of most Cretaceous rocks (basalt to trachydacite). However, magma mixing or crustal contamination was required to explain some andesites from the Jiamusi Block showing extremely low Cr, Ni and Mg#. When integrated with the coeval blueschist-facies metamorphism, the Early Jurassic volcanism indicate an active continental margin in the Lesser Xing'an-Zhangguangcai Range due to the westward subduction of the Mudanjiang Ocean. After the closure of the Mudanjiang Ocean, two

NE/NNE trending sinistral strike-slip faults in NE China were triggered, accompanied by the slab roll-back of the Paleo-Pacific oceanic plate. The Jurassic continental arc and accretionary complexes in NE China were cut through by the two strike-slip faults and bended to form small oroclines. At ca. 100 Ma, numerous accretionary complexes were accreted along the eastern margin of the CAOB, further forcing the retreat of trench and slab roll-back. The middle Cretaceous intra-continental volcanism was generated in the Lesser Xing'an-Zhangguangcai Range and Jiamusi Block during this roll-back process.

4.1 Introduction

The eastern Heilongjiang Province, NE China is located in the eastern margin of the Central Asian Orogenic Belt (CAOB; Fig. 4.1). It is bounded by the Sikhote-Alin orogenic belt of the Russian Far East, which is a Paleo-Pacific accretionary complex comprising several NNE trending belts with different origins (Figs. 1 and 2). The Songliao Basin limits the study area (NE China) to the west. The area includes the Lesser Xing'an-Zhangguangcai Range in the west and the Jiamusi-Khanka Block in the east (Fig. 4.3). Magmatic rocks are the most important components in the eastern CAOB and occupy up to ~80 % of the area (Fig. 4.3). These magmatic rocks are the products of several major tectonothermal events, especially the subduction and back-arc extension related to the Paleo-Pacific plates (Farallon, Izanagi and Pacific plates). The magmatic rocks record both the materials reworked from the continental crust and input from the mantle (Jahn, 2004; Jahn et al., 2000; Kröner et al., 2014; Wu et al., 2000). They are the most essential evidence concerning crustal growth and the subduction process of the NW Paleo-Pacific Ocean (Wu et al., 2011; Liu et al., 2017a, b).

The eastern CAOB was influenced by several major tectonic regimes, namely the Paleo-Asian Ocean, Mongol-Okhotsk Ocean and Paleo-Pacific Ocean (Xu et al., 2015). The Paleo-Asian Ocean included all the various oceanic components and continental

fragments between the Siberia and North China cratons, and was finally closed in the late Paleozoic (Wilde, 2015; Xiao et al., 2004; Zhao et al., 2013) along the Solonker-Changchun-Yanji Fault (SCYF in Fig. 4.2).

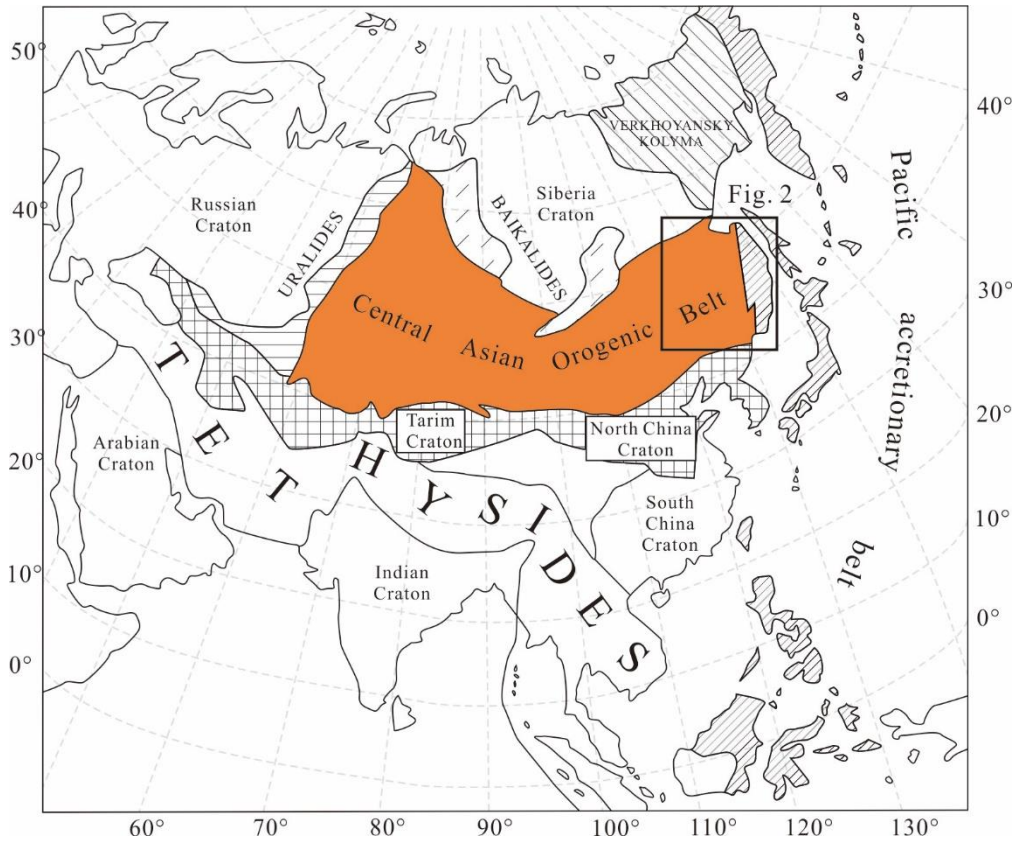

Fig. 4.1 Sketch map showing Asian tectonics and the Central Asian Orogenic Belt (CAOB). Modified after Sengör and Natal'in, (1996) and Wilde (2015).

The Mongol-Okhotsk Ocean was located between the southeastern Siberia Craton and the combined blocks of NE China and Mongolia, and was closed in the Late Jurassic to Early Cretaceous (Cogné et al., 2005; Kravchinsky et al., 2002; Tomurtogoo et al., 2005; van der Voo et al., 1999), leaving a narrow suture zone in the northeastern part of the CAOB (Fig. 4.2). The effects of subduction and post-collisional events related to the Mongol-Okhotsk Ocean produced NE and E-W trending magmatic belts in northeastern Mongolia, the Trans-Baikal area in Russia and the Great Xing'an Range in China (Donskaya et al., 2012; Tang et al., 2014; Tomurtogoo et al., 2005; Xu et al., 2013; Zorin, 1999). Closure of both the Paleo-Asian and Mongol-Okhotsk oceans resulted in generally E-W trending magmatic arcs and suture zones. Whereas the N-S trending magmatic belts in the eastern CAOB mainly resulted from the subduction of

the Paleo-Pacific and the Mudanjiang oceans. The former was subducted along the eastern margin of the Bureya-Jiamusi-Khanka Block marked by the Sikhote-Alin accretioanry belt (Fig. 4.2) and the latter was located between this block and the Lesser Xing'an-Zhangguangcai Range, indicated by the Heilongjiang Complex (Fig. 4.2). Most studies indicate that the Paleo-Pacific and Mudanjiang oceans dominated the Mesozoic tectonics in NE China and Sikhote-Alin after closure of the Paleo-Asian Ocean (Zhou et al., 2009; Khanchuk et al., 2015; Wilde, 2015; Wilde and Zhou, 2015; Sun et al., 2018).

However, the tectonic settings of the Zhangguangcai Range and Bureya-Jiamusi-Khanka Block during the Mesozoic remains controversial and is one of the key questions to be resolved in geological study of the eastern CAOB. Some researchers consider that the Lesser Xing'an-Zhangguangcai Range and the Jiamusi Block were active continental margins in the Early Jurassic (Wu et al., 2007; Zhou et al., 2009; Liu et al., 2016), whereas others argue that this area was in extension during the Late Triassic to Early Jurassic (Wu et al., 2002; Xu et al., 2009; Yu et al., 2012; Wang et al., 2015). As for the tectonic environment in the Cretaceous, only a few studies (e.g. Sun et al., 2013) have been carried out. The age and geochemical features of most Cretaceous volcanic rocks, as well as the relationship between the volcanic rocks and subduction in the area remain unclear.

In an attempt to resolve these issues, Mesozoic volcanic rocks in the Lesser Xing'an-Zhangguangcai Range and the Jiamusi Block were the focus of this study. Zircon U-Pb dating and whole-rock geochemical data for the Mesozoic volcanic rocks are presented here in order to determine the sequence of events and geodynamic setting.

4.2 Geological background

The study area is bounded by the Songliao basin to the west, Mongol-Okhotsk belt to the north, the Solonker-Changchun-Yanji Fault to the south and the Sikhote-Alin

accretionary complexes to the east (Figs. 2 and 3), tectonically including the Lesser Xing'an-Zhangguangcai Range and the Bureya-Jiamusi-Khanka Block (Fig. 4.2).

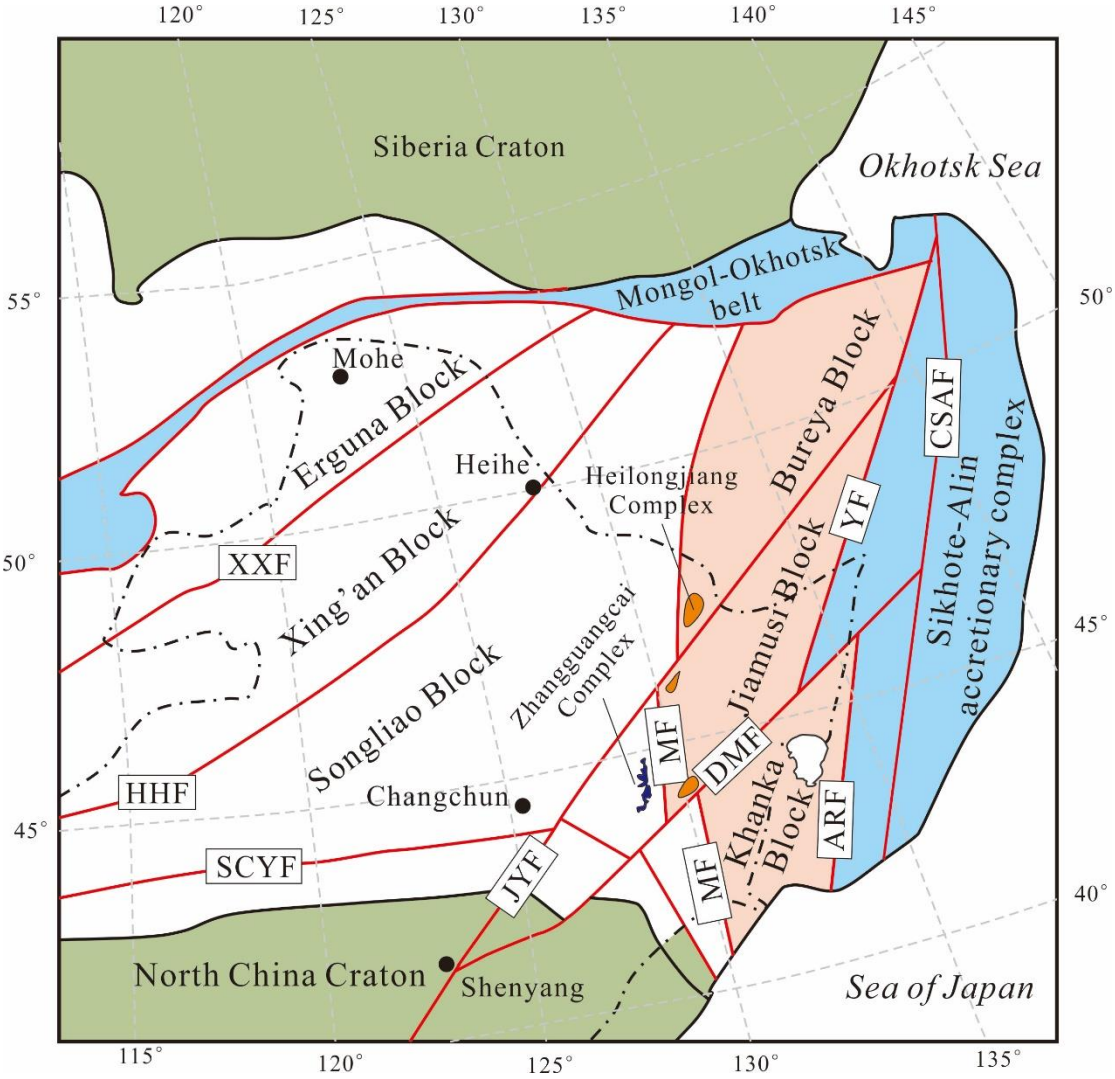

Fig. 4.2 Major geological units in the eastern CAOB. Faults: XXF = Xinlin-Xiguitu Fault; HHF = Hegenshan-Heihe Fault; SCYF = Solonker-Changchun-Yanji Fault; JYF = Jia-Yi Fault; DMF = Dun-Mi Fault; MF = Mudanjiang Fault; WTF = West Turan Fault; ARF = Arsen'evsky Fault; YF = Yuejinshan Fault; CSAF = Central Sikhote-Alin Fault.

4.2.1 Continental blocks

The Songliao Block is composed of two components, the Lesser Xing'an-Zhangguangcai Range in the eastern margin and the remainder covered by the Songliao Basin (Fig. 4.3). Some research suggested that the basement of the Songliao Basin is juvenile crust consisting of late Paleozoic to Mesozoic metavolcano-sedimentary rocks and granitic gneiss without Precambrian components (Wu et al.,

2001a). However, more recent work has shown that the oldest age for the basement is ~1.8 Ga, recorded by a rhyolitic volcanic breccia and meta-diorite obtained from drill holes in the southern part of the basin (Pei et al., 2007; Wang et al., 2006b). In the Middle Jurassic to Cenozoic, the Songliao Basin experienced rifting, postrift subsidence and structural inversion due to changes in the movement direction of the Paleo-Pacific plate (Wang et al., 2006b; Kirillova, 2003). Nonmarine volcanic and sedimentary rocks were deposited in both basins from the Middle to Late Jurassic. The most important episode of volcanism is the Early Cretaceous (135 – 110 Ma; Li et al., 2015; Pei et al., 2008; Sorokin et al., 2013; Zhang et al., 2011), with minor volcanic rocks formed in the Middle Jurassic (~165 Ma; Gao et al., 2007; Wu et al., 2000). The Lesser Xing'an-Zhangguangcai Range is located at the eastern margin of the Songliao Block (Fig. 4.3), in which the most important components are the magmatic rocks (Wei et al., 2012; Wu et al., 2011; Xu et al., 2013), formed in the early Paleozoic (500 – 470 Ma), early Permian (280 – 290 Ma), late Pemian to Early Triassic (260 – 240 Ma), Late Triassic to Early Jurassic (220 – 170 Ma), and middle Cretaceous (~100 Ma). The most widespread component is the Late Triassic to Early Jurassic magmatic rocks.

The Bureya-Jiamusi-Khanka Block is dissected by the northern branches of the Tan-Lu Fault, namely the Dun-Mi and Jia-Yi faults (DMF and JYF in Fig. 4.2, respectively). High-grade orthogneisses exposed in the southern Jiamusi Block yield zircon U-Pb ages of 898 – 891 Ma (Yang et al., 2017), whereas a ~933 Ma gabbro-granite complex is also reported in the northern Bureya Block (Sorokin et al., 2016a). Thus, early Neoproterozoic rocks are the oldest known basement in this united block. The more widespread but younger basement shared by the three blocks is formed by late Pan-African (~500 Ma; Wilde et al., 1997, 2000, 2003) granulite and early Paleozoic granitoids (Tsutsumi et al., 2014; Xu et al., 2018).

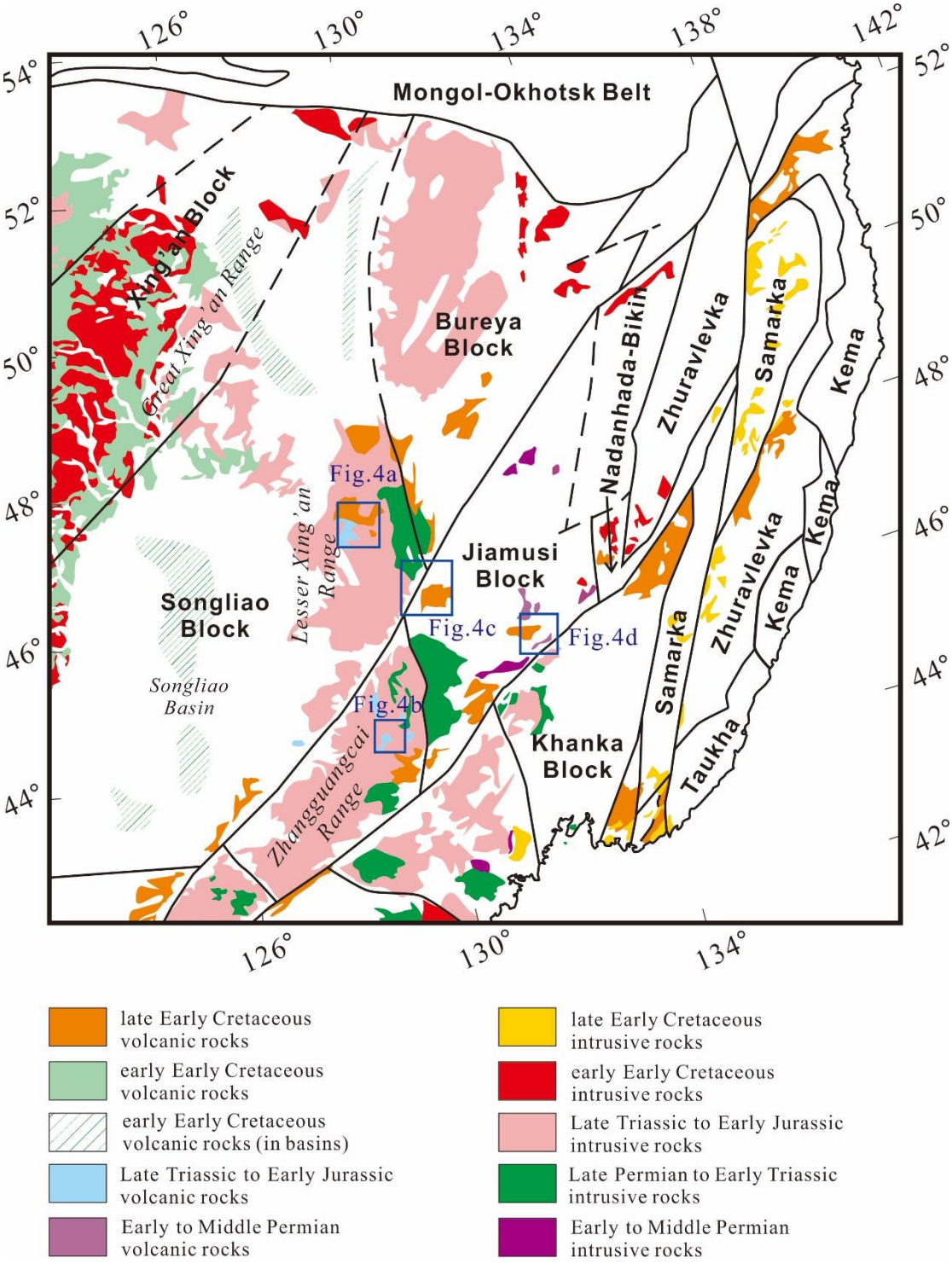

Fig. 4.3 The magmatic rocks (Permian to Cretaceous) in the eastern CAOB and Sikhote-Alin orogenic belt.

Paleozoic sedimentary cover was deposited along the eastern margin of the Jiamusi and the Khanka blocks, including Early Paleozoic marbles, non-marine terrigenous rocks and late Paleozoic volcano-sedimentary strata (Khanchuk et al., 2016; Meng et al., 2008; Yang et al., 2015a; Zhang et al., 2015). Some N-S trending late Permian to

Early Triassic granitoids intruded into the western Jiamusi and Khanka blocks (Liu et al., 2017a; Huang et al., 2008; Wu et al., 2001b; Yang et al., 2016; Xu et al., 2018), whereas the Late Triassic to Early Jurassic magmatic rocks are exposed rarely in the Jiamusi Block but extensively in the western Bureya and Khanka blocks (Liu et al., 2017a; Ma et al., 2016; Yang et al., 2015b; Sorokin et al., 2007, 2010, 2016b). The middle Cretaceous magmatism, including a ~100 Ma basalt-andesite-dacite association, is widespread in the Jiamusi Block (Sun et al., 2013).

4.2.2 Accretionary complexes/terranes related to the Mudanjiang Ocean and Paleo-Pacific Ocean

Between the Songliao and Bureya-Jiamusi-Khanka blocks, two accretionary complexes are recognized near the Mudanjiang Fault, namely, the Heilongjiang Complex and the Zhangguangcai Complex (Fig. 4.2), which are the remnants of the Mudanjiang Ocean. The Heilongjiang Complex is located on the western margin of the Jiamusi Block, and is composed of metagabbro, amphibolite, marble, quartzite, blueschist and mica schist. The protolith ages of the blueschist range from the early Permian to Triassic, whereas the high-pressure metamorphic ages are Early Jurassic (Ge et al, 2016; Zhou et al., 2009). A recent study has suggested the youngest zircon age of the blueschist is latest Jurassic (ca. 140 Ma; Zhu et al., 2015). In this case, the protolith is younger than the blueschist-facies metamorphism, indicating further research is required to resolve this issue. The Zhangguangcai Complex is a N-S trending tectonic mélange consisting of amphibolite, biotite-plagioclase metamorphic rocks, marble, schists and meta-volcanic rocks (HBGMR, 1993). The protolith age of components in this accretionary complex ranges from Paleozoic to Early Mesozoic, whereas the timing of the mélange is estimated between the Late Triassic and Early Jurassic (Wang et al., 2012).

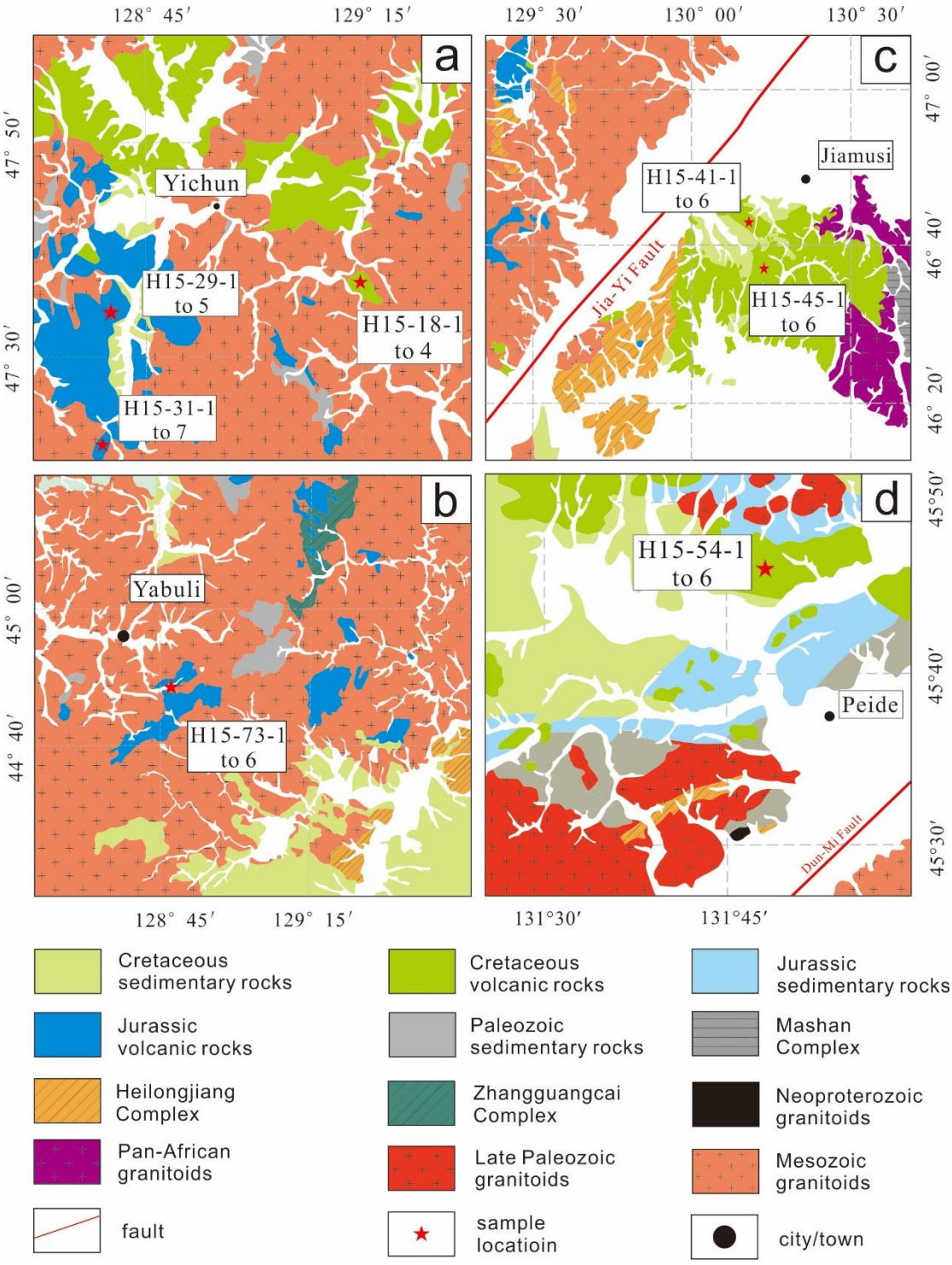

Fig. 4.4 The geological maps of the sample locations. (a) Samples H15-18-1 to H15-18-4, H15-29-1 to H15-29-5 and H15-31-1 to H15-31-7 in the Yichun area. Modified from the 1:200, 000 Yichun and Jinshantun geological maps; (b) Sample H15-73-1 to H15-73-6 in the Yabuli area. Modified from the 1:200, 000 Yimianpo geological map; (c) Samples H15-41-1 to H15-41-6 and H15-45-1 to H15-45-6 in the Jiamusi area. Modified from the 1:200, 000 Jiamusi and Huanan geological maps; (d) Sample H15-54-1 to H15-54-6 in the Peide area. Modified from the 1:200, 000 Hulin geological map.

Numerous accretionary belts (or "tectonostratigraphic terranes" in Russian literatures) related to the Paleo-Pacific plate mainly occur in the Sikhote-Alin area of the Russian Far East and only partly in NE China. They are mainly Jurassic to Cretaceous in age. Three different kinds of belts are present: 1) accretionary complexes, 2) turbidite basins related to strike-slip faults and, 3) arc-related basins resulting from subduction of the Paleo-Pacific Ocean. For the first type, continuous sedimentary strata can be recognized in some local areas, which consists of, from bottom to top, basalt, chert, mudstone, sitstone and turbiditic sandstone, revealing changing sedimentary facies from ocean to continental margin (Kemkin, 2008; Kojimo, 1989; Matsuda and Isozaki, 1991). These accretionary complexes are deformed strongly, including abundant faults and folds. The second kind of belt is turbidite basins deposited along, and then transported by, the Central Sikhote-Alin Fault. The main rock type is sandstone interlayered by siltstone (Malinovsky and Golozubov, 2011). The third type is composed of arc-related basins and components of island arcs (Malinovsky et al., 2006, 2008). The main rock types are siltstone, sandstone, conglomerate, tuff and basaltic volcanic flows (Malinovsky et al., 2005). The Sikhote-Alin terranes were accreted one by one to the eastern margin of the Bureya-Jiamusi-Khanka Block before the Late Cretaceous (Golozoubov et al., 1999; Khanchuk et al., 2001, 2016). Cretaceous to Cenozoic magmatism is widespread in the whole area, which is mainly recorded by plutons and their extrusive equivalents, in which most of them are rhyolitic to andesitic (Jahn et al., 2015; Kruk et al., 2014; Fig. 4.3). The known zircon U-Pb ages of the magmatic rocks range from the Early Cretaceous in the west to Paleogene in the southeast (Jahn et al., 2015; Khanchuk et al., 2016; Tang et al., 2016).

4.3 Sample locations and petrography

Fourty samples of volcanic rocks were collected from the Lesser Xing'an-Zhangguangcai Range and the Jiamusi Block, using for zircon U-Pb dating and whole-rock geochemical analysis (Supplementary Table 1). The sample locations are shown

on their local geological maps (Fig. 4.4).

4.3.1 Samples from the Lesser Xing'an-Zhangguangcai Range

Sample H15-18-1, H15-18-2, H15-18-3 and H15-18-4 were collected from the lower Youhao Formation that crops out to the southwest of Yichun (Fig. 4.4a). The lower Youhao Formation consists of basalt, basaltic andesite, andesite and andesitic tuff, whereas the upper Youhao Formation is more felsic, and the rock types are mainly andesite, trachyandesite with minor rhyolite. The samples in this study are fine-grained basaltic andesites (Fig. 4.5a), consisting of plagioclase, clinopyroxene, hornblende and biotite.

In the Yichun area, the Taiantun Formation is distributed in a N-S trending belt (Fig. 4.4a). Sample H15-29-1 to H15-29-5 were collected from the lower part of the formation and are grey porphyritic rhyolite (Fig. 4.5b). The phenocrysts are quartz and K-feldspar, up to 1.5 mm in length, and make up 40% by volume. The groundmass is mainly composed of K-feldspar, plagioclase and quartz. Sample H15-31-1 to H15-31-7 (Fig. 4.4a) were collected from the upper part of the Taiantun Formation that is composed of trachydacite, andesite and rhyolitic tuff. It is transitional between andesite and dacite and is porphyritic with phenocrysts of plagioclase (Fig. 4.5c). The groundmass is mainly composed of plagioclase and hornblende, with minor quartz and K-feldspar.

The Taiantun Formation is also exposed in the southern Zhangguangcai Range (Fig. 4.4b). To the south of Yabuli town, the lower Taiantun Formation is composed of andesite, siltstone and slate, with andesitic tuff interlayers. The upper Taiantun Formation in this area is composed of andesitic to rhyolitic lava and tuff. Sample H15-73-1 to H15-73-6 were collected from the lower Taiantun Formation and are andesites in composition. They have a porphyritic texture, with phenocrysts of clinopyroxene and plagioclase, set in a groundmass of plagioclase, hornblende and clinopyroxene.

The plagioclase phenocrysts reach 2 mm in length, whereas the size of hornblende and clinopyroxene range from 0.2 – 0.5 mm in diameter (Fig. 4.5g).

4.3.2 Samples from the Jiamusi Block

In the Jiamusi Block, volcanic rocks crop out extensively near Jiamusi city and the town of Peide.

To the south of Jiamusi city, the volcano-sedimentary strata are widely distributed over an area of ~1000 km^2 (Fig. 4.4c). The lower strata (the Xigemu Formation) are mainly composed of basalt, basaltic andesite and dacite, with minor volcanic agglomerate. The middle part, the Aoqi Formation is mainly felsite and rhyolite. The upper sequences, including the Sifengshan and Furao fomations are mainly composed of sedimentary rocks, including sandstone, siltstone, conglomerate, shale, with thin layers of coal. Samples H15-41-1 to H15-41-6 and H15-45-1 to H15-45-6 were collected from the lower strata. Sample H15-41-1 to H15-41-6 are basalts which are black in color with porphyritic cryptocrystalline texture and massive structure. The mineral assemblage is plagioclase, hornblende, clinopyroxene and ilimenite (Fig. 4.5d). Sample H15-45-1 to H15-45-6 are greyish-yellow dacite with a porphyritic texture. The phenocrysts are quartz and K-feldspar up to 0.8 – 1.5 mm in length and the groundmass consists of plagioclase, quartz and K-feldspar (Fig. 4.5e).

To the north of Peide town, the Songmuhe Formation crops out and the main rock types are andesite and dacite, with minor rhyolite and andesitic tuff (Fig. 4.4d). Sample H15-54-1 is andesite that is light grey in color with a porphyritic texture. The phenocrysts are mainly plagioclase, and the main minerals in the groundmass are plagioclase, clinopyroxene, hornblende, biotite, magnetite and minor quartz (Fig. 4.5f).

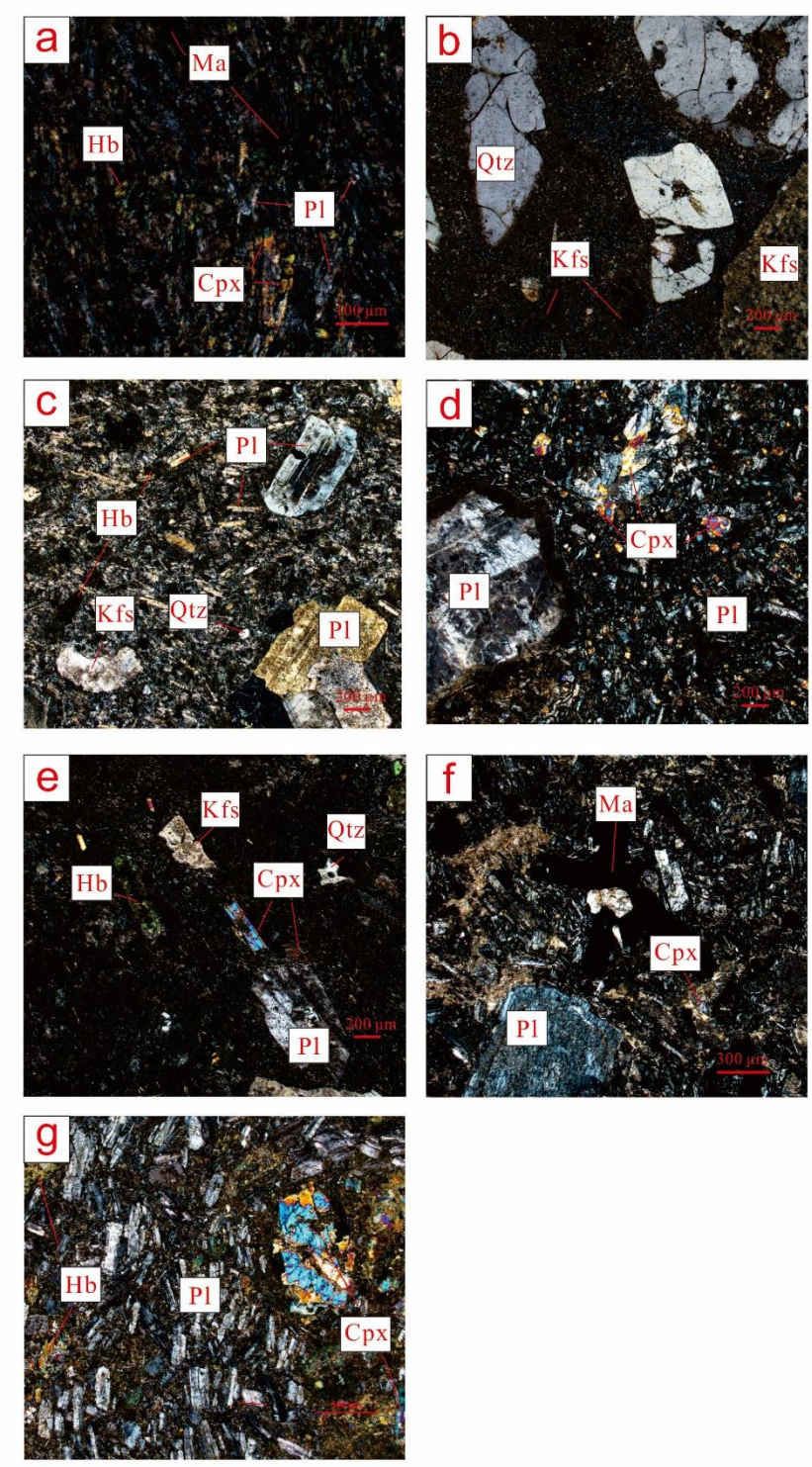

Fig. 4.5 Micrographs of the thin sections. (a) Sample H15-18-1 (basaltic andesite); (b) Sample H15-29 (rhyolite); (c) Sample H15-31-1 (andesite); (d) Sample H15-41-1 (basalt); (e) Sample H15-45-1 (dacite); (f) Sample H15-54-1 (andesite); (g) Sample H15-73-1 (andesite). Abbreviations: Pl = plagioclase; Hb = Horblende; Cpx = clinopyroxene; Ma = magnetite; Qtz = quartz; Kfs = K-feldspar.

4.4 Analytical techniques

Samples H15-18-1, H15-29-1, H15-30-1, H15-41-1, H15-45-1, H15-54-1 and H15-73-1 were selected for zircon U-Pb analysis and other 33 fresh samples were selected for analysis of whole-rock major and trace elements (Table 2).

Zircon was extracted by crushing, followed by heavy liquid and magnetic separation at the Honesty Geological Services Corporation, Langfang, Hebei Province, China. Zircons from dacite and rhyolite were abundant with more than 500 grains. However, there were less than 100 zircons available from the basalt, basaltic andesite and andesite samples, including H15-18-1, H15-54-1 and H15-73-1. The zircons were mounted in epoxy resin along with the BR266 standard (Stern, 2001) and polished to reveal the center of the grains. Cathodoluminescence (CL) images were taken using a Philips XL30 Scanning Electron Microscopy at Curtin University before SHRIMP zircon U-Pb analysis. Zircon U-Pb dating was conducted using a SHRIMP II ion microprobe at Curtin University following standard procedures (Nelson et al., 1995). The mass resolution was ca. 5000 at 1% peak height. The spot size of the ion beam was ~30 μm. Six scans through the mass stations were used during the data collection. Standard BR266 (559 Ma, U = 909 ppm) was used for U concentration and age calibration. Ages and concordia diagrams were calculated using the programs SQUID 2 (Ludwig, 2009) and ISOPLOT 3.0 (Ludwig, 2003).

For each sample prepared for geochemical analysis, the fresh rocks were crushed to powder. The geochemical analyses were performed at the Wuhan Sample Solution Analytical Technology Co., Ltd., Wuhan, China. The major elements were analyzed using a Rigaku-100e XRF whereas the trace elements were analyzed using an Agilent 7700e inductively-coupled plasma mass spectrometer (ICP-MS). The analytical precision for all major oxides was better than 0.5%. The analytical precisions were 5–10% for REEs, Rb, Sr, Cs, Ba, U, Th, Pb, Zr and Hf, and 20% for other trace elements.

4.5 Results

4.5.1 SHRIMP zircon U-Pb dating

Zircons from the volcanic rocks are transparent (or pale yellow) and tabular in shape. Most zircons have oscillatory zonation in cathodoluminescence (CL) images, showing typical magmatic features (Fig. 4.6).

In sample H15-18-1, zircons range in length from 50-250 μm (Fig. 4.6), and the length to width ratios range from 1:1 to 5:1. Seventeen zircons were analyzed from this sample, and four zircons are excluded from the calculations because of low U (21-90 ppm) and Th (11-31 ppm) concentrations. For the other 13 zircons, one shows no zonation and have low Th/U ratio (0.05), suggesting a possible metamorphic origin. The $^{206}Pb/^{238}U$ age of this zircon is 565 Ma. The other 12 zircons show higher U and Th concentrations ranging from 126-1478 ppm and 50-617 ppm, respectively. The Th/U ratios vary from 0.31-1.16, indicating a magmatic origin. Most of the magmatic zircons are inherited grains, having $^{206}Pb/^{238}U$ ages from 174 to 440 Ma (Fig. 4.7a). However, two somewhat discordant zircons with clear oscillatory zoning have $^{206}Pb/^{238}U$ age of 106 Ma and 104 Ma with a weighted mean age of 105±8 Ma, taken to represent the age of the sample H15-18-1, i.e. late Early Cretaceous (Fig. 4.7b).

Zircons from sample H15-29-1 are tabular and 100-250 μm in length with typical oscillatory zonation, indicating a magmatic origin (Fig. 4.6). Fifteen zircons were analyzed from this sample and the U and Th concentrations range from 88-1059 ppm and 30-621 ppm, respectively. The Th/U ratios vary from 0.27-0.61, suggesting a magmatic origin. There is one inherited zircon with a $^{206}Pb/^{238}U$ age of 322 Ma. The other zircons have $^{206}Pb/^{238}U$ ages ranging from 196-206 Ma, with a weighted mean age of 203±1 Ma (Fig. 4.7c), hence the age of sample H15-29-1 is end Triassic.

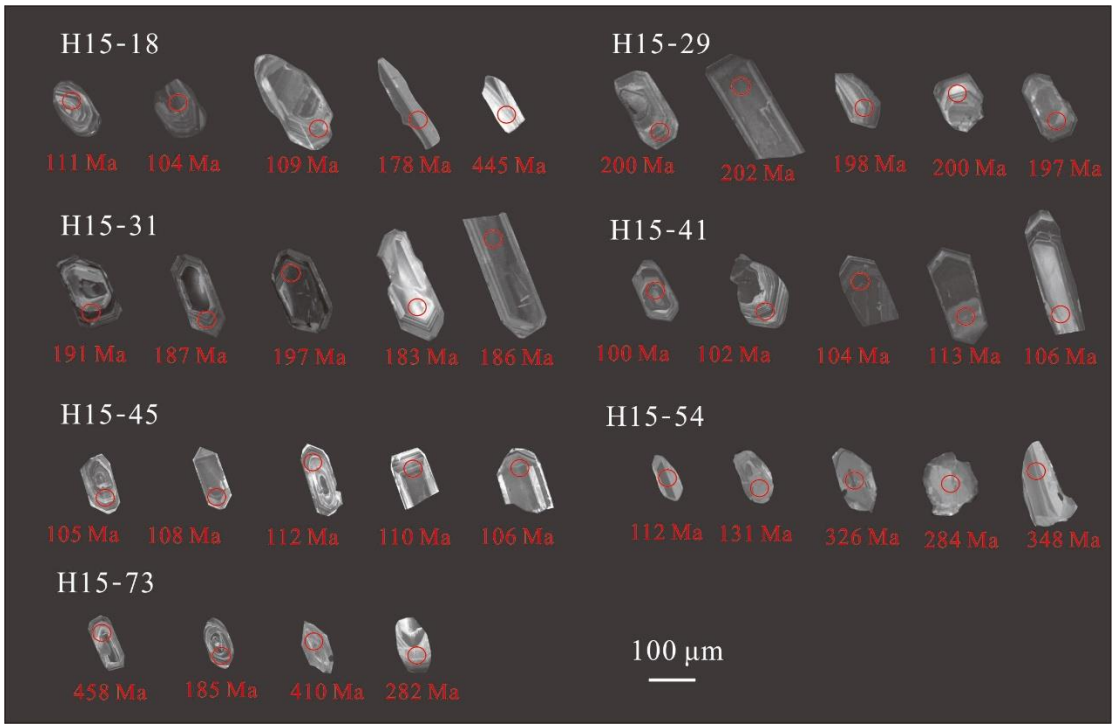

Fig. 4.6 Cathodoluminescence (CL) images for analyzed zircons by SHRIMP.

Fifteen zircons were analyzed from sample H15-31-1, which were tabular, 50-300 μm in length, and with length to width ratios ranging from 1:1 to 3:1. All zircons have oscillatory zonation, indicating a magmatic origin. The U concentrations range from 113-1036 ppm, whereas the Th concentrations range from 48-338 ppm. The Th/U ratios vary from 0.34-0.61, which supports their magmatic origin. The 15 zircons have $^{206}Pb/^{238}U$ ages ranging from 175-189 Ma, with a weighted mean age of 183±3 Ma (Fig. 4.7d). Thus, sample H15-31 is Early Jurassic in age.

Zircons in sample H15-41-1 are tabular, 40-200 μm in length, and with length to width ratios ranging from 1:1 to 4:1. All zircons have oscillatory zonation (Fig. 4.6). Twelve zircons were analyzed, and the U and Th concentrations range from 177-2393 ppm and 38-1741 ppm, respectively. The Th/U ratios vary from 0.24-1.85, suggesting a magmatic origin. The zircons have $^{206}Pb/^{238}U$ ages from 100-113 Ma with a weighted mean age of 101±2 Ma (Fig. 4.7e), indicating eruption at the end of the Early Cretaceous.

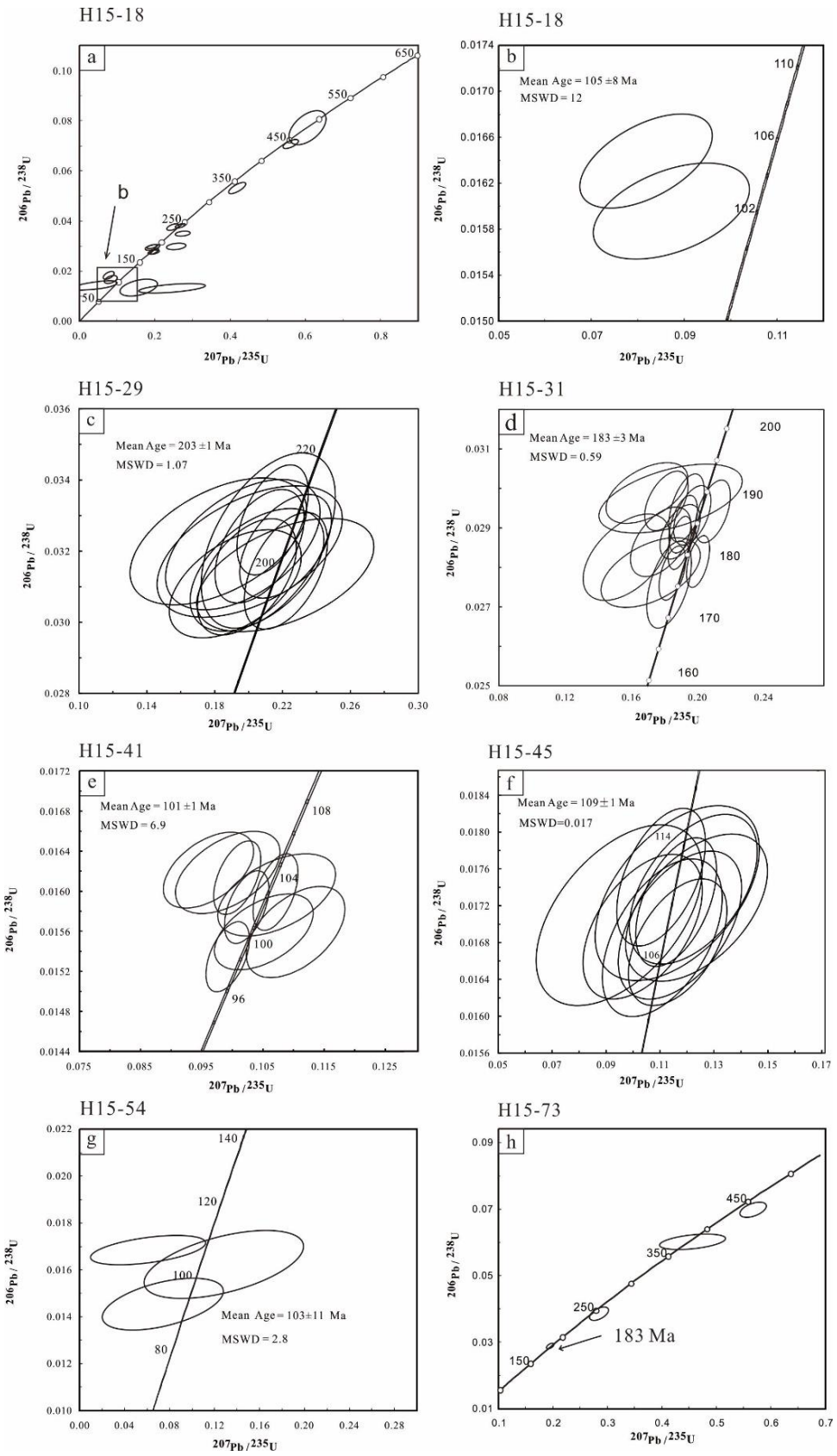

Fig. 4.7 SHRIMP U-Pb diagrams for (a) and (b) sample H15-18-1; (c) sample H15-29-1; (d) sample H15-31-1; (e) sample H15-41-1; (f) sample H15-45-1; (g) sample H15-54-1; (h) sample H15-73-1.

For sample H15-45, zircons are elongated and 50-200 μm in length, with length to width ratios ranging from 1:1 to 2:1 (Fig. 4.6). All zircons show magmatic oscillatory zonation. Fourteen zircons were analyzed, and the U and Th concentrations vary from 121-1291 ppm and 100-2391 ppm, respectively, with the Th/U ratios ranging from 0.67 to 1.16, indicating a magmatic origin. The zircons have $^{206}Pb/^{238}U$ ages ranging from 105-116 Ma, with a weighted mean age of 109±1 Ma (Fig. 4.7f). Thus, the age of sample H15-45 is late Early Cretaceous.

The zircons in sample H15-54 are stubby to euhedral, 50-180 μm in length, with length to width ratios ranging from 1:1 to 4:1. Most zircons have magmatic oscillatory zonation, however, there are some zircons showing only weak zonation, whereas some others show core-rim structure with oscillatory zonation in the core but no zonation in the rim (Fig. 4.6). Eight concordant ages were obtained for this sample. Five zircons have $^{206}Pb/^{238}U$ ages ranging from 116-340 Ma, which are interpreted as inherited zircons. The other 3 zircons with oscillatory zonation have $^{206}Pb/^{238}U$ ages ranging from 95-110 Ma with an imprecise weighted mean age of 103±11 Ma (Fig. 4.7g). Thus, sample H15-54 also formed in the late Early Cretaceous.

There were only 9 zircons extracted from sample H15-73-1. The length of these zircons ranges from 20-100 μm, with length to width ratios of 1:1 to 2:1. The zircons show magmatic oscillatory zonation (Fig. 4.6). There are 4 concordant ages: 185 Ma, 282 Ma, 410 Ma and 458 Ma (Fig. 4.7h). Only the 185 Ma zircon has typical oscillatory zonation suggesting a magmatic origin and the other 3 zircons have core-rim structure, indicating they are inherited zircons. Thus, the age of sample H15-73-1 should be the Early Jurassic or later, but cannot be well constrained.

4.5.2 Geochemistry

4.5.2.1 Jurassic volcanic rocks

All the Jurassic volcanic rocks in this study, including samples H15-29-2 to H15-29-

6, H15-31-2 to H15-31-7 and H15-73-2 to H15-73-6, are from the Lesser Xing'an-Zhangguangcai Range. There are no Jurassic magmatic rocks found in the Jiamusi Block.

In the Na_2O+K_2O vs. SiO_2 diagram (Fig. 4.8a), sample H15-29-2 to H15-29-6 are classified as rhyolite, whereas sample H15-31-2 to H15-31-7 are transitional from andesite to trachydacite and sample H15-73-2 to H15-73-6 are trachyandesite.
The rhyolite (H15-29-2 to H15-29-6) has high contents of SiO_2 (74.4 – 76.8 %), K_2O (4.8 – 6.5 %) and total alkalis (8.6 – 9.2 %), whereas the contents of total Fe_2O_3 (0.72 – 1.54 %), MgO (0.04 – 0.07 %) and CaO (0.24 – 0.52 %) are low. The Na_2O/K_2O and A/CNK ratios vary from 0.4 to 0.8 and 1.06 to 1.13, respectively, indicating they are weakly peraluminous. In the primitive mantle-normalized diagram and chondrite-normalized diagram (Fig. 4.8b, c), the rhyolite is enriched in large ion lithophile elements (LILEs) and light rare earth elements (LREEs) and depleted in high field strength elements (HFSEs) and heavy rare earth elements (HREEs). Negative anomalies of Ba, Nb-Ta, Sr and Eu (Eu/*Eu=0.26–0.31, with positive anomalies of Rb, Th, U, Pb are observed (Fig. 4.8b, c).

The andesite, trachyandesite and trachydacite (H15-31-2 to H15-31-7) have lower contents of SiO_2 (58.6 – 65.7 %), K_2O (1.8 – 3.2 %) and total alkalis (5.4 – 7.7 %) with higher contents of total Fe_2O_3 (4.6 – 6.8 %). However, the contents of MgO in trachyandesite (sample H15-31-2 to H15-31-7) is in the range of 0.9 – 3.25 %, lower than that in andesite-trachydacite (from 2.87 to 5.65 % in sample H15-73-2 to H15-73-6). Correspondingly, in the samples H15-31-2 to H15-31-7, the Mg# of the trachyandesite varies from 31.3 to 51.0, also lower than the range of 58.7 – 66.1 in the andesite-trachydacite. In the primitive mantle-normalized diagram and chondrite-normalized diagram (Fig. 4.8b, c), both samples show similar enriched LILEs and LREES with depleted HFSEs and HREES. They both have strong negative anomalies of Nb-Ta and positive anomalies of Th, U and Pb. However, there are negative anomalies of Sr and Eu in the trachyandesite, whereas positive anomalies of Sr and Eu

are present in the andesite-trachydacite.

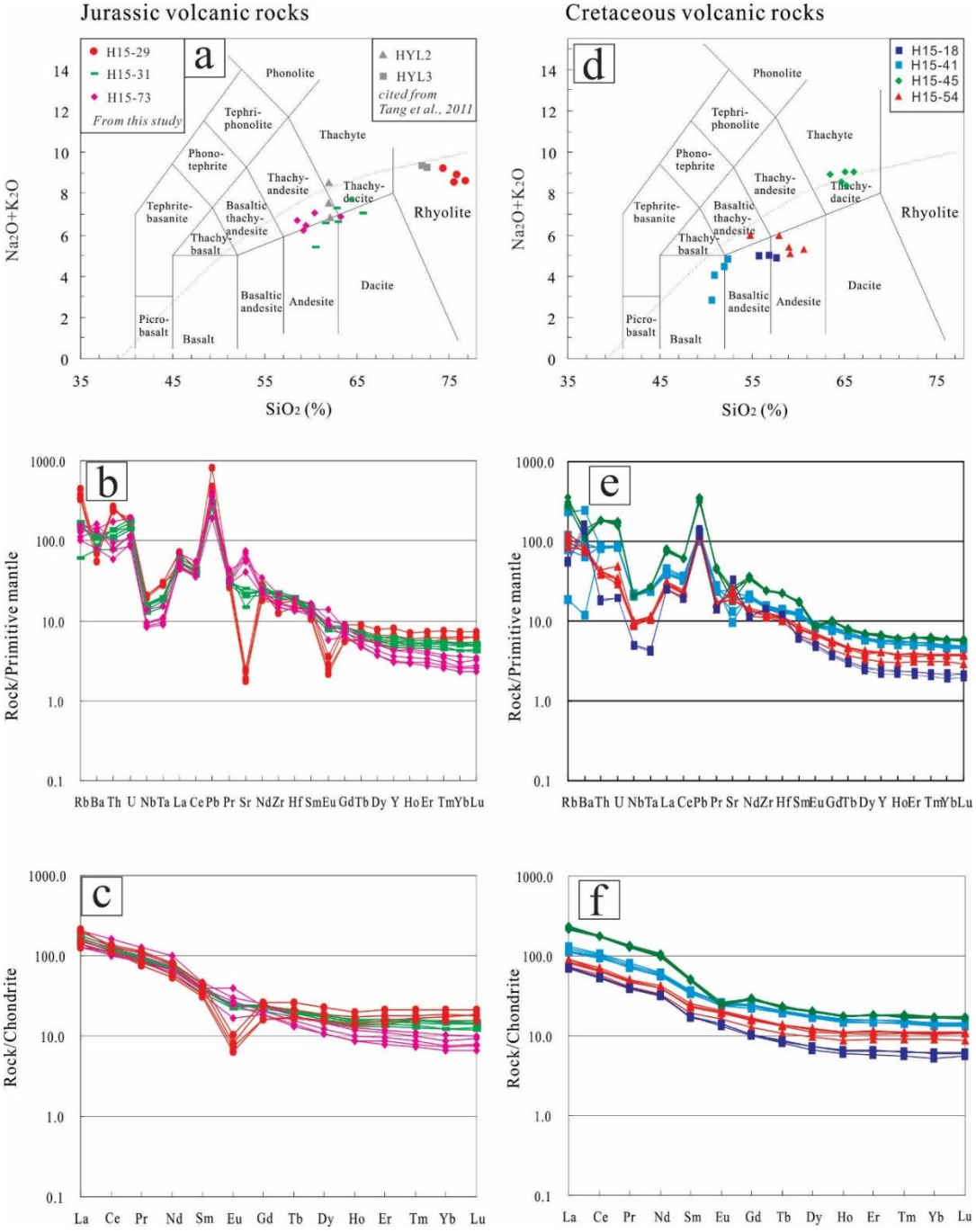

Fig. 4.8 (a) Total alkalis vs. silica classification diagram, (b) chondrite-normalized REE patterns and (c) primitive mantle-normalized trace element spider diagrams for the Jurassic volcanic rocks. (d) Total alkalis vs. silica classification diagram, (e) chondrite-normalized REE patterns and (f) primitive mantle-normalized trace element spider diagrams for the Cretaceous volcanic rocks (Middlemost, 1994; Sun and McDonough, 1989).

4.5.1.2 Cretaceous volcanic rocks

The Cretaceous volcanic rocks in this study represented by all the samples from the

Jiamusi Block (H15-41-2 to H15-41-6, H15-45-2 to H15-41-6 and H15-54-2 to H15-54-6) and one sample from the Lesser Xing'an Range (H15-18-2 to H15-18-6).
In the Na_2O+K_2O vs. SiO_2 diagram (Fig. 4.8d), samples H15-18-2 to H15-18-6 are basalt. Samples H15-41-2 to H15-41-6 are basaltic andesites. Samples H15-45-2 to H15-45-6 are trachydacites, and H15-54-2 to H15-54-6 are andesites.

Samples H15-18-2 to H15-18-6 (basalt), H15-41-2 to H15-41-6 (basaltic andesites), and H15-54-2 to H15-54-6 have low contents of SiO_2 in the range of 50.7 to 59.2 %, and high contents of total Fe_2O_3 (5.3 – 7.6 %) and MgO (1.6 – 4.6 %). The samples H15-45-2 to H15-45-6 (trachydacites) have higher contents of SiO_2 from 63.6 to 66.1 %, lower contents of total Fe_2O_3 (4.3 – 4.5 %) and MgO (1.5 – 2.2 %). The andesitic samples H15-54-2 to H15-54-6 have the lowest Mg# values (38.4 to 47.5), Cr (<2 ppm) and Ni (<3 ppm). However, the Mg# of other Cretaceous rocks, even the trachydacite (H15-45-2 to H15-45-6) are mostly > 48, with a mean value of 51.7. The contents of Cr and Ni are >50 ppm and >38 ppm, respectively, much higher than those in the andesite (H15-54-2 to H15-54-6). In the primitive mantle-normalized spider diagram and chondrite-normalized REE diagram (Fig. 4.8e, f), all the Cretaceous volcanic rocks share similar patterns, i.e. enrichment of LREE and LILEs and depletion of HREEs and HFSEs. There are strong negative anomalies for Nb-Ta and positive anomalies for Th, U and Pb. The trachydacites (H15-45-2 to H15-45-6) have negative anomalies of Sr and Eu, however, the basaltic andesite (H15-41-2 to H15-41-6) and andesite (H15-54-2 to H15-54-6) have positive anomalies of Sr and Eu. The basalt (H15-18-2 to H15-18-6) shows negative to weakly positive Sr anomalies without an Eu anomaly.

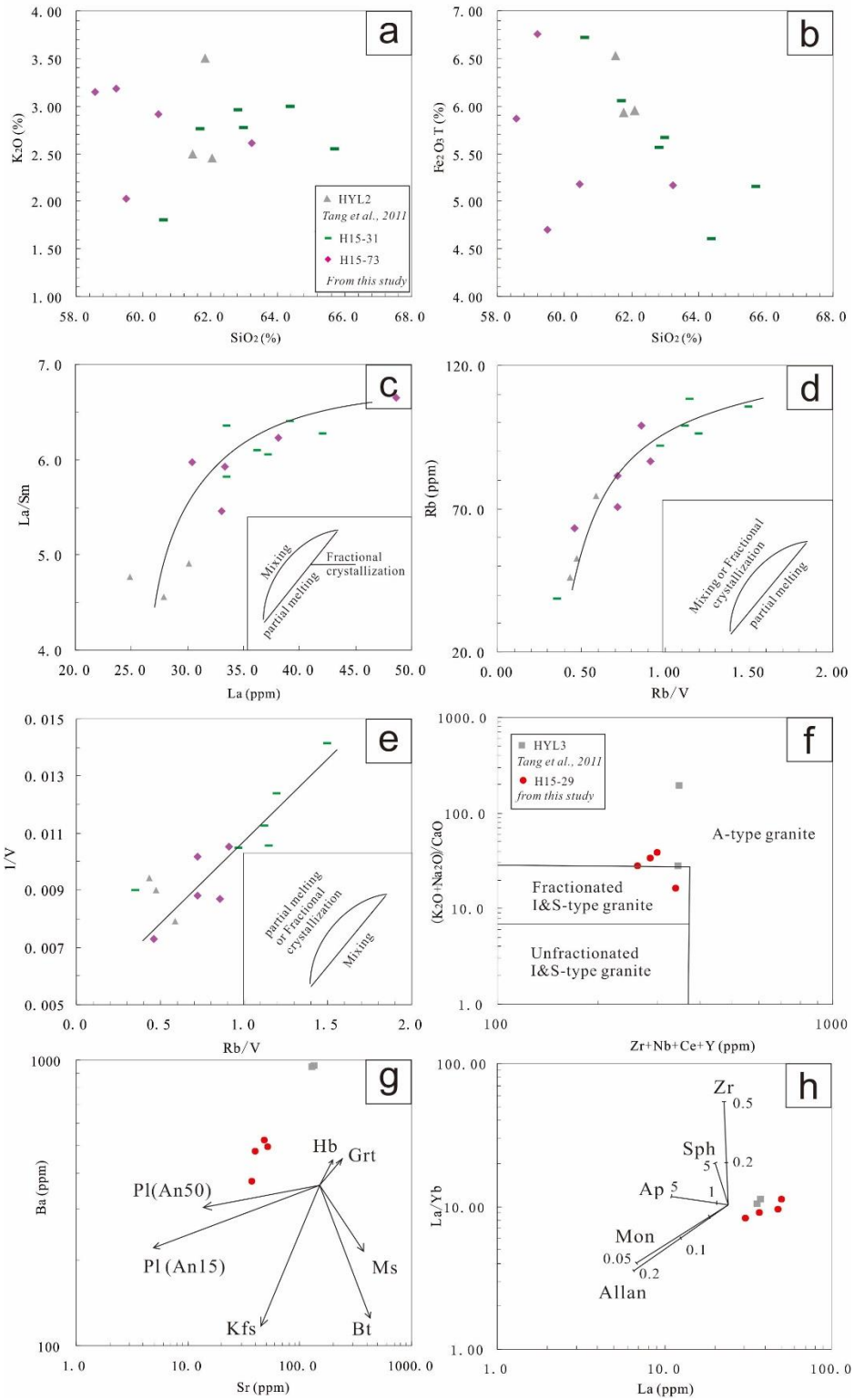

Fig. 4.9 Geochemical diagrams for the Jurassic lava. (a) The K_2O vs. SiO_2 diagram, (b) $Fe_2O_3^T$ vs. SiO_2 diagram, (c) La/Sm vs. La diagram, (d) Rb vs. Rb/V diagram and (e) 1/V vs. Rb/V diagram are for the Jurassic basaltic andesite, andesite and dacite (Schiano et al., 2010); (f) The $(K_2O + Na_2O)/CaO$ vs. Zr + Nb + Ce + Y diagram, (g) Ba vs. Sr diagram and (h) La/Yb vs. La diagram are for the Jurassic rhyolite (Whalen et al., 1987; Wu et al., 2003a).

4.6 Discussion

4.6.1 Petrogenesis of the Jurassic volcanic rocks

In addition to the Jurassic volcanic rocks analyzed in this study, trachyte, trachyandesite and rhyolite with zircon U-Pb ages of 179 – 184 Ma are reported from the Maoershan area (~100 km west to the sample H15-73-1) in the middle Zhangguangcai Range (Tang et al., 2011). These will be cited and discussed with our data together in this section.

4.6.1.1 Petrogenesis of the andesitic lava

The Early Jurassic volcanic rocks in the Lesser Xing'an-Zhangguangcai Range are characterized by moderate abundances of SiO_2, moderate to high contents of K_2O and total alkalis, enriched LILEs and LREEs and depleted HFSEs and HREEs, similar to igneous rocks formed at active continental margins, which is further supported by the strong negative anomalies of Nb-Ta and positive anomalies of Th and U (Fig. 4.8b, c; Pearce and Peate, 1995).

Generally, andesite-trachyandesite-trachydacite at active continental margins can be generated from two kinds of primary magma: 1) basaltic magma which evolves into andesitic magma through different mechanisms, such as fractional crystallization, with or without crustal assimilation, or magma mixing between mafic and felsic magma (Gill, 1981; Graham and Cole, 1991; Hildreth and Moorbath, 1988; Plank and Langmuir, 1988; Reubi and Blundy, 2009); or 2) andesitic primary magma melted from upper mantle peridotite under water-saturated conditions to generate high-magnesian andesitic magma with residual harzburgite in the source (Grove et al., 2002; Hirose, 1997; Kelemen, 1995), or melted from subducted oceanic crust with garnet amphibolite or eclogite as residuals, producing adakitic magma (Defant and Drummond, 1990; Shimoda et al., 1998).

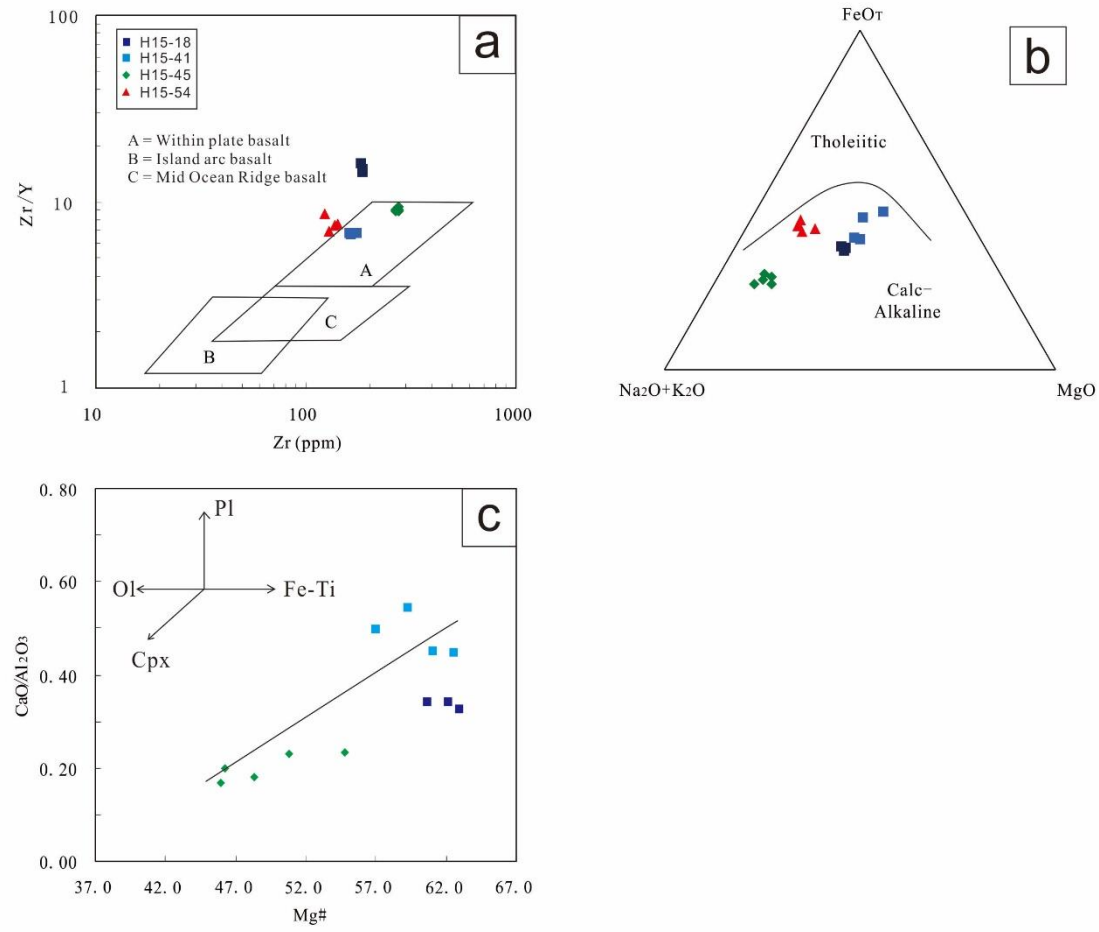

Fig. 4.10 Geochemical diagrams for the Cretaceous lava (a) the Zr/Y vs. Zr diagram for the Cretaceous volcanic rocks (Pearce and Norry, 1979). (b) AFM diagram shows the calc-alkaline series for the Cretaceous volcanic rocks. (c) CaO/Al2O3 vs. Mg# diagram shows the fractional crystallization of clinopyroxene (Sun et al., 2013).

However, the low Sr/Y ratios (< 200) of the andesites in the Lesser Xing'an-Zhangguangcai Range are distinct from adakitic magma (Defant and Drummond, 1990). The andesites have low contents of MgO (< 6%) and Mg# (< 66) with high FeO_T/MgO ratios (1.08 – 5.10), which is also inconsistent with high-magnesian andesitic magma generated from the interaction between subducted slab-melting/fluids and overlying mantle peridotite (Hirose, 1997; Jolly et al., 2007). Thus, the primary magma in this study is likely to be basaltic rather than andesitic.

Either magma mixing or fractional crystallization, accompanied by crustal assimilation (AFC process), can produce andesitic lava from basaltic primary magma. However, the following lines of evidence argue against fractional crystallization and

instead support a magma mixing model. First of all, Sr/Nd in the andesite, trachyandesite and trachydacite from the Lesser Xing'an-Zhangguangcai Range varies from 14 to 47 (except for 8.5 in one sample), higher than that of the mid- to upper-crust (~10; Rudnick and Gao, 2003), indicating that assimilation during magma ascent was not important. Secondly, the volume of andesitic lava should be much smaller than that of basaltic lava if the former is fractionated from the latter. However, basalt derived from the mantle wedge is rare in the study region and the andesite-dacite-rhyolite series is dominant, which suggests the importance of continental crust, changes the composition of primary basaltic magma in the source region. Thirdly, if AFC processes affected the primary basaltic magma, there should be a clear linear relation between SiO_2 and major elements oxides, such as MgO, Fe_2O_3T, K_2O and Na_2O. However, this is not shown in the Harker diagrams (Fig. 4.9a, b). Finally, fractional crystallization and magma mixing can be distinguished by trace elements because of the distinct behaviors of the elements with distinct partition coefficients (Treuil and Joron, 1975; Allègre and Minster, 1978). In the La/Sm vs. La, Rb vs. Rb/V and 1/V vs. Rb/V diagrams (Fig. 4.9c-e), magma mixing is shown to be more significant than fractional crystallization or partial melting for the andesitic-dacitic magma (Schiano et al., 2010).

Sample H15-73-3 is more similar to basaltic primary magma because of its low SiO_2 (59 %) and high Mg# (66.1), whereas sample H15-31-1 is closer to the felsic end-member in composition, with high SiO_2 (ca. 65%) and low Mg# (31.3). Thus, the basaltic end-member derived from the partial melting of the mantle wedge is characterized by low SiO_2 and Al_2O_3 and high MgO, Fe_2O_3T, Mg#, Cr and Ni. The felsic end-member which is melted from the lower crust heated by the ascending basaltic magma has higher SiO_2 and Al_2O_3 and lower MgO, Fe_2O_3T, Mg#, Cr and Ni. The andesitic lava is therefore the product of magma mixing of two end-members and crustal assimilation was insignificant.

4.6.1.2 Petrogenesis of the rhyolitic lava

Early Jurassic rhyolite in the Lesser Xing'an-Zhangguangcai Range is a minor component compared to the andesite and dacite. However, contemporaneous granite is widely exposed in this region, which has similar features in major and trace elements to the rhyolite. Thus, the granitoids should be treated as the intrusive equivalents of the rhyolites (Wu et al., 2003a, b, 2011).

The A/CNK value of the rhyolite ranges from 1.06 to 1.11, indicating it is weakly peraluminous. The 10000*Ga/Al ratio of rhyolite (~2.6) is near the boundary between A- and I&S-type granite (Whalen et al., 1987), indicating that the rhyolite is transitional between A- and highly fractionated I-type granite (Fig. 4.9f). Tang et al. (2011) proposed that the rhyolite in the Maoershan area is A-type rhyolite (Fig. 4.9f). However, aluminous A-type granite is difficult to distinguish from highly fractionated I-type granite/rhyolite (Chappell and White, 1992; King et al., 1997), which is widely distributed in NE China (Wu et al., 2003a, b). In the Lesser Xing'an-Zhangguangcai Range, Early Jurassic granite/rhyolite is closely associated with hornblende-bearing gabbro, diorite, granodiorite and syenogranite (Wu et al., 2003a, b). However, no alkaline mafic mineral, such as arfvedsonite or aegirine-augite, is present in the rhyolite, indicating that it is a highly fractionated I-type granite, and not an A-type granitoid.

The highly fractionated I-type rhyolite (sample H15-29) has high SiO_2 (>74 %), K_2O (4.8 – 6.5 %) and low MgO (<0.1 %), Fe_2O_3T (<2 %) and Mg# (< 25), indicating that the granitic magma was derived from the lower crust without any mantle participation. The strongly negative anomalies of Sr and Eu suggest fractionation of plagioclase and/or K-feldspar (Fig. 4.8b, c). The fractionation of K-feldspar can also be recognized in the Ba vs. Sr diagram (Fig. 4.9g). The extremely low contents of MgO and Fe_2O_3T are the result of fractionated mafic minerals, such as hornblende. The contents of P_2O_5 decrease with increasing SiO_2, suggesting the fractional crystallization of apatite or titanite (Supplementary table 2). In the La/Yb vs. La diagram, there is evidence of minor fractionation of monazite and/or allanite (Fig. 4.9h; Wu et al., 2003b). Thus, the

Early Jurassic rhyolite is a highly fractionated I-type rhyolite derived from lower continental crust without mantle input, and the granitic magma experienced fractional crystallization of plagioclase, K-feldspar, hornblende and accessory minerals, including apatite, titanite, monazite and allanite.

4.6.2 Petrogenesis of the Cretaceous volcanic rocks

The middle Cretaceous volcanic rocks mainly consist of basalt (samples H15-41-2 to H15-41-6 from the Jiamusi Block), basaltic andesite (sample H15-18-2 to H15-18-6 from the Lesser Xing'an Range), andesite (H15-54-2 to H15-54-6 from the Jiamusi Block) and dacite (H15-45-2 to H15-45-6 from the Jiamusi Block). These contemporaneous volcanic rocks are widely distributed in the Lesser Xing'an-Zhangguangcai Range, Jiamusi Block and Khanka Block (Fig. 4.3).

In the Zr/Y vs. Zr diagram (Fig. 4.10a), the basaltic and andesitic lava shows intra-plate characteristics, indicating they formed in an extensional setting (Pearce and Norry, 1979). This is consistent with the bimodal composite dykes with an age of 100 Ma found to the south of Jiamusi city, indicating extensional settings in the western Jiamusi Block and the Lesser Xing'an-Zhangguangcai Range (Sun et al., 2013). Rather than tholeiite, the Cretaceous mafic volcanic rocks are calc-alkaline, which is common at active continental margins (Fig. 4.10b). The negative anomalies of Nb-Ta, enrichment of LILEs and LREEs and depletion of HFSEs and HREEs indicate the influence of fluids released from subducted slab/sediments (Pearce and Peate, 1995). Thus, the basaltic and andesitic magma was likely produced in a back-arc extensional environment.

The basalts (samples H15-41-2 to H15-41-6) and basaltic-andesites (sample H15-18-2 to sample H15-18-6) are characterized by low SiO_2 (51 – 60.7 %), high MgO (3.7 – 4.5 %), Fe_2O_{3T} (5.3 – 7.6 %), Mg# (57 – 63), Cr (150 – 295 ppm) and Ni (37 – 107 ppm). They may represent a primary basaltic magma that was less contaminated by

continental crust than the andesite and dacite. In subduction zones, basaltic melt is attributed to fluids that released from the slab, which lowers the solidus of peridotite in the mantle wedge and thus results in the basaltic melts enriched in LILE/HFSE ratios (Gill, 1981; Saunders et al., 1980). The crystallization of Fe-rich minerals (such as clinopyroxene, hornblende and magnetite) under water-saturated conditions contributes to the calc-alkaline trend, namely the absence of Fe-enrichment in the basalt and andesite (Sission and Grove, 1993). In the CaO/Al_2O_3 vs. Mg# diagram, the fractionation of clinopyroxene can be recognized (Fig. 4.10c). This also explains the varying concentrations of Cr with constant concentration of Ni in samples H15-41-2 to H15-41-6 and H15-18-2 to H15-18-6, because Cr is much more compatible than Ni in clinopyroxene (Green, 1980).

The dacite (samples H15-45-2 to H15-45-6) could have been generated after the fractionation of the mafic minerals. Fractional crystallization lowers the contents of Fe, Mg, Mg#, Cr and Ni with increasing SiO_2 (Supplementary table 2). However, fractional crystallization cannot explain the geochemical features of the andesite collected north of Peide (samples H15-54-2 to H15-54-6). According to fractional crystallization models, the concentrations of incompatible elements (such as Cr, Ni and Mg) in dacite should be lower than those in andesite. However, the Mg# values, concentrations of Cr and Ni are lower in the andesite (samples H15-54-2 to H15-54-6) than those in the dacite (samples H15-45-2 to H15-45-6) in this study. Thus, magma mixing with felsic magma melted from continental crust is necessary to reduce the Mg#, Cr and Ni. In the adjacent area, magma mixing is also recognized in Huanan, the central Jiamusi Block. In this area, a ~100 Ma andesitic dike intruded into the contemporaneous granitic wall rocks, whereas numerous andesitic enclaves are found near the contact (Sun, 2013). From the central part of the andesitic dike to the granitic wall rock, the contents of SiO_2 become higher and the $\varepsilon Nd(t)$ more positive, indicating the interaction between mafic and felsic magma from different magmatic sources (Sun, 2013). The andesitic enclaves have similar SiO_2 but slightly lower Mg#, Cr and Ni to the andesite north of Peide in this study, suggesting a similar magma mixing process.

4.7 Tectonic implications

4.7.1 Tectonic environment of the Jurassic volcanic rocks

It is important to discuss the Heilongjiang Complex and the Sikhote-Alin accretionary complexes (or "Sikhote-Alin orogenic belt"; Jahn et al., 2015; Tang et al., 2016; Liu et al, 2017b) before discussing the tectonic environment of the volcanic rocks in this area.

The Heilongjiang Complex is located in the western Jiamusi Block, marking the remnants of the Mudanjiang Ocean (Fig. 4.2). It consists of components from the oceanic crust which experienced high-pressure metamorphism, including lenses of mafic-ultramafic rocks, quartz-feldspathic schists, blueschists and other sedimentary rocks. The blueschists were metamorphosed to epidote-blueschist facies with P–T conditions of approximately T = 320 – 450 °C and P = 0.9 – 1.1 GPa (Zhou et al., 2009; Ge et al., 2016). The zircon U-Pb ages of the blueschists, representing the age of their protoliths (E-MORB and OIB), range from 281 Ma to 213 Ma (Ge et al., 2016; Zhou et al., 2009). The timing of metamorphism, which is recorded by hornblende and muscovite Ar-Ar ages, ranges from 198 Ma to 165 Ma, indicating subduction of the Mudanjiang Ocean during the Early to Middle Jurassic (Li et al., 2010; Ge et al., 2016; Wu et al., 2007; Zhou et al., 2009). Arc-related intrusive rocks in the Early Jurassic also includes the mafic-ultramafic intrusions and the giant granitic plutons in the Lesser Xing'an-Zhangguangcai Range. The mafic-ultramafic rocks, such as olivine gabbro, gabbro and gabbro-diorite show important enrichment of LILEs and LREEs and depletion of Nb-Ta and Ti, suggesting arc-related features due to the influence of fluids from the subducted sediments (Yu et al., 2012). The occurrence of I-type granitoids in NE China is well documented, indicating they are highly-fractionated I-type granites (Wu et al., 2003a, b; Liu et al., 2016). The geochemical characteristics of enriched LILEs, LREEs and depleted Nb-Ta are similar to arc magmas. The positive $\varepsilon Nd(t)$ and $\varepsilon Hf(t)$ data suggest that they formed by melting of juvenile crust (Wu et al.,

2003a, b; Liu et al., 2016). Yu et al. (2012) proposed that the I-type granitoids and the mafic-ultramafic rocks represent typical bimodal magmatism and thus were the products of back-arc extension. However, the extensive andesite and dacite analyzed in our study do not support this view. The lack of intermediate intrusive rocks, such as diorite and granodiorite, can be attributed to only weak mixing between the felsic and mafic magma in the chamber.

Based on spatial relationships between the volcanic rocks in the Lesser Xing'an-Zhangguangcai Range and the Heilongjiang Complex, along with the arc-related geochemical features of the volcanic rocks, it is proposed that the Early Jurassic volcanic rocks were formed in a magmatic arc at an active continental margin. The late Triassic to Early Jurassic granitoids (Wu et al., 2011; Ge et al., 2017, 2018) and Early Jurassic volcanic rocks in the Lesser Xing'an-Zhangguangcai Range (Xu et al., 2013; Tang et al., 2011 and data in this study) represents a continental arc. To the east of this arc, the Heilongjiang Complex was the remnant of the coeval mélange. Hence, the Mudanjiang Ocean was subducted westwards below this active margin and the fluid released from the slab was released into the mantle wedge. Partial melting of the upper mantle and overlying crust together produced the Early Jurassic andesite and the I-type rhyolite.

Along the east margin of the Jiamusi-Khanka Block, the Paleo-Pacific Oceanic plate also began its subduction during the Early Jurassic (Wu et al., 2007; Guo et al., 2015; Zhou et al., 2014; Liu et al., 2017a). The direct evidence for this subduction is the Sikhote-Alin accretionary complexes. The Sikhote-Alin orogenic belt is consisted of several NNE trending accretionary prisms and basins, with ages ranging from Middle Jurassic to Early Cretaceous. Unlike the Heilongjiang complex, there is no Jurassic or Cretaceous high-pressure metamorphism reported yet in this area. However, paleontological and radio-isotopic dating indicate that these NNE trending accretionary belts were continuously accreted to the eastern Jiamusi-Khanka Block from west to east during Jurassic to Cretaceous (Khanchuk et al., 2016; Jahn et al.,

2015; Liu et al., 2017b). The Early Jurassic (187 to 174 Ma) arc-related volcanic rocks were generated in the Nadanhada accretionary complex (the west part of the Sikhote-Alin accretionary complexes; Wang et al., 2017), including calc-alkaline andesite-dacites-rhyolite associations, Nb-enriched andesites and high-Mg andesites. In the south Khanka Block, Guo et al. (2015) reported a mafic intrusive complex with age of ca. 187 Ma in the Tumen area, which was evolved from a water-saturated parental magma because of the dehydration of the subducted Paleo-Pacific slab.

Thus, there were two subduction zones along the western and eastern margin of the Jiamusi-Khanka Block in the Early Jurassic, namely the subduction of the Mudanjiang and Paleo-Pacific oceans, respectively (Fig. 4.11a).

4.7.2 Tectonic environment of the Cretaceous volcanic rocks

The closing time of the Mudanjiang Ocean is now constrained well. Some research indicates that the collision between the Songliao and Jiamusi-Khanka blocks is 210-180 Ma (Zhou et al., 2009, 2013, 2017). Recently, Zhu et al. (2015, 2016) suggested that the closure should be as late as Early Cretaceous because the protolith age of the blueschist was dated to ca. 142 Ma. Thus, the final closure timing needs further research. However, the consensus is that eastern CAOB began to be dominated by the advance and roll-back of the Paleo-Pacific slab from the Early Cretaceous (Wu et al., 2005; Sun et al., 2018).

Because of subduction of the Paleo-Pacific Ocean, magmatism in both arc and back-arc (intra-continental) areas were generated extensively. The Sikhote-Alin accretionary complexes, including the Nadanhada Terrane, were accreted to the eastern margin of the Bureya-Jiamusi-Khanka Block from the Late Jurassic to middle Cretaceous.

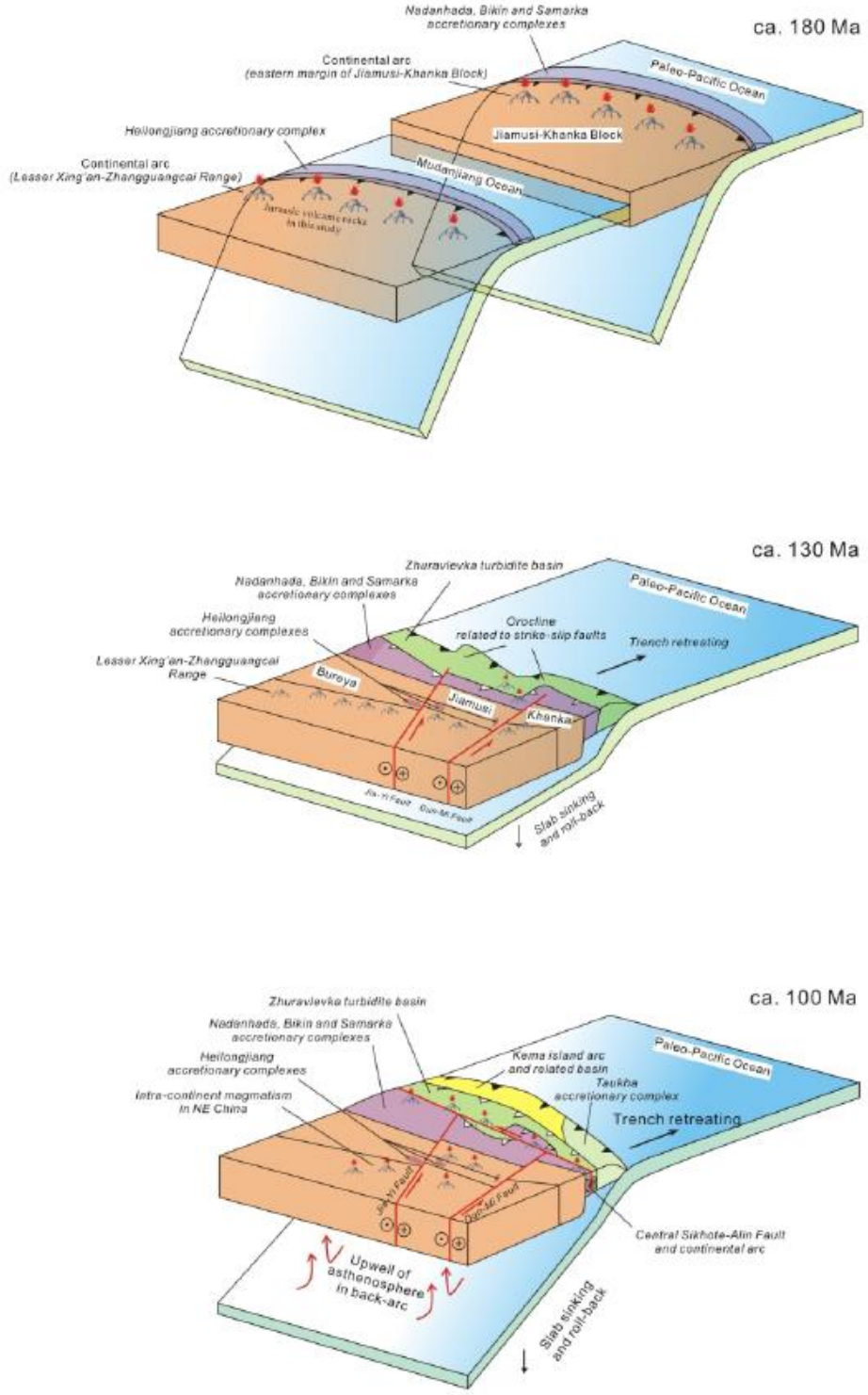

Fig. 4.11 Tectonic model about the subduction of Mudanjiang and Paleo-Pacific oceans during the Early Jurassic to middle Cretaceous.

This process forced the trench to retreat oceanwards and intensified the roll-back of the Paleo-Pacific slab. Because of the roll-back process, arc-related magmatism

migrated eastwards from the eastern Jiamusi Block (Early Jurassic) to the Sikhote-Alin accretionary complexes in the Early to Late Cretaceous (Cheng et al., 2006; Golozoubov et al., 1999; Kemkin and Kemkina, 2000; Khanchuk et al., 2001, 2016; Sun et al., 2015b; Zhou et al., 2014; Jahn et al., 2015). Contemporarily, intra-continental magmatism in the back-arc area was also moved eastwards from the Great Xing'an Range (Late Jurassic to Early Cretaceous) to the Lesser Xing'an-Zhangguangcai Range and Jiamusi Block (middle Cretaceous). In NE Asia, widely distributed metamorphic core complexes and extensional basins indicate a regionally extensional event due to the slab roll-back (Wang et al., 2011, 2012). The intra-plate basalt and andesite in this study, integrated with the ~100 Ma bimodal dikes and A-type rhyolite in the Jiamusi Block (Sun et al., 2013), reveal that extension related to back-arc roll-back was active in the middle Cretaceous NE China.

4.7.3 Summary of previous models of the Paleo-Pacific subduction

The correlation between the eastwards migrating magmatism and the subduction of the Paleo-Pacific Ocean in NE China has been discussed for decades. Several models are summarized below.

1. Delamination model. Wang et al. (2006a) and Zhang et al. (2010) proposed that lithospheric delamination was triggered in the Late Jurassic and the flat slab of the Paleo-Pacific Oceanic plate was broken off and sank into asthenosphere. The delamination was initiated under the Great Xing'an Range at first and then extended eastwards to the Lesser Xing'an-Zhangguangcai Range, Bureya-Jiamusi-Khanka Block and Korean Peninsula, responded by the migration of magmatism.

2. Slab roll-back model. Some studies proposed that the younger tendency of magmatism in NE China resulted from the roll-back of the Paleo-Pacific slab, whereas the delamination and break-off of the flat slab is not necessary (Sun et al., 2013; Ma et al., 2016). As the subduction angle of the slab became steeper,

the trench retreated eastwards, causing the back-arc or intra-continental extension in NE China. The magmatism with ages ranging from 150 to 80 Ma recorded the intra-continental extension. As the slab became steeper, the magmatic belt migrated more eastwards from the interior of the eastern CAOB to Korean Peninsula and even Japanese Islands.

3. Roll-back with migrating continental arc and intra-continental magmatism model. Recently, Sun et al. (2018) proposed a tectonic model emphasizing the closure of the Mudanjiang Ocean and the eastward migration of the continental arc in Sikhote-Alin, not only the migration of intra-continental magma as proposed by previous models. This model firstly considered the migration of the continental arc along with the intra-continental magmatism.

The first model neglected the importance of the Mudanjiang Ocean when explaining Jurassic to Cretaceous magmatism in the eastern CAOB. According to our study, the Early Jurassic volcanic rocks in the Lesser Xing'an-Zhangguangcai Range was related to the subduction of the Mudanjiang Ocean, rather than the subduction of the Paleo-Pacific Oceanic plate (the Izanagi Plate). This is also evidenced by the Early Jurassic granitoids in the Lesser Xing'an-Zhangguangcai Range (Wu et al., 2011; Xu et al., 2013; Liu et al., 2017a) and the Heilongjiang accretionary complex (Zhou et al., 2009, 2017). Thus, it was not possible for the Paleo-Pacific slab to "ignore" the Mudanjiang Ocean and reach far west to the Great Xing'an Range.

For both the first and second model, the sharing issue is that the migration of magmatism is more complicated than previously estimated, based on the new geochronological and geochemical data. For instance, previous studies showed that the volcanic rocks with ages of 135 to 110 Ma were mainly located in the western NE China (mainly in the Great Xing'an Range and Songliao Basin). However, recent studies reveal that the arc-related granitoids in the western the Sikhote-Alin area also have ages from 135 to 110 Ma (Cheng et al., 2006; Kruk et al., 2014; Jahn et al., 2015).

Thus, the migration of magmatism in NE Asia should include both the continental arc and back-arc areas, like suggested by the third model (Sun et al., 2018).

However, one of the most notable tectonic events in NE Asia is that the sinistral strike-slip faulting was activated from the Late Jurassic to Early Cretaceous. The strike-slip faults cut across the Lesser Xing'an-Zhangguangcai Range, Bureya-Jiamusi-Khanka Block and the Sikhote-Alin orogenic belt (Figs. 2 and 3). This strike-slip faulting event followed the closure of the Mudanjiang Ocean, and was coeval with the roll-back of the Paleo-Pacific slab and migrating magmatism. This important event and its influence to tectonics was not discussed in the previous models. In our new model, the role played by these strike-slip faults will be estimated, together with the slab roll-back process and magmatism.

4.8 New tectonic model of NE Asia from Jurassic to Cretaceous

In the Early Jurassic, the westward subduction of the Mudanjiang Ocean generated the continental arc in the Lesser Xing'an-Zhangguangcai Range and the Heilongjiang accretionary complex (Fig. 4.11). The other arc was formed along the eastern margin of the Jiamusi Block, recorded by the arc-related volcanic rocks now preserved in the Nadanhada accretionary complex (Wang et al., 2017).

The closure of the Mudanjiang Ocean needs more research in future. However, it is proposed that the final closure happened between the Middle Jurassic to early Early Cretaceous according to the following evidence. The youngest age of the high-pressure metamorphism of the Heilongjiang Complex is ca. 180-170 Ma (Zhou et al., 2009; Ge et al., 2016), which coincide with the end time of the continental arc magma in the Lesser Xing'an-Zhangguangcai Range (Wu et al., 2011). Thus, the lower limit of the closure event should be Middle Jurassic. At ca. 130 Ma, the basins to the east of Heilongjiang Complex began to accept sediments from the Lesser Xing'an Zhangguangcai Range, indicating the Mudanjiang Ocean had been closed before the

early Early Cretaceous (Zhang et al., 2015).

After the closure of the Mudanjiang Ocean, the slab of the Paleo-Pacific Ocean extended westwards to the Lesser Xing'an-Zhangguangcai Range (Fig. 4.11), even as far as the Great Xing'an Range (Sun et al., 2013). The Dun-Mi and Jia-Yi faults, two northern branches of the Tan-Lu Fault, were triggered during this period. The earliest active age of the Dun-Mi Fault is 161±3 Ma dated by the biotite Ar-Ar method from a mylonite in the Mishan area, which is a cooling age of the ductile shear zone, suggesting that the initiation of this strike-slip fault was early Middle Jurassic or earlier (Sun et al., 2010). More recent researches propose that the most important large-scale sinistral strike-slip faulting of the Dun-Mi and Jia-Yi faults happened in the early Early Cretaceous, constrained by several deformed and undeformed plutons/dikes (Liu et al., 2018; Gu et al., 2016; Zhang et al., 2018). It was followed by a regional extension due to the slab roll-back from the Early Cretaceous, evidenced by the depression of numerous basins and oldest volcanic rocks in the Songliao basin dated to ca. 133 Ma (Pei et al., 2008), as well as the structural geological survey (Sun et al., 2010, 2016). We propose that the two faults cut through the Jurassic continental arc (Lesser Xing'an-Zhangguangcai Range), the Bureya-Jiamusi-Khanka Block and the Jurassic accretionary complexes in Sikhote-Alin into several components. The Jurassic continental arc and accretionary complexes were bended to for a convex in the eastern Jiamusi-Khanka Block and Sikhote-Alin accretionary complexes. An orocline was thus created in the Early Cretaceous (Fig. 4.11), similar to the present Tonga area and this orocline structure is now preserved in the Nadanhada-Bikin accretionary complex and Zhuravlevka turbidite basin (Fig. 4.3).

During the late Early Cretaceous, the Zhuravlevka turbidite basin, Kema island arc and Taukha accretionary complex were accreted from west to east along the Paleo-Pacific margin, forcing the trench to retreat eastwards (Fig. 4.11). The most important strike-slip fault in Sikhote-Alin, the Central Sikhote-Alin Fault and its branches began to move the eastern Sikhote-Alin orogenic belt northwards. The continental arc with ages ranging from 110 to 100 Ma was located within/near the fault zone (Jahn et al., 2015;

Khanchuk et al., 2016). The Fault was active along with the arc volcanos and responsible for the lateral component of the oblique subduction of the Izanagi Plate, alike to the present tectonics in the Sumatra Island. The intra-continental extension continued to move to east, causing the volcanism of ca. 100 Ma in the Lesser Xing'an-Zhangguangcai Range and adjacent Jiamusi Block (Fig. 4.11).

4.9 Conclusions

The andesite, trachyandesite, trachydacite and rhyolite in the Lesser Xing'an-Zhangguangcai Range are Early Jurassic in age (178 – 189 Ma). The andesitic lava was product of magma mixing between the basaltic magma from mantle and granitic magma from lower crust, whereas the rhyolitic lava was I-type granite which was melted from the lower crust and then experienced highly fractionation of plagioclase, K-feldspar, hornblende, biotite and accessory minerals, such as apatite, titanite, monazite and allanite. The Early Jurassic volcanic rocks were generated in the active continental margin and were associated with the westward subduction of the Mudanjiang Ocean.

The basalt, basaltic andesite, andesite and trachydacite in the Lesser Xing'an-Zhangguangcai Range and the Jiamusi Block are middle Cretaceous in age (ca. 100 Ma). These volcanic rocks show important calc-alkaline trending which is attributed to the crystallization of Fe-enriched minerals, such as hornblende, clinopyroxene and magnetite. The andesite in the north of Peide may experience higher proportion of magma mixing of the felsic magma. The middle Cretaceous volcanic rocks are intra-continental volcanic rocks generated in the extensional setting.

In the Early Jurassic, continental arc-related magmatic rocks were generated in the Lesser Xing'an-Zhangguangcai Range due to the subduction of the Mudanjiang Ocean. During the Late Jurassic to Early Cretaceous, the Mudajiang Ocean was closed and the Bureya-Jiamusi-Khanka Block collided with the Songliao Block. Afterwards the slab

of the Paleo-Pacific Ocean reached the interior of the eastern CAOB. At the same time, two strike-slip faults were triggered and cut through the previous geological units. Oroclines were formed due to the slab roll-back and sinistral strike-slip faults. This process resulted in the eastwards migrating of both arc and intra-continental magmatism. In the late Early Cretaceous, the Central Sikhote-Alin Fault began to slide along the continental arc and the intra-continental magmatism migrated to the Lesser Xing'an-Zhangguangcai Range and the adjacent Jiamusi Block.

4.10 Reference

Allegre, C., Minster, J., 1978. Quantitative models of trace element behavior in magmatic processes. Earth and Planetary Science Letters 38, 1-25.

Bi, J.H., Ge, W.C., Yang, H., Wang, Z.H., Xu, W.L., Yang, J.H., Xing, D.H., Chen, H.J., 2016. Geochronology and geochemistry of late Carboniferous–middle Permian I- and A-type granites and gabbro–diorites in the eastern Jiamusi Massif, NE China: Implications for petrogenesis and tectonic setting. Lithos 266, 213-232.

Bi, J.H., Ge, W.C., Yang, H., Zhao, G.C., Xu, W.L., Wang, Z.H., 2015. Geochronology, geochemistry and zircon Hf isotopes of the Dongfanghong gabbroic complex at the eastern margin of the Jiamusi Massif, NE China: Petrogensis and tectonic implications. Lithos 234, 27-46.

Chappell, B., White, A., 1992. I-and S-type granites in the Lachlan Fold Belt. Geological Society of America Special Papers 272, 1-26.

Cheng, R., Wu, F., Ge, W., Sun, D., Liu, X., Yang, J., 2006. Emplacement age of the Raohe Complex in eastern Heilongjiang Province and the tectonic evolution of the eastern part of Northeastern China. Acta Petrologica Sinica 22, 353-376 (In Chinese with English abstract).

Cogné, J.P., Kravchinsky, V.A., Halim, N., Hankard, F., 2005. Late Jurassic-Early Cretaceous closure of the Mongol-Okhotsk Ocean demonstrated by new Mesozoic palaeomagnetic results from the Trans-Baikal area (SE Siberia). Geophysical Journal International 163, 813-832.

Defant, M.J., Drummond, M.S., 1990. Derivation of some modern arc magmas by melting of young subducted lithosphere. Nature 347, 662-665.

Dong, Y., Ge, W.C., Yang, H., Xu, W.L., Bi, J.H., Wang, Z.H., 2016. Geochemistry and geochronology of the Late Permian mafic intrusions along the boundary area of Jiamusi and Songnen-Zhangguangcai Range massifs and adjacent regions, northeastern China: Petrogenesis and implications for the tectonic evolution of the Mudanjiang Ocean. Tectonophysics.

Donskaya, T., Gladkochub, D., Mazukabzov, A., De Waele, B., Presnyakov, S., 2012. The Late Triassic Kataev volcanoplutonic association in western Transbaikalia, a fragment of the active continental margin of the Mongol-Okhotsk Ocean. Russian Geology and Geophysics 53, 22-36.

Gao, F., Xu, W., Yang, D., Pei, F., Liu, X., Hu, Z., 2007. LA-ICP-MS zircon U-Pb dating from granitoids in southern basement of Songliao basin: Constraints on ages of the basin basement. Science in China Series D: Earth Sciences 50, 995-1004 (In Chinese with English abstract).

Ge, M.H., Zhang, J.J., Liu, K., Ling, Y.Y., Wang, M., Wang, J.M., 2016. Geochemistry and geochronology of the blueschist in the Heilongjiang Complex and its implications in the late Paleozoic tectonics of eastern NE China. Lithos 261, 232-249.

Gill, J.B., 1981. Orogenic andesites and plate tectonics. Springer, Berlin, pp. 1-390.

Golozoubov, V., Markevich, V., Bugdaeva, E., 1999. Early Cretaceous changes of vegetation and environment in East Asia. Palaeogeography, Palaeoclimatology, Palaeoecology 153, 139-146.

Gu, C., Zhu, G., Zhai, M., Lin, S., Song, L., & Liu, B., 2016. Features and origin time of Mesozoic strike-slip structures in the Yilan-Yitong Fault Zone. Science China Earth Sciences, 59(12), 2389-2410.

Graham, I., Cole, J., 1991. Petrogenesis of andesites and dacites of White Island volcano, Bay of Plenty, New Zealand, in the light of new geochemical and isotopic data. New Zealand journal of geology and geophysics 34, 303-315.

Grebennikov, A.V., Khanchuk, A.I., Gonevchuk, V.G., Kovalenko, S.V., 2016. Cretaceous and Paleogene granitoid suites of the Sikhote-Alin area (Far East Russia): Geochemistry and tectonic implications. Lithos 261, 250-261.

Green, T., 1980. Island arc and continent-building magmatism—A review of petrogenic models based on experimental petrology and geochemistry. Tectonophysics 63, 367-385.

Grove, T., Parman, S., Bowring, S., Price, R., Baker, M., 2002. The role of an H2O-rich fluid component in the generation of primitive basaltic andesites and andesites from the Mt. Shasta region, N California. Contributions to Mineralogy and Petrology 142, 375-396.

HBGMR (Heilongjiang Bureau of Geology and Mineral Resources), 1993. Regional Geology of Heilongjiang Province. Geological Publishing House, Beijing, pp. 148–191 (in Chinese with English abstract).

Hildreth, W., Moorbath, S., 1988. Crustal contributions to arc magmatism in the Andes of central Chile. Contributions to mineralogy and petrology 98, 455-489.

Hirose, K., 1997. Melting experiments on lherzolite KLB-1 under hydrous conditions and generation of high-magnesian andesitic melts. Geology 25, 42-44.

Huang, Y., Ren, D., Zhang, X., Xiong, X., Zhang, C., Wang, Y., Zhao, L., 2008. Zircon U–Pb dating of the Meizuo granite and geological significance in the Huanan uplift, east Heilongjiang Province. Journal of Jilin University (Earth Science Edition) 38, 631-638 (In Chinese with English abstract).

Jahn, B.M., 2004. The Central Asian Orogenic Belt and growth of the continental crust in the Phanerozoic. Geological Society, London, Special Publications 226, 73-100.

Jahn, B.M., Valui, G., Kruk, N., Gonevchuk, V., Usuki, M., Wu, J.T., 2015. Emplacement ages, geochemical and Sr–Nd–Hf isotopic characterization of Mesozoic to early Cenozoic granitoids of the Sikhote-Alin Orogenic Belt, Russian Far East: Crustal growth and regional tectonic evolution. Journal of Asian Earth Sciences 111, 872-918.

Jahn, B.M., Wu, F.Y., Chen, B., 2000. Granitoids of the Central Asian Orogenic Belt

and continental growth in the Phanerozoic. Geological Society of America Special Papers 350, 181-193.

Shao, J.A., Li, Y.F., Tang, K.D., 2013. Restoration of the orogenic processes of Zhangguangcai Range. Acta Petrologica Sinica 29, 2959-2970 (In Chinese with English abstract).

Jolly, W.T., Schellekens, J.H., Dickin, A.P., 2007. High-Mg andesites and related lavas from southwest Puerto Rico (Greater Antilles Island Arc): Petrogenetic links with emplacement of the Late Cretaceous Caribbean mantle plume. Lithos 98, 1-26.

Kaplun, V., 2012. Geoelectric section of the lithosphere of the Amur-Zeya sedimentary basin deduced from magnetotelluric sounding along the Blagoveshchensk-Birakan profile. Russian Journal of Pacific Geology 6, 131-142.

Kaplun, V., 2013. Geoelectric section of the lithosphere of the Amur-Zeya sedimentary basin deduced from magnetotelluric soundings. Russian Journal of Pacific Geology 7, 151-166.

Kelemen, P.B., 1995. Genesis of high Mg# andesites and the continental crust. Contributions to Mineralogy and Petrology 120, 1-19.

Kemkin, I., Kemkina, R., 2000. Taukha Terrane of Southern Sikhote Alin: Geology and Evolution. Geotectonics 34, 407-414.

Kemkin, I.V., Taketani, Y., 2008. Structure and age of lower structural unit of Taukha terrane of Late Jurassic–Early Cretaceous accretionary prism, southern Sikhote–Alin. Island Arc 17, 517-530.

Khanchuk, A.I., 2001. Pre-Neogene tectonics of the Sea-of-Japan region: a view from the Russian side. Earth Sci 55, 275-291.

King, P., White, A., Chappell, B., Allen, C., 1997. Characterization and origin of aluminous A-type granites from the Lachlan Fold Belt, southeastern Australia. Journal of petrology 38, 371-391.

Kirillova, G.L., 2003. Late Mesozoic–Cenozoic sedimentary basins of active continental margin of Southeast Russia: paleogeography, tectonics, and coal–oil–gas presence. Marine and Petroleum Geology 20, 385-397.

Kojima, S., 1989. Mesozoic terrane accretion in northeast China, Sikhote-Alin and

Japan regions. Palaeogeography, Palaeoclimatology, Palaeoecology 69, 213-232.

Kröner, A., Kovach, V., Belousova, E., Hegner, E., Armstrong, R., Dolgopolova, A., Seltmann, R., Alexeiev, D., Hoffmann, J., Wong, J., 2014. Reassessment of continental growth during the accretionary history of the Central Asian Orogenic Belt. Gondwana Research 25, 103-125.

Kröner, A., Windley, B., Badarch, G., Tomurtogoo, O., Hegner, E., Jahn, B., Gruschka, S., Khain, E., Demoux, A., Wingate, M., 2007. Accretionary growth and crust formation in the Central Asian Orogenic Belt and comparison with the Arabian-Nubian shield. Geological Society of America Memoirs 200, 181-209.

Kravchinsky, V.A., Cogné, J.-P., Harbert, W.P., Kuzmin, M.I., 2002. Evolution of the Mongol-Okhotsk Ocean as constrained by new palaeomagnetic data from the Mongol-Okhotsk suture zone, Siberia. Geophysical Journal International 148, 34-57.

Kruk, N., Simanenko, V., Gvozdev, V., Golozubov, V., Kovach, V., Serov, P., Kholodnov, V., Moskalenko, E.Y., Kuibida, M., 2014. Early Cretaceous granitoids of the Samarka terrane (Sikhote-Alin'): geochemistry and sources of melts. Russian Geology and Geophysics 55, 216-236.

Li, J.Y., 2006. Permian geodynamic setting of Northeast China and adjacent regions: closure of the Paleo-Asian Ocean and subduction of the Paleo-Pacific Plate. Journal of Asian Earth Sciences 26, 207-224.

Li, S.Q., Yang, Y.Z., Xie, Q.L., Wang, Y., Chen, F., 2015. Age Constraints on Late Mesozoic Lithospheric Extension and Origin of Felsic Volcanism in the Songliao Basin, NE China. The Journal of Geology 123, 153-175.

Li, W., Takasu, A., Liu, Y., Guo, X., 2010. Newly discovered garnet-barroisite schists from the Heilongjiang Complex in the Jiamusi Massif, northeastern China. Journal of mineralogical and petrological sciences 105, 86-91.

Liu, C., Zhang, X.Z., Liu, Y., Yang, B.J., Feng, X., Wang, D., Liu, D.M., 2009. Geoelectrical evidence for characteristics of lithospheric structure beneath the Yuejinshan collage zone and its vicinity in Northeast Asia. Chinese Journal of Geophysics 52, 403-412 (In Chinese with English abstract).

Liu, C., Zhu, G., Zhang, S., Gu, C., Li, Y., Su, N., & Xiao, S., 2018. Mesozoic strike-slip movement of the Dunhua–Mishan Fault Zone in NE China: A response to oceanic plate subduction. Tectonophysics, 723, 201-222.

Liu, K., Zhang, J., Wilde, S.A., Zhou, J., Wang, M., Ge, M., Wang, J., Ling, Y., 2017a. Initial subduction of the Paleo-Pacific Oceanic plate in NE China: Constraints from whole-rock geochemistry and zircon U-Pb and Lu-Hf isotopes of the Khanka Lake granitoids. Lithos, 274-275, 254-270.

Liu, K., Zhang, J., Wilde, S. A., Liu, S., Guo, F., Kasatkin, S. A., Golozoubov, V.V., Ge, M., Wang, M., Wang, J., 2017b. U-Pb Dating and Lu-Hf Isotopes of Detrital Zircons From the Southern Sikhote-Alin Orogenic Belt, Russian Far East: Tectonic Implications for the Early Cretaceous Evolution of the Northwest Pacific Margin. Tectonics, 36(11), 2555-2598.

Ma, X.H., Zhu, W.P., Zhou, Z.H., Qiao, S.L., 2016. Transformation from Paleo-Asian Ocean closure to Paleo-Pacific subduction: New constraints from granitoids in the eastern Jilin–Heilongjiang Belt, NE China. Journal of Asian Earth Sciences, in press.

Malinovsky, A., Golozoubov, V., Simanenko, V., 2006. The Kema island-arc terrane, eastern Sikhote Alin: Formation settings and geodynamics, Doklady earth sciences. Springer, pp. 1026-1029.

Malinovsky, A., Golozubov, V., 2011. Lithology and depositional settings of the terrigenous sediments along transform plate boundaries: Evidence from the early cretaceous Zhuravlevka terrane in Southern Sikhote Alin. Russian Journal of Pacific Geology 5, 400-417.

Malinovsky, A., Golozubov, V., Simanenko, V., 2005. Composition and depositional settings of Lower Cretaceous terrigenous rocks of the Kema River Basin, eastern Sikhote Alin. Lithology and Mineral Resources 40, 429-447.

Malinovsky, A.I., Golozoubov, V.V., Simanenko, V.P., Simanenko, L.F., 2008. Kema terrane: A fragment of a back‐arc basin of the early Cretaceous Moneron–Samarga island‐arc system, East Sikhote–Alin range, Russian Far East. Island Arc 17, 285-304.

Matsuda, T., Isozaki, Y., 1991. Well‐documented travel history of Mesozoic pelagic chert in Japan: from remote ocean to subduction zone. Tectonics 10, 475-499.

Meng, E., Xu, W.L., Yang, D.B., Pei, F.P., Ji, W.Q., Yu, Y., Zhang, X.Z., 2008. Permian volcanisms in eastern and southeastern margins of the Jiamusi Massif, northeastern China: Zircon U-Pb chronology, geochemistry and its tectonic implications. Chinese Science Bulletin 53, 956-965 (In Chinese with English abstract).

Meng, E., Xu, W.L., Pei, F.P., Yang, D.B., Wang, F., Zhang, X.Z., 2011. Permian bimodal volcanism in the Zhangguangcai Range of eastern Heilongjiang Province, NE China: zircon U–Pb–Hf isotopes and geochemical evidence. Journal of Asian Earth Sciences 41, 119-132.

Natal'in, B., 1993. History and modes of Mesozoic accretion in southeastern Russia. Island Arc 2 (1), 15-34.

Pearce, J.A., Norry, M.J., 1979. Petrogenetic implications of Ti, Zr, Y, and Nb variations in volcanic rocks. Contributions to mineralogy and petrology 69, 33-47.

Pearce, J.A., Peate, D.W., 1995. Tectonic implications of the composition of volcanic arc magmas. Annual Review of Earth and Planetary Sciences 23, 251-286.

Pei, F., Xu, W., Yang, D., Ji, W., Yu, Y., Zhang, X., 2008. Mesozoic volcanic rocks in the southern Songliao basin: zircon U–Pb ages and their constraints on the nature of basin basement. Earth Science (Journal of China University of Geosciences) 5, 603-617 (In Chinese with English abstract).

Pei, F., Xu, W., Yang, D., Zhao, Q., Liu, X., Hu, Z., 2007. Zircon U-Pb geochronology of basement metamorphic rocks in the Songliao Basin. Chinese Science Bulletin 52, 942-948 (In Chinese with English abstract).

Petrishchevsky, A., 2011. Rheological model of the crust beneath southern Sikhote-Alin: Evidence from gravity data. Russian Journal of Pacific Geology 5(3), 210-224.

Petrishchevsky, A., 2013. Gravity models of two-level collision of lithospheric plates in northeastern Asia. Geotectonics 47(6), 465-484.

Plank, T., Langmuir, C.H., 1988. An evaluation of the global variations in the major element chemistry of arc basalts. Earth and Planetary Science Letters 90, 349-370.

Reubi, O., Blundy, J., 2009. A dearth of intermediate melts at subduction zone volcanoes and the petrogenesis of arc andesites. Nature 461, 1269-1273.

Rudnick, R.L., Gao, S., 2003. Composition of the Continental Crust, In: Rudnick, R. L. (Eds.), Treatise on Geochemistry, Volume 3. Elsevier, pp. 1-64.

Saunders, A.D., Tarney, J., Weaver, S.D., 1980. Transverse geochemical variations across the Antarctic Peninsula: implications for the genesis of calc-alkaline magmas. Earth and Planetary Science Letters 46, 344-360.

Schiano, P., Monzier, M., Eissen, J.-P., Martin, H., Koga, K., 2010. Simple mixing as the major control of the evolution of volcanic suites in the Ecuadorian Andes. Contributions to Mineralogy and Petrology 160, 297-312.

Şengör, A., Natal'In, B., Burtman, V., 1993. Evolution of the Altaid tectonic collage and Palaeozoic crustal growth in Eurasia. Nature 364, 299-307.

Shimoda, G., Tatsumi, Y., Nohda, S., Ishizaka, K., Jahn, B., 1998. Setouchi high-Mg andesites revisited: geochemical evidence for melting of subducting sediments. Earth and Planetary Science Letters 160, 479-492.

Sisson, T., Grove, T., 1993. Experimental investigations of the role of H2O in calc-alkaline differentiation and subduction zone magmatism. Contributions to Mineralogy and Petrology 113, 143-166.

Sorokin, A., Kotov, A., Kudryashov, N., Kovach, V., 2016a. Early Mesozoic granitoid and rhyolite magmatism of the Bureya Terrane of the Central Asian Orogenic Belt: Age and geodynamic setting. Lithos.

Sorokin, A., Kotov, A., Sal'nikova, E., Kudryashov, N., Anisimova, I., Yakovleva, S., Fedoseenko, A., 2010. Granitoids of the Tyrma–Bureya complex in the northern Bureya–Jiamusi superterrane of the Central Asian fold belt: age and geodynamic setting. Russian Geology and Geophysics 51, 563-571.

Sorokin, A., Kudryashov, N., Kotov, A., 2007. Age and geochemistry of the Early Mesozoic granitoid massifs of the southern Bureya terrane of the Russian Far

East. Russian Journal of Pacific Geology 1, 454-463.

Sorokin, A., Malyshev, Y.F., Kaplun, V., Sorokina, A., Artemenko, T., 2013. Evolution and deep structure of the Zeya-Bureya and Songliao sedimentary basins (East Asia). Russian Journal of Pacific Geology 7, 77-91.

Sorokin, A., Ovchinnikov, R., Kudryashov, N., Sorokina, A., 2016b. An Early Neoproterozoic gabbro–granite association in the Bureya Continental Massif (Central Asian fold belt): First geochemical and geochronological data, Doklady Earth Sciences. Springer, pp. 1307-1311.

Sun, M.D., Chen, H.L., Zhang, F.Q., Wilde, S.A., Dong, C.W., Yang, S.F., 2013a. A 100Ma bimodal composite dyke complex in the Jiamusi Block, NE China: An indication for lithospheric extension driven by Paleo-Pacific roll-back. Lithos 162, 317-330.

Sun, M.D., 2013. Late Mesozoic magmatism and its tectonic implication for the Jiamusi Block and adjacet areas of NE China. Thesis, Zhejiang University, pp. 1-202 (In Chinese with English abstract).

Sun, M.D., Xu, Y.G., Wilde, S.A., Chen, H.L., Yang, S.F., 2015. The Permian Dongfanghong island-arc gabbro of the Wandashan orogen, NE China: implications for Paleo-Pacific subduction. Tectonophysics 659, 122-136.

Sun, M., Chen, H., Milan, L. A., Wilde, S. A., Jourdan, F., Xu, Y., 2018. Continental Arc and Back-Arc Migration in Eastern NE China: New Constraints on Cretaceous Paleo‐Pacific Subduction and Rollback. Tectonics 37, 3893-3915.

Sun, S.S., McDonough, W.S., 1989. Chemical and isotopic systematics of oceanic basalts: implications for mantle composition and processes. Geological Society, London, Special Publications 42, 313-345.

Tang, J., Xu, W.L., Wang, F., Wang, W., Xu, M.J., Zhang, Y.H., 2014. Geochronology and geochemistry of Early–Middle Triassic magmatism in the Erguna Massif, NE China: constraints on the tectonic evolution of the Mongol–Okhotsk Ocean. Lithos 184, 1-16.

Tang, J., Xu, W.L, Niu, Y.L., Wang, F., Ge, W.C, Sorokin, A., Chekryzhov, I., 2016. Geochronology and geochemistry of Late Cretaceous–Paleocene granitoids in the

Sikhote-Alin Orogenic Belt: Petrogenesis and implications for the oblique subduction of the paleo-Pacific plate. Lithos 266, 202-212.

Tang, J., Xu, W.L., Wang, F., Gao, F.H., Cao, H.H., 2011. Petrogenesis of bimodal volcanic rocks from Maoershan Formation in Zhangguangcai Range: Evidence from geochronology and geochemistry. Global Geology 30, 508-520 (In Chinese with English abstract).

Tomurtogoo, O., Windley, B., Kröner, A., Badarch, G., Liu, D., 2005. Zircon age and occurrence of the Adaatsag ophiolite and Muron shear zone, central Mongolia: constraints on the evolution of the Mongol–Okhotsk ocean, suture and orogen. Journal of the Geological Society 162, 125-134.

Treuil, M., Joron, J., 1975. Utilisation des elements hygromagmatophiles pour la simplification de la modélisation quantitative des processus magmatiques: exemples de l'Afar et de la dorsale médio-atlantique. Soc. Ital. Mineral. Petrol 31, 125-174.

Tsutsumi, Y., Yokoyama, K., Kasatkin, S. A., Golozubov, V. V., 2014. Zircon U–Pb age of granitoids in the Maizuru Belt, southwest Japan and the southernmost Khanka Massif, Far East Russia. Journal of Mineralogical and Petrological Sciences, 109(2), 97-102.

Utkin, V., 2013. Shear structural paragenesis and its role in continental rifting of the East Asian margin. Russian Journal of Pacific Geology 7, 167-188.

Van der Voo, R., Spakman, W., Bijwaard, H., 1999. Mesozoic subducted slabs under Siberia. Nature 397, 246-249.

Wang, F., Xu, W.L., Meng, E., Cao, H.H., Gao, F.H., 2012. Early Paleozoic amalgamation of the Songnen–Zhangguangcai Range and Jiamusi massifs in the eastern segment of the Central Asian Orogenic Belt: Geochronological and geochemical evidence from granitoids and rhyolites. Journal of Asian Earth Sciences 49, 234-248.

Wang, F., Xu, W.L., Xu, Y.G., Gao, F.H., Ge, W.C., 2015. Late Triassic bimodal igneous rocks in eastern Heilongjiang Province, NE China: implications for the initiation of subduction of the Paleo-Pacific Plate beneath Eurasia. Journal of

Asian Earth Sciences 97, 406-423.

Wang, F., Zhou, X.H., Zhang, L.C., Ying, J.F., Zhang, Y.T., Wu, F.Y., Zhu, R.X., 2006a. Late Mesozoic volcanism in the Great Xing'an Range (NE China): timing and implications for the dynamic setting of NE Asia. Earth and Planetary Science Letters 251, 179-198.

Wang, P.J., Chen, F., Chen, S.M., Siebel, W., Satir, M., 2006b. Geochemical and Nd-Sr-Pb isotopic composition of Mesozoic volcanic rocks in the Songliao basin, NE China. Geochemical Journal 40, 149-159.

Wang, T., Zheng, Y., Zhang, J., Zeng, L., Donskaya, T., Guo, L., Li, J., 2011. Pattern and kinematic polarity of late Mesozoic extension in continental NE Asia: Perspectives from metamorphic core complexes. Tectonics, 30.

Wang, T., Guo, L., Zheng, Y., Donskaya, T., Gladkochub, D., Zeng, L., J., Wang, Y., Mazukabzov, A., 2012. Timing and processes of late Mesozoic mid-lower-crustal extension in continental NE Asia and implications for the tectonic setting of the destruction of the North China Craton: mainly constrained by zircon U–Pb ages from metamorphic core complexes. Lithos, 154, 315-345.

Wei, H., Sun, D., Ye, S., Yang, Y., Liu, Z., Liu, X., Hu, Z., 2012. Zircon U-Pb ages and its geological significance of the granitic rocks in the Yichun-Hegang region, southeastern Xiao Hinggan Mountains. Earth Science-Journal of China University of Geosciences 37, 50-59 (In Chinese with English abstract).

Wilde, S., Dorsett-Bain, H., Liu, J., 1997. The identification of a Late Pan-African granulite facies event in northeastern China: SHRIMP U–Pb zircon dating of the Mashan Group at Liu Mao, Heilongjiang Province, China, Proceedings of the 30th IGC: Precambrian Geology and Metamorphic Petrology, pp. 59-74.

Wilde, S.A., 2015. Final amalgamation of the Central Asian Orogenic Belt in NE China: Paleo-Asian Ocean closure versus Paleo-Pacific plate subduction—a review of the evidence. Tectonophysics 662, 345-362.

Wilde, S.A., Wu, F.Y., Zhang, X.Z., 2003. Late Pan-African magmatism in northeastern China: SHRIMP U–Pb zircon evidence from granitoids in the Jiamusi Massif. Precambrian Research 122, 311-327.

Wilde, S.A., Zhang, X.Z, Wu, F.Y, 2000. Extension of a newly identified 500Ma metamorphic terrane in North East China: further U–Pb SHRIMP dating of the Mashan Complex, Heilongjiang Province, China. Tectonophysics 328, 115-130.

Wilde, S.A., Zhou, J.B., 2015. The late Paleozoic to Mesozoic evolution of the eastern margin of the Central Asian Orogenic Belt in China. Journal of Asian Earth Sciences 113, 909-921.

Windley, B.F., Alexeiev, D., Xiao, W.J., Kröner, A., Badarch, G., 2007. Tectonic models for accretion of the Central Asian Orogenic Belt. Journal of the Geological Society 164, 31-47.

Wu, F.Y., Jahn, B.M., Wilde, A.S., Sun, D.Y., 2000. Phanerozoic crustal growth: U–Pb and Sr–Nd isotopic evidence from the granites in northeastern China. Tectonophysics 328, 89-113.

Wu, F.Y., Jahn, B.M., Wilde, S.A., Lo, C.H., Yui, T.F., Lin, Q., Ge, W.C., Sun, D.Y., 2003a. Highly fractionated I-type granites in NE China (I): geochronology and petrogenesis. Lithos 66, 241-273.

Wu, F.Y., Jahn, B.M., Wilde, S.A., Lo, C.H., Yui, T.F., Lin, Q., Ge, W.C., Sun, D.Y., 2003b. Highly fractionated I-type granites in NE China (II): isotopic geochemistry and implications for crustal growth in the Phanerozoic. Lithos 67, 191-204.

Wu, F.Y., Sun, D.Y., Ge, W.C., Zhang, Y.B., Grant, M.L., Wilde, S.A., Jahn, B.M., 2011. Geochronology of the Phanerozoic granitoids in northeastern China. Journal of Asian Earth Sciences 41, 1-30.

Wu, F.Y., Sun, D.Y., Li, H.M., Wang, X.L., 2001a. The nature of basement beneath the Songliao Basin in NE China: geochemical and isotopic constraints. Physics and Chemistry of the Earth, Part A: Solid Earth and Geodesy 26, 793-803 (In Chinese with English abstract).

Wu, F.Y., Wilde, A.S., Sun D.Y., 2001b. Zircon SHRIMP U-Pb ages of gneissic granites in Jiamusi massif , northeastern China. Acta Petrologica Sinica, 17: 443-452 (In Chinese with English abstract).

Wu, F.Y., Yang, J.H., Lo, C.H., Wilde, S.A., Sun, D.Y., Jahn, B.M., 2007. The

Heilongjiang Group: a Jurassic accretionary complex in the Jiamusi Massif at the western Pacific margin of northeastern China. Island Arc 16, 156-172.

Xiao, W.J, Windley, B.F., Hao, J., Zhai, M., 2003. Accretion leading to collision and the Permian Solonker suture, Inner Mongolia, China: termination of the central Asian orogenic belt. Tectonics 22.

Xu, B., Zhao, P., Wang, Y., Liao, W., Luo, Z., Bao, Q., Zhou, Y., 2015. The pre-Devonian tectonic framework of Xing'an–Mongolia orogenic belt (XMOB) in north China. Journal of Asian Earth Sciences 97, 183-196.

Xu, J., Zhu, G., Tong, W., Cui, K., Liu, Q., 1987. Formation and evolution of the Tancheng-Lujiang wrench fault system: a major shear system to the northwest of the Pacific Ocean. Tectonophysics 134(4), 273-310.

Xu, T., Xu, W. L., Wang, F., Ge, W. C., Sorokin, A. A., 2018. Geochronology and geochemistry of early Paleozoic intrusive rocks from the Khanka Massif in the Russian Far East: Petrogenesis and tectonic implications. Lithos, 300, 105-120.

Xu, W.L., Ji, W.Q., Pei, F.P., Meng, E., Yu, Y., Yang, D.B., Zhang, X., 2009. Triassic volcanism in eastern Heilongjiang and Jilin Provinces, NE China: chronology, geochemistry, and tectonic implications. Journal of Asian Earth Sciences 34, 392-402.

Xu, W.L., Pei, F.P., Wang, F., Meng, E., Ji, W.Q., Yang, D.B., Wang, W., 2013. Spatial–temporal relationships of Mesozoic volcanic rocks in NE China: constraints on tectonic overprinting and transformations between multiple tectonic regimes. Journal of Asian Earth Sciences 74, 167-193.

Yang, H., Ge, W.C., Zhao, G.C., Bi, J.H., Wang, Z.H., Dong, Y., Xu, W.L., 2017. Zircon U–Pb ages and geochemistry of newly discovered Neoproterozoic orthogneisses in the Mishan region, NE China: Constraints on the high-grade metamorphism and tectonic affinity of the Jiamusi–Khanka Block. Lithos 268, 16-31.

Yang, H., Ge, W.C., Zhao, G.C., Yu, J.J., Zhang, Y., 2015a. Early Permian–Late Triassic granitic magmatism in the Jiamusi–Khanka Massif, eastern segment of the Central Asian Orogenic Belt and its implications. Gondwana Research 27,

1509-1533.

Yang, H., Ge, W.C., Zhao, G.C., Dong, Y., Xu, W.L., Ji, Z., Yu, J.J., 2015b. Late Triassic intrusive complex in the Jidong region, Jiamusi–Khanka Block, NE China: Geochemistry, zircon U–Pb ages, Lu–Hf isotopes, and implications for magma mingling and mixing. Lithos 224, 143-159.

Yang, H., Ge, W.C, Dong, Y., Bi, J.H., Wang, Z.H., Ji, Z., 2016. Record of Permian–Early Triassic continental arc magmatism in the western margin of the Jiamusi Block, NE China: petrogenesis and implications for Paleo-Pacific subduction. International Journal of Earth Sciences, doi:10.1007/s00531-016-1396-y.

Yu, J.J., Hou, X., Ge, W.C., Zhang, Y., Liu, J., 2013. Magma mixing genesis of the Early Permian Liulian pluton at the northeastern margin of the Jiamusi massif in NE China: evidences from petrography, geochronology and geochemistry. Acta Petrologica Sinica 29, 2971-2986 (In Chinese with English abstract).

Zhang, F., Chen, H., Yu, X., Dong, C., Yang, S., Pang, Y., Batt, G., 2011. Early Cretaceous volcanism in the northern Songliao Basin, NE China, and its geodynamic implication. Gondwana Research 19, 163-176.

Zhang, F. Q., Chen, H. L., Batt, G. E., Dilek, Y., Min-Na, A., Sun, M. D., ... & Zhao, X. Q., 2015. Detrital zircon U–Pb geochronology and stratigraphy of the Cretaceous Sanjiang Basin in NE China: Provenance record of an abrupt tectonic switch in the mode and nature of the NE Asian continental margin evolution. Tectonophysics, 665, 58-78.

Zhang, J.H., Gao, S., Ge, W.C., Wu, F.Y., Yang, J.H., Wilde, S.A., Li, M., 2010. Geochronology of the Mesozoic volcanic rocks in the Great Xing'an Range, northeastern China: implications for subduction-induced delamination. Chemical Geology 276, 144-165.

Zhang, S., Zhu, G., Liu, C., Li, Y., Su, N., Xiao, S., & Gu, C., 2018. Strike-slip motion within the Yalu River Fault Zone, NE Asia: The development of a shear continental margin. Tectonics 37, 1771-1796.

Zhang, X.Z., Guo, Y., Zhou, J.B., Zeng, Z., Pu, J.B., Fu, Q.L., 2015. Late Paleozoic-Early Mesozoic tectonic evolution in the east margin of the Jiamusi massif,

eastern northeastern China. Russian Journal of Pacific Geology 9, 1-10.

Zhao, P., Chen, Y., Xu, B., Faure, M., Shi, G., Choulet, F., 2013. Did the Paleo‐Asian Ocean between North China Block and Mongolia Block exist during the late Paleozoic? First paleomagnetic evidence from central‐eastern Inner Mongolia, China. Journal of Geophysical Research: Solid Earth 118, 1873-1894.

Zhou, J.B., Wilde, S.A., 2013. The crustal accretion history and tectonic evolution of the NE China segment of the Central Asian Orogenic Belt. Gondwana Research 23, 1365-1377.

Zhou, J.B., Wilde, S.A., Zhang, X.Z., Zhao, G.C., Zheng, C.Q., Wang, Y.J., Zhang, X.H., 2009. The onset of Pacific margin accretion in NE China: evidence from the Heilongjiang high-pressure metamorphic belt. Tectonophysics 478, 230-246.

Zhou, J.B., Cao, J.L., Wilde, S.A., Zhao, G.C., Zhang, J.J., Wang, B., 2014. Paleo‐Pacific subduction‐accretion: Evidence from Geochemical and U‐Pb zircon dating of the Nadanhada accretionary complex, NE China. Tectonics 33, 2444-2466.

Zhu, C.Y., Zhao, G., Sun, M., Liu, Q., Han, Y., Hou, W., Zhang, X., Eizenhofer, P.R., 2015. Geochronology and geochemistry of the Yilan blueschists in the Heilongjiang Complex, northeastern China and tectonic implications. Lithos 216, 241-253.

Zhu, C. Y., Zhao, G., Sun, M., Eizenhöfer, P. R., Liu, Q., Zhang, X., ... & Hou, W., 2017. Geochronology and geochemistry of the Yilan greenschists and amphibolites in the Heilongjiang complex, northeastern China and tectonic implications. Gondwana Research, 43, 213-228.

Zhu, C. Y., Zhao, G., Sun, M., Han, Y., Liu, Q., Eizenhöfer, P. R., ... & Hou, W., 2017. Detrital zircon U–Pb and Hf isotopic data for meta-sedimentary rocks from the Heilongjiang Complex, northeastern China and tectonic implications. Lithos, 282, 23-32.

Zorin, Y.A., 1999. Geodynamics of the western part of the Mongolia–Okhotsk collisional belt, Trans-Baikal region (Russia) and Mongolia. Tectonophysics 306, 33-56.

Chapter5 Izanagi-Pacific ridge subduction in NE Asia in the early Cenozoic: A review of geological evidence from NE Asia

5.0 Abstract

The subduction of a spreading ridge beneath continental margin can significantly modify the arc magma source, deformation styles and thermal conditions of the overriding plate. In NE Asia, the Izanagi-Pacific Ridge (IPR) subduction is important to re-organize the plate motions. However, the geological evidence from the continental margin is not well constrained. In this paper, we review the recently published data, and recognize four magma/deformation stages during the Late Cretaceous to Eocene. It is proposed that the trench-sub-parallel IPR subduction led to the remarkable change of tectono-thermal conditions in early Cenozoic NE Asian margin. At stage 1 (Late Cretaceous), the N- or NNW-directed subduction of the Izanagi plate generated the arc magma involving important old crustal materials and leading to the NNE-striking sinistral strike-slip faults. At stage 2 (Paleocene), the NWW-striking transform faults between the IPR segments were subducted, developing small slab windows and facilitating the initial input of the depleted mantle materials. MORB-like gabbros from the spreading ridge intruded into the trench in the latest Paleocene. Local nearly N-S extension was active above these windows. At stage 3 (Early Eocene), the IPR was totally subducted, forming a margin-wide slab window initially in Sikhote-Alin and then SW Japan, which interrupted the arc magma and generated the trench-parallel extension. At stage 4 (Middle to Late Eocene), the lateral slip faults changed to dextral due to the W-directed subduction of the Pacific plate. Igneous rocks show strongly depleted isotopic features after the IPR subduction, indicating the replacement of the magma source region.

5.1 Introduction

Several oceanic plates were created in the Pacific domain during the Mesozoic to Cenozoic, such as the Farallon, Izanagi, Kula and Pacific plates. The long-term subduction and consumption of the oceanic plates were accompanied by frequent ridge subduction in the circum-Pacific region, which is generally used to explain the episodic magmatism, tectonic erosion and accretionary orogeny along the eastern Asian margin (Maruyama et al., 1997; Isozaki et al., 2010). Nowadays, ridge subduction can be observed around the Pacific Ocean, for instance, the ridges between the Nazca and Cocos, Nazca and Antarctic plates are subducting beneath the Andeas (Fig. 5.1). Slab window are created in the subducted ridge segment and mantle upwelling follows, changing the tectono-thermal condition of the overriding plate and feature of magmatism derived from mantle wedge or crust level.

Fig. 5.1 Ridge subduction in the Pacific Domain (Sisson and Pavlis, 1993; Windley and Xiao, 2018).

In the west Pacific, the Izanagi-Pacific Ridge subduction event is the most recent and

important one. The regional geological events in NE Asia related the Izanagi-Pacific ridge subduction include: 1) the porphyry copper-gold mineralization (Sun et al., 2007; 2009), the A-type granitoids, adakite and Nb-enriched basalt in Early Cretaceous along the Lower Yangtz River belt (Ling et al., 2009); 2) the magmatism related to the destruction of the North China Craton at ca. 130 Ma (Ling et al., 2013); and 3) the accretionary orogeny in SW Japan. In these models, the Izanagi/Kula-Pacific spreading ridge was nearly perpendicular to the eastern Asian margin and moved northwards with the N-directed subduction of the Izanagi plate from the Late Cretaceous to Early Cenozoic. The ages of felsic magma and metamorphism become younger northeastwards along the Median Tectonic Line in SW Japan (Kinoshita, 1995 and 2002). Maruyama et al. (1997) and Isozaki et al. (2010) attributed the episodic gap of arc magma and tectonic erosion in Japan to several times of ridge subduction.

However, new plate reconstruction models are proposed by more recently published data on oceanic island chains, magnetic anomaly bands and tectonic numerical simulation (Fig. 5.2). The Izanagi-Pacific ridge is now believed to be parallel/sub-parallel to the Eurasian continental margin, whereas the arriving time of the ridge to NE Asia is revised to 60 Ma (Whittaker et al., 2007). After the Izanagi subducted rapidly and sank beneath the Asian continent, the young Pacific Plate began its subduction at ca. 50 Ma. The most significant influence of this ridge subduction is the abrupt change of subduction motion of oceanic plates, from NNW to NWW or nearly W. This “50 Ma event” is related to plate reorganization in the Pacific domain, such as the changing motion of the Australian plate (Whittaker et al., 2007); the initial subduction of the western intra-ocean island arc system, including the Izu-Bonin-Mariana (Ishizuka et al., 2011; Arculus et al., 2015) and Tonga-Kermadec arcs (Meffre et al., 2012); the intraplate deformation in the Pacific Plate and the Hawaii-Emperor Bend (O’Connor et al., 2013; Sharp and Clauge, 2006), although some research proposed that the ca. 60° bend of this volcano chain should be attributed to mantle plume motion or the combined change of both plume/hot spot and plate motion direction (Steinberger et al., 2004; Tarduno et al., 2003 and 2009).

Although the new model about the Izanagi-Pacific ridge subduction had been proposed since a decade ago, the already published evidence was mainly limited within the oceanic plate, such as the magnetic chron, oceanic arc or volcano chain. Evidence from the continental side is very lack, which leads to various models proposed recently to explain the "plate reorganization event at ca. 50 Ma". For example, one model emphasized that it was the dock of an intra-oceanic island arc system in the north Pacific, rather than the Izanagi-Pacific Ridge subduction that reconstructed the motion of the Pacific plates (Domeier et al., 2017). Some other studies argue that the "50 Ma event" in the Pacific domain coincides with the Indian-Eurasian collision at ca. 60-50 Ma and the plate motion change in NE Asia was caused by the far-field effect of the Tibetan plateau building (Tapponnier and Molnar, 1976; Jolivet et al., 1990).

The most important reason for the controversy is that the geological evidence supporting different models does not derive from the NE Asian continental margin, a key area directly influenced by the Pacific plate reorganization event. In reality, a large amount of new data has been published in this essential area on major basins and faults, geochemistry and isotope of magmatic rocks and paleomagnetism. This paper aims to summarize the recently published data and provides the geological records from NE China, Russian Far East and adjacent areas related to the plate reorganization event in the early Cenozoic and assess possibility of the Izanagi-Pacific ridge subduction, as well as other proposed models so far.

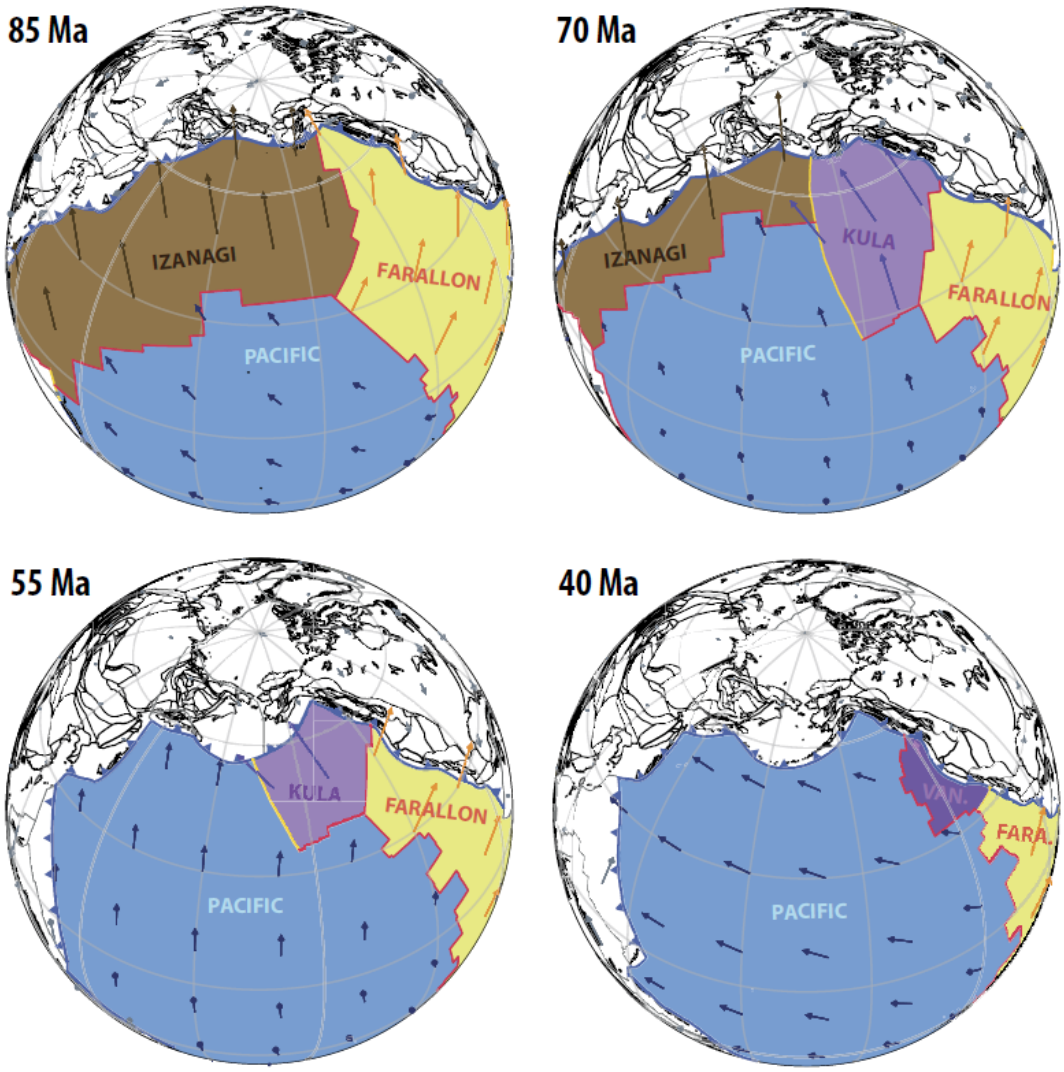

Fig. 5.2 Reconstruction of Izanagi-Pacific Ridge subduction in the early Cenozoic and the plate motion from the Late Cretaceous to Eocene (Domeier et al., 2017; Müller et al., 2016)

5.2 General influences of ridge subduction

5.2.1 Slab window formation and mantle flow

The most remarkable and direct result of a spreading center dragged into a subduction zone is the formation of a slab window. The formation of slab windows varies with several factors, 1) the geometric configuration of the trench-ridge-trench or trench-ridge-transform triple junction, 2) the motion vector of convergent plates and 3) subducted slab angles (Throkelson, 1996). A uniform and large slab window is developed from originally separated small and local windows opening along the

subducted segments of ridge and transform (Fig. 5.3). The geometry of the window is important because the scope on the overriding plate influenced by ridge subduction depends on the how large the window opens. Furthermore, intraplate magma, rift/extension and any other manifestations of ridge subduction events are always restricted in the window. Slab window, hot asthenosphere upwelling through it and their geological responses on the overriding plate facilitate our recognition of a ridge subduction event in an ancient orogen.

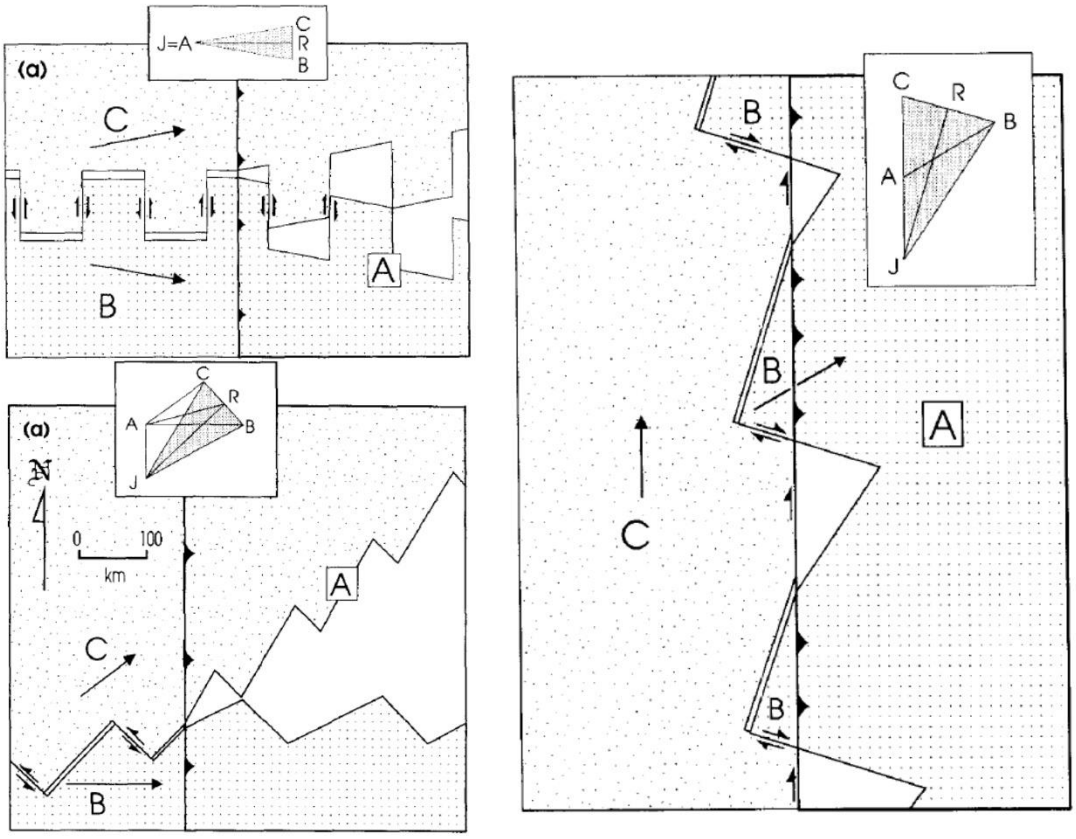

Fig. 5.3 The shapes of slab windows in different convergent directions (Thorkelson, 1996)

Once a slab window is generated, asthenosphere mantle can ascend through it, changing the chemical and rheological structure in/near the subduction zone. This is visualized by body-wave travel-time tomography conducted in the Patagonian Andes (Russo et al., 2010). The window between the Nazca and Antarctic plates show much slower P-wave velocity than the adjacent slab at the same depth (100 and 200 km depth), and the boundary between the Nazca slab and the Patagonian slab window clearly coincides with the transform. In some cases, mantle also can flow laterally

through the slab window and affect the deep structure of the subducted oceanic lithosphere. In the Solomon Sea of SW Pacific, mantle beneath arc flows across the slab window, mixing the sub-slab mantle on the subducted Australian plate side. This unusual mantle exchange generates submarine volcanoes with geochemical and Sr-Nd-Pb isotopic compositions similar to the arc magma on the other side of the trench (Chadwick et al., 2009).

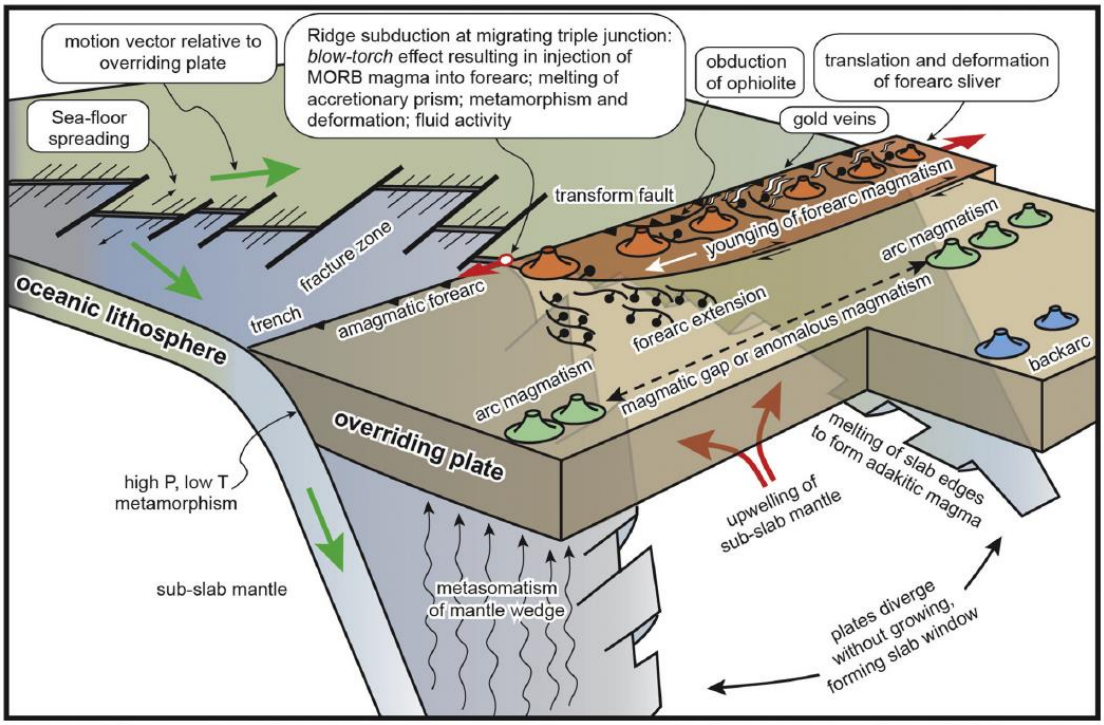

Fig. 5.4 Magmatism in a spreading ridge subduction zone (Thorselkon, 1996; Sisson and Pavils, 1993; Windley and Xiao, 2018)

5.2.2 Change of magmatism in continental arc and fore-arc area

The dehydration of subducted oceanic sediments and partial melting of mantle wedge cause arc magmatism along the active plate margin. However, when a slab window is formed in the subduction zone, the normal dehydration and melting of mantle wedge reaction will be interrupted or replaced by intra-plate magmatism related to hot and anhydrous asthenosphere (Fig. 5.4).

A very unique feature when an active ridge arrives at a trench is the fore-arc magmatism, namely, the MORB-like pluton invades into a coeval or slightly older

fore-arc sediments or accretionary wedge. In the arc area, intra-plate magmatism may be dominant because of the upwelling asthenosphere and regional extension/rifting. The magmatic genesis indicated by trace elements and isotopes can be distinguished from the arc magma (Klein and Karsten, 1995; Thorkelson et al., 2011; Tang et al., 2012). Adakite is also usually observed, which is considered to represent the melting of the thin slab edge on the both boundaries of the slab window.

Because of the geometric configuration and subduction direction, the triple junction tends to migrate along the trench in most cases. As well, the corresponded deformation in the upper plate and ridge subduction related magma always show migration process along the convergent margin.

5.2.3 Deformation in the overriding plate

In the idealized ridge-subduction model, extension and even rifting upon the slab window should be the typical setting in the upper plate. This is common feature because asthenosphere upwelling is prone to generate environment alike to an active rift.

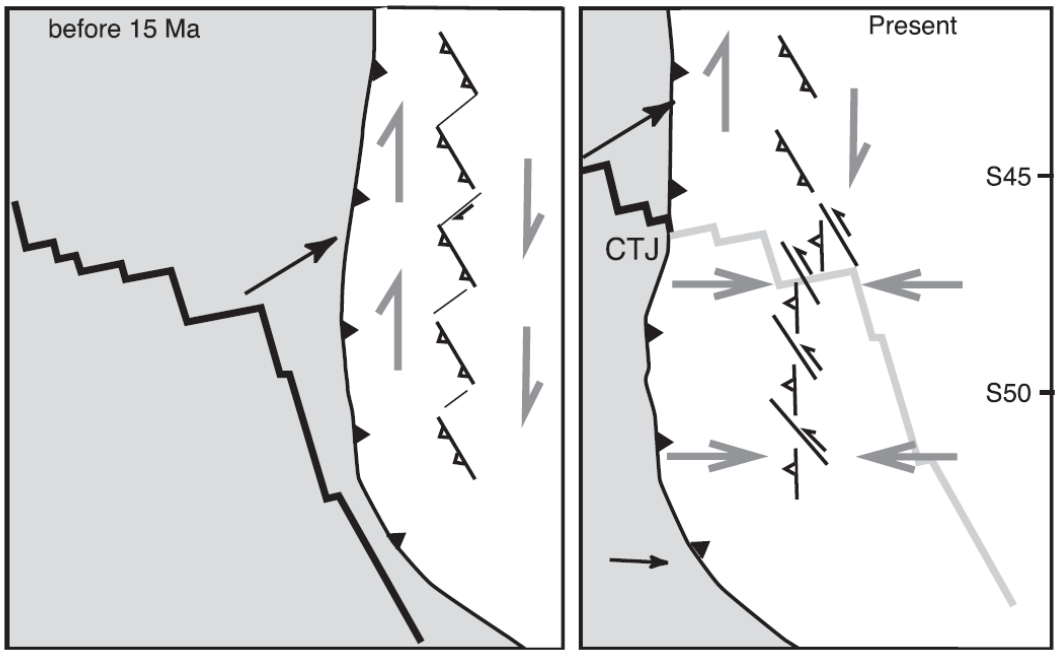

Fig. 5.5 The varying regional stress field in Chile with the migrating of triple junction

(Lagabrielle et al., 2004)

More often, however, the deformation styles are multiple and variable because extension caused by slab window is not the only mechanical mechanism near the triple-junction area, the changing convergent direction also matters. In many cases, the subduction of one plate is replaced by the other one following the migration of the triple junction, or after the consumption of the trailing plate. This process can contribute to the dramatically change of the local stress direction on the overriding plate margin. A famous example is the Farallon-Pacific-North American triple junction in Alaska. Before 56-63 Ma, the junction moved to north along the trench. After, the direction of migration was inversed and thus enlarged the slab window, resulting in trench-parallel extension in Alaska. When the junction moved away from this local area, thrusts and folds caused by the Farallon subduction superposed the early structures (Sisson and Pavlis, 1995). In Chile, the subduction direction of the Nazca plate is oriented at ~N60°E before the Chile triple junction reached the South American margin. The margin-parallel motion component gave rise to N-S trending dextral strike-slip faults. However, after the junction arrived and then moved northwards, the southern Chile was dominated by the subduction of the Antarctic plate, which is almost at E-W direction and the N-S faults became mainly thrusts/reverse faults (Lagabrielle et al., 2004).

Accelerated tectonic erosion in the fore-arc area is also an important geological process in the ridge subduction zone. This is attributed to the positive-negative topography of the ridge-transform structure and the mechanically weakening of the overriding plate due to the overpressuring and hot fluids derived from the subducted active ridge (Bourgois et al., 1996). The subduction of the Chile ridge in Patagonian Andes caused very rapid erosion rate of 231 to 443 km3·km-1 ·Ma-1, which is at 2.3 times higher than the Peru and Japan subduction erosion rate (von Huene and Lallemand, 1990; Sosson et al., 1994).

5.3 Brief geological outline of NE China and Sikhote-Alin

The continental blocks with Neoproterozoic basements include the Bureya, Jiamusi and Khanka blocks mainly in NE China and extend into the Russian Far East (Fig. 5.6). The three blocks are separated by two branches of the Tan-Lu Fault in NE China, the Jia-Yi and Dun-Mi faults (Fig. 5.6), and thus sometimes they are referred as the "Bureya-Jiamusi-Khanka Block". The oldest basement outcrop is found in the southeast margin of the Jiamusi Block in NE China. The U–Pb dating of the magmatic cores of zircons in an orthogneiss yields an age of 898 ± 4 to 891 ± 13 Ma. Whereas the rims or metamorphic zircons have ages of 563 Ma and 518-496 Ma (Yang et al., 2017). Similar Neoproterozoic magmatic ages with Pan-African metamorphic ages of zircons are reported in the Khanka Block as well (Khanchuk et al., 2010). Because of other extensively distributed khondalitic sequences (~500 Ma) in the eastern Central Asian Orogenic Belt (CAOB), the Bureya-Jiamusi-Khanka Block is proposed to be a part amalgamated with other blocks in NE China since 500 Ma (Wilde et al., 2003; Zhou et al., 2011; Zhou and Wilde, 2013).

During the Permian to Triassic, a new oceanic basin, the Mudanjiang Ocean, was opened between the Bureya-Jiamusi-Khanka Block and the rest of the eastern CAOB (Ge et al., 2016; Zhou et al., 2009). The subduction of the Mudanjiang Ocean was initiated in the latest Permian to Early Triassic and lasted > 100 Ma until the ocean was closed in the Middle to Late Jurassic (Liu et al., 2017; Sun et al., 2018). Afterwards, the Paleo-Pacific oceanic slab began to influence the whole eastern CAOB. Continental arcs, intra-ocean arcs, fore-arc basins and trenches were generated during the long-term westward subduction of the Paleo-Pacific plates, such as the Farallon, Izanagi/Kula and Pacific plates. The continuous lateral accretion of subduction-related materials to the continental margin extended the territory of NE Asian continent towards the ocean side, forming the wide accretionary complexes in Sikhote-Alin, Japanese Islands and Sakhalin Island (Maruyama et al., 1997; Isozaki et al., 2010; Khanchuk et al., 2016). Typical trench retreat and eastward migration of arc/back-arc

magma was resulted in this process during the Cretaceous (Sun et al., 2018).

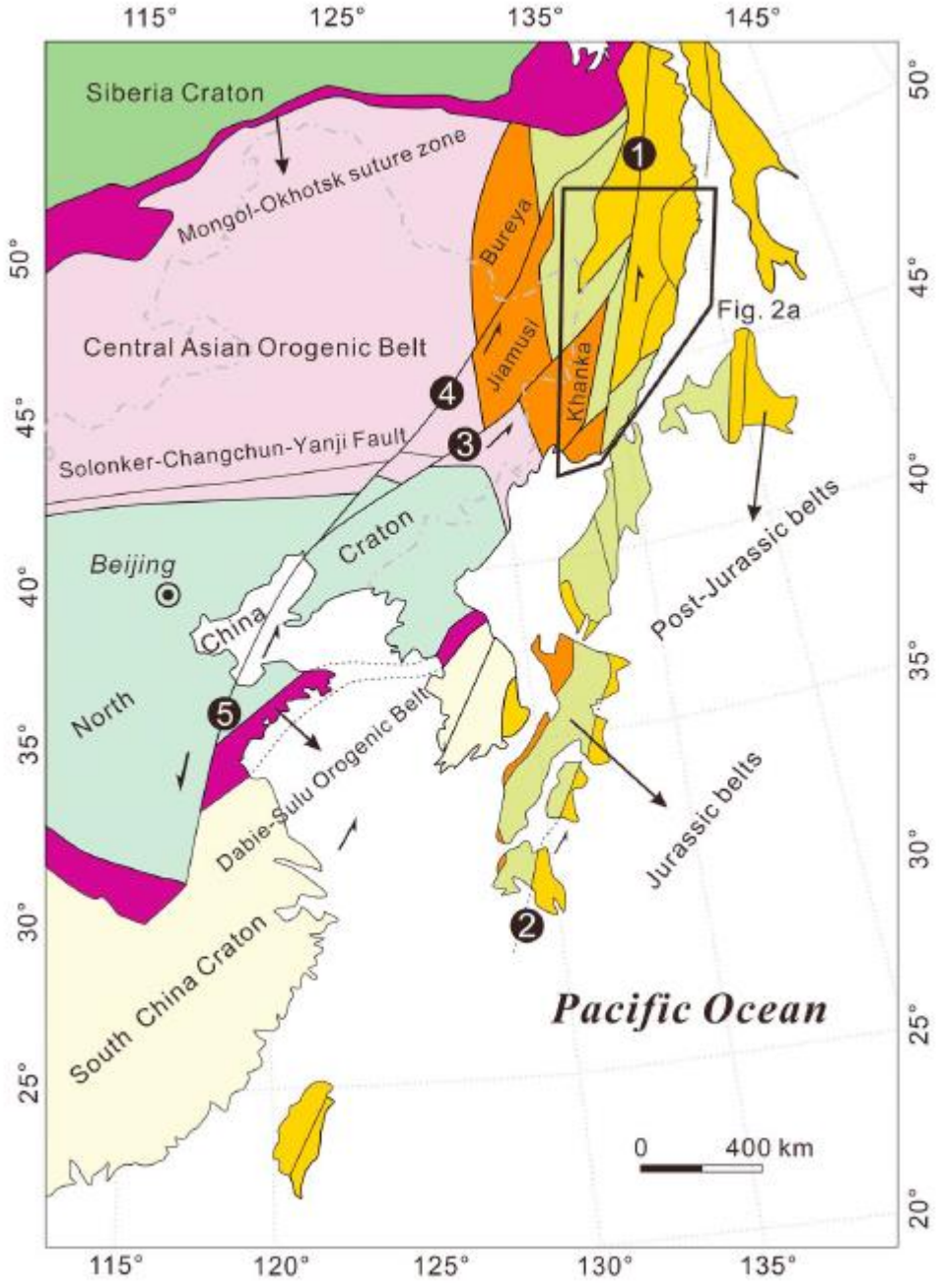

Fig. 5.6 The tectonic framework of the eastern Asian margin before the open of Sea of Japan (Liu et al., 2017b). Numbers in black circles represent major strike-slip faults: 1. The Central Sikhote-Alin Fault; 2. The Median Tectonic Line; 3. The Dun-Mi Fault; 4. The Jia-Yi Fault; 5: The Tan-Lu Fault

The Cenozoic history of the NE Asian continental margin was highlighted by important tectono-thermal change in the Paleocene to Eocene. The specific manifestations are summarized in details in the next sectors, including the changes of regional stress field expressed by the fault kinematics and basin uplifts, geochemical

and isotopic features of magmatic rocks, and the relationship between arc magma alignments and structures.

5.4 Change of convergent direction of the oceanic plate in the early Cenozoic

Regional stress field in the NE Asian margin is mainly controlled by the convergence between the Eurasian and (Paleo-) Pacific plates. Once the convergent rate or direction was changed, the principle compressional stress and its components in different directions followed to change abruptly. Thus, the geological records on structural geology, especially the major faults and basins in NE Asian, provide us an opportunity to uncover this process.

The eastern Asian continent is characterized by a giant NE to NNE trending strike-slip system and related sedimentary basins. The most celebrated faults (>1000 km long) in this fault system include the Tan-Lu Fault and its segments in northeast China, the Median Tectonic Line in SW Japan and the Central Sikhote-Alin Fault in Russian Far East (Fig. 5.6). Parallel or sub-parallel branch faults are limited by these major fault zones. They were most active during the Jurassic to early Cenozoic, and Quaternary seismic events are also frequently observed for the major faults. The strike-slip fault system is located between the Eurasian continent and oceanic plates in the Pacific domain, importantly adjusting the deformation of the lithosphere of the eastern Eurasian plate and recording the change of stress field dominated by the subduction of oceanic plates. Thus, the major kinematic change of the strike-slip fault system during the early Cenozoic is used to reflect the interaction between Asian continent and Pacific plates.

Basins with various sizes were formed due to the complicated interaction between the continental margin and the subducted oceanic plate and specifically controlled by the Mesozoic to Cenozoic faults. The change of regional stress field dominated not only

the kinematics of the faults, but also the depression and uplift of the basins. Some major basins are especially sensitive to these tectonic events. For example, back-arc extension in NE China caused the fault-depression and depression of the Songliao Basin in the Early Cretaceous. The change of Pacific plate motion later resulted into several times of basin inversion from the Late Cretaceous.

Thus, some major faults in Russian Far East, Korea and Sakhalin-Hokkaido and basin inversion/uplift events are summarized below to uncover the abrupt change of kinematics during the early Cenozoic.

5.4.1 Kinematic change of major faults in NE Asia

In the north Sikhote-Alin, Sakhalin, NE China and Korea, available data shows that a transition from sinistral to dextral strike-slip motion for the major NE or NNE trending faults took place during the late Paleocene to Eocene, reflecting that the regional principle compression direction changed from NNW to WNW or nearly W.

The Kiselevka Fault is a NE trending fault, parallel to the north segment of the Tan-Lu Fault in NE China (Fig. 5.7). The Kiselevka Fault bounds the north margin of the Kiselevka-Manoma terrane, a Cretaceous accretionary complex constituted by Jurassic to Cretaceous volcano-sedimentary assemblages (Filippov et al., 2010; Filippov and Kemkin, 2009). This accretionary complex is related to an intra-ocean arc, not the Asian continent because there are very few clasts with mature continental signatures found in the terrigenous sediments. The island arc barriered the Kiselevka-Manoma complex from the mainland of NE Asia, and then they were docked to the continental margin together. The Kiselevka Fault acted as a strike-slip fault between the accreted assemblages and the continent after the accretionary orogenic process. Detailed structural investigations were conducted near the Udyl Lake and the Amur River bank (Kudymov, 2010). In the early Cenozoic, two major deformation stages are recognized based on the attitudes of fractures, faults, folds and some en echelon structures along the fault zone and grabens. The first-stage deformation style of the fault zone matches

a simple shear stress field in the Paleocene. Sinistral shear dominated the fault at this stage, accompanied by nearly N-S trending compression and E-W trending extension, which was attributed to the NNW- or nearly N-directed motion of the Izanagi Plate. The second-stage deformation is characterized by "latitudinal" compression and "meridional" extension. During the later stage, the Kiselevka Fault experienced a dextral strike-slip motion, consistent with the W-directed subduction of the Pacific plate in the Eocene.

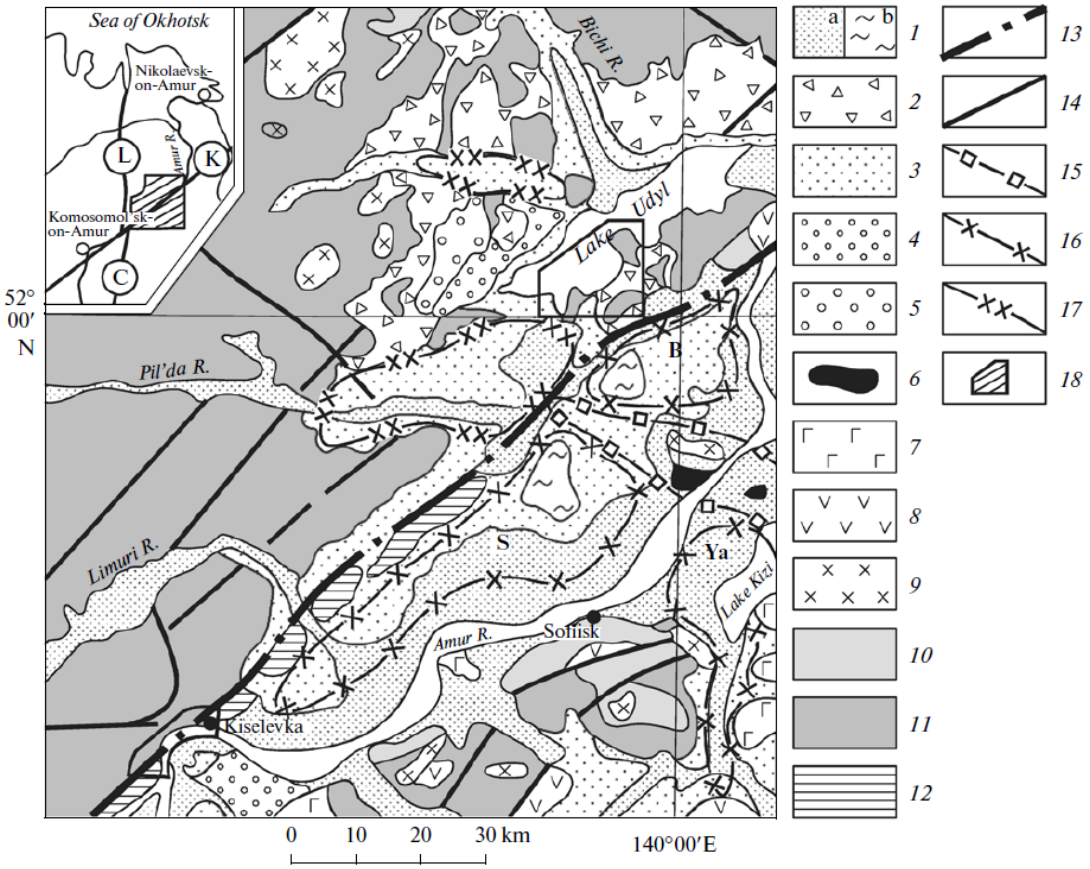

Fig. 5.7 The Kiselevka Fault in the north Sikhote-Alin orogenic belt (Kudymov, 2010)

In the west Sakhalin, it is noted that the geological meaning of the angular unconformity between Late Cretaceous and Eocene remains unclear. However, predominantly NE-directed (30° to 45°) compression and resultant dextral displacement were generated along the **West Sakhalin and Tym'-Poronai fault systems**, two N-S trending major fault zones (extend >200 km) bounding the West Sakhalin accretionary complex (Golozoubov et al., 2016). Oligocene to Miocene

basaltic and rhyolitic dikes or veins striking NE 30°, as well as the NE-SW striking grabens or half-grabens are consistent with the regional compression direction and dextral strike-slip motion in the west Sakhalin Island. All these structures or sedimentary basins were reworked in the Pleistocene when WNW-directed compression prevailed and the previous strike-slip faults were dominated by thrusting (Golozoubov et al., 2012).

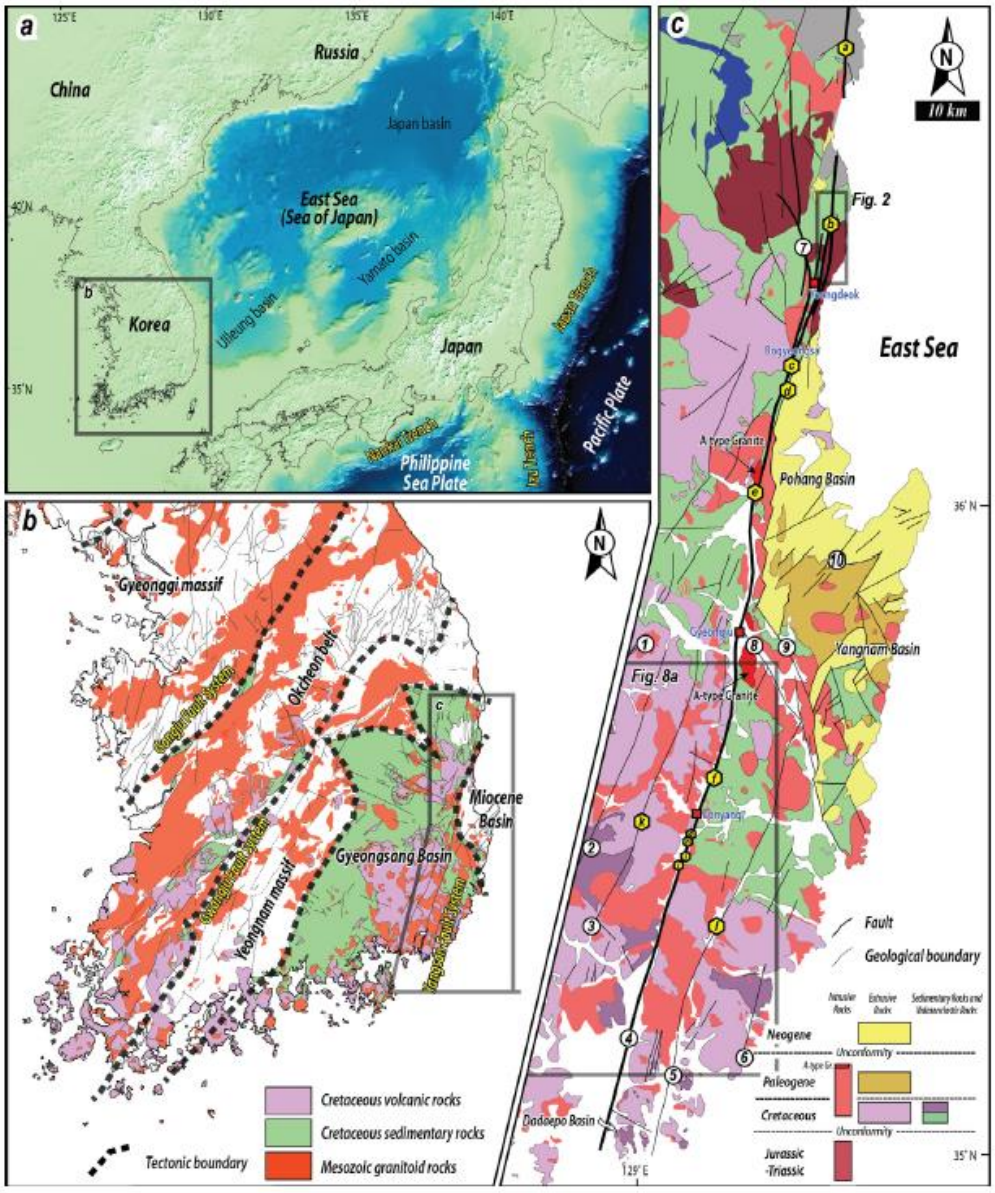

Fig. 5.8 The location and geological map of the Yansan Fault zone in SE Korea (Cheon et al., 2019)

The **Yansan Fault** in SE Korea extends >170 km in the Gyeongsang Basin with right-lateral offset of 20-30 km and is hidden in the Sea of Japan at its north and south ends

(Fig. 5.8). The fault is the largest one of the Yansan Fault System which includes 6 or more parallel strike-slip faults or shear zones that cur through the Mesozoic to Cenozoic sedimentary, volcanic and intrusive rocks in the basin (Hwang et al., 2007). The fault system experienced several episodes during the Cretaceous to Cenozoic. Sinistral strike-slip motion in the Late Cretaceous is recognized by the magnetic fabrics research on the 70-60 Ma granitoids, showing that the NE-SW trending compression resulted in a NE–SW-trending magnetic foliation (Cho et al., 2007). Cho et al. (2016) further explains how the syndepositional tilting and growth fault were generated during the deposition of the Dadaepo Formation during the Late Cretaceous. Anisotropic magnetic susceptibility (AMS) research on the fault gouge was also used by Cheon et al. (2019) to suggest the sinistral fabrics followed by later dextral ones. After the early Paleocene, the SE Korean Peninsula was characterized by regional extension and dextral strike-slip motion along the NNE- or N-trending faults. The first notable evidence is the dense NE-striking andesitic dikes with ages of 51-44 Ma, accommodating the NE-directed compression derived from the regional dextral shear domain (Cheon et al., 2019). The second evidence is the A-type granitoids (50 Ma in age) cut by the dextral strike-slip fault (Cho et al., 2016). The dextral shear also triggered some extensional basins with sedimentary and volcanic fills. Thus, the transition from sinistral to dextral motion of the NNE-trending strike-slip faults is confined to ca. 50-44 Ma (Fig. 5.9).

The Yalu River Fault, a NE-trending strike-slip fault running along the China-North Korea border, experienced dextral strike-slip motion in the early Cenozoic after a rift stage. This fault is roughly parallel to the Dun-Mi Fault in NE China and extends ~700 km along the Yalu River. The known earliest movement of the Yalu River Fault was initiated in the Early Cretaceous under a regional N-S compression (Zhang et al., 2018). The fault zone was dominated by N-S extension in the Late Cretaceous. However, the normal faulting and rifting was replaced by E-W compression and dextral strike-slip motion after the Late Cretaceous. The precise time of this transition has not been constrained well because of the lack of early Cenozoic basin fills. However, the end of

the Cretaceous basins and angular unconformities in them indicate that the E-W compression accompanied by dextral shear took place in the early Cenozoic (Zhang et al., 2018).

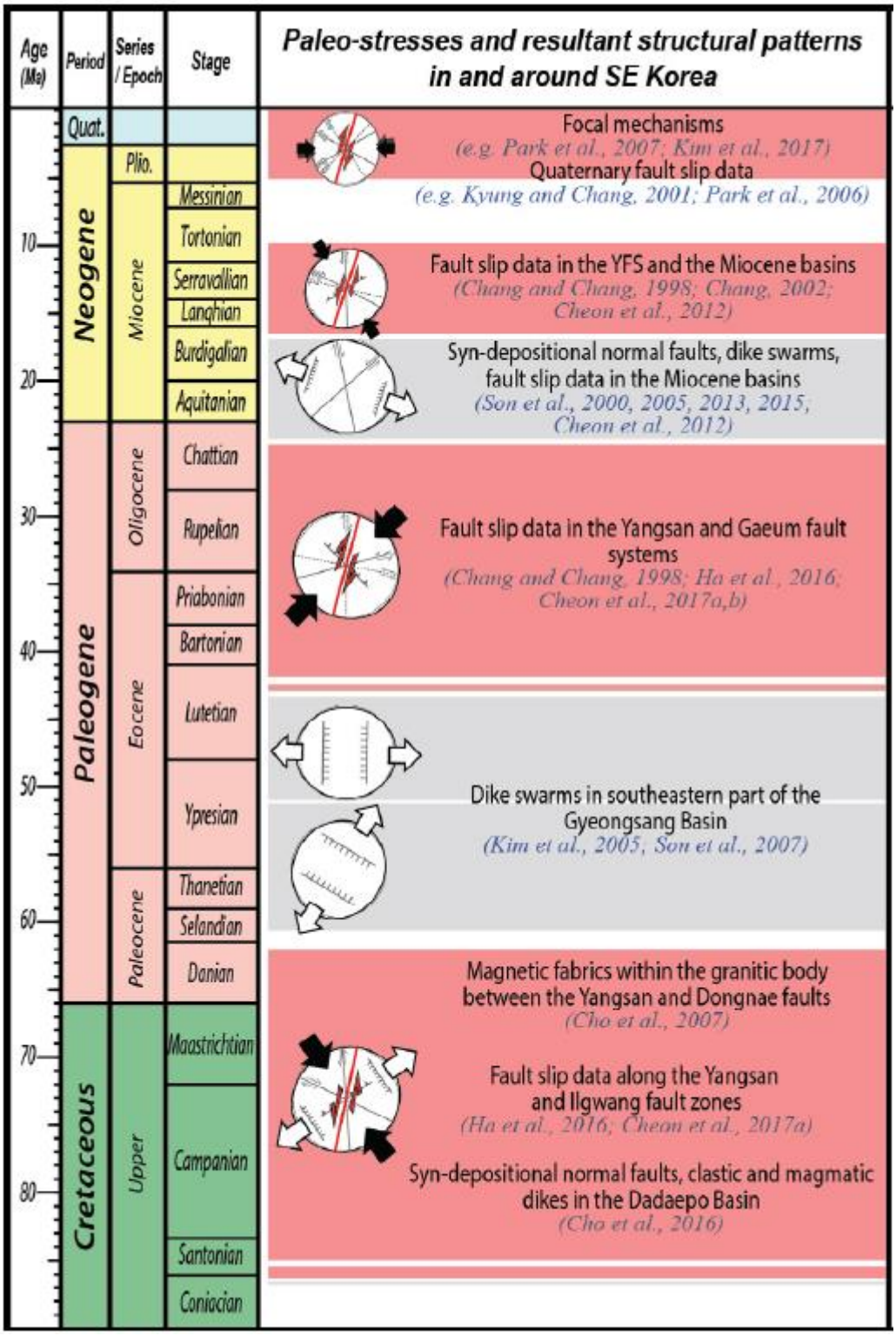

Fig. 5.9 The stress history of the Yansan Fault zone (Cheon et al., 2019)

Initial dextral displacement during the early Cenozoic was also commonly seen in

the interior of the NE Asian margin. The north segment of the **Tan-Lu Fault** experienced a transition from sinistral strike-slip motion in the Cretaceous to dextral or extension in the early Cenozoic, including the Jia-Yi Fault in NE China (Gu et al., 2017) and the buried fault zone in the Bohai Bay Basin (Gilder et al., 1999; Hsiao et al., 2004; Hsiao et al., 2010; Cheng et al., 2018). The Tan-Lu Fault Zone is famous for its giant sinistral strike-slip displacement reaching 400-700 km during the Mesozoic (Xu et al., 1987; Xu and Zhu, 1994). The Sulu and Dabie orogens were displaced by this fault zone, as well as the north margin of the North China Craton. Although the detailed tectonic models vary from each other, the sinistral strike-slip motion along with regional compression is verified by geometric, kinematic and geochronological data (Gilder et al., 1999; Zhu et al., 2005, 2009, 2012).

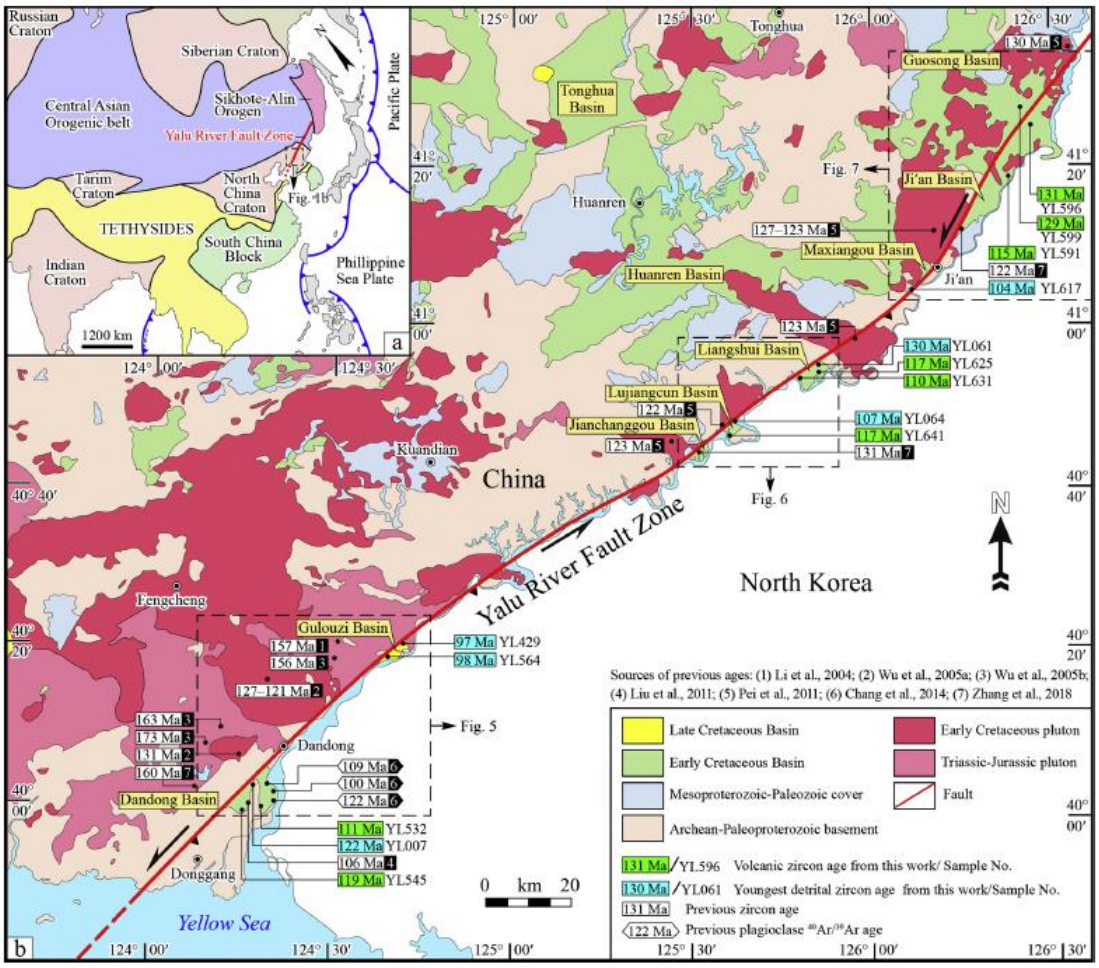

Fig. 5.10 Geological map of the Yalu River Fault (Zhang et al., 2019)

However, the sinistral motion is inversed by extensively extension and dextral motion

in the Cenozoic. The offshore 3-D seismic data in the Bohai Bay Basin shows that at least 18 en echelon bends along the Tan-Lu Fault Zone are developed in the Cenozoic basins, including both the releasing and restraining bends (Fig. 5.11). The right-step restraining bends demonstrate that the dextral strike-slip motion of the Tan-Lu Fault Zone was active during the late Paleocene to Eocene sediments were deposited (Huang et al., 2015). The dextral shear is estimated to be initiated at ca. 40 Ma and became intense until ca. 25 Ma when the Sea of Japan was open. The syn-depositional fault map based on the seismic data also suggests an abrupt increase of the quantity of NNE-trending strike-slip faults and their dextral motion shifted from the sinistral in the Cretaceous Bohai Bay Basin (Cheng et al., 2018). In NE China, however, the transition is different. The Dun-Mi and Jia-Yi faults are two major branches of the Tan-Lu Fault across the Bohai Bay Basin. Evidence for sinistral shear of both two faults is strong in the Cretaceous, such as the macro- and micro-shear indicators, c-axis fabrics of quartz, mylonitic foliations and mineral lineations along the fault zones (Gu et al., 2016). Geochronological data indicates that the sinistral strike-slip motion was active during 160 to 126 Ma for the Jia-Yi Fault (Gu et al., 2016) and 102-96 Ma for the Dun-Mi Fault (Liu et al., 2018). Especially, for the Jia-Yi Fault zone, several small-scale basins or grabens are developed along the strike. Regional compression in the Late Cretaceous resulted in the absence of Upper Cretaceous strata in the basins. Then the Paleogene sediments were deposited and deformed and overlain by the Neogene sedimentary rocks. Most basins/grabens are bounded by two NE-striking transtensional faults, whereas the most popular faults in the interior of the basins/grabens are E-W trending normal faults and small NE-trending normal faults along the basin margin (Gu et al., 2017). Based on the growth strata and outcrops of the faults, it is suggested that N-S extension derived from NE-SW trending dextral strike-slip simple shear was responsible for the growth of the basins/grabens (Sun et al., 2010; Gu et al., 2017).

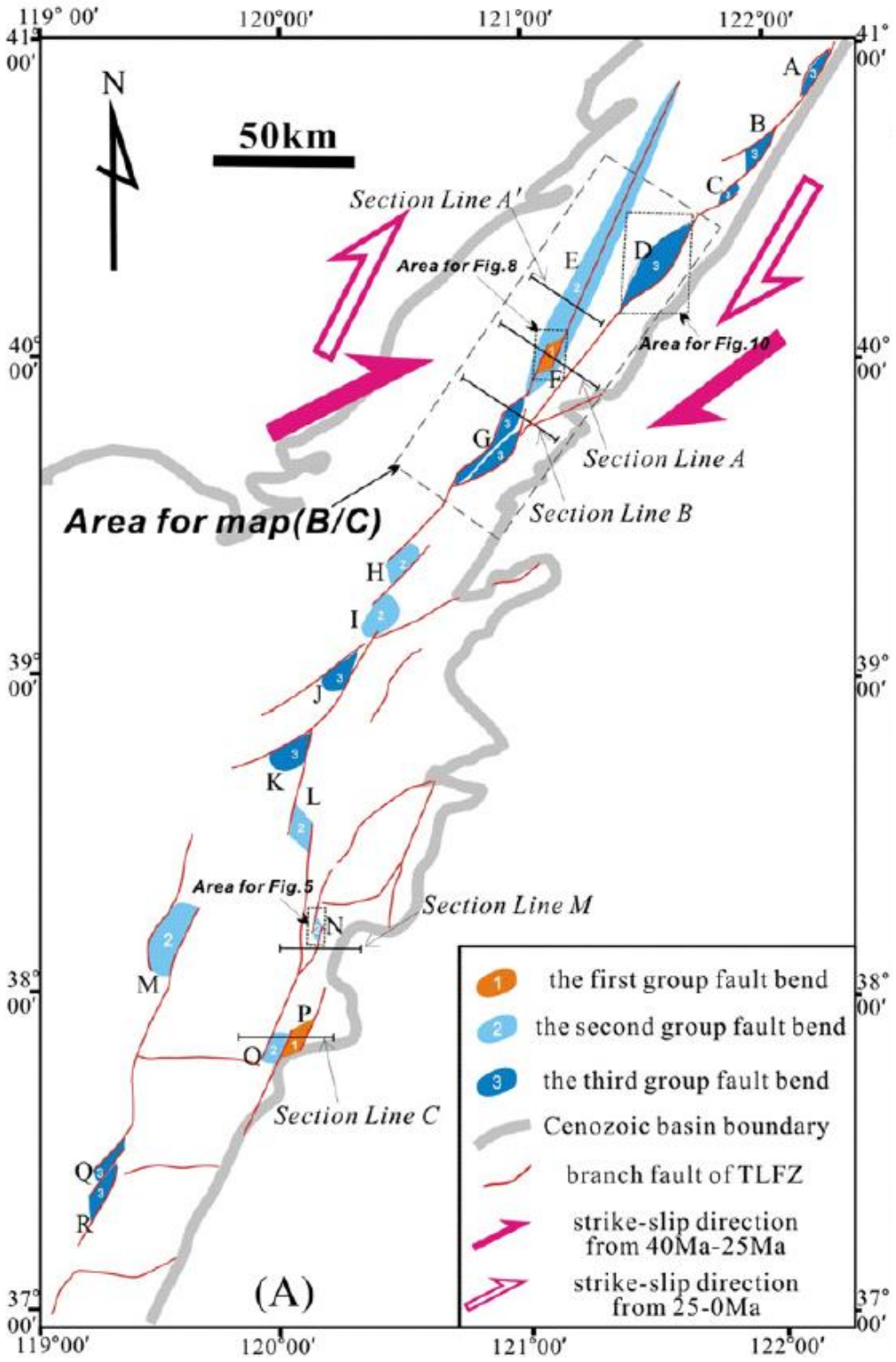

Fig. 5.11 The en echelon patterns of bends along the Tan-Lu Fault zone in the Bohai Bay Basin (Huang et al., 2015)

5.4.2 Basin inversion and abrupt uplift during the Paleocene to Eocene in NE China

The eastern margin of NE China was influenced by the subduction of Paleo-Pacific plates and had been an active continental margin until the Early Cretaceous, when the Sikhote-Alin accretionary complexes were accreted, which afterwards forced the trench and arc magma to migrate eastwards (Khanchuk et al., 2016; Sun et al., 2018). Thus, after the Early Cretaceous, basins in NE China were developed in a back-arc setting.

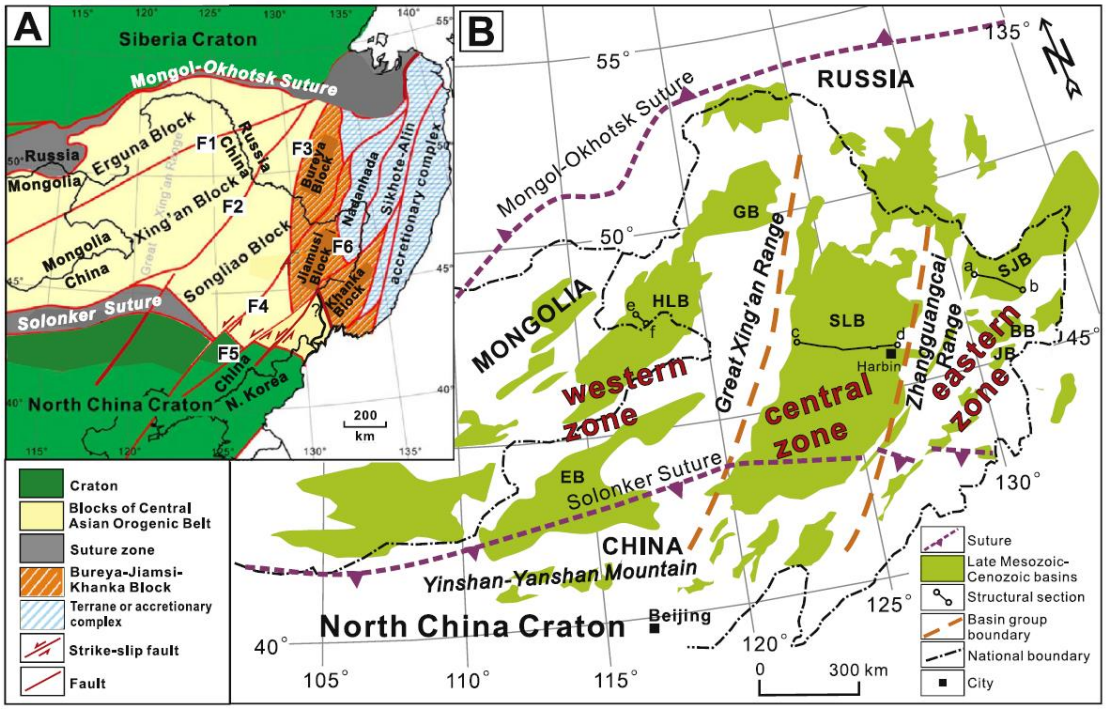

Fig. 5.12 Major Mesozoic to Cenozoic basins in NE China (Zhang et al., 2017)

During the whole Early Cretaceous, the back-arc area of NE China experienced a widespread regional extension (Fig. 5.12). Main evidence includes the rift basins, grabens along strike-slip faults and metamorphic core complexes in Transbaikalia region, China-Mongolia border and NE China (Wang et al., 2011). The extension event is attributed to post-collisional collapse of the Mongol-Okhotsk orogen and roll-back of the Izanagi slab (Wang et al., 2006; Zhang et al., 2010; Sun et al., 2013, 2018). However, from the Late Cretaceous, episodic uplift/basin inversion happened in NE China. The most important uplift/basin inversion events are the early Late Cretaceous

during 88-86 Ma and early Cenozoic during 65-50 Ma (Song et al., 2018). Basaltic volcanic rocks erupted at 76-74 Ma and 48-44 Ma immediately following the uplift events. Both basin inversion events are recorded by the regional angular unconformities, such as the T11 and T02 reflectors in the seismic profile of the Songliao Basin (Fig. 5.13; Song et al., 2014; Zhang et al., 2017) and ES3 and ES4 reflectors in the Sanjiang Basin (Zhang et al., 2012). The Late Cretaceous even is also called "Nenjiang movement" in Chinese literatures, and is related to the increase of the ridge spreading rate of in the Pacific domain (Müller et al., 2016), the change of the NE Asian margin from a Pacific-type to Andean type (Song et al., 2018) or the dock of the Okhotomorsk block/microcontinent to the NE Asian margin (Zhang et al., 2017). The early Ceonozoic one gave birth to the most widespread angular unconformity in the Songliao and adjacent basins (such as the Erlian Basin to the west and Sanjiang-Amur Basin to the east). The interrupt of sedimentary fills began from the earliest Paleocene and continued to the earliest Eocene (Li, 2016; Bai et al., 2017). Abrupt uplift of basins or surrounding mountains are revealed by low-temperature geochronological data (Fig. 5.14). In the Songliao Basin, thermal modeling based on apatite and zircon fission tracks indicate the cooling age of the sedimentary rocks focus on 65-50 Ma (Song et al., 2018), as well as the zircon/apatite U-Th/He data showing similar results (Song et al., 2014). Biotite $^{40}Ar/^{39}Ar$ and zircon U-Th/He dating are used in some Early Cretaceous plutons in the Jiaodong Peninsula, near the Tan-Lu Fault zone and the results indicate that the final-stage cooling of the granitoid plutons was abruptly rapid during 65-40 Ma (Wu et al., 2018). Similar uplift and exhumation are also recorded in the Great and Lesser Xing'an ranges on both the west and east sides of the Songliao Basin, respecitively (Li and Gong, 2011; Li et al., 2011) and the Huachuan-Fujin uplift in the Sanjiang Basin (Chen, 2016).

The important uplift/basin inversion event in the early Cenozoic marks a regional E-W compressional stress, replacing the long-term deposition in the Cretaceous. The time of this event coincides with the initiation of dextral motion of most NE- or NNE-trending faults in NE Asia. It is indicated that the regional principle compressional

stress changed from NNW to NW/W, possibly related to the change of plate motion in the west Pacific.

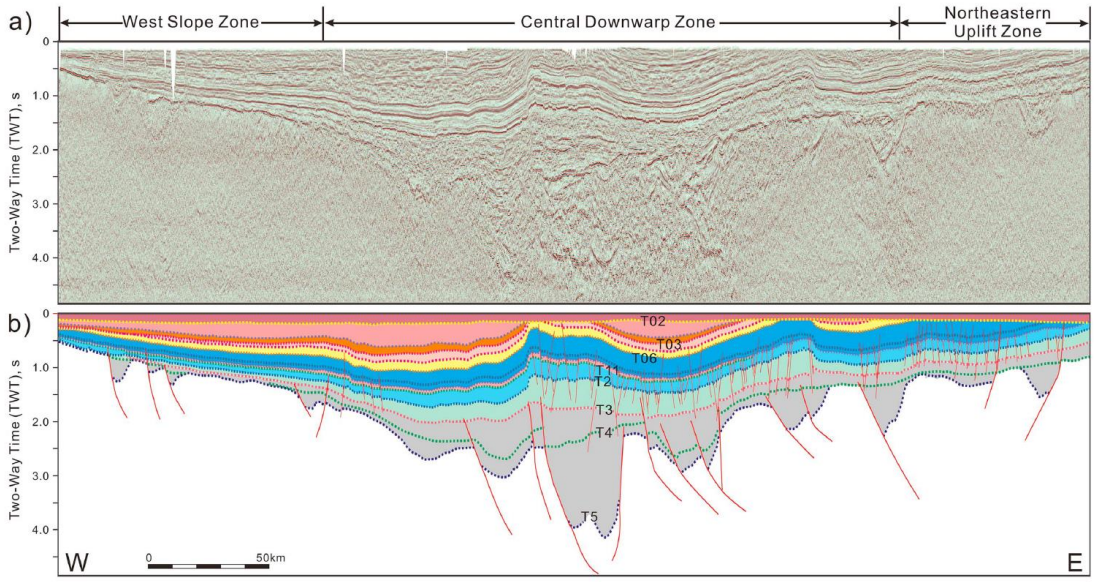

Fig. 5.13 Seismic profile of the Central Songliao Basin (Song et al., 2018)

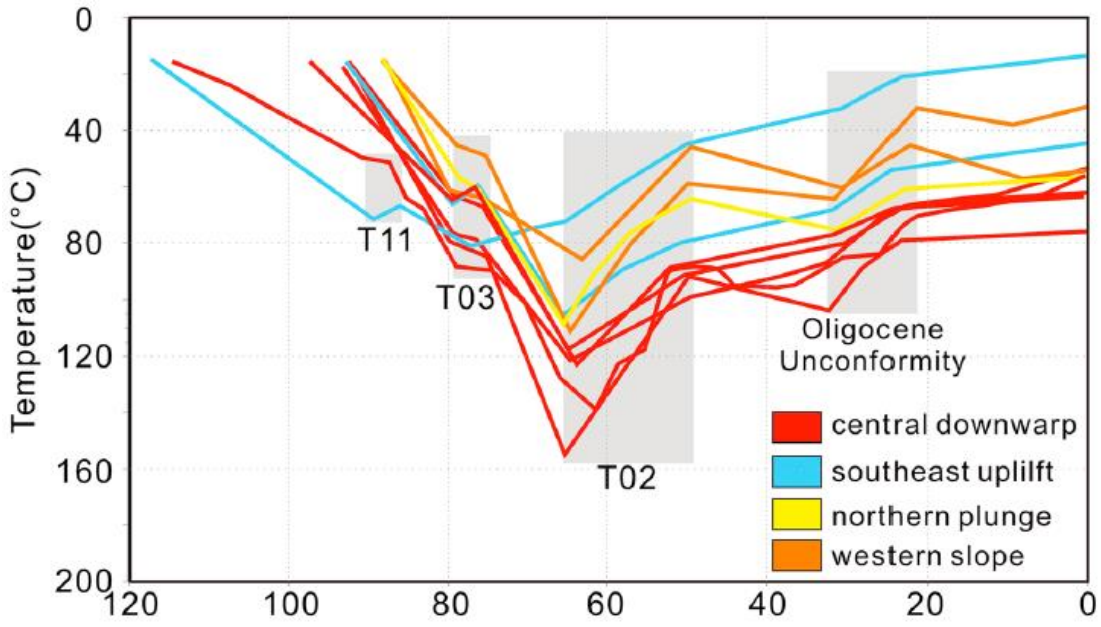

Fig. 5.14 The cooling rate based on zircon and apatite fission track and angular unconformities in the Songliao Basin (Song et al., 2018)

5.5 Change of magma genesis from Cretaceous to Eocene in Russian Far East

From Early Cretaceous, the quasi-continuous magmatism in Sikhote-Alin, Russian Far East was active and generated voluminous intrusive rocks into the Late Jurassic to Cretaceous accretionary assemblages as well as the equivalent volcanic rocks covering them, implying frequent and persistent tectonothermal events in the NW Pacific margin. Summarizing the published research on zircon U-Pb geochronology, geochemistry and Sr-Nd-Hf isotope, the Sikhote-Alin volcanic and plutonic rocks are subdivided into two major episodes, the older one is Early Cretaceous to Paleocene and the younger one is the latest Paleocene to Eocene (Fig. 5.15).

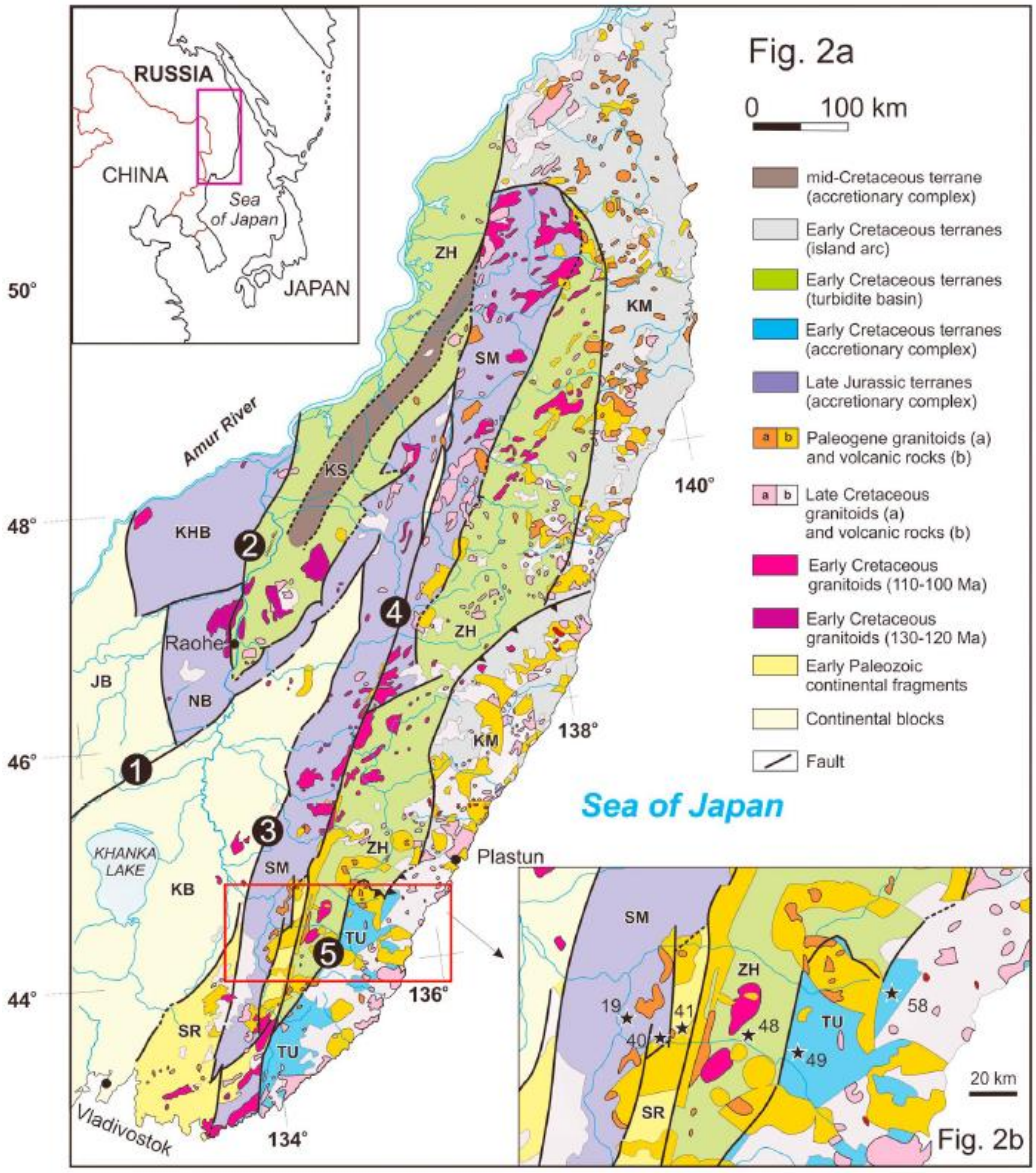

Fig. 5.15 The accretionary assemblages and magmatic rocks in Sikhote-Alin (Liu et al., 2017b)

5.5.1 Early Cretaceous to Paleocene: eastwards migrated arc magma related to the subduction of the Izanagi Plate

The earliest magmatic rocks (131 to 110 Ma) in this area are only reported in the **west Sikhote-Alin**, including several silicic plutons/batholiths and andesite-dacite-rhyolite sequences in the Nadanhada accretionary complex in NE China, the Amur turbidite basin and north Samarka accretionary complex in Russian Far East (Fig. 5.15). The oldest granitoid massif (131 Ma) intrudes into the Nadanhada accretionary complex and its adjacent area in the Amur turbidite basin in Lermontovka (Jahn et al., 2015). Pyroxene-amphibole monzodiorite and quartz monzodiorite represent the minor mafic association in the massif. The felsic association is the majority, comprised of biotite or two-mica granodiorite and granite. Particularly, cordierite, a typical mineral of peraluminous granite is found to the north of Bikin, Russian Far East (Jahn et al., 2015) and the Hamahe pluton in Nadanhada, NE China (Cheng et al., 2006), indicating their S-type infinity. Geochemical data of these granitic rocks also show S-type characteristics with high K/Na, Al and low Ca concentrations (Cheng et al., 2006; Kruk et al., 2014a). This may indicate the anatexis of meta-sedimentary rocks from the accretionary complex (Kruk et al., 2014a), or the existence of the unknown old basement in Sikhote-Alin (Jahn et al., 2015).

During 110-75 Ma, the magmatism rocks became more voluminous and moved to east, concentrating along the **Central Sikhote-Alin Fault** zone. Plutons/batholiths at this stage intruded in the eastern Samarka accretionary complex, the western Zhuravlevka turbidite basin and locally, the Sergeevka nappes, forming a long and narrow magmatic belt (Fig. 5.15).

In the **north part** of the belt, several large plutons occur in the Dalnensky area which are dated to 106 and 109 Ma (Jahn et al., 2015). The main lithology includes hornblende-biotite diorite, monzodiorite, granodiorite and monzonite, which are intruded by younger dikes and smaller intrusions of granite (Soloviev and

Krivoshchekov, 2011). In the **central part**, principle rock types belong to granitoids, mainly biotite-hornblende granites associated with gabbro and diorite. The central part has the densest intrusive bodies in the Central Sikhote-Alin Fault zone in the middle Cretaceous. In the ~100 km long belt, at least 13 large plutons occur at the both sides of the Central Sikhote-Alin Fault. In the **south part** of the magmatic belt, a few batholiths intruded the Sergeevka nappes and the southern Samarka accretionary complex in Uspensky area. The ages of the Uspensky massif vary from 103 to 91 Ma (Khanchuk et al., 2008; Jahn et al., 2015; Tang et al., 2016). The massif is bounded by two major NNE trending faults, the Arsenyev Fault to the west and the Central Sikhote-Alin Fault to the east. Khanchuk et al. (2008) connected the deformation in the granitoids with the strike-slip faulting, proposing that this massif as well as all the magmatic rocks in the middle Cretaceous represents "syn-orogenic" or "syn-strike-slip" magmatism. Biotite (± amphibolite) granodiorite and garnet-two-mica/biotite granite are the typical lithology.

Unlike the cordierite-bearing "S-type" granites at the early stage, the 110-75 Ma granitoids along the Central Sikhote-Alin Fault zone are more diverse on geochemical features. The K/Na and A/CNK ratios range within wide fields, showing a transition feature from S- to I-type (Kruk et al., 2014a). According to the data of Jahn et al. (2015) and Zhao et al. (2017), most of these granitoids are metaluminous to weakly peraluminous, belonging to I-type and they argue that the samples with peraluminous (S-type) and "within-plate" features are actually resulted from highly fractionation of originally I-type arc magma, characterized by tetrad effects and important Eu negative anomalies (Jahn et al., 2015).

The Late Cretaceous to Paleocene magmatic episode (83-55 Ma) migrated more eastwards to the eastmost Sikhote-Alin area, along **the margin of the Japan Sea**. A number of volcanic rocks erupted upon the middle Cretaceous Kema island arc assemblage and the Early Cretaceous Taukha accretionary complex, with many coeval plutons/batholiths covered by these volcanic sequences (Fig. 5.15). The eruptive and

intrusive rocks constitute the majority of a linear huge magmatic belt, the East Sikhote-Alin Volcaonic-Plutonic Belt (ESAVPB), involving the ~1500 km long continental margin of Sikhote-Alin with width of ~20-90 km (Khanchuk, 2001; Martynov et al., 2017). The ESAVPB, along with the volcanic-plutonic belt along the Okhotsk Sea margin, is considered to be a Silicic Large Igneous Provinces related to the subduction of the Paleo-Pacific Ocean (Grebennikov and Popov, 2014). Granodiorite and granite are the most extensive intrusive rocks. Equivalent volcanic sequences mainly include dacite, rhyolite, andesite and a few basalt. These granitoids and equivalent volcanic rocks are high-K calc-alkaline series with high SiO_2 (> 70%) and metaluminous to weak peraluminous feature (A/CNK<1.1). I-type are dominant at this stage, similar to the granitoids with ages of 110-75 Ma. However, the volume of eruptive rocks, including lava, tuff and ignimbrite, are much more abundant than the older stage.

Above all, the Early Cretaceous to Paleocene magmatic rocks in Sikhote-Alin are dominated by I-type felsic granitoids, accompanied by S-type at the earliest stage. All of them belong to the high-K calc-alkaline series, accompanied by diorites or gabbros and associated with subduction and continental arc settings. This is also supported by the common geochemical features, like the enriched Light Rare Earth Elements (LREEs) and depleted Nb-Ta-Ti for both granitic and basaltic rocks (Jahn et al., 2015; Khanchuk et al., 2016; Tang et al., 2016; Zhao et al., 2017).

An essential issue about these magmatic rocks is that whether their protoliths involving an old basement or not. A microcontinent named “Anuy” was proposed to explain the formation of the Anuy dome in north Sikhote-Alin (Faure and Natal’in, 1992; Faure et al., 1995). The dome consists of a metamorphic core assemblage with multiple metamorphic grades, including migmatite, ophiolite nappe, gneiss and micaschist. However, later research analyzed the field structures, geochemistry and Nd isotopes of both the metamorphic dome and its surrounding sedimentary rocks of the Samarka accretionary complex, based on which they argue that the Anuy dome is not the remnant of a microcontinent but a metamorphic core complex (Kruk et al., 2014b). The $\varepsilon_{Nd}(t)$ values of the 131-55 Ma rocks in Sikhote-Alin range from -5 to +3, but

mostly <0 (Fig. 5.16; Jahn et al., 2015; Khanchuk et al., 2016; Zhao et al., 2017). The clearly enriched Nd isotope features reveal that Sikhote-Alin may have an old basement covered by the Jurassic to Cretaceous accretionary assemblages, showing infinity with granitoids in SW Japan (Jahn et al., 2015). Another evidence to speculate the existence of an old basement is that the crustal thickness of Sikhote-Alin is about 38 km (Rodnikov et al., 2008), which is too thick if this area is only constituted of deformed sediments without a mature crustal basement. Khanchuk et al. (2016), however, argues that the enriched Nd isotopes may be the result of anatexis of the accretionary sediments derived from old terrigenous continental blocks, instead of the inherited feature from an old basement. Zircon Hf isotopes of the granitoids show large variations but mostly positive $\varepsilon_{Hf}(t)$ values (Fig. 5.17; Jahn et al., 2015; Tang et al., 2016), opposite to the whole-rock Nd isotopes and may indicate the important juvenile component in the magma. Thus, for now, the existence of a hidden mature crustal basement is still highly debated. The decoupling of the Nd-Hf isotopes and missing outcrop of old basement rocks are the keys to solve this issue. But no matter it exists or not, it is widely accepted by these studies that the Early Cretaceous to Paleocene magmatic rocks were formed in an active continental margin with important mixing feature between reworked crust-derived material and juvenile or mantle-derived components.

Significantly, these arc magma (131-55 Ma) is characterized by their spatial migration from west to east. As described above, the earliest stage of S- and I-type granitoids (131-110 Ma) are located in the west Sikhote-Alin and NE China. Later, the Central Sikhote-Alin Fault zone became the most important magmatic belt from 110 Ma to 75 Ma. From ca. 83 Ma to 55 Ma, more and more lava and ignimbrite were erupted to the east of the Fault zone and eventually the Late Cretaceous to Paleocene magmatism was restricted along the coastal margin. Trench retreat and slab roll-back are thus proposed by many previous studies to be responsible for the magmatic migration in not only Sikhote-Alin, but also NE China and the Korean Peninsula initiated in the Early Cretaceous. In South Korea, Early Jurassic granitoids are most widely

distributed, representing the arc magma caused by subduction. But after a long magma gap from ca. 160 to 120 Ma, the Cretaceous to Paleocene granitoids, including mainly I-type with minor A-type, intruded in the Proterozoic basement and Mesozoic basins in South Korea (Sagong et al., 2005). Four groups of intrusive rocks are identified, namely, 119-106 Ma, 99-87 Ma, 85-82 Ma and 76-67 Ma. The four NE trending magma belts become younger from NW to SE, which is attributed to the change of subduction slab angle from shallow (100-85 Ma) to steep (85-65 Ma) and coeval trench retreat (Kim et al., 2016). In NE China, the magma migration is clear and has been recognized by many published studies. In the early research, it is believed that the volcanic rocks migrated from the Great Xing'an Range (150 Ma) to Korea and Japan (80 Ma), involving a >1000 km wide region (Wang et al., 2006). But more recent research finds out that the Great Xing'an Range may be influenced by the Mongol-Okhotsk Ocean realm, rather than the Paleo-Pacific Ocean. New data about the Cretaceous volcanic rocks in NE China reveals that the magma in this area is not arc magma but back-arc and intra-plate magma. The ages of these back-arc andesite and basalt range from 130 Ma in the Songliao Basin to 100 Ma in the Jiamusi-Khanka Block, corresponding to the eastward migration of arc magma in Sikhote-Alin (Sun et al., 2018).

In summary, the NE Asia, including the NE China, Sikhote-Alin and Korean Peninsula, was controlled by the long-term oblique subduction of the Paleo-Pacific Oceanic plate from Early Cretaceous to Paleocene. The arc magma in Sikhote-Alin and the back-arc magma in NE China migrate eastwards contemporarily, possibly caused by the slab roll-back and trench retreat. Particularly, the arc-related granitoids in Sikhote-Alin are characterized by negative $\varepsilon_{Nd}(t)$ values, indicating important assimilation of crust-derived material or the existence of mature basement beneath the accretionary assemblages.

5.5.2 Late Paleocene to Eocene: abrupt increasing juvenile component

input and mantle upwelling

The Early Cretaceous to Paleocene plutonic and volcanic rocks in Sikhote-Alin are homogenously I-type granitic although their spatial migration and various lithology. In the late Paleocene to Eocene, however, the magmatic associations, geochemical and isotopic features changed significantly. Lava, tuff and ignimbrite became more basic from the late Paleocene and basalt-andesite-dacite sequence was dominant, other than rhyolite-dacite associations in the Cretaceous and early Paleocene (Grebennikov and Popov, 2014). Granitoids from the late Paleocene to Eocene are characterized by higher potassium and silicon than the arc magma in the Cretaceous. Main lithology includes alkali-feldspar granite, syenogranite, leucogranite with minor aegirine-riebeckite granite (Grebennikov et al., 2016).

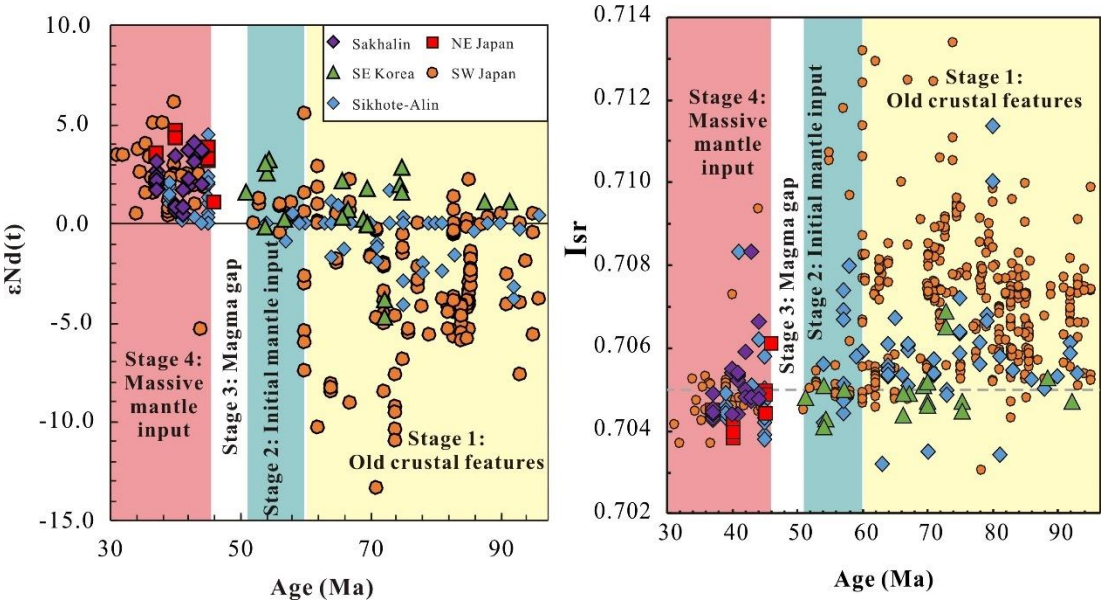

Fig. 5.16 The whole-rock Sr-Nd isotopes of the magmatic rocks in Sikhote-Alin and adjacent areas

Two main types of granitoids and equivalent volcanic rocks can be distinguished in the early Cenozoic Sikhote-Alin area, the A-type and adakite-like rocks. The A-type granitoids/rhyolites are widespread in the eastern Sikhote-Alin from Paleocene to Eocene (Fig. 5.18). Their SiO_2 contents are mostly >70% and reach 76% in some massifs. High Ga/Al values (typically >2.6) of these granitoids show A-type infinity (Whalen et al., 1987), whereas most of them also have high FeO/(FeO+MgO) values,

classified as ferroan granite. The A/CNK ratios range largely from 0.9 to 1.4 and show various features from peralkaline to peraluminous. Most of these alkali-enriched granitoids belong to A_2 type in the discrimination diagrams of A-type granite, related to the magma that have been through a cycle of subduction-zone or continent-continent collision (Eby, 1992). Adakite-like volcanic rocks, characterized by high Sr/Y and $(La/Yb)_N$ values are mostly dated to early Eocene (46-39 Ma; Chashchin et al., 2011; Wu et al., 2017). These volcanic rocks are mainly dacite and rhyodacite, associated with coeval basalt, andesite and dacite which show no adakitic features. Most of the adakitic rocks are presented in the Khanka Block, appearing as small extrusive bodies in local basins and only a few in the eastern Sikhote-Alin area. Geochemical data indicates that they belong to the "high-SiO_2 adakite" with high SiO_2 (>60%), low MgO (<4%) and K/Rb ratios (130-400). The positive correlation between Sr/Y and SiO_2 of the Eocene volcanic rocks reveals the importance of fractional crystallization from andesite or basalt during the formation of the adakitic characteristics, (Wu et al., 2017).

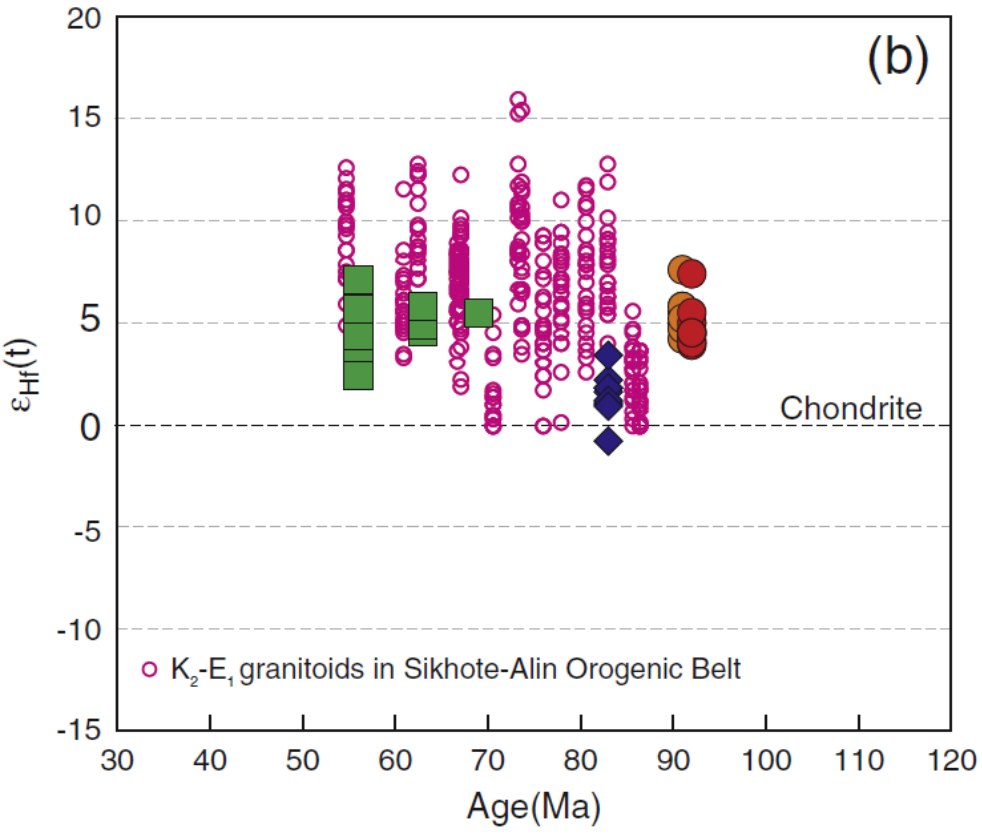

Fig. 5.17 The zircon Hf isotopes of the Sikhote-Alin granitoids (Tang et al., 2016)

Despite of the predominantly negative $\varepsilon_{(Nd)}t$ values in the Cretaceous to early Paleocene, the Eocene igneous rocks show importantly depleted Nd isotopic features. Some trachyandesite and andesite samples without adakitic signatures have $\varepsilon_{(Nd)}t$ values ranging from -2.08 to 4.48 (Fig. 5.16). The adakite-like rocks also show a similar large range, suggesting the protolith of the Eocene rocks are various, including both juvenile meta-basaltic rocks for the adakites and ultramafic rocks with significant crustal mixture for the calc-alkaline basalt and andesite (Wu et al., 2017).

In the adjacent areas, such as Sakhalin and Hokkaido, the abrupt change of isotopic features is also recognized. Eocene is the most important magmatic episode for the Sakhalin and Hokkaido areas, marked by voluminous emplacement of granitoids. In Sakhalin, granodiorite, granite and tonalite with positive $\varepsilon_{(Nd)}t$ values ranging from 1.7 to 3.1 was emplaced into the eastern Sakhalin accretionary complex during 43-37 Ma (Zhao et al., 2019; Liao et al., 2018). The initial $^{87}Sr/^{86}Sr$ ratios are low, varying from 0.7042 to 0.7049. The Sr-Nd isotope shows clearly juvenile signatures, indicating that mantle-derived component or remelting of juvenile basaltic crust is more important than the old crustal component. The geochemical data shows that their protoliths are metasedimentary rocks or amphibolite in the accretionary complex. In the southern Sakhalin, an Eocene A-type granitic pluton (Okhotsk pluton) intruded into the Cretaceous to Paleocene accretionary complex, shows mantle-derived characteristics with ε_{Nd} (T) values of 3.1 to 3.7 and initial $^{87}Sr/^{86}Sr$ ratios from 0.7047–0.7048. Zircon Hf isotopes further verify the "juvenile" features by very positive ε_{Hf} (T) values ranging from +12 to +16 (Liao et al., 2018). The granitoids in Hokkaido are comparable to those in Sakhalin. Granites in the Hikada belt, the central Hokkaido show ε_{Nd} (T) values of 1 to 4.7 and initial $^{87}Sr/^{86}Sr$ ratios from 0.7044–0.7061 and zircon ε_{Hf}(T) values of 8 to 19 (Jahn et al., 2014), suggesting a largely juvenile feature. Considering that Sakhalin and Hokkaido represent the Paleocene to Eocene island arc built upon the Cretaceous accretionary complex, these important juvenile characteristics imply crust growth addition to the older continental crust.

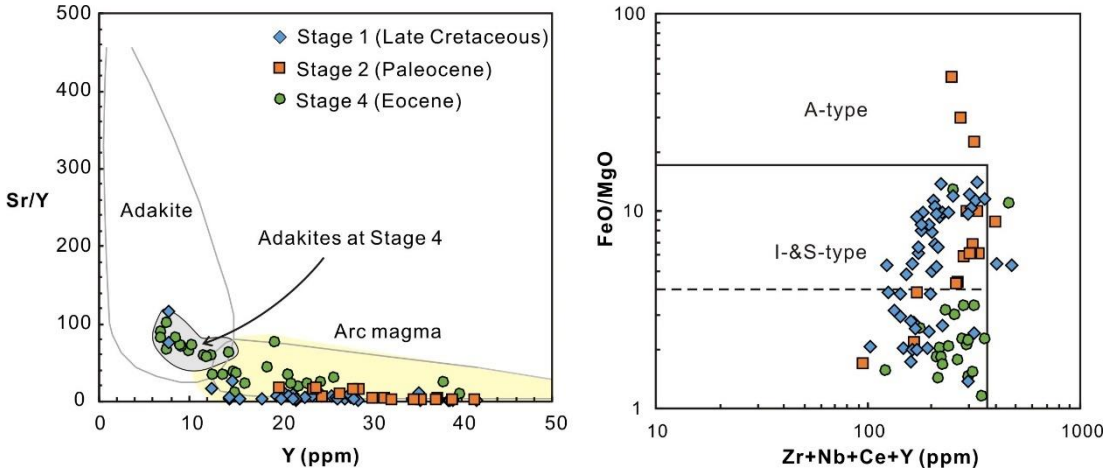

Fig. 5.18 The A-type granitoids and adakites in Sikhote-Alin

Crustal growth is a common feature in the accretionary orogens, such as the Central Asian Orogenic Belt (CAOB). Previous studies propose that the CAOB is one of the most important area contributing to the Phanerozoic crustal growth all over the world (Jahn et al., 2004; Wu et al., 2011). This is explained by the special orogenic process and architecture in the CAOB. Liner arc, fore- and back-arc basins, microcontinental blocks were formed during the prolonged subduction in the Paleo-Asian Ocean domain. Precambrian basement is very lack in most areas of this giant accretionary orogen. Thus, the subduction-related magmatism is characterized by juvenile features and believed to be derived from the reworked juvenile crust or the direct input of mantle component.

Both Sikhote-Alin and SW Japan belong to typical accretionary orogens and were named Nipponides" by Sengör and Natal'in, 1996, similar to the CAOB. However, in Sikhote-Alin, Sakhalin and Hokkaido, the crustal nature is different. The older igneous rocks in Sikhote-Alin is comparable to SW Japan, showing typically negative whole-rock $\varepsilon_{Nd}(T)$ values and high initial $^{87}Sr/^{86}Sr$ ratios (Jahn et al., 2015). Some previous studies argue that old basement existed in the Early Cretaceous in Sikhote-Alin and SW Japan (Jahn et al., 2015; Jahn, 2010), although no precise zircon U-Pb dating age of old basement has been reported so far. During the late Paleocene to Eocene, however, the old crust signatures disappear and are replaced by obviously juvenile features. The

abrupt change is proposed to represent mantle upwelling under the crustal lithosphere, consistent with a possible slab window formed during ridge subduction. After the ridge encountered the trench in NE Asia, the downgoing slab was totally consumed beneath the Asian continent margin. The subducted ridge was teared by the drag of slab to form a slab window. Hot asthenosphere passed the window and heated the overriding plate to generate voluminous granitoids and equivalent volcanic rocks with important mantle signatures. In both Sakhalin and Hokkaido, trench-ridge interaction during the ridge subduction is recorded by the emplacement of intrusive rocks. The S- and A-type granites intruded into the Paleocene accretionary complex in the central Sakhalin Island (Liao et al., 2018; Zhao et al., 2018 and 2019). It is implied that shallow-level crust was melted due under high temperature, probably due to the active spreading ridge beneath the trench. In the Hidaka belt, Hokkaido, the MORB-like gabbro-diorite associations were found to be emplaced into the Late Cretaceous to Paleogene accretionary complex at ca. 55 Ma (Maeda and Kagami, 1996). High temperature metamorphism took place contemporarily, generating both pelitic and mafic granulite. The Sr-Nd isotope of gabbro and granulite vary largely, suggesting the mantle component from the subducted ridge and crustal component from the anatexis of sediments in accretionary complex (Maeda and Kagami, 1996).

5.6 Change of magma chamber/volcano alignments and their relationship with structures in Sikhote-Alin

The relationship between magma and major structures, namely, the alignment of volcanos/magma chambers and faults/fractures, has been discussed for long time. However, it remains a question that the major controlling role is played by magma or structure. In this section, the change of distribution of magmatic rocks in Sikhote-Alin is outlined and discussed the significant change of regional stress field in Sikhote-Alin from the Cretaceous to Paleocene. In this area, it is shown that major structures can dominate the distribution of magmatism in continental arc.

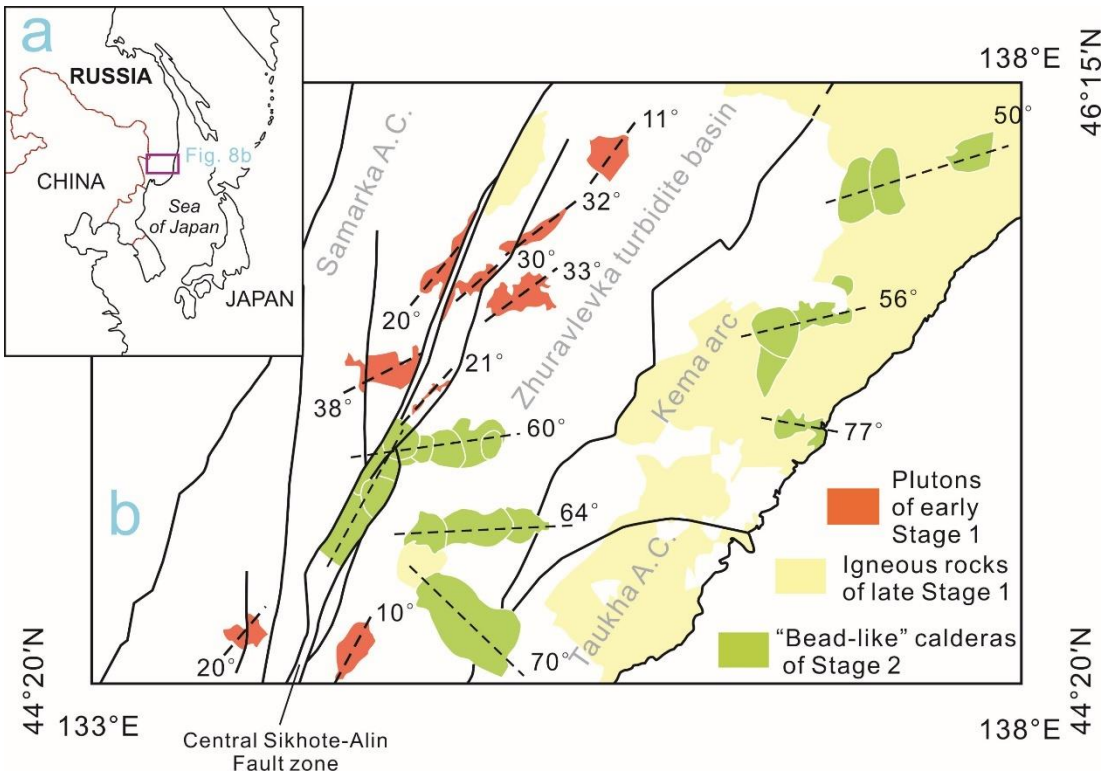

Fig. 5.19 The relationship between pluton/caldera alignments with structures. The middle Cretaceous plutons are shown by orange color and the Paleocene calderas are green.

According to the volcanos/plutons alignments and their relationship with structures, three magmatic associations are identified in Sikhote-Alin.

1) In the middle Cretaceous (110-75 Ma), granitoids and felsic volcanic rocks were regularly presented along the Central Sikhote-Alin Fault and its branches, comprising a narrow magmatic band/linear area (Fig. 5.19). The rock types include mainly diorite, granodiorite, monzogranite, syenogranite and a few gabbros. Most of them are classified to I type and some are S type or the transition between the two (Kruk et al., 2014a; Jahn et al., 2015). In addition to the linear area as a whole, the most important feature of their occurrence is the shape of intrusive bodies and their spatial distribution. Most plutons are elliptic or elongated with length/width ratios ranging from 2:1 to 5:1. The long axes of most plutons are usually oblique to the Fault with small angles, vary from 10-38° and form typical en echelon patterns (Fig. 5.19). In some local areas, there are also a few plutons parallel with

or confined by the Fault zone, showing different long-axis direction from the en echelon ones (Fig. 5.19). About 70% of the plutons are not more than ~50 km from the Central Sikhote-Alin Fault. The distance between ca. 15% of the plutons and the Fault, however, reaches as far as 80 km, which seems unrelated to this major fault.

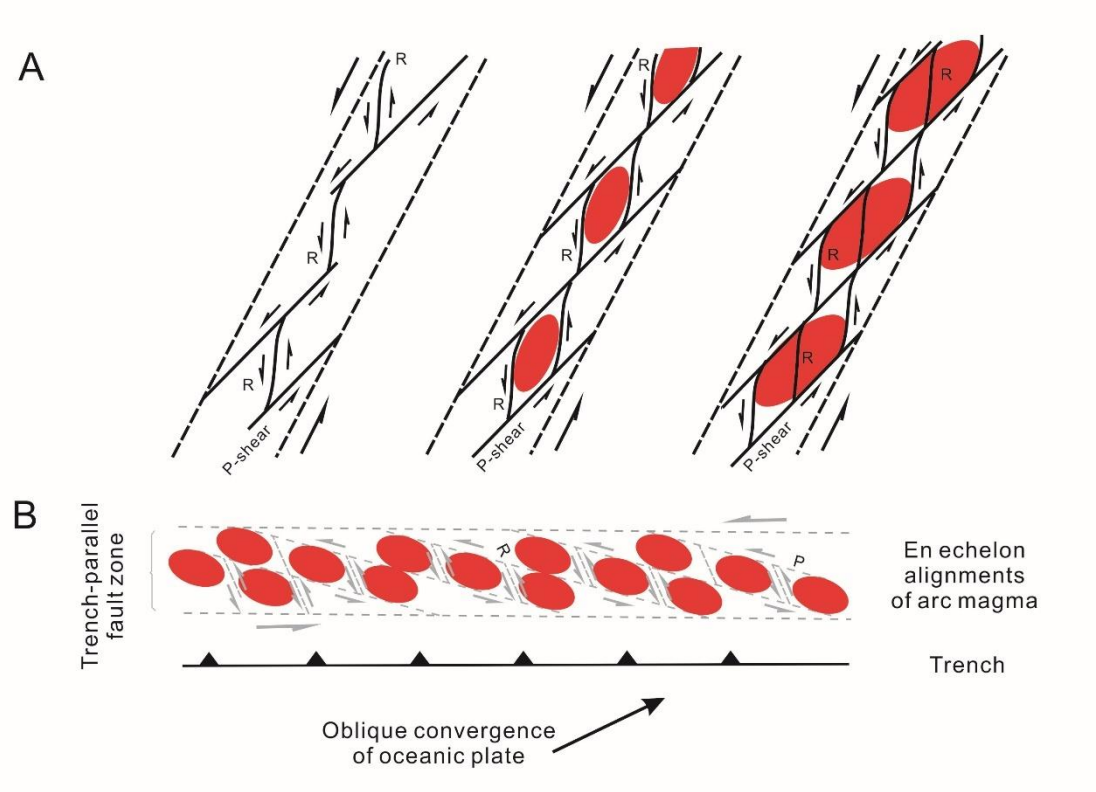

Fig. 5.20 The P shear, R-shear bridge and magmatic intrusions in a sinistral strike-slip zone, similar to the Cretaceous pluton alignments in the central Sikhote-Alin

2) The second type is called plateau-ignimbrite (Grebennikov and Popov, 2014), which occupy a more widespread area along the margin of Sea of Japan, striding the major NNE trending faults and accretionary complexes in Sikhote-Alin. The age of these volcanic rocks and granitoids in Sikhote-Alin are Late Cretaceous, ranging from ca. 85 to 65 Ma. Unlike to narrow linear belt in middle Cretaceous, the Late Cretaceous magmatic rocks are mainly to the east of the Central Sikhote-Alin Fault, with some intrusive or eruptive rocks in the fault zone. The ages become younger from NW to SE, which is attributed to the roll-back of the Izanagi slab and retreat of trench (Jahn et al., 2015; Tang et al., 2016). I-type granitoids

and volcanic rocks are dominant in this period, similar with but more felsic than the middle Cretaceous magma. These magmatic rocks are known as the East Sikhote-Alin Volcanic-Plutonic Belt (ESAVPB) in some literatures (Khanchuk, 2001; Jahn et al., 2015), emphasizing the feature that they intruded into or erupted upon the NNE trending accretionary complexes after the accretionary orogeny before the Late Cretaceous.

3) The third magmatic episode is from the Paleocene to Eocene. The Paleocene rocks (65-55 Ma) are andesite-dominated (Fig. 5.19). An important feature of the Paleocene rocks is that many of them still keep the ancient caldera-shapes with radial or circular faults in the volcano structures. Usually three or more calderas cluster in a narrow belt to be a bead-like shape, trending nearly E-W or SE. The skew angles of the beads to the Central Sikhote-Alin Fault are large, ranging from 50° to 77° (Fig. 5.19). However, some other volcanic structures are isolated and related to the tectonic depressions or intersects of faults in the east Sikhote-Alin, along the margin of Sea of Japan. Whether the volcanos gather together or not, the volcanic rocks and ignimbrites are always associated with granitic pluton/batholith in the volcano structures, showing possible collapse of overlying eruptive rocks on the magma chamber or just simple uplift and erosion of the old volcano structures and intrusive bodies.

The Eocene lava (ca. 50-30 Ma), however, changes to basaltic rocks with intra-plate features and there is no bead-shape found. The Late Cretaceous to Paleocene intrusive/eruptive rocks are constrained to the east of the Central Sikhote-Alin Fault. But the Eocene volcanic rocks are both extensive in the northeast Sikhote-Alin and southern Khanka Block. Martynov et al. (2017) divide the Eocene basalts into the East zone (NE Sikhote-Alin) and Southwest zone (south Khanka). The later one has a long distance from the Late Cretaceous volcanic front, about 300 km. This is abnormal because the magmatism shows eastwards or southeastwards migration from the Late Cretaceous to Paleocene and most of the young magmatic

rocks (<80 Ma) are limited to the east of the Fault. Whereas previous research clearly shows that the southwest Eocene basalts were found to the west of the Fault and importantly related to the local dextral strike-slip depressions (Utkin et al., 2007).

Three stages of magma are characterized by different distribution patterns and relationships with regional structures.

The first-stage magmatic rocks are closely related to the Central Sikhote-Alin Fault, not only because of the short distance between most plutons and the Fault, but also their distribution patterns. For example, there are nine plutons in the central and southern Sikhote-Alin dated to 105 to 85 Ma by zircon U-Pb method (Fig. 5.19). All these plutons are located very near or within the ~20 km wide strike-slip fault zone. On both sides of the fault zone, plutons are always elongated oblique to the fault with small angles and the most popular angles range from 10° to 33°, consistent with the P-shear in the simple shear model. These plutons have close association with the major sinistral strike-slip fault and its branches. This type of magmatic distribution is commonly observed in modern and ancient arcs, for example, the modern Sumatra, Kuril arcs and Late Cretaceous Sierra Nevada. These subduction zones are characterized by oblique subduction of oceanic plate, major strike-slip fault/shear zone in arc and en echelon volcanic arrays (Fig. 5.19). The emplacement and ascent of magma is most facilitated by tensional cracks in middle-upper crust. However, the P-shear in Riedel shear model is a transpressional fracture, not benefitting the emplacement of magma chamber. We use the model proposed by Tikoff and Teyssier (1992) to explain this issue. In a strike-slip arc, continental-scale P shears are formed as en echelon patterns. Although P shears are transpressional, the bridges between the spaced P shears must be tensional and dilational jogs or small pull-apart basins are developed in the narrow spaces between P shears (Fig. 5.20). The bridges, in reality, are small-scale strike-slip fractures (R-shear in the Riedel shear model) with opposite directions against the overall strike-slip motion. In this hypothesis, the elongated

plutons eventually tend to be parallel with P shears and show an en echelon pattern with small angles to the major strike-slip faults. The model is verified in Sierra Nevada by the dextral shear zone (the Rosy Finch shear zone) running through the three Late Cretaceous en echelon plutons. In Sikhote-Alin, transpressional branches of the major strike-slip fault are extensively developed. For instance, in the north part of the fault zone, the plutons are either bordered or cut by the major fault and the P-shear transpressional fault. The bend of the P-shear faults created local extension and supplied space for magmatic emplacement and eruption.

The Late Cretaceous magmatic rocks are extensively and irregularly distributed in the southeastern Sikhote-Alin, and no particular pattern or array is observed. Most of them are located to the east of the Central Sikhote-Alin Fault, with minor near or within the Fault zone. These plutonic-volcanic rocks in Sikhote-Alin are quasi-continuous from 80 Ma. The granitoids, as well as the dacites and rhyolites, in this period were generated intensively in the southeast Sikhote-Alin accretionary orogen, especially in the Taukha accretionary complex (Fig. 5.15). Stable and active oblique subduction of the Izanagi slab was responsible for the silicic magma. It should be noticed that the spatial migration of magmatism is important in the Cretaceous. During 110-85 Ma, the majority of arc magma concentrated along the Central Sikhote-Alin Fault. Whereas the Late Cretaceous to Early Paleocene magma migrated to the east of the Fault, indicating a roll-back of the Izanagi slab. The accretionary complexes (< 100 Ma) include the fore-arc basins and prisms in Sakhalin and Hokkaido, also verifying the retreat of trench. After this process, the east Sikhote-Alin continental margin changed from arc/fore arc to arc/back arc settings.

The third magmatic episode is characterized by bead-like Paleocene volcanic arrays (65-55 Ma), quite different from the Cretaceous ones. The en echelon pattern common in middle Cretaceous (110-85 Ma) was replaced by volcano clusters with high oblique angles to the Central Sikhote-Alin Fault, varying from 50° to 70°. It is implied that the previous P-shear-bridge model does not work for these new volcano alignments and

the regional stress field may have significantly changed. In Riedel shear model, T-shear is a potential tensional crack for these high-angle volcano belts. However, regional geological evidence does not support this possibility because previous sinistral strike-slip faulting was not active at that time. Trench-normal subduction, instead, is proposed to be responsible for the Paleocene bead-like volcano clusters (Fig. 5.19). Nearly E-W compression caused by westwards orthogonal subduction may strengthen the N-S trending thrusts and subordinately initiate the E-W trending extension. The extension was second-order and only focused on some local areas where previous fractures existed, such as the Cretaceous pull-apart basins within/close to the Central Sikhote-Alin Fault zone. Magma generated in this period was facilitated to intrude the middle-upper crust through these extensional cracks and aligned as nearly E-W trending, which is thus oblique to the Central Sikhote-Alin Fault at high angle. Regional E-W trending extensional faults/fractures are crustal scale to accommodate the emplacement of several magma chambers and eruption of corresponding lava. Thus, the bead-like volcano clusters may represent important change of maximum principle stress in NW Pacific in the early Cenozoic, from NNE-SSW to nearly E-W. The change of volcanic alignments took place in other arcs due to the different stress field. The NE Honshu, Japan, is taken as an example here. During the Late Miocene to Pliocene, dextral strike-slip was dominant in this area because the strain was controlled by not only the westwards subduction of the Pacific plate, but also the SW compression of the Kuril arc, and the latter one was significantly stronger. Dextral strike-slip and local extensional faults led to the NE-SW alignment of volcanos in NE Honshu in this period. However, the Pacific plate sped up during the Quaternary and the orthogonal compression was thus strengthened. N-S trending thrusts imposed the N-S trending strike-slip faults and many local E-W trending extensional fractures were generated. Volcano clusters in these local areas were aligned to E-W and the overall strike of the arc was N-S, consistent with the direction of trench.

5.7 Discussion: potential models for the tectonic transition in the early Cenozoic NE Asia

5.7.1 Summary of the Cretaceous to early Cenozoic tectonic-thermal change in the NE Asian continental margin

We have reviewed the major changes of kinematics of structures, magmatic genesis and the structure-magma relationship in NE China, Sikhote-Alin and some adjacent areas in Korea, Russia and Japan. The geological records in the region indicate an important tectonic-thermal condition change during the early Cenozoic.

In summary, the numerous NE- or NNE-striking strike-slip faults in the region were characterized by sinistral strike-slip motion in the Cretaceous and afterwards replaced by a reversed direction. Examples are the Tan-Lu Fault segment in the Bohai Bay Basin, Dun-Mi and Jia-Yi faults in NE China, Kiselevka Fault in north Sikhote-Alin, West Sakhalin and Tym'-Poronai fault systems in Sakhalin and Yansan Fault system in SE Korea. The major basins, such as the Songliao and Sanjiang-Amur basins experienced important inversion event during ca. 65-50 Ma, accompanied by abrupt cooling/uplift event of the surrounding mountains in NE China and Jiaodong Peninsula. It should be note that all the reviewed Cretaceous to Paleogene basins are located in the back-arc area (NE China), not in the arc or fore-arc area (Sikhote-Alin) because of the available data of seismic profile and outcrop investigation are more abundant in the Chinese side. For the magmatic genesis in the arc area, intense magmatic intrusion or eruption, especially the A-type and adakite-like granitoids appeared more abundantly after a short magmatic gap during ca. 55-50 Ma in Sikhote-Alin and Japan and ca. 60-50 Ma in SE Korea. Cenozoic volcanism shows more various tectonic origins including intra-plate features, rather than the typical supra-subduction features in the Cretaceous. Fore-arc MORB gabbros and diorites intruded into the accretionary prisms in Hokkaido at ca. 55 Ma. Anatexis of upper crust and fore-arc/trench sediments resulted in the A- and S-type granitoid intrusions in Sakhalin during the early Eocene. Importantly, the Sr-Nd isotopes of all these arc and fore-arc magmatic rocks reveal an abrupt change from enriched to depleted chracteristics, following the magmatic gap during 55-50 Ma. The zircon $\varepsilon_{(Hf)}t$ values show a consistently increasing trend from the Early Cretaceous to Eocene. All these geochemical and isotopic data indicate a

significant increase of mantle component in the protolith area in the early Cenozoic, replacing the clear crustal signatures in the Cretaceous.

The relationship between the arc caldera/plutons and local structures in Sikhote-Alin also verifies the change of regional stress field. The middle Cretaceous (110-75 Ma) plutons/batholiths are limited within a ~100 km wide belt with NNE trending as a whole along the Central Sikhote-Alin Fault zone. The plutons show clearly en echelon patterns. Their long-axis directions are oblique to the major fault zone with small angle (10° to 33°), indicating regional sinistral motion of the arc-parallel strike-slip fault. This arc magma chamber pattern is similar to the volcano alignments in the present oblique-subduction arcs, such as Sumatra and Kuril and the Cretaceous pluton alignments in Sierra Nevada, corresponding with the magma-control depressions developed by the R-shear extensional bridges connecting the transpressional P shears. In the rest of the Late Cretaceous, the magmatism migrated to the east of the Central Sikhote-Alin Fault and were widespread in the whole southeastern Sikhote-Alin area. In the late Paleocene, however, the en echelon patterns were replaced by nearly E-W striking magma chambers in the east Sikhote-Alin. Afterwards, the volcanic rocks became scattered and show no clear liner patterns in the Eocene. The dramatic change of volcano/pluton alignment represents the regional stress field varied from sinistral simple shear related to NNE-directed oblique subduction to nearly E-W compression related to the orthogonal subduction.

5.7.2 Potential models to explain the tectonic-thermal condition change in the NE Asian margin

5.7.2.1 Model 1: The two-stage transform margin in Sikhote-Alin and slab windows

The transform margin model is proposed by most Russian literatures and firstly comprehensively summarized by Khanchuk (2001), further improved by later studies

on magmatic rocks and structural analysis. They proposed that the continental margin in Sikhote-Alin was very similar to the present California at two stages, the middle Cretaceous and the Paleocene to Eocene (Fig. 5.21). The evolution of this transform margin at the first stage was dominated by a large sinistral strike-slip fault which was later cut and dismembered by the open of the Sea of Japan. The Central Sikhote-Alin Fault, Tanakura and Median Tectonic lines in Japan are three segements of the Early Cretaceous fault (Khanchuk, 2001). According to this prospect, the middle Cretaceous magma was generated by the weak subduction and strong sinistral strike-slip motion related to the northward rapid subduction of the Izanagi Plate (Simanenko and Khanchuk, 2003). The Late Cretaceous continental margin became Andean-type and generated plateau-ignimbrites with equivalent intrusions showing typical supra-subduction features (Grebennikov and Popov, 2014). In the Paleocene to Eocene, the previous subduction was ended by a rifting regime. The special A-type granite and volcanic rocks were resulted from the regional extensional settings related to a dextral strike-slip motion along the second-stage transform margin from 65 to 40 Ma (Grebennikov et al., 2016). In the meantime, the subducted slab behaved differently from the oceanic plate, which triggered the break of slab and formation of slab windows, which provided important pathways for the materials from the asthenosphere. Martynov et al. (2017), however, indicates that the intense extension and basaltic volcanism reached their peaks at around the middle Eocene and last a long time until the open of Sea of Japan (ca. 15 Ma). Slab window related to large-scale dextral strike-slip motion facilitated the mantle input with Pacific-MORB features into the previously prevalent Indian-MORB type region beneath the Sikhote-Alin orogen (Martynov and Khanchuk, 2013).

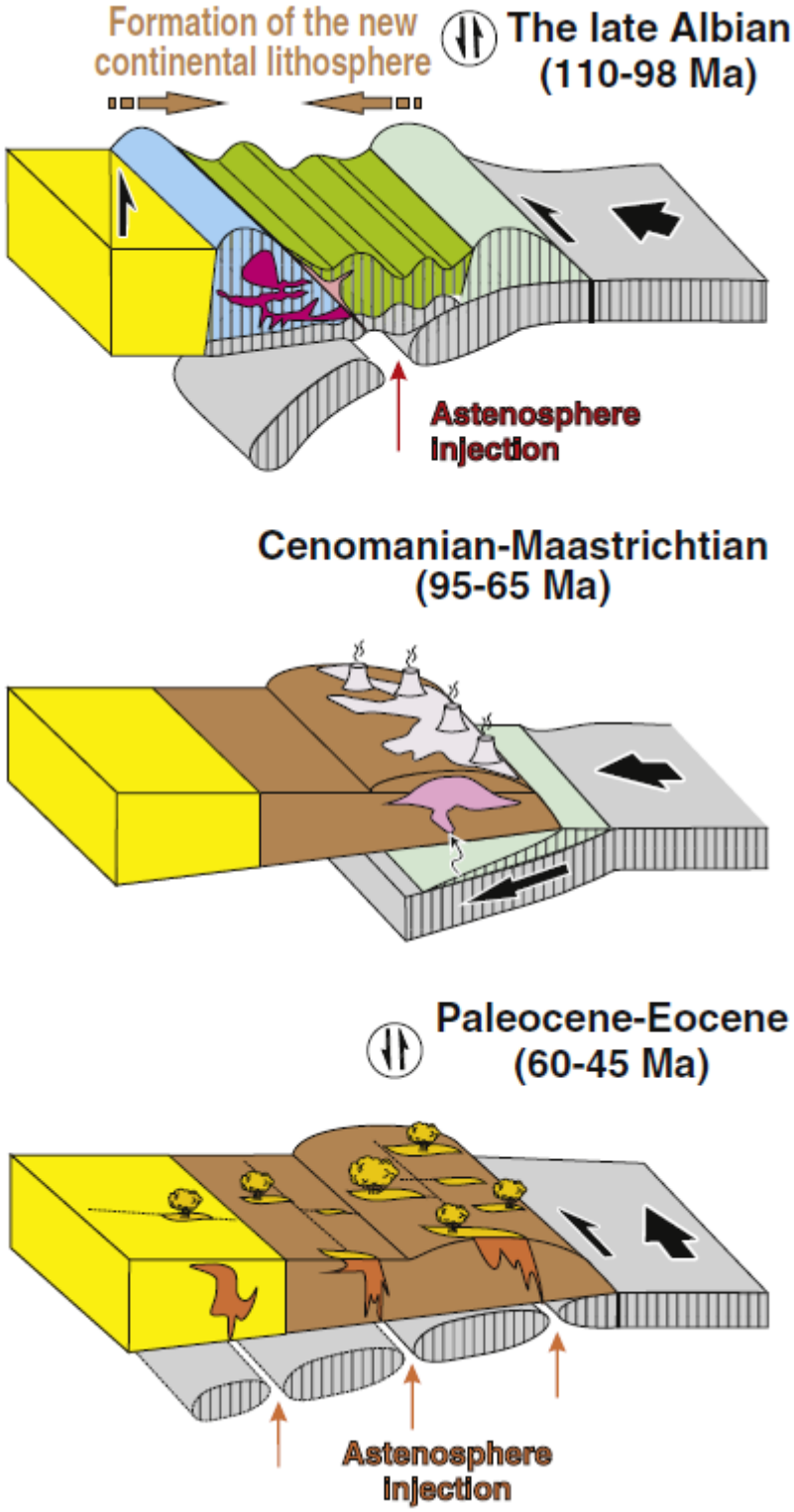

Fig. 5.21 Model 1: two-stage transform in NE Asian continental margin (Grebennikov et al., 2016)

5.7.2.2 Model 2: Far-field effect of the Indian-Eurasian collision

Most studies focusing on the strike-slip faults in NE Asia argue that the abrupt change of sinistral to dextral motion in the early Cenozoic should be attributed to the Indian-Eurasian collision during 60-50 Ma (Fig. 5.22). The collision forced the major blocks in eastern Asia escaped eastwards and large-scale strike-slip faults accommodated most of the deformation and extrusion (Tapponnier and Molnar, 1976; Tapponnier et al., 1990). The eastern margin of the Eurasian continent played a free boundary to escape and the dextral shear zones in the Okhotsk, Sakhalin and Hokkaido were resulted to adjust the regional deformation (Jolivet et al., 1990). Under this tectonic regime, the crust of NE Asia was shortened and dominated by E-W compression (Gu et al., 2017).

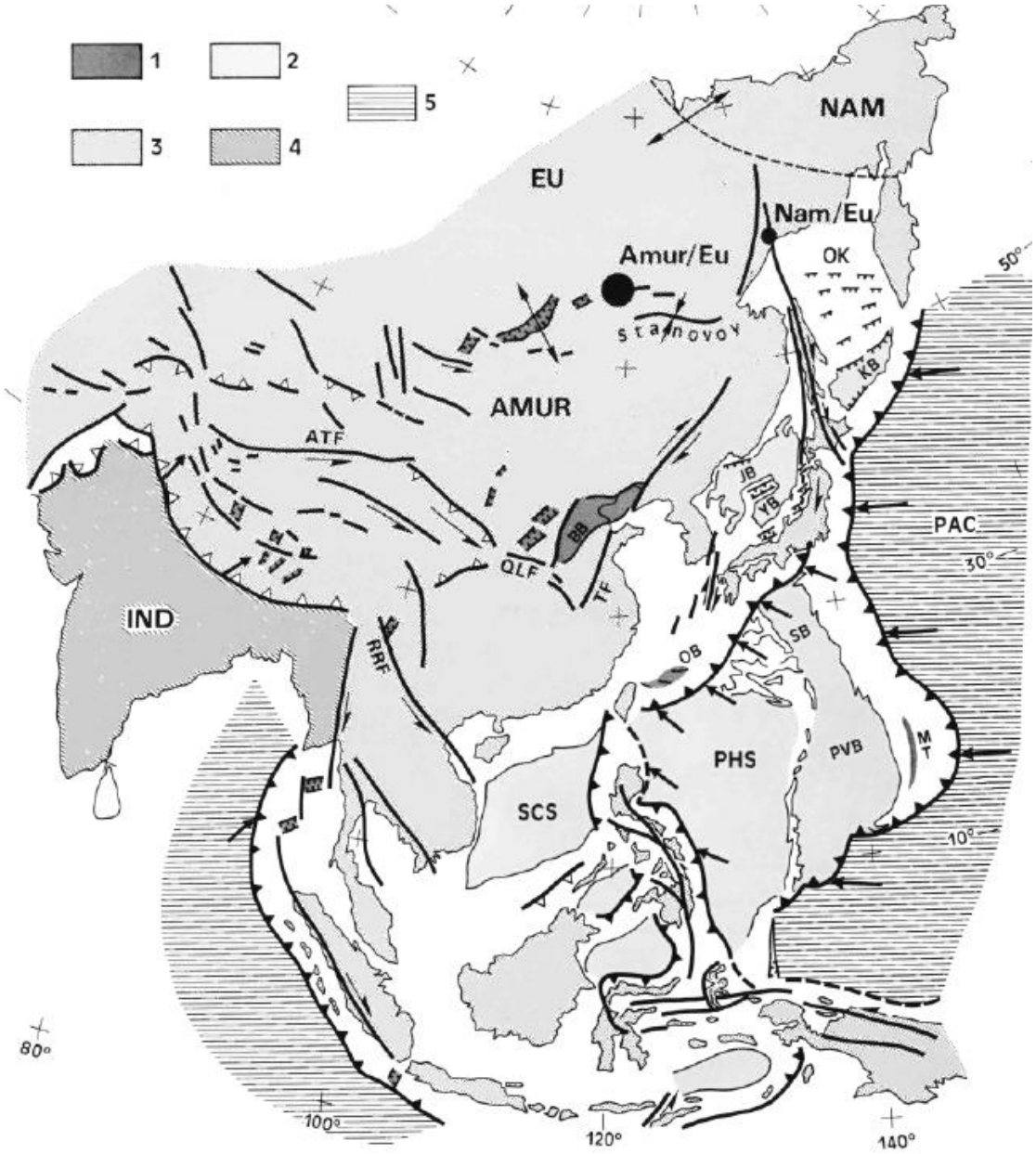

Fig. 5.22 Model 2: the far-field effect of Indian-Eurasian collision (Jolivet al., 1990)

5.7.2.3 Model 3: Dock of the Pacific intra-oceanic arcs to the NE Asian margin

Exotic intra-oceanic arcs were widely distributed in the north Pacific during the Late Cretaceous to Paleocene, involving a ~3000 km long subduction zone from Japan, Hokkaido, Kamchatka and Aleutian (Fig. 5.23; Konstantinovskaia, 2000). Reconstructions of these ancient island arcs are based on paleomagnetic, geological and kinematic data preserved in the volcanic and sedimentary rocks (Domeier et al., 2017). The south-dip Kronotsky and Olutorsky intra-ocean subduction zones were

developed initially far from the NE Asian continent where the north- and west-dip subduction zones were active in the Late Cretaceous to Paleocene. Domeier et al. (2017) also argued that the Izanagi-Pacific ridge was reversed to form this long intra-ocean subduction zone at ca. 80 Ma, which gave birth to the Kula plate in the north Pacific domain. The intra-oceanic island arc system arrived at the NE Asian margin in the early Eocene (Alexeiev et al., 2006). Thus, the abrupt change of stress field and oceanic plate motion from north-directed to NW- or NWW-directed were the results of the dock of this island arc system.

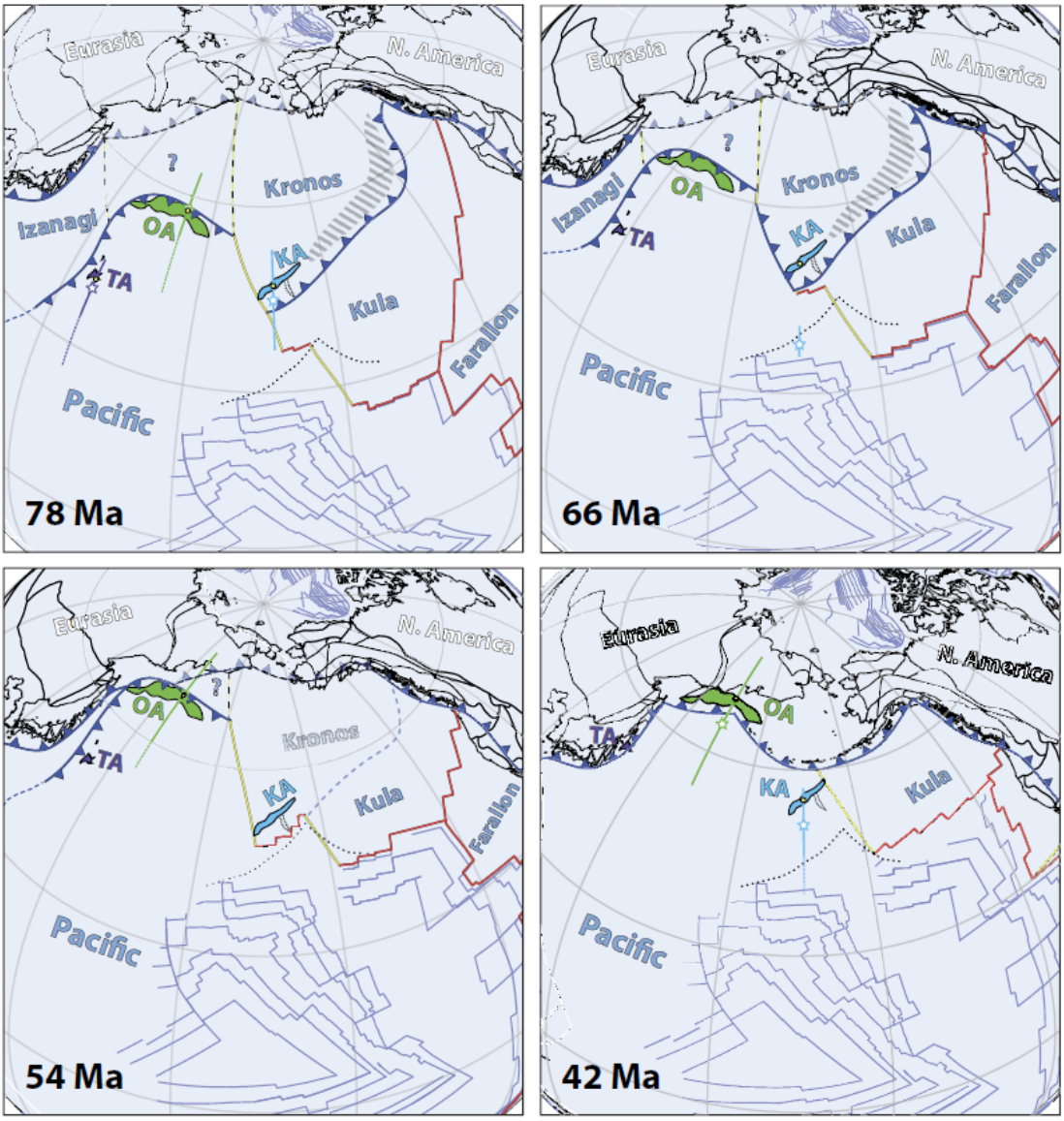

Fig. 5.23 Model 3: the dock of an intra-ocean island arc system in the north Pacific (Domeier et al., 2017)

5.7.2.4 Model 4: Izanagi-Pacific ridge subduction in NE Asia

The fourth model mainly attributes the early Cenozoic event to the arrival of the Izanagi-Pacific Ridge (IPR) to the NE Asian margin (Fig. 5.2; Whittaker et al., 2007). The IPR is proposed to extend over 2000 km long and be parallel or sub-parallel to the Asian continental margin. The ridge subduction and coeval slab break-off happened during ca. 60 to 55 Ma at the Japanese trench. The previous ridge-push force in the Cretaceous was replaced by slab-pull after the Izanagi plate was totally consumed beneath the continental margin, triggered the oceanic plate motion varied from NW to W. Seton et al. (2015) further explained this process using numerical simulation. It is proposed that the arrival of the IPR resulted in a short interrupt of subduction during 60 to 50 Ma. Before the ridge subduction, the Pacific plate was surrounded by a circus of spreading ridges. But afterwards, the initial subduction of the Izu-Bonin-Marianas and Tonga arcs increased the west-directed slab-pull force after ca. 50 Ma. The plate motion changes in the Pacific regime were also responsible for the rapid reorganization of the mid-mantle flow. So, the IPR subduction in the early Cenozoic was not a response to the plate-mantle interaction in this model, but the trigger of the hemisphere-scale event (Seton et al., 2015; Müller et al., 2016). The major changes of no matter magmatic genesis or the regional stress conditions were caused by the IPR subduction in the Paleocene to early Eocene.

5.7.3 Examination of Model 1, 2 and 3 based on the reviewed geological evidence

Slab window related to transform margin is the most important feature in the first-type model (two-stage transform margin model). This model explains why the mantle signatures of these magmatic rocks were abruptly enhanced in the early Cenozoic and connected the slab window with the dextral strike-slip motion. However, important and basic questions remain that how the windows were opened and what was the geodynamic factor that forced the sinistral faults to act inversely in the Paleocene to Eocene. Some studies attribute the slab windows to the strike-slip motion or the different deformation behaviors of the oceanic plates at variant depths (Grebennikov

et al., 2016). However, the proposed differences are not observed to generate any similar window structures in the modern subduction zones. Generally, the formation of slab windows is caused by the trench-ridge-trench or trench-transform-trench triple junction motion when a trench is encountered by a spreading ridge or a transform fault (Thorkelson, 1996). After the ridge or transform fault is subducted and teared beneath a subduction zone, the different motion vectors of the two subducted plates separated by the ridge or transform will force the open of a slab window. The shape and size of the window depends on the direction and speed of plate motions (Thorkelson, 1996). The other problem of this model is that no explanation is made for the change of major faults from sinistral in the Cretaceous to dextral in the early Cenozoic, although this event is regarded as an important signature of tectonic reorganization. In summary, the transform margin model (Model 1) solves the problem of the abrupt geochemical and isotopic changes of magmatism by proposing slab window formation, but keeps the questions open that why slab windows were generated in the early Cenozoic and what is the relationship between the changes of the fault kinematics and magmatism.

Model 2 can easily explain the kinematic change of major faults in NE Asia by extrusion of Asian continental blocks to the Pacific margin which is set up as a free boundary (Tapponnier and Molnar, 1976; Jolivet et al., 1990). However, the Indian-Eurasian collision generated intense deformation along the Himalayas and its foreland basin, which is > 5000 km away from the eastern Asian margin. It remains unclear that if the far-field effect of the collision was strong enough or not to inverse the rift basins as large as the Songliao and Sanjiang basins. The stress decays after such a long travel and compressional deformation should become much weaker in NE Asia. However, the volcano/pluton alignments controlled by the E-W trending structures are limited to the eastern Sikhote-Alin, showing the regional principle compression was E-W and the strongest deformation was concentrated in the east, not the west.

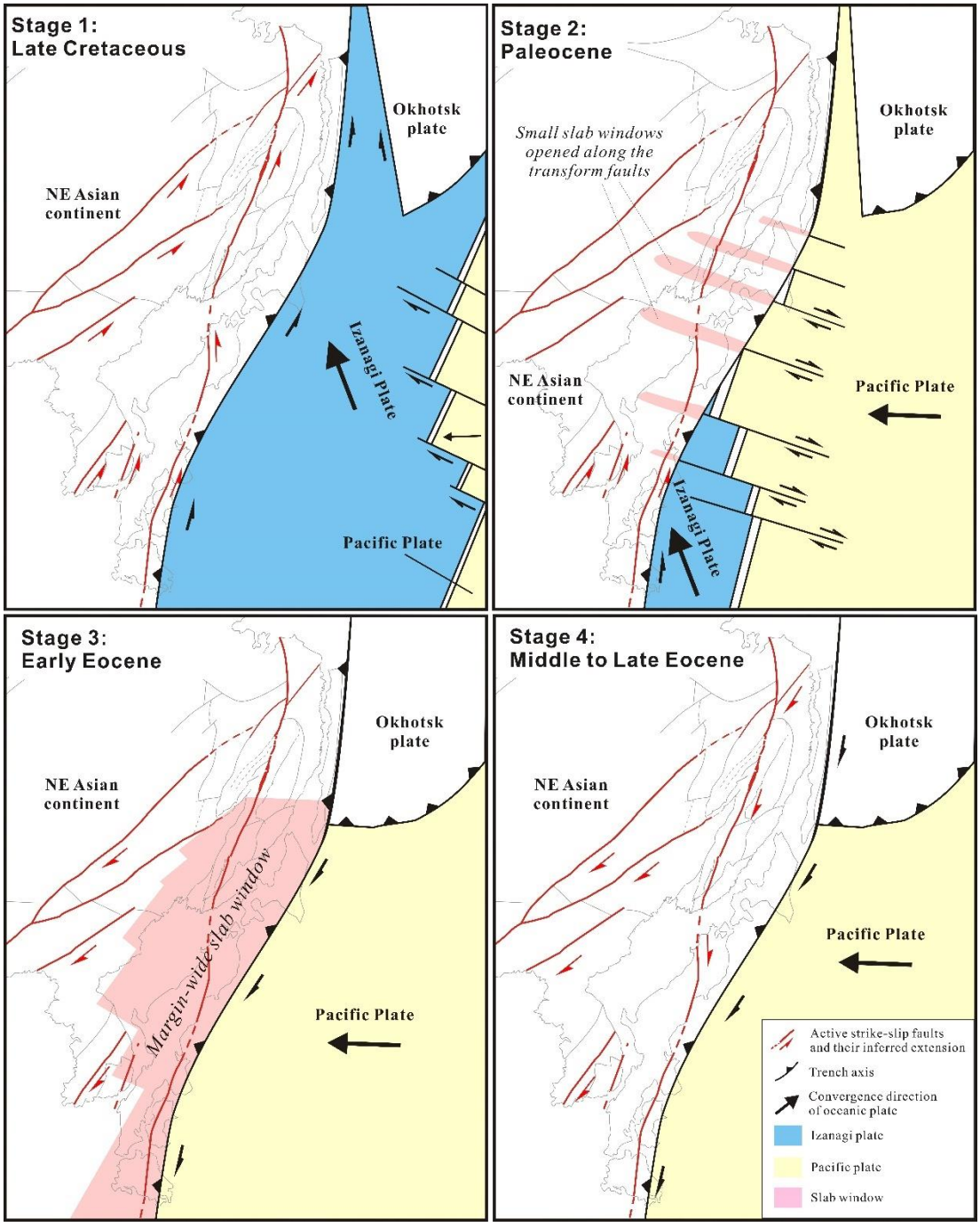

Fig. 5.24 The Izanagi-Pacific ridge subduction model.

On the other hand, the dramatic change of magmatism from enriched to depleted isotopic features is also hard to understand if the Indian-Eurasian collision was the major force. The dextral strike-slip faults in Sakhalin, Hokkaido and Sikhote-Alin were born to accommodate the escape deformation in Asian continent. In this scenario, the deformation would be limited within the crust or lithosphere level because they are rigid to be displaced. Whereas the tectonic-thermal conditions of the mantle wedge

and subducted slab would maintain the status quo, making the isotopic and geochemical features of magmatism consistent in the NE Asian margin.

Model 3 introduces an >3000 km long island-arc system into the Late Cretaceous to Paleocene tectonic context in the north Pacific regime, including the eastern Hokkaido, Kamchatka and Aleutian. The most important feature in this model is that the Izanagi-Pacific Ridge was believed to be inversed to a south-dip intra-ocean subduction zone and a bi-directional subduction system existed in the north Pacific. The dock of the island arc system in the Paleocene to Eocene is important to explain the history of the volcanic arcs and deformations within the oceanic plate. The collision between the island arc system and Asian mainland terminated this intra-oceanic subduction and thus enhanced the northwest movement of the Pacific plate. This process meets the change of regional stress field in NE Asia. However, how the arc-continent collision affected the magmatism in the NE Asian margin is unclear. After the arc-continent collision, the westward subduction was still active in the NW Pacific margin and thus is difficult to explain the extensive magmatic gap between ca. 60-50 Ma in Sikhote-Alin, SE Korea and Japan. It is also ambiguous that if the geochemical and isotopic features of the mantle wedge would be changed after the collision or not. At a word, the intra-ocean island arc model is feasible to reconstruct the motion of the Pacific plate, but needs more details for the switch from bi-directional subduction to W- and NW-directed subduction and its geological influences on the continental side.

5.7.4 Geological responses of the Izanagi-Pacific Ridge subduction in the NE Asian margin: Examination from the magmatic, structural and paleomagnetic data

In this paper, it is proposed that Model 4, the Izanagi-Pacific Ridge subduction model is the most appropriate one to understand the tectono-magma change in the early Cenozoic. The ridge is estimated to reach the eastern Asian trenches at about 60 Ma and be totally subducted under the continent at ca. 55-50 Ma. The time coincides with

the fore-arc MORB intrusions in Hokkaido, sediments anataxis in Sakhalin and adakite-like and A-type rocks in Sikhote-Alin. The lithological associations match well the predicted ones by the ridge subduction model. Slab window proposed by Model 1 can be attributed to the widen ridge and transform fault after they were subducted beneath the continent, which provides a pathway for the mantle-derived materials with highly depleted Sr-Nd-Hf isotopic features. The Izanagi plate moved in N- or NNW-direction in the Cretaceous can explain the giant sinistral strike-slip before the ridge subduction. Whereas the initiation of the west-dip subduction of the Pacific plate changed the regional compression direction from northwest to nearly west. A new dextral strike-slip motion was developed due to the geometric relationship between the E-W convergence direction and the NNE striking of the continental arc in the NE Asian margin. Also, the NNE-trending alignments of plutons in Cretaceous was replaced by the nearly E-W trending alignments of calderas in Sikhote-Alin. Recently and previously published paleomagnetic data which were ignored more or less in the previous reconstructions further verifies the ridge-subduction scenario. In the Cretaceous, all the paleomagnetic data show a long northward travel of terranes in Sikhote-Alin and Sakhalin, consistent with the NNW-directed motion of the Izanagi plate (Didenko et al., 2014; Ichihashi et al., 2015; Khanchuk et al., 2015). In the latest Cretaceous to Paleocene, the Sikhote-Alin terranes were proposed to experience a counterclockwise rotation of 20.5°±17.7° from 66 to 51 Ma (Uno et al., 1999), or 41°±16° from 53 to 50 Ma (Otofuji et al., 2003). After ca. 50 Ma, the relative position of the Sikhote-Alin terranes had been fixed to the Eurasian continent and they behaved as a unified unit until the open of Sea of Japan in the Miocene (Otofuji et al., 1995). Whereas a vertical axis rotation of blocks in the interior of Sakhalin and Hokkaido was detected during Eocene to Miocene and explained by the micro-block rotations within the dextral shear zones (Takeuchi et al., 1999). The rapid rotation of the Sikhote-Alin terranes in the early Cenozoic may be resulted from the rapid NNW-directed subduction of the remnant Izanagi plate and the onset of the NWW- or W-directed subduction of the Pacific plate. The counterclockwise rotation of convergent direction from NNW to NWW or W triggered the counterclockwise rotation of the Sikhote-Alin

orogenic belt. This process can be responsible for the intense uplift and basin inversion events in the back-arc area (NE China) and the E-W compression in the arc area (Sikhote-Alin). After ca. 50 Ma when the switch of convergent direction was finished, the Sikhote-Alin terranes began to be influenced by the mantle upwelling across the slab window and the increased orthogonal subduction with dextral strike-slip component.

5.8 Conclusions

In this paper, we reviewed major changes of kinematics of major strike-slip faults, basin inversion/uplift events, geochemical and isotopic features of magmatic rocks, and the relationship between volcano/pluton alignments and local structures in NE Asia, especially in NE China and Sikhote-Alin orogenic belt in Russian Far East.

The changes of tectono-thermal conditions in NE Asia are represented by the following evidence:

1) the large-scale strike-slip faults dominated by sinistral motion in the Cretaceous were then inversed to dextral in the early Cenozoic;

2) abrupt uplift from ca. 65 to 50 Ma resulted into regional angular unconformity in the Songliao, Sanjiang-Amur and adjacent small basins in NE China, as well as the dramatically increase of cooling rate of the surrounding mountains;

3) the long-term arc magmatism with supra-subduction features during the Cretaceous was replaced by various magmatic associations after a short magmatic gap during 60-50 Ma in the NE Asian margin, such as the A-type, adakite-like granitoids, basaltic volcanic rocks with intra-plate infinity in Sikhote-Alin and SE Korea, fore-arc MORB intrusions in Hokkaido and A- and S-type granitoids in Sakhalin;

4) the Sr-Nd-Hf isotopes of the magmatic rocks show important increase of mantle-derived component after the magmatic gap whereas the Cretaceous rocks were characterized by strongly enriched features;

5) the plutons in the middle Cretaceous were distributed along the Central Sikhote-Alin Fault zone with en echelon patterns, showing sinistral simple shear context. In the Paleocene to early Eocene, the alignments of calderas changed to roughly E-W trending, almost perpendicular to the fault zone, implying an E-W principle compression.

The changes of regional structures and magmatic genesis were proposed to be the geological evidence of Izanagi-Pacific Ridge subduction sub-parallel to the continental margin at ca. 65 to 50 Ma. The slab window formed during the ridge subduction facilitated the mantle upwelling, overprinting the Cretaceous arc-magma geochemical and enriched isotopic features in NE Asian continental margin. After the consumption of the Izanagi plate, the Pacific subduction was initiated at ca. 50 Ma and the convergence direction was NWW-SEE or nearly E-W. The sudden change of oceanic plate motion forced the Sikhote-Alin terranes rotated counterclockwise in the early Cenozoic, enhancing the E-W compressive component to trigger the E-W trending local depressions and volcano alignments in Sikhote-Alin, regional angular unconformity and uplift in NE China and extensively dextral strike-slip motion along the major NNE-trending faults in NE Asia.

5.9 References

Alexeiev, D. V., Gaedicke, C., Tsukanov, N. V., & Freitag, R. (2006). Collision of the Kronotskiy arc at the NE Eurasia margin and structural evolution of the Kamchatka–Aleutian junction. International Journal of Earth sciences, 95(6), 977-993.

Arculus, R. J., Ishizuka, O., Bogus, K. A., Gurnis, M., Hickey-Vargas, R., Aljahdali, M. H., ... & do Monte Guerra, R. (2015). A record of spontaneous subduction initiation in the Izu–Bonin–Mariana arc. Nature Geoscience, 8(9), 728.

Bai, B., Wang, Y. Q., Mao, F. Y., & Meng, J. (2017). New material of Eocene Helaletidae (Perissodactyla, Tapiroidea) from the Irdin Manha Formation of the Erlian Basin, Inner Mongolia, China and comments on related localities of the Huheboerhe area. American Museum Novitates, 2017(3878), 1-45.

Bourgois, J., Martin, H., Lagabrielle, Y., Le Moigne, J., & Frutos Jara, J. (1996). Subduction erosion related to spreading-ridge subduction: Taitao peninsula (Chile margin triple junction area). Geology, 24(8), 723-726.

Chadwick, J., Perfit, M., McInnes, B., Kamenov, G., Plank, T., Jonasson, I., & Chadwick, C. (2009). Arc lavas on both sides of a trench: Slab window effects at the Solomon Islands triple junction, SW Pacific. Earth and Planetary Science Letters, 279(3-4), 293-302.

Chashchin, A. A., Nechaev, V. P., Nechaeva, E. V., & Blokhin, M. G. (2011). Discovery of Eocene adakites in Primor'e. Doklady Earth Sciences, 438(2), 744-749.

Chen, D. (2016). Mesozoic-Cenozoic Tectonic Evolution and Low Temperature Thermochronological Study of Eastern Heilongjiang, NE China (in Chinese with English Abstract). Geology, Zhejiang: Zhejiang University Hangzhou.

Cheng, R. Y., Wu, F. Y., Ge, W. C., Sun, D. Y., Liu, X. M., & Yang, J. H. (2006). Emplacement age of the Raohe Complex in eastern Heilongjiang Province and the tectonic evolution of the eastern part of Northeastern China. Acta Petrologica Sinica, 22(2), 353-376.

Cheng, Y., Wu, Z., Lu, S., Li, X., Lin, C., Huang, Z., ... & Wang, S. (2018). Mesozoic to Cenozoic tectonic transition process in Zhanhua Sag, Bohai Bay Basin, East China. Tectonophysics, 730, 11-28.

Cheon, Y., Cho, H., Ha, S., Kang, H. C., Kim, J. S., & Son, M. (2019). Tectonically controlled multiple stages of deformation along the Yangsan Fault Zone, SE Korea, since Late Cretaceous. Journal of Asian Earth Sciences, 170, 188-207.

Cho, H. S., Son, M., & Kim, I. S. (2007). Anisotropy of magnetic susceptibility (AMS)

of granitic rocks in the eastern region of the Yangsan Fault. Economic and Environmental Geology, 40(2), 171-189.

Cho, H., Son, M., Cheon, Y., Sohn, Y. K., Kim, J. S., & Kang, H. C. (2016). Evolution of the Late Cretaceous Dadaepo Basin, SE Korea, in response to oblique subduction of the proto-Pacific (Izanagi/Kula) or Pacific plate. Gondwana Research, 39, 145-164.

Didenko, A. N., Khanchuk, A. I., Tikhomirova, A. I., & Voinova, I. P. (2014). Eastern segment of the Kiselevka-Manoma terrane (Northern Sikhote Alin): Paleomagnetism and geodynamic implications. Russian Journal of Pacific Geology, 8(1), 18-37.

Domeier, M., Shephard, G. E., Jakob, J., Gaina, C., Doubrovine, P. V., & Torsvik, T. H. (2017). Intraoceanic subduction spanned the Pacific in the Late Cretaceous–Paleocene. Science advances, 3(11), eaao2303.

Domeier, M., Shephard, G. E., Jakob, J., Gaina, C., Doubrovine, P. V., & Torsvik, T. H. (2017). Intraoceanic subduction spanned the Pacific in the Late Cretaceous–Paleocene. Science advances, 3(11), eaao2303.

Eby, G. N. (1992). Chemical subdivision of the A-type granitoids: petrogenetic and tectonic implications. Geology, 20(7), 641-644.

Faure, M., & Natal'in, B. (1992). The geodynamic evolution of the eastern Eurasian margin in Mesozoic times. Tectonophysics, 208(4), 397-411.

Faure, M., Natal'In, B. A., Monie, P., Vrublevsky, A. A., Borukaiev, C., & Prikhodko, V. (1995). Tectonic evolution of the Anuy metamorphic rocks (Sikhote Alin, Russia) and their place in the Mesozoic geodynamic framework of East Asia. Tectonophysics, 241(3-4), 279-301.

Filippov, A. N., & Kemkin, I. V. (2009). Siliceous-volcanogenic complexes of western Sikhote Alin: Their stratigraphy and origin. Russian Journal of Pacific Geology, 3(2), 154-168.

Filippov, A. N., Govorov, G. I., Chashchin, A. A., & Punina, T. A. (2010). Composition and formation settings of the siliceous-volcanogenic complexes of the Nizhneussuriisk segment, Kiselevka-Manoma terrane, West Sikhote Alin.

Russian Journal of Pacific Geology, 4(4), 289-303.

Ge, M. H., Zhang, J. J., Liu, K., Ling, Y. Y., Wang, M., & Wang, J. M. (2016). Geochemistry and geochronology of the blueschist in the Heilongjiang Complex and its implications in the late Paleozoic tectonics of eastern NE China. Lithos, 261, 232-249.

Gilder, S. A., Leloup, P. H., Courtillot, V., Chen, Y., Coe, R. S., Zhao, X., ... & Zhu, R. (1999). Tectonic evolution of the Tancheng‐Lujiang (Tan‐Lu) fault via middle Triassic to Early Cenozoic paleomagnetic data. Journal of Geophysical Research: Solid Earth, 104(B7), 15365-15390.

Golozubov, V. V., Kasatkin, S. A., Grannik, V. M., & Nechayuk, A. E. (2012). Deformation of the Upper Cretaceous and Cenozoic complexes of the West Sakhalin terrane. Geotectonics, 46(5), 333-351.

Golozubov, V. V., Kasatkin, S. A., Malinovskii, A. I., Nechayuk, A. E., & Grannik, V. M. (2016). Dislocations of the Cretaceous and Cenozoic complexes of the northern part of the West Sakhalin Terrane. Geotectonics, 50(4), 439-452.

Grebennikov, A. V., & Popov, V. K. (2014). Petrogeochemical aspects of the Late Cretaceous and Paleogene ignimbrite volcanism of East Sikhote-Alin. Russian Journal of Pacific Geology, 8(1), 38-55.

Grebennikov, A. V., Khanchuk, A. I., Gonevchuk, V. G., & Kovalenko, S. V. (2016). Cretaceous and Paleogene granitoid suites of the Sikhote-Alin area (Far East Russia): Geochemistry and tectonic implications. Lithos, 261, 250-261.

Gu, C., Zhu, G., Zhai, M., Lin, S., Song, L., & Liu, B. (2016). Features and origin time of Mesozoic strike-slip structures in the Yilan-Yitong Fault Zone. Science China Earth Sciences, 59(12), 2389-2410.

Gu, C., Zhu, G., Zhang, S., Liu, C., Li, Y., Lin, S., & Wang, W. (2017). Cenozoic evolution of the Yilan–Yitong Graben in NE China: An example of graben formation controlled by pre-existing structures. Journal of Asian Earth Sciences, 146, 168-184.

Hsiao, L.Y., Graham, S.A., Tilander, N., 2004. Seismic reflection imaging of a major strike-slip fault zone in a rift system: Paleogene structure and evolution of the

Tan-Lu fault system, Liaodong Bay, Bohai, offshore China. AAPG Bull. 88, 71–97.

Hsiao, L.Y., Graham, S.A., Tilander, N., 2010. Stratigraphy and sedimentation in a rift basin modified by synchronous strike-slip deformation: southern Xialiao basin, Bohai, offshore China. Basin Res. 22, 61–78.

Huang, L., Liu, C. Y., & Kusky, T. M. (2015). Cenozoic evolution of the Tan–Lu Fault Zone (East China)—constraints from seismic data. Gondwana Research, 28(3), 1079-1095.

Hwang, B. H., McWilliams, M., Son, M., & Yang, K. (2007). Tectonic implication of A-type granites across the Yangsan fault, Gigye and Gyeongju areas, southeast Korean Peninsula. International Geology Review, 49(12), 1094-1102.

Ichihashi, R. J., Zaman, H., Wada, Y., Sugamori, Y., Kajikawa, Y., Ahn, H. S., ... & Otofuji, Y. I. (2015). Paleomagnetic evidence for post-early cretaceous tectonic rotation of the Sikhote-Alin superterrane, Far East Russia. Journal of Asian Earth Sciences, 111, 88-99.

Ishizuka, O., Tani, K., Reagan, M. K., Kanayama, K., Umino, S., Harigane, Y., ... & Dunkley, D. J. (2011). The timescales of subduction initiation and subsequent evolution of an oceanic island arc. Earth and Planetary Science Letters, 306(3-4), 229-240.

Isozaki, Y., Aoki, K., Nakama, T., & Yanai, S. (2010). New insight into a subduction-related orogen: a reappraisal of the geotectonic framework and evolution of the Japanese Islands. Gondwana Research, 18(1), 82-105.

Jahn, B. M. (2004). The Central Asian Orogenic Belt and growth of the continental crust in the Phanerozoic. Geological Society, London, Special Publications, 226(1), 73-100.

Jahn, B. M. (2010). Accretionary orogen and evolution of the Japanese Islands: Implications from a Sr-Nd isotopic study of the Phanerozoic granitoids from SW Japan. American Journal of Science, 310(10), 1210-1249.

Jahn, B. M., Usuki, M., Usuki, T., & Chung, S. L. (2014). Generation of Cenozoic granitoids in Hokkaido (Japan): Constraints from zircon geochronology, Sr-Nd-

Hf isotopic and geochemical analyses, and implications for crustal growth. American Journal of Science, 314(2), 704-750.

Jahn, B. M., Valui, G., Kruk, N., Gonevchuk, V., Usuki, M., & Wu, J. T. (2015). Emplacement ages, geochemical and Sr–Nd–Hf isotopic characterization of Mesozoic to early Cenozoic granitoids of the Sikhote-Alin Orogenic Belt, Russian Far East: Crustal growth and regional tectonic evolution. Journal of Asian Earth Sciences, 111, 872-918.

Jolivet, L., Davy, P., & Cobbold, P. (1990). Right‐lateral shear along the northwest Pacific margin and the India‐Eurasia collision. Tectonics, 9(6), 1409-1419.

Khanchuk, A. I. (2001). Pre-Neogene tectonics of the Sea-of-Japan region: A view from the Russian side. in Special issue: *Geotectonic framework of eastern Asia before the opening of the Japan Sea*, *Part 2*, Earth Science (Chikyu Kagaku), 55(5), 275-291.

Khanchuk, A. I., Kemkin, I. V., & Kruk, N. N. (2016). The Sikhote-Alin orogenic belt, Russian South East: Terranes and the formation of continental lithosphere based on geological and isotopic data. Journal of Asian Earth Sciences, 120, 117-138.

Khanchuk, A. I., Kruk, N. N., Valui, G. A., Nevolin, P. L., Moskalenko, E. Y., Fugzan, M. M., ... & Travin, A. V. (2008). The Uspensk intrusion in South Primorye as a reference petrotype for granitoids of the transform continental margins. Doklady Earth Sciences, 421(1), 734-737).

Khanchuk, A. I., Vovna, G. M., Kiselev, V. I., Mishkin, M. A., & Lavrik, S. N. (2010). First results of zircon LA-ICP-MS U-Pb dating of the rocks from the Granulite complex of Khanka massif in the Primorye region. In Doklady Earth Sciences, 434 (1), 1164-1167.

Kim, S. W., Kwon, S., Park, S. I., Lee, C., Cho, D. L., Lee, H. J., ... & Kim, S. J. (2016). SHRIMP U–Pb dating and geochemistry of the Cretaceous plutonic rocks in the Korean Peninsula: a new tectonic model of the Cretaceous Korean Peninsula. Lithos, 262, 88-106.

Kinoshita, O. (1995). Migration of igneous activities related to ridge subduction in Southwest Japan and the East Asian continental margin from the Mesozoic to the

Paleogene. Tectonophysics, 245(1-2), 25-35.

Kinoshita, O. (2002). Possible manifestations of slab window magmatisms in Cretaceous southwest Japan. Tectonophysics, 344(1-2), 1-13.

Klein, E. M., & Karsten, J. L. (1995). Ocean-ridge basalts with convergent-margin geochemical affinities from the Chile Ridge. Nature, 374(6517), 52.

Konstantinovskaia, E. A. (2000). Geodynamics of an Early Eocene arc–continent collision reconstructed from the Kamchatka Orogenic Belt, NE Russia. Tectonophysics, 325(1-2), 87-105.

Kruk, N. N., Simanenko, V. P., Golozubov, V. V., Kovach, V. P., Vladimirov, V. G., & Kasatkin, S. A. (2014b). Geochemistry of rocks in the Anuy metamorphic dome, Sikhote-Alin: Composition of the protoliths and the possible nature of metamorphism. Geochemistry International, 52(3), 229-246.

Kruk, N. N., Simanenko, V. P., Gvozdev, V. I., Golozubov, V. V., Kovach, V. P., Serov, P. I., ... & Kuibida, M. L. (2014a). Early Cretaceous granitoids of the Samarka terrane (Sikhote-Alin'): geochemistry and sources of melts. Russian Geology and Geophysics, 55(2), 216-236.

Kudymov, A. V. (2010). Cenozoic stress fields in the Kiselevka fault zone, Lower Amur region. Russian Journal of Pacific Geology, 4(6), 495-501.

Lagabrielle, Y., Suárez, M., Rossello, E. A., Hérail, G., Martinod, J., Régnier, M., & de la Cruz, R. (2004). Neogene to Quaternary tectonic evolution of the Patagonian Andes at the latitude of the Chile Triple Junction. Tectonophysics, 385(1-4), 211-241.

Li, Q. (2016). Eocene fossil rodent assemblages from the Erlian Basin (Inner Mongolia, China): biochronological implications. Palaeoworld, 25(1), 95-103.

Li, X. M., & Gong, G. L. (2011). Late Mesozoic‐Cenozoic exhumation history of the Lesser Hinggan Mountains, NE China, revealed by fission track thermochronology. Geological Journal, 46(4), 277-287.

Li, X., Yang, X., Xia, B., Gong, G., Shan, Y., Zeng, Q., ... & Sun, W. (2011). Exhumation of the Dahinggan Mountains, NE China from the Late Mesozoic to the Cenozoic: New evidence from fission-track thermochronology. Journal of

Asian Earth Sciences, 42(1-2), 123-133.

Liao, J. P., Jahn, B. M., Alexandrov, I., Chung, S. L., Zhao, P., Ivin, V., & Usuki, T. (2018). Petrogenesis of Mid-Eocene granites in South Sakhalin, Russian Far East: Juvenile crustal growth and comparison with granitic magmatism in Hokkaido and Sikhote-Alin. Journal of Asian Earth Sciences, 167, 103-129.

Ling, M. X., Li, Y., Ding, X., Teng, F. Z., Yang, X. Y., Fan, W. M., ... & Sun, W. (2013). Destruction of the North China Craton induced by ridge subductions. The Journal of Geology, 121(2), 197-213.

Ling, M. X., Wang, F. Y., Ding, X., Hu, Y. H., Zhou, J. B., Zartman, R. E., ... & Sun, W. (2009). Cretaceous ridge subduction along the lower Yangtze River belt, eastern China. Economic Geology, 104(2), 303-321.

Liu, C., Zhu, G., Zhang, S., Gu, C., Li, Y., Su, N., & Xiao, S. (2018). Mesozoic strike-slip movement of the Dunhua–Mishan Fault Zone in NE China: A response to oceanic plate subduction. Tectonophysics, 723, 201-222.

Liu, K., Zhang, J., Wilde, S. A., Zhou, J., Wang, M., Ge, M., ... & Ling, Y. (2017). Initial subduction of the Paleo-Pacific Oceanic plate in NE China: Constraints from whole-rock geochemistry and zircon U–Pb and Lu–Hf isotopes of the Khanka Lake granitoids. Lithos, 274, 254-270.

Maeda, J. I., & Kagami, H. (1996). Interaction of a spreading ridge and an accretionary prism: Implications from MORB magmatism in the Hidaka magmatic zone, Hokkaido, Japan. Geology, 24(1), 31-34.

Martynov, Y. A., & Khanchuk, A. I. (2013). Cenozoic volcanism of the eastern Sikhote Alin: petrological studies and outlooks. Petrology, 21(1), 85-99.

Martynov, Y. A., Khanchuk, A. I., Grebennikov, A. V., Chashchin, A. A., & Popov, V. K. (2017). Late Mesozoic and Cenozoic volcanism of the East Sikhote-Alin area (Russian Far East): a new synthesis of geological and petrological data. Gondwana Research, 47, 358-371.

Maruyama, S., Isozaki, Y., Kimura, G., & Terabayashi, M. (1997). Paleogeographic maps of the Japanese Islands: plate tectonic synthesis from 750 Ma to the present. Island arc, 6(1), 121-142.

Meffre, S., Falloon, T. J., Crawford, T. J., Hoernle, K., Hauff, F., Duncan, R. A., ... & Wright, D. J. (2012). Basalts erupted along the Tongan fore arc during subduction initiation: Evidence from geochronology of dredged rocks from the Tonga fore arc and trench. Geochemistry, Geophysics, Geosystems, 13(12).

Müller, R. D., Seton, M., Zahirovic, S., Williams, S. E., Matthews, K. J., Wright, N. M., ... & Bower, D. J. (2016). Ocean basin evolution and global-scale plate reorganization events since Pangea breakup. Annual Review of Earth and Planetary Sciences, 44, 107-138.

O'Connor, J. M., Steinberger, B., Regelous, M., Koppers, A. A., Wijbrans, J. R., Haase, K. M., ... & Garbe‐Schönberg, D. (2013). Constraints on past plate and mantle motion from new ages for the Hawaiian‐Emperor Seamount Chain. Geochemistry, Geophysics, Geosystems, 14(10), 4564-4584.

Otofuji, Y. I., Matsuda, T., Itaya, T., Shibata, T., Matsumoto, M., Yamamoto, T., ... & Sakhno, V. G. (1995). Late Cretaceous to early Paleogene paleomagnetic results from Sikhote Alin, far eastern Russia: implications for deformation of East Asia. Earth and Planetary Science Letters, 130(1-4), 95-108.

Otofuji, Y. I., Takaaki, M., Ryo, E., Koji, U., Nishihama, K., Halim, N., ... & Matunin, A. P. (2003). Late Cretaceous palaeomagnetic results from Sikhote Alin, far eastern Russia: tectonic implications for the eastern margin of the Mongolia Block. Geophysical Journal International, 152(1), 202-214.

Pavlis, T. L., & Sisson, V. B. (1995). Structural history of the Chugach metamorphic complex in the Tana River region, eastern Alaska: A record of Eocene ridge subduction. Geological Society of America Bulletin, 107(11), 1333-1355.

Rodnikov, A. G., Sergeyeva, N. A., Zabarinskaya, L. P., Filatova, N. I., Piip, V. B., & Rashidov, V. A. (2008). The deep structure of active continental margins of the Far East (Russia). Russian Journal of Earth Sciences, 10(4).

Russo, R. M., Gallego, A., Comte, D., Mocanu, V. I., Murdie, R. E., & VanDecar, J. C. (2010). Source-side shear wave splitting and upper mantle flow in the Chile Ridge subduction region. Geology, 38(8), 707-710.

Sagong, H., Kwon, S. T., & Ree, J. H. (2005). Mesozoic episodic magmatism in South

Korea and its tectonic implication. Tectonics, 24(5).

Seton, M., Flament, N., Whittaker, J., Müller, R. D., Gurnis, M., & Bower, D. J. (2015). Ridge subduction sparked reorganization of the Pacific plate‐mantle system 60–50 million years ago. Geophysical Research Letters, 42(6), 1732-1740.

Sharp, W. D., & Clague, D. A. (2006). 50-Ma initiation of Hawaiian-Emperor bend records major change in Pacific plate motion. Science, 313(5791), 1281-1284.

Simanenko, V. P., & Khanchuk, A. I. (2003). Cenomanian volcanism of the Eastern Sikhote-Alin volcanic belt: geochemical features. Geochemistry International, 41(8), 787-798.

Soloviev, S. G., & Krivoshchekov, N. N. (2011). Vostok-2 gold-base-metal-tungsten skarn deposit, Central Sikhote-Alin, Russia. Geology of Ore Deposits, 53(6), 478-500.

Song, Y., Ren, J., Stepashko, A. A., & Li, J. (2014). Post-rift geodynamics of the Songliao Basin, NE China: Origin and significance of T11 (Coniacian) unconformity. Tectonophysics, 634, 1-18.

Song, Y., Stepashko, A., Liu, K., He, Q., Shen, C., Shi, B., & Ren, J. (2018). Post‐rift Tectonic History of the Songliao Basin, NE China: Cooling Events and Post‐rift Unconformities Driven by Orogenic Pulses From Plate Boundaries. Journal of Geophysical Research: Solid Earth, 123(3), 2363-2395.

Sosson, M., Bourgois, J., & de Lépinay, B. M. (1994). SeaBeam and deep-sea submersible Nautile surveys in the Chiclayo canyon off Peru (7 S): subsidence and subduction-erosion of an Andean-type convergent margin since Pliocene times. Marine Geology, 118(3-4), 237-256.

Steinberger, B., Sutherland, R., & O'connell, R. J. (2004). Prediction of Emperor-Hawaii seamount locations from a revised model of global plate motion and mantle flow. Nature, 430(6996), 167.

Sun, M. D., Chen, H. L., Zhang, F. Q., Wilde, S. A., Dong, C. W., & Yang, S. F. (2013). A 100 Ma bimodal composite dyke complex in the Jiamusi Block, NE China: an indication for lithospheric extension driven by Paleo-Pacific roll-back. Lithos, 162, 317-330.

Sun, M., Chen, H., Milan, L. A., Wilde, S. A., Jourdan, F., & Xu, Y. (2018). Continental Arc and Back‐Arc Migration in Eastern NE China: New Constraints on Cretaceous Paleo‐Pacific Subduction and Rollback. Tectonics, 37(10), 3893-3915.

Sun, W., Ding, X., Hu, Y. H., & Li, X. H. (2007). The golden transformation of the Cretaceous plate subduction in the west Pacific. Earth and Planetary Science Letters, 262(3-4), 533-542.

Sun, W., Ling, M., Yang, X., Fan, W., Ding, X., & Liang, H. (2010). Ridge subduction and porphyry copper-gold mineralization: An overview. Science China Earth Sciences, 53(4), 475-484.

Sun, X., Wang, S., Wang, Y., Du, J., & Xu, Q. (2010). The structural feature and evolutionary series in the northern segment of Tancheng-Lujiang fault zone. Acta Petrologica Sinica, 26(1), 165-176. (In Chinese with English Abstract).

Takeuchi, T., Kodama, K., & Ozawa, T. (1999). Paleomagnetic evidence for block rotations in central Hokkaido–south Sakhalin, Northeast Asia. Earth and Planetary Science Letters, 169(1-2), 7-21.

Tang, G. J., Wyman, D. A., Wang, Q., Li, J., Li, Z. X., Zhao, Z. H., & Sun, W. D. (2012). Asthenosphere–lithosphere interaction triggered by a slab window during ridge subduction: trace element and Sr–Nd–Hf–Os isotopic evidence from Late Carboniferous tholeiites in the western Junggar area (NW China). Earth and Planetary Science Letters, 329, 84-96.

Tang, J., Xu, W., Niu, Y., Wang, F., Ge, W., Sorokin, A. A., & Chekryzhov, I. Y. (2016). Geochronology and geochemistry of Late Cretaceous–Paleocene granitoids in the Sikhote-Alin Orogenic Belt: Petrogenesis and implications for the oblique subduction of the paleo-Pacific plate. Lithos, 266, 202-212.

Tapponnier, P., & Molnar, P. (1976). Slip-line field theory and large-scale continental tectonics. Nature, 264(5584), 319.

Tapponnier, P., Lacassin, R., Leloup, P. H., Schärer, U., Dalai, Z., Haiwei, W., ... & Jiayou, Z. (1990). The Ailao Shan/Red River metamorphic belt: tertiary left-lateral shear between Indochina and South China. Nature, 343(6257), 431.

Tarduno, J. A., Duncan, R. A., Scholl, D. W., Cottrell, R. D., Steinberger, B., Thordarson, T., ... & Carvallo, C. (2003). The Emperor Seamounts: Southward motion of the Hawaiian hotspot plume in Earth's mantle. Science, 301(5636), 1064-1069.

Tarduno, J., Bunge, H. P., Sleep, N., & Hansen, U. (2009). The bent Hawaiian-Emperor hotspot track: Inheriting the mantle wind. Science, 324(5923), 50-53.

Thorkelson, D. J. (1996). Subduction of diverging plates and the principles of slab window formation. Tectonophysics, 255(1-2), 47-63.

Thorkelson, D. J., Madsen, J. K., & Sluggett, C. L. (2011). Mantle flow through the Northern Cordilleran slab window revealed by volcanic geochemistry. Geology, 39(3), 267-270.

Tikoff, B., & Teyssier, C. (1992). Crustal-scale, en echelon" P-shear" tensional bridges: A possible solution to the batholithic room problem. Geology, 20(10), 927-930.

Uno, K., Otofuji, Y. I., Matsuda, T., Kuniko, Y., Enami, R., Kulinich, R. G., ... & Sakhno, V. G. (1999). Late Cretaceous paleomagnetic results from Northeast Asian continental margin: the Sikhote Alin mountain range, eastern Russia. Geophysical research letters, 26(5), 553-556.

Utkin, V. P., Nevolin, P. L., & Mitrokhin, A. N. (2007). Late Paleozoic and Mesozoic deformations in the southwestern Primorye region. Russian Journal of Pacific Geology, 1(4), 307-323.

von Huene, R., & Lallemand, S. (1990). Tectonic erosion along the Japan and Peru convergent margins. Geological Society of America Bulletin, 102(6), 704-720.

Wang, F., Zhou, X. H., Zhang, L. C., Ying, J. F., Zhang, Y. T., Wu, F. Y., & Zhu, R. X. (2006). Late Mesozoic volcanism in the Great Xing'an Range (NE China): timing and implications for the dynamic setting of NE Asia. Earth and Planetary Science Letters, 251(1-2), 179-198.

Wang, T., Zheng, Y., Zhang, J., Zeng, L., Donskaya, T., Guo, L., & Li, J. (2011). Pattern and kinematic polarity of late Mesozoic extension in continental NE Asia: Perspectives from metamorphic core complexes. Tectonics, 30(6).

Whalen, J. B., Currie, K. L., & Chappell, B. W. (1987). A-type granites: geochemical

characteristics, discrimination and petrogenesis. Contributions to mineralogy and petrology, 95(4), 407-419.

Whittaker, J. M., Müller, R. D., Leitchenkov, G., Stagg, H., Sdrolias, M., Gaina, C., & Goncharov, A. (2007). Major Australian-Antarctic plate reorganization at Hawaiian-Emperor bend time. Science, 318(5847), 83-86.

Wilde, S. A., Wu, F., & Zhang, X. (2003). Late Pan-African magmatism in northeastern China: SHRIMP U–Pb zircon evidence from granitoids in the Jiamusi Massif. Precambrian Research, 122(1-4), 311-327.

Wu, F. Y., Sun, D. Y., Ge, W. C., Zhang, Y. B., Grant, M. L., Wilde, S. A., & Jahn, B. M. (2011). Geochronology of the Phanerozoic granitoids in northeastern China. Journal of Asian Earth Sciences, 41(1), 1-30.

Wu, J. T. J., Jahn, B. M., Nechaev, V., Chashchin, A., Popov, V., Yokoyama, K., & Tsutsumi, Y. (2017). Geochemical characteristics and petrogenesis of adakites in the Sikhote-Alin area, Russian Far East. Journal of Asian Earth Sciences, 145, 512-529.

Wu, L., Monié, P., Wang, F., Lin, W., Ji, W., & Yang, L. (2018). Multi-phase cooling of Early Cretaceous granites on the Jiaodong Peninsula, East China: Evidence from 40Ar/39Ar and (U-Th)/He thermochronology. Journal of Asian Earth Sciences, 160, 334-347.

Xu, J., & Zhu, G. (1994). Tectonic models of the Tan-Lu fault zone, eastern China. International Geology Review, 36(8), 771-784.

Xu, J., Zhu, G., Tong, W., Cui, K., & Liu, Q. (1987). Formation and evolution of the Tancheng-Lujiang wrench fault system: a major shear system to the northwest of the Pacific Ocean. Tectonophysics, 134(4), 273-310.

Yang, H., Ge, W. C., Zhao, G. C., Bi, J. H., Wang, Z. H., Dong, Y., & Xu, W. L. (2017). Zircon U–Pb ages and geochemistry of newly discovered Neoproterozoic orthogneisses in the Mishan region, NE China: Constraints on the high-grade metamorphism and tectonic affinity of the Jiamusi–Khanka Block. Lithos, 268, 16-31.

Zhang, F. Q., Chen, H. L., Yang, S. F., Feng, Z. Q., Wu, H. Y., Batt, G. E., ... & Yang,

J. G. (2012). Late Mesozoic–Cenozoic evolution of the Sanjiang Basin in NE China and its tectonic implications for the West Pacific continental margin. Journal of Asian Earth Sciences, 49, 287-299.

Zhang, F. Q., Dilek, Y., Chen, H. L., Yang, S. F., & Meng, Q. A. (2017). Structural architecture and stratigraphic record of Late Mesozoic sedimentary basins in NE China: Tectonic archives of the Late Cretaceous continental margin evolution in East Asia. Earth-Science Reviews, 171, 598-620.

Zhang, J. H., Gao, S., Ge, W. C., Wu, F. Y., Yang, J. H., Wilde, S. A., & Li, M. (2010). Geochronology of the Mesozoic volcanic rocks in the Great Xing'an Range, northeastern China: implications for subduction-induced delamination. Chemical Geology, 276(3-4), 144-165.

Zhang, S., Zhu, G., Liu, C., Li, Y., Su, N., Xiao, S., & Gu, C. (2018). Strike‐Slip Motion Within the Yalu River Fault Zone, NE Asia: The Development of a Shear Continental Margin. Tectonics, 37(6), 1771-1796.

Zhao, P., Alexandrov, I., Jahn, B. M., Liao, J. P., & Ivin, V. (2019). Late Eocene granites in the Central Sakhalin Island (Russian Far East) and its implication for evolution of the Sakhalin-Hokkaido orogenic belt. Lithos, 324, 684-698.

Zhao, P., Jahn, B. M., & Xu, B. (2017). Elemental and Sr-Nd isotopic geochemistry of Cretaceous to Early Paleogene granites and volcanic rocks in the Sikhote-Alin Orogenic Belt (Russian Far East): implications for the regional tectonic evolution. Journal of Asian Earth Sciences, 146, 383-401.

Zhou, J. B., & Wilde, S. A. (2013). The crustal accretion history and tectonic evolution of the NE China segment of the Central Asian Orogenic Belt. Gondwana Research, 23(4), 1365-1377.

Zhou, J. B., Wilde, S. A., Zhang, X. Z., Zhao, G. C., Liu, F. L., Qiao, D. W., ... & Liu, J. H. (2011). A > 1300 km late Pan-African metamorphic belt in NE China: New evidence from the Xing'an block and its tectonic implications. Tectonophysics, 509(3-4), 280-292.

Zhou, J. B., Wilde, S. A., Zhang, X. Z., Zhao, G. C., Zheng, C. Q., Wang, Y. J., & Zhang, X. H. (2009). The onset of Pacific margin accretion in NE China: evidence

from the Heilongjiang high-pressure metamorphic belt. Tectonophysics, 478(3-4), 230-246.

Zhu, G., Jiang, D., Zhang, B., & Chen, Y. (2012). Destruction of the eastern North China Craton in a backarc setting: Evidence from crustal deformation kinematics. Gondwana Research, 22(1), 86-103.

Zhu, G., Liu, G. S., Niu, M. L., Xie, C. L., Wang, Y. S., & Xiang, B. (2009). Syn-collisional transform faulting of the Tan-Lu fault zone, East China. International Journal of Earth Sciences, 98(1), 135-155.

Zhu, G., Wang, Y., Liu, G., Niu, M., Xie, C., & Li, C. (2005). $^{40}Ar/^{39}Ar$ dating of strike-slip motion on the Tan–Lu fault zone, East China. Journal of Structural Geology, 27(8), 1379-1398.

Chapter 6 Major conclusions and future work

The oceanic plates in the Pacific domain have dominated the tectonic evolution of the northeast Asian margin since the Mesozoic, including the continental blocks, arcs and arc-related basins in NE China and Sikhote-Alin, Russian Far East. Field investigation, petrological observations, whole-rock geochemistry, zircon U-Pb dating and Lu-Hf isotopic analyses were conducted on rocks from this area to unravel the magmatic genesis, sedimentary provenance and regional subduction history.

The earliest arc magmatism in the area is represented by the Khanka Lake granitoids in the northern Khanka Block. Zircon LA-ICP-MS dating yields two major magmatic episodes corresponding to the two major lithologies, the earliest Triassic (ca. 249 Ma) granodiorite and Late Triassic to Early Jurassic (209-199 Ma) syenogranite. Later felsic veins intruded into throughout the batholith during 195-184 Ma. The granodiorite (ca. 249 Ma) has abundant mafic enclaves in the outcrop and shows adakite-like geochemical features, such as high Sr, Sr/Y and La/Yb, with zircon εHf(t) values of −0.65 to 1.61, indicating that magma mixing between old lower crust and juvenile basaltic magma was important. The syenogranite (209-199 Ma) belongs to the highly fractionated I-type granites, showing high SiO_2, Na_2O, K_2O and very low Mg, Fe, Ni and Cr. The zircon εHf(t) values are positive, ranging from 1.72 to 5.12, suggesting the importance of juvenile materials in its source. The zircon εHf(t) values from granodiorite, syenogranite and felsic veins become more positive as the zircon ages become younger, recording the consistent increase of juvenile crust melting. The Khanka Lake granitoids are proposed to be evidence of the early-stage subduction of the Paleo-Pacific plate in NE China and the eastern CAOB.

Subduction-related magmatism was also active along the eastern margin of the Songliao Block, namely in the Lesser Xing'an-Zhangguangcai Range. The ancient Mudanjiang Ocean was located between the Songliao and Jiamusi-Khanka blocks

before the Cretaceous, and was part of the Paleo-Pacific Ocean in NE China. The volcanic rocks here were sampled and analyzed to understand their genesis and relationship with subduction. Zircon SHRIMP U-Pb dating and whole-rock geochemical analysis were carried out on these volcanic rocks. The results show that most samples are Early Jurassic in age (189-178 Ma), including andesite, trachyandesite, trachydacite and rhyolite. The rhyolite is highly fractionated I-type, similar to the coeval granites in the Lesser Xing'an-Zhangguangcai Range, whereas the andesite to trachytic rocks were mainly affected by magma mixing processes at an active continental margin. The samples from the Jiamusi Block and one sample from the Lesser Xing'an Range yield late Early Cretaceous (ca. 100 Ma) ages. Fractional crystallization was the most important genesis mechanism for these basalts and trachydacites. However, evidence of magma mixing or crustal contamination was also recorded in several andesitic samples. The Jurassic arc magma was generated by the westward subduction of the Mudanjiang Ocean. After closure of the Mudanjiang Ocean, the Paleo-Pacific Ocean began to govern the tectonic evolution of the eastern CAOB. Roll-back of the slab triggered back-arc extension in NE China and resulted in extensive volcanism in the Jiamusi Block during the late Early Cretaceous.

During the Jurassic to Cretaceous, numerous accretionary components were accreted along the eastern margin of the Jiamusi-Khanka Block to form the Sikhote-Alin accretionary orogenic belt. These accretionary belts are mainly N-S trending and separated by thrusts and strike-slip faults. Sandstone samples were collected along an E-W traverse in the southern Sikhote-Alin orogenic belt for zircon U-Pb dating and Lu-Hf isotopic analysis. The results indicate that the Jiamusi-Khanka Block was the most important source area for the sediments in the Samarka accretionary complex, whereas the Zhuravlevka turbidite basin, separated by the Central Sikhote-Alin Fault from the Samark belt, was supplied by both the Jiamusi-Khanka Block and North China Craton. The eastmost belt, the Taukha accretionary complex, however, shows no signal of the Jiamusi-Khanka Block, but was only fed from the North China Craton. The E-W trending accretionary process cannot explain all the data. Thus, it is proposed

that the eastern Sikhote-Alin belts were initially deposited farther south during the Early Cretaceous. Afterwards sinistral strike-slip faulting transported the eastern Sikhote-Alin belts northward after their deposition and formed a tectonic collage.

The magmatic rocks migrated eastwards into the coastal Sikhote-Alin area after major sinistral strike-slip motion during the late Early Cretaceous, related to subduction of the Izanagi Plate. The whole-rock Nd and zircon Hf isotopes of the granitoids show significant enriched features in the Late Cretaceous. However, after a magmatic gap between 55 and 45 Ma, mantle input increased abruptly indicated by the dramatically depleted isotopic characteristics. Meanwhile, I&S-type granitoids and volcanic rocks were replaced by A-type granite and intra-plate basalts and adakitic volcanic rocks. This change in magmatism is considered tobe the result of a slab window opening during the early Cenozoic under the continental margin, caused by Izanagi-Pacific ridge subduction. At ca. 55 Ma, MORB-like gabbros intruded into the coeval accretionary complexes in Hokkaido, Japan, whereas A- and S-type granites were emplaced into the coeval fore-arc basins in Sakhalin in Far East Russia, further supporting a ridge subduction model. Ridge subduction and the migration of a triple junction caused a change in the regional stress field. The Pacific plate moved in the NWW or W after consumption of the Izanagi plate, which was subducted to the NNW. This important change triggered a change in the sinistral strike-slip faults in Sikhote-Alin, NE China and Korea to dextral or extensional settings. Emplacement of Cretaceous en echelon plutons related to the strike-slip faulting ceased and the arc region was dominated by nearly E-W trending caldera alignments, corresponding to the change in plate motion. Ridge subduction between 60 and 45 Ma is supported by evidence from the ocean side. Specifically, new research based on magnetic anomalies, seamount chains and plate reconstructions proposes that the Izanagi-Pacific ridge arrived at the eastern Asian margin at ca. 60 Ma, resulting in the plate reorganization in the west Pacific domain.

Although the Mesozoic to early Cenozoic subduction history is explained by thse data,

the model still needs to be improved in details and tested by further studies. The future work in this area should include:

1. The details about the ridge subduction should be improved by collecting more data on the Cenozoic volcanism. The main data in Chapter 5 were derived from previous studies which focus on Late Cretaceous and Paleocene granitoids. The Eocene and later volcanism is still not precisely dated and new geochemical analyses are required. Structural data to determine the regional stress field change is also not sufficient at present, but is vital for working out the detailed geodynamic history of the area.

2. The strike-slip faults in NE China were also active during the Cretaceous, similar to the Central Sikhote-Alin Fault on Russian side. But a detailed structural investigation should be carried out to understand the relationship between these faults and the tectonic dynamics of the major sinistral strike-slip system.

3. The local Cretaceous basins in NE China are located between two NE trending faults and locally controlled by early-stage normal faults and late-stage thrusts. However, the relationship between basins and faults is not fully understood and the timing of faults and their dynamics is not well studied. Field investigations, kinematics and geochronology need to be carried out in NE China to solve this issue.

Chapter 7 References

Alexeiev, D. V., Gaedicke, C., Tsukanov, N. V., & Freitag, R. (2006). Collision of the Kronotskiy arc at the NE Eurasia margin and structural evolution of the Kamchatka–Aleutian junction. International Journal of Earth sciences, 95(6), 977-993.

Allegre, C., Minster, J., 1978. Quantitative models of trace element behavior in magmatic processes. Earth and Planetary Science Letters 38, 1-25.

Aoki, K., Isozaki, Y., Kofukuda, D., Sato, T., Yamamoto, A., Maki, K., … Hirata, T. (2014). Provenance diversification within an arc-trench system induced by batholith development: The Cretaceous Japan case. Terra Nova, 26(2), 139–149. https://doi.org/10.1111/ter.12080

Arculus, R. J., Ishizuka, O., Bogus, K. A., Gurnis, M., Hickey-Vargas, R., Aljahdali, M. H., ... & do Monte Guerra, R. (2015). A record of spontaneous subduction initiation in the Izu–Bonin–Mariana arc. Nature Geoscience, 8(9), 728.

Argentov, V., Gnibidenko, G., Popov, A., & Potap'ev, S. (1976). Deep Structure of Primorye. Moscow (in Russian): Nauka.

Atherton, M.P., Petford, N., 1993. Generation of sodium-rich magmas from newly underplated basaltic crust. Nature 362, 144–146.

Bai, B., Wang, Y. Q., Mao, F. Y., & Meng, J. (2017). New material of Eocene Helaletidae (Perissodactyla, Tapiroidea) from the Irdin Manha Formation of the Erlian Basin, Inner Mongolia, China and comments on related localities of the Huheboerhe area. American Museum Novitates, 2017(3878), 1-45.

Barnes, C.G., Petersen, S.W., Kistler, R.W., Murray, R., Kays, M.A., 1996. Source and tectonic implications of tonalite-trondhjemite magmatism in the Klamath Mountains. Contributions to Mineralogy and Petrology 123, 40–60.

Batten, D. (1984). Palynology, climate and the development of Late Cretaceous floral provinces in the Northern Hemisphere; a review. In Fossils and Climate, (pp. 127–164). Chichester, UK: John Wiley.

Berger, W., & Winterer, E. (1974). Plate stratigraphy and the fluctuating carbonate line. In Pelagic sediments: On land and under the sea (pp. 11–48). International Association of Sedimentologists. Special Publication Number 1, Oxford, UK: Blackwell Scientific Publications.

Bi, J. H., Ge, W. C., Yang, H., Zhao, G. C., Xu, W. L., & Wang, Z. H. (2015). Geochronology, geochemistry and zircon Hf isotopes of the Dongfanghong gabbroic complex at the eastern margin of the Jiamusi Massif, NE China: Petrogensis and tectonic implications. Lithos, 234, 27–46.

Bi, J., Ge, W., Yang, H., Zhao, G., Yu, J., Zhang, Y., Wang, Z., Tian, D., (2014). Petrogenesis and tectonic implications of early Paleozoic granitic magmatism in the Jiamusi Massif, NE China: geochronological, geochemical and Hf isotopic evidence. Journal of Asian Earth Sciences 96, 308–331.

Bi, J.H., Ge, W.C., Yang, H., Wang, Z.H., Xu, W.L., Yang, J.H., Xing, D.H., Chen, H.J., (2016). Geochronology and geochemistry of late Carboniferous–middle Permian I-and A-type granites and gabbro–diorites in the eastern Jiamusi Massif, NE China: Implications for petrogenesis and tectonic setting. Lithos 266, 213-232.

Bingen, B., Birkeland, A., Nordgulen, & Sigmond, E. M. (2001). Correlation of supracrustal sequences and origin of terranes in the Sveconorwegian orogen of SW Scandinavia: SIMS data on zircon in clastic metasediments. Precambrian Research, 108(3-4), 293–318. https://doi.org/10.1016/S0301-9268(01)00133-4

Blichert-Toft, J., & Albarède, F. (1997). The Lu-Hf isotope geochemistry of chondrites and the evolution of the mantle-crust system. Earth and Planetary Science Letters, 148(1-2), 243–258. https://doi.org/10.1016/S0012-821X(97)00040-X

Bourgois, J., Martin, H., Lagabrielle, Y., Le Moigne, J., & Frutos Jara, J. (1996). Subduction erosion related to spreading-ridge subduction: Taitao peninsula (Chile margin triple junction area). Geology, 24(8), 723-726.

Cao, H., Wenliang, X., Fuping, P., & Xingzhou, Z. (2011). Permian tectonic evolution in southwestern Khanka Massif: Evidence from Zircon U-Pb chronology, Hf isotope and Geochemistry of gabbro and diorite. Acta Geologica Sinica (English Edition), 85(6), 1390–1402.

Castillo, P.R., Janney, P.E., Solidum, R.U., 1999. Petrology and geochemistry of Camiguin island, southern Philippines: insights to the source of adakites and other lavas in a complex arc setting. Contributions to Mineralogy and Petrology 134, 33–51.

Cawood, P. A., Hawkesworth, C., & Dhuime, B. (2012). Detrital zircon record and tectonic setting. Geology, 40(10), 875–878. https://doi.org/ 10.1130/G32945.1

Chadwick, J., Perfit, M., McInnes, B., Kamenov, G., Plank, T., Jonasson, I., & Chadwick, C. (2009). Arc lavas on both sides of a trench: Slab window effects at the Solomon Islands triple junction, SW Pacific. Earth and Planetary Science Letters, 279(3-4), 293-302.

Chappell, B., White, A., 1992. I-and S-type granites in the Lachlan Fold Belt. Geological Society of America Special Papers 272, 1-26.

Chappell, B.W., 1999. Aluminium saturation in I- and S-type granites and the characterization of fractionated haplogranites. Lithos 46, 535–551.

Charvet, J. (2013). The neoproterozoic–early paleozoic tectonic evolution of the South China Block: An overview. Journal of Asian Earth Sciences, 74, 198–209.

Charvet, J., Shu, L., Faure, M., Choulet, F., Wang, B., Lu, H., & Le Breton, N. (2010). Structural development of the Lower Paleozoic belt of South China: Genesis of an intracontinental orogen. Journal of Asian Earth Sciences, 39(4), 309–330. https://doi.org/10.1016/ j.jseaes.2010.03.006

Chashchin, A. A., Nechaev, V. P., Nechaeva, E. V., & Blokhin, M. G. (2011). Discovery of Eocene adakites in Primor'e. Doklady Earth Sciences, 438(2), 744-749.

Chen, D. (2016). Mesozoic-Cenozoic Tectonic Evolution and Low Temperature Thermochronological Study of Eastern Heilongjiang, NE China (in Chinese with English Abstract). Geology, Zhejiang: Zhejiang University Hangzhou.

Chen, J.Y., Tang, J.H., (2015). Petrogenesis of the Fogang highly fractionated I-type granitoids: constraints from Nb, Ta, Zr and Hf. Acta Petrologica Sinica 31, 846–854 (in Chinese with English abstract).

Chen, Y., Zhang, Z., Li, K., Yu, H., & Wu, T. (2016). Detrital zircon U–Pb ages and Hf isotopes of Permo-Carboniferous sandstones in central Inner Mongolia, China:

Implications for provenance and tectonic evolution of the southeastern Central Asian Orogenic Belt. Tectonophysics, 671, 183–201. https://doi.org/10.1016/j.tecto.2016.01.018

Chen, Z. H., Xing, G. F., & Zhao, X. L. (2015). Palaeoproterozoic A-type magmatism in northern Wuyishan terrane, Southeast China: Petrogenesis and tectonic implications. International Geology Review, 1–14.

Cheng, R. Y., Wu, F. Y., Ge, W. C., Sun, D. Y., Liu, X. M., & Yang, J. H. (2006). Emplacement age of the Raohe Complex in eastern Heilongjiang Province and the tectonic evolution of the eastern part of Northeastern China. Acta Petrologica Sinica, 22(2), 353-376.

Cheng, Y., Wu, Z., Lu, S., Li, X., Lin, C., Huang, Z., ... & Wang, S. (2018). Mesozoic to Cenozoic tectonic transition process in Zhanhua Sag, Bohai Bay Basin, East China. Tectonophysics, 730, 11-28.

Cheon, Y., Cho, H., Ha, S., Kang, H. C., Kim, J. S., & Son, M. (2019). Tectonically controlled multiple stages of deformation along the Yangsan Fault Zone, SE Korea, since Late Cretaceous. Journal of Asian Earth Sciences, 170, 188-207.

Cheong, C. S., Kim, N., Jo, H. J., Cho, M., Choi, S. H., Zhou, H., & Geng, J. Z. (2015). Lithospheric mantle signatures as revealed by zircon Hf isotopes of Late Triassic post-collisional plutons from the central Korean peninsula, and their tectonic implications. Terra Nova, 27(2), 97–105. https://doi.org/10.1111/ter.12135

Cheong, C. S., Kim, N., Kim, J., Yi, K., Jeong, Y. J., Park, C. S., … Cho, M. (2014). Petrogenesis of Late Permian sodic metagranitoids in southeastern Korea: SHRIMP zircon geochronology and elemental and Nd–Hf isotope geochemistry. Journal of Asian Earth Sciences, 95, 228–242. https://doi.org/10.1016/j.jseaes.2014.06.005

Cheong, C. s., Yi, K., Kim, N., Lee, T. H., Lee, S. R., Geng, J. Z., & Li, H. K. (2013). Tracking source materials of Phanerozoic granitoids in South Korea by zircon Hf isotopes. Terra Nova, 25(3), 228–235. https://doi.org/10.1111/ter.12027

Cho, H. S., Son, M., & Kim, I. S. (2007). Anisotropy of magnetic susceptibility (AMS) of granitic rocks in the eastern region of the Yangsan Fault. Economic and

Environmental Geology, 40(2), 171-189.

Cho, H., Son, M., Cheon, Y., Sohn, Y. K., Kim, J. S., & Kang, H. C. (2016). Evolution of the Late Cretaceous Dadaepo Basin, SE Korea, in response to oblique subduction of the proto-Pacific (Izanagi/Kula) or Pacific plate. Gondwana Research, 39, 145-164.

Chung, S., Zhang, Q., Liu, D., Ji, J., Chu, M., Lee, H.Y., Lo, C., Lee, T., Qian, Q., 2003. Adakites from continental collision zones: melting of thickened lower crust beneath southern Tibet. Geology 31, 1021–1024.

Cogné, J.P., Kravchinsky, V.A., Halim, N., Hankard, F., 2005. Late Jurassic-Early Cretaceous closure of the Mongol-Okhotsk Ocean demonstrated by new Mesozoic palaeomagnetic results from the Trans-Baikal area (SE Siberia). Geophysical Journal International 163, 813-832.

Condie, K.C., 2005. TTGs and adakites: are they both slab melts? Lithos 80, 33–44.

Darby, B. J., & Gehrels, G. (2006). Detrital zircon reference for the North China block. Journal of Asian Earth Sciences, 26(6), 637–648. https://doi.org/10.1016/j.jseaes.2004.12.005

Defant, M.J., Drummond, M.S., 1990. Derivation of some modern arc magmas by melting of young subducted lithosphere. Nature 347, 662-665.

Deng, Z., Liu, S., Zhang, L., Wang, Z., Wang, W., Yang, P., Luo, P., Guo, B., 2014. Geochemistry, zircon U–Pb and Lu–Hf isotopes of an Early Cretaceous intrusive suite in northeastern Jiangxi Province, South China Block: implications for petrogenesis, crust/mantle interactions and geodynamic processes. Lithos 200–201, 334–354.

Dickinson, W. R. (1985). Interpreting provenance relations from detrital modes of sandstones. In G. G. Zuffa (Eds.), Provenance of Arenites (pp. 333–361). Dordrecht, Netherlands: Reidel. https://doi.org/10.1007/978-94-017-2809-6_15

Dickinson, W. R., & Gehrels, G. E. (2009). Use of U–Pb ages of detrital zircons to infer maximum depositional ages of strata: A test against a Colorado Plateau Mesozoic database. Earth and Planetary Science Letters, 288(1-2), 115–125. https://doi.org/10.1016/j.epsl.2009.09.013

Dickinson, W. R., Beard, L. S., Brakenridge, G. R., Erjavec, J. L., Ferguson, R. C., Inman, K. F., … Ryberg, P. T. (1983). Provenance of North American Phanerozoic sandstones in relation to tectonic setting. Geological Society of America Bulletin, 94(2), 222–235.

Didenko, A., Khanchuk, A., Tikhomirova, A., & Voinova, I. (2014). Eastern segment of the Kiselevka-Manoma terrane (Northern Sikhote Alin): Paleomagnetism and geodynamic implications. Russian Journal of Pacific Geology, 8(1), 18–37. https://doi.org/10.1134/ S1819714014010023

Domeier, M., Shephard, G. E., Jakob, J., Gaina, C., Doubrovine, P. V., & Torsvik, T. H. (2017). Intraoceanic subduction spanned the Pacific in the Late Cretaceous–Paleocene. Science advances, 3(11), eaao2303.

Dong, Y., Ge, W.C., Yang, H., Xu, W.L., Bi, J.H., Wang, Z.H., 2016. Geochemistry and geochronology of the Late Permian mafic intrusions along the boundary area of Jiamusi and Songnen-Zhangguangcai Range massifs and adjacent regions, northeastern China: Petrogenesis and implications for the tectonic evolution of the Mudanjiang Ocean. Tectonophysics.

Donskaya, T., Gladkochub, D., Mazukabzov, A., & Ivanov, A. (2013). Late Paleozoic–Mesozoic subduction-related magmatism at the southern margin of the Siberian continent and the 150 million-year history of the Mongol-Okhotsk Ocean. Journal of Asian Earth Sciences, 62, 79–97. https://doi.org/10.1016/j.jseaes.2012.07.023

Donskaya, T., Gladkochub, D., Mazukabzov, A., De Waele, B., Presnyakov, S., 2012. The Late Triassic Kataev volcanoplutonic association in western Transbaikalia, a fragment of the active continental margin of the Mongol-Okhotsk Ocean. Russian Geology and Geophysics 53, 22-36.

Eby, G. N. (1992). Chemical subdivision of the A-type granitoids: petrogenetic and tectonic implications. Geology, 20(7), 641-644.

Faure, M., & Natal'in, B. (1992). The geodynamic evolution of the eastern Eurasian margin in Mesozoic times. Tectonophysics, 208(4), 397-411.

Faure, M., Caridroit, M., & Charvet, J. (1986). The late Jurassic oblique collisional orogen of SW Japan—New structural data and synthesis. Tectonics, 5(7), 1089–

1114. https://doi.org/10.1029/TC005i007p01089

Faure, M., Natal'In, B. A., Monie, P., Vrublevsky, A. A., Borukaiev, C., & Prikhodko, V. (1995). Tectonic evolution of the Anuy metamorphic rocks (Sikhote Alin, Russia) and their place in the Mesozoic geodynamic framework of East Asia. Tectonophysics, 241(3–4), 279–301. https://doi. org/10.1016/0040-1951(94)00186-D

Fernández, R. D., Catalán, J. R. M., Gerdes, A., Abati, J., Arenas, R., & Fernández-Suárez, J. (2010). U–Pb ages of detrital zircons from the Basal allochthonous units of NW Iberia: Provenance and paleoposition on the northern margin of Gondwana during the Neoproterozoic and Paleozoic. Gondwana Research, 18(2–3), 385–399. https://doi.org/10.1016/j.gr.2009.12.006

Fernandez-Suarez, J., Alonso, G. G., Cox, R., & Jenner, G. A. (2002). Assembly of the Armorica microplate: A strike-slip terrane delivery? Evidence from U-Pb ages of detrital zircons. The Journal of Geology, 110(5), 619–626. https://doi.org/10.1086/341760

Filippov, A. N., & Kemkin, I. V. (2009). Siliceous-volcanogenic complexes of western Sikhote Alin: Their stratigraphy and origin. Russian Journal of Pacific Geology, 3(2), 154-168.

Filippov, A. N., Govorov, G. I., Chashchin, A. A., & Punina, T. A. (2010). Composition and formation settings of the siliceous-volcanogenic complexes of the Nizhneussuriisk segment, Kiselevka-Manoma terrane, West Sikhote Alin. Russian Journal of Pacific Geology, 4(4), 289-303.

Fujisaki, W., Isozaki, Y., Maki, K., Sakata, S., Hirata, T., & Maruyama, S. (2014). Age spectra of detrital zircon of the Jurassic clastic rocks of the Mino-Tanba AC belt in SW Japan: Constraints to the provenance of the mid-Mesozoic trench in East Asia. Journal of Asian Earth Sciences, 88, 62–73. https://doi.org/10.1016/j.jseaes.2014.02.006

Gao, F., Xu, W., Yang, D., Pei, F., Liu, X., Hu, Z., 2007. LA-ICP-MS zircon U-Pb dating from granitoids in southern basement of Songliao basin: Constraints on ages of the basin basement. Science in China Series D: Earth Sciences 50, 995-

1004 (In Chinese with English abstract).

Ge, M. H., Zhang, J. J., Liu, K., Ling, Y. Y., Wang, M., & Wang, J. M. (2016). Geochemistry and geochronology of the blueschist in the Heilongjiang Complex and its implications in the late Paleozoic tectonics of eastern NE China. Lithos, 261, 232-249.

Ge, W.C., Wu, F.Y., Zhou, C.Y., Zhang, J., 2007. Porphyry Cu-Mo deposits in the eastern Xing'an-Mongolian Orogenic Belt: mineralization ages and their geodynamic implications. Chinese Science Bulletin 52, 3416–3427 (in Chinese with English abstract).

Gehrels, G. (2014). Detrital zircon U-Pb geochronology applied to tectonics. Annual Review of Earth and Planetary Sciences, 42(1), 127–149. https://doi.org/10.1146/annurev-earth-050212-124012

Geology of Heilongjiang Province. Geological Publishing House, Beijing, pp. 148–191 (in Chinese with English abstract).

Gilder, S. A., Leloup, P. H., Courtillot, V., Chen, Y., Coe, R. S., Zhao, X., … Zhu, R. (1999). Tectonic evolution of the Tancheng-Lujiang (Tan-Lu) fault via middle Triassic to Early Cenozoic paleomagnetic data. Journal of Geophysical Research, 104(B7), 15,365–15,390. https://doi.org/ 10.1029/1999JB900123

Gill, J.B., 1981. Orogenic andesites and plate tectonics. Springer, Berlin, pp. 1-390.

Golozoubov, V. V. (2006). Tectonics of the Jurassic and Lower Cretaceous Complexes of the North-Western Farming of the Pacific Ocean (p. 231). Vladivostok: Dal'nauka. (in Russian)

Golozoubov, V. V., Khanchuk, A. I., Kemkin, I. V., Panchenko, I. V., & Simanenko, V. P. (1992). Taukha and Zhuravlevka Terranes (South SikhoteAlin), (p. 83). Vladivostok: Preprint. (in Russian)

Golozoubov, V. V., Markevich, V. S., & Bugdaeva, E. (1999). Early Cretaceous changes of vegetation and environment in East Asia. Palaeogeography, Palaeoclimatology, Palaeoecology, 153(1–4), 139–146. https://doi.org/10.1016/S0031-0182(99)00074-7

Golozubov, V. V., Kasatkin, S. A., Grannik, V. M., & Nechayuk, A. E. (2012).

Deformation of the Upper Cretaceous and Cenozoic complexes of the West Sakhalin terrane. Geotectonics, 46(5), 333-351.

Golozubov, V. V., Kasatkin, S. A., Malinovskii, A. I., Nechayuk, A. E., & Grannik, V. M. (2016). Dislocations of the Cretaceous and Cenozoic complexes of the northern part of the West Sakhalin Terrane. Geotectonics, 50(4), 439-452.

Graham, I., Cole, J., 1991. Petrogenesis of andesites and dacites of White Island volcano, Bay of Plenty, New Zealand, in the light of new geochemical and isotopic data. New Zealand journal of geology and geophysics 34, 303-315.

Grasse, S. W., Gehrels, G. E., Lahren, M. M., Schweickert, R. A., & Barth, A. P. (2001). U-Pb geochronology of detrital zircons from the Snow Lake pendant, central Sierra Nevada—Implications for Late Jurassic–Early Cretaceous dextral strike-slip faulting. Geology, 29(4), 307–310.

Grebennikov, A. V., & Popov, V. K. (2014). Petrogeochemical aspects of the Late Cretaceous and Paleogene ignimbrite volcanism of East Sikhote-Alin. Russian Journal of Pacific Geology, 8(1), 38-55.

Grebennikov, A. V., Khanchuk, A. I., Gonevchuk, V. G., & Kovalenko, S. V. (2016). Cretaceous and Paleogene granitoid suites of the Sikhote-Alin area (Far East Russia): Geochemistry and tectonic implications. Lithos, 261, 250–261. https://doi.org/10.1016/j.lithos.2015.12.020

Green, T., (1980). Island arc and continent-building magmatism—A review of petrogenic models based on experimental petrology and geochemistry. Tectonophysics 63, 367-385.

Griffin, W. L., Zhang, A., O'Reilly, S. Y., Ryan, C. G., Flower, M., Chung, S. L., … Lee, T. Y. (1998). Phanerozoic evolution of the lithosphere beneath the Sino-Korean Craton. In Mantle dynamics and plate interactions in East Asia, Geographical Series (Vol. 27, pp. 107–126). Washington, DC: American Geophysical Union.

Griffin, W., Belousova, E., Shee, S., Pearson, N., & O'reilly, S. (2004). Archean crustal evolution in the northern Yilgarn Craton: U–Pb and Hf- isotope evidence from detrital zircons. Precambrian Research, 131(3–4), 231–282.

https://doi.org/10.1016/j.precamres.2003.12.011

Griffin, W.L., Pearson, N.J., Belousova, E., Jackson, S.E., Achterbergh, E., O'Reilly, S.Y., Shee, S.R., (2000). The Hf isotope composition of cratonic mantle: LAM–MC–PIMCS analysis of zircon megacrysts in kimberlites. Geochimica et Cosmochimica Acta 64, 133–147.

Grove, T., Parman, S., Bowring, S., Price, R., Baker, M., (2002). The role of an H2O-rich fluid component in the generation of primitive basaltic andesites and andesites from the Mt. Shasta region, N California. Contributions to Mineralogy and Petrology 142, 375-396.

Grove, T.L., Elkins-Tanton, L.T., Parman, S.W., Cartterjee, N., Muntener, O., Gaetani, G.A., (2003). Fractional crystallization and mantle melting controls on calk-alkaline differentiation trends. Contributions to Mineralogy and Petrology 145, 515–533.

Gu, C., Zhu, G., Zhai, M., Lin, S., Song, L., & Liu, B. (2016). Features and origin time of Mesozoic strike-slip structures in the Yilan-Yitong Fault Zone. Science China Earth Sciences, 59(12), 2389-2410.

Gu, C., Zhu, G., Zhang, S., Liu, C., Li, Y., Lin, S., & Wang, W. (2017). Cenozoic evolution of the Yilan–Yitong Graben in NE China: An example of graben formation controlled by pre-existing structures. Journal of Asian Earth Sciences, 146, 168-184.

Guo, F., Fan, W., Gao, X., Li, C., Miao, L., Zhao, L., Li, H., (2010). Sr–Nd–Pb isotope mapping of mesozoic igneous rocks in NE China: constraints on tectonic framework and Phanerozoic crustal growth. Lithos 120, 563–578.

Guo, F., Li, H., Fan, W., Li, J., Zhao, L., Huang, M., Xu, W., (2015). Early Jurassic subduction of the Paleo-Pacific Ocean in NE China: petrologic and geochemical evidence from the Tumen mafic intrusive complex. Lithos 224–225, 46–60.

Guo, F., Nakamura, E., Fan, W., Kobayashi, K., Li, C., (2007). Generation of Palaeocene adakitic andesites by magma mixing, Yanji area, NE China. Journal of Petrology 48, 661–692.

Guo, F., Nakamura, E., Fan, W., Kobayashi, K., Li, C., Gao, X., (2009). Mineralogical

and geochemical constraints on magmatic evolution of Paleocene adakitic andesites from the Yanji area, NE China. Lithos 112, 321–341.

Gutiérrez-Alonso, G., Fernández-Suárez, J., Jeffries, T., Jenner, G., Tubrett, M., Cox, R., & Jackson, S. (2003). Terrane accretion and dispersal in the northern Gondwana margin. An Early Paleozoic analogue of a long-lived active margin. Tectonophysics, 365(1–4), 221–232. https://doi. org/10.1016/S0040-1951(03)00023-4

H.H., Zhou, L., Yang, L., (2012). Improved in situ Hf isotope ratio analysis of zircon using newly designed X skimmer cone and jet sample cone in combination with the addition of nitrogen by laser ablation multiple collector ICP–MS. Journal of Analytical Atomic Spectrometry 27, 1391–1399.

HBGMR (Heilongjiang Bureau of Geology and Mineral Resources), 1993. Regional

Hildreth, W., Moorbath, S., (1988). Crustal contributions to arc magmatism in the Andes of central Chile. Contributions to mineralogy and petrology 98, 455-489.

Hirose, K., (1997). Melting experiments on lherzolite KLB-1 under hydrous conditions and generation of high-magnesian andesitic melts. Geology 25, 42-44.

Horie, K., Yamashita, M., Hayasaka, Y., Katoh, Y., Tsutsumi, Y., Katsube, A., … Cho, M. (2010). Eoarchean–Paleoproterozoic zircon inheritance in Japanese Permo-Triassic granites (Unazuki area, Hida Metamorphic Complex): Unearthing more old crust and identifying source terrranes. Precambrian Research, 183(1), 145–157. https://doi.org/10.1016/j.precamres.2010.06.014

Hou, Z.Q., Gao, Y.F., Qu, X.M., Rui, Z.Y., Mo, X.X., 2004. Origin of adakitic intrusives generated during mid-Miocene east–west extension in southern Tibet. Earth and Planetary Science Letters 220, 139–155.

Howell, D. G., Jones, D. L., & Schermer, E. R. (1985). Tectonostratigraphic Terranes of the Circum-Pacific Region. In D. G. Howell (Ed.), Tectonostratigraphic terranes of the Circum-Pacific region. Circum-Pacific Council for Energy and Mineral Resources, Earth Science Series 1 (pp. 3–30). Houston, TX: AAPG.

Hsiao, L.Y., Graham, S.A., Tilander, N., (2004). Seismic reflection imaging of a major strike-slip fault zone in a rift system: Paleogene structure and evolution of the

Tan-Lu fault system, Liaodong Bay, Bohai, offshore China. AAPG Bull. 88, 71–97.

Hsiao, L.Y., Graham, S.A., Tilander, N., (2010). Stratigraphy and sedimentation in a rift basin modified by synchronous strike-slip deformation: southern Xialiao basin, Bohai, offshore China. Basin Res. 22, 61–78.

Hu, Z., Liu, Y., Gao, S., Liu, W., Zhang, W., Tong, X., … Chen, H. (2012). Improved in situ Hf isotope ratio analysis of zircon using newly designed X skimmer cone and jet sample cone in combination with the addition of nitrogen by laser ablation multiple collector ICP-MS. Journal of Analytical Atomic Spectrometry, 27(9), 1391–1399. https://doi.org/10.1039/c2ja30078h

Huang, L., Liu, C. Y., & Kusky, T. M. (2015). Cenozoic evolution of the Tan–Lu Fault Zone (East China)—constraints from seismic data. Gondwana Research, 28(3), 1079-1095.

Huang, Y., Ren, D., Zhang, X., Xiong, X., Zhang, C., Wang, Y., Zhao, L., (2008). Zircon U–Pb dating of the Meizuo granite and geological significance in the Huanan uplift, east Heilongjiang Province. Journal of Jilin University (Earth Science Edition) 38, 631-638 (In Chinese with English abstract).

Hwang, B. H., McWilliams, M., Son, M., & Yang, K. (2007). Tectonic implication of A-type granites across the Yangsan fault, Gigye and Gyeongju areas, southeast Korean Peninsula. International Geology Review, 49(12), 1094-1102.

Ichihashi, R. J., Zaman, H., Wada, Y., Sugamori, Y., Kajikawa, Y., Ahn, H. S., ... & Otofuji, Y. I. (2015). Paleomagnetic evidence for post-early cretaceous tectonic rotation of the Sikhote-Alin superterrane, Far East Russia. Journal of Asian Earth Sciences, 111, 88-99.

Iizuka, T., Yamaguchi, T., Hibiya, Y., & Amelin, Y. (2015). Meteorite zircon constraints on the bulk Lu—Hf isotope composition and early differentiation of the Earth. Proceedings of the National Academy of Sciences, 112(17), 5331–5336. https://doi.org/10.1073/pnas.1501658112

Ishizuka, O., Tani, K., Reagan, M. K., Kanayama, K., Umino, S., Harigane, Y., ... & Dunkley, D. J. (2011). The timescales of subduction initiation and subsequent

evolution of an oceanic island arc. Earth and Planetary Science Letters, 306(3-4), 229-240.

Isozaki, Y. (1997). Contrasting two types of orogen in Permo-Triassic Japan: Accretionary versus collisional. Island Arc, 6(1), 2–24. https://doi.org/10.1111/j.1440-1738.1997.tb00038.x

Isozaki, Y., Aoki, K., Nakama, T., & Yanai, S. (2010). New insight into a subduction-related orogen: a reappraisal of the geotectonic framework and evolution of the Japanese Islands. Gondwana Research, 18(1), 82-105.

Isozaki, Y., Maruyama, S., & Furuoka, F. (1990). Accreted oceanic materials in Japan. Tectonophysics, 181(1–4), 179–205. https://doi.org/ 10.1016/0040-1951(90)90016-2

Jahn, B. M. (2004). The Central Asian Orogenic Belt and growth of the continental crust in the Phanerozoic. Geological Society, London, Special Publications, 226(1), 73-100.

Jahn, B. M. (2010). Accretionary orogen and evolution of the Japanese Islands: Implications from a Sr-Nd isotopic study of the Phanerozoic granitoids from SW Japan. American Journal of Science, 310(10), 1210–1249.

Jahn, B. M., Usuki, M., Usuki, T., & Chung, S. L. (2014). Generation of Cenozoic granitoids in Hokkaido (Japan): Constraints from zircon geochronology, Sr-Nd-Hf isotopic and geochemical analyses, and implications for crustal growth. American Journal of Science, 314(2), 704-750.

Jahn, B. M., Valui, G., Kruk, N., Gonevchuk, V., Usuki, M., & Wu, J. T. (2015). Emplacement ages, geochemical and Sr–Nd–Hf isotopic characterization of Mesozoic to early Cenozoic granitoids of the Sikhote-Alin Orogenic Belt, Russian Far East: Crustal growth and regional tectonic evolution. Journal of Asian Earth Sciences, 111, 872–918. https://doi.org/10.1016/j.jseaes.2015.08.012

Jahn, B.M., (2001). Highly evolved juvenile granites with tetrad REE patterns: the Woduhe and Baerzhe granites from the Great Xing'an Mountains in NE China. Lithos 59, 171–198.

Jahn, B.M., Griffin, W.L., Windley, B., (2000). Continental growth in the Phanerozoic:

evidence from Central Asia. Tectonophysics 328, vii–vix.

Janoušek, V., Finger, F., Roberts, M., Frýda, J., Pin, C., Dolejš, D., (2004). Deciphering the petrogenesis of deeply buried granites: whole-rock geochemical constraints on the origin of largely undepleted granulites from the Moldanubian Zone of the Bohemian Massif. Transactions of the Royal Society of Edinburgh: Earth Sciences 95, 141–159.

Jia, J., Zheng, H., Huang, X., Wu, F., Yang, S., Wang, K., & He, M. (2010). Detrital zircon U-Pb ages of Late Cenozoic sediments from the Yangtze delta: Implication for the evolution of the Yangtze River. Chinese Science Bulletin, 55(15), 1520–1528. https://doi.org/10.1007/s11434-0103091-x

Jolivet, L., Davy, P., & Cobbold, P. (1990). Right‐lateral shear along the northwest Pacific margin and the India‐Eurasia collision. Tectonics, 9(6), 1409-1419.

Jolly, W.T., Schellekens, J.H., Dickin, A.P., (2007). High-Mg andesites and related lavas from southwest Puerto Rico (Greater Antilles Island Arc): Petrogenetic links with emplacement of the Late Cretaceous Caribbean mantle plume. Lithos 98, 1-26.

Kaplun, V., (2012). Geoelectric section of the lithosphere of the Amur-Zeya sedimentary basin deduced from magnetotelluric sounding along the Blagoveshchensk-Birakan profile. Russian Journal of Pacific Geology 6, 131-142.

Kaplun, V., (2013). Geoelectric section of the lithosphere of the Amur-Zeya sedimentary basin deduced from magnetotelluric soundings. Russian Journal of Pacific Geology 7, 151-166.

Kato, K., & Saka, Y. (2003). Kurosegawa terrane as a transform fault zone in southwest Japan. Gondwana Research, 6(4), 669–686. https://doi. org/10.1016/S1342-937X(05)71016-9

Kato, K., & Saka, Y. (2006). New model for the Early Cretaceous development of SW Japan based on basic rocks of the Chichibu Composite Terrane. Geosciences Journal, 10(3), 275–289. https://doi.org/10.1007/BF02910370

Kelemen, P.B., (1995). Genesis of high Mg# andesites and the continental crust. Contributions to Mineralogy and Petrology 120, 1-19.

Kemkin, I. (2008). Structure of terranes in a Jurassic accretionary prism in the Sikhote-Alin-Amur area: Implications for the Jurassic geodynamic history of the Asian eastern margin. Russian Geology and Geophysics, 49(10), 759–770. https://doi.org/10.1016/j.rgg.2007.12.014

Kemkin, I. V., & Kemkina, R. A. (2015). Geochemistry of chert rocks from the Sikhote-Alin Taukha terrane, Russia far east: Significance for determination of their depositional environment. Environmental Earth Sciences, 73(5), 2253–2268. https://doi.org/10.1007/s12665-014-3574-1

Kemkin, I., & Kemkina, R. (2000). Jurassic-Early Cretaceous biostratigraphic cherty and terrigenous deposits of the Dalnegorsk Ore region (Southern Sikhote-Alin). Geology of the Pacific Ocean, 15(1), 85–106.

Kemkin, I., Filippov, A., & Khanchuk, A. (2006). New data on the structure of the Khabarovsk Terrane of the Jurassic accretionary prism (Sikhote-Alin). Doklady Earth Sciences, 406(1), 28–31. https://doi.org/10.1134/S1028334X06010089

Kemkin, I., Khanchuk, A., & Kemkina, R. (2016). Accretionary prisms of the Sikhote-Alin Orogenic Belt: Composition, structure and significance for reconstruction of the geodynamic evolution of the eastern Asian margin. Journal of Geodynamics, 102, 202–230. https://doi.org/ 10.1016/j.jog.2016.10.002

Kemkin, I.V., (2008). Structure of terranes in a Jurassic accretionary prism in the Sikhote- Alin-Amur area: implications for the Jurassic geodynamic history of the Asian eastern margin. Russian Geology and Geophysics 49, 759–770.

Khanchuk, A. I. (2001). Pre-Neogene tectonics of the Sea-of-Japan region: A view from the Russian side. in Special issue: *Geotectonic framework of eastern Asia before the opening of the Japan Sea*, *Part 2*, Earth Science (Chikyu Kagaku), 55(5), 275-291.

Khanchuk, A. I., & Vysotskiy, S. (2016). Different-depth gabbro–ultrabasite associations in the Sikhote-Alin ophiolites (Russian Far East). Russian Geology and Geophysics, 57(1), 141–154. https://doi.org/10.1016/j.rgg.2016.01.010

Khanchuk, A. I., Didenko, A. N., Popeko, L. I., Sorokin, A. A., & Shevchenko, B. F.

(2015). Structure and evolution of the Mongol-Okhotsk Orogenic Belt. In A. Kroner (Ed.), The Central Asian Orogenic Belt. Contributions to the Regional Geology of the Earth (pp. 211–234). Stuttgart, Germany: E. Schweitzerbart Science Publishers.

Khanchuk, A. I., Didenko, A. N., Tikhomirova, A. I., & Voinova, I. P. (2015). Paleomagnetism and geochemistry of the Kiselevka block of the Kiselevka-Manoma terrane (northern Sikhote-Alin): Geodynamic significance. Geological Society of America Special Papers, 513, 513–514.

Khanchuk, A. I., Kruk, N. N., Valui, G. A., Nevolin, P. L., Moskalenko, E. Y., Fugzan, M. M., ... & Travin, A. V. (2008). The Uspensk intrusion in South Primorye as a reference petrotype for granitoids of the transform continental margins. Doklady Earth Sciences, 421(1), 734-737).

Khanchuk, A. I., Ratkin, V. V., Ryazantseva, M. D., Golozubov, V. V., & Gonokhova, N. G. (1996). Geology and Mineral Deposits of Primorskiy Krai, (p. 61). Dalnauka: Vladivostok.

Khanchuk, A. I., Vovna, G. M., Kiselev, V. I., Mishkin, M. A., & Lavrik, S. N. (2010). First results of zircon LA-ICP-MS U-Pb dating of the rocks from the Granulite complex of Khanka massif in the Primorye region. In Doklady Earth Sciences, 434 (1), 1164-1167.

Khanchuk, A.I., (2010a). First SHRIMP U–Pb zircon dating of magmatic complexes in the southwestern Primor'e region. Russian Geology and Geophysics 49, 759–770.

Khanchuk, A.I., (2010b). First results of zircon LA ICP MS U–Pb dating of the rocks from the granulite complex of Khanka massif in the Primorye region. Doklady Earth Sciences 434, 1164–1167.

Kim, S. W., Kwon, S., Koh, H. J., Yi, K., Jeong, Y. J., & Santosh, M. (2011). Geotectonic framework of Permo–Triassic magmatism within the Korean Peninsula. Gondwana Research, 20(4), 865–889. https://doi.org/10.1016/j.gr.2011.05.005

Kim, S. W., Kwon, S., Park, S. I., Lee, C., Cho, D. L., Lee, H. J., ... & Kim, S. J. (2016).

SHRIMP U–Pb dating and geochemistry of the Cretaceous plutonic rocks in the Korean Peninsula: a new tectonic model of the Cretaceous Korean Peninsula. Lithos, 262, 88-106.

Kim, S. W., Kwon, S., Park, S. I., Yi, K., Santosh, M., & Ryu, I. C. (2015). Early to Middle Paleozoic arc magmatism in the Korean Peninsula: Constraints from zircon geochronology and geochemistry. Journal of Asian Earth Sciences, 113, 866–882. https://doi.org/10.1016/ j.jseaes.2015.09.017

Kim, S. W., Williams, I. S., Kwon, S., & Oh, C. W. (2008). SHRIMP zircon geochronology, and geochemical characteristics of metaplutonic rocks from the south-western Gyeonggi Block, Korea: Implications for Paleoproterozoic to Mesozoic tectonic links between the Korean Peninsula and eastern China. Precambrian Research, 162(3–4), 475–497. https://doi.org/10.1016/j.precamres.2007.10.006

Kimura, T. (1979). Late Mesozoic palaeofloristic provinces in east Asia. Proceedings of the Japan Academy, Series B Physical and Biological Sciences, 55(9), 425–430. https://doi.org/10.2183/pjab.55.425

Kimura, T. (2000). Early Cretaceous climatic provinces in Japan and adjacent regions on the basis. Cretaceous Environments of Asia, 17, 155. https://doi.org/10.1016/S0920-5446(00)80029-1

Kimura, T., Ohana, T., & Mimoto, K. (1988). Discovery of a podocarpaceous plant from the Lower Cretaceous of Kochi Prefecture, in the Outer Zone of southwest Japan. Proceedings of the Japan Academy, Series B, 64(8), 213–216.

King, P., White, A., Chappell, B., Allen, C., (1997). Characterization and origin of aluminous A-type granites from the Lachlan Fold Belt, southeastern Australia. Journal of petrology 38, 371-391.

Kinoshita, O. (1995). Migration of igneous activities related to ridge subduction in Southwest Japan and the East Asian continental margin from the Mesozoic to the Paleogene. Tectonophysics, 245(1-2), 25-35.

Kinoshita, O. (2002). Possible manifestations of slab window magmatisms in Cretaceous southwest Japan. Tectonophysics, 344(1-2), 1-13.

Kirillova, G. L. (2003). Cretaceous tectonics and geological environments in East Russia. Journal of Asian Earth Sciences, 21(8), 967–977. https:// doi.org/10.1016/S1367-9120(02)00093-7

Kirillova, G.L., (2003). Late Mesozoic–Cenozoic sedimentary basins of active continental margin of Southeast Russia: paleogeography, tectonics, and coal–oil–gas presence. Marine and Petroleum Geology 20, 385-397.

Klein, E. M., & Karsten, J. L. (1995). Ocean-ridge basalts with convergent-margin geochemical affinities from the Chile Ridge. Nature, 374(6517), 52.

Kojima, S. (1989). Mesozoic terrane accretion in northeast China, Sikhote-Alin and Japan regions. Palaeogeography, Palaeoclimatology, Palaeoecology, 69, 213–232. https://doi.org/10.1016/0031-0182(89)90165-X

Kojima, S., Igor'V, K., Kametaka, M., & Ando, A. (2000). A correlation of accretionary complexes of southern Sikhote-Alin of Russia and the Inner Zone of Southwest Japan. Geosciences Journal, 4(3), 175–185. https://doi.org/10.1007/BF02910136

Kojima, S., Tsukada, K., Otoh, S., Yamakita, S., Ehiro, M., Dia, C., … Eichwald, L. P. (2008). Geological relationship between Anyui metamorphic complex and Samarka terrane, Far East Russia. Island Arc, 17(4), 502–516. https://doi.org/10.1111/j.1440-1738.2008.00644.x

Konstantinovskaia, E. A. (2000). Geodynamics of an Early Eocene arc–continent collision reconstructed from the Kamchatka Orogenic Belt, NE Russia. Tectonophysics, 325(1-2), 87-105.

Kravchinsky, V. A., Cogné, J.-P., Harbert, W. P., & Kuzmin, M. I. (2002). Evolution of the Mongol-Okhotsk Ocean as constrained by new palaeomagnetic data from the Mongol-Okhotsk suture zone, Siberia. Geophysical Journal International, 148(1), 34–57. https://doi.org/ 10.1046/j.1365-246x.2002.01557.x

Kröner, A., Kovach, V., Belousova, E., Hegner, E., Armstrong, R., Dolgopolova, A., Seltmann, R., Alexeiev, D., Hoffmann, J., Wong, J., (2014). Reassessment of continental growth during the accretionary history of the Central Asian Orogenic Belt. Gondwana Research 25, 103-125.

Kröner, A., Windley, B., Badarch, G., Tomurtogoo, O., Hegner, E., Jahn, B., Gruschka, S., Khain, E., Demoux, A., Wingate, M., (2007). Accretionary growth and crust formation in the Central Asian Orogenic Belt and comparison with the Arabian-Nubian shield. Geological Society of America Memoirs 200, 181-209.

Kruk, N. N., Simanenko, V. P., Golozubov, V. V., Kovach, V. P., Vladimirov, V. G., & Kasatkin, S. A. (2014a). Geochemistry of rocks in the Anuy metamorphic dome, Sikhote-Alin: Composition of the protoliths and the possible nature of metamorphism. Geochemistry International, 52(3), 229–246. https://doi.org/10.1134/S0016702914010030

Kruk, N. N., Simanenko, V. P., Golozubov, V. V., Kovach, V. P., Vladimirov, V. G., & Kasatkin, S. A. (2014b). Geochemistry of rocks in the Anuy metamorphic dome, Sikhote-Alin: Composition of the protoliths and the possible nature of metamorphism. Geochemistry International, 52(3), 229-246.

Kudymov, A. V. (2010). Cenozoic stress fields in the Kiselevka fault zone, Lower Amur region. Russian Journal of Pacific Geology, 4(6), 495-501.

Kusky, T., Windley, B., & Zhai, M. G. (2007). Tectonic evolution of the North China Block: From orogen to craton to orogen. Geological Society, London, Special Publications, 280(1), 1–34. https://doi.org/10.1144/SP280.1

Lagabrielle, Y., Suárez, M., Rossello, E. A., Hérail, G., Martinod, J., Régnier, M., & de la Cruz, R. (2004). Neogene to Quaternary tectonic evolution of the Patagonian Andes at the latitude of the Chile Triple Junction. Tectonophysics, 385(1-4), 211-241.

Lee, D. W. (1999). Strike–slip fault tectonics and basin formation during the Cretaceous in the Korean Peninsula. Island Arc, 8(2), 218–231. https://doi.org/10.1046/j.1440-1738.1999.00233.x

Lee, K. S., Chang, H. W., & Park, K. H. (1998). Neoproterozoic bimodal volcanism in the central Ogcheon belt, Korea: Age and tectonic implication. Precambrian Research, 89(1–2), 47–57. https://doi.org/10.1016/S0301-9268(97)00077-6

Lee, S. R., Cho, M., Cheong, C. S., Kim, H., & Wingate, M. T. (2003). Age, geochemistry, and tectonic significance of Neoproterozoic alkaline granitoids in

the northwestern margin of the Gyeonggi massif, South Korea. Precambrian Research, 122(1–4), 297–310. https://doi.org/ 10.1016/S0301-9268(02)00216-4

Lee, T. H., Park, K. H., Yi, K., Geng, J. Z., & Li, H. K. (2015). SHRIMP U-Pb ages and Hf isotopic composition of the detrital zircons from the Myogok Formation, SE Korea: Development of terrestrial basin and igneous activity during the early Cretaceous. Geosciences Journal, 19(2), 189–203. https://doi.org/10.1007/s12303-014-0042-6

Li, B.L., Sun, F.Y., Yao, F.L., 2002. Large scale sinistral strike-slip movement of Dunhua-Mishan fracture zone and its control on gold metallogeny in the Mesozoic. Geotectonica et Metallogenia 26, 390–395 (in Chinese with English abstract).

Li, H. Y., & Huang, X. L. (2013). Constraints on the paleogeographic evolution of the North China Craton during the Late Triassic–Jurassic. Journal of Asian Earth Sciences, 70, 308–320.

Li, J.Y., (2006). Permian geodynamic setting of Northeast China and adjacent regions: closure of the Paleo-Asian Ocean and subduction of the Paleo-Pacific Plate. Journal of Asian Earth Sciences 26, 207–224.

Li, Q. (2016). Eocene fossil rodent assemblages from the Erlian Basin (Inner Mongolia, China): biochronological implications. Palaeoworld, 25(1), 95-103.

Li, S. Z., Zhao, G. C., Sun, M., Wu, F. Y., Hao, D. F., Han, Z. Z., … Xia, X. P. (2005). Deformational history of the Paleoproterozoic Liaohe Group in the Eastern Block of the North China Craton. Journal of Asian Earth Sciences, 24, 654–669.

Li, S. Z., Zhao, G. C., Sun, M., Wu, F. Y., Liu, J. Z., Hao, D. F., … Luo, Y. (2004). Mesozoic, not Paleoproterozoic SHRIMP U–Pb zircon ages of two Liaoji granites, Eastern Block, North China Craton. International Geology Review, 46(2), 162–176. https://doi.org/10.2747/0020- 6814.46.2.162

Li, S. Z., Zhao, G. C., Sun, M., Zhao, G. T., & Hao, D. F. (2006). Are the South and North Liaohe Groups of the North China Craton different exotic terranes? Nd isotope constraints. Gondwana Research, 9(1–2), 198–208. https://doi.org/10.1016/j.gr.2005.06.011

Li, S., Wilde, S.A., He, Z., Jiang, X., Liu, R., Zhao, L., (2014). Triassic sedimentation and postaccretionary crustal evolution along the Solonker suture zone in Inner Mongolia, China. Tectonics 33, 960–981.

Li, S.Q., Yang, Y.Z., Xie, Q.L., Wang, Y., Chen, F., (2015). Age Constraints on Late Mesozoic Lithospheric Extension and Origin of Felsic Volcanism in the Songliao Basin, NE China. The Journal of Geology 123, 153-175.

Li, W., Takasu, A., Liu, Y., Guo, X., (2010). Newly discovered garnet-barroisite schists from the Heilongjiang Complex in the Jiamusi Massif, northeastern China. Journal of mineralogical and petrological sciences 105, 86-91.

Li, X. H., Li, Z. X., Zhou, H., Liu, Y., & Kinny, P. D. (2002). U–Pb zircon geochronology, geochemistry and Nd isotopic study of Neoproterozoic bimodal volcanic rocks in the Kangdian Rift of South China: Implications for the initial rifting of Rodinia. Precambrian Research, 113(1–2), 135–154. https://doi.org/10.1016/S0301-9268(01)00207-8

Li, X. M., & Gong, G. L. (2011). Late Mesozoic - Cenozoic exhumation history of the Lesser Hinggan Mountains, NE China, revealed by fission track thermochronology. Geological Journal, 46(4), 277-287.

Li, X., Li, Z., Li, W., Liu, Y., Yuan, C., Wei, G., Qi, C., (2007). U–Pb zircon, geochemical and Sr–Nd–Hf isotopic constraints on age and origin of Jurassic I- and A-type granites from central Guangdong, SE China: a major igneous event in response to foundering of a subducted flat-slab? Lithos 96, 186–204.

Li, X., Yang, X., Xia, B., Gong, G., Shan, Y., Zeng, Q., ... & Sun, W. (2011). Exhumation of the Dahinggan Mountains, NE China from the Late Mesozoic to the Cenozoic: New evidence from fission-track thermochronology. Journal of Asian Earth Sciences, 42(1-2), 123-133.

Li, Z. X., & Li, X. H. (2007). Formation of the 1300-km-wide intracontinental orogen and postorogenic magmatic province in Mesozoic South China: A flat-slab subduction model. Geology, 35(2), 179–182. https://doi.org/10.1130/G23193A.1

Li, Z. X., Li, X. H., Chung, S. L., Lo, C. H., Xu, X., & Li, W. X. (2012). Magmatic switch-on and switch-off along the South China continental margin since the

Permian: Transition from an Andean-type to a Western Pacific-type plate boundary. Tectonophysics, 532, 271–290.

Li, Z. X., Li, X. H., Zhou, H., & Kinny, P. D. (2002). Grenvillian continental collision in south China: New SHRIMP U-Pb zircon results and impli- cations for the configuration of Rodinia. Geology, 30(2), 163–166.

Li, Z., Li, X., Kinny, P., & Wang, J. (1999). The breakup of Rodinia: Did it start with a mantle plume beneath South China? Earth and Planetary Science Letters, 173(3), 171–181. https://doi.org/10.1016/S0012-821X(99)00240-X

Liao, J. P., Jahn, B. M., Alexandrov, I., Chung, S. L., Zhao, P., Ivin, V., & Usuki, T. (2018). Petrogenesis of Mid-Eocene granites in South Sakhalin, Russian Far East: Juvenile crustal growth and comparison with granitic magmatism in Hokkaido and Sikhote-Alin. Journal of Asian Earth Sciences, 167, 103-129.

Ling, M. X., Li, Y., Ding, X., Teng, F. Z., Yang, X. Y., Fan, W. M., ... & Sun, W. (2013). Destruction of the North China Craton induced by ridge subductions. The Journal of Geology, 121(2), 197-213.

Ling, M. X., Wang, F. Y., Ding, X., Hu, Y. H., Zhou, J. B., Zartman, R. E., ... & Sun, W. (2009). Cretaceous ridge subduction along the lower Yangtze River belt, eastern China. Economic Geology, 104(2), 303-321.

Liu, C., Zhang, X.Z., Liu, Y., Yang, B.J., Feng, X., Wang, D., Liu, D.M., 2009. Geoelectrical evidence for characteristics of lithospheric structure beneath the Yuejinshan collage zone and its vicinity in Northeast Asia. Chinese Journal of Geophysics 52, 403-412 (In Chinese with English abstract).

Liu, C., Zhu, G., Zhang, S., Gu, C., Li, Y., Su, N., & Xiao, S. (2018). Mesozoic strike-slip movement of the Dunhua–Mishan Fault Zone in NE China: A response to oceanic plate subduction. Tectonophysics, 723, 201-222.

Liu, F., & Liou, J. (2011). Zircon as the best mineral for P–T–time history of UHP metamorphism: A review on mineral inclusions and U–Pb SHRIMP ages of zircons from the Dabie–Sulu UHP rocks. Journal of Asian Earth Sciences, 40(1), 1–39. https://doi.org/10.1016/ j.jseaes.2010.08.007

Liu, K., Zhang, J., Wilde, S. A., Zhou, J., Wang, M., Ge, M., ... & Ling, Y. (2017a).

Initial subduction of the Paleo-Pacific Oceanic plate in NE China: Constraints from whole-rock geochemistry and zircon U–Pb and Lu–Hf isotopes of the Khanka Lake granitoids. Lithos, 274, 254-270.

Liu, K., Zhang, J., Wilde, S. A., Liu, S., Guo, F., Kasatkin, S. A., Golozoubov, V.V., Ge, M., Wang, M., Wang, J., (2017b). U-Pb Dating and Lu-Hf Isotopes of Detrital Zircons From the Southern Sikhote-Alin Orogenic Belt, Russian Far East: Tectonic Implications for the Early Cretaceous Evolution of the Northwest Pacific Margin. Tectonics, 36(11), 2555-2598.

Liu, Y., Gao, S., Hu, Z., Gao, C., Zong, K., Wang, D., (2010). Continental and oceanic crust recycling-induced melt–peridotite interactions in the Trans-North China Orogen: U–Pb dating, Hf isotopes and trace elements in zircons from mantle xenoliths. Journal of Petrology egp082.

Luan, J. P., Wang, F., Xu, W. L., Ge, W. C., Sorokin, A. A., Wang, Z. W., & Guo, P. (2017). Provenance, age, and tectonic implications of Neoproterozoic strata in the Jiamusi Massif: evidence from U–Pb ages and Hf isotope compositions of detrital and magmatic zircons. Precambrian Research, 297, 19–32.

Ludwig, K. (2001). Isoplot 3.0—A geochronological toolkit for Microsoft Excel, Special Publication No. 4, Berkeley Geochronology Center, Berkeley, Calif.

Ma, Q., Zheng, J.P., Xu, Y.G., Griffin, W.L., Zhang, R.S., 2015. Are continental "adakites" de- rived from thickened or foundered lower crust? Earth and Planetary Science Letters 419, 125–133.

Ma, X.H., Zhu, W.P., Zhou, Z.H., Qiao, S.L., 2016. Transformation from Paleo-Asian Ocean closure to Paleo-Pacific subduction: New constraints from granitoids in the eastern Jilin–Heilongjiang Belt, NE China. Journal of Asian Earth Sciences, in press.

Maeda, J. I., & Kagami, H. (1996). Interaction of a spreading ridge and an accretionary prism: Implications from MORB magmatism in the Hidaka magmatic zone, Hokkaido, Japan. Geology, 24(1), 31-34.

Malinovsky, A., & Golozubov, V. (2011). Lithology and depositional settings of the terrigenous sediments along transform plate boundaries: Evidence from the early

cretaceous Zhuravlevka terrane in Southern Sikhote Alin. Russian Journal of Pacific Geology, 5(5), 400–417. https:// doi.org/10.1134/S1819714011050058

Malinovsky, A., Golozoubov, V., Simanenko, V., (2006). The Kema island-arc terrane, eastern Sikhote Alin: Formation settings and geodynamics, Doklady earth sciences. Springer, pp. 1026-1029.

Malinovsky, A., Golozubov, V., Simanenko, V., (2005). Composition and depositional settings of Lower Cretaceous terrigenous rocks of the Kema River Basin, eastern Sikhote Alin. Lithology and Mineral Resources 40, 429-447.

Malinovsky, A.I., Golozoubov, V.V., Simanenko, V.P., Simanenko, L.F., (2008). Kema terrane: A fragment of a back‐arc basin of the early Cretaceous Moneron–Samarga island‐arc system, East Sikhote–Alin range, Russian Far East. Island Arc 17, 285-304.

Maniar, P.D., Piccoli, P.M., 1989. Tectonic discrimination of granitoids. Geological Society of America Bulletin 101, 635–643.

Martynov, Y. A., & Khanchuk, A. I. (2013). Cenozoic volcanism of the eastern Sikhote Alin: petrological studies and outlooks. Petrology, 21(1), 85-99.

Martynov, Y. A., Khanchuk, A. I., Grebennikov, A. V., Chashchin, A. A., & Popov, V. K. (2017). Late Mesozoic and Cenozoic volcanism of the East Sikhote-Alin area (Russian Far East): a new synthesis of geological and petrological data. Gondwana Research, 47, 358-371.

Maruyama, S. (1997). Pacific-type orogeny revisited: Miyashiro-type orogeny proposed. Island Arc, 6(1), 91–120. https://doi.org/10.1111/ j.1440-1738.1997.tb00042.x

Maruyama, S., Isozaki, Y., Kimura, G., & Terabayashi, M. (1997). Paleogeographic maps of the Japanese Islands: plate tectonic synthesis from 750 Ma to the present. Island arc, 6(1), 121-142.

Matsuda, T., Isozaki, Y., (1991). Well‐documented travel history of Mesozoic pelagic chert in Japan: from remote ocean to subduction zone. Tectonics 10, 475-499.

Meffre, S., Falloon, T. J., Crawford, T. J., Hoernle, K., Hauff, F., Duncan, R. A., ... & Wright, D. J. (2012). Basalts erupted along the Tongan fore arc during subduction

initiation: Evidence from geochronology of dredged rocks from the Tonga fore arc and trench. Geochemistry, Geophysics, Geosystems, 13(12).

Meng, E., Xu, W., Pei, F., Yang, D., Wang, F., & Zhang, X. (2011). Permian bimodal volcanism in the Zhangguangcai Range of eastern Heilongjiang Province, NE China: Zircon U–Pb–Hf isotopes and geochemical evidence. Journal of Asian Earth Sciences, 41(2), 119–132. https://doi.org/10.1016/j.jseaes.2011.01.005

Meng, E., Xu, W., Yang, D., Pei, F., Yu, Y., & Zhang, X. (2008). Permian volcanisms in eastern and southeastern margins of the Jiamusi Massif, northeastern China: Zircon U-Pb chronology, geochemistry and its tectonic implications. Chinese Science Bulletin, 53(8), 1231–1245.

Meng, E., Xu, W.L., Pei, F., Yang, D., Yu, Y., Zhang, X., (2010). Detrital-zircon geochronology of Late Paleozoic sedimentary rocks in eastern Heilongjiang Province, NE China: implications for the tectonic evolution of the eastern segment of the Central Asian Orogenic Belt. Tectonophysics 485, 42–51.

Menzies, M. A., Fan, W., & Zhang, M. (1993). Palaeozoic and Cenozoic lithoprobes and the loss of >120 km of Archaean lithosphere,

Miao, L., Zhang, F., Zhu, M., & Liu, D. (2015). Zircon SHRIMP U–Pb dating of metamorphic complexes in the conjunction of the Greater and Lesser Xing'an ranges, NE China: Timing of formation and metamorphism and tectonic implications. Journal of Asian Earth Sciences, 114, 634–648. https://doi.org/10.1016/j.jseaes.2014.09.035

Middlemost, E., 1994. Naming materials in the magma/igneous rock system. Earth-Science Reviews 37, 215–224.

Mizutani, S. (1987). Mesozoic terranes in the Japanese Islands and neighbouring East Asia. In E. Scheibner (Eds). Terrane accretion and oro- genic belts, American Geophysical Union, Geodynamic Series 19, (pp. 263–273). https://doi.org/10.1029/GD019p0263

Müller, R. D., Sdrolias, M., Gaina, C., Steinberger, B., & Heine, C. (2008). Long-term sea-level fluctuations driven by ocean basin dynamics. Science, 319(5868), 1357–1362. https://doi.org/10.1126/science.1151540

Müller, R. D., Seton, M., Zahirovic, S., Williams, S. E., Matthews, K. J., Wright, N. M., ... & Bower, D. J. (2016). Ocean basin evolution and global-scale plate reorganization events since Pangea breakup. Annual Review of Earth and Planetary Sciences, 44, 107-138.

Nakama, T., Hirata, T., Otoh, S., Aoki, K., Yanai, S., & Maruyama, S. (2010). Paleogeography of the Japanese Islands: Age spectra of detrital zircon and provenance history of the orogen. Journal of Geography, 119(6), 1161–1172. https://doi.org/10.5026/jgeography.119.1161

Natal'in, B. (1993). History and modes of Mesozoic accretion in southeastern Russia. Island Arc, 2(1), 15–34. https://doi.org/10.1111/ j.1440-1738.1993.tb00072.x

O'Connor, J. M., Steinberger, B., Regelous, M., Koppers, A. A., Wijbrans, J. R., Haase, K. M., ... & Garbe‐Schönberg, D. (2013). Constraints on past plate and mantle motion from new ages for the Hawaiian‐Emperor Seamount Chain. Geochemistry, Geophysics, Geosystems, 14(10), 4564-4584.

Otofuji, Y. I., Matsuda, T., Itaya, T., Shibata, T., Matsumoto, M., Yamamoto, T., ... & Sakhno, V. G. (1995). Late Cretaceous to early Paleogene paleomagnetic results from Sikhote Alin, far eastern Russia: implications for deformation of East Asia. Earth and Planetary Science Letters, 130(1-4), 95-108.

Otofuji, Y. I., Takaaki, M., Ryo, E., Koji, U., Nishihama, K., Halim, N., ... & Matunin, A. P. (2003). Late Cretaceous palaeomagnetic results from Sikhote Alin, far eastern Russia: tectonic implications for the eastern margin of the Mongolia Block. Geophysical Journal International, 152(1), 202-214.

Pavlis, T. L., & Sisson, V. B. (1995). Structural history of the Chugach metamorphic complex in the Tana River region, eastern Alaska: A record of Eocene ridge subduction. Geological Society of America Bulletin, 107(11), 1333-1355.

Peacock, S.M., Rusher, T., Thompson, A.B., (1994). Partial melting of subducting oceanic crust. Earth and Planetary Science Letters 121, 224–227.

Pearce, J.A., (1982). Trace Element Characteristics of Lavas From Destructive Plate Boundaries. John Wiley & Sons, Chichester, United Kingdom (GBR), pp. 525–548.

Pearce, J.A., Norry, M.J., (1979). Petrogenetic implications of Ti, Zr, Y, and Nb variations in volcanic rocks. Contributions to mineralogy and petrology 69, 33-47.

Pearce, J.A., Peate, D.W., (1995). Tectonic implications of the composition of volcanic arc magmas. Annual Review of Earth and Planetary Sciences 23, 251-286.

Peccerillo, A., Taylor, S.R., (1976). Geochemistry of Eocene calc-alkaline volcanic rocks from the Kastamonu area, northern Turkey. Contributions to Mineralogy and Petrology 58, 63–81.

Pei, F., Xu, W., Yang, D., Ji, W., Yu, Y., Zhang, X., (2008). Mesozoic volcanic rocks in the southern Songliao basin: zircon U–Pb ages and their constraints on the nature of basin basement. Earth Science (Journal of China University of Geosciences) 5, 603-617 (In Chinese with English abstract).

Pei, F., Xu, W., Yang, D., Zhao, Q., Liu, X., Hu, Z., (2007). Zircon U-Pb geochronology of basement metamorphic rocks in the Songliao Basin. Chinese Science Bulletin 52, 942-948 (In Chinese with English abstract).

Peng, P., Bleeker, W., Ernst, R. E., Söderlund, U., & McNicoll, V. (2011). U–Pb baddeleyite ages, distribution and geochemistry of 925Ma mafic dykes and 900Ma sills in the North China craton: Evidence for a Neoproterozoic mantle plume. Lithos, 127(1–2), 210 – 221. https://doi.org/ 10.1016/j.lithos.2011.08.018

Peng, P., Zhai, M., Ernst, R. E., Guo, J., Liu, F., & Hu, B. (2008). A 1.78 Ga large igneous province in the North China craton: The Xiong'er Volcanic Province and the North China dyke swarm. Lithos, 101(3–4), 260–280. https://doi.org/10.1016/j.lithos.2007.07.006

Petrishchevsky, A., (2011). Rheological model of the crust beneath southern Sikhote-Alin: Evidence from gravity data. Russian Journal of Pacific Geology 5(3), 210-224.

Petrishchevsky, A., (2013). Gravity models of two-level collision of lithospheric plates in northeastern Asia. Geotectonics 47(6), 465-484.

Plank, T., Langmuir, C.H., (1988). An evaluation of the global variations in the major element chemistry of arc basalts. Earth and Planetary Science Letters 90, 349-

370.

Qi, G., Zhang, J., & Wang, M. (2015). Mesozoic tectonic setting of rift basins in eastern North China and implications for destruction of the North China Craton. Journal of Asian Earth Sciences, 111, 414–427. https://doi.org/10.1016/j.jseaes.2015.06.022

Qian, Q., Hermann, J., (2013). Partial melting of lower crust at 10–15 kbar: constraints on adakite and TTG formation. Contributions to Mineralogy and Petrology 165 (6), 1195–1224.

Qiu, Y. M., Gao, S., McNaughton, N. J., Groves, D. I., & Ling, W. (2000). First evidence of> 3.2 Ga continental crust in the Yangtze craton of south China and its implications for Archean crustal evolution and Phanerozoic tectonics. Geology, 28(1), 11–14.

Rapp, R.P., Watson, E.B., (1995). Dehydration melting of metabasalt at 8–32 kbar, implications for continental growth and crust–mantle recycling. Journal of Petrology 36, 891–931.

Rapp, R.P., Watson, E.B., Miller, C.F., (1991). Partial melting of amphibolite/eclogite and the origin of Archaean trondhjemites and tonalites. Precambrian Research 51, 1–25.

Reubi, O., Blundy, J., (2009). A dearth of intermediate melts at subduction zone volcanoes and the petrogenesis of arc andesites. Nature 461, 1269-1273.

Rodnikov, A. G., Sergeyeva, N. A., Zabarinskaya, L. P., Filatova, N. I., Piip, V. B., & Rashidov, V. A. (2008). The deep structure of active continental margins of the Far East (Russia). Russian Journal of Earth Sciences, 10(4).

Rojas-Agramonte, Y., Kröner, A., Demoux, A., Xia, X., Wang, W., Donskaya, T., … Sun, M. (2011). Detrital and xenocrystic zircon ages from Neoproterozoic to Palaeozoic arc terranesof Mongolia: Significance for the origin of crustal fragments in the Central Asian Orogenic Belt. Gondwana Research, 19(3), 751–763. https://doi.org/10.1016/j.gr.2010.10.004

Rowley, D. B., Raymond, A., Parrish, J. T., Lottes, A. L., Scotese, C. R., & Ziegler, A. M. (1985). Carboniferous paleogeographic, phytogeographic, and paleoclimatic

reconstructions. International Journal of Coal Geology, 5(1–2), 7–42. https://doi.org/10.1016/0166-5162(85)90009-6

Rudnick, R.L., Gao, S., (2003). Composition of the Continental Crust, In: Rudnick, R. L. (Eds.), Treatise on Geochemistry, Volume 3. Elsevier, pp. 1-64.

Russo, R. M., Gallego, A., Comte, D., Mocanu, V. I., Murdie, R. E., & VanDecar, J. C. (2010). Source-side shear wave splitting and upper mantle flow in the Chile Ridge subduction region. Geology, 38(8), 707-710.

Sagong, H., Kwon, S. T., & Ree, J. H. (2005). Mesozoic episodic magmatism in South Korea and its tectonic implication. Tectonics, 24(5).

Sano, Y., Hidaka, H., Terada, K., Shimizu, H., & Suzuki, M. (2000). Ion microprobe U-Pb zircon geochronology of the Hida gneiss: Finding of the oldest minerals in Japan. Geochemical Journal, 34(2), 135–153. https://doi.org/10.2343/geochemj.34.135

Saunders, A.D., Tarney, J., Weaver, S.D., 1980. Transverse geochemical variations across the Antarctic Peninsula: implications for the genesis of calc-alkaline magmas. Earth and Planetary Science Letters 46, 344-360.

Schiano, P., Monzier, M., Eissen, J.-P., Martin, H., Koga, K., 2010. Simple mixing as the major control of the evolution of volcanic suites in the Ecuadorian Andes. Contributions to Mineralogy and Petrology 160, 297-312.

Segal, I., Halicz, L., & Platzner, I. T. (2003). Accurate isotope ratio measurements of ytterbium by multiple collection inductively coupled plasma mass spectrometry applying erbium and hafnium in an improved double external normalization procedure. Journal of Analytical Atomic Spectrometry, 18(10), 1217–1223. https://doi.org/10.1039/b307016f

Sengör, A. C., & Natal'In, B. A. (1996). Turkic-type orogeny and its role in the making of the continental crust. Annual Review of Earth and Planetary Sciences, 24(1), 263–337. https://doi.org/10.1146/annurev.earth.24.1.263

Şengör, A., Natal'In, B., & Burtman, V. (1993). Evolution of the Altaid tectonic collage and Palaeozoic crustal growth in Eurasia. Nature, 364, 22.

Seton, M., Flament, N., Whittaker, J., Müller, R. D., Gurnis, M., & Bower, D. J. (2015).

Ridge subduction sparked reorganization of the Pacific plate‐mantle system 60–50 million years ago. Geophysical Research Letters, 42(6), 1732-1740.

Shao, J., & Tang, K. (1995). Terranes in Northeast China and Evolution of Northeast Asia Continental Margin, edited, Seismic Press, Beijing.

Shao, J.A., Li, Y.F., Tang, K.D., (2013). Restoration of the orogenic processes of Zhangguangcai Range. Acta Petrologica Sinica 29, 2959-2970 (In Chinese with English abstract).

Shao, J.A., Tang, K.D., Wang, C.Y., Zang, Q.J., Zhang, Y.P., (1991). The tectonic characteristics and evolution of Nadanhada Terrane. Science in China. Series B 7, 744 (in Chinese).

Shao, J.A., Tang, K.D., Zhan, L.P., (1995). Reconstruction of an ancient continental margin and its implication: new progress on the study of geology of Yanbian region, northeast China. Science in China. Series B 25, 548–555.

Sharp, W. D., & Clague, D. A. (2006). 50-Ma initiation of Hawaiian-Emperor bend records major change in Pacific plate motion. Science, 313(5791), 1281-1284.

Shimoda, G., Tatsumi, Y., Nohda, S., Ishizaka, K., Jahn, B., (1998). Setouchi high-Mg andesites revisited: geochemical evidence for melting of subducting sediments. Earth and Planetary Science Letters 160, 479-492.

Simanenko, V. P., & Khanchuk, A. I. (2003). Cenomanian volcanism of the Eastern Sikhote-Alin volcanic belt: geochemical features. Geochemistry International, 41(8), 787-798.

Menzies, M., Xu, Y., Zhang, H., & Fan, W. (2007). Integration of geology, geophysics and geochemistry: A key to understanding the North China Craton. Lithos, 96(1–2), 1–21. https://doi.org/10.1016/j.lithos.2006.09.008

Sisson, T., Grove, T., (1993). Experimental investigations of the role of H2O in calc-alkaline differentiation and subduction zone magmatism. Contributions to Mineralogy and Petrology 113, 143-166.

Smithies, R.H., (2000). The Archaean tonalite–trondhjemite–granodiorite (TTG) series is not an analogue of Cenozoic adakite. Earth and Planetary Science Letters 182 (1), 115–125.

Söderlund, U., Patchett, P. J., Vervoort, J. D., & Isachsen, C. E. (2004). The 176 Lu decay constant determined by Lu–Hf and U–Pb isotope systematics of Precambrian mafic intrusions. Earth and Planetary Science Letters, 219(3–4), 311–324. https://doi.org/10.1016/S0012- 821X(04)00012-3

Soloviev, S. G., & Krivoshchekov, N. N. (2011). Vostok-2 gold-base-metal-tungsten skarn deposit, Central Sikhote-Alin, Russia. Geology of Ore Deposits, 53(6), 478-500.

Song, B., Niu, B.G., Li, J.Y., Xu, W.X., (1994). Isotope geochronology of granitoids in Mudanjiang-Jixi area. Acta Petrologica et Mineralogica 13, 204–213 (in Chinese with English abstract).

Song, S., Wang, M. M., Xu, X., Wang, C., Niu, Y., Allen, M. B., & Su, L. (2015). Ophiolites in the Xing'an-Inner Mongolia accretionary belt of the CAOB: Implications for two cycles of seafloor spreading and accretionary orogenic events. Tectonics, 34, 2221–2248. https://doi.org/ 10.1002/2015TC003948

Song, Y., Ren, J., Stepashko, A. A., & Li, J. (2014). Post-rift geodynamics of the Songliao Basin, NE China: Origin and significance of T11 (Coniacian) unconformity. Tectonophysics, 634, 1-18.

Song, Y., Stepashko, A., Liu, K., He, Q., Shen, C., Shi, B., & Ren, J. (2018). Post‐rift Tectonic History of the Songliao Basin, NE China: Cooling Events and Post‐rift Unconformities Driven by Orogenic Pulses From Plate Boundaries. Journal of Geophysical Research: Solid Earth, 123(3), 2363-2395.

Sorokin, A., Kotov, A., Kudryashov, N., Kovach, V., (2016a). Early Mesozoic granitoid and rhyolite magmatism of the Bureya Terrane of the Central Asian Orogenic Belt: Age and geodynamic setting. Lithos.

Sorokin, A., Ovchinnikov, R., Kudryashov, N., Sorokina, A., (2016b). An Early Neoproterozoic gabbro–granite association in the Bureya Continental Massif (Central Asian fold belt): First geochemical and geochronological data, Doklady Earth Sciences. Springer, pp. 1307-1311.

Sorokin, A., Kotov, A., Sal'nikova, E., Kudryashov, N., Anisimova, I., Yakovleva, S., Fedoseenko, A., (2010). Granitoids of the Tyrma–Bureya complex in the northern

Bureya–Jiamusi superterrane of the Central Asian fold belt: age and geodynamic setting. Russian Geology and Geophysics 51, 563-571.

Sorokin, A., Kudryashov, N., Kotov, A., (2007). Age and geochemistry of the Early Mesozoic granitoid massifs of the southern Bureya terrane of the Russian Far East. Russian Journal of Pacific Geology 1, 454-463.

Sorokin, A., Malyshev, Y.F., Kaplun, V., Sorokina, A., Artemenko, T., (2013). Evolution and deep structure of the Zeya-Bureya and Songliao sedimentary basins (East Asia). Russian Journal of Pacific Geology 7, 77-91.

Sosson, M., Bourgois, J., & de Lépinay, B. M. (1994). SeaBeam and deep-sea submersible Nautile surveys in the Chiclayo canyon off Peru (7 S): subsidence and subduction-erosion of an Andean-type convergent margin since Pliocene times. Marine Geology, 118(3-4), 237-256.

Steinberger, B., Sutherland, R., & O'connell, R. J. (2004). Prediction of Emperor-Hawaii seamount locations from a revised model of global plate motion and mantle flow. Nature, 430(6996), 167.

Sun, M. D., Chen, H. L., Zhang, F. Q., Wilde, S. A., Dong, C. W., & Yang, S. F. (2013). A 100 Ma bimodal composite dyke complex in the Jiamusi Block, NE China: an indication for lithospheric extension driven by Paleo-Pacific roll-back. Lithos, 162, 317-330.

Sun, M. D., Xu, Y. G., Wilde, S. A., & Chen, H. L. (2015a). Provenance of Cretaceous trench slope sediments from the Mesozoic Wandashan Orogen, NE China: Implications for determining ancient drainage systems and tectonics of the Paleo-Pacific. Tectonics, 34, 1269–1289. https://doi.org/10.1002/2015TC003870

Sun, M. D., Xu, Y. G., Wilde, S. A., Chen, H. L., & Yang, S. F. (2015b). The Permian Dongfanghong island-arc gabbro of the Wandashan Orogen, NE China: Implications for Paleo-Pacific subduction. Tectonophysics, 659, 122–136. https://doi.org/10.1016/j.tecto.2015.07.034

Sun, M., Chen, H., Milan, L. A., Wilde, S. A., Jourdan, F., & Xu, Y. (2018). Continental Arc and Back‐Arc Migration in Eastern NE China: New Constraints on

Cretaceous Paleo‐Pacific Subduction and Rollback. Tectonics, 37(10), 3893-3915.

Sun, M.D., (2013). Late Mesozoic magmatism and its tectonic implication for the Jiamusi Block and adjacet areas of NE China. Thesis, Zhejiang University, pp. 1-202 (In Chinese with English abstract).

Sun, S., McDonough, F., (1989). Chemical and isotopic systematics of oceanic basalts: implication for mantle composition and processes. In: Saunders, A.D., Norry, M.J. (Eds.), Magmatism in the Ocean Basins. Geological Society London: Special Publications 42, pp. 313–345.

Sun, W., Ding, X., Hu, Y. H., & Li, X. H. (2007). The golden transformation of the Cretaceous plate subduction in the west Pacific. Earth and Planetary Science Letters, 262(3-4), 533-542.

Sun, W., Ling, M., Yang, X., Fan, W., Ding, X., & Liang, H. (2010). Ridge subduction and porphyry copper-gold mineralization: An overview. Science China Earth Sciences, 53(4), 475-484.

Sun, X., Wang, S., Wang, Y., Du, J., & Xu, Q. (2010). The structural feature and evolutionary series in the northern segment of Tancheng-Lujiang fault zone. Acta Petrologica Sinica, 26(1), 165-176. (In Chinese with English Abstract).

Taira, A. (2001). Tectonic evolution of the Japanese island arc system. Annual Review of Earth and Planetary Sciences, 29(1), 109–134. https://doi.org/10.1146/annurev.earth.29.1.109

Takeuchi, T., Kodama, K., & Ozawa, T. (1999). Paleomagnetic evidence for block rotations in central Hokkaido–south Sakhalin, Northeast Asia. Earth and Planetary Science Letters, 169(1-2), 7-21.

Tang, G. J., Wyman, D. A., Wang, Q., Li, J., Li, Z. X., Zhao, Z. H., & Sun, W. D. (2012). Asthenosphere–lithosphere interaction triggered by a slab window during ridge subduction: trace element and Sr–Nd–Hf–Os isotopic evidence from Late Carboniferous tholeiites in the western Junggar area (NW China). Earth and Planetary Science Letters, 329, 84-96.

Tang, J., Xu, W., Niu, Y., Wang, F., Ge, W., Sorokin, A. A., & Chekryzhov, I. Y. (2016).

Geochronology and geochemistry of Late Cretaceous–Paleocene granitoids in the Sikhote-Alin Orogenic Belt: Petrogenesis and implications for the oblique subduction of the paleo-Pacific plate. Lithos, 266, 202-212.

Tang, J., Xu, W.L., Wang, F., Gao, F.H., Cao, H.H., 2011. Petrogenesis of bimodal volcanic rocks from Maoershan Formation in Zhangguangcai Range: Evidence from geochronology and geochemistry. Global Geology 30, 508-520 (In Chinese with English abstract).

Tang, J., Xu, W.L., Wang, F., Wang, W., Xu, M.J., Zhang, Y.H., (2014). Geochronology and geochemistry of Early–Middle Triassic magmatism in the Erguna Massif, NE China: constraints on the tectonic evolution of the Mongol–Okhotsk Ocean. Lithos 184, 1-16.

Tapponnier, P., & Molnar, P. (1976). Slip-line field theory and large-scale continental tectonics. Nature, 264(5584), 319.

Tapponnier, P., Lacassin, R., Leloup, P. H., Schärer, U., Dalai, Z., Haiwei, W., ... & Jiayou, Z. (1990). The Ailao Shan/Red River metamorphic belt: tertiary left-lateral shear between Indochina and South China. Nature, 343(6257), 431.

Tarduno, J. A., Duncan, R. A., Scholl, D. W., Cottrell, R. D., Steinberger, B., Thordarson, T., ... & Carvallo, C. (2003). The Emperor Seamounts: Southward motion of the Hawaiian hotspot plume in Earth's mantle. Science, 301(5636), 1064-1069.

Tarduno, J., Bunge, H. P., Sleep, N., & Hansen, U. (2009). The bent Hawaiian-Emperor hotspot track: Inheriting the mantle wind. Science, 324(5923), 50-53.

Thorkelson, D. J. (1996). Subduction of diverging plates and the principles of slab window formation. Tectonophysics, 255(1-2), 47-63.

Thorkelson, D. J., Madsen, J. K., & Sluggett, C. L. (2011). Mantle flow through the Northern Cordilleran slab window revealed by volcanic geochemistry. Geology, 39(3), 267-270.

Tikoff, B., & Teyssier, C. (1992). Crustal-scale, en echelon" P-shear" tensional bridges: A possible solution to the batholithic room problem. Geology, 20(10), 927-930.

Tomurtogoo, O., Windley, B., Kröner, A., Badarch, G., Liu, D., (2005). Zircon age and

occurrence of the Adaatsag ophiolite and Muron shear zone, central Mongolia: constraints on the evolution of the Mongol–Okhotsk ocean, suture and orogen. Journal of the Geological Society 162, 125-134.

Treuil, M., Joron, J., (1975). Utilisation des elements hygromagmatophiles pour la simplification de la modélisation quantitative des processus magmatiques: exemples de l'Afar et de la dorsale médio-atlantique. Soc. Ital. Mineral. Petrol 31, 125-174.

Tsutsumi, Y., Yokoyama, K., Kasatkin, S. A., & Golozubov, V. V. (2016). Provenance study of accretionary complexes in Primorye, Far East Russia, using ages and compositions of detrital minerals. Memoirs of the National Museum of Nature and Science, 51, 79–87.

Tsutsumi, Y., Yokoyama, K., Kasatkin, S. A., Golozubov, V. V., (2014). Zircon U–Pb age of granitoids in the Maizuru Belt, southwest Japan and the southernmost Khanka Massif, Far East Russia. Journal of Mineralogical and Petrological Sciences, 109(2), 97-102.

Turek, A., & Kim, C.-B. (1996). U-Pb zircon ages for Precambrian rocks in southwestern Ryeongnam and southwestern Gyeonggi massifs, Korea. Geochemical Journal, 30(4), 231–249. https://doi.org/10.2343/geochemj.30.231

Uno, K., Otofuji, Y. I., Matsuda, T., Kuniko, Y., Enami, R., Kulinich, R. G., ... & Sakhno, V. G. (1999). Late Cretaceous paleomagnetic results from Northeast Asian continental margin: the Sikhote Alin mountain range, eastern Russia. Geophysical research letters, 26(5), 553-556.

Utkin, V. (1993). Wrench faults of Sikhote-Alin and accretionary and destructive types of fault dislocation in the Asia-Pacific transition zone. The Tancheng-Lujiang wrench fault system, 225–237.

Utkin, V. (2013). Shear structural paragenesis and its role in continental rifting of the East Asian margin. Russian Journal of Pacific Geology, 7(3), 167–188. https://doi.org/10.1134/S181971401303007X

Utkin, V. P., Nevolin, P. L., & Mitrokhin, A. N. (2007). Late Paleozoic and Mesozoic deformations in the southwestern Primorye region. Russian Journal of Pacific

Geology, 1(4), 307-323.

Vakhrameev, V. (1987). Climates and the distribution of some gymsosperms in Asia during the Jurassic and Cretaceous. Review of Palaeobotany and Palynology, 51(1–3), 205–212. https://doi.org/10.1016/0034-6667(87)90030-3

Van Achterbergh, E., Ryan, C., & Griffin, W. (2001). GLITTER On-Line Interactive Data Reduction for the LA-ICPMS Microprobe. Sydney: Macquarie Research Ltd.

Van der Voo, R., Spakman, W., Bijwaard, H., (1999). Mesozoic subducted slabs under Siberia. Nature 397, 246-249.

Von Huene, R., & Lallemand, S. (1990). Tectonic erosion along the Japan and Peru convergent margins. Geological Society of America Bulletin, 102(6), 704-720.

Wang, F., Xu, W.L., Meng, E., Cao, H.H., Gao, F.H., (2012). Early Paleozoic amalgamation of the Songnen–Zhangguangcai Range and Jiamusi massifs in the eastern segment of the Central Asian Orogenic Belt: Geochronological and geochemical evidence from granitoids and rhyolites. Journal of Asian Earth Sciences 49, 234-248.

Wang, F., Xu, W.L., Xu, Y.G., Gao, F.H., Ge, W.C., (2015). Late Triassic bimodal igneous rocks in eastern Heilongjiang Province, NE China: implications for the initiation of subduction of the Paleo-Pacific Plate beneath Eurasia. Journal of Asian Earth Sciences 97, 406-423.

Wang, F., Zhou, X. H., Zhang, L. C., Ying, J. F., Zhang, Y. T., Wu, F. Y., & Zhu, R. X. (2006). Late Mesozoic volcanism in the Great Xing'an Range (NE China): timing and implications for the dynamic setting of NE Asia. Earth and Planetary Science Letters, 251(1-2), 179-198.

Wang, J., Chang, S.-C., Lu, H.-B., & Zhang, H.-C. (2016). Detrital zircon provenance of the Wangshi and Laiyang groups of the Jiaolai basin: Evidence for Early Cretaceous uplift of the Sulu orogen, Eastern China. International Geology Review, 58(6), 719–736. https://doi.org/ 10.1080/00206814.2015.1105728

Wang, M., Zhang, J., Zhang, B., Qi, G., (2015). An Early Paleozoic collisional event along the northern margin of the Central Tianshan Block: constraints from

geochemistry and geochronology of granitic rocks. Journal of Asian Earth Sciences 113, 325–338.

Wang, P.J., Chen, F., Chen, S.M., Siebel, W., Satir, M., (2006). Geochemical and Nd-Sr-Pb isotopic composition of Mesozoic volcanic rocks in the Songliao basin, NE China. Geochemical Journal 40, 149-159.

Wang, Q., Deng, J., Li, C., Li, G., Yu, L., & Qiao, L. (2014). The boundary between the Simao and Yangtze blocks and their locations in Gondwana and Rodinia: Constraints from detrital and inherited zircons. Gondwana Research, 26(2), 438–448. https://doi.org/10.1016/ j.gr.2013.10.002

Wang, Q.H., (2004). Recycling lower continental crust in the North China craton. Nature 432, 892–897.

Wang, T., Guo, L., Zheng, Y., Donskaya, T., Gladkochub, D., Zeng, L., J., Wang, Y., Mazukabzov, A., (2012). Timing and processes of late Mesozoic mid-lower-crustal extension in continental NE Asia and implications for the tectonic setting of the destruction of the North China Craton: mainly constrained by zircon U–Pb ages from metamorphic core complexes. Lithos, 154, 315-345.

Wang, T., Zheng, Y., Zhang, J., Zeng, L., Donskaya, T., Guo, L., & Li, J. (2011). Pattern and kinematic polarity of late Mesozoic extension in continental NE Asia: Perspectives from metamorphic core complexes. Tectonics, 30(6).

Wang, X.F., Li, Z.J., Chen, B.L., (2000). Tan-Lu Fault Zone. Geol. Publ. House, Beijing, pp. 122–258 (in Chinese).

Wei, H., Sun, D., Ye, S., Yang, Y., Liu, Z., Liu, X., Hu, Z., (2012). Zircon U-Pb ages and its geological significance of the granitic rocks in the Yichun-Hegang region, southeastern Xiao Hinggan Mountains. Earth Science-Journal of China University of Geosciences 37, 50-59 (In Chinese with English abstract).

Wei, H.Y., Sun, D.Y., Ye, S.Q., Yang, Y.C., Liu, Z.H., Liu, X.M., Liu, Z.C., (2008). Zircon U–Pb ages and its geological significance of the granitic rocks in the Yichun-Hegang region, southeastern Xiao Hinggan Mountains. Earth Science - Journal of China University of Geosciences 37, 50–59 (in Chinese with English abstract).

Whalen, J. B., Currie, K. L., & Chappell, B. W. (1987). A-type granites: geochemical characteristics, discrimination and petrogenesis. Contributions to mineralogy and petrology, 95(4), 407-419.

Whittaker, J. M., Müller, R. D., Leitchenkov, G., Stagg, H., Sdrolias, M., Gaina, C., & Goncharov, A. (2007). Major Australian-Antarctic plate reorganization at Hawaiian-Emperor bend time. Science, 318(5847), 83-86.

Wilde, S. A. (2015). Final amalgamation of the Central Asian Orogenic Belt in NE China: Paleo-Asian Ocean closure versus Paleo-Pacific plate subduction—A review of the evidence. Tectonophysics, 662, 345–362. https://doi.org/10.1016/j.tecto.2015.05.006

Wilde, S. A., Dorsett-Bain, H. L., & Lennon, R. G. (1999). Geological setting and controls on the development of graphite, sillimanite and phosphate mineralization within the Jiamusi Massif: An exotic fragment of Gondwanaland located in north-eastern China? Gondwana Research, 2(1), 21–46. https://doi.org/10.1016/S1342-937X(05)70125-8

Wilde, S. A., Wu, F., & Zhang, X. (2003). Late Pan-African magmatism in northeastern China: SHRIMP U–Pb zircon evidence from granitoids in the Jiamusi Massif. Precambrian Research, 122(1-4), 311-327.

Wilde, S. A., Zhang, X., & Wu, F. (2000). Extension of a newly identified 500Ma metamorphic terrane in North East China: Further U–Pb SHRIMP dating of the Mashan Complex, Heilongjiang Province, China. Tectonophysics, 328(1–2), 115–130. https://doi.org/10.1016/S0040- 1951(00)00180-3

Wilde, S. A., Zhao, G., & Sun, M. (2002). Development of the North China Craton during the late Archaean and its final amalgamation at 1.8 Ga: Some speculations on its position within a global Palaeoproterozoic supercontinent. Gondwana Research, 5(1), 85–94. https://doi.org/ 10.1016/S1342-937X(05)70892-3

Wilde, S., Dorsett-Bain, H., & Liu, J. (1997). The identification of a Late Pan-African granulite facies event in northeastern China: SHRIMP U–Pb zircon dating of the Mashan Group at Liu Mao, Heilongjiang Province, China. Proceedings of the 30th IGC: Precambrian Geology and Metamorphic Petrology, 17, 59–74.

Wilde, S.A., (2015). Final amalgamation of the Central Asian Orogenic Belt in NE China: Paleo-Asian Ocean closure versus Paleo-Pacific plate subduction—a review of the evidence. Tectonophysics 662, 345-362.

Wilde, S.A. and Zhou, J.B., (2015). The late Paleozoic to Mesozoic evolution of the eastern margin of the Central Asian Orogenic Belt in China. Journal of Asian Earth Sciences 113, 909-921.

Windley, B. F., Alexeiev, D., Xiao, W., Kröner, A., & Badarch, G. (2007). Tectonic models for accretion of the Central Asian Orogenic Belt. Journal of the Geological Society, 164(1), 31–47. https://doi.org/10.1144/0016-76492006-022

Wolf, M., London, D., (1994). Apatite dissolution into peraluminous haplogranitic melts: an experimental study of solubilities and mechanisms. Geochimica et Cosmochimica Acta 58, 4127–4145.

Wu, F. Y., Han, R. H., Yang, J. H., Wilde, S. A., Zhai, M. G., & Park, S. C. (2007). Initial constraints on the timing of granitic magmatism in North Korea using U–Pb zircon geochronology. Chemical Geology, 238(3–4), 232–248. https://doi.org/10.1016/j.chemgeo.2006.11.012

Wu, F. Y., Jahn, B. M., Wilde, S. A., Lo, C. H., Yui, T. F., Lin, Q., … Sun, D. Y. (2003a). Highly fractionated I-type granites in NE China (I): Geochronology and petrogenesis. Lithos, 66(3–4), 241–273. https://doi.org/10.1016/S0024-4937(02)00222-0

Wu, F. Y., Jahn, B. M., Wilde, S. A., Lo, C. H., Yui, T. F., Lin, Q., … Sun, D. Y. (2003b). Highly fractionated I-type granites in NE China (II): Isotopic geochemistry and implications for crustal growth in the Phanerozoic. Lithos, 67(3–4), 191–204. https://doi.org/10.1016/S0024- 4937(03)00015-X

Wu, F. Y., Sun, D. Y., Ge, W. C., Zhang, Y. B., Grant, M. L., Wilde, S. A., & Jahn, B. M. (2011). Geochronology of the Phanerozoic granitoids in northeastern China. Journal of Asian Earth Sciences, 41(1), 1-30.

Wu, F. Y., Zhang, Y. B., Yang, J. H., Xie, L. W., & Yang, Y. H. (2008). Zircon U–Pb and Hf isotopic constraints on the Early Archean crustal evolution in Anshan of the North China Craton. Precambrian Research, 167(3–4), 339–362.

https://doi.org/10.1016/j.precamres.2008.10.002

Wu, F., Wilde, S.A., Sun, D.Y., (2001). Zircon SHRIMP U–Pb ages of gneissic granites in Jiamusi Massif, northeastern China. Acta Petrologica Sinica 17, 443–452 (in Chinese with English abstract).

Wu, F., Yang, J., Lo, C., Wilde, S.A., Sun, D., Jahn, B., (2007). The Heilongjiang Group: a Jurassic accretionary complex in the Jiamusi Massif at the western Pacific margin of northeastern China. Island Arc 16, 156–172.

Wu, F.Y., Jahn, B.M., Wilde, A.S., Sun, D.Y., (2000). Phanerozoic crustal growth: U–Pb and Sr–Nd isotopic evidence from the granites in northeastern China. Tectonophysics 328, 89-113.

Wu, J. T. J., Jahn, B. M., Nechaev, V., Chashchin, A., Popov, V., Yokoyama, K., & Tsutsumi, Y. (2017). Geochemical characteristics and petrogenesis of adakites in the Sikhote-Alin area, Russian Far East. Journal of Asian Earth Sciences, 145, 512-529.

Wu, L., Monié, P., Wang, F., Lin, W., Ji, W., & Yang, L. (2018). Multi-phase cooling of Early Cretaceous granites on the Jiaodong Peninsula, East China: Evidence from 40Ar/39Ar and (U-Th)/He thermochronology. Journal of Asian Earth Sciences, 160, 334-347.

Wu, Y. B., & Zheng, Y. F. (2013). Tectonic evolution of a composite collision orogen: An overview on the Qinling–Tongbai–Hong'an–Dabie– Sulu orogenic belt in central China. Gondwana Research, 23(4), 1402–1428. https://doi.org/10.1016/j.gr.2012.09.007

Wyld, S. J., & Wright, J. E. (2001). New evidence for Cretaceous strike-slip faulting in the United States Cordillera and implications for terrane- displacement, deformation patterns, and plutonism. American Journal of Science, 301(2), 150–181. https://doi.org/10.2475/ajs.301.2.150

Xiao, L., Clemens, J.D., (2007). Origin of potassic C-type. adakite magmas: experimental and field constraints. Lithos 95, 399–414.

Xiao, W., Windley, B. F., Hao, J., & Zhai, M. (2003). Accretion leading to collision and the Permian Solonker suture, Inner Mongolia, China: termination of the

central Asian orogenic belt. Tectonics, 22(6), 1069. https://doi.org/10.1029/2002TC001484

Xiong, X.L., (2006). Trace element evidence for the growth of early continental crust by melting of rutile-bearing hydrous eclogite. Geology 34, 945–948.

Xu, B., Zhao, P., Bao, Q.Z., Zhou, Y.H., Wang, Y.Y., Luo, Z.W., (2014). Preliminary study on the pre-Mesozoic tectonic unit division of the Xing-Meng Orogenic Belt XMOB. Acta Petrologica Sinica 30, 1841–1857 (in Chinese with English abstract).

Xu, B., Zhao, P., Wang, Y., Liao, W., Luo, Z., Bao, Q., & Zhou, Y. (2015). The pre-Devonian tectonic framework of Xing'an–Mongolia orogenic belt (XMOB) in north China. Journal of Asian Earth Sciences, 97, 183–196. https://doi.org/10.1016/j.jseaes.2014.07.020

Xu, J. W., & Zhu, G. (1994). Tectonic models of the Tan-Lu fault zone, eastern China. International Geology Review, 36(8), 771–784.

Xu, J., & Zhu, G. (1994). Tectonic models of the Tan-Lu fault zone, eastern China. International Geology Review, 36(8), 771-784.

Xu, J., Zhu, G., Tong, W., Cui, K., & Liu, Q. (1987). Formation and evolution of the Tancheng-Lujiang wrench fault system: a major shear system to the northwest of the Pacific Ocean. Tectonophysics, 134(4), 273-310.

Xu, T., Xu, W. L., Wang, F., Ge, W. C., Sorokin, A. A., (2018). Geochronology and geochemistry of early Paleozoic intrusive rocks from the Khanka Massif in the Russian Far East: Petrogenesis and tectonic implications. Lithos, 300, 105-120.

Xu, W. L., Pei, F. P., Wang, F., Meng, E., Ji, W. Q., Yang, D. B., & Wang, W. (2013). Spatial–temporal relationships of Mesozoic volcanic rocks in NE China: Constraints on tectonic overprinting and transformations between multiple tectonic regimes. Journal of Asian Earth Sciences, 74, 167–193. https://doi.org/10.1016/j.jseaes.2013.04.003

Xu, W.L., Ji, W., Pei, F.P., Meng, E., Yu, Y., Yang, D., Zhang, X., (2009). Triassic volcanism in eastern Heilongjiang and Jilin provinces, NE China: chronology, geochemistry, and tectonic implications. Journal of Asian Earth Sciences 34, 392–

402.

Yabe, A., Terada, K., & Sekido, S. (2003). The Tetori-type flora, revised: A review. Memoir of the Fukui Prefectural Dinosaur Museum, 2, 23–42. Yang, J. H., Wu, F. Y., Shao, J. A., Wilde, S. A., Xie, L. W., & Liu, X. M. (2006). Constraints on the timing of uplift of the Yanshan Fold and Thrust

Yang, H., Ge, W. C., Zhao, G. C., Bi, J. H., Wang, Z. H., Dong, Y., & Xu, W. L. (2017). Zircon U–Pb ages and geochemistry of newly discovered Neoproterozoic orthogneisses in the Mishan region, NE China: Constraints on the high-grade metamorphism and tectonic affinity of the Jiamusi–Khanka Block. Lithos, 268, 16-31.

Yang, H., Ge, W., Zhao, G., Yu, J., & Zhang, Y. (2015a). Early Permian–Late Triassic granitic magmatism in the Jiamusi–Khanka Massif, eastern segment of the Central Asian Orogenic Belt and its implications. Gondwana Research, 27(4), 1509–1533. https://doi.org/10.1016/j. gr.2014.01.011

Yang, H., Ge, W.C., Zhao, G.C., Dong, Y., Xu, W.L., Ji, Z., Yu, J.J., (2015b). Late Triassic intrusive complex in the Jidong region, Jiamusi–Khanka Block, NE China: Geochemistry, zircon U–Pb ages, Lu–Hf isotopes, and implications for magma mingling and mixing. Lithos 224, 143-159.

Yang, H., Ge, W.C, Dong, Y., Bi, J.H., Wang, Z.H., Ji, Z., (2016). Record of Permian–Early Triassic continental arc magmatism in the western margin of the Jiamusi Block, NE China: petrogenesis and implications for Paleo-Pacific subduction. International Journal of Earth Sciences, doi:10.1007/s00531-016-1396-y.

Yang, H., Zhang, Y.L., Chen, H.J., Ge, W.C., (2012). Zircon U–Pb ages of Khanka Lake granitic complex and its geological implication. Global Geology 31, 621–630 (in Chinese with English abstract).

Yang, J. H., Wu, F. Y., Wilde, S. A., Belousova, E., & Griffin, W. L. (2008). Mesozoic decratonization of the North China block. Geology, 36(6), 467–470. https://doi.org/10.1130/G24518A.1

Yang, J., Gao, S., Chen, C., Tang, Y., Yuan, H., Gong, H., … Wang, J. (2009). Episodic crustal growth of North China as revealed by U–Pb age and Hf isotopes of detrital

zircons from modern rivers. Geochimica et Cosmochimica Acta, 73(9), 2660–2673. https://doi.org/10.1016/ j.gca.2009.02.007

Yang, S., Zhang, F., & Wang, Z. (2012). Grain size distribution and age population of detrital zircons from the Changjiang (Yangtze) River system, China. Chemical Geology, 296, 26–38.

Yin, A., & Nie, S. (1993). An indentation model for the North and South China collision and the development of the Tan-Lu and Honam fault systems, eastern Asia. Tectonics, 12(4), 801–813. https://doi.org/10.1029/93TC00313

Yu, J., Hou, X., Zhang, Y., & Liu, J. (2013). Magma mixing genesis of the Early Permian Liulian pluton at the northeastern margin of the Jiamusi massif in NE China: Evidence from petrology, geochronology and geochemistry. Acta Petrologica Sinica, 29(9), 2971–2986.

Yu, J., Wang, F., Xu, W., Gao, F., & Pei, F. (2012). Early Jurassic mafic magmatism in the Lesser Xing'an–Zhangguangcai Range, NE China, and its tectonic implications: Constraints from zircon U–Pb chronology and geochemistry. Lithos, 142, 256–266.

Yu, J.J., Hou, X., Ge, W.C., Zhang, Y., Liu, J., (2013). Magma mixing genesis of the Early Permian Liulian pluton at the northeastern margin of the Jiamusi massif in NE China: evidences from petrography, geochronology and geochemistry. Acta Petrologica Sinica 29, 2971-2986 (In Chinese with English abstract).

Yui, T., Maki, K., Lan, C., Hirata, T., Chu, H., Kon, Y., … Ernst, W. (2012). Detrital zircons from the Tananao metamorphic complex of Taiwan: Implications for sediment provenance and Mesozoic tectonics. Tectonophysics, 541, 31–42.

Zhai, M. G., & Santosh, M. (2011). The early Precambrian odyssey of the North China Craton: A synoptic overview. Gondwana Research, 20(1), 6–25. https://doi.org/10.1016/j.gr.2011.02.005

Zhai, M. G., Guo, J. H., Peng, P., & Hu, B. (2007). U-Pb zircon age dating of a rapakivi granite batholith in Rangnim massif, North Korea. Geological Magazine, 114, 547–552.

Zhang, F. Q., Chen, H. L., Batt, G. E., Dilek, Y., Min-Na, A., Sun, M. D., ... & Zhao,

X. Q., (2015). Detrital zircon U–Pb geochronology and stratigraphy of the Cretaceous Sanjiang Basin in NE China: Provenance record of an abrupt tectonic switch in the mode and nature of the NE Asian continental margin evolution. Tectonophysics, 665, 58-78.

Zhang, F. Q., Chen, H. L., Yang, S. F., Feng, Z. Q., Wu, H. Y., Batt, G. E., ... & Yang, J. G. (2012). Late Mesozoic–Cenozoic evolution of the Sanjiang Basin in NE China and its tectonic implications for the West Pacific continental margin. Journal of Asian Earth Sciences, 49, 287-299.

Zhang, F. Q., Dilek, Y., Chen, H. L., Yang, S. F., & Meng, Q. A. (2017). Structural architecture and stratigraphic record of Late Mesozoic sedimentary basins in NE China: Tectonic archives of the Late Cretaceous continental margin evolution in East Asia. Earth-Science Reviews, 171, 598-620.

Zhang, F., Chen, H., Yu, X., Dong, C., Yang, S., Pang, Y., Batt, G., (2011). Early Cretaceous volcanism in the northern Songliao Basin, NE China, and its geodynamic implication. Gondwana Research 19, 163-176.

Zhang, H. F., Zhu, R. X., Santosh, M., Ying, J. F., Su, B. X., & Hu, Y. (2013). Episodic widespread magma underplating beneath the North China Craton in the Phanerozoic: Implications for craton destruction. Gondwana Research, 23(1), 95–107. https://doi.org/10.1016/j.gr.2011.12.006

Zhang, J. H., Gao, S., Ge, W. C., Wu, F. Y., Yang, J. H., Wilde, S. A., & Li, M. (2010). Geochronology of the Mesozoic volcanic rocks in the Great Xing'an Range, northeastern China: implications for subduction-induced delamination. Chemical Geology, 276(3-4), 144-165.

Zhang, Q. S., & Yang, Z. S. (1988). Early Crust and Mineral Deposits of Liaodong Peninsula, China. Beijing: Geological Publishing House.

Zhang, Q., Wang, Y., Li, C.D., Wang, Y.L., Jin, W.J., Jia, X.Q., (2006). Granite classification on the basis of Sr and Yb contents and its implications. Acta Petrologica Sinica 22, 2249–2269 (in Chinese with English abstract).

Zhang, R., Liou, J., & Ernst, W. (2009). The Dabie–Sulu continental collision zone: A comprehensive review. Gondwana Research, 16(1), 1–26.

https://doi.org/10.1016/j.gr.2009.03.008

Zhang, S. H., Zhao, Y., Davis, G. A., Ye, H., & Wu, F. (2014). Temporal and spatial variations of Mesozoic magmatism and deformation in the North China Craton: Implications for lithospheric thinning and decratonization. Earth-Science Reviews, 131, 49–87. https://doi.org/10.1016/j.earscirev.2013.12.004

Zhang, S. H., Zhao, Y., Song, B., Hu, J. M., Liu, S. W., Yang, Y. H., … Liu, J. (2009). Contrasting Late Carboniferous and Late Permian–Middle Triassic intrusive suites from the northern margin of the North China craton: Geochronology, petrogenesis, and tectonic implications. Geological Society of America Bulletin, 121(1–2), 181–200.

Zhang, S. H., Zhao, Y., Song, B., Yang, Z. Y., Hu, J. M., & Wu, H. (2007). Carboniferous granitic plutons from the northern margin of the North China block: Implications for a late Palaeozoic active continental margin. Journal of the Geological Society, 164(2), 451–463. https://doi.org/ 10.1144/0016-76492005-190

Zhang, S., Zhu, G., Liu, C., Li, Y., Su, N., Xiao, S., & Gu, C. (2018). Strike‐Slip Motion Within the Yalu River Fault Zone, NE Asia: The Development of a Shear Continental Margin. Tectonics, 37(6), 1771-1796.

Zhang, S., Zhu, G., Liu, C., Li, Y., Su, N., Xiao, S., & Gu, C., (2018). Strike-slip motion within the Yalu River Fault Zone, NE Asia: The development of a shear continental margin. Tectonics 37, 1771-1796.

Zhang, X.Z., Guo, Y., Zhou, J.B., Zeng, Z., Pu, J.B., Fu, Q.L., (2015). Late Paleozoic-Early Mesozoic tectonic evolution in the east margin of the Jiamusi massif, eastern northeastern China. Russian Journal of Pacific Geology 9, 1-10.

Zhao, G. C., Cao, L., Wilde, S. A., Sun, M., Choe, W. J., & Li, S. Z. (2006). Implications based on the first SHRIMP U-Pb zircon dating on Precambrian granitoid rocks in North Korea. Earth and Planetary Science Letters, 251(3–4), 365–379. https://doi.org/10.1016/j. epsl.2006.09.021

Zhao, G., & Zhai, M. (2013). Lithotectonic elements of Precambrian basement in the North China Craton: Review and tectonic implications. Gondwana Research,

23(4), 1207–1240. https://doi.org/10.1016/j.gr.2012.08.016

Zhao, G., Cawood, P. A., Li, S., Wilde, S. A., Sun, M., Zhang, J., … Yin, C. (2012). Amalgamation of the North China Craton: Key issues and discussion. Precambrian Research, 222, 55–76.

Zhao, G., Sun, M., Wilde, S. A., & Sanzhong, L. (2005). Late Archean to Paleoproterozoic evolution of the North China Craton: Key issues revisited. Precambrian Research, 136(2), 177–202. https://doi.org/10.1016/j.precamres.2004.10.002

Zhao, G., Wilde, S. A., Cawood, P. A., & Sun, M. (2001). Archean blocks and their boundaries in the North China Craton: Lithological, geochemical, structural and P–T path constraints and tectonic evolution. Precambrian Research, 107(1–2), 45–73. https://doi.org/10.1016/ S0301-9268(00)00154-6

Zhao, P., Alexandrov, I., Jahn, B. M., Liao, J. P., & Ivin, V. (2019). Late Eocene granites in the Central Sakhalin Island (Russian Far East) and its implication for evolution of the Sakhalin-Hokkaido orogenic belt. Lithos, 324, 684-698.

Zhao, P., Chen, Y., Xu, B., Faure, M., Shi, G., & Choulet, F. (2013). Did the Paleo-Asian Ocean between North China Block and Mongolia Block exist during the late Paleozoic? First paleomagnetic evidence from central-eastern Inner Mongolia, China. Journal of Geophysical Research: Solid Earth, 118, 1873–1894.

Zhao, P., Jahn, B. M., & Xu, B. (2017). Elemental and Sr-Nd isotopic geochemistry of Cretaceous to Early Paleogene granites and volcanic rocks in the Sikhote-Alin Orogenic Belt (Russian Far East): implications for the regional tectonic evolution. Journal of Asian Earth Sciences, 146, 383-401.

Zhao, Y.L., Liu, Y.J., Han, G.Q., Wen, Q.B., Li, W., Liang, J.D., (2009). 3D finite element simulation on sinistral strike-slip of Dunhua-Mishan fault. Global Geology 28, 310–317 (in Chinese with English abstract).

Zheng, J., Griffin, W., O'Reilly, S. Y., Lu, F., Yu, C., Zhang, M., & Li, H. (2004). U–Pb and Hf-isotope analysis of zircons in mafic xenoliths from Fuxian kimberlites: Evolution of the lower crust beneath the North China Craton. Contributions to Mineralogy and Petrology, 148(1), 79–103. https://doi.org/10.1007/s00410-004-

0587-x

Zheng, J., Griffin, W., O'Reilly, S. Y., Zhang, M., Pearson, N., & Pan, Y. (2006). Widespread Archean basement beneath the Yangtze craton. Geology, 34(6), 417–420. https://doi.org/10.1130/G22282.1

Zhou, J. B., & Li, L. (2017). The Mesozoic accretionary complex in Northeast China: Evidence for the accretion history of Paleo-Pacific subduction. Journal of Asian Earth Sciences, 145, 91–100. https://doi.org/10.1016/j.jseaes.2017.04.013

Zhou, J. B., & Wilde, S. A. (2013). The crustal accretion history and tectonic evolution of the NE China segment of the Central Asian Orogenic Belt. Gondwana Research, 23(4), 1365-1377.

Zhou, J. B., Cao, J. L., Wilde, S. A., Zhao, G. C., Zhang, J. J., & Wang, B. (2014). Paleo-Pacific subduction-accretion: Evidence from Geochemical and U-Pb zircon dating of the Nadanhada accretionary complex, NE China. Tectonics, 33, 2444–2466. https://doi.org/10.1002/ 2014TC003637

Zhou, J. B., Wilde, S. A., Zhang, X. Z., Zhao, G. C., Liu, F. L., Qiao, D. W., ... & Liu, J. H. (2011). A > 1300 km late Pan-African metamorphic belt in NE China: New evidence from the Xing'an block and its tectonic implications. Tectonophysics, 509(3-4), 280-292.

Zhou, J. B., Wilde, S. A., Zhang, X. Z., Zhao, G. C., Zheng, C. Q., Wang, Y. J., & Zhang, X. H. (2009). The onset of Pacific margin accretion in NE China: evidence from the Heilongjiang high-pressure metamorphic belt. Tectonophysics, 478(3-4), 230-246.

Zhou, J.B., Wilde, S.A., Zhao, G., Zhang, X., Zheng, C., Wang, H., Zeng, W., (2010). Pan-African metamorphic and magmatic rocks of the Khanka Massif, NE China: further evidence regarding their affinity. Geological Magazine 147, 737–749.

Zhu, C. Y., Zhao, G., Sun, M., Eizenhöfer, P. R., Liu, Q., Zhang, X., ... & Hou, W., (2017a). Geochronology and geochemistry of the Yilan greenschists and amphibolites in the Heilongjiang complex, northeastern China and tectonic implications. Gondwana Research, 43, 213-228.

Zhu, C. Y., Zhao, G., Sun, M., Han, Y., Liu, Q., Eizenhöfer, P. R., ... & Hou, W., (2017b).

Detrital zircon U–Pb and Hf isotopic data for meta-sedimentary rocks from the Heilongjiang Complex, northeastern China and tectonic implications. Lithos, 282, 23-32.

Zhu, C.Y., Zhao, G., Sun, M., Liu, Q., Han, Y., Hou, W., Zhang, X., Eizenhofer, P.R., (2015). Geochronology and geochemistry of the Yilan blueschists in the Heilongjiang Complex, northeastern China and tectonic implications. Lithos 216, 241-253.

Zhu, D., Mo, X., Wang, L., Zhao, Z., Niu, Y., Zhou, C., Yang, Y., (2009). Petrogenesis of highly fractionated I-type granites in the Chayu area of eastern Gangdese, Tibet: constraints from zircon U–Pb geochronology, geochemistry and Sr-Nd-Hf isotopes. Science in China Series D-Earth Sciences 39, 833–848.

Zhu, G., Jiang, D., Zhang, B., & Chen, Y. (2012). Destruction of the eastern North China Craton in a backarc setting: Evidence from crustal deformation kinematics. Gondwana Research, 22(1), 86-103.

Zhu, G., Liu, G. S., Niu, M. L., Xie, C. L., Wang, Y. S., & Xiang, B. (2009). Syn-collisional transform faulting of the Tan-Lu fault zone, East China. International Journal of Earth Sciences, 98(1), 135-155.

Zhu, G., Wang, Y., Liu, G., Niu, M., Xie, C., & Li, C. (2005). $^{40}Ar/^{39}Ar$ dating of strike-slip motion on the Tan–Lu fault zone, East China. Journal of Structural Geology, 27(8), 1379-1398.

Zhu, R. X., Yang, J. H., & Wu, F. Y. (2012). Timing of destruction of the North China Craton. Lithos, 149, 51–60. https://doi.org/10.1016/ j.lithos.2012.05.013

Zonenshain, L. (1973). The evolution of Central Asiatic geosynclines through sea-floor spreading. Tectonophysics, 19(3), 213–232. https://doi. org/10.1016/0040-1951(73)90020-6

Zonenshain, L.P., Kuzmin, M.I., Natapov, L.M. (Eds.), 1990. Geology of the USSR: a plate tectonic synthesis. American Geophysical Union, Geodynamics Series 21.

Zorin, Y.A., (1999). Geodynamics of the western part of the Mongolia–Okhotsk collisional belt, Trans-Baikal region (Russia) and Mongolia. Tectonophysics 306, 33-56.